HARVARD UNIVERSITY
Graduate School of Arts and Sciences

DISSERTATION ACCEPTANCE CERTIFICATE

The undersigned, appointed by the

Department of Molecular and Cellular Biology

have examined a dissertation entitled

"Molecular Controls over Developmental Acquisition of Diverse Callosal Projection Neuron Subtype Identities"

presented by Ryan Marie Fame,

candidate for the degree of Doctor of Philosophy and hereby

certify that it is worthy of acceptance.

Signature Jeffrey D. Macklis

Typed name: Prof. Jeffrey Macklis

Signature

Typed name: Prof. Jeff Lichtman

Signature

Typed name: Prof. Paola Arlotta

Signature John E. Dowling

Typed name: Prof. John Dowling

Date: August 30, 2012

Molecular Controls over Developmental Acquisition of Diverse Callosal Projection Neuron Subtype Identities

A dissertation presented

by

Ryan Marie Fame

to

The Department of Molecular and Cellular Biology

in partial fulfillment of the requirements

for the degree of

Doctor of Philosophy

in the subject of

Biochemistry

Harvard University

Cambridge, Massachusetts

August 2012

Dissertation Advisor Doctoral Candidate

Professor Jeffrey D. Macklis Ryan Marie Fame

Molecular Controls over Developmental Acquisition of Diverse Callosal Projection Neuron Subtype Identities

Abstract

The mammalian neocortex is an exquisite, highly organized brain structure composed of hundreds of subpopulations of neurons and glia, precisely connected to enable motor control, sensory perception, information integration, and planning. Unique molecular, structural, and anatomical neuronal properties underlie diverse functionality, endowing much of the neocortex's complex processing power. Neocortical size correlates with information processing capacity, suggesting that increased neuronal number and diversity begets increased sophistication. One excitatory projection neuron type, callosal projection neurons (CPN), has disproportionately expanded with cortical size increase.

CPN directly connect homotypic regions of the two neocortical hemispheres by sending axons via the largest white matter fiber tract in the brain, the corpus callosum (CC), allowing quick relay, integration, and comparison of information. In humans, the CC contains over 300,000 axons, CPN have been centrally implicated in autism spectrum disorders, and absence or surgical disruption of CPN connectivity in humans is associated with defects in abstract reasoning, problem solving, and generalization. Therefore, CPN are critical to complex brain functions, and their diversity likely contributes to these roles.

Work presented in this dissertation addresses molecular controls over CPN development, specifically genes that are expressed by, and function in, particular subpopulations of CPN. While much progress has been made in identifying molecular controls over neocortical arealization, lamination, and broad subtype specification, CPN diversity has remained largely unaddressed. Therefore, this work begins by

identifying genes more highly expressed in CPN than other closely related projection neuron populations, and uncovers molecular diversity within CPN. From this molecular diversity, functional analysis of three candidate molecular controls over CPN subtype diversity follows. *Cited2* acts broadly in neocortical progenitor development and postnatally in refining somatosensory CPN identity. *Caveolin1* identifies a population of CPN with dual axonal projections. *Tmtc4* is mutated in human CC disease and can function in CPN axonal development. These analyses of CPN molecular diversity in mouse then expand to an investigation of which molecular subpopulations are conserved, expanded, or uncommon between rodent and primate, allowing both for comparative evolutionary theories of CPN function, and indicating which CPN populations critical for human brain function can be best studied in rodent models.

Table of Contents

Abstract iii
Table of Contents v
Figures and Tables vii
List of Abbreviations xi
Acknowledgements xii
Chapter 1: Introduction 1
- 1.1 Overview 2
- 1.2 Neocortical Progenitors 4
- 1.3 Specification of Neocortical Projection Neuron Progenitor Domains 16
- 1.4 Molecular Controls over Neocortical Projection Neuron Subtype Specification and Development 21
- 1.5 Areal Diversity of Neocortical Projection Neurons 66
- 1.6 Progressive Restriction and Refinement of Cortical Projection Neuron Subtypes 72
- 1.7 Disease Relevance 74
- 1.8 Dissertation Overview 75

Chapter 2: Novel Subtype-Specific Genes Identify Distinct Subpopulations of Callosal Projection Neurons 77
- 2.1 Abstract 78
- 2.2 Introduction 79
- 2.3 Materials and Methods 82
- 2.4 Results 88
- 2.5 Discussion 114

Chapter 3: Cited2 Functions Broadly in Early Intermediate Progenitor Cell Development and in Somatosensory Callosal Projection Neuron Identity Acquisition 119
- 3.1 Abstract 120
- 3.2 Introduction 121
- 3.3 Materials and Methods 127
- 3.4 Results 136
- 3.5 Discussion 172

Chapter 4: Caveolin1 identifies a specific subpopulation of CPN including dual projecting CPN/FPN 179
- 4.1 Abstract 180
- 4.2 Introduction 181
- 4.3 Materials and Methods 185
- 4.4 Results 191
- 4.5 Discussion 219

Chapter 5: TMTC4 is Critical for Human Corpus Callosum Formation and Functions in Axonal Development of a Subpopulation of Callosal Projection Neurons in Mice 224
- 5.1 Abstract 225
- 5.2 Introduction 226
- 5.3 Materials and Methods 232
- 5.4 Results 240
- 5.5 Discussion 260

Chapter 6: Subtype-Specific Genes that Identify Distinct Subpopulations of Callosal Projection Neurons in Mice Identify Molecularly Homologous Populations in Macaque 266
- 6.1 Abstract 267
- 6.2 Introduction 268
- 6.3 Materials and Methods 273
- 6.4 Results 278

6.5 Discussion 292
Chapter 7: Discussion **297**
7.1 Progressive acquisition of neocortical projection neuron identity 299
7.2 Callosal projection neuron diversity 302
7.3 Mechanisms of progressive generation of diverse callosal projection neuron subpopulations 304
7.4 Evolutionary neocortical expansion, implications for callosal projection neuron disease, and future directions 306

References **309**
Appendix/ Chapter 8: SOX6 Controls Dorsal Progenitor Identity and Interneuron Diversity During Neocortical Development **343**
8.1 Abstract 344
8.2 Introduction 345
8.3 Materials and Methods 348
8.4 Results 353
8.5 Discussion 396
8.6 Appendix References 401

Figures and Tables

Figure 1.1: Progenitors residing in the VZ and SVZ produce projection neurons in an "inside-out" fashion 6

Figure 1.2: Cortical projection neuron progenitors 8

Figure 1.3: Establishment of the pallial progenitor domain 18

Figure 1.4: Major subtypes of projection neurons within the neocortex 24

Figure 1.5: Schematic representation of an experimental approach used to identify projection neuron-specific genes 30

Figure 1.6: CPN development and diversity....36

Figure 1.7: Spatially-restricted genes identify novel CPN subpopulations 44

Table 1.1: Genes expressed by callosal projection neurons (CPN) and their progenitors 46

Figure 1.8: Comparison of developing and adult mammalian neocortex of mouse, macaque, and human shows correlations between SVZ expansion, superficial neocortical layer expansion, and white matter expansion 54

Figure 1.9: Evolutionary expansion of callosal projection neuron populations 56

Figure 1.10: Molecular controls over layer V cortical projection neuron subtype development 64

Figure 1.11: Functional and molecularly defined neocortical areas 68

Table 2.1: Detailed information about the clones used for *in situ* hybridization 86

Figure 2.1: Schematic of the experimental approach used to identify CPN-specific genes 90

Table 2.2: Selected subset of the genes identified by microarray analysis that are expressed at higher levels in callosal projection neurons compared to corticospinal motor neurons and corticotectal projection neurons 92

Figure 2.2: CPN-genes that label most callosal projection neurons across layers II/III and V 96

Figure 2.3: CPN-genes that selectively label callosal neurons of the superficial layers II/III and IV......100

Figure 2.4: CPN-genes that preferentially label the outermost portion of layer II/III and layer I 102

Figure 2.5: CPN-genes that preferentially label the deepest portion of layer II/III and layer IV 104

Figure 2.6: Genes that preferentially label CPN of the deep layers V and VI 106

Figure 2.7: Specific expression of Plexin-D1 and Dkk3 in retrogradely labeled CPN of the deep layers V and VI....108

Figure 2.8: Gene combinations identify CPN within sub-compartments of canonical cortical laminae..112

Figure 3.1: CPN areal diversity 122

Figure 3.2: *Cited2* is developmentally expressed by CPN and excluded from CSMN 138

Figu**re 3.3:** *Cited2* is expressed at early and mid-stage CPN development 140

Figure 3.4: At E15.5, peak time of neocortical *Cited2* expression, *Cited2* is most highly expressed in immature neurons of the SVZ....142

Figure 3.5: *Cited2* expression becomes progressively restricted to sensory neocortical areas................144

Figure 3.6: Conditional deletion of *Cited2* via *Emx1* driven cre recombinase expression results in specific loss of *Cited2* expression in the forebrain 146

Figure 3.7: Specific reduction in IPCs in E15.5 *Cited2* cKO 148

Figure 3.8: Loss of *Cited2* function results in a loss of Tbr2+ intermediate progenitors at E15.5...........150

Figure 3.9: Loss of *Cited2* function results in increased cell death at E15.5 154

Figure 3.10: Loss of *Cited2* function results reduced superficial layer thickness at P3 156

Figure 3.11: Loss of *Cited2* function results in reduced cortical length at P3 that is maintained at least until P21 158

Figure 3.12: Loss of *Cited2* function results in reduced cortical length in somatosensory neocortex at P3 that is restricted to the unrefined sensorimotor cortex at P0 and maintained until at least P8 160

Figure 3.13: Loss of *Cited2* function results in reduced cortical length in somatosensory neocortex only in superficial layer neurons and not in acallosal layer IV...162

Figure 3.14: Loss of *Cited2* function results increased somatosensory superficial layer cellular density at P3 166

Figure 3.15: Loss of *Cited2* function results in call-autonomous migration delay 168

Figure 3.16: Loss of *Cited2* function results in cell-autonomous axon extension delay 170

Figure 4.1: *Caveolin1* is expressed by a restricted population of caudo-lateral CPN 192

Figure 4.2: CAV1 is expressed in an areally restricted fashion at P8, and is excluded from motor cortex 194

Figure 4.3: A subset of CAV1-expressing neurons co-express CTIP2, but CAV1 is not expressed by SCPN 198

Figure 4.4: Caveolin1-expressing neurons are born between days E12.5 and E13 200

Figure 4.5: Caveolin1 is expressed in neuronal cell-bodies and dendrites at postnatal ages 202

Figure 4.6: CAV1 developmental expression includes overlap with dual projecting CPN/FPN 206

Figure 4.7: CAV1 is expressed in restricted subpopulations of neocortical neurons including dual projecting CPN/FPN at P8 208

Figure 4.8: Loss of *Cav1* function does not disrupt formation of dual projecting CPN/FPN axonal projections at P8 210

Figure 4.9: Caveolin family members are expressed in non-overlapping patterns in the developing brain, and do not appear to compensate for loss of *Cav1* function 212

Figure 4.10: Correct *Cav1* expression is not dependent on corpus callosum formation at P4 214

Figure 4.11: Exogenous CAV1 expression leads to delayed neuronal migration and excess axonal branching in the CC 216

Figure 5.1: Tmtc4 has a predicted structure of 12 transmembrane domains and 8 tetra-trico-peptide repeats ; human mutations occur in the TPR domain 228

Figure 5.2: *Tmtc4* is expressed by CPN at mid-stage CPN development 242

Figure 5.3: *Tmtc4* is not expressed at the midline at the time of midline structure formation, and is expressed postnatally by superficial layer and layer Va neurons 244

Figure 5.4: Overexpression scheme for analyzing human mutations of *Tmtc4*, which produce full-length protein 246

Figure 5.5: Wildtype Tmtc4-2A and human mutations of Tmtc4-2A are localized to neuronal endoplasmic reticulum 248

Figure 5.6: shRNA construct that provides eighty percent knockdown of *Tmtc4 in vitro* does not result in significant *Tmtc4* mRNA knockdown *in vivo* 252

Figure 5.7: Human mutations of $Tmtc4^{\Delta R506Q}$ result in aberrant axonal branching/ failure to stop in mouse superficial layer neurons at P8 254

Figure 5.8: Human mutations of $Tmtc4^{\Delta E463K}$ result in aberrant axonal targeting in mouse superficial layer neurons at P8 258

Figure 6.1: Schematic representation and cytoarchitectural view of mouse and macaque somatosensory neocortex 270

Table 6.1: Detailed information about the clones used for *in situ* hybridization 276

Figure 6.2: *Fezf2* is detectable in macaque tissue using current *in situ* hybridization approach 280

Figure 6.3: At E14.5 and E94, early expressed CPN genes are similarly expressed in mouse and macaque 282

Figure 6.4: At early postnatal times in mouse and E108 CPN genes reveal related CPN populations in mouse and macaque superficial and deep cortical layers 286

Figure 6.5: Subcellular and functional areal localization of CPN-expressed proteins suggest related functions for conserved genes expressed in CPN populations 290

Figure A1: SOX6 and SOX5 are expressed in complementary populations of telencephalic progenitors and neuronal progeny during corticogenesis 354

Figure A2: Sox6, expressed in pallial progenitors, and SOX5 expressed in subpallial progenitors, overlap in the dorsal subpallial VA, and are not sufficient to repress expression of eachother 358

Figure A3: SOX6 subpallial mantle zone expression is postmitotic 360

Figure A4: SOX6 and SOX5 are cross-repressive in pallial and subpallial telencephalic progenitor domains 364

Figure A5: Loss of SOX6 function results in ectopic proneural gene expression in pallial progenitors and subpallial mantle zones 366

Figure A6: SOX6 regulates transcription factor expression during development 368

Figure A7: Pallium –derived cortical neuron specification and laminar location is broadly normal in $Sox6^{-/-}$ neocortex 370

Table A1: Loss of SOX6 function cuases a partial ventralization of the pallial VZ 372

Figure A8: Loss of SOX6 function results in abnormal early cortical interneuron differentiation, without a change in interneuron number 376

Figure A9: Measurement of the tangential distance between the leading edge of the MZ and IZ/SVZ cortical interneuron migratory streams, and the number of interneurons migrating within each of these streams 378

Figure A10: Loss of SOX6 function disrupts the normal laminar position and morphology of cortical interneurons...380

Figure A11: SOX6 controls interneuron subtype development and laminar location 382

Figure A12: SOX6 is necessary for cortical interneuron subtype development 384

Figure A13: Loss of SOX6 function produces an increased number of early- and late-born NPY-positive cortical interneurons 386

Figure A14: SOX6 control over MGE-derived cortical interneuron subtype differentiation is population autonomous 388

Figure A15: NPY$^+$ neurons in *Sox6*$^{-/-}$ cortex are not pallium-born 390

Figure A16: Schematic model for cross-repressive and network interactive function of SOX6 and SOX5 in progenitors and postmitotic cortical neurons 392

List of Abbreviations

I-VI	neocortical layers 1-6
ACN	anterior commissure neurons
AgCC	agenesis of the corpus callosum
ASD	autism spectrum disorders
bp	base pairs
Cav1	caveolin 1
CβA	chicken beta-actin
CBP	CREB binding protein
CC	corpus callosum
CITED2	CBP interacting transactivator with Glu/Asp rich c-terminal domain 2
CP	cortical plate
CPN	callosal projection neurons
CPN/FPN	dual projecting callosal and frontal projection neurons
CSMN	corticospinal motor neurons
CStrPNi	interhemispheric corticostriatal projection neurons
CTB	B subunit of cholera toxin
CTPN	corticotectal projection neurons
CThPN	corticothalamic projection neurons
ER	endoplasmic reticulum
FACS	fluorescence activated cell sorting
IPC	intermediate progenitor cell (basal progenitor)
IZ	intermediate zone
M1	primary motor cortical area
MZ	marginal zone
RG	radial glia (apical progenitor)
S1	primary somatosensory cortical area
S2	secondary somatosensory cortical area
SCPN	subcerebral projection neurons
SP	subplate
SVZ	subventricular zone
Tmtc4	transmembrane and TPR containing 4
TPR	tetra-trico-peptide repeat
VZ	ventricular zone

Acknowledgements

Gentle reader: I am appreciative for this space to express my thanks to a great many people who have journeyed with me and supported the endeavor of my doctoral education.

First, many thanks go to my mentor Jeffrey Macklis. His precise mixture of scientific rigor and thoughtful communication, motivated by excited curiosity and clinical compassion has been inspirational and educational to me on many levels. I always learn something from our conversations. He is a thoughtful mentor and a wonderful advocate.

Another credit to Jeff is the unique, collaborative environment of the Macklis lab that he has established and fostered. I am truly grateful to have spent years researching alongside such impressively talented, uncommonly kind scientists. I thank Drs. Eiman Azim and Denis Jabauadon for training me early in my career in the lab. I very much enjoyed collaborating with and learning from them. It has been a rare privilege to collaborate with Dr Jessica MacDonand on many projects; I am so glad she agreed to join me. She is a good friend and an outstanding scientist, experimentalist, and writer. I truly enjoyed every moment of mentoring an exceptional Harvard College student, Miss Eva Gilles-Buck, who brought much joy, excellence, and creativity to our team. Many thanks to my fellow graduate students both past and present: Mollie Woodworth, Eiman Azim, Sara Shnider, Cameron Sadegh, Luciano Custo-Greig, Alex Murphy, Kadir Ozkan, and Zhaoying Xu, it has been wonderful to journey alongside you. I learn something new in almost every conversation with our postdoctoral fellows: Drs. Noriyuki Kishi, Jason Emsley, Denis Jabaudon, Tina Lai, P. Hande Özdinler, U. Shivraj Sohur, Maria José Galazo, Jessica MacDonald, Suzanne Tharin, Hari Padmanabhan, Vibhu Sahni, and Alex Poulopoulos. Discussions with many of these labmates have encouraged and enlightened the work that follows. The careful work and support of technicians: Alyssa Meleski, Katy Quinn, Lincoln Pasquina, Ryan Richardson, Chloé Greppi, Tim Keefe, Patrick Davis, and Ben Noble have contributed greatly to this dissertation. The unfailing assistance of Deb Schuback, Kelly Deneen, and Dr. Karen Ye has supported diverse aspects of my research and has lifted many burdens of logistics in a reliable way, with unfailing positivity.

Much gratitude goes to my Dissertation Advisory Committee: Professors Jeff Lichtman, Paola Arlotta, and Andy McMahon; it has been a real treat to work so closely with three remarkable thinkers, who are also caring mentors. I also thank my Dissertation Examining Committee: Professors Jeff Lichtman, Paola Arlotta, and John Dowling, for all of their time and care for this dissertation. Many thanks go also to the Department of Molecular and Cellular Biology, in particular the incoming class of 2006 who have shown only friendship and support of one another; Corinna Rohse, Suzanne Shaw Smith, Chris McCartney-Melstad, and Mike Lawrence for their unfailing departmental support at all stages of my graduate career; and Susan Foster, Nancy Hegarty, Debra Maddalena, and Ronnie Mugimu for their help in processing my NSF and NRSA fellowship applications.

I close by thanking those outside of the lab who support me. Thanks to the groups of scholar-athletes who allowed me to swim, row, and cycle with you; you have helped keep my mind and body well. Thanks to the St. Paul's Catholic community for keeping my soul well. Ryan, you continuously fill my life with unconditional love, silly humor, and homemade meals; you keep me strong. Karen, Billy, Leslie, Allison, and Meagan; your friendship brings home to me. Lastly, all of my thanks go to my family. To my sisters, Rachel and Michelle: growing up with your curiosity, creativity, and love has always been inspirational. I am amazed at how as adults we three have triangulated our interests to understanding biology, human nature, and geology. Mom and Dad, you have made everything possible. You gave me life and filled it with love, encouragement, support, accountability, and enthusiasm.

Thank you.

“For the real amazement, if you wish to be amazed, is this process: You start out as a single cell derived from the coupling of a sperm and an egg; this divides in two, then four, then eight, and so on, and at a certain stage there emerges a single cell that has as all its progeny the human brain. The mere existence of such a cell should be one of the great astonishments of Earth. People ought to be walking around all day, all through their waking hours calling to each other in endless wonderment, talking of nothing except that cell.” ~Lewis Thomas (1913-1993)

This page has been intentionally left blank.

Chapter 1:

Introduction

Publication:

- **Fame RM***, MacDonald, JL*, and Macklis, JD. 2011 "Development, Specification, and Diversity of Callosal Projection Neurons." *Trends in Neurosciences.* 34(1):41-50.

- MacDonald JL*, **Fame RM***, Azim E, Shnider SJ, Molyneaux BJ, Arlotta P, and Macklis JD. "Specification of cortical projection neurons: transcriptional mechanisms." *Developmental Neuroscience: A Comprehensive Reference, Volume 1. Elsevier in press*. Rubenstein J, Rakic P, eds. Elsevier. (in press).

1.1 Overview

The human cerebral cortex is the region of the brain responsible for cognitive function, sensory perception, voluntary motor control, spatial reasoning, language, and consciousness. It contains over two-thirds of the neuronal mass of the whole nervous system, and three-quarters of all synaptic connections(Rakic, 1988). About 90% of the cerebral cortex is contained in a structure unique to mammals that has undergone dramatic expansion and elaboration throughout evolution, the neocortex(Finlay and Darlington, 1995). The mammalian neocortical capacity for high-order processing emerges from its complex, yet highly organized, six-layered structure and the unique connections between its hundreds of different neuronal subtypes, and their association with diverse glial populations that support and enable appropriate neuronal function and communication (Peters and Jones, 1984; Ramón y Cajal, 1995). Neocortical expansion in primates has occurred both radially and longitudinally throughout evolution, transitioning to a thicker cellular layer, more white matter, as well as to more surface area from lissensephalic (smooth brain) to gyrencephalic (wrinked brain). As this neocortical expansion proceeded, the diverse population of interhemispheric connecting callosal projection neurons (CPN) has expanded disproportionately more than other populations of long-distance neocortical projection neurons, likely representative of their functional contribution to increased neocortical processing capability(Smart et al., 2002b).

Two broad classes of neurons make up the neocortex: interneurons, GABAergic inhibitory non-pyramidal neurons that make local connections; and projection neurons, glutamatergic excitatory pyramidal neurons that extend axons to distant intracortical, subcortical, and subcerebral targets to transmit information from the neocortex to other neocortical areas, or to other regions of the central nervous system (Molyneaux et al., 2007). During development, these two broad classes of neurons are generated from different progenitor zones; interneurons are generated primarily from progenitors in the ventral (subpallial) telencephalon, and migrate tangentially over long distances to their final locations within the neocortex (Wonders and Anderson, 2006), while projection neurons are generated from progenitors of the neocortical germinal zone located in the dorsolateral (pallial) wall of the telencephalon, and migrate radially to their final neocortical position (Rakic, 1972; Tan et al., 1998; Ware et al., 1999; Anderson et al., 2002; Gorski et al., 2002a; Molyneaux et al., 2007; Leone et al., 2008).

Different subpopulations of projection neurons are born in overlapping temporal waves, with newly born projection neurons migrating past the earlier born neurons to form more superficial layers of neurons, thus progressively establishing the six layered structure of the mature neocortex in an "inside-out" manner, with layers VI and V generated first, followed by layers IV, III, and II (Angevine and Sidman, 1961; Molyneaux et al., 2007; Leone et al., 2008) (See Figure 1.1). Within the mature neocortex, distinct populations of projection neurons are located in different cortical layers and areas (with many subtypes intermingled in each layer and area), have unique morphological features, express and are controlled by different complements of transcription factors, and ultimately serve different functions. The complexity and diversity of projection neuron subtypes makes any classification scheme difficult, but the most accurate system likely extends beyond the most commonly used system of hodology (anatomical projections) to include a combination of hodology, morphology, electrophysiological properties, and combinatorial patterns of gene expression that most likely represent yet-unrecognized functional differences (Peters and Jones, 1984; Migliore and Shepherd, 2005; Molyneaux et al., 2007).

Establishing this complex neocortical circuitry requires tightly regulated spatial and temporal developmental programs that not only generate the requisite cellular diversity, but also appropriately integrate the components into functioning networks. In order to understand the development of the neocortex, it is essential to understand molecular controls that guide these developmental programs, and precisely regulate neuronal fate specification, differentiation, maturation, and connectivity.

Here, in this introduction, I review the development of the rodent neocortex in the context of recent data revealing roles of individual and combinatorial sets of genes in controlling specification and development of distinct projection neuron subtypes. In this dissertation, I focus on molecular controls over development of subtypes of one diverse population of neocortical projection neurons, the callosal projection neurons (CPN), which are critical for long-distance bilateral transfer and integration of cortical information, and have been centrally implicated in autism spectrum disorders (ASD).

First, I describe the diversity of progenitors that give rise to the projection neurons of the neocortex. Next, I discuss current knowledge on molecular programs that instruct early steps of progenitor specification, and extensively review molecular controls over neuronal subtype and layer specific identity. Finally, I focus on the distinct projection neuron population that is the focus of this dissertation, CPN, and one comparative population, subcerebral projection neurons, and describe recent advances in understanding the interplay of combinatorial molecular controls over the generation of precision and diversity of these developmentally and clinically important neuronal subtypes, and, by extension, neocortical diversity more broadly.

1.2 Neocortical Progenitors

During early mammalian brain development, the cerebral cortex arises from the dorsal aspect of the rostral forebrain (telencephalon), a brain structure formed by evagination of the two cerebral hemispheres at the rostral end of the neural tube surrounding the lateral ventricles. The six-layered neocortex ("new cortex", as opposed to evolutionarily older and perhaps less refined cortical areas like "archicortex"), which makes up the majority of the cerebral cortex, is initially composed of a thin neuroepithelium lining the dorsal wall of the lateral ventricles, called the ventricular zone (VZ; Figure 1.1). As neurogenesis proceeds, an additional proliferative layer known as the subventricular zone (SVZ) forms superficial to the VZ (Bayer and Altman, 1991). Progenitors residing in the VZ and SVZ produce projection neurons of the different neocortical layers in a tightly controlled temporal order from approximately E10.5 to E17.5 in mouse (Angevine and Sidman, 1961; Rakic, 1974; Caviness and Takahashi, 1995). Post-mitotic neurons then position themselves in the developing neocortex via defined modes of radial and tangential migration (Rakic, 1972; Noctor et al., 2001; Rakic, 2003; Britanova et al., 2006). The earliest born neurons appear around E10.5 in the mouse, and form a layered structure called the preplate (PP), which is later split into the more superficial marginal zone, and the deeply located subplate (SP). The cortical plate, which will give rise to the multilayered neocortex, develops in between these two layers (Bayer and Altman, 1991), such that later born neurons arriving at the cortical plate migrate past earlier born neurons, progressively establishing the six layered structure of the mature cortex in an “inside-out” manner (Angevine and Sidman, 1961; Rakic, 1974).

1.2 a. Neocortical Progenitor Types

Three broad classes of progenitors give rise to cortical projection neurons, characterized by different competency states and proliferative properties: neuroepithelial cells, radial glia, and intermediate progenitors (Gotz and Huttner, 2005) (Figure 1.2). Neuroepithelial progenitors are multipotent, (i.e. able to generate neurons, astroglia, and oligodendroglia) (Williams and Price, 1995), and have epithelial morphological features with a clear apical-basal polarity. They primarily undergo symmetric divisions, producing two neuroepithelial progenitors, thereby expanding the progenitor pool whose progeny will ultimately populate the neocortex. In addition, a minority undergoes asymmetric division, generating two different daughter cells, a neuroepithelial progenitor and a neuron of the deep layers of the neocortex (Smart, 1973; Chenn and McConnell, 1995; Gotz and Huttner, 2005).

As neurogenesis progresses, these neuroepithelial progenitors differentiate into radial glial cells, maintaining some neuroepithelial properties, such as expression of the intermediate filament protein nestin (Hartfuss et al., 2001), and an apical-basal cell polarity, but also acquiring astroglial properties, including expression of astrocytic molecular markers such as glial fibrillary acidic protein (GFAP), the calcium-binding protein S100β, and the glutamate transporter GLAST (Hartfuss et al., 2001; Noctor et al., 2002; Kriegstein and Parnavelas, 2003). Radial glial cells reside on the apical surface of the VZ, and extend a long process to the pia; this process has a well-characterized role in guiding migrating neurons from their site of production in the VZ to their final laminar destination, by serving as a migratory scaffolding (Rakic, 1972; Rakic, 2003). More recently, radial glial cells have been shown to have properties of neuronal progenitors, and, depending on the stage of development, divide either symmetrically to produce two radial glia, or asymmetrically to generate another radial glia

Figure 1.1: **Progenitors residing in the VZ and SVZ produce projection neurons in an "inside-out" fashion**

(A-C) From approximately E10 to E12, pallial ventricular zone (VZ) progenitors divide asymmetrically and generate neurons that migrate radially and form the preplate (PP). At approximately E12.5, a second wave of postmitotic neurons migrates radially and intercalates into the preplate, splitting it into the superficial marginal zone (MZ) and a deep subplate (SP), forming the cortical plate (CP), which will expand over the next several days and the first week postnatal week into the mature, six-layered neocortex. The subventricular zone (SVZ) develops superficial to the primary VZ, providing a secondary germinal zone composed of intermediate progenitor cells (IPCs). Over the next approximately five days, diverse cortical projection neuron subtypes are born in sequential and overlapping waves. At approximately E12.5, cortical projection neurons destined for layer VI are born, including corticothalamic projection neurons and a subset of callosal projection neurons (CPN). At approximately E13.5, an additional subpopulation of CPN and subcerebral projection neurons (SCPN), including corticospinal motor neurons (CSMN), destined for layer V are generated. At approximately E14.5, layer IV pyramidal neurons are born. Finally, between approximately E15.5 and E17.5, heterogeneous subpopulations of CPN and other intracortical projection neurons destined for layers II/III are generated. WM, white matter. Adapted from (Molyneaux et al., 2007).

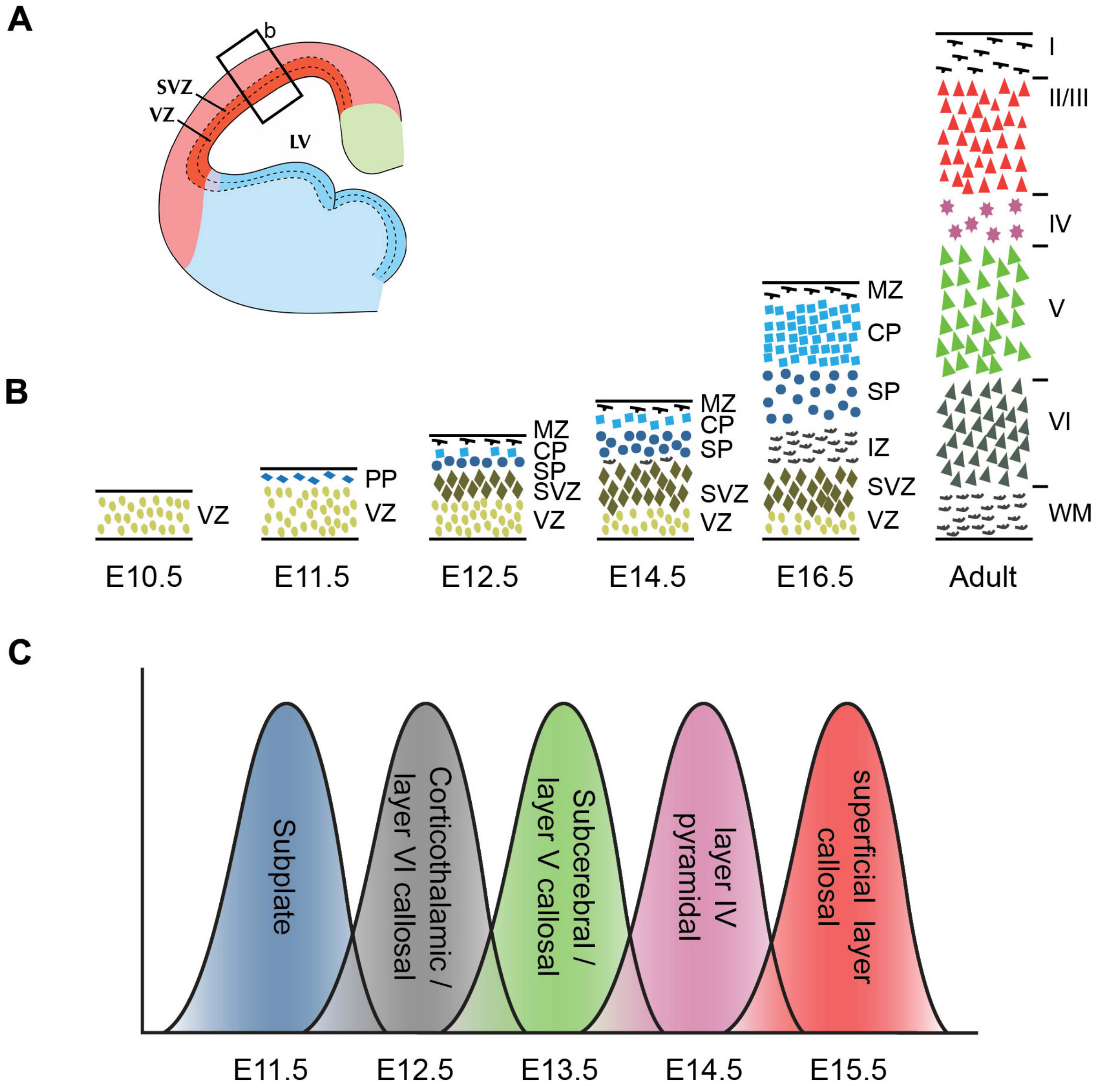

Figure 1.1 (Continued)

Figure 1.2: Cortical projection neuron progenitors

Neuroepithelial cells (green) in early cortical development largely divide symmetrically (dark green; circular arrow) to generate more neuroepithelial cells, while some neuroepithelial cells increasingly over time likely divide asymmetrically (lighter green; thin arrow) to generate immature neurons (pink) that will differentiate into early, deep layer projection neurons (brown). As the developing cortical epithelium thickens, neuroepithelial cells elongate and differentiate into radial glial progenitors (blue). Radial glial progenitors either 1) self-renew (dark blue; circular arrow), 2) divide asymmetrically (medium blue) to directly generate immature neurons (pink) that migrate along the maintained pial process, then mature into deep layer projection neuron subtypes (brown), or 3) divide asymmetrically to generate intermediate progenitors (yellow; also “basal progenitors”), which divide symmetrically to produce two immature neurons that migrate radially along the radial glial progenitor and mature into superficial layer projection neurons (red). A distinct population of cortical progenitors has been described, short neural precursors (dark purple), which generally produce neurons directly from the VZ rather than producing intermediate progenitor cells, generating progeny that predominantly reside in layer IV.

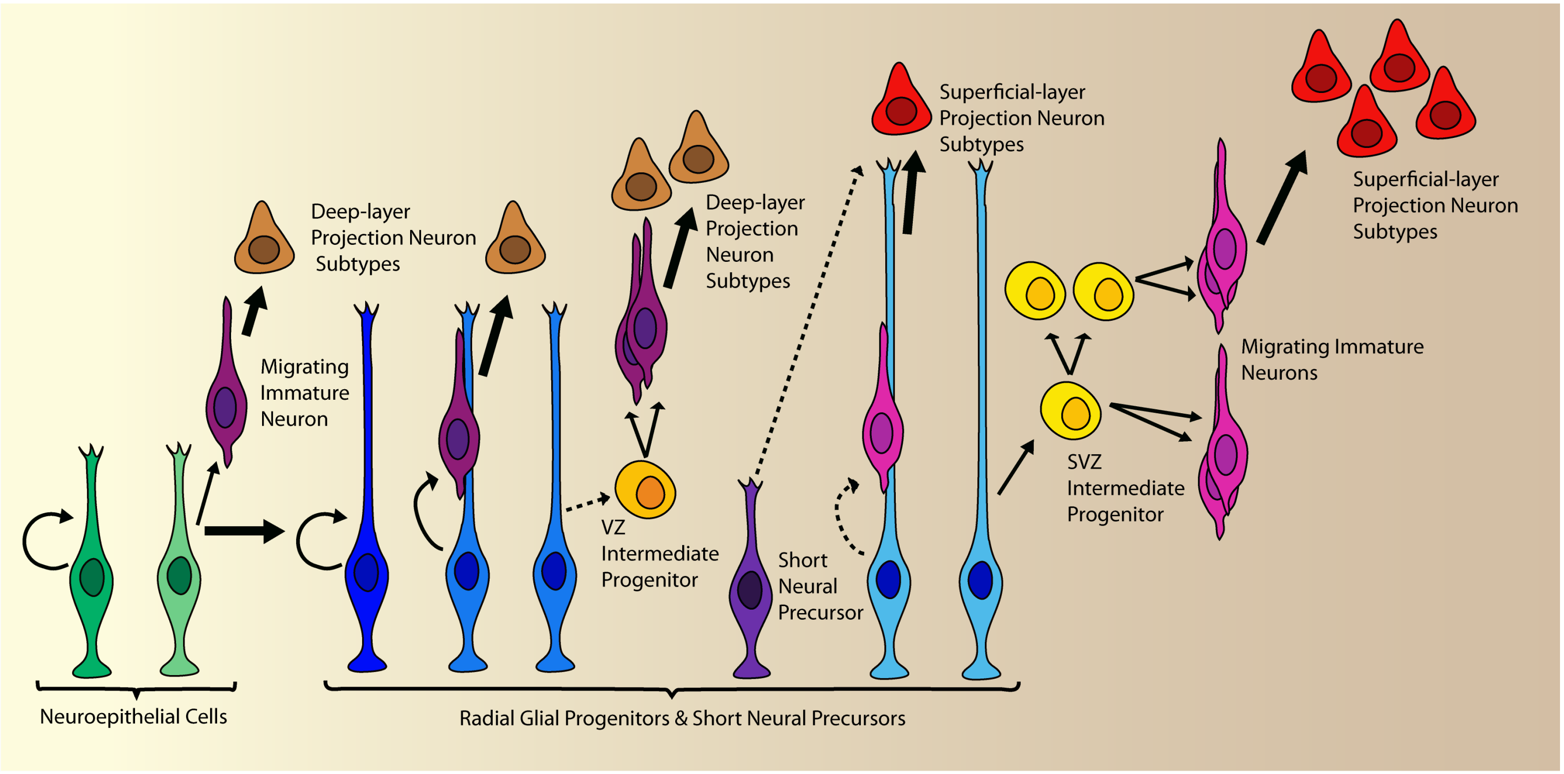

Figure 1.2 (Continued)

and either a postmitotic neuron or an intermediate progenitor cell (Malatesta et al., 2000; Hartfuss et al., 2001; Noctor et al., 2001; Heins et al., 2002; Noctor et al., 2002; Malatesta et al., 2003; Anthony et al., 2004; Miyata et al., 2004; Noctor et al., 2004; Mo et al., 2007; Noctor et al., 2008). During neurogenic divisions, the radial glial cell maintains its pial process, and the newly born neuron migrates along the parent glial scaffold to its destination layer (Noctor et al., 2001; Noctor et al., 2004).

In addition to the typical radial glia, other neuron-producing progenitors have been described within the VZ (Hinds and Ruffett, 1971; Gotz and Huttner, 2005; Gal et al., 2006; Mo et al., 2007). Recently, a subpopulation of progenitors that can be distinguished from radial glia cells by absence of a full-length pial process, and by the ability to drive the *Tα1* α-tubulin promoter has been identified (Gal et al., 2006; Stancik et al., 2010). These short neural precursors, or SNPs, have a longer cell cycle length than radial glial cells, and they generally produce neurons directly from the VZ rather than producing intermediate progenitor cells (Stancik et al.). Further, SNPs and radial glial cells fate-mapped at E14.5 generate neurons in distinct lamina of the cortex, with SNP progeny residing predominantly in layer IV, and radial glial progeny in layer II/III (Stancik et al.). Although further study is needed to clarify the extent of progenitor diversity, and the relationships between currently identified and likely further to-be-identified subtypes of progenitors within the VZ, there is growing evidence to indicate that progenitor heterogeneity might be critical in generation of the full and rich diversity of cortical projection neuron subtypes.

In addition, intermediate progenitors (also called basal progenitors because they divide without touching the apical surface) are the other major type of neuron-producing progenitor. Intermediate progenitors are located throughout the proliferative zones (the basal VZ early in corticogenesis and SVZ later in corticogenesis) (Haubensak et al., 2004; Pontious et al., 2008; Kowalczyk et al., 2009), and are the primary component of the SVZ. Intermediate progenitors of the VZ, which contribute to early-born, deep layer projection neuron subtypes, and intermediate progenitors of the SVZ, which give rise to later-born, superficial layer projection neuron subtypes, are molecularly distinct, although both have been shown to express Tbr2/ Eomes during G1 (Kawaguchi et al., 2008). The SVZ begins to form as a distinct region at approximately E13.5 in mouse, and expands significantly during late corticogenesis (Smart and McSherry, 1982; Bayer and Altman, 1991). Smart and McSherry (1982) proposed that the SVZ might be a site of neurogenesis for superficial layer neurons (Smart and McSherry, 1982), but solid evidence supporting this hypothesis was lacking. Instead, cell divisions in the SVZ were thought to primarily contribute to gliogenesis, not neurogenesis (Takahashi et al., 1995). More recently, however, elegant studies in slice culture have shown that radial glia frequently undergo an asymmetric division to generate an intermediate progenitor, which then can migrate into the SVZ before pausing and undergoing a symmetric cell division to produce two more intermediate progenitors or two neurons (Miyata et al., 2004; Noctor et al., 2004). The SVZ might not be the sole source of superficial layer neurons, as low-level radial glia progenitor neurogenic divisions have also been observed throughout corticogenesis (Kowalczyk et al., 2009). By observing neurogenesis in *Tis21*-green fluorescent protein (GFP) knock-in mice that only express nuclear-GFP in cells undergoing a neuron-producing division, Haubensak *et al*. (2004) identified intermediate progenitors dividing at the basal side of the VZ (the developing SVZ) that undergo symmetric cell divisions to give rise to two post-mitotic neurons (Haubensak et al., 2004), confirming and extending the slice culture results *in vivo*.

Circumstantial evidence that this observed neurogenesis in the SVZ contributes to generation of superficial layer neurons came from identification of several genes that are expressed in the SVZ during superficial layer neurogenesis, and are also expressed by superficial layer post-mitotic neurons. For example, the genes *Svet1* and *Cux2* are expressed by a subset of dividing cells in the SVZ during generation of superficial layer neurons, and postnatally in some neurons of layers II-IV, suggesting that *Svet1* and *Cux2* might be markers for superficial layer progenitors within the SVZ (Tarabykin et al., 2001; Nieto et al., 2004; Zimmer et al., 2004; Franco et al., 2012). Interestingly, *Cux2* expression is detected in the basal VZ starting at E11.5, suggesting that progenitors committed to the generation of superficial layer neurons might be present early in cortical neurogenesis, before formation of the SVZ, and several days before the production of superficial layer neurons (Nieto et al., 2004; Zimmer et al., 2004), though more definitive fate mapping experiments are needed to explore this possibility.

A separate set of *in vivo* fate mapping experiments used the promoter regions of the *Nex* gene to obtain *Cre* recombinase expression in progenitors of the SVZ, combined with a floxed reporter delivered by adenovirus at E14, to label progenitors during generation of superficial layer neurons. GFP reporter expression was mapped to neurons residing in the superficial layers, providing more definitive support for the SVZ origin of superficial layer neurons (Wu et al., 2005). Studies of the evolution of mammalian cortex suggest that superficial layer neurons are a recent evolutionary addition, while layer V and VI projection neurons might be related to pyramidal neurons of a primitive cortex(Reiner, 1991; Marín-Padilla, 1992; Aboitiz and Montiel, 2003; Aboitiz et al., 2003). Thus, expansion of the SVZ might represent an evolutionary mechanism to increase the number of neurons within the neocortex, especially during generation of neurons of superficial layers (Smart et al., 2002a; Kriegstein et al., 2006).

The SVZ has further expanded in primates (and some gyrencephalic non-primate mammals) to include two progenitor regions - an inner and an outer SVZ, the progenitors of which are distinct (Smart et al., 2002a; Fietz et al.; Hansen et al.). The progenitors of the inner SVZ (ISVZ) more closely resemble rodent SVZ intermediate progenitors; they express *Tbr2*, but down-regulate *Pax6* (Fietz et al., 2010). The progenitors of the primate outer SVZ (OSVZ), on the other hand, are more similar to radial glial cells, both in morphology and molecular identity (Smart et al., 2002a; Fietz et al.; Hansen et al.). Further, the radial glial-like progenitors of the OSVZ can undergo both symmetric, self-renewing divisions, as well as asymmetric, neurogenic and self-renewing divisions (Fietz et al., 2010; Hansen et al.). This capacity of OSVZ progenitors to undergo self-renewing asymmetric divisions to also generate progenitors that can further proliferate greatly enhances neuronal output, and may have been an important evolutionary step in the expansion of the neocortex.

1.2 b. Neocortical Progenitor Cell Fate Plasticity

The precise relationships among progenitors, and the identities of distinct progenitor populations that give rise to broad classes and restricted sets of projection neuron subtypes, are still largely unknown, though recent results are beginning to clarify progenitor heterogeneity. Lineage tracing of clonally related populations indicates that, at the earliest stages of cortical neurogenesis (approximately E11.5 in mouse), individual progenitors are able to give rise to pyramidal neurons across layers II-VI (Tan et al., 1998; Reid and Walsh, 2002). As development progresses, progenitors become progressively restricted in their competence states(Azim et al., 2009b). Some early cortical progenitors at the time of generation of deep layer neurons are still multipotent and can generate later-born neurons of superficial layers when transplanted into the niche of late progenitors (McConnell and Kaznowski, 1991); progenitors of the superficial layers possess less plasticity (Frantz and McConnell, 1996; Mizutani and Saito, 2005), but appear to retain some ability to generate earlier fates under the appropriate conditions (Molyneaux et al., 2005; Fukumitsu et al., 2006).

A delicate balance of cell intrinsic and extrinsic factors act in concert on cortical progenitors to determine, and progressively restrict, fate of their neuronal progeny. Elegant transplantation experiments in the 1990s demonstrated that progenitors are partially responsive to environmental factors in determining laminar fate of their progeny, in a cell-cycle dependent manner. Prior to completion of S-phase of the cell cycle, transplanted progenitors can generate progeny more appropriate to the age of the host, but upon cell-cycle exit, they are more committed to their normal fate (McConnell and Kaznowski, 1991). The progressive increase in the length of cell cycle, and in G1 phase in particular, throughout cortical neurogenesis (Takahashi et al., 1994; Caviness and Takahashi, 1995; Takahashi et al., 1995), is strongly correlated with a shift to differentiative rather than proliferative division of progenitors (Lukaszewicz et al., 2002; Calegari et al., 2005), and long G1 length might provide an extended plastic period of sensitivity to the influence of extrinsic and intrinsic cell-fate determining signals (Dehay and Kennedy, 2007).

In agreement with findings demonstrating extrinsic control over early cortical progenitor plasticity, recent experiments have revealed that manipulation of extracellular signals can also alter fate of neurons born late in cortical neurogenesis. BDNF delivered to progenitors during birth of later born neurons shifts them to laminar fate with some characteristics of earlier born neurons if progenitors are exposed to BDNF before the S phase of the cell cycle (Fukumitsu et al., 2006). Some extrinsic signals regulating progenitor development and fate may come in the form of feedback regulation by postmitotic neurons of the cortical plate (Morrow et al., 2001; Barnabe-Heider et al., 2005; Seuntjens et al., 2009). For example, newly born cortical neurons produce the neurotrophic cytokine cardiotrophin-1, which instructs cortical progenitors to produce astrocytes rather than neurons, thereby ensuring that gliogenesis does not occur until neurogenesis is largely complete (Barnabe-Heider et al., 2005). Further, conditional deletion of the transcription factor *Sip1* from postmitotic cortical projection neurons results in over-expression of *neurotrophin-3* at E14.5, resulting in precocious generation of superficial layer projection neurons at the expense of deep layer projection neurons, while at E16.5 there is an over-expression of *Fgf9,* leading to precocious gliogenesis (Seuntjens et al., 2009). Thus, Sip1 might repress the expression of signaling factors in postmitotic neurons that regulate sequential fate decisions of progenitors to ensure the generation of appropriate numbers of neurons and glia throughout corticogenesis (Seuntjens et al., 2009).

Throughout corticogenesis, neocortical progenitors also undergo intrinsic, progressive restriction in their competence state. As mentioned previously, heterochronic transplantation experiments from McConnell and colleagues demonstrated that progenitors of early-born, deep-layer neurons have the potential to give rise to superficial layer neurons when transplanted into the germinal zone of an older host, but progenitors of later-born neurons are restricted to generating superficial layers, even when transplanted into the germinal zone of a younger host at the time of deep layer neuron birth (Frantz and McConnell, 1996; Desai and McConnell, 2000), suggesting an intrinsic restriction of potential. Further, *in vitro* analysis of single cortical progenitor clones using time-lapse microscopy combined with molecular analysis, suggests that the temporal sequence of generating broad neuronal classes is, to a significant extent, intrinsically programmed in the progenitors, and this level of determination is not easily malleable by cell-extrinsic factors outside the immediate environment of the progenitor clone (Shen et al., 2006). These single cortical progenitor clones exhibit a similar timeline of progressive restriction in potential as seen *in vivo*, in that neurons that express at least the broadest laminar markers are produced after the same number of cell divisions *in vitro* as their *in vivo* counterparts. However, now that much more is known about projection neuron subtype development and combinatorial molecular markers of distinct subtypes, it remains to be seen whether individual clones generate multiple lineages or only distinct subtypes within a layer in an *in vitro* environment. Additional experiments are necessary to investigate the clonal relationships among neuronal subtypes of different layers, and to determine whether single progenitors can progress through generation of different subtypes of pyramidal neurons with full cortical phenotypes *in vitro* (Hack et al., 2004).

Transplantation studies support the principle of environmental influence on defining neurogenic and non-neurogenic regions in adult cortex, and provide evidence for a critical role of the microenvironment in influencing potential of neural progenitors. When adult neural progenitors are transplanted into distinct neurogenic regions, they can differentiate into neurons in a manner somewhat appropriate to the region of transplantation (Gage et al., 1995; Suhonen et al., 1996; Takahashi et al., 1998; Shihabuddin et al., 2000). Some SVZ progenitors generate what appear morphologically to be dentate gyrus neurons when transplanted into the dentate gyrus, and, reciprocally, some dentate gyrus subgranular zone progenitors generate what appear morphologically to be olfactory bulb interneurons after transplantation into the rostral migratory stream (RMS) (Suhonen et al., 1996). When implanted outside these constitutively neurogenic regions, both types of progenitors generate only glia, highlighting the importance of the microenvironment, and suggesting that at least some progenitors might be able to be directed to differentiate into specific fates other than their normal fate during development.

Glia and neurons share a common lineage in corticogenesis, yet, unlike neurons, glia are continuously produced throughout adulthood, suggesting glial progenitors as another source of plastic cortical progenitors potentially capable of producing neurons. Thus, neocortical progenitors might be manipulated much later in development, or even during adulthood, to produce specific, diverse types of neurons. In support of this idea, previous experiments have shown that with the appropriate stimuli, progenitors in the adult mouse neocortex can be induced to generate new projection neurons (Magavi et al., 2000; Chen et al., 2004; Brill et al., 2009), demonstrating the existence of at least some manipulable progenitors within the adult neocortex.

1.3 Specification of Neocortical Projection Neuron Progenitor Domains

Upon induction of the telencephalon by gradients of extracellular signaling molecules such as sonic hedgehog, fibroblast growth factors, and bone morphogenetic proteins (Rallu et al., 2002), a number of repressive transcription factor interactions, of which key examples are discussed here, establish a dorsal, or pallial, neocortical progenitor identity as distinct from ventral, or subpallial progenitor identity (Figure 1.3). These transcription factors include *Lhx2*, *FoxG1*, *Emx2*, *Pax6*, and *Sox6*, each of which has crucial roles in specifying the progenitors that give rise to projection neurons of the neocortex. Together, these five transcriptional regulators establish the neocortical progenitor domain by repressing dorsal midline (*Lhx2* and *FoxG1*) and subpallial fates (*Emx2*, *Pax6,* and *Sox6*), a critical first step in the initial specification of neocortical projection neuron identity.

Lhx2 functions as an essential intrinsic determinant of cortical identity, acting cell-autonomously to specify cortical identity and suppress alternative fates in a spatially dependent manner, during an early critical period when progenitors comprise the cortical neuroepithelium (Mangale et al., 2008). In the absence of *Lhx2*, the majority of the neocortical VZ is absent (Vyas et al., 2003), and *Lhx2* null cells adopt “antihem” identity laterally (at the lateral cortical boarder). Medially they become cortical “hem” cells (at the border with the hippocampus), which can induce and organize ectopic hippocampal fields (Bulchand et al., 2001; Monuki et al., 2001; Mangale et al., 2008). Additionally, *Lhx2* functions at a critical period, before neuroepithelial cells are converted to telencephalic progenitors, to determine their region-specific differentiation into neocortical rather than olfactory progenitors (Chou et al., 2009). Similarly, in the absence of *FoxG1*, neocortical progenitors are not specified, while progenitors of the archicortex (which give rise to the hippocampus and other evolutionarily older cortical regions) and the cortical hem (one major source of Cajal-Retzius cells) are expanded (Dou et al., 1999; Muzio and Mallamaci, 2005). Remarkably, *FoxG1* removal as late as E13.5 from progenitors that already possess a neocortical identity results in the production of cells with characteristics of Cajal-Retzius cells (Hanashima et al., 2004; Shen et al., 2006), indicating that persistent expression of *FoxG1* throughout neurogenesis is required for maintenance of neocortical progenitor identity. This suggests that progenitors, though seemingly progressively fate-restricted, retain a tremendous degree of plasticity.

Emx2 and *Pax6*, key determinants of the proper development of cortical areas, are expressed in opposite and overlapping gradients in the dorsal telencephalon (reviewed in (Mallamaci and Stoykova, 2006)), and are also required for establishing the identity of pallial progenitors (Muzio et al., 2002). In the absence of both genes, the cortex does not form, and subpallial progenitor domains expand across the entire dorsal telencephalon (Muzio et al., 2002; Schuurmans and Guillemot, 2002). The absence of *Pax6* alone results in the expression of markers of subpallial progenitors, such as *Mash1*, *Gsh2,* and *Dlx2*, in the pallium, and abnormalities in the production of projection neurons most pronounced in rostral cortex (Stoykova et al., 2000; Toresson et al., 2000; Yun et al., 2001; Muzio et al., 2002; Schuurmans et al., 2004). This is not due to migration of subpallial cells into cortical territory (Kroll and O'Leary, 2005), but, rather, to a cell autonomous failure to repress subpallial genes in the absence of *Pax6* expression (Quinn et al., 2007). Cross-repression between *Pax6*, expressed in the pallial VZ, and *Gsh2*, expressed in the subpallial VZ, helps establish the pallial-subpallial boundary (PSB) (Yun et al., 2001). *Pax6* also activates expression of the basic helix-loop-helix (bHLH) transcription factor *Ngn2*, which, in coordination with *Ngn1*, establishes the PSB, largely by repressing subpallial expression of the bHLH transcription factor *Mash1* (Ma et al., 1996; Fode et al., 2000; Monuki et al., 2001; Schuurmans and Guillemot, 2002).

The SRY-type HMG box (SOX)-containing transcription factors *Sox5* and *Sox6* also play a critical cross-repressive role in parcellation of the proliferative neuroepithelium at the PSB(Azim et al., 2009a). *Sox6* and *Sox5* are complementarily expressed in pallial and subpallial progenitors, respectively, and

Figure 1.3: Establishment of the pallial progenitor domain

(**A**) During neocortical development, shown here at ~E11, the telencephalon is parcellated into pallial (dorsal; red) and subpallial (ventral; blue) domains. The pallium gives rise to excitatory projection neurons of the cortex, with the dorsal midline region (green), including the archicortex and cortical hem, giving rise to neurons of the hippocampus and choroid plexus, and Cajal-Retzius cells. The subpallium, subdivided into the medial, lateral, and caudal ganglionic eminences (MGE, LGE, and CGE), gives rise to the basal ganglia and associated limbic regions, as well as the inhibitory interneurons that migrate tangentially to populate the neocortex. This spatial segregation of proliferative domains (dark red and dark blue) enables distinct molecular programs to generate diverse populations of excitatory and inhibitory cortical neuron subtypes via cross-repressive actions of combinatorial molecular controls. (**B**) A number of the key transcriptional regulators that establish the pallial progenitor domain through repression of dorsal midline and subpallial molecular programs have now been elucidated. PSB, pallial-subpallial boundary; LGE/MGE, lateral/medial ganglionic eminence. Portion of figure adapted from(Schuurmans and Guillemot, 2002; Azim et al., 2009a).

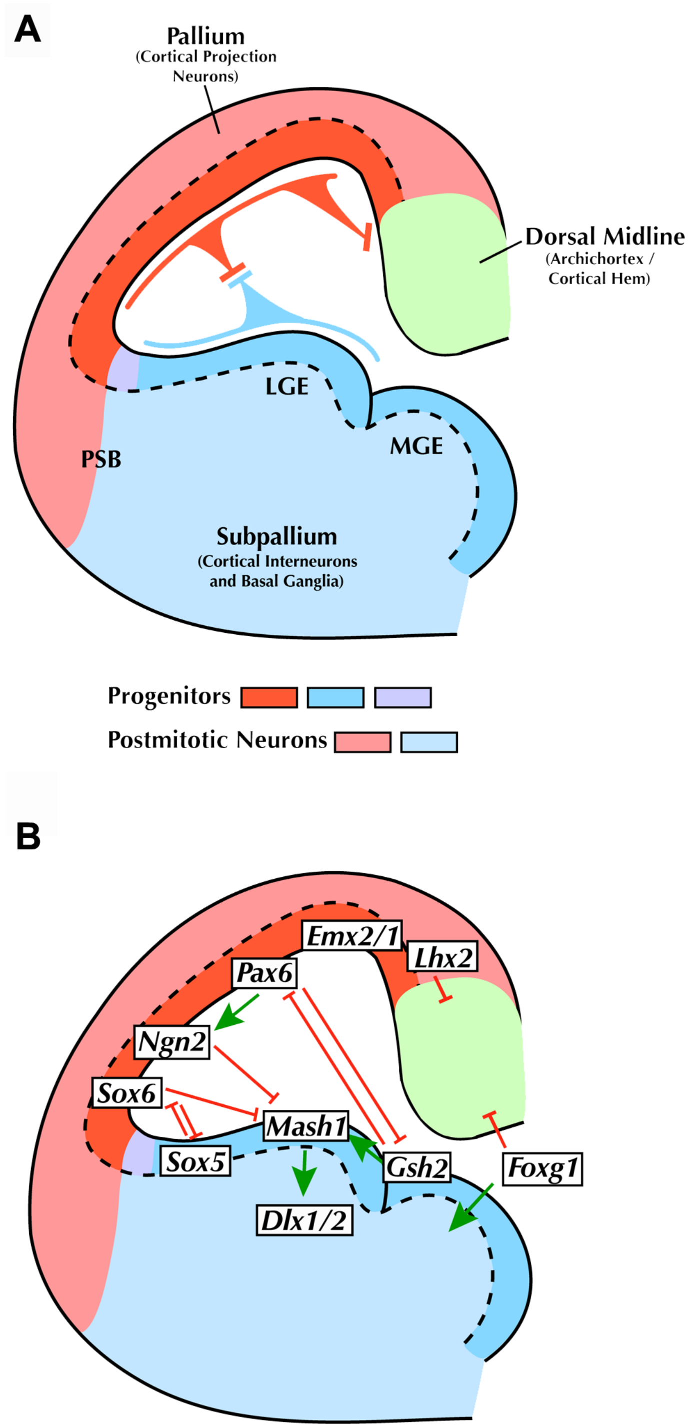

Figure 1.3 (Continued)

Sox6 controls the segregation of pallial from subpallial progenitors by repressing the expression of *Mash1* and downstream subpallium-specific programs in pallial progenitors(Azim et al., 2009a). Interestingly, despite the partial ventralization of *Sox6* null pallial progenitors, *Pax6* and *Ngn2* are expressed normally in the *Sox6* null pallium, and projection neuron laminar distribution and subtype- and layer-specific molecular expression are largely normal. Thus, *Sox6* critically maintains pallial progenitor identity by repressing subpallial programs of gene expression, but redundant and/or compensatory controls (for example, *Ngn2* and *Ngn1*) persist that are sufficient to ensure largely appropriate pallial corticogenesis, indicating that *Sox6* likely acts cooperatively with *Ngn2* to control the segregation of telencephalic progenitor domains during development(Azim et al., 2009a).

During corticogenesis, *Pax6*, along with *Nr2e1* (previously called *Tlx)*, also controls the proliferation of VZ progenitors during the establishment and expansion of the SVZ. In both *Pax6* mutants and *Nr2e1* mutants, deep layer neurons are generated normally, while the superficial cortical layers are decreased in thickness (Caric et al., 1997; Tarabykin et al., 2001; Land and Monaghan, 2003; Nieto et al., 2004; Schuurmans et al., 2004; Zimmer et al., 2004). There is a global decrease in superficial layer neurons in both the *Pax6* and *Nr2e1* single mutants, including a reduction in the number of *Cux1, Cux2,* and *Svet1* expressing neurons in the *Pax6* mutants (Tarabykin et al., 2001; Nieto et al., 2004), with an even more severe phenotype in the double mutants (Schuurmans et al., 2004).

Investigations into the mechanisms underlying the decrease in superficial layer neuron number in the *Pax6* and *Nr2e1* mutants indicates that these genes control the kinetics of cell division of VZ progenitors, and the decision of a progenitor to divide symmetrically or asymmetrically. Therefore, they appear to regulate the expansion of the SVZ, and the number of pyramidal neurons in the superficial layers. In *Nr2e1* mutants, the SVZ is decreased in size, progenitors proliferate less, and they undergo premature differentiation, producing the most superficial layers of the neocortex one to two days early (Land and Monaghan, 2003; Roy et al., 2004). Similarly, in *Pax6* mutants, there is an increase in the proportion of progenitors undergoing asymmetrical cell division between E12.5 and E15.5 (Estivill-

Torrus et al., 2002), with a premature decrease in the number of *Cux2* expressing cells in the SVZ of *Pax6* mutants (Nieto et al., 2004), despite an apparent expansion of the SVZ in the mutants due to the defective migration of late born cells (Caric et al., 1997).

Recent work has begun to offer some insight into the temporal sequence of molecular controls that regulate these decisions. For example, *Pax6* is expressed at high levels in progenitors dividing at the ventricular surface, while it is largely excluded from intermediate progenitors in the SVZ. The progressive loss of *Pax6* as cells migrate into the SVZ is associated with the initiation of *Tbr2* expression, identifying the transition to intermediate progenitor cells (Englund et al., 2005). This observation, combined with the recent finding that there is a reduction in the number of *Tbr2* intermediate progenitors in the absence of *Pax6* (Englund et al., 2005; Quinn et al., 2007), suggests that *Pax6* regulates the formation and expansion of the SVZ. In further support of this transcription factor regulating the development of the superficial layers, conditional disruption of *Pax6* at the onset of neurogenesis leads to premature cell cycle exit, increased production of deep layer neurons, and a near complete loss of superficial layer neurons (Tuoc et al., 2009). Interestingly, loss of *Pax6* after generation of the deep layer neurons does not affect specification or numbers of superficial layer neurons, suggesting that the severe reduction in superficial layer neurons in the *Pax6* null neocortex results from a depletion of the progenitor pool available for late neurogenesis (Tuoc et al., 2009).

1.4 Molecular Controls Over Neocortical Projection Neuron Subtype Specification and Development

Within the broad class of neocortical projection neurons, many subtypes of projection neurons exist with distinct connectivity, soma laminar location, and gene expression. Three broad classes of projection neurons exist, based on anatomical classification: (1) corticofugal projection neurons, which are located exclusively in deep layers, and extend their axons away from the cortex to subcortical (e.g. striatum, thalamus) and subcerebral targets (e.g. brainstem and spinal cord); (2) callosal projection neurons (CPN), which are located in layers II/III, V and VI, and extend an axon to the contralateral hemisphere; and (3) associative projection neurons, which extend their axon within a single cortical hemisphere (Figure 1.4) (Molyneaux et al., 2007; Fame et al., 2011).

The corticofugal projection neurons include subplate neurons, which form the deepest cortical layer and send pioneering axons to the thalamus (McConnell et al., 1989; McConnell et al., 1994); corticothalamic projection neurons (CThPN), located primarily in layer VI, which project to different nuclei of the thalamus; and subcerebral projection neurons, which reside in deep layer V (Vb) and extend their primary axon to targets in the midbrain, hindbrain, and spinal cord. Although all subcerebral projection neurons have a common laminar position, and are born within the same developmental time frame, they are themselves quite diverse and include several unique subtypes. Corticospinal motor neurons (CSMN) are large pyramidal neurons that reside in sensory and motor areas and extend their primary axon to the spinal cord, with some extending secondary collaterals to the striatum, red nucleus, caudal pons and medulla, whereas corticopontine and corticobulbar projection neurons extend a primary axon to brainstem targets in the pons and medulla, respectively. Corticotectal projection neurons reside in layer V of visual cortex, and extend their primary axon to the superior colliculus in the midbrain (Arlotta et al., 2005; Molyneaux et al., 2007).

CPN are heterogeneous with respect to their birth dates and their final laminar destinations, and include several subtypes with distinct projection patterns. CPN with a single contralateral axonal projection reside in layer II/III (~80%), V (~20%) and VI (a small %), while CPN with an additional ipsilateral frontal projection reside primarily in layer Va (Mitchell and Macklis, 2005; Molyneaux et al., 2007; Molyneaux et al., 2009). Other subtypes of CPN with distinct dual projections are now being identified anatomically and molecularly (Fame et al., 2011). Another subtype, a subtype of corticostriatal projection neurons (CStrPN) called intratelencephalic corticostriatal projection neurons (CStrPNi), which also reside primarily in layer Va, have axonal projections with shared characteristics of both CPN and subcerebral projection neurons: their axons project across the midline to the contralateral hemisphere, but extend collaterals subcortically to the ipsilateral or contralateral striatum and may display hybrid molecular properties(Wilson, 1987; Molyneaux et al., 2007; Azim et al., 2009b;

Reiner et al., 2010). Approximately 60% of all corticostriatal inputs are CStrPNi, whereas the other 40% arise from striatal collaterals of CSMN (Jinnai and Matsuda, 1979; Reiner et al.). It has been suggested that as a population, CStrPN express *Etv1*, but no molecular distinction has yet been identified between the two distinct populations of CStrPN (Gong et al., 2007), although electrophysiological and physical dichotomy exists (Reiner et al., 2010).

The molecular mechanisms that direct neocortical progenitors toward this remarkable diversity of projection neuron phenotypes are only recently becoming elucidated. Despite the discovery of genes that identify neocortical progenitors as global populations (e.g. *Pax6*, *Tbr2,* and *Sox6*), as of yet, there are only a few markers to distinguish among progenitors generating different projection neuron subtypes (e.g. *Fezf2* and *Svet1).* Therefore, much less is known about genes that control the progressive commitment of progenitors to give rise to distinct subtypes of post-mitotic projection neurons. A number of neuronal subtype specific genes are expressed in what appear to be subpopulations in the VZ and SVZ, where they might label progenitors or early post-mitotic neurons of that same neuronal subtype, suggestive of a role in their fate determination. FEZ family zinc finger 2 (*Fezf2*) is a transcription factor expressed both by a subpopulation of VZ progenitors during generation of deep layers (presumed to be the progenitors for all corticofugal neuron subtypes), and selectively by postmitotic subcerebral projection neurons at high level, and by corticothalamic and other corticofugal projection neurons at lower level (Chen et al., 2005a; Chen et al., 2005b; Molyneaux et al., 2005). *Fezf2* controls specification of subcerebral projection neurons, and, in its absence, this entire broad neuronal population is not specified during development (Chen et al., 2005a; Molyneaux et al., 2005; Chen et al., 2008a). The transcription factors *Cux2* and *Tbr2*, as well as the non-coding RNA *Svet1,* located in an intronic sequence of the *Unc5d* gene (Sasaki et al., 2008), are specifically expressed in the SVZ and by superficial layer neurons, suggesting a role in SVZ intermediate progenitor cell neurogenesis, and development of superficial layer neurons (Tarabykin et al., 2001; Nieto et al., 2004; Englund et al., 2005).

Figure 1.4: **Major subtypes of projection neurons within the neocortex**

Classified by hodology, there are three basic classes of cortical projection neurons: associative, commissural, and corticofugal. Some principal subtypes are:

(A) **Callosal Projection Neurons (commissural)**

Callosal projection neurons are projection neurons of small to medium pyramidal size that are primarily located in layers II/III (~80%), V (~20%) and VI (a small %) and extend an axon across the corpus callosum. At least four major types of callosal neurons can be classified that maintain (1) single projections to the contralateral cortex (red); (2) dual projections to the contralateral cortex and ipsilateral frontal cortex (blue); (3) dual projections to the contralateral cortex and ipsilateral caudal cortex (pink); (4) dual projections to the contralateral cortex and ipsilateral or contralateral striatum (green). These are not thought to project axons to targets outside of the telencephalon.

(B) Corticofugal (projections away from the cerebral cortex)

Corticothalamic projection neurons: projection neurons primarily located in cortical layer VI, with a smaller population in layer V, that project subcortically to different nuclei of the thalamus (purple).

Subcerebral Projection Neurons: (also referred to as Type I layer V projection neurons) include pyramidal neurons of the largest size, which are located in deep layer V and extend projections to the brainstem and spinal cord. They can be even further subdivided into several distinct projection neuron subtypes. Among them (1) *corticospinal motor neurons* (light blue) are located in the sensorimotor area of cortex and maintain primary projections to the spinal cord, with some extending secondary collaterals to the striatum, red nucleus, caudal pons and medulla; *corticopontine projection neurons* (orange) maintain primary projections to the pons; *corticotectal projection neurons* (teal) are located in the visual area of cortex and maintain primary projections to the superior colliculus, with secondary collateral projections to the rostral pons. Many other subtypes of subcerebral projection neurons exist that send axons to different areas of the brainstem or with different combinations of collaterals, but are not depicted here for simplicity. Adapted from (Molyneaux et al., 2007).

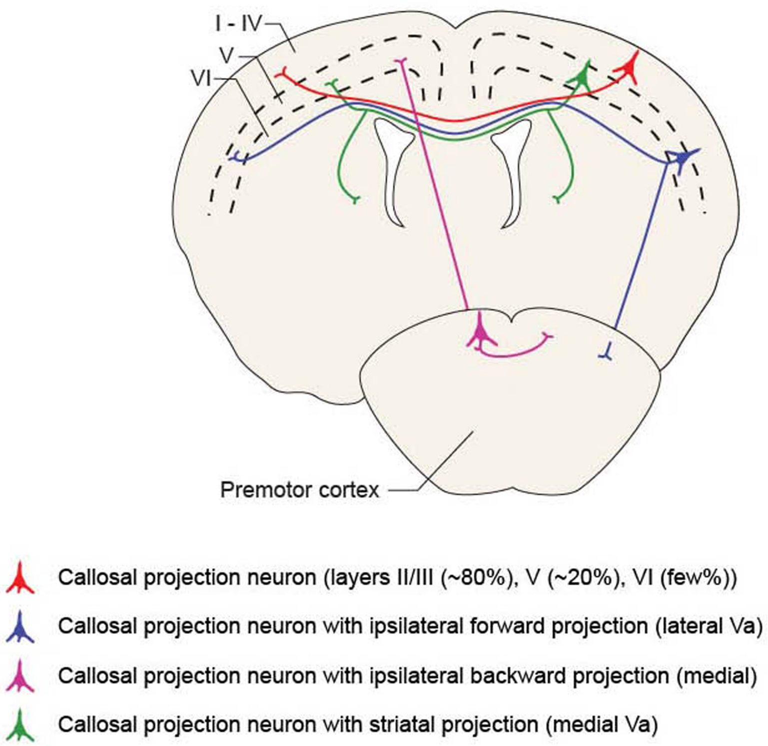

A **Callosal projection neurons**

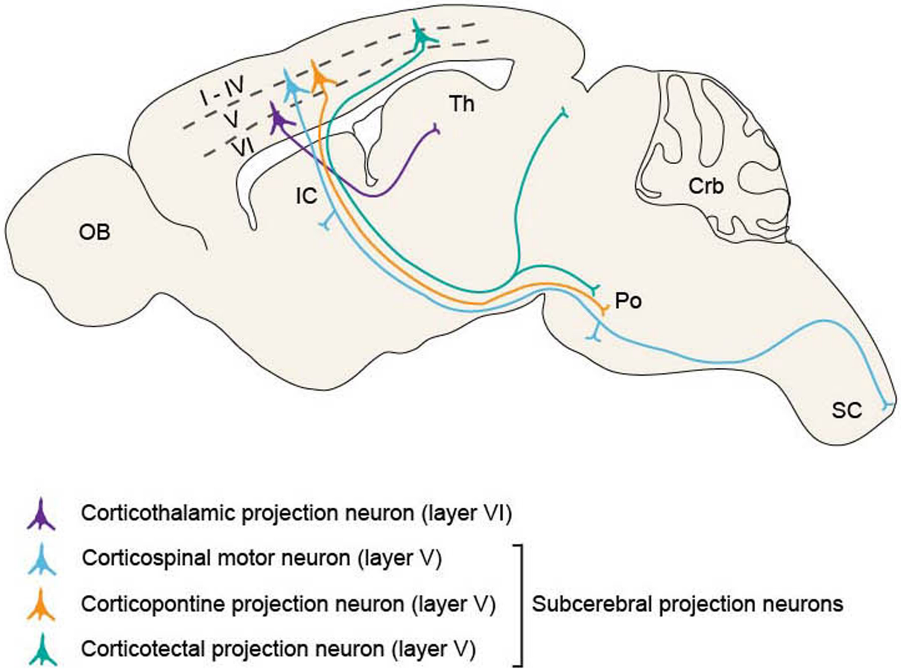

B **Corticofugal projection neurons**

Figure 1.4 (Continued)

However, it is important not to directly infer that a gene plays a role in specification of subtypes at the progenitor level based on restricted expression that is later observed in that particular neuronal subtype; it is entirely possible that the gene has two independent functions during development (Alvarez-Bolado et al., 1995). This is best illustrated by considering *Lhx2*, which is expressed in the VZ and SVZ prior to and during the generation of superficial layers, and is also expressed by postmitotic neurons of the superficial layers. The finding that loss of *Lhx2* results in absence of neurons of all layers (Bulchand et al., 2001; Monuki et al., 2001) suggests that *Lhx2* likely has two functions during development: in the VZ, it is required to establish neocortical identity of progenitors of all layers, while later in development it might control more specific aspects of superficial layer differentiation. Furthermore, genes expressed by neocortical progenitors at the time a subpopulation is born may not directly regulate their specification, as is the case with *Otx1*. *Otx1* is a transcription factor that is expressed by VZ progenitors and postmitotic subcerebral projection neurons, but controls a later stage of differentiation - the pruning of exuberant axonal projections (Frantz et al., 1994b; Weimann et al., 1999). On the other hand, as discussed above, there is better evidence that genes like *Cux2* and *Svet1* might be identifiers of SVZ progenitors destined to give rise to a superficial layer pyramidal neuron. For each of these genes, further study is required to define the relationship between progenitors and post-mitotic neurons expressing the same genes, and fate-mapping experiments combined with molecular analysis will be an important step in linking molecular identity of distinct progenitors to direct fate determination of specific neuronal lineages.

A critical step for understanding developmental processes that govern projection neuron specification and differentiation is the delineation of the postmitotic gene expression profiles of distinct projection neuron subtypes, and characterization of the functions of these genes in the pathways from progenitors to differentiation of the multitude of mature neuronal phenotypes. Recently, tremendous advances have been made in identification of laminar- and subtype-specific markers through multiple approaches: large scale *in situ* hybridization projects (Gray et al., 2004; Visel et al., 2004; Magdaleno et al., 2006; Lein et al., 2007); the creation of transgenic mouse lines expressing GFP under the control of promoters of lineage or layer restricted genes (Gong et al., 2003); gene expression studies comparing microdissected regions of neocortex (Liu et al., 2000; Zhong et al., 2004; Bedogni et al., 2010); and comparison of purified neuronal subtypes by microarray analysis (Arlotta et al., 2005; Sugino et al., 2006; Molyneaux et al., 2009). The Brain Gene Expression Map (BGEM) (Magdaleno et al., 2006), the Allen Brain Atlas (ABA) (Lein et al., 2007), and Genepaint (Visel et al., 2004) are three notable databases providing comprehensive digital atlases of gene expression in the developing and adult central nervous system via *in situ* hybridization of thousands of transcripts, facilitating identification of spatio-temporal expression of lamina and region-specific genes, as well as genes that are coordinately expressed in specific regions. These data have been leveraged by the GENSAT project (Heintz, 2004) to generate bacterial artificial chromosome (BAC) transgenic reporter lines, in which the gene coding region has been replaced with an enhanced GFP driven by the endogenous regulatory promoter regions, for all genes expressed in the nervous system. The select mouse lines that recapitulate *in vivo* expression (not all do) provide a powerful tool for analysis of axonal projections from neurons expressing the gene of interest, as well as fate-mapping of these subpopulations of neurons in mutant mice.

Until recently, molecular classification of projection neurons in the neocortex largely consisted of lamina-specific genes, such as *Er81*, which is expressed throughout layer V in both CPN and subcerebral projection neurons (Yoneshima et al., 2006), and *Cux2*, which is expressed by SVZ progenitors, as well as in superficial layers (Nieto et al., 2004; Zimmer et al., 2004). However, this broad parcellation does not reflect the complexity of neocortical circuitry, where neurons born at the same time, and that share final laminar location and partial overlap of gene expression, differ significantly with respect to axonal projections, areal location in neocortex, and expression of subtype-specific genes that control specification and differentiation of that particular neuron subtype. This is particularly striking in layer V, where neurons with a shared birthdate project to such diverse targets as contralateral hemisphere and spinal cord.

A substantial advance in identifying genes that are unique to, and potentially control development and function of, diverse projection neuron subtypes in the neocortex came from recent work demonstrating that combinatorial programs of gene expression unique to each projection neuron subtype control specificity and precision of differentiation and connectivity of distinct subtypes of projection neurons in the neocortex(Arlotta et al., 2005; Molyneaux et al., 2005; Ozdinler and Macklis, 2006; Molyneaux et al., 2007; Arlotta et al., 2008; Joshi et al., 2008b; Lai et al., 2008; Azim et al., 2009a; Azim et al., 2009b; Molyneaux et al., 2009; Tomassy et al., 2010; MacDonald et al., in press). These specific cell-intrinsic programs were identified by selective purification of projection neuron subtypes during development of neocortex, using retrograde labeling followed by fluorescence-activated cell sorting (FACS), and microarray comparisons of gene expression for distinct subtypes of projection neurons at critical stages of differentiation (embryonic day [E] 18, postnatal day [P] 3, P6, and P14) (Arlotta et al., 2005) (Figure 1.5). This approach has been extremely successful at identifying many critical molecular controls over specification and development of distinct projection neuron subtypes; these include *Fezf2* (Chen et al., 2005a; Chen et al., 2005b; Molyneaux et al., 2005; Chen et al., 2008a), *Ctip2* (Arlotta et al., 2005; Arlotta et al., 2008), *Sox5* (Lai et al., 2008), *Bhlhb5* (Joshi et al., 2008b), *Lmo4* (Azim et al., 2009b), *Clim1* (Azim et al., 2009b), *Sox6*(Azim et al., 2009a), among others (Molyneaux et al., 2009; Tomassy et al., 2010). The remarkably fine resolution of this approach is demonstrated by the identification of unique molecular controls over CSMN development, even as compared to the closely-related subcerebral projection neurons, CTPN, which reside in layer V, and extend an early projection to the spinal cord that is later pruned (O'Leary, 1992; O'Leary and Koester, 1993).

In addition to cell type-specific molecular controls over cortical specification, layer-specific genes give insight into development and specification of restricted populations of cortical neurons. Examples of layer-specific genes include, among many others: *Cux1*, *Cux2*, and *Lhx2*, markers of layers II/III to IV (Nakagawa et al., 1999; Bulchand et al., 2003; Nieto et al., 2004; Zimmer et al., 2004); *Brn2*, a marker of layer II/III and V(McEvilly et al., 2002; Sugitani et al., 2002); *RORβ*, a marker of layer IV

(Schaeren-Wiemers et al., 1997; Jabaudon et al., 2012); *6430573F11Rik* and *Encephalopsin*, markers of layer V (Arlotta et al., 2005; Magdaleno et al., 2006); and *Foxp2*, a marker of layer VI (Ferland et al., 2003). Among these genes, some have been described as being expressed by one specific neuronal type within a layer or across layers, including a large number of genes that exhibit varying degrees of restricted expression to CSMN (Arlotta et al., 2005) and others with restricted expression by all CPN or a series of progressively more precise CPN subpopulations (Molyneaux et al., 2009); discussed further below. Genes with expression known to be restricted to individual subtypes include: *Ctip2* and *Fezf2*, which are both expressed at high levels by subcerebral neurons of layer V, and at much lower levels by corticothalamic neurons of layer VI (Arlotta et al., 2005; Molyneaux et al., 2005); *Scip*, which is primarily expressed by subcerebral projection neurons of layer V, in addition to lower levels of expression by neurons of layers II-III (Frantz et al., 1994a); *Otx1*, which is expressed by 40-50% of subcerebral neurons, as well as a number of cells in layer VI (Weimann et al., 1999); *Er81*, which is expressed by cortico-cortical as well as subcerebral projection neurons of layer V (Hevner et al., 2003); *Nfh*, which is expressed by subcerebral projection neurons of layer V (Voelker et al., 2004); *Lmo4*, which is expressed by callosal neurons of layers II/III, V, and VI, and is excluded from CSMN (Bulchand et al., 2003; Arlotta et al., 2005); *Sox5*, which is expressed at high levels in developing CFuPN, and is excluded from CPN (Lai et al., 2008); and *Lpl, Hspb3, Nectin3, Plxnd1,* and *Dkk3,* expressed by distinct subpopulations of CPN and excluded from CSMN (Molyneaux et al., 2009). The subplate neurons also exhibit molecular diversity: some genes, including *Ctgf* and *Cplx3,* are specifically expressed by subplate neurons (Heuer et al., 2003; Hoerder-Suabedissen et al., 2008), while *Tmem163* and *MoxD1* are expressed by both subplate neurons and by a subpopulation of layer V neurons (Hoerder-Suabedissen et al., 2009).

Investigations into functions of layer and subtype-restricted genes are starting to provide insight into how neuronal subtypes are specified in the neocortex. *Brn1* and *Brn2*, which are expressed primarily by neurons of layers II-V (McEvilly et al., 2002; Sugitani et al., 2002; Hevner et al., 2003), are involved in directing differentiation and migration of neurons within these layers. *Brn1*/*Brn2* double

Figure 1.5: Schematic representation of an experimental approach used to identify projection neuron-specific genes. CPN (red), corticothalamic projection neurons (purple), corticospinal motor neurons (green), and corticotectal projection neurons (blue) were retrogradely labeled at distinct stages of development from the contralateral hemisphere, the thalamus, the spinal cord, and the superior colliculus, respectively. Labeled neurons were dissociated, purified using fluorescence activated cell sorting (FACS), and followed by comparative microarray genetic expression analysis(Catapano et al., 2001; Catapano et al., 2004; Arlotta et al., 2005; Ozdinler and Macklis, 2006; Molyneaux et al., 2007; Molyneaux et al., 2009). Adapted with permission from Ref.. (Molyneaux et al., 2009).

1. Retrograde labeling of projection neuron subtypes

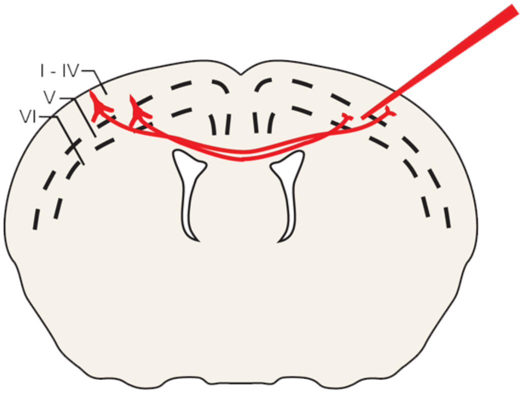

Callosal projection neuron (layers II/III (~80%), V (~20%), VI (few%))

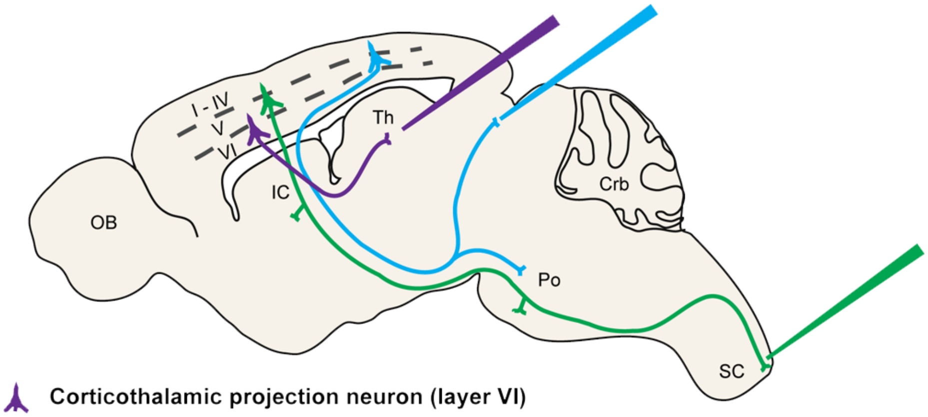

Corticothalamic projection neuron (layer VI)

Corticospinal motor neuron (layer V)

Corticotectal projection neuron (layer V)

2. FACS purification of labeled projection neurons

3. Comparative microarray analysis

Figure 1.5 (Continued)

knockouts possess decreased numbers of neurons of layers II-V, and those that are born exhibit abnormalities in migration, arresting in the VZ/SVZ (McEvilly et al., 2002; Sugitani et al., 2002). Additionally, some markers of superficial layer neurons are expressed in these mutants, while others (e.g. *mSorLa*) are absent, suggesting subtype specific abnormalities in differentiation of different populations of superficial neurons. In contrast, *Tle4* and *Tbr1* expressing neurons of layer VI appear to form and migrate normally into the cortical plate in the absence of *Brn1* and *Brn2* (McEvilly et al., 2002; Sugitani et al., 2002). Further analysis of *Brn1*/*Brn2* mutants with recently identified markers is needed to illuminate precisely which subtypes of neurons are affected in the absence of *Brn1* and *Brn2*.

While it has been proposed that *Ngn1* and *Ngn2* play key roles in regulating deep layer neurogenesis (Schuurmans et al., 2004; Guillemot et al., 2006), the majority of *Er81* positive and *Tbr1* positive neurons of layers V and VI are clearly generated in their absence (Fode et al., 2000; Schuurmans et al., 2004). *Ngn1* and *Ngn2* likely function, therefore, to maintain dorsal glutamatergic fate within deep layer neurons (Schuurmans et al., 2004), rather than playing a primary role in specifying laminar or projection neuron subtype fate. *Mdga1*, a recently identified cell adhesion molecule, is required for layer II/III projection neurons to migrate to their appropriate position in the neocortex (Takeuchi and O'Leary, 2006). Knockdown of *Mdga1* by RNAi results in migrational arrest in the intermediate zone and deep layers of the neocortex (Takeuchi and O'Leary, 2006).

Interestingly, many genes are expressed across multiple projection neuron subtypes, and are likely to cooperate with distinct partners expressed in a more restricted pattern to exert a subtype-specific function. For example, *Tbr1* is expressed at high levels by subplate and layer VI, but in rostral cortex is also expressed in layers II/III (Bulfone et al., 1995), and it accordingly has multiple described functions across different subtypes and cortical layers; this includes regulating preplate splitting, development of corticothalamic projections, and guidance of developing CPN axons across the midline to form the corpus callosum (Hevner et al., 2001; Bedogni et al.). *Id2* codes for a helix-loop-helix transcription factor that is expressed in layer V in intermediate and caudal regions of neocortex, with an abrupt boundary in the rostral region, yet in layer II/III it exhibits a complementary pattern of high rostral expression and low expression levels in intermediate and caudal areas. *Bhlhb5* is expressed in an area-restricted pattern across layers II-V, but exerts specific developmental control over CSMN in layer V (Joshi et al., 2008b). *Clim1* and *Lmo4* are both expressed broadly, but progressively delineate CSMN from CPN in layer V (Azim et al., 2009b). Such examples illustrate that combinatorial programs of gene expression across layers and subtypes of projection neurons delineate a molecular complexity that parallels the known anatomical and functional complexity of neocortical projection neurons (Koester and O'Leary, 1992; O'Leary and Koester, 1993; Arlotta et al., 2005; Mitchell and Macklis, 2005; Molyneaux et al., 2007). Similar investigations for each of the other subtype-specific genes are needed in order to delineate programs of gene expression that direct subtype-specific differentiation. As more evidence accumulates regarding functional roles played by the many subtype-specific genes that are being discovered, we will likely witness rapid progress in understanding programs of molecular controls that direct neuronal subtype differentiation in the neocortex.

1.4 a. Callosal Projection Neuron Specification, Development, and Diversity

In contrast to subcerebral projection neurons (discussed in more detail in the following section), callosal projection neurons (CPN) are heterogeneous with respect to their birthdate and laminar postion. CPN are the largest class of commissural neurons in placental mammals (Aboitiz et al., 2003), connecting homotopic regions of the two cerebral hemispheres via the corpus callosum, the principal white matter fiber tract in the brain that, in human, is composed of over 300,000 fibers (Swenson, 2006). CPN are critical for bilateral transfer and integration of cortical information, and they have been centrally implicated in autism spectrum disorders (ASD). One of only a few anatomically identified pathologies of ASD is a reduced corpus callosum relative to overall brain volume (Egaas et al., 1995; Vidal et al., 2006; Herbert and Kenet, 2007; Minshew and Williams, 2007; Freitag et al., 2009; Mcalonan et al., 2009). Absence, or surgical disruption, of CPN connectivity in humans is also associated with defects in abstract reasoning, problem solving, and generalization (Paul et al., 2007).

Early Development and Axon Guidance

CPN maturation follows a set of discrete sequential steps as CPN establish correct circuitry and synaptic connections with their targets in the contralateral hemisphere. CPN are born throughout corticogenesis at the same times in development as other neurons with cell bodies residing in their same cortical layers: in the mouse, layer VI CPN are born at approximately embryonic day 12.5 (E12.5) along with corticothalamic projection neurons (CThPN); layer V CPN are born around E13.5 along with corticospinal motor neurons (CSMN); and superficial layer CPN are born from approximately E15.5 to E17.5(Angevine and Sidman, 1961; Molyneaux et al., 2007). As CPN are born, the two telencephalic hemispheres begin fusing, aided in part by two populations of glia - midline zipper glia and indusium griseum glia(Silver et al., 1982; Shu et al., 2003b; Richards et al., 2004; Lindwall et al., 2007) (Figure 1.6A). While cellular and molecular mechanisms of midline fusion have not been completely identified, it is clear that, if the midline is not fully fused, callosal axons have no substrate and cannot cross to the contralateral hemisphere. Many midline fusion and glial defects cause partial or complete agenesis of the corpus callosum, independent from abnormalities of CPN themselves (see Ref. (Donahoo and Richards, 2009) for review).

As the hemispheres continue to fuse, populations of glia and local neurons form the transient bridge-like subcallosal sling across the midline (Silver et al., 1982; Shu et al., 2003a; Niquille et al., 2009). CPN send axons ventrally toward the intermediate zone guided, in part, by signals from indusium griseum glia dorsally at the midline, and glial wedge and subcallosal sling populations ventrally(Shu et al., 2003a; Richards et al., 2004; Niquille et al., 2009). Upon reaching the intermediate zone, callosal axons turn toward the midline to cross at the corticoseptal boundary, rather than projecting laterally as CFuPN do. Upon encountering the contralateral glial wedge, CPN axons turn dorsally and extend into the neocortex toward homotopic targets. Mechanisms of precise CPN targeting to contralateral homotopic regions are still largely unknown, but callosal axons have been shown to follow the trajectory of radial glia in the contralateral hemisphere as they extend their axons to appropriate targets(Norris and Kalil, 1991). During development (at E17 in mouse), axons from neurons of the cingulate cortex begin the process of midline crossing(Silver et al., 1982; Koester and O'Leary, 1994; Ozaki and Wahlsten, 1998; Rash and Richards, 2001) and might act as pioneers for neocortical CPN(Piper et al., 2009) (Figure 1.6A), which begin to cross one day later(Silver et al., 1982). First-born, deep-layer cingulate pioneers and neocortical CPN are the first of each respective population to cross the midline and, therefore, reach final targets before superficial layer CPN.

Processes of midline crossing and targeting are mediated by a large number of long-range and short-range signals that, while highly studied, are not completely known. Key molecular regulators controlling midline crossing and targeting are best studied for deep layer, early-crossing CPN; it is not evident whether or not superficial layer, later-born CPN employ the same mechanisms. These processes have been extensively reviewed elsewhere(Rash and Richards, 2001; Richards et al., 2004; Lindwall et al., 2007; Niquille et al., 2009) and I will only briefly summarize that body of work here. Studies over the past decade have uncovered some midline crossing and targeting controls that operate at several different levels of CPN function. At the level of growth cone dynamics in callosal axons themselves, *Mammalian Enabled* (*Mena*) plays a role in actin cytoskeletal dynamics in neurons of neocortical layers II/III and V, and is required for proper formation of the corpus callosum as well as the hippocampal commissure(Lanier et al., 1999). Long-range guidance molecules, such as members of the Slit/ Robo, Wnt, and Netrin families also play active roles in axon guidance across the corpus callosum. Slits, including Slit2, are enriched along the midline, surrounding the area through which CPN axons pass; these axons express the Slit receptor Robo1 (Bagri et al., 2002; Shu et al., 2003c; Sundaresan et al., 2004; Andrews et al., 2006; Lindwall et al., 2007; López-Bendito et al., 2007). Wnts, particularly Wnt5a, are necessary for formation of all forebrain commissures, both through canonical, Frizzled3-mediated(Wang et al., 2006), and non-canonical, related to tyrosine kynase (Ryk)-mediated(Keeble et al., 2006; Li et al., 2009), receptor transduction pathways(Lindwall et al., 2007). In addition to Slits and Wnts, Netrin1 and its receptor, deleted in colorectal cancer (DCC), are also required for all forebrain commissure formation(Serafini et al., 1996; Fazeli et al., 1997; Lindwall et al., 2007; Ren et al., 2007); however, although CPN express DCC, there is no evidence that DCC-mediated mechanisms

Figure 1.6: CPN development and diversity (**A**) During development, callosal axons (red) turn toward the midline. Multiple glial populations (blue) and mixed neuronal/glial populations (purple) play critical roles in CPN axon guidance and midline crossing. Pioneering axons (brown) from neurons of the cingulate cortex begin the process of midline crossing. This schematic represents processes that occur across multiple embryonic times during mouse CPN development. Abbreviations: CP, cortical plate; IZ, intermediate zone; SVZ, subventricular zone; VZ, ventricular zone; IGG, indusium griseum glia; GW, glial wedge; SCS, subcallosal sling; MZG, midline zipper glia. (**B)** At least four major types of adult CPN can be classified based on projection patterns. These include: single projections to the contralateral cortex (red); dual projections to the contralateral cortex and ipsilateral or contralateral striatum (green); dual projections to the contralateral cortex and ipsilateral premotor cortex (blue); or dual projections to the contralateral cortex and ipsilateral sensorimotor cortex (purple).

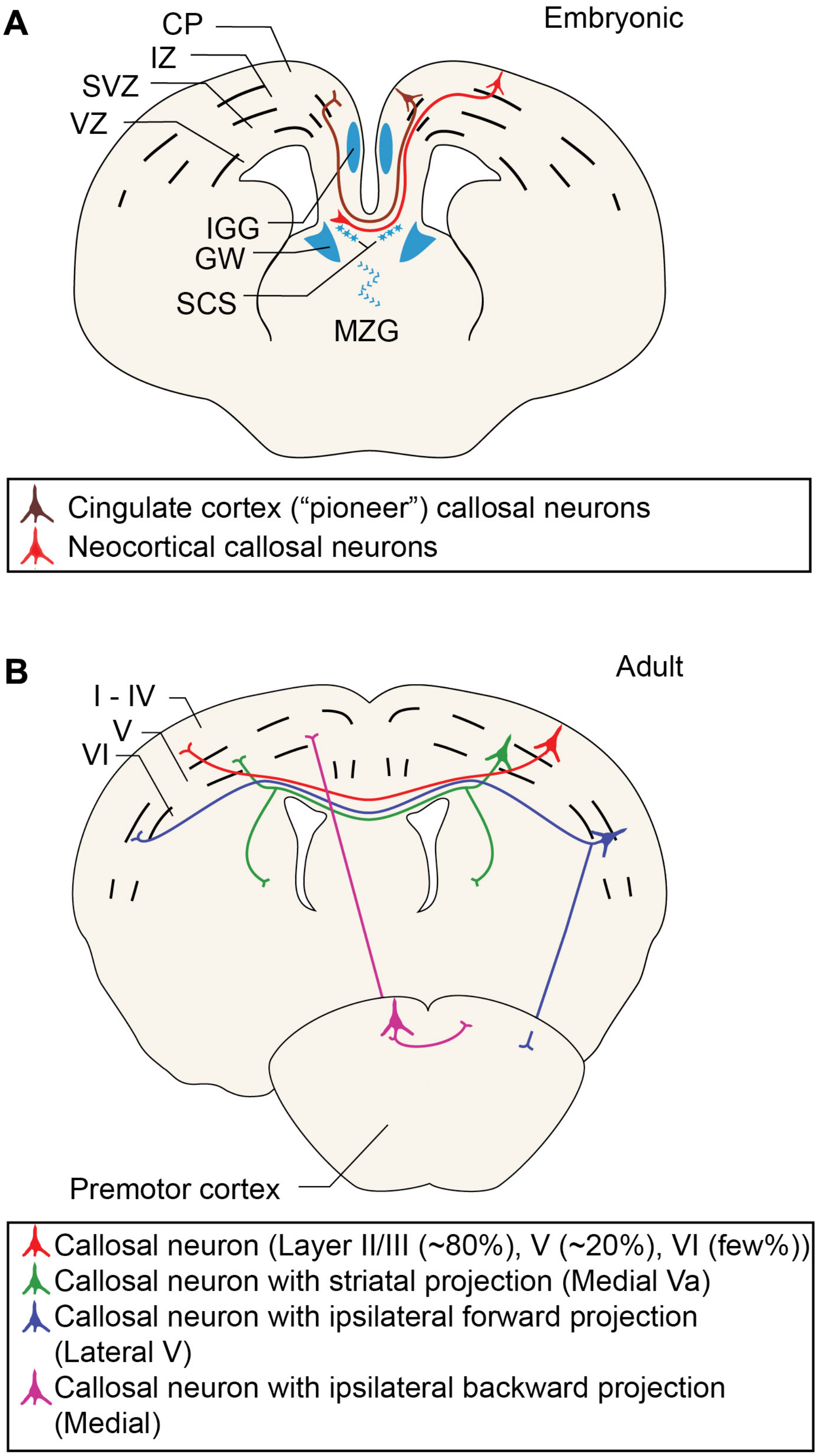

Figure 1.6 (Continued)

of guidance are the same in the corpus callosum as they are for Netrin1 in commissure formation of the spinal cord(Serafini et al., 1996; Shu et al., 2000). At least some guidance roles of the subcallosal sling are mediated by Semaphorin-3C (Sema3C) attraction through the Neuropilin1 receptor on CPN(Gu et al., 2003; Niquille et al., 2009). In addition to long-range signals, short-range, local interactors – in particular ephrins and their receptors (EphA5, EphB1, and EphrinB3)– are essential for corpus callosum formation(Hu et al., 2003; Mendes et al., 2006; Lindwall et al., 2007). Notably, it appears rare for guidance defects in corpus callosum formation to be callosum-specific; rather, they typically affect broader populations of commissures.

As a broad population, CPN extend exuberant projections throughout development, with the maximal number of CPN with dual projections occurring at approximately postnatal day 8 (P8) in mice(Innocenti and Price, 2005; Mitchell and Macklis, 2005). Dual projections are progressively refined until approximately P21, when the adult projection pattern for CPN is established; this process is thought to occur largely through activity-dependant, Hebbian mechanisms(Innocenti and Price, 2005; Mizuno et al., 2007; Wang et al., 2007; Mizuno et al., 2010). Interestingly, laterally located CPN that are furthest from the midline and the many signaling molecules present there, extend a bifurcated axon early in development that projects toward both the midline and the internal capsule. Only later (approximately P11 in mice) do lateral developing CPN retract axonal segments projecting to the internal capsule(Garcez et al., 2007).

Anatomical Diversity

While CPN have long been regarded as a single, relatively uniform population, substantial diversity within this broad population is being increasingly revealed, and molecular controls underlying development of CPN and these distinct subpopulations are beginning to be elucidated (Molyneaux et al., 2009; Fame et al., 2011). All CPN extend an axon to the homotopic region of the contralateral neocortex; thus, the locations and laminar positions of CPN within the neocortex define the targets of their callosal axons. The corpus callosum is often broadly categorized in six regions from rostral to caudal, named for homotopic regions these axons connect: frontal, motor, somatosensory, auditory, temporoparietal, and visual. Callosal fibers vary in density and diameter across these regions, both in rodents and humans(Aboitiz and Montiel, 2003).

In addition to homotopic, interhemispheric projections extended by all CPN, subpopulations of CPN can be defined by the variety of long-range dual axonal projections they extend. Subpopulations of CPN send dual projections to contra- or ipsilateral striatum (here, referred to as CStrPNi)(Wilson, 1987), caudally to contra- and/or ipsilateral primary somatosensory cortex (here, referred to as BPN)(Cauller et al., 1998; Mitchell and Macklis, 2005), or rostrally to contra- or ipsilateral frontal areas (here, referred to as FPN)(Mitchell and Macklis, 2005) (Figure 1.6B). CPN with dual projections reside preferentially in the deep layers of the neocortex. For example, in adult mice, only about 4% of layer II/III CPN extend dual axonal projections to the frontal premotor cortex, while approximately 40% of layer V CPN do(Mitchell and Macklis, 2005). CStrPNi reside almost exclusively in layer Va(Wilson, 1987), which supports the hypothesis that CPN with dual projections reside in evolutionarily-older deep layers, and, therefore, are more likely to have been evolutionarily co-opted from existing CFuPN. Additionally, deep layer CPN (layers V and VI) provide about 80% of the collaterals connecting primary motor cortex to primary somatosensory cortex, and some deep layer CPN have also been shown to project to secondary somatosensory cortex and the claustrum, in addition to the striatum(Veinante and Deschenes, 2003). In patients with partial agenesis of the corpus callosum, diffusion tensor imaging detects heterotopic axonal projections that are not detectable in healthy subjects(Wahl et al., 2008). It is possible that, in healthy subjects, these heterotopic projections are still present, but undetectable over overwhelming signal from intact, homotopic axons. If this is the case, there might be much more diversity of connectivity within the human corpus callosum than investigators have been able to detect with current technology. However, recent data using diffusion spectrum magnetic resonance imaging (DSI) provides compelling evidence that axons in the corpus callosum tract run exclusively longitudinally or perpendicular to those longitudinal fibers, with no other orientations(Wedeen et al., 2012).

While many deep layer CPN have long-distance dual projecting axons, superficial layer CPN participate in local column circuitry. Layer II/III CPN send collaterals to pyramidal neurons within layer II/III, more strongly to layer V, and to pyramidal and stellate neurons in layer VI, in both ipsilateral and contralateral hemispheres (Petreanu et al., 2007). Thus, in addition to their role in connecting two homotopic regions of the neocortical hemispheres, CPN are responsible for functional association and integration among different neuronal types in ipsilateral and contralateral cortical hemispheres.

This laminar, anatomical, and connectivity diversity within the broad population of CPN demonstrates that it is not a homogenous population of projection neurons. Rather, CPN are a strikingly diverse set of subpopulations requiring precise control of their neuronal diversity by a complex and interactive set of molecular controls.

Molecular Controls over CPN Development and Diversity

Although, as discussed earlier, much progress has been made in beginning to understand the anatomical trajectory of developing CPN axons and cellular and molecular controls over midline crossing(Silver et al., 1982; Norris and Kalil, 1991; Lanier et al., 1999; Shu et al., 2000; Rash and Richards, 2001; Richards et al., 2004; Sundaresan et al., 2004; Andrews et al., 2006; Smith et al., 2006; Tole et al., 2006; Lindwall et al., 2007; López-Bendito et al., 2007; Plachez et al., 2008; Niquille et al., 2009), considerably less is known about molecular controls that specify CPN subtype identity and control this precise development. Because the majority of CPN reside in superficial layers, the first identified molecular controls over CPN generation and development were identified as laminar-specific genes such as *Brn1, Brn2, Cux1,* and *Cux2*, as discussed above (Table 1.1). In 2008, the first critical molecular regulator of broad CPN specification, special AT-rich sequence-binding protein 2 (SATB2), was identified and characterized as a DNA-binding transcription factor expressed by CPN. SATB2 is necessary for specification of CPN through repression of COUP-TF interacting protein 2 (CTIP2)(Alcamo et al., 2008; Britanova et al., 2008), a transcription factor critical for CSMN axon outgrowth and fasciculation(Arlotta et al., 2005; Chen et al., 2005a; Chen et al., 2005b; Molyneaux et al., 2005; Molyneaux et al., 2007). In the absence of SATB2 function, neurons that would have extended axons across the corpus callosum instead project subcortically through the internal capsule and take on some molecular and electrophysiological characteristics of CFuPN(Chen et al., 2008a). Identification of SATB2 as a molecular regulator of CPN identity across all layers, especially axonal connectivity through inhibition of CTIP2, significantly advanced the characterization of CPN at a molecular level. However, many interesting questions about instructive molecular signals responsible for midline crossing and precise homo- and heterotopic connections remain to be answered. Importantly, mechanisms by which this and other still-uncharacterized signals govern general CPN development are still largely unknown.

Recently, molecular controls that act specifically in subclasses of CPN have begun to be identified. The transcription factor activator enhancing binding protein 2 gamma (AP2γ) acts specifically in a subset of radial glia cortical progenitors to specify SVZ intermediate progenitors and enable the switch from proliferative to neurogenic division, and to generate a specific subpopulation of superficial layer CPN in visual cortex (Pinto et al., 2009). Interestingly, while the action of AP2γ is highly area specific, the expression of AP2γ is not, suggesting an areally-restricted partner or compensatory activity. In addition, *Cux1* and *Cux2,* previously discussed as layer-specific identifiers, regulate dendrite branching, spine development, and synapse formation specifically in layer II/III CPN (Cubelos et al., 2010). These subtype-specific controls are important for understanding the diversity that exists within and is integral to the broad CPN population.

Multiple approaches have been used successfully to identify molecular controls over temporal and/or laminar stages of neocortical projection neuron development. Investigators have screened gene expression databases for transcriptional regulators expressed in relevant laminae or progenitor zones of the neocortex, or have investigated functions of guidance molecules known to play critical roles in guiding neuronal populations in other regions of the nervous system. However, in order to identify molecular controls over development of specific, individual populations of neocortical projection neurons in a more direct and unbiased manner, approaches to isolate and purify individual neuronal populations have provided substantial power and sensitivity. As discussed above, one approach that has proven useful for isolating distinct populations of cortical projection neurons has been to first retrogradely label them from their developmental axonal trajectories and final axonal targets, and then to purify them using fluorescence activated cell sorting (FACS) (Figure 1.5). For a variety of reasons discussed in more detail in Chapter 2 (Arlotta et al., 2005; Molyneaux et al., 2005; Molyneaux et al., 2007), this approach was first used to label and isolate CPN (Catapano et al., 2001; Catapano et al., 2004; Arlotta et al., 2005; Molyneaux et al., 2009), CSMN (Arlotta et al., 2005; Molyneaux et al., 2005; Ozdinler and Macklis, 2006), corticotectal projection neurons (CTPN(Arlotta et al., 2005)), CThPN, CStrPN, and segmentally specific cervical or lumbar CSMN. These purified neurons were submitted to comparative microarray analysis to identify genes differentially expressed by each population at four key embryonic and postnatal developmental stages (E18.5, P3, P6, P14). Other purification methods have also proven fruitful for isolating distinct populations of cortical projection neurons (Barres et al., 1988; Dugas et al., 2008).

Purification of specific neuronal populations, followed by comparative gene expression analyses has not only led to the identification of genes expressed by each population at distinct stages in development, but has also enriched for critical subtype-specific molecular controls by comparing gene expression between very closely related cortical projection neuron populations. This work has already identified a set of genes that, in combination, define a progressively restricting program of molecular controls (or a “molecular-logic”) over development of important populations of cortical projection neurons including CPN (Arlotta et al., 2005; Molyneaux et al., 2005; Arlotta et al., 2008; Joshi et al., 2008b; Lai et al., 2008; Molyneaux et al., 2009; Tomassy et al., 2010). These data were collected symmetrically with regard to development of the neocortical projection neuron populations compared, and provides equivalent (but not yet functionally investigated) information regarding molecular controls over CPN development both as a broad population and in specific subpopulations(Molyneaux et al., 2009) (Figure 1.7, Table 1.1).

CPN genes identified in this way have been analyzed based on their laminar- and sublaminar-specific distributions across different stages of maturation (Molyneaux et al., 2009) (Figure 1.7, Table 1.1). Temporal information from these analyses identifies distinct molecular stages of CPN development that likely reflect known processes occurring during CPN maturation. Molecular controls expressed most highly early in CPN development (i.e.. at or before E18.5 in the mouse, such as *Inhba*, *Btg1*, *Frmd4b*, *Epha3*, and *Ptn*) likely act during neuronal subtype specification, refinement of differentiation, migration, or initial axonal extension. Genes whose expression sharply rises and falls (i.e.. are specifically expressed only during the mid-stages of CPN development, such as *Cpne4*, *Tmtc4*, *Nnmt*, *Cav1*, *Nectin*-3, and *Chn2)* might be hypothesized to function when CPN have already crossed the midline and are extending toward their specific targets. Genes expressed specifically late in CPN development (e.g. *Plexin-D1*, *Gfra2*, *TcrB*, and *Dkk3*) might more likely function in final CPN maturation and refinement of adult connectivity.

In addition to temporal gene expression data, this work identifies differential subtype-specific laminar gene expression. A subset of the identified CPN genes appear specific to CPN in all layers in which CPN reside (i.e. layers II/III and V-VI), while others discriminate between CPN of deep layers and those of superficial layers (Figure 1.7). Further, several genes finely subdivide CPN within individual layers, and appear to label discrete CPN subpopulations that have not been previously described using anatomical or morphological criteria(Mitchell and Macklis, 2005; Molyneaux et al., 2009). Interestingly, while a number of the genes expressed specifically in superficial layer CPN are expressed throughout the entirety of layers II/III, some genes are restricted to only the most superficial portion of layers II/III, while other genes are restricted to the deeper portion of superficial layers (Figure 1.7).

In isolation, differences in laminar expression might merely reflect birthdate differences. However, in light of being specific to CPN versus other neocortical projection neurons, and considering the existence of diverse hodological CPN subpopulations already identified, these differentially expressed

Figure 1.7: Spatially-restricted genes identify novel CPN subpopulations.

Schematic representation of neocortical layers depicting laminar-specific expression of 20 selected, representative genes expressed by early postnatal CPN within the neocortex (Molyneaux et al., 2009). Dark and light blue bands indicate high and low levels of expression, respectively. Grey oblique stripes demarcate layers in which CPN reside. Most of these genes have dynamic patterns of expression through development; therefore, developmental stage must be considered when using these genes to identify specific populations of CPN. Representative genes are depicted with multiple patterns of laminar expression: most cortical layers; and deep cortical layers only (top row); superficial cortical layers only (middle row); and subdivisions of superficial layers (bottom row). See text and table S1 for more detailed expression and references. Abbreviations: roman numerals indicate neocortical layers (I-VI); SP, subplate.

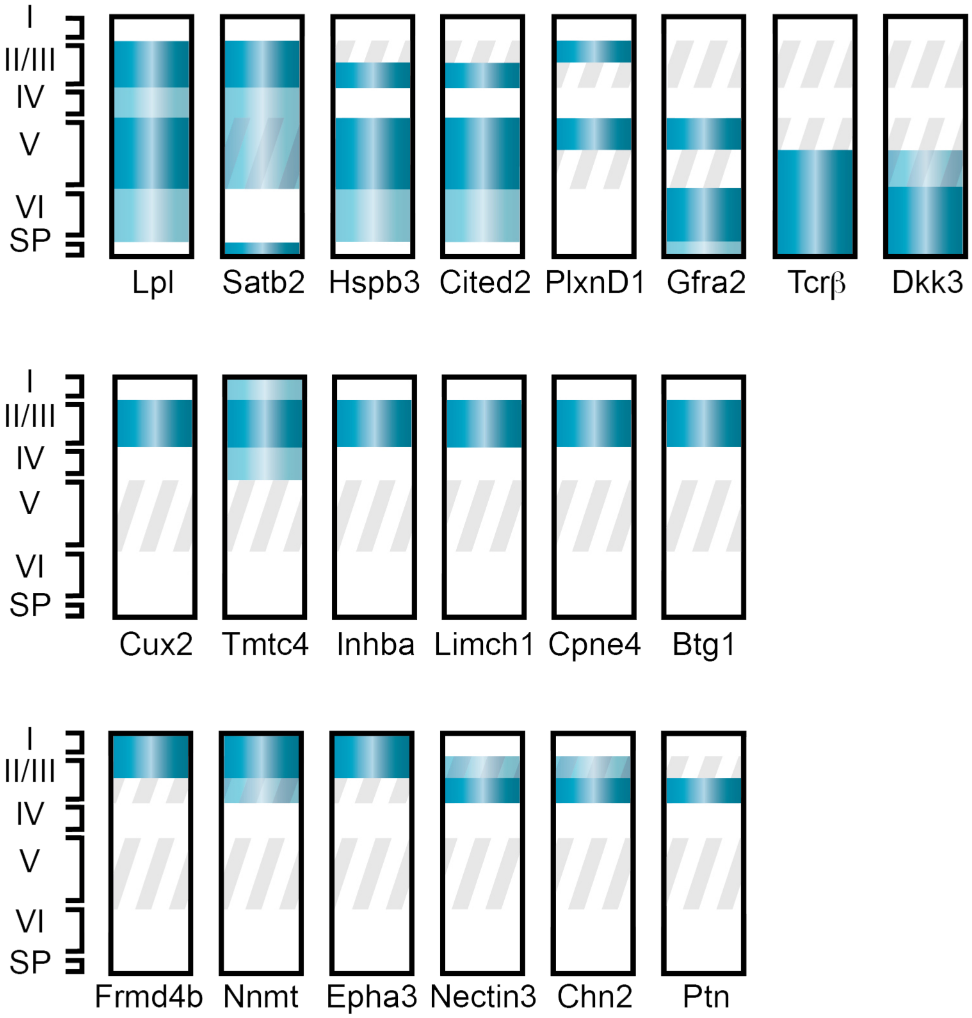

Figure 1.7 (Continued)

Table 1.1 Genes expressed by callosal projection neurons (CPN) and their progenitors

Abbreviations: VZ, ventricular zone; SVZ, subventricular zone; IPC, intermediate progenitor cell; E, embryonic day; P, postnatal day; S1, primary somatosensory cortex; roman numerals (I-VI) label neocortical layers.

	Gene	Expression	Developmental Stage	Published Function in CPN/progenitors	References
CPN Progenitors	*Ap2γ*	VZ progenitors	embryonic	regulates basal progenitor fate, and formation of layer II/III CPN in the occipital cortex	(Pinto et al., 2009)
	Brn1	SVZ IPCs and migrating neuroblasts	embryonic	together with *Brn2*, regulates generation and migration of layers II-IV	(McEvilly et al., 2002; Sugitani et al., 2002)
	Brn2	SVZ IPCs and migrating neuroblasts	embryonic	together with *Brn1*, regulates generation and migration of layers II-IV	(McEvilly et al., 2002; Sugitani et al., 2002)
	Cux1	mitotic SVZ IPCs	embryonic	unknown	(Nieto et al., 2004)
	Cux2	mitotic SVZ IPCs	embryonic	regulates SVZ progenitor proliferation and generation of superficial layers	(Nieto et al., 2004; Zimmer et al., 2004; Cubelos et al., 2007)
	Lhx2	VZ and SVZ progenitors	embryonic	regulates cortical hem formation	(Bulchand et al., 2001; Bulchand et al., 2003)
	Svet1	SVZ IPCs	embryonic	unknown	(Tarabykin et al., 2001)
	Tbr2	SVZ IPCs	embryonic	regulates IPC specification, and expansion of all cortical layers.	(Englund et al., 2005; Sessa et al., 2008; Chou et al., 2009)
	Tlx	VZ and SVZ progenitors	embryonic	Regulates generation of layers II/III and size of corpus callosum	(Land and Monaghan, 2003; Roy et al., 2004)
	Unc5d	SVZ IPCs	embryonic	unknown	(Zhong et al., 2004)
Post-mitotic CPN	*Brn1*	layers II/III and IV	maintained through early postnatal development	unknown	(McEvilly et al., 2002; Sugitani et al., 2002)
	Brn2	layers II/III and IV	maintained through early postnatal development	unknown	(McEvilly et al., 2002; Sugitani et al., 2002)
	Btg1	CPN in layers II/III	high at E18, decreasing postnatally	unknown	(Molyneaux et al., 2009)

Table 1.1 (Continued)

	Cav1	CPN in deep sublamina of II/III, and Va	high at P3, and decreased by P14	unknown	(Molyneaux et al., 2009)
	Chn2	CPN in deep sublamina of II/III	high at P6, with expression maintained at P14	unknown	(Molyneaux et al., 2009)
	Cited2	CPN in layers II/III, V, and VI	high at E18, decreasing postnatally	unknown	(Molyneaux et al., 2009)
	Cux1	layers II/III and IV	from embryonic development through adulthood	regulates dendritic branching, and synapse formation of layer II/III CPN	(Nieto et al., 2004; Cubelos et al., 2010)
	Cux2	layers II/III and IV	from embryonic development through adulthood	regulates dendritic branching, and synapse formation of layer II/III CPN	(Nieto et al., 2004; Zimmer et al., 2004; Cubelos et al., 2010)
	Dkk3	CPN in layer VI	increasing expression postnatally	unknown	(Molyneaux et al., 2009)
	Dtx4	cortical plate and superficial sublamina of II/II, layer IV	early post-mitotic until early postnatal (decreased by P14)	unknown	(Zhong et al., 2004)
	EphA3	CPN in superficial sublamina of II/III	high at E18, decreasing postnatally	unknown	(Molyneaux et al., 2009)
	Frmd4b	CPN in superficial sublamina of II/III	high at E18, decreasing postnatally	unknown	(Molyneaux et al., 2009)
	Gfra2	CPN in Layers V and VI	increasing expression postnatally	unknown	(Molyneaux et al., 2009)
	Gpr6	layers II/III, highest occipital	expressed from P3-P15, with highest expression at P6.	unknown	(Chenn et al., 2001)
	Hspb3	CPN in layers II/III, V, and VI	high at P3, with expression maintained at P14	unknown	(Molyneaux et al., 2009)
	Inhba	CPN in layers II/III	high at P3, and decreased by P14	unknown	(Molyneaux et al., 2009)

Table 1.1 (Continued)

	Kitl	layers II/III, IV, and early VI	early post-mitotic until early postnatal (decreased by P14)	unknown	(Zhong et al., 2004)
	Limch1	CPN in layers II/III	high at E18, decreasing postnatally	unknown	(Molyneaux et al., 2009)
	Lhx2	layers II-IV	high embryonic and early postnatal expression, decreasing by adulthood	necessary to specify neocortex	(Bulchand et al., 2003; Chou et al., 2009)
	Lmo4	CPN in layers II/III and V	Increases in CPN throughout postnatal development, with hightest expression medially	regulates area identities and connectivity of somatosensory cortex	(Arlotta et al., 2005; Kashani et al., 2006; Azim et al., 2009b; Huang et al., 2009)
	Lpl	CPN in layers II/III, V, and VI	high at P3, and decreased by P14	unknown	(Molyneaux et al., 2009)
	Mdga1	preplate, IZ, and cortical plate. Layers II/III, and layers IV and VIa in S1	high preplate expression at E13.5 and high cortical expression by P7	controls correct migration of layer II/III neurons	(Takeuchi and O'Leary, 2006)
	Mef2c	cortical plate and layers II/III, IV	early post-mitotic until early postnatal (decreased by P14)	critical for differentiation of neocortical neurons	(Zhong et al., 2004; Vlamings et al., 2008)
	Mena	layers II/III, and V	from embryonic development through adulthood	plays a role in actin cytoskeletal dynamics, and is necessary for formation of the corpus callosum	(Lanier et al., 1999)
	miR-189	layers II-IV	high broad neocortical expression at P9 becoming restricted to layers II-IV by P14	binds to *Slitrk1*, whose overexpression increases dendrite length	(Abelson et al., 2005)
	Nectin-3	CPN in the middle sublamina of II/III	high at P6, and decreased by P14	unknown	(Molyneaux et al., 2009)

Table 1.1 (Continued)

	Nnmt	CPN in the superficial sublamina of II/III	high at P3 and P6, and decreased by P14	unknown	(Molyneaux et al., 2009)
	PlexinD1	CPN in Va, and the superficial sublamina of II/III	high at P3, with expression maintained at P14	unknown	(Molyneaux et al., 2009)
	Ptn	CPN in deep sublamina of II/III	high E18-P6, and decreased by P14	unknown	(Molyneaux et al., 2009)
	Satb2	layers II-IV, V, and VI	early post-mitotic until early postnatal (decreased by P7)	represses *Ctip2* to regulate CPN identity and axonal midline crossing	(Britanova et al., 2005; Alcamo et al., 2008; Britanova et al., 2008)
	Svet1	layers II-IV	maintained from progenitors into adulthood (not observed after P60)	unknown	(Tarabykin et al., 2001)
	Tcrβ	CPN in layers Vb and VI	increasing expression postnatally	unknown	(Molyneaux et al., 2009)
	Unc5d	cortical plate and layers II/III, IV	early post-mitotic until early postnatal (decreased by P14)	unknown	(Zhong et al., 2004)

Table 1.1 (Continued)

genes might be hypothesized to be molecular controls and/or functional hallmarks of these previously identified subpopulations, as well as of novel, as-of-yet unidentified subpopulations of CPN. Molecular controls expressed by all CPN are more likely to control top-level, unifying properties of CPN, such as midline crossing and avoidance of corticofugal fate and connectivity. Alternatively, these broadly expressed genes might have more restricted action due to combinatorial intersection with areally restricted binding partners and/or co-factors (such precedents exist with *Bhlhb5* (Joshi et al., 2008b), *Clim1* and *Lmo4* (Azim et al., 2009b), and AP2γ (Pinto et al., 2009)). Since superficial layers have undergone substantial evolutionary expansion in comparison to deep layers, as discussed in more detail below, genes with expression restricted to deep layers might reflect transcriptional changes that allowed CPN to arise from evolutionarily older corticofugal projection neuron populations (Molnár et al., 2006; Lai et al., 2008; Azim et al., 2009b). The deep layers also contain the overwhelming majority of CPN with dual-projecting axons (Wilson, 1987; Mitchell and Macklis, 2005), and, as such, genes expressed by subpopulations of deep layer CPN might identify and control development of these dual-projecting populations. In contrast, genes restricted to superficial layer CPN might serve as controls over development of columnar collaterals, or subpopulations of CPN that evolved later and are born later in cortical development than deep layer CPN. Additionally, different combinations of these genes identify even more sublaminae than are observed by examining single genes in isolation. Thus, it is evident that there is striking molecular, and likely hodological and functional, diversity within the broad population of CPN. Investigation of functions of these combinatorial molecular controls will allow for better characterization and understanding of functions and clinical relevance of each of these and other unique subpopulations of CPN.

Evolution

CPN and their associated axonal pathway in the corpus callosum arose relatively recently in evolution; observed first in placental mammals(Aboitiz and Montiel, 2003). The corpus callosum is not unique in its ability to connect the two neocortical hemispheres, but is the only fiber tract devoted solely to integration of information from the two cortical hemispheres. In non-placental mammals, such as marsupials, the dominant interhemispheric fiber tract in the brain is the much smaller anterior commissure (AC), consisting of interhemispheric fibers from the amygdala, olfactory tract, and temporal lobes, as well as long-distance connections from the neocortex that take a convoluted route to project to the contralateral neocortex(Aboitiz and Montiel, 2003). The hippocampal commissure also plays a role, albeit much smaller than the anterior commissure, in enabling interhemispheric communication in animals lacking a corpus callosum (Aboitiz and Montiel, 2003; Mihrshahi, 2006). Pre-existence of these other commissural tracts might have more readily allowed for evolution and establishment of cortical commissural projection neurons that became CPN. For example, hippocampal commissure axons, in addition to cingulate axons, might pioneer the path that neocortical CPN later follow across the corpus callosum, suggesting that these hippocampal commissural neurons might have fasciculated with emerging early CPN to enable their crossing of the midline barrier to first project across the region that is now the corpus callosum (Rash and Richards, 2001; Mihrshahi, 2006; Donahoo and Richards, 2009).

The broad laminar distribution of CPN speaks not only to a broad time window of CPN generation during development from diverse progenitor populations, but also suggests preferential evolutionary expansion of this neuronal population as the cortex expanded throughout evolution. The telencephalon of sauropsids (e.g. reptiles and birds) is a three-layered structure that is evolutionarily related to layers I, V, and VI in the mammalian neocortex, but is devoid of CPN (Molnár et al., 2006; Charvet et al., 2009). The evolutionarily novel cortical layers II/III, which are present in rodents, are greatly expanded in primates (Smart et al., 2002a; Molnár et al., 2006) (Figure 1.8), as is the volume of white matter in the corpus callosum(Schoenemann et al., 2005), with over 190 million axons in the human (Tomasch, 1954). These mammalian neocortical superficial layers arise primarily from progenitors of the SVZ (Tarabykin et al., 2001), which is a distinct progenitor zone present in mammals and some sauropsids (including birds and crocodilians, but not turtles), but not in amphibians(Charvet et al., 2009). The SVZ itself has greatly expanded and diversified in primates to include two distinct regions, the inner and the outer SVZ, which generate the expanded cortical diversity, particularly in superficial layers, found in primates(Smart et al., 2002a; Fietz et al., 2010; Hansen et al., 2010) (Figure 1.8). The outer SVZ contains unique self-renewing, proliferative, radial glia-like progenitors that are distinct from those in the inner SVZ(Fietz et al., 2010; Hansen et al.). A number of molecular controls over SVZ populations have been identified as discussed above, including *T-box brain gene* 2 (*Tbr2, also known as Eomes)*(Baala et al., 2007; Arnold et al., 2008; Sessa et al., 2008), and *subventricular-expressed transcript 1* (*Svet1)*(Tarabykin et al., 2001). Given that the majority of CPN reside in the evolutionarily expanded superficial layers generated from this progressively expanded population of intermediate progenitors, it is logical to hypothesize that CPN have undergone extensive expansion throughout evolution of the cerebral cortex. Thus, compared to deep layer-restricted CFuPN, CPN might be predicted to serve especially important roles in primate cognitive function.

Expansion of superficial neocortical layers in primate evolution far exceeds expansion of deep layers (Molnár et al., 2006). A large portion of CPN with known heterotopic long-range dual-projecting axons reside in deep neocortical layers, suggesting that deep layer CPN might have been evolutionarily co-opted from existing populations of CFuPN to project not only to subcortical targets, but also across the midline to connect and integrate the two hemispheres of the neocortex. Once the early, deep population(s) of CPN were established, their presence might have favored expansion of the neocortex, and addition of more subtypes of CPN to augment the functionally advantageous rapid and precise integration of neocortical hemispheres, perhaps first in primary visual cortex(Aboitiz and Montiel, 2003) or newly evolving motor cortex(Mihrshahi, 2006). Interestingly, there is a large group of CPN-enriched genes expressed in sublaminae within superficial neocortical layers in mouse(Molyneaux et al., 2009) (Figure 1.9). In the mouse, neocortical layers II and III are not typically distinguished as distinct, but they are expanded and obviously distinct in primates. While developmental expression of these sublaminar CPN genes in primate cortex is not currently known, some (e.g. *Cux2, Nectin-3,* and *Plxnd1)* display similar expression in adult human cortex as in mouse cortex (Arion et al., 2007; Allen-Institute-for-Brain-Science, ©2009b). It is interesting to speculate that sublaminarly-distributed genes

Figure 1.8: Comparison of developing and adult mammalian neocortex of mouse, macaque, and human shows correlations between SVZ expansion, superficial neocortical layer expansion, and white matter expansion.

Schematic comparison of histological sections of (**A**) developing and adult mouse, (**B**) developing and adult rhesus macaque monkey, and (**C**) adult human neocortex. Adult cross-sections are from visual cortex. The thicknesses are represented relative to a common scale. Callosal projection neurons (red) reside mostly in layers II/III (~80%), V (~20%), and VI (few %) in the adult neocotex. There is a strong correlation between the expansion of the SVZ and the expansion of the superficial layer thickness and neocortical white matter. Abbreviations: E, embryonic; PP, preplate; VZ, ventricular zone; MZ, marginal zone; CP, cortical plate; SP, subplate; SVZ, subventricular zone; OSVZ, outer SVZ; ISVZ, inner SVZ; OFL, outer fibrous layer; IFL, inner fibrous layer; WM, white matter; Roman numerals denote neocortical layers (I-VI). Adapted and expanded with permission from (Smart et al., 2002a) (macaque) with data from (Allen-Institute-for-Brain-Science, ©2009a) (mouse), and (Schoenemann et al., 2005; Allen-Institute-for-Brain-Science, ©2009b) (human).

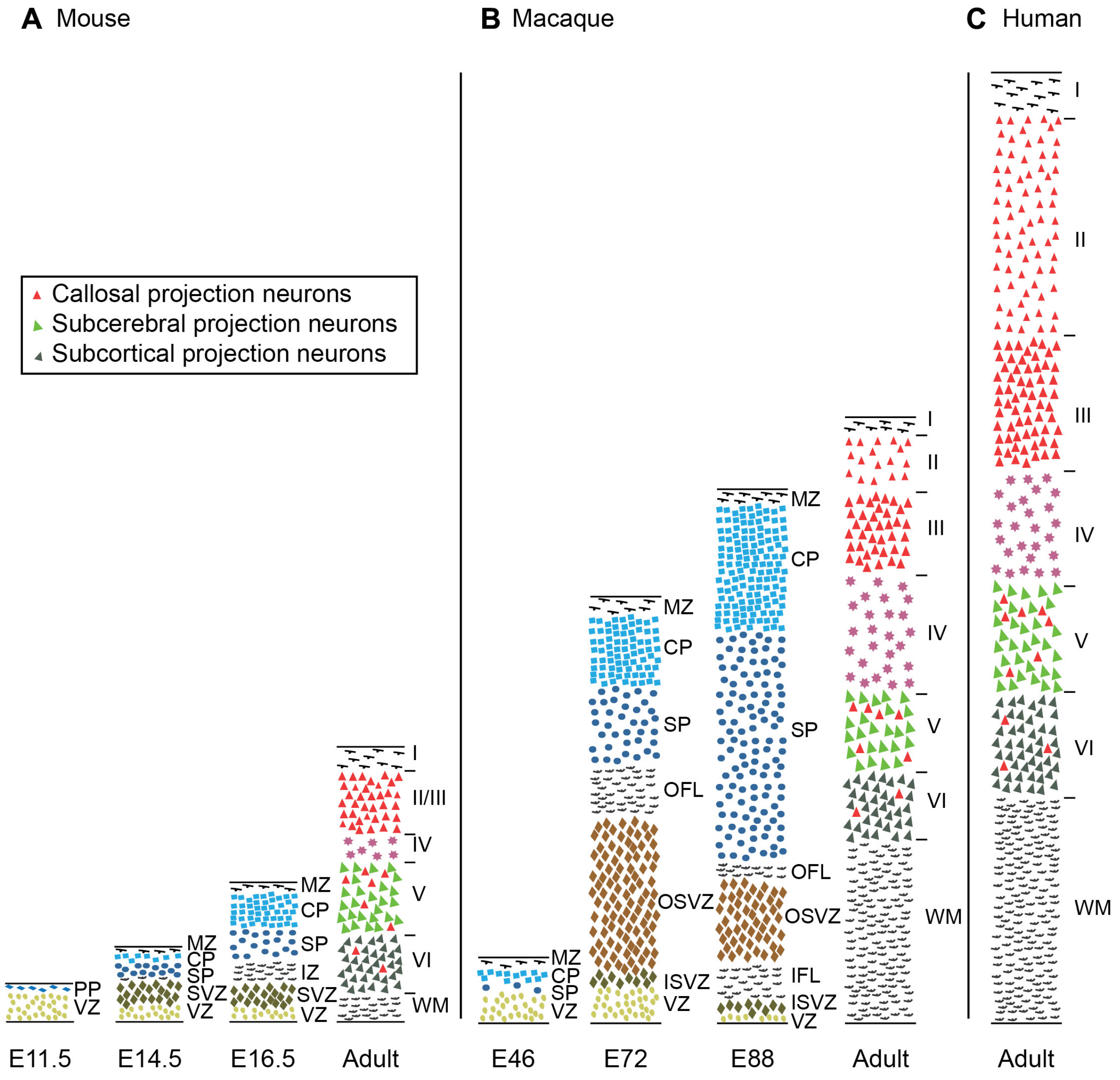

Figure 1.8 (Continued)

Figure 1.9 : Evolutionary expansion of callosal projection neuron populations

(**A**) Schematic comparison of histological sections of adult sauropsid (in particular, turtle, reptile) cortex, and mouse, monkey, and human neocortex (visual cortex), with thicknesses represented relative to a common scale. Sauropsids have a three-layered cortex, with no callosal projection neurons (CPN). In mammals, CPN (red) reside in layers II/III, V, and VI. The majority (~80%) of CPN reside in the superficial layers II/III, where they are the predominant projection neuron population. Approximately 20% (in mouse) of CPN reside in layer V, co-mingled with subcerebral projection neurons (green), with a small population of CPN found among the corticothalamic neurons (grey) in layer VI. There is a dramatic expansion of the layer II/III CPN population between mouse and primates (with layers II and III becoming distinct lamina), while the overall thickness of layers V and VI remains relatively constant. Adapted and expanded from (Smart et al., 2002a) (Macaque), with data from (Allen-Institute-for-Brain-Science, ©2009a) (mouse), and (Schoenemann et al., 2005) and (Allen-Institute-for-Brain-Science, ©2009b) (human). (**B**) Schematic of genes expressed specifically by CPN in early postnatal mouse neocortex layers, depicting the substantial molecular heterogeneity of CPN subpopulations. Some genes are expressed only in CPN of layers V and VI (potentially evolutionarily older CPN derived from CFuPN), others are expressed by CPN of all layers, while others distinguish between CPN of the superficial layers II/III and the deep layers V and VI. Interestingly, other CPN genes finely subdivide the canonical cortical layers, revealing new sublayers. For example, *Frmd4b*, *Nnmt*, and *Epha3* are expressed in superficial layer II/III, while *Nectin-3*, *Chn2*, and *Ptn* are expressed in deep layer II/III, perhaps reflecting a molecular subdivision of layers II and III in the mouse, serving as evolutionarily early molecular identifiers of the further expansion and specialization of superficial layers in primates.

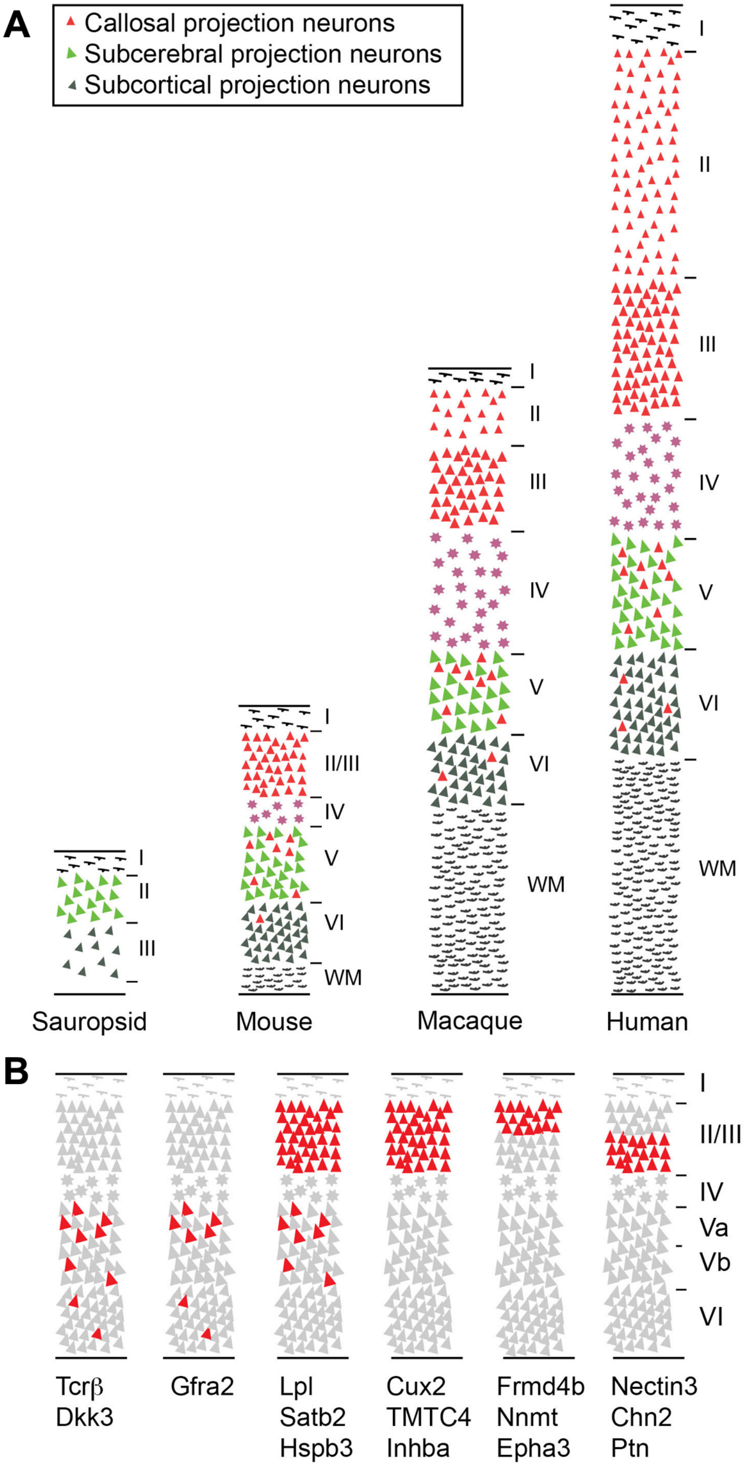

Figure 1.9 (Continued)

might serve as evolutionarily early molecular identifiers of the further expansion and specialization of superficial layers in primates.

Recent evidence supports a growing understanding and new appreciation of the striking diversity within the broad population of CPN. CPN as a population are defined by their homotopically projecting axons across the corpus callosum, but, as mentioned above, some subpopulations of CPN have dual-projecting axons to long distance ipsilateral and contralateral targets, while other subpopulations participate in local column circuitry, both ipsilaterally and contralaterally. The progressive evolutionary emergence of complexity and increased diversity of connectivity in the cerebral cortex also suggests diversity in the origin of CPN. Deep-layer CPN might have arisen from evolutionarily older CFuPN(Lai et al., 2008; Azim et al., 2009b), while superficial-layer CPN expanded greatly with the expansion of the SVZ in the progression from lower mammals to primates and humans.

Currently, molecular controls over CPN as a broad population, as well as over specific subpopulations of CPN, are being discovered and functionally investigated. This work elucidating the connectivity, guidance, and molecular characteristics of CPN, both as a broad population, and as distinct hodological and functional subpopulations of CPN, will greatly contribute to the understanding of CPN and complex associative functions in which they play critical roles. More in-depth understanding of distinct, critical functions of specific CPN subpopulations will enable more sophisticated understanding of cortical function, and insight into neurological abnormalities involving CPN and the corpus callosum, including agenesis of the corpus callosum, autism spectrum disorders, and likely other syndromes of high-level dysfunction of associative connectivity.

1.4 b. Molecular Controls Over Subcerebral Projection Neuron Specification and Differentiation

Among the different types of cortical projection neurons, subcerebral projection neurons have been a good model population for studying subtype specification in the neocortex. They are a readily identifiable, prototypical projection neuron population, located within layer Vb of the neocortex (Figure 1.4). They are defined by axons that project caudal to the cerebrum to targets in spinal cord or brainstem, including tectum, red nucleus, and pons(Wise and Jones, 1977; Killackey et al., 1989; Legg et al., 1989; O'Leary and Koester, 1993; Arlotta et al., 2005; Molnár et al., 2006). All subcerebral projection neurons extend a primary axon through the internal capsule, cerebral peduncle, and pyramidal tract toward the spinal cord. Inappropriate connections are later eliminated, such that subcerebral projection neurons in sensorimotor cortex project to caudal pons and spinal cord, while those in visual cortex maintain projections to rostral pons and superior colliculus (O'Leary and Terashima, 1988; Schreyer and Jones, 1988; O'Leary and Koester, 1993). Given this common pattern of initial development, many of the molecular controls regulating early specification and differentiation are likely to be shared among different subtypes of subcerebral projection neurons (Arlotta et al., 2005; Molyneaux et al., 2007; Joshi et al., 2008b).

The most well studied subtype of subcerebral projection neuron is corticospinal motor neurons (CSMN), a developmentally and clinically important population. CSMN are of great interest since they control precise voluntary movement in humans, they degenerate in motor neuron degenerative diseases including amyotrophic lateral sclerosis (ALS), and their injury contributes centrally to the loss of motor function following spinal cord injury. The precise point in development at which CSMN begin to differ molecularly from other subcerebral projection neurons, and mechanisms that initiate this difference, have only recently begun to be elucidated (e.g. (Arlotta et al., 2005; Joshi et al., 2008b)). Recently, identification of a large number of subcerebral and CSMN specific genes has enabled an expanding effort to decipher programs controlling CSMN development (Molyneaux et al., 2007). The expression patterns of these genes indicate that fate specification and differentiation of subcerebral projection neurons in general, and CSMN in particular, is directed by a combinatorial integration of transcription factors and other molecular controls. These molecular controls are expressed in patterns that together uniquely identify CSMN. For example, a small number of CSMN genes appear restricted to sensorimotor cortex (e.g. *Diap3*, *Igfbp4*, and *Crim1*), distinguishing CSMN from other subcerebral projection neurons of layer V (Arlotta et al., 2005). Other genes are expressed by subcerebral projection neurons across the full extent of layer V (e.g. *Ctip2, Encephalopsin*, *Fezf2*, *Clim1*, *Pcp4*, and *S100a10*), indicating restriction to all or most subcerebral projection neurons (Arlotta et al., 2005). Thus far, functions of only a minority of these genes have been reported, but these studies are already revealing key roles for these genes in subcerebral specification and differentiation (Weimann et al., 1999; Arlotta et al., 2005; Chen et al., 2005a; Chen et al., 2005b; Molyneaux et al., 2005; Ozdinler and Macklis, 2006; Molyneaux et al., 2007; Chen et al., 2008a; Joshi et al., 2008b; Lai et al., 2008; Azim et al., 2009b; Tomassy et al., 2010).

Fezf2, a transcription factor expressed by all subcerebral projection neurons from early stages of development through adulthood (Inoue et al., 2004; Arlotta et al., 2005), is required for specification of all subcerebral projection neurons (Chen et al., 2005a; Chen et al., 2005b; Molyneaux et al., 2005). In the absence of *Fezf2* function in null mutant mice, the entire population of subcerebral projection neurons is absent, and there are no projections from the cerebral cortex to either spinal cord or brainstem (Chen et al., 2005a; Molyneaux et al., 2005). Importantly, without *Fezf2*, neocortical progenitors still produce similar numbers of layer V neurons (Chen et al., 2005b; Molyneaux et al., 2005); however, lineage tracing of the normally *Fezf2* positive neurons and axons using a *Fezf2* mutant with a human placental alkaline phosphatase (hPLAP) insertion at the *Fezf2* locus demonstrates that these neurons adopt CPN-like properties, including axonal extension across the midline via the anterior commissure, and expression of the CPN-specific molecular marker *Satb2* (Chen et al., 2008a), a critical transcriptional regulator of CPN identity (Alcamo et al., 2008; Britanova et al., 2008). In contrast, superficial layer pyramidal neurons are born correctly and appear normal (Chen et al., 2005a; Molyneaux et al., 2005). Thus, *Fezf2* does not affect ability of progenitors to generate glutamatergic neurons that position themselves in layer V; it likely acts to direct the next step in the program of specification, defining characteristics of a subcerebral projection neuron. As additional support for *Fezf2* in directing subcerebral projection neuron specification, over-expression of *Fezf2* is sufficient to induce birth of entirely new deep layer projection neurons that express *Ctip2* and *Tbr1,* and extend axons through the internal capsule (Chen et al., 2005b; Molyneaux et al., 2005). Interestingly, layer VI neurons and subplate neurons, which express *Fezf2* at lower levels than subcerebral projection neurons, exhibit disorganization and abnormalities in gene expression in *Fezf2* null mutant mice, but are much less seriously affected (Hirata et al., 2004; Chen et al., 2005a; Molyneaux et al., 2005), suggesting that the level of *Fezf2* protein is directly linked to its function, and it exerts different functions in distinct neuronal populations in a dose-dependent manner.

A second set of molecular controls has been identified that control later aspects of subcerebral projection neuron development, including axon fasciculation and extension to the spinal cord. One important member of this set is *Ctip2,* which likely acts downstream of *Fezf2,* as *Ctip2* is not expressed in *Fezf2* null mutant mice (Molyneaux et al., 2005; Chen et al., 2008a). In the absence of *Ctip2*, subcerebral projection neuron axons exhibit defects in fasciculation, outgrowth, and pathfinding, with most axons misrouted in the forebrain, and only very few axons even reaching the brainstem; none reach the spinal cord (Arlotta et al., 2005). In addition, reduced *Ctip2* expression in *Ctip2* heterozygous mice results in a defect in pruning of transient projections to the spinal cord from subcerebral projection neurons residing in somatosensory cortex, further demonstrating different functions for these transcription factors at different levels of expression (Arlotta et al., 2005). Interestingly, *Ctip2* also controls proper differentiation of striatal medium spiny neurons (MSN), including their patch-matrix organization through which CSMN axons traverse, and the expression by MSN of a set of axon and migrational guidance and repulsive signals; these results implicate *Ctip2* as potentially having additional non cell-autonomous function in CSMN axon growth and fasciculation (Arlotta et al., 2008; Woodworth and Macklis, 2009). These experiments identified *Ctip2* as a critical regulator of subcerebral axon extension and refinement of collaterals as these neurons mature.

Another central transcriptional regulator known to function in target choice of subcerebral projection neurons is *Otx1*. This protein is expressed by putative deep layer progenitors in the VZ, exhibiting decreasing levels of expression in the VZ during generation of superficial layer neurons (Weimann et al., 1999; Inoue et al., 2004). As deep layer projection neurons mature, localization of OTX1 shifts from cytoplasm to nucleus, indicating a fine regulation of the activity of this protein (Frantz et al., 1994b; Weimann et al., 1999). Postnatally within layer V, *Otx1* is expressed by 40-50%

of subcerebral projection neurons, primarily those within visual cortex, while it is not expressed by callosal projection neurons (Weimann et al., 1999). Mice lacking the gene for *Otx1* have defects in development of corticotectal projection neurons. Without *Otx1*, corticotectal projection neurons maintain an axon to the spinal cord and caudal pontine nuclei, collaterals that are only appropriate for CSMN and are normally eliminated by corticotectal projection neurons (Weimann et al., 1999). These results indicate that *Otx1* might function later in subcerebral projection neuron development than *Fezf2* and *Ctip2,* controlling refinement and pruning of axonal collaterals. Additional axon outgrowth and guidance molecules, such as IGF-I and RYK, have been described to function in extension and guidance of subcerebral projection neuron axons to targets in the brainstem and spinal cord (Liu et al., 2005; Harel and Strittmatter, 2006; Ozdinler and Macklis, 2006).

Sox5 controls another critical element in proper differentiation of CSMN and all other corticofugal projection neuron subtypes: post-mitotic regulation of their sequential generation from subplate neurons (earliest born corticofugal projection neurons), through corticothalamic neurons to corticospinal motor neurons and corticostriatal projection neurons. *Sox5* controls this sequential generation of corticofugal projection neuron subtypes by progressively reducing its repression (via Sox5 down-regulation) of genes required for differentiation of later generated subtypes, ultimately CSMN, preventing premature emergence of normally later-born neurons during early stages of corticogenesis (Lai et al., 2008). *Sox5* loss-of-function causes striking overlap of the identities of the three principal sequentially born corticofugal neuron subtypes (subplate, corticothalamic, corticospinal); in the *Sox5* null cortex, subplate neurons aberrantly develop molecular hallmarks and connectivity of subcerebral projection neurons, CThPN are imprecisely differentiated, while differentiation of subcerebral projection neurons is accelerated (Lai et al., 2008). *Sox5* over-expression at late stages of corticogenesis causes re-emergence of neurons with corticofugal features, reinforcing the critical role of *Sox5* in controlling the sequential generation of corticofugal neurons. Thus, *Sox5* functions in immature post-mitotic neurons to control coordinate regulation of subtype-specific genes, and timing of critical fate decisions in different subtypes of corticofugal projection neurons, thereby enabling these closely related neuronal populations to differentiate into distinct neuronal subtypes.

Studies of motor neuron development in *Drosophila melanogaster* provide insight into how cortical progenitors might progressively generate distinct classes of pyramidal neurons over time (e.g. corticofugal projection neurons as a class, with multiple subtypes determined postmitotically). In this system, progenitors express a sequential series of transcription factors during neurogenesis, including *hunchback*, *krüppel, pdm1*, and *castor,* followed by maintained expression of these same transcription factors in post-mitotic progeny that were born during the window of expression of each gene by the progenitors (Isshiki et al., 2001). Similarly, it is conceivable that, in mammalian neocortex, radial glia progenitors might express a sequential series of transcription factors that are maintained in intermediate progenitors and post-mitotic neurons, imparting class identity. Thus, during generation of corticofugal projection neurons from *Sox6+/Fezf2+* progenitors, genes such as *Otx1, Ctip2, Sox5, Clim1/Lmo4, Bhlhb5* might act on partially specified progenitors to determine further aspects of laminar and projection identity as individual subtypes of corticofugal and other pyramidal neurons are generated (Figure 1.10). *Fezf2,* with these other regulators, specifies the precise subcerebral projection neuron lineage within a layer (e.g. layer V), enabling development of the molecular, morphological, and anatomical projection properties of subcerebral projection neurons and other subtypes. Later, once this cascade is initiated, the regulated and level-dependent expression of genes such as *Ctip2* and *Otx1*, which govern subcerebral axonal outgrowth, fasciculation, pruning, and, ultimately, connectivity, function to establish precise connectivity and later morphological features of subcerebral and other projection neurons. The direct relationships between these transcriptional regulators and the many not-yet-functionally characterized genes that act in cascades of subcerebral and other projection neuron development remains to be determined. Together, the transcriptional regulators above comprise first elements of the molecular program that controls subcerebral projection neuron development modeled and described anatomically almost two decades ago by O’Leary and colleagues (O'Leary and Koester, 1993).

Figure 1.10: Molecular controls over layer V cortical projection neuron subtype development

The sequential actions of a combinatorial set of molecular controls regulate the generation of distinct layer V subcerebral projection neuron (SCPN) and callosal projection neuron (CPN) subtypes. As layer V projection neurons are generated from the VZ, *Pax6*, *Ngn2*, and *Sox6* maintains the dorsal identity of pallial progenitors. *Fezf2* is expressed by a subpopulation of VZ progenitors and in postmitotic subcerebral PN, specifying subcerebral PN fate over CPN fate. Simultaneously, *Sox5* acts postmitotically to regulate the sequential acquisition of distinct corticofugal projection neurons subtype fates. Downstream of *Fezf2*, *Ctip2* postmitotically controls SCPN differentiation, regulating axonal extension and fasciculation, potentially in coordination with *Otx1*. *Bhlhb5* functions postmitotically in acquisition of the caudal motor areal identity of CSMN, as well as the areal identity of neurons in somatosensory cortex. In neighboring CPN, *Satb2* postmitotically controls CPN differentiation over subcerebral PN fate, at least in part by directly repressing *Ctip2* expression. Yellow neurons at E15.5 represent the gradual refinement of molecular identity between SCPN and CPN during postmitotic differentiation. VZ, ventricular zone; CP, cortical plate. The outline on the whole brain inset on the top right illustrates the cortical region described in the figure. Figure adapted from (Azim, 2009, Dissertation).

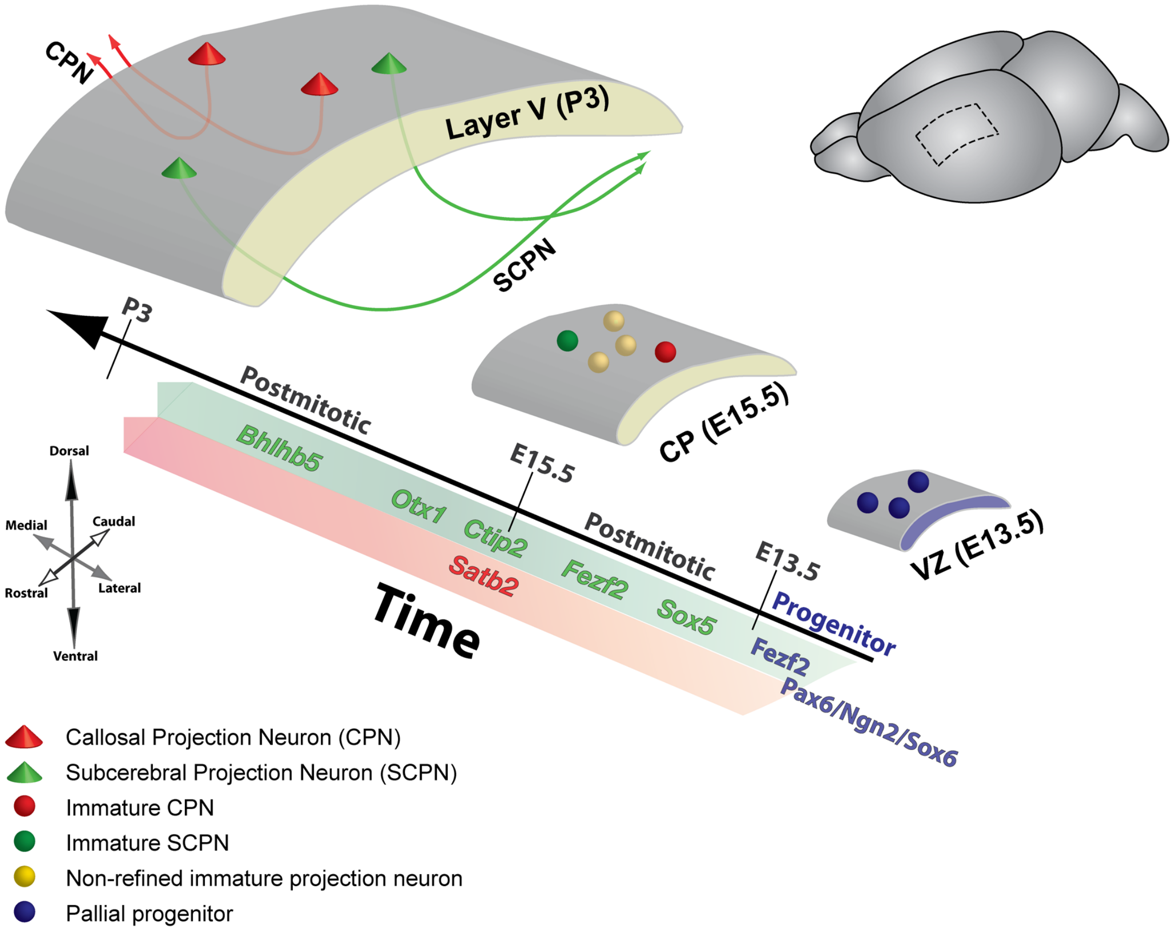

Figure 1.10 (Continued)

1.5 Areal Diversity of Neocortical Projection Neurons

The complexity of neocortical circuitry is further magnified by neuronal diversity across areas along tangential axes of the neocortex. Each area is characterized by distinct cytoarchitecture, connectivity, gene expression, and laminar composition and, as such, imparts a unique functional capacity to the neocortex. The neocortex has four primary areas (three sensory and one motor): somatosensory cortex (S1), which processes sensory information from the body; visual cortex (V1), which processes visual information relayed from the retina; auditory cortex (A1), which receives input from the ears; and primary motor cortex (M1), which controls voluntary movement (Figure 1.11). Each area is innervated by thalamocortical afferents from distinct thalamic nuclei, which convey modality-specific sensory information from the periphery, a reciprocal area-specific/nucleus-specific relationship that is critical for both development of cortical areas, as well as their adult function (O'Leary and Nakagawa, 2002).

Arealization of the neocortex is controlled by the interplay of intrinsic and extrinsic factors, working in combination to regulate specification and development of neocortical areas.
During early stages, prior to innervation from thalamocortical afferents, area identity is broadly the tangential axes at later stages of area-specific neuronal differentiation.

Morphogens, such as fibroblast growth factors (FGFs) and Wnts secreted from the commissural plate, and bone morphogenic proteins (BMPs) secreted from the cortical hem, initiate graded transcription factor expression tangentially across the telencephalon, influencing identity and size of cortical areas (Rash and Grove, 2006). *Emx2* displays low rostro-lateral to high caudo-medial expression, and *Pax6* shows a complementary high rostro-lateral to low caudo-medial expression profile. These opposing gradients influence downstream molecular patterning that confers areal identity to regions of neuroepithelium, regulating subsequent establishment of projections, and, therefore, function of cortical areas (Bishop et al., 2000; Mallamaci et al., 2000; Rash and Grove, 2006). Similarly, a high caudal to low rostral gradient of *Coup-TF1* expression is important for establishing the proper balance between caudal and rostral cortical areas (Armentano et al., 2007). The zinc-finger transcription factor *Sp8* is expressed in a high rostro-medial to low caudo-lateral gradient, and has been shown to specify rostral motor identity, at least partially via direct activation of *Fgf8* (Sahara et al., 2007; Zembrzycki et al., 2007). Additional, or complementary, arealization might be conferred by caudo-rostral gradients of *Lhx2* and *Emx1* expression, a rostro-caudal gradient of *Tbr1* expression (Donoghue and Rakic, 1999b; Bishop et al., 2002), and spatially restricted compartmental expression of *Dlx1*, *Dlx2*, and *Gbx2* (Bulchand et al., 2003).

As development progresses, these broad gradients are refined to sharp boundaries of gene expression, which parallel sharpening of anatomical and cytoarchitectonic boundaries of primary sensory areas. Mechanisms by which these broad gradients are converted to sharp boundaries of expression in the cortex are still largely unknown. Attempts to identify genes with restricted expression in clearly defined 'protoareas' of the VZ have been unsuccessful, instead finding only genes with graded regional expression in proliferative layers of the developing neocortex (Sansom et al., 2005). As such, area identities are likely controlled by complex programs of overlapping spatial and temporal molecular controls (Rash and Grove, 2006; Joshi et al., 2008b; Tomassy et al., 2010). Studies in *Drosophila* have demonstrated that sharp borders of expression can be established by combinatorial action of multiple broadly-expressed transcriptional regulators, even generating, in the case of the pair-rule gene *even-skipped* (*Eve*), a discrete stripe pattern (Stanojevic et al., 1991). Similar pathways have been identified in developing spinal cord, where graded, partially overlapping expression of multiple transcription factors, induced by a morphogen gradient of secreted Sonic hedgehog (SHH) from the notocord and floor plate, gradually refines into sharp boundaries of transcription factor expression in VZ progenitors, which in turn specifies discrete lineages of progenitors of motorneurons and interneurons (Jessell, 2000).

Such mechanisms are beginning to come to light in the neocortex with the identification of molecular controls that regulate specification and development of distinct subtypes of projection neurons in both a laminar and area-specific manner. For example, although the transcription factor AP2γ (also known as Tcfap2c) is expressed by a subset of apical ventricular zone progenitors

Figure 1.11: Functional and molecularly defined neocortical areas
(A) Functional and molecularly defined cortical areas

The neocortex has four primary areas (three sensory and one motor): the somatosensory cortex (S1, blue), which processes sensory information from the body; the visual cortex (V1, yellow), which processes visual information relayed from the retina; the auditory cortex (A1, green), which receives input from the ears; and the primary motor cortex (M1, red) which controls voluntary movement. Many molecular controls act early in progenitors to define these areas, while others act postmitotically to refine cortical areas. Two examples of molecular controls that act in part postmitotically to refine precise neuronal differentiation and identity within cortical areas are *Coup-tf1* (grey) and *Bhlhb5* (pink). *Coup-tf1* is expressed in a high caudal to low rostral gradient throughout layers II-IV, and is highly expressed in layer IV in S1. *Bhlhb5* is expressed throughout layers II-V, high in S1 and V1.

(B) Molecular controls over area identity

Molecular controls determine refinement of areal identity and, subsequently, the identity of projection neurons. In the absence of *Coup-tf1* expression, for example, M1 (red) expands at the expense of the S1 area. Therefore, fated S1 CThPN "motorize" and extend axons to the spinal cord, while both rostral and caudal fated CSMN axons arrest at or before the pons. Areally disrupted caudal CSMN are most severely affected and do not even reach the pons. In the absence of *Bhlhb5,* in contrast, S1 is selectively disrupted. Fated CSMN on the boarder of M1 and S1 do not extend axons to the spinal cord, while rostral CSMN in less-affected central M1 maintain projections to the pyramidal decussation.

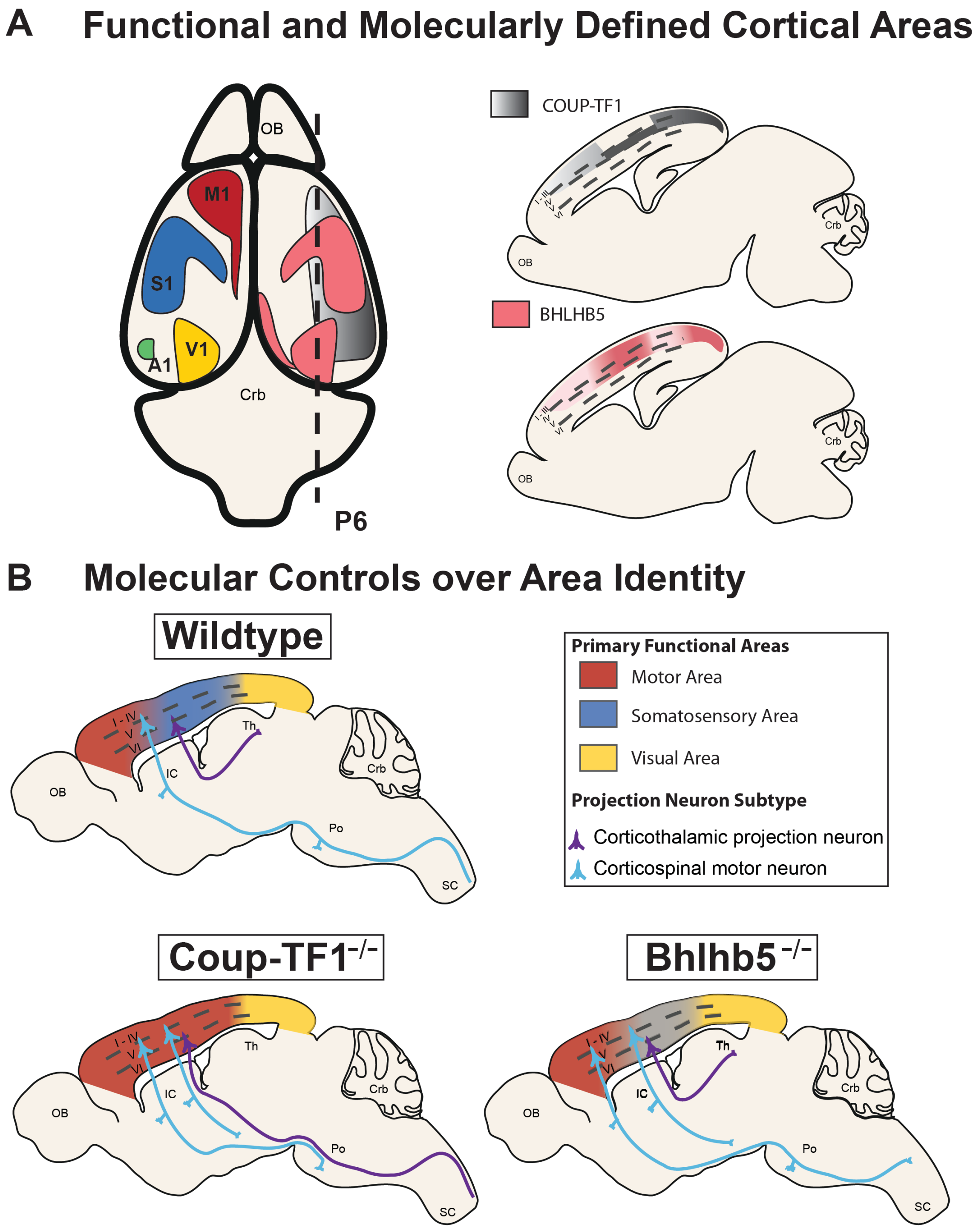

Figure 1.11 (Continued)

throughout the cortex at mid-neurogenesis, deletion of AP2γ leads to a specific reduction of superficial layer neurons in occipital (visual) cortex, resulting in impaired function of adult visual cortex (Pinto et al., 2009). AP2γ**,** acting in apical progenitors, directly regulates expression of basal progenitor fate determinants *Math3* and *Tbr2*, and loss of AP2γ results in a mis-specification of basal progenitors in occipital cortex at the time of superficial layer neuron generation. This leads to a significant reduction of CPN in layers II/III in occipital cortex, while leaving layer V CPN and more rostral layer II/III CPN unaltered. The area-restricted role of AP2γ is further emphasized by over-expression experiments, which demonstrate that AP2γ is sufficient to induce increased generation of superficial layer neurons in caudal, but not rostral, cortex. This may be due to interaction of AP2γ with *Pax6* and partial redundancy in regulation of basal cell determinants (Pinto et al., 2009). *Pax6* also directly regulates expression of *Tbr2* and *Math3*, in addition to regulating AP2γ itself. As such, *Pax6* might compensate for loss of AP2γ in rostral cortex, where *Pax6* expression is high, but would be unable to fully compensate for AP2γ in caudal regions, where its expression is low.

The transcription factor *CoupTF-I* also imparts area-specific temporal control over development of a specific projection neuron subtype, namely CSMN (Figure 1.11). In contrast to AP2γ, *CoupTF-I* is expressed in a gradient in the neocortex, with highest expression in progenitors and postmitotic neurons in parietal (presumptive sensory) and occipital areas of the neocortex, and lowest expression in frontal (presumptive motor) cortex (Zhou et al., 2001; Armentano et al., 2007). Forebrain-specific loss of function of *CoupTF-I* results in a marked expansion of motor areas, occupying most of the neocortex, concomitant with a compression of sensory areas to the caudal occipital cortex (Armentano et al., 2007). These shifts are accompanied by changes in molecular profiles and axonal projections of parietal cortical neurons to match their new modified motor identity: layer IV neurons in this region do not express *Rorβ*, an orphan nuclear receptor specifically expressed in primary sensory areas (Nakagawa and O'Leary, 2003), but express cadherin 8 (*cad8*), a cell adhesion molecule that demarcates rostral motor areas (Hamasaki et al., 2004); layer VI corticothalamic projection neurons express elevated levels of *Fezf2* typical of motor areas, and preferentially project to motor rather than sensory thalamic nuclei (Armentano et al., 2007). CSMN are also born prematurely in somatosensory cortex in the absence of *CoupTF-I*, thus expanding layer V at the expense of layer VI corticothalamic neurons (Tomassy et al., 2010). Axons of these aberrantly specified corticothalamic neurons project to subcerebral structures, including the spinal cord, while CSMN differentiate imprecisely and do not project beyond the pons. These results indicate that *CoupTF-I* plays a critical role in regulating area-specific temporal development of CSMN by repressing a 'motorizing' genetic program of differentiation in neurons of somatosensory cortex. That adult *CoupTF-I* conditional mutant mice display impaired fine motor skills further reinforces the necessity for precision in both areal and temporal control of projection neuron differentiation (Tomassy et al., 2010).

In addition to identifying molecular controls that function at the progenitor level to govern development of areal-specific projection neuron subtypes, there is growing knowledge of molecular controls that function post-mitotically to sharpen the boundaries between these areas. *Bhlhb5* is a class B helix-loop-helix TF (Brunelli et al., 2003) that is expressed by postmitotic projection neurons in layer II-V, and exhibits a dramatic refinement in expression from a high caudo-medial to low rostro-lateral gradient, similar to the *Emx2* expression gradient in VZ progenitors, which transforms into to a sharp border between motor and sensory cortex. *Bhlhb5* regulates postmitotic acquisition of identity in sensory and caudal motor neocortical projection neurons, where it is expressed in discrete domains (Figure 1.11). These areas are mis-specified in the absence of *Bhlhb5* function, without significantly affecting frontal motor identity, resulting in area-specific changes in molecular identity of projection neurons across layers II-V, as well as abnormal differentiation of CSMN located in caudal motor cortex (Joshi et al., 2008b). *Bhlhb5,* therefore, translates the graded transcription factor expression in progenitors and early postmitotic neurons to sharply delineated area-specific molecular and anatomical properties. It is likely that *Bhlhb5* acts in a combinatorial manner with other area and lamina restricted postmitotic transcription factors to control precise areal identity of projection neurons in a lamina and projection neuron subtype-specific manner.

One such postmitotic transcription factor might be *Tbr1*. *Tbr1* is expressed in an opposing gradient to *Bhlhb5* in embryonic cortical plate (high rostral), with a complementary laminar expression profile in later embryonic development (Bedogni et al.). In frontal cortex, *Tbr1* is highly expressed in all layers, while in more caudal regions, *Tbr1* is highly detected in layer VI, subplate, and Cajal-Retzius neurons, with much lower expression in layers II – V. In the absence of *Tbr1* function, there is a loss of rostral identity, and an expansion in caudal gene expression, including *Bhlhb5* (Bedogni et al.). Furthermore, there is an increase in subcerebral projection neurons (layer V) at the expense of earlier born corticothalamic projection neurons (layer VI), as determined by both projection pattern and gene expression profiles (including up-regulation of *Fezf2* and down-regulation of *Sox5*) (Bedogni et al.). Together, these findings further underscore the incredibly refined, progressive differentiation of neocortical projection neurons, not only along the radial axis, but also within a single layer in different tangential areas. These post-mitotic arealizing programs enable developing neurons to gradually acquire their mature identity, specialized to perform a specific sensory or motor function within the intricate neocortical circuitry.

1.6 Progressive Restriction and Refinement of Cortical Projection Neuron Subtypes

Progressive restriction of neuronal identity at multiple progressive levels of specification suggests that populations of dividing progenitors, transitioning progenitors, and early post-mitotic neurons have increasingly restricted plasticity. The initial subtype fate decisions early in the life of a neuron, and potential malleability of this fate when the balance of key signals is modified, reveals not only that a neuron is deterministically set on a general developmental path at its birth, but also that this program must be precisely executed during postmitotic differentiation (Figure 1.10). As an example, CPN and subcerebral projection neurons in layer V of the neocortex share aspects of molecular identity that are progressively resolved during differentiation. The LIM-HD-related genes *Lmo4* and *Clim1,* as well as the transcription factors *Ctip2* and *Satb2,* are initially expressed by both CPN and subcerebral projection neurons in layer V, and only during mid to late differentiation does expression of *Lmo4,* *Satb2, Clim1, and Ctip2* become largely segregated into these two distinct neuronal subtypes (Arlotta et al., 2005; Alcamo et al., 2008; Britanova et al., 2008; Azim et al., 2009b). This progressive postmitotic resolution of molecular identity reveals similarities and possible shared evolutionary origin between layer V CPN and subcerebral projection neurons, and provides insight into how and when these neuronal subtypes achieve their distinct identities during cortical development.

At many stages of neocortical projection neuron specification, manipulation of specific molecular controls can fully or partially fate-switch a progenitor, transitioning progenitor, or immature post-mitotic neuron, indicating even more cortical plasticity than previously detected through transplantation studies. These directed misexpression experiments suggest that late progenitors that are normally fated to generate late-born, superficial layer neurons can still be induced to generate early fates (e.g. Molyneaux et al., 2005). In *Drosophila*, expression of *Hunchback*, which is normally expressed by early progenitors and their neuronal progeny, is sufficient to allow later progenitors to generate neurons with an early phenotype. However, this plasticity decreases over time; progenitors at advanced stages of development are resistant to *Hunchback* expression, and do not revert to an earlier phenotype (Isshiki et al., 2001; Pearson and Doe, 2003). In an analogous fashion in the mammalian neocortex, overexpression of *Fezf2* in progenitors soon after the generation of layer V and VI is completed (i.e. in progenitors that give rise to layer IV neurons), or in progenitors that would normally give rise to layers II/III, is sufficient to at least partially override the fate restriction, and induce later-stage progenitors to produce neurons with some molecular and anatomical features of earlier-born neurons (Chen et al., 2005a; Molyneaux et al., 2005). Further analysis of *Fezf2* transfected neurons with additional positive and negative markers of subcerebral projection neurons is needed to determine the extent of the effect of *Fezf2* on neuronal phenotype. Interestingly, in contrast to the more restricted window of *Hunchback* effect, *Fezf2* appears to, at least in part, affect progenitor plasticity late in development; forced expression of *Fezf2* in E17 progenitors results in generation of superficial layer neurons that inappropriately express *Tbr1* at a higher frequency than is normally observed in superficial layer neurons, and extend axonal projections to the pons (a feature of deep layer neurons) (Chen et al., 2005b). In agreement with the limitations of plasticity seen with *Hunchback* in *Drosophila*, *Fezf2* over-expressing neurons are still able to migrate to the layer appropriate for their late birth date instead of layer V. While the extent to which these late born neurons change their identity in response to *Fezf2* over-expression remains to be elucidated, together, these experiments indicate that cortical progenitors might be more plastic than previously suspected, even late in neurogenesis, if manipulated by the appropriate molecular controls (Molyneaux et al., 2007).

There is also increasing evidence that cortical plasticity is maintained to a certain extent in post-mitotic differentiating neurons. Normally, *Sox5* acts post-mitotically to control sequential generation of corticofugal neurons. Gain-of-function analysis reinforces this critical role of *Sox5,* as over-expression at late stages of corticogenesis causes re-emergence of neurons with corticofugal features (Lai et al., 2008). Further, *Ctip2* and *Satb2*, post-mitotic effector molecular controls specifically expressed by CSMN and CPN (Arlotta et al., 2005; Alcamo et al., 2008), respectively, are able to redirect these projection neuron axons to abnormal, reciprocal targets when over-expressed in embryonic development (Alcamo et al., 2008; Chen et al., 2008a), suggesting postmitotic, early neuronal plasticity in the cortex.

1.7 Disease Relevance

Autism spectrum disorders (ASD) are increasingly viewed as due in substantial part to anatomically and cellularly subtle, but functionally overt, disorders of cortical associative connectivity, especially of higher cognitive and social integrative systems(Geschwind and Levitt, 2007). Cortical connectivity in ASD has been described as over-connectivity in local circuits, with disconnection in long-distance circuits(Courchesne and Pierce, 2005). Such long distance disconnection is highlighted by weak functional connectivity and synchronization between the cerebral hemispheres (Dinstein et al., 2011; Schipul et al.).

Since CPN are the cortical commissural neurons that connect the two cerebral hemispheres via the corpus callosum, and since they are critical for long-distance bilateral transfer and integration of cortical information, they have been centrally implicated in ASD. A smaller CC relative to overall brain volume is one of only a few anatomically identified pathologies in a substantial number of ASD patients (Egaas et al., 1995; Vidal et al., 2006; Herbert and Kenet, 2007; Minshew and Williams, 2007; Frazier and Hardan, 2009; Freitag et al., 2009; Mcalonan et al., 2009), and absence of the CC in humans is associated with defects in abstract reasoning, problem solving, and generalization (Paul et al., 2007). Currently, little is known about the molecular development and heterogeneity of CPN, and even less is known about subpopulations of CPN with distinct and likely important associative functions, and potentially important roles in subtypes of ASD. Thus, CPN and callosal biology have very substantial significance in ASD.

Increased knowledge of specific neuronal subpopulations affected in this heterogeneous set of disorders, and of functions of genes playing a role in their development will likely allow specific subclasses of disorders to be separated from the broader spectrum of disorders. This increasing division of these diseases will enable work toward directed preventative and therapeutic approaches based on knowledge of specific neuronal and molecular subtypes. Identification of *Mecp2* as the gene mutated in ASD Rett's syndrome (Amir et al., 1999) enabled increased understanding and directed research on this branch of ASD. Continuing to break down the spectrum into individual disorders has great potential to encourage directed research of this type for many such unique disorders.

1.8 Dissertation Overview

In this dissertation, I identify and begin to functionally characterize molecular controls over diverse subpopulations of midline-crossing callosal neocortical projection neurons (CPN), and I investigate expansion of CPN subpopulations in primates, employing some of these specifically expressed genes. I investigate functions of three of these candidate molecular controls in mice (*Cited2, Caveolin1,* and *TMTC4)* over specific identity acquisition of CPN subpopulations.

I open with an introduction of neocortical neuronal subtypes, their generation, diversity, and some of the progress made in identifying molecular controls over the development of these subpopulations.

In Chapter 2, I focus on identification and analysis of molecular controls over CPN subtype diversity. This work includes identification of novel molecular controls over CPN development, and newly identified molecular subtypes of CPN, as serves as the basis for functional analysis of CPN controls in the following chapters.

In Chapter 3, I investigate functions of one candidate molecular control, *Cited2*, over somatosensory CPN fate acquisition. The transcriptional co-activator *Cited2* acts early in corticogenesis to control neuronal birth and survival. It is also required later in development to specifically ensure somatosensory CPN territory.

In Chapters 4 and 5, I examine functions of two additional controls, *Cav1* and *TMTC4,* over unique populations of frontal / callosally projecting CPN and disease relevant superficial layer CPN, respectively.

In Chapter 6, I investigate molecular evolution of CPN by examining similarities and differences between a select number of molecular CPN subpopulations throughout evolution, using comparative gene expression analysis between mouse and macaque sensory cortex.

I conclude with a discussion of the implications of these results for understanding neocortical development and function, and disorders of precise cortical connectivity such as ASD and agenesis of the corpus callosum.

The contents of the Appendix covers work I joined early in my doctoral studies, expanding the understanding of parcellation of progenitor domains in the forebrain, and generation of interneuron diversity, through functions of the SRY-box transcription factor *Sox6*.

Chapter 2:

Novel Subtype-specific Genes Identify Distinct Subpopulations of Callosal Projection Neurons

Author contributions: I joined this project in the revisions stage when the FACS purification, comparative microarray analysis, candidate selection, and single *in situ* hybridization characterization were complete. I worked closely with first author Bradley Molyneaux and co-second author Jessica MacDonald to strengthen the paper by adding all of the neuron type-specific validation by using fluorescent *in situ* hybridization with fluorescent retrograde label, an approach that I had been developing for other use, and was optimizing with Jessica MacDonald. We also tested many antibodies and optimized staining for the Nectin-3 primary antibody combined with retrograde labeling. All of the double *in situ* hybridization co-expression analysis is new, and was not included in the publication. This approach was developed in collaboration between the Allen Brain Institute for Brain Science's Zachary Riley, co-second author Jessica MacDonald, and me.

Publication: Bradley J. Molyneaux*, Paola Arlotta*, Ryann M. Fame†, Jessica L. MacDonald†, Kyle L. MacQuarrie, and Jeffrey D. Macklis. "Novel Subtype-specific Genes Identify Distinct Subpopulations of Callosal Projection Neurons." *J. Neurosci*. 2010. Sept. 30; 29(39):12343-12354. (* equally-contrubuting first authors, †equally-contributing second authors)

This chapter has been kept largely unchanged from its published form, with the exception of double *in situ* hybridization data and minor changes in figure organization and numbering.

2.1 Abstract

Little is known about the molecular development and heterogeneity of callosal projection neurons (CPN), cortical commissural neurons that connect homotopic regions of the two cerebral hemispheres via the corpus callosum, and that are critical for bilateral integration of cortical information. Here we report on the identification of a series of genes that individually and in combination define CPN and novel CPN subpopulations during embryonic and postnatal development. We used *in situ* hybridization analysis, immunocytochemistry, and retrograde labeling to define the layer-specific and neuron-type-specific distribution of this series of newly identified CPN genes across different stages of maturation. We demonstrate that a subset of these genes (e.g. *Hspb3* and *Lpl*) appear specific to all CPN (in layers V-VI and II/III), while others (e.g. *Nectin-3, PlexinD1,* and *Dkk3*) discriminate between CPN of the deep layers and those of the upper layers. Further, the data show that several genes finely subdivide CPN within individual layers, and appear to label CPN subpopulations that have not been previously described using anatomical or morphological criteria. The genes identified here likely reflect the existence of distinct programs of gene expression governing the development, maturation, and function of the newly identified subpopulations of CPN. Together, these data define the first set of genes that identify and molecularly subcategorize distinct populations of callosal projection neurons, often located in distinct subdivisions of the canonical cortical laminae.

2.2 Introduction

The neocortex is the region of the brain responsible for cognitive function, sensory perception, and consciousness, and, as such, it has undergone pronounced expansion and development during evolution. The cortex is composed of many different subtypes of neurons, which are organized in six cortical layers and numerous cortical areas (Molyneaux et al., 2007). In addition to locally integrated neurons, which include multiple subclasses of GABAergic interneurons across all layers, and Cajal-Retzius cells located in layer I (Ramón y Cajal, 1995; Markram et al., 2004), a rich variety of glutamatergic projection neuron subtypes exist. Projection neurons, representing approximately 80% of all neuron types of the cortex, can be classified by the target of their axonal projections to distinct intracortical, subcortical, and subcerebral targets, as well as by their location in specific cortical layers and areas (Molyneaux et al., 2007). The molecular identity of distinct projection neuron types, and the signals that control lineage-restricted neurogenesis are only beginning to be defined for most projection neuron types of the cortex(Weimann et al., 1999; Hevner et al., 2001; Arlotta et al., 2005; Chen et al., 2005a; Chen et al., 2005b; Molyneaux et al., 2005; Szemes et al., 2006; Alcamo et al., 2008; Britanova et al., 2008; Joshi et al., 2008b; Lai et al., 2008).

In this report, we focus on the molecular development of callosal projection neurons (CPN), a broad population of cortical commissural neurons that connect homotopic regions of the two cerebral hemispheres via the corpus callosum, the largest fiber tract of the brain (Richards et al., 2004). While all callosal projection neurons have axonal projections through the corpus callosum, they show substantial heterogeneity in their axonal projection properties, with some CPN having single projections to the contralateral cortex, and others maintaining either dual projections to the contralateral cortex and ipsilateral/contralateral striatum, or dual projections to the contralateral cortex and ipsilateral frontal cortex (Wilson, 1987; Koralek et al., 1990; Reiner et al., 2003; Gao and Zheng, 2004; Mitchell and Macklis, 2005). Adding further to this diversity of subtypes, CPN are found across multiple cortical layers, with the vast majority located in layers II/III (~80%) and V (~20%), and a smaller population present in layer VI (Conti and Manzoni, 1994; Ramos et al., 2008). Of interest, the origin and time of birth of CPN destined to populate these different layers is distinct. While deep layer CPN (located in layers VI and V) are born during early stages of corticogenesis (between E12 and E14 in the mouse), primarily from progenitors located in the ventricular zone (VZ) of the dorsal pallium, upper layer CPN (located in layers II/III) are born later (between E15 and E17), and many of them derive from intermediate progenitors (also known as basal progenitors) located in the subventricular zone (SVZ), a second germinal zone that develops above the VZ during late neurogenesis (Smart and McSherry, 1982; Wu et al., 2005; Kriegstein et al., 2006). Together, these data indicate that CPN are highly heterogeneous, and potentially as diverse as the many subtypes of corticofugal projection neurons (e.g. corticospinal, corticothalamic, corticostriatal, and subplate). CPN are likely composed of multiple molecularly distinct subpopulations that are not currently resolved at the anatomical level.

It is likely, but yet unclear, that CPN populations located in different cortical layers, or presenting different patterns of connectivity, ultimately play different functional roles. Substantial previous work demonstrates that callosal connections are central for the bilateral integration of cortical information in response to incoming sensory input from the thalamus (Nicolelis and Shuler, 2001; Hlushchuk and Hari, 2006). This is evident in cases of agenesis or surgical transection of the corpus callosum in humans, often associated with abnormal emotional and social behavior, and with the impairment of higher cognitive function (Paul et al., 2007). Abnormalities of CPN have been one of the central neuroanatomic findings in autism spectrum disorders, including Rett syndrome, and are implicated in abnormalities of associative function in autism (Saitoh and Courchesne, 1998). Detailed functional and molecular studies of the roles of different CPN subpopulations have been complicated by the heterogeneity of neuron types that are present within individual cortical layers, and by the scarcity of CPN-specific antigenic markers to define neurons of this broad class as they develop *in vivo*.

To discover sub-type specific molecular controls over the development of CPN and corticofugal populations and to identify new markers of these neuronal populations, we previously purified CPN and two subtypes of subcerebral projection neurons – corticospinal motor neurons (CSMN) and corticotectal projection neurons (CTPN) – from the murine neocortex at distinct stages of late-embryonic and early postnatal development (Arlotta et al., 2005). Using microarrays, we identified genes that in specific combinations mark CSMN and control development of this neuron type and related corticofugal projection neuron populations *in vivo*, but are excluded from CPN (Arlotta et al., 2005; Molyneaux et al., 2005; Lai et al., 2008).

Here we report on the identification of a set of genes that are progressively restricted to CPN, and that are novel markers of this broad projection neuron lineage during embryonic and postnatal development. Some of these genes appear specific to all CPN (in layers V-VI and II/III), whereas others discriminate between CPN of the deep layers and those of the upper layers. Further, we show that a subset of genes finely subdivides CPN within individual layers, and appear to label CPN subpopulations that have not been previously described using anatomical and morphologic criteria. Together, these data define the first set of genes that identify and likely play central roles in the subtype-specific development of CPN, providing molecular evidence for the presence of multiple CPN subpopulations often located in distinct subdivisions of the canonical cortical laminae.

2.3 Materials and Methods

2.3 a. Retrograde labeling

All procedures to retrogradely label and purify CPN and the comparative populations CSMN and CTPN are previously described in Arlotta et al. (2005). In brief, for CPN, neurons were retrogradely labeled at E18, P3, P6, and P14 by injection of green fluorescent microspheres (Lumafluor Corp., FL) into contralateral cortex (E17, P1, P4, P12) of C57BL/6 mice (Charles River Laboratories, MA), as previously described (Catapano et al., 2001). Cholera toxin subunit B conjugated to Alexa 555 (CTB555; Invitrogen) was used for retrograde labeling of CPN and CSMN for *in situ* hybridization and immunocytochemistry experiments. Embryonic injections were performed using a Vevo 660 ultrasound system (VisualSonics, Toronto). All animal studies were approved by the Massachusetts General Hospital Institutional Animal Care and Use Committee and performed in accordance with institutional and federal guidelines.

2.3 b. CPN dissociation and FACS purification

Labeled areas of somatosensory cortex were dissociated essentially as described (Catapano et al., 2001). In brief, dissociated cortex was enzymatically digested with 0.16 gm/L L-cysteine HCl and 11.7 U/ml papain at 37°C for 30 min. Neurons were mechanically dissociated to create a single cell suspension by gentle trituration in iced OptiMem (Life Technologies, Gaithersburg, MD) containing 20 mM glucose and both 0.4 mM kynurenic acid and 0.025 mM APV to protect against glutamate-induced neurotoxicity. Microsphere-labeled CPN were purified from the cortical cell suspension by fluorescence-activated cell sorting (FACS), and neurons were collected directly in RNAlater (Ambion). Additional details and methods to purify CSMN and CTPN are reported in (Arlotta et al., 2005).

2.3 c. Microarrays

Microarray probe synthesis and microarray analysis were all previously performed and are described in Arlotta et al. (2005). In order to optimize identification of CPN specific genes, the same hybridization solutions were now applied to the newly available Affymetrix 430 2.0 microarrays, and hybridized and processed according to Affymetrix protocols. Microarray data were normalized using two independent methods: the RMA function within Bioconductor (Irizarry et al., 2003) and the "error model" method within Rosetta Resolver (version 5.0; Rosetta Biosoftware, Seattle, WA). Statistical significance of gene expression differences between neuronal subtypes was determined by pair-wise comparisons at each age using statistical analysis of microarrays (SAM) (Tusher et al., 2001). Using a SAM D-score cutoff of greater than 2 or less than -2, we selected significantly differentially expressed genes, and further analyzed their temporal dynamics of expression to identify a refined set of genes for further analysis (Arlotta et al., 2005). For example, genes with similar dynamics of expression that are simply shifted a few days later in CPN compared with CSMN demonstrate statistical difference at each independent time point but likely represent the same biological process in each population, shifted simply due to population birthdate and developmental stage. All microarray data have been deposited in the Gene Expression Omnibus database at the National Center for Biotechnology Information, and are available via accession numbers GDS1076 (Affymetrix 430a microarray data) and Affymetrix 430 2.0 microarrays will be submitted upon acceptance of this manuscript.

2.3 d. In situ hybridization and immunocytochemistry

All clones for *in situ* hybridization (ISH) were generated by RT-PCR. Sequences of all primers used are listed in table 2.1. Nonradioactive colorimetric *in situ* hybridization was performed using reported methods (Berger and Hediger, 2001). Probes were labeled with dig-UTP for all single ISH, and second probes were labeled with DNP-UTP for double fluorescent ISH. Sense probes were used as negative controls in all experiments.

For fluorescent single and double *in situ* hybridization, 14 μm cryosections mounted on superfrost plus slides were postfixed in 4% PFA in PBS for 20 min., rinsed in PBS for 3 min., rinsed for 3 min. in 0.1M triethanolamine (Sigma St.Louis,MO), acetylated for 10 min. in 0.1M triethanolamine/ 0.25% acetic anhydride (Sigma), and then dehydrated through a series of increasing concentrations of EtOH in DEPC-treated double distilled H_2O for 3 min. in each solution: 50% EtOH, 70% EtOH, 95% EtOH, 100% EtOH.

Sections were dried completely and stored at -20°C. Slides were warmed to RT, then secured in capillary flow-through chambers (Tecan, Männedorf), and slides remained in the chambers for the remainder of the procedure. Endogenous peroxidases were inactivated by incubation in 3% H_2O_2 in MeOH (Sigma). After a PBS rinse, tissue was permeabilzed first in 0.2M HCl, followed by proteinase K (Sigma) treatment [0.0175U/mL in 0.005M EDTA, 0.05M Tris, 0.005% Tween 20]. Sections were then postfixed in 4% PFA in PBS for 20 min., and preybridizied in 63.5°C hybridization buffer (Ambion custom mix B8807G). Slides were incubated overnight at 63.5°C in 300ng/mL in hybridization buffer in a well-humidified oven. Slides were then subjected to stringency washes in decreasing salt concentrations at 61°C: 5x SSC (Ambion), 4x SSC in 50% diFormamide (Fisher Scientific, Pittsburgh, PA), 2x SSC in 50% diFormamide, 0.1x SSC, and 0.1x SSC at RT. Sections were then blocked in 0.1g blocking reagent (Roche) / mL maleate [0.9M maleic acid (Sigma), 0.1M NaCl (Sigma), 0.0005% Tween 20 (Sigma), 0.175M NaOH (Sigma)], rinsed in maelate, then in NTE [0.5M NaCl, 0.01 Trizma, 0.005M EDTA, 0.005% Tween 20], followed by incubation in 20mM iodoacetamide in NTE. Sections were rinsed in TNT [0.1M Trizma, 0.15M NaCl, 0.00075% Tween 20], blocked in TNB [0.05g NEN blocking buffer (Perkin Elmer) / mL TNT], and incubated for 1 hour in horseradish peroxidase-conjugated anti-dig (Roche) primary antibody, rinsed with TNT, followed by signal amplification using a tyramide amplification system, TSA-plus ® biotin (Perkin Elmer), TNT rinse, and streptavidin labeled with alexa flurophore 647, followed by 4% PFA fixation. Single fluorescence *in situ* ends here with PBS rinse. For double *in situ*, peroxidases were inactivated in 3% H_2O_2 in PBS, rinsed in PBS, blocked in TNB, incubated for 1hour in horseradish peroxidase-conjugated anti-DNP (Roche), rinsed in TNT, amplified with TSA-plus ® DNP for 45 min., rinsed in TNT, incubated in anti-DNP secondary antibody labeled with alexa flurophore 488, rinsed in TNT, postfixed in 4% PFA, and rinsed in PBS. Slides were coverslipped with Fluromount ®, dried, and edges were protected with clear nailpolish.

For Nectin-3 immunocytochemistry, brains were fixed and stained using standard methods (Fricker-Gates et al., 2002). Briefly, brains were fixed by transcardial perfusion with PBS, followed by 4% paraformaldehyde, and postfixed overnight at 4°C in 4% paraformaldehyde. Brains were sectioned coronally at 50 μm a vibrating microtome (Leica). Sections were blocked in 0.3% BSA (Sigma), 8% goat serum, and 0.3% Triton X-100 (Sigma) for 30 min. at room temperature, before incubation in rabbit-anti-Nectin-3 primary antibody at 1:100 (Abcam ab63931). Secondary antibodies were from the Invitrogen Alexa series. Images were acquired using a Nikon E1000 microscope, using a cooled CCD digital camera (QImaging Retiga) and Openlab acquitsition software (Improvision).

Table 2.1: Detailed Information About the Clones Used for In Situ Hybridization

Gene	**GenBank ID**	**Left primer**	**Right primer**	**Amplicon(bp)**
Btg1	NM_007569	TGCCATAGTTTGGACAGTACC	CAAAATAGATGGTGGTTTGTGG	635
Cav1	NM_007616	ACCTCTCTGGACTGGCAGAA	AGTGTCGGCAAGACTGAAGG	653
Chn2	NM_023543	GCATGAGATTTCCACACCAA	TTTCCTTCCATTACACTGTCATAA	407
Cited2	NM_010828	TGCTGCCACTTTTTCCTATTC	TCTGTGAAATGTTTGCCACTG	501
Cpne4	NM_028719	TGACACAAATTCCTGGACAATC	CAGTGAGCTCAAAGACCAAGC	551
Cux2	NM_007804	TCAGTCAACAGCTCCATTCG	GACAGCGAGAAAGTCCTTGG	626
Dkk3	NM_015814	ATTGGGTTCACCATTTCAGG	CAGGCGTTTAAGAGGTACTCG	617
Epha3	NM_010140	GTCCAAATGCCTTAAAATGG	CAATAGCATTTGGCACTTGG	595
Frmd4b	NM_145148	AGCTCCTGAATCGTGGCTTA	TCCTGCAGCTCGGAGTAAAT	603
Gfra2	NM_008115	GATGTGAACATGTCTCCCAAAG	ATTTTGTCAGGCGGGAGTTC	382
Gm879	NM_001034874	AATGGGTTTGGCATTGTAGC	AATTTCCATTGGTGCTTTGC	523
Gpr88	NM_022427	CAAATGAAACCAATGGTCAGG	TATCTGTTTCCCGTGTCTCC	514
Hspb3	NM_019960	TGATTCAGCCCCAATTAAGC	CTGGGGTATGAAGAGCAACC	632
Inhba	NM_008380	GCGATCAGAAAGCTTCATGTG	AGACTGGCACCACTCTCCTG	506
Limch1	NM_001001980	AGCCAGACACGAAAGGAATG	GCAAACACCTCCGAGAGAAG	509
Lpl	NM_008509	TGCTGTGCAAAGAGAAGAGC	CGGACACAAAGTTAGCACCA	658
Nectin-3	NM_021495	AAACAACCTGATCCGCAAAG	CAGTGAAAACTGTAAAGCAGCTC	466
Nnmt	NM_010924	CCTATGTGTGTGATCTTGAAGG	AGATCTGCCTGGCTTTCG	455
PlxnD1	NM_026376	CAGGAAATGAACGCACACC	TGAGGGACACAGACAACTGC	656
Ptn	NM_008973	GCCTACCCGTCCAAATATCC	GCCAGTTCTGGTCTTCAAGG	590
TcrB	X67128	GGGTTCTGTCTGCAACCATC	AAGGTGTCAACGAGGAAGGA	244
Tmtc4	NM_028651	GAAGCAGAGCAGAGCTACCG	TCTGAACAGAGGCTTCATGC	579

Table 2.1 (Continued)

2.4 Results

2.4 a. Purification and Microarray Analysis of Callosal Projection Neurons, Corticospinal Motor Neurons, and Corticotectal Projection Neurons.

To identify genes that control the cell-type specification and differentiation of callosal projection neurons, we compared the gene expression profiles of CPN to two other pure populations of cortical projection neurons: corticospinal motor neurons and corticotectal projection neurons. The general approach used, and the analysis of data to identify genes involved in the development of the corticospinal motor neuron and related corticofugal populations, was previously described (Arlotta et al., 2005). Here, we report on the identification and further characterization of genes that define the broad population and distinct subtypes of interhemispheric callosal projection neurons.

CPN were retrogradely labeled via injections of green fluorescent microspheres into their axonal projection fields in contralateral sensorimotor cortex at four different stages of development, followed by dissociation and FACS of the labeled neurons to typically greater than 99% purity (Catapano et al., 2001; Catapano et al., 2004; Arlotta et al., 2005; Ozdinler and Macklis, 2006). Specifically, callosal projection neurons that were purified at multiple stages of development, including E18, P3, P6, and P14, were labeled as schematically depicted in Figure 2.1. For precise targeting and purification of E18 CPN, fluorescent microspheres were microinjected in the contralateral hemisphere of E17 embryos, *in utero*, under high-resolution ultrasound backscatter microscopic guidance (Arlotta et al., 2005). Similar methods were used to label corticospinal motor neurons and corticotectal projection neurons [Figure 2.1; (Arlotta et al., 2005)].

In the study by Arlotta et al. (2005), we previously used these pure neuronal preparations to compare the molecular development of corticospinal motor neurons and callosal projection neurons using Affymetrix 430A microarrays (data available at NCBI Gene Expression Ominbus accession number GDS1076). In order to optimize identification of CPN-specific genes, and to maximize the number of genes examined by microarray to provide the most inclusive investigation of gene expression through development, we now hybridized samples to the newly available and more inclusive Affymetrix 430 2.0

arrays, which contain a substantially expanded probe set. Using this approach, we identified a large number of genes that are expressed at higher levels in callosal projection neurons compared to CSMN and corticotectal projection neurons. The forty genes with the most biologically significant and distinctive expression profiles following temporal analysis (see methods) are listed in Table 2.2. These genes can be classified in several ontology groups and include, among others, transcription factors (e.g. *Cux1, Cux2, Lhx2, Pdzrn3, Cited 2)*, cell signaling molecules and receptors (e.g. *Gfra 2, Gpr6, Gpr88, Ptprk, TCRβ*), and axon guidance molecules (e.g. *Chimerin 2, Dcc, EphA3, Plxdc2, PlxnD1*). Although many of these genes are relatively uncharacterized in the cortex, and none of them has been previously demonstrated to specifically label the broad CPN population or CPN subtypes, we find that selected genes previously demonstrated to be restricted to the upper layers (where most CPN are located), are specifically and highly expressed in CPN within those layers [e.g. *Cux1, Cux2 – (Nieto et al., 2004; Zimmer et al., 2004)*, confirming the validity of our approach in identifying candidates with restricted expression to CPN and distinct CPN subtypes.

2.4 b. Many CPN specific genes identify anatomic diversity and distinct CPN populations.

Previous anatomical and birthdating analysis have shown that the broad CPN population is heterogeneous, including neurons born at different developmental times (e.g. E12.5-13.5 for layer VI and V CPN, E15.5 for layer II/III CPN), located in different cortical layers (e.g. II/III, V, and VI), with some extending collateral projections to distinct targets (e.g. striatum, ipsilateral frontal cortex) (Wise and Jones, 1976; Mitchell and Macklis, 2005). This is in striking contrast to the much more homogeneous population of corticospinal motor neurons, which are born at ~E13.5, populate one layer (layer V) and a limited area (sensorimotor) of cortex, and extend projections to the spinal cord (though with a range of spinal segmental specificity)(O'Leary and Koester, 1993). Based on such previous anatomical data, we reasoned that CPN specific genes might fall into at least two general categories: (i) broad CPN "identity genes" that might label most or all CPN; and (ii) genes that subparcellate CPN into multiple subtypes,

Figure 2.1: Schematic representation of the experimental approach used to identify CPN-specific genes. Callosal projection neurons (CPN), corticospinal motor neurons (CSMN), and corticotectal projection neurons (CTPN) were retrogradely labeled at distinct stages of development from the contralateral hemisphere, the spinal cord, and the superior colliculus, respectively. Labeled neurons were dissociated, FACS purified, and submitted to comparative microarray analysis.

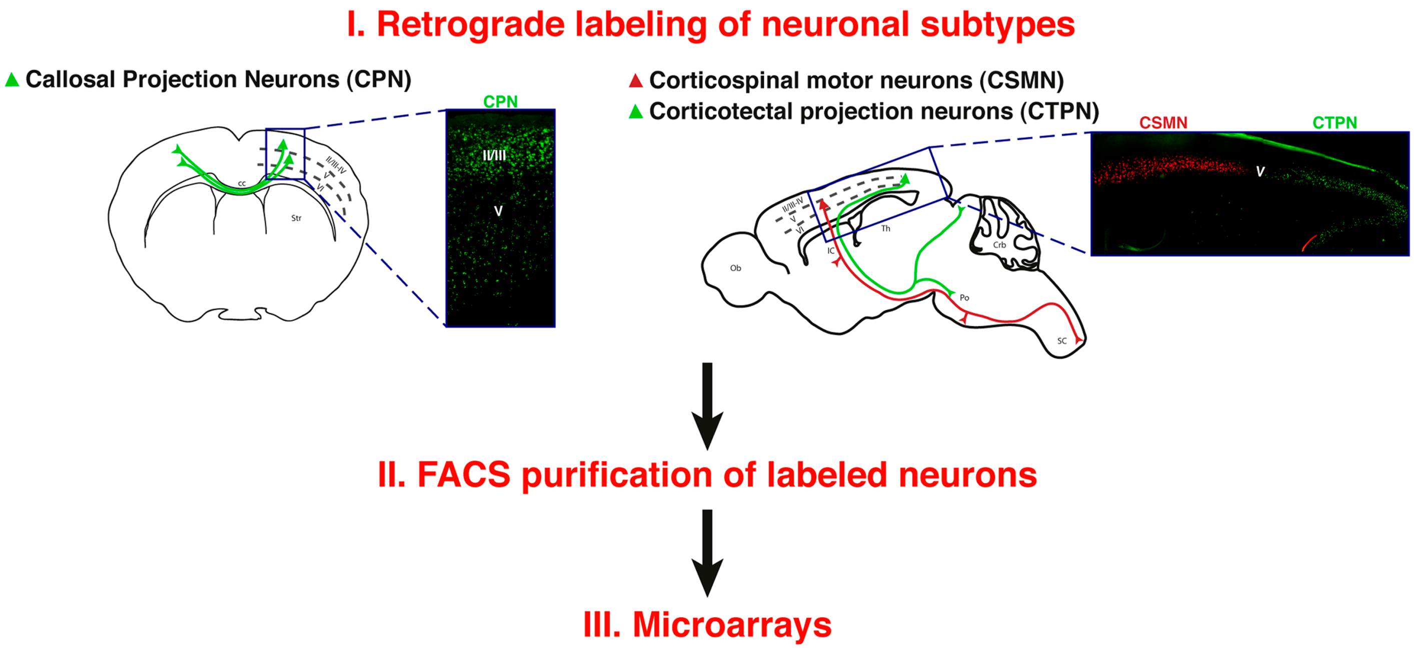

I. Retrograde labeling of neuronal subtypes

▲ Callosal Projection Neurons (CPN)

▲ Corticospinal motor neurons (CSMN)

▲ Corticotectal projection neurons (CTPN)

II. FACS purification of labeled neurons

III. Microarrays

Figure 2.1 (Continued)

Table 2.2: Selected subset of the genes identified by microarray analysis that are expressed at higher levels in callosal projection neurons compared to corticospinal motor neurons and corticotectal projection neurons. The forty genes listed are those with the most biologically significant and distinctive expression profiles following temporal analysis of gene expression data. Genes that were further investigated here with *in situ* hybridization are listed in bold.

Gene Name	**Full Name**	**GenBank ID**
Adamts3	ADAM metallopeptidase with thrombospondin type 1 motif, 3	NM_001081401
Btg1	**B-cell translocation gene 1**	**NM_007569**
C030017B01Rik	EST (located 3' of Kctd16)	AK046738
Cav1	Caveolin (caveolae protein 1)	**NM_007616**
Cdh10	Cadherin 10	NM_009865
Chn2	**Chimerin 2**	**NM_023543**
Cited2	**Cbp/p300-interacting transactivator, with Glu/Asp-rich carboxy-terminal domain, 2**	**NM_010828**
Coup-tfl	Chicken ovalbumin upstream promoter-transcription-factor 1	NM_010151
Cpne4	**Copine 4**	**NM_028719**
Cux1	Cut-like 1	NM_009986
Cux2	**Cut-like 2**	**NM_007804**
DCC	Deleted in colorectal carcinoma	NM_007831
Dkk3	**Dickkopf homolog 3**	**NM_015814**
Epha3	**Eph receptor A3**	**NM_010140**
Frmd4b	**FERM domain containing 4B**	**NM_145148**
Gfra2	**Glial cell line derived neurotrophic factor family receptor alpha 2**	**NM_008115**
Gm879	**Gene model 879**	**NM_001034874**
Gpr6	G-protein-coupled receptor 6	NM_199058
Gpr88	**G-protein coupled receptor 88**	**NM_022427**
Gria4	Glutamate receptor, ionotropic, AMPA4	BB130399
Grp	Gastrin releasing peptide	NM_175012
Hspb3	**Heat shock protein 3**	**NM_019960**
Inhba	**Inhibin beta-A**	**NM_008380**
Kcnh1	Potassium voltage-gated channel, subfamily H, member 1	NM_001038607
Klhl4	Kelch-like 4	NM_172781
Lhx2	LIM homeobox protein 2	NM_010710
Limch1	**LIM and calponin homology domains 1**	**NM_001001980**
Lpl	**Lipoprotein lipase;**	**NM_008509**
Nectin-3	**Nectin-3**	**NM_021495**
Nnmt	**Nicotinamide N-methyltransferase**	**NM_010924**
Pdzrn3	PDZ domain containing RING finger 3	NM_018884
Plxdc2	plexin domain containing 2	NM_026162
PlxnD1	**Plexin D1**	**NM_026376**
Ptn	**Pleiotrophin**	**NM_008973**
Ptprk	Protein tyrosine phosphatase, receptor type, K	NM_008983
Satb2	Special AT-rich sequence binding protein 2	NM_139146
TcrB	**T-cell receptor beta**	**X67128**
Tmtc4 (J22rik)	**transmembrane and tetratricopeptide repeat containing 4**	**NM_028651**
Unc5d	Unc-5 homolog D	NM_153135
Vglut2	Vesicular glutamate transporter 2	NM_080853

Table 2.2 (Continued)

potentially reflecting anatomic, connectivity, and functional heterogeneity. Genes in the second set would only be expressed in distinct subtypes of CPN.

To investigate this possibility and determine whether the anatomical complexity of the broad CPN population is mirrored at the molecular level, we investigated the fine spatial expression of a subset of these newly identified CPN genes via *in situ* hybridization. We find that a small number of these genes are expressed in a laminar distribution suggestive of their presence in all CPN (Fig. 2.2), showing high levels of expression in layers II/III, the CPN proportion of V, and in a smaller number of layer VI neurons consistent with CPN. These include the genes *Lpl* (lipoprotein lipase) (Figure 2.2A), an enzyme involved in lipoprotein metabolism with unknown function in the brain (Vilaro et al., 1990); *Hspb3* (Figure 2.2B), a small heat shock protein not previously described in the brain (Sugiyama et al., 2000); and *Cited2* (Figure 2.2C), thought to function as a transcriptional coactivator and interact with *Lhx2* (Glenn and Maurer, 1999). The spatial expression of these genes matches the distribution of CPN obtained *via* retrograde tracing of all CPN from the contralateral hemisphere (Figure 2.2D).

In addition to genes that label all CPN and distinguish them from other types of cortical projection neurons within the same layers, *in situ* hybridization for 20 additional CPN genes reveals that they are distributed in distinct, individual laminar and sublaminar patterns within the cortex (Figures 2.2-2.6). These data confirm and extend at the molecular level previous anatomical data on the heterogeneity of connections and functional diversity of CPN, and provide the first demonstration that distinct CPN populations exist in the cortex that can be identified by the combinatorial expression of newly identified CPN genes (see Figure 2.8).

2.4 c. CPN-specific genes mark distinct temporal stages of CPN development.

To identify genes expressed by CPN at distinct stages of development, and thus likely functioning to control distinct aspects of cell-fate specification and differentiation of this neuronal lineage *in vivo*, we further investigated by *in situ* hybridization the fine spatial expression of genes that by microarray appear to be preferentially expressed at early (E18), mid (P3, P6), or late (P14) stages of CPN development. We identified several CPN-restricted genes that, aside from subdividing the CPN population spatially in layers and sublayers, are also expressed selectively at distinct times of development (Figures 2.3-2.6 and Table 2.1). Genes expressed early during CPN development, and thus potentially functioning in lineage specification, neuronal migration, and initial axonal extension, include to following: *Cux2*, *Inhba*, *Btg1* (see Figure 2.3A, 2.3B, and G); *Frmd4b, EphA3* (see Figure 2.4A and C); and *Ptn* (see Figure 2.5C). Other genes are virtually absent at E18, but are highly expressed at P3, by which time CPN have already reached their final location in the neocortex, have sent axonal projections through the corpus callosum, and are connecting to targets in the contralateral hemisphere. These genes expressed at mid-stage of CPN development include the following: *Cpne4* and *Tmtc4* (see Figure 2.3D and E); *Nnmt, Cav1* (see Figure 2.4B and D); *Nectin-3, Chn2, Gm879* (see Figure 2.5A, B, and F). Finally, genes highly expressed at later stages of CPN development, and thus that might be important in later CPN maturation, maintenance, and/or control of late events of CPN connectivity include: *Plexin-D1, Gfra2, Tcrβ,* and *Dkk3* (see Figure 2.6A-D).

2.4 d. Genes that distinguish upper layer from deep layer CPN

CPN are located in both superficial (II/III) and deep (V and VI) layers of neocortex, but those of layers II/III are very different in their time and place of origin from those of V and VI. CPN of the deep layers are born during early corticogenesis (E11.5- E13.5 in the mouse) from progenitors located in the ventricular zone underlying neocortex (Angevine and Sidman, 1961; Caviness and Takahashi, 1995). In contrast, superficial layer CPN are born later, with a peak of birth around E15.5, and they derive largely from a second pool of progenitors (basal progenitors; also known as intermediate progenitors) located in the subventricular zone (SVZ), a second germinal layer that develops above the VZ during late corticogenesis (Kriegstein et al., 2006). The SVZ and its intermediate progenitors are thought to be central to the marked expansion of the superficial cortical layers of late evolution (Kriegstein et al., 2006).

Figure 2.2: CPN-genes that label most callosal projection neurons across layers II/III and V.

(A-C), Temporal profiles of gene expression from microarray analysis in CPN (red) versus CSMN (blue) during embryonic (E18) and early postnatal (P3, P6, P14) stages of development. Bars indicate standard errors of the mean. **(A'-C')**, *in situ* hybridization in coronal sections of cortex showing that the expression of selected genes closely resembles the typical distribution of the retrogradely labeled, broad CPN population **(D)**. **(A''-C'')**, magnification of selected areas from **A'-C'**. Ages are as indicated in **A'-C'**. ***E*–*N***, *Lpl* and *Hspb3* are expressed by CPN across layers II/III and V and not in CSMN. ***E***, Fluorescent *in situ* hybridization for *Lpl* (green) in a coronal section of P8 cortex demonstrates that it is expressed in CPN identified by retrograde labeling via injection of CTB555 (red) in the contralateral cortex at P6. ***F***, ***G***, Magnification of selected areas in layers II/III and V from ***E***; arrows indicate *Lpl*-expressing CPN. ***H***, Fluorescent *in situ* hybridization for *Hspb3* (green) in a coronal section of P8 cortex demonstrates that it is expressed in retrogradely labeled CPN (red). ***I***, ***J***, Magnification of selected areas in layers II/III and V from ***H***; arrows indicate *Hspb3*-expressing CPN. ***K***, Fluorescent *in situ* hybridization for *Lpl* (green) in a coronal section of P8 cortex demonstrates that it is not expressed in CSMN identified by retrograde labeling via injection of CTB555 (red) in the spinal cord at P4 (high magnification shown in ***L***).***M***, Fluorescent *in situ* hybridization for *Hspb3* (green) in a coronal section of P8 cortex demonstrates that it is also not expressed in retrogradely labeled CSMN (red) (high magnification shown in ***N***). Scale bars: ***A"-C",*** 100 µm; ***E***, ***H***, ***K***,***M***, 200 µm; ***F***, ***G***, ***I***, ***J***, ***L***, ***N***, 50 µm.

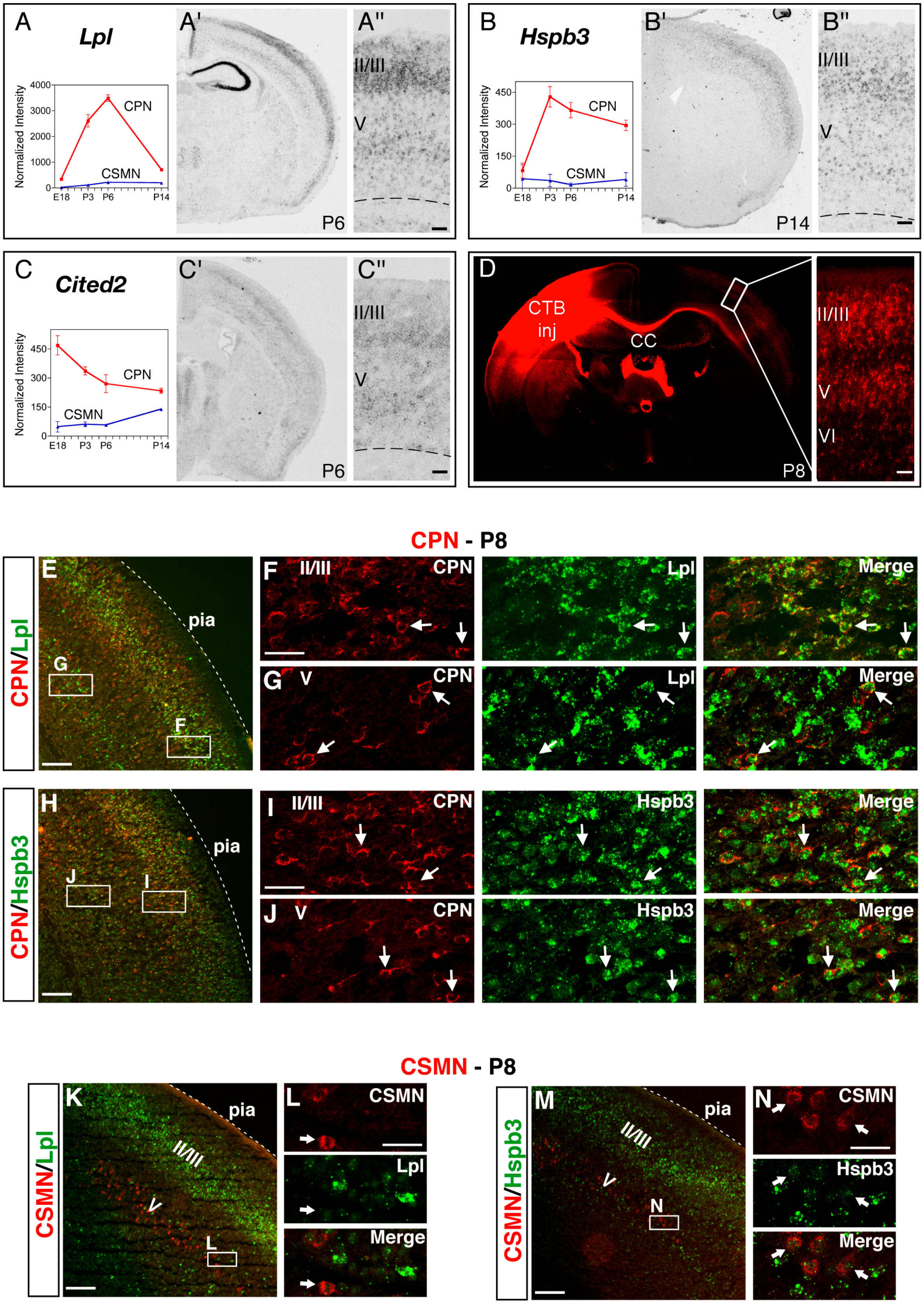

Figure 2.2 (Continued)

To determine whether CPN of the superficial and deep layers are distinct at the molecular level, and to identify potential molecular-genetic controls over the subtype-specific differentiation of these distinct CPN populations, we investigated whether any of the newly-identified CPN-specific genes are restricted to CPN in either superficial or deep laminae. Indeed, we identified several genes that label only superficial layer CPN (Figure 2.3). These include early expressed genes like *Cux2* (Figure 2.3A) and *Inhba* (Figure 2.3B), as well as *Btg1* (Figure 2.3G), a transcriptional coactivator that regulates myoblast differentiation and might play a similar role in CPN development. In addition, later genes like *Cpne4* and *Tmtc4* specifically label superficial layer CPN (Figure 2.3D, E), suggesting potential functional roles in the maturation of these CPN. While *Cux2* was previously reported to label the upper layers of the neocortex (Nieto et al., 2004; Zimmer et al., 2004), acting as a confirmatory positive control for the current analysis, here we refine the prior results by demonstrating that *Cux2* is expressed by CPN within the superficial layers. Other genes identified here are both novel markers of CPN and, more broadly, of superficial cortical layers. Together, expression of these genes as superficial layer CPN markers enables the demarcation and molecular classification of CPN of the superficial layers, and indicates that upper layer CPN are molecularly distinct even at early stages of differentiation from CPN located in deep layers of neocortex

2.4 e. A subset of CPN-specific genes defines novel sub-lamina within the normally unresolved murine upper layer II/III.

Although many of the newly identified upper layer CPN genes are broadly expressed across the thickness of layer II/III, we find, interestingly, that several CPN-specific genes label only narrow sub-lamina, subparcellating what has been traditionally termed layer II/III in rodents. For example, *Frmd4b, Nnmt,* and *EphA3* (Figure 2.4A-C) label only a very thin strip of CPN in the most superficial portion of layer II/III. In contrast, other genes label CPN populations in the middle (*Nectin-3, Chn2*; Figure 2.5A and B), or deeper (*Ptn, Cav1, Gm879*; Figure 2.5 C, D, F) portions of nominal layer II/III. Genes that distinguish the most superficial and deepest aspects of nominal layer II/III from the broader middle portion of the layer are of particular interest, since retrograde labeling of CPN from contralateral cortex indicates that the largest number and concentration of CPN are located within the middle portion of layer II/III, suggesting special functional and connectivity roles for the most superficial and deepest layer II/III CPN compared with the predominant layer II/III population.

To further investigate the specificity of expression of these genes within upper layer CPN, we chose *Nectin-3* as a prototypical gene and evaluated its cell-type-specific expression. We retrogradely labeled CPN using a cholera toxin subunit B Alexa 555 conjugate, which clearly labels upper layer CPN and their axons coursing through the corpus callosum (Fig. 2.5*G*). Immunocytochemistry for Nectin-3 demonstrates colocalization with CPN axons in the corpus callosum, as well as within the somas and apical dendrites of superficial cortical CPN (Fig. 2.5*H–K*).

Together, these genes define a previously unrecognized molecular parcellation of the superficial cortical layers, refining previous histological and anatomical definitions, and enabling new functional and evolutionary hypotheses regarding distinct CPN populations.

2.4 f. Other CPN-specific genes are expressed only in deep layer CPN, and identify distinct populations in layers Va, Vb, and VI.

In a complementary fashion to genes expressed selectively by CPN of upper layers, many of the newly identified CPN genes are specifically expressed in deep layers V and VI, and are excluded from layers II/III, thus defining distinct sets of early-born CPN of the deep layers. These genes include *Plexin-D1, Gfra2, Tcrβ,* and *Dkk3* (Figure 2.6 A-D). Quite interestingly, layer V and VI CPN can be further defined by combinatorial expression of selected deep layer CPN genes, and thus classified into subpopulations occupying distinct sub-portions of these canonical layers. For example, *in situ* hybridization reveals that CPN in layer Va express the unique combination of *Plexin-D1* and *Gfra2* (Figure 2.6 A, B); they likely represent callosal neurons that maintain collateral projections to ipsilateral and/or contralateral striatum (Gao and Zheng, 2004). CPN located in deeper positions within layer V (e.g. layer Vb) can be defined by the expression of *Gfra2, Dkk3,* and *TcrB* (Figure 2.3 C-D), and by the

Figure 2.3: CPN-genes that selectively label callosal neurons of the superficial layers II/III and IV. **(A-F)**, Temporal profiles of gene expression from microarray analysis in CPN (red) versus CSMN (blue) during embryonic (E18) and early postnatal (P3, P6, P14) stages of development. Bars indicate standard errors of the mean. **(A'-F')**, *in situ* hybridization in coronal sections of cortex showing preferential CPN-gene expression in the superficial layers. **(A''-F'')**, magnification of selected areas from **A'-F'**. Ages are as indicated in **A'-F'**. Scale bars: **A"-F"**, 100 µm.

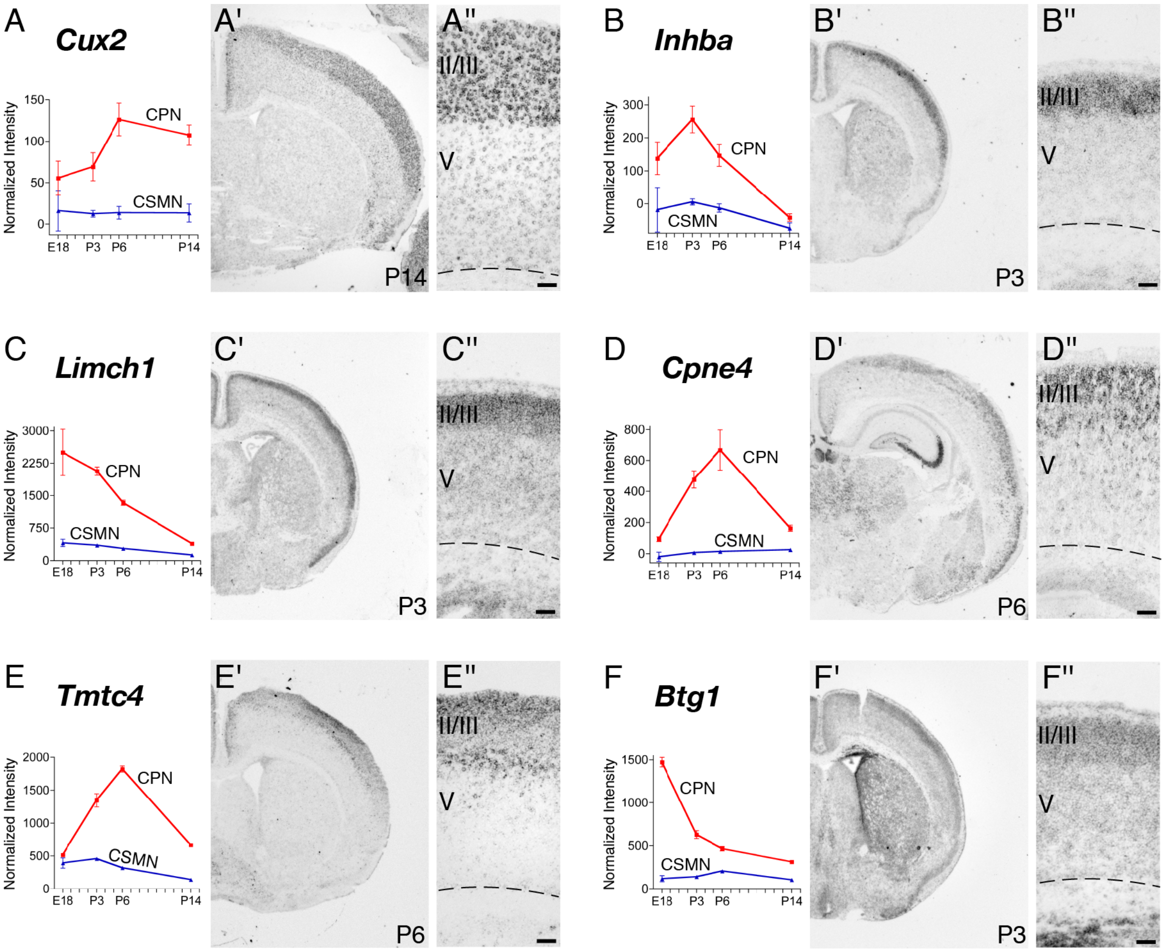

Figure 2.3 (Continued)

Figure 2.4: CPN-genes that preferentially label the outermost portion of layer II/III and layer I. **(A-C)**, Temporal profiles of gene expression from microarray analysis in CPN (red) versus CSMN (blue) during embryonic (E18) and early postnatal (P3, P6, P14) stages of development. Bars indicate standard errors of the mean. **(A'-C'),** *in situ* hybridization in coronal sections of cortex showing preferential CPN-gene expression in the most superficial portions of layer II/III. **(A''-D'')**, magnification of selected areas from **A'-C'**. Ages are as indicated in **A'-C'**. Scale bars: **A"-C"**, 100 μm.

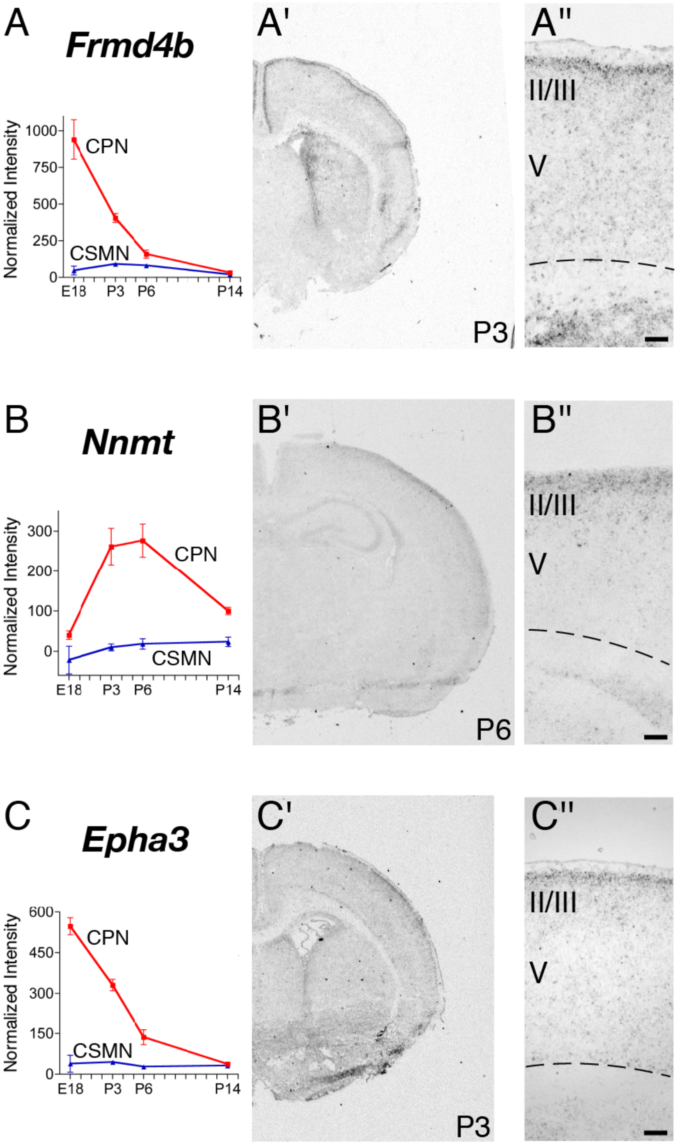

Figure 2.4 (Continued)

Figure 2.5: CPN-genes that preferentially label the deepest portion of layer II/III and layer IV. **(A-F)**, Temporal profiles of gene expression from microarray analysis in CPN (red) versus CSMN (blue) during embryonic (E18) and early postnatal (P3, P6, P14) stages of development. Bars indicate standard errors of the mean. **(A'-F')**, *in situ* hybridization in coronal sections of cortex showing preferential CPN-gene expression in the deepest portions of layer II/III and IV. **(A''-E'')**, magnification of selected areas from **A'-F'**. ***G–K***, Nectin-3 is expressed in CPN in layer II/III and in CPN axons in the corpus callosum at P1.***G***, CPN retrogradely labeled with CTB555 (red) via injections into contralateral cortex at P0.***H***, ***I***, Nectin-3 immunocytochemistry (green) detects Nectin-3 expression in CPN in layer II/III, as well as in CPN axons in the corpus callosum. ***J***, Magnification of selected area in ***I***. ***J***_, Magnification of selected area in ***J***, showing expression of Nectin-3 in a subset of CPN axons in the corpus callosum. ***K***, Magnification of selected area in ***I***. ***K***_, Magnification of selected area in ***K***, showing expression of Nectin-3 in CPN in layer II/III. CTB inj, Site of CTB555 injection; CC, corpus callosum; LV, lateral ventricle; Str, striatum. Ages are as indicated in **A'-E'**, and ***G***. Scale bars: **A"-E"**, 100 µm; ***G–I***, 500 µm; ***J***, ***K***, 100 µm; ***J'***, ***K'***, 50 µm.

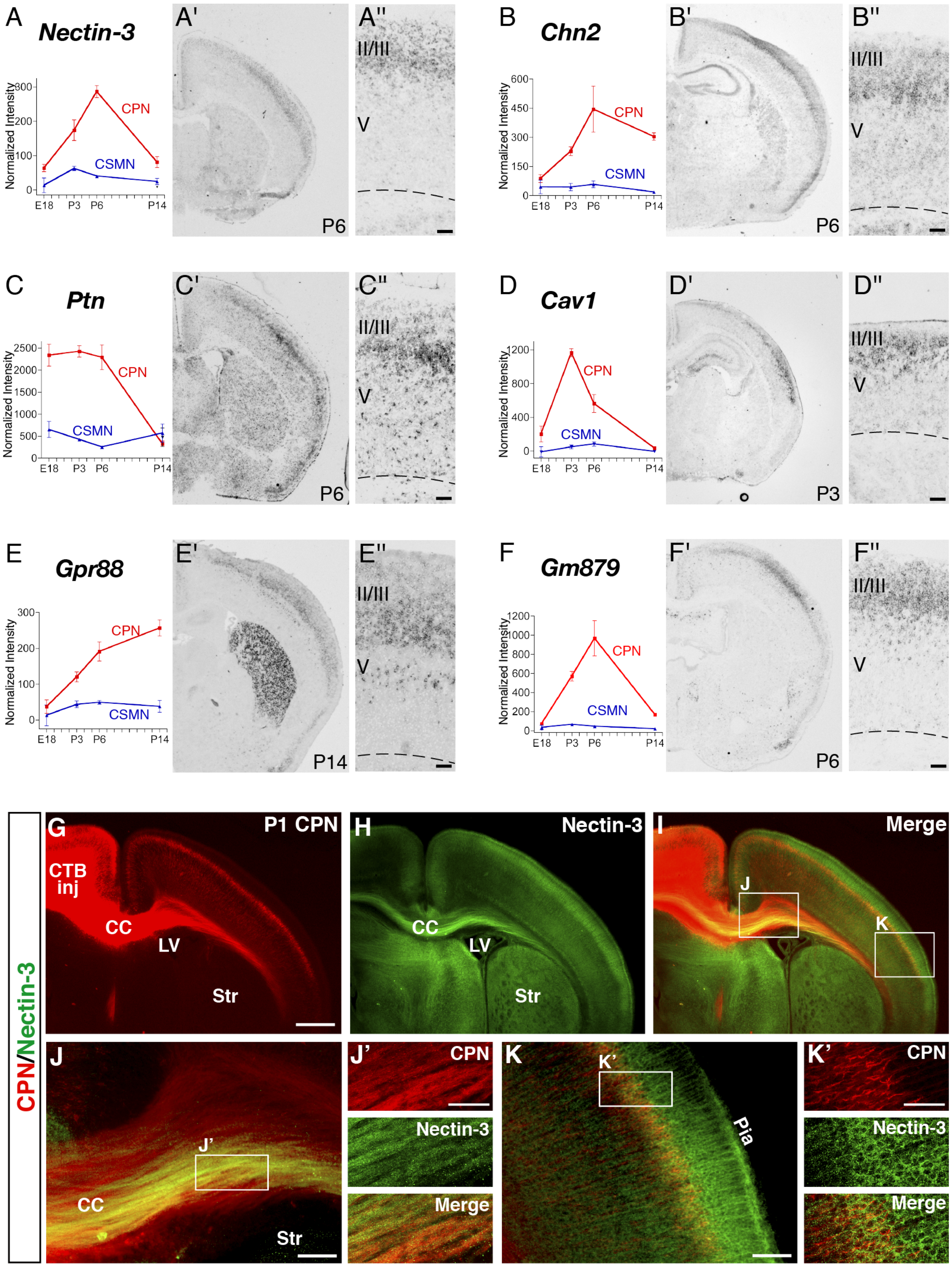

Figure 2.5 (Continued)

Figure 2.6: Genes that preferentially label CPN of the deep layers V and VI. **(A-D)**, Temporal profiles of gene expression from microarray analysis in CPN (red) versus CSMN (blue) during embryonic (E18) and early postnatal (P3, P6, P14) stages of development. Bars indicate standard errors of the mean. **(A'-D')**, *in situ* hybridization in coronal sections of cortex showing preferential CPN-gene expression in the deep layers V and VI. **(A''-D'')**, magnification of the areas boxed in **A'-D'**. Ages are as indicated in A'-D'. Scale bars: **A"-D"**, 100 μm.

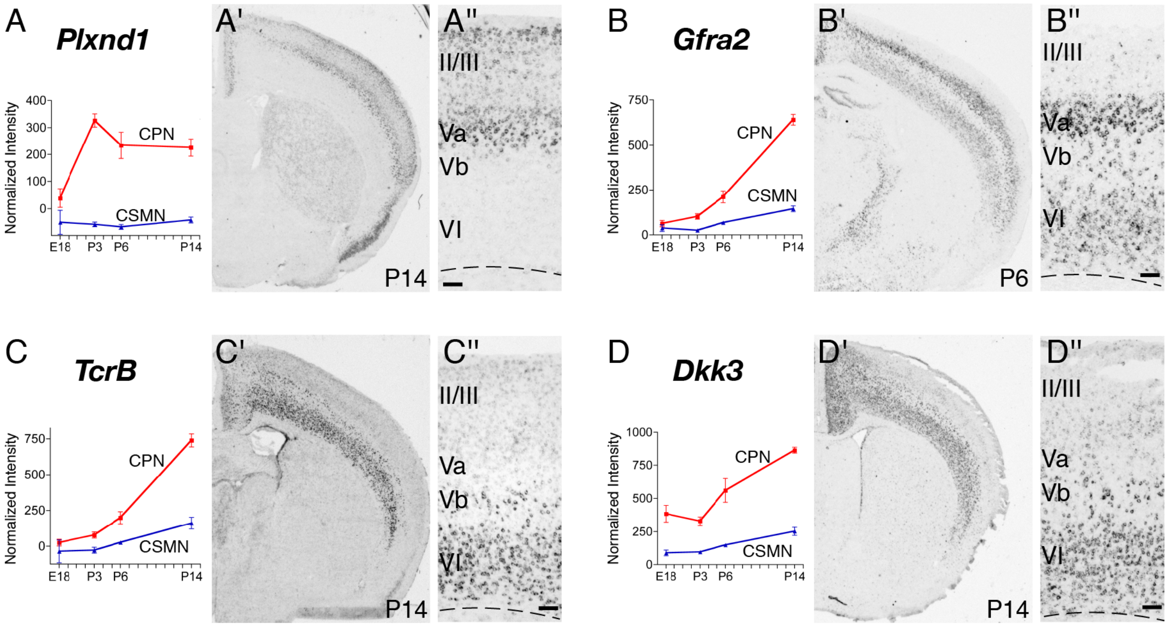

Figure 2.6 (Continued)

Figure 2.7: Specific expression of Plexin-D1 and Dkk3 in retrogradely labeled CPN of the deep layers V and VI.***A–H***, *Plexin-D1* is expressed by CPN of the deep layer V and not by CSMN.***A***, Fluorescent *in situ* hybridization for *Plexin-D1* (green) in a coronal section of P8 cortex demonstrates that it is expressed within CPN (red) identified via injection of CTB555 into contralateral cortex at P6. ***B–D***, Magnification of selected area from ***A*** reveals that essentially all *Plexin-D1*-expressing cells are CPN (arrows). ***E–H***, Fluorescent *in situ* hybridization for *Plexin-D1* (green) in a coronal section of P8 cortex demonstrates that it is not expressed in CSMN (red) identified retrogradely labeled via spinal cord injection of CTB555. ***F–H***, Magnification of selected area from ***E***, with the arrow indicating a CSMN that is adjacent to a *PlexinD1*-expressing cell (arrowhead). ***I–P***, *Dkk3* is expressed by CPN of the deep layers V and VI and not by CSMN. ***I***, Fluorescent *in situ* hybridization for *Dkk3* (green) in a coronal section of P8 cortex demonstrates that it is expressed in CPN (red) identified via injection of CTB555 into contralateral cortex at P6. ***J–L***, Magnification of selected area from ***I***, with arrows indicating *Dkk3*-positive CPN; notably, a subset of *Dkk3*-expressing cells are not retrogradely labeled. ***M***, Fluorescent *in situ* hybridization for *Dkk3* (green) in a coronal section of P8 cortex demonstrates that *Dkk3* is not expressed in CSMN (red) retrogradely labeled via spinal cord injection of CTB555.***N–P***, Magnification of selected area from***M***, with arrows indicating CSMN that do not express *Dkk3.* Scale bars: ***A***, ***E***, ***I***,***M***, 200 µm; ***B–D***, ***F–H***, ***J–L***, ***N–P***, 50 µm.

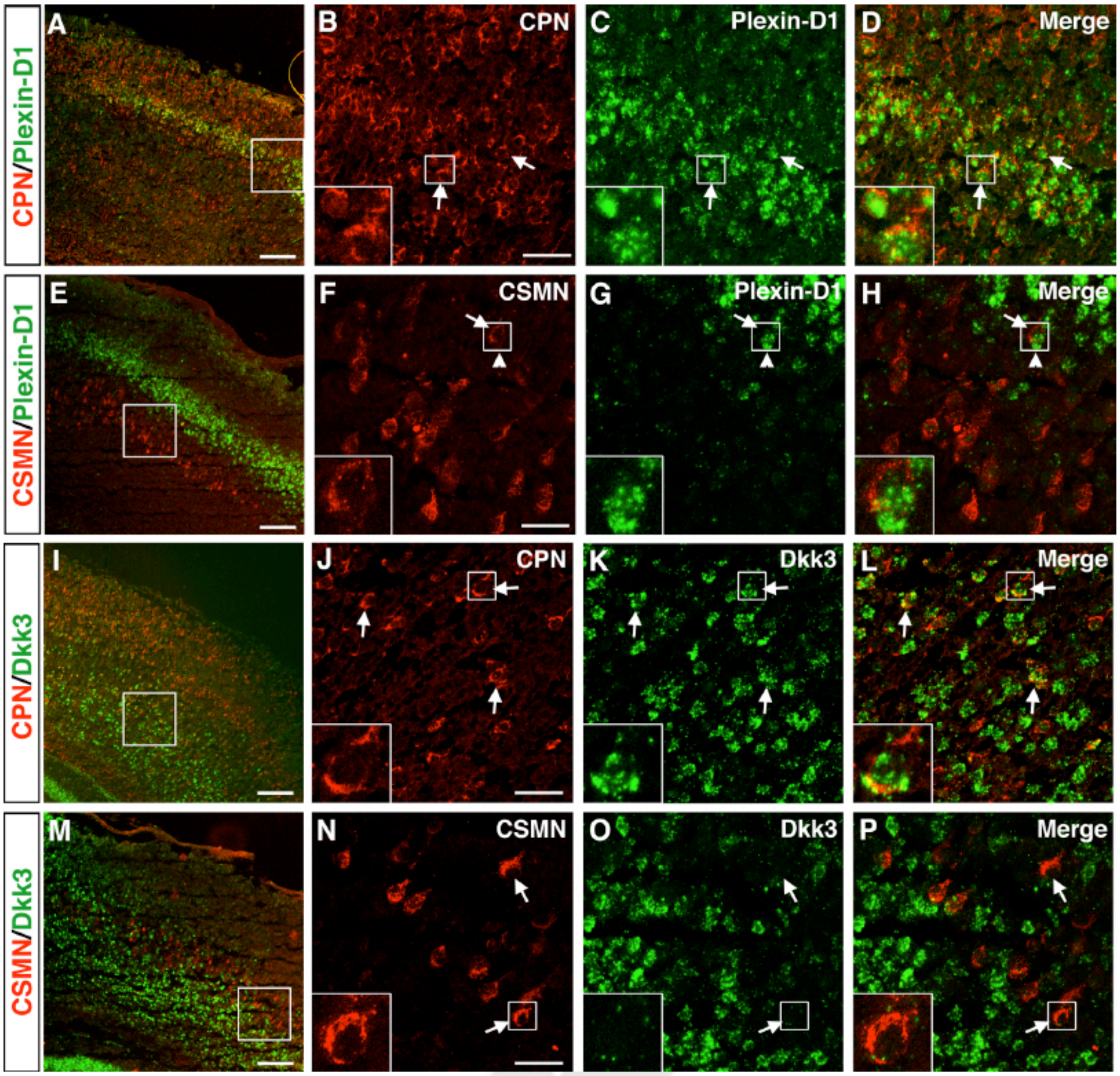

Figure 2.7 (Continued)

absence of *Plexin-D1* expression (Figure 2.3A). The relatively small population of CPN located in layer VI appears to express higher levels of *Gfra2, Tcrβ,* and *Dkk3* (Figure 2.6B-D), and lack *Plexin-D1*.

We further investigated cell-type-specific expression of the representative genes *Plexin-D1* and *Dkk3*.We find that *Plexin-D1* RNA is expressed at high levels within retrogradely labeled CPN in layer Va and at lower levels within CPN of more superficial layers (Fig. 2.7*A–D*). In contrast, retrograde labeling of CSMN demonstrates that they are located in layer Vb, below the *Plexin- D1*-positive layer Va. Of note, the border between these two layers is indistinct, with CSMN intermingled with *PlexinD1*-expressing CPN. Even at this interface, CSMN do not express *Plexin-D1*, clearly demonstrating the true cell-type specificity of this CPN marker. In addition, we examined the cell-type-specific expression of *Dkk3* and find that it labels a large portion of layerV and VI retrogradely labeled CPN (Fig. 2.7*I–L*), whereas layer V CSMN do not express *Dkk3* (Fig. 2.7*M–P*).

It is intriguing to note that each of the genes expressed highly and somewhat selectively in layer VI appears to label more cells than the number of CPN estimated to be located in this layer from many prior retrograde tracing experiments. This suggests 1) that each gene might also label other neuronal and glial types within layer VI, including perhaps the preponderant population of corticothalamic projection neurons of layer VI, and 2) that this layer VI subset (and perhaps other subsets) of CPN might be molecularly related to, or even evolutionary derived from, corticofugal projection neurons. Expression of genes such as Dkk3 with other CPN genes (e.g., *Hsbp3)* may be used to further delineate subtypes of CPN within deep cortical layers.

2.4 g. Combinatorial codes of genes define distinct subpopulations of CPN, and identify novel subdivisions of canonical cortical layers.

To directly compare the laminar and sublaminar distribution of individual CPN genes and to provide a first spatial map of combinatorial molecular expression by these distinct CPN subpopulations, we investigated the cellular level of expression of a selected set of CPN genes within the same brain. We chose genes that have distinct laminar distributions, also selecting for those that show a similar temporal expression, enabling detection and comparison at the same stage of development. We chose P6 as a mid-point in CPN development at which a large number of CPN-specific genes are expressed, and we performed *in situ* hybridization for all selected genes on 10 μm thick serial sections from the same brain (Figure 2.8 A). Cresyl violet staining of the first section of the series was used to distinguish canonical cortical layers at the histological level. For this analysis, we chose 8 representative genes: *Nectin-3, Cav1,* and *Chn2* (all expressed in distinct sub-lamina of layer II/III); *Hspb3* and *Lpl* (both expressed in layers II/III and V); *Plexin-D1* (expressed in layer Va); *Tmtc4* (expressed in layers II/III and Va); and *Dkk3* (expressed in layer VI). This series of *in situ* hybridizations allowed us to delineate the relative laminar location of the cells expressing each of the genes. For example, we found that, at P6, *Cav1*-expressing cells are overlapping with *Plexin-D1* labeling within layer Va . To investigate whether these partially overlapping gene expression domains reflect distinct populations of neurons expressing only one or a restricted combination of these genes, we performed double fluorescent *in situ* hybridization for a select set of genes at P8. We find that, indeed, with only *Lpl* and *Plexin-D1* expression, there exist three distinct populations of CPN, a superficial population expressing *Lpl* a deep population expressing *Plexin-D1,* and a middle population expressing both (Figure 2.8B). Additionally, even though *Hspb3* is expressed by CPN in layers II/III, and V, a very superficial portion of layer II/III is devoid of *Hspb3*-expressing neurons, but contains cells highly expressing *Inhba* (Figure 2.8C). This analysis reveals that distinct subpopulations of CPN can be identified at the molecular level that express unique combinations of these genes; these distinct CPN populations occupy different layers, and, in some cases, different sub-laminae of the same layer (Figure 2.8). Together, these results demonstrate that CPN are a molecularly diverse set of populations and suggest that functionally and connectionally distinct subgroups of CPN are defined during their differentiation by distinct combinatorial codes of gene expression that govern their development. These data provide a new “molecular anatomy” of CPN via the expression of genes that classify this highly diverse set of neuronal populations at the molecular level with a precision not previously possible using standard anatomical and histological criteria.

Figure 2.8: Combinations of genes identify CPN within sub-compartments of canonical cortical laminae. **(A)**, *in situ* hybridization at P6 for representative genes in sequential coronal sections of cortex from the same mouse, showing molecularly distinct populations of CPN identify subcompartments within the canonical cortical layers. Solid lines identify layers, and dotted lines identify subdivisions of the layers demarcated by CPN-gene expression. (B-C) Double fluorescent *in situ* hybridization at P8 for *Lpl* and *Plexin-D1* (B-B'), and *Inhba* and *Hspb3* (C-C') in coronal sections of P8 cortex demonstrates distinct laminar distributions of these CPN genes, with only partial overlap. Scale bars: B,C, 200 µm; B',C', 50 µm.

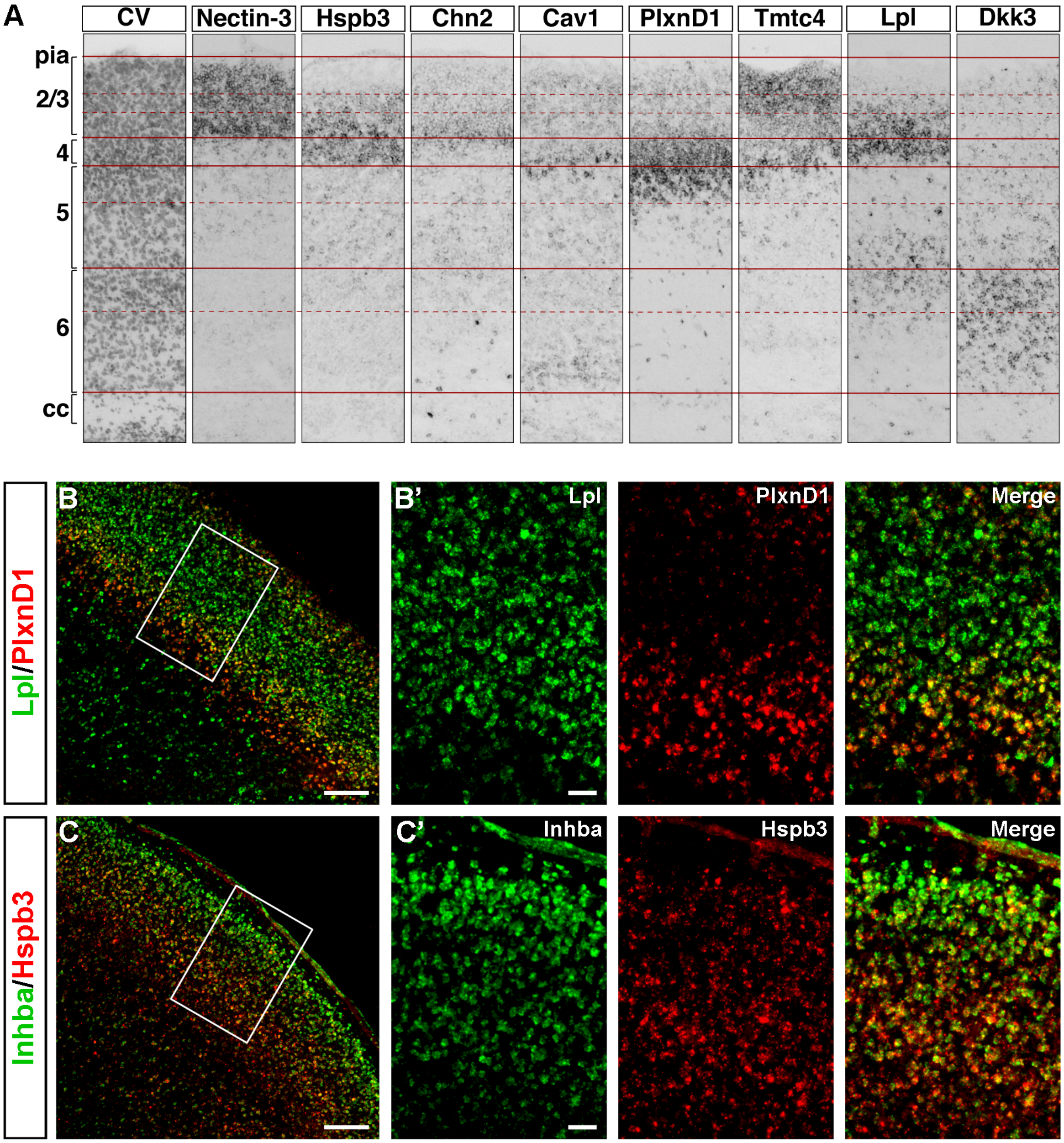

Figure 2.8 (Continued)

2.5 Discussion

Despite knowledge of the developmental and anatomical properties of some broad classes of projection neurons types of the cortex, the genes that distinguish individual neuronal lineages and that instruct their lineage-specific development are only beginning to be identified. We previously reported on the identification of genes that mark and control the development of the lineage of corticospinal motor neurons, a major corticofugal projection neuron population of layer V(Arlotta et al., 2005). Here we report on the identification of genes that identify at the molecular level the lineage of inter-hemispheric callosal projection neurons of the cortex.

Previous anatomical, histological, and birthdating analyses have highlighted the anatomical complexity and the cellular heterogeneity of the broad population of callosal projection neurons (Koralek et al., 1990; Conti and Manzoni, 1994; Reiner et al., 2003; Mitchell and Macklis, 2005; Ramos et al., 2008). However, detailed functional and molecular studies of different CPN subpopulations have been complicated by the heterogeneity of neuron types within individual cortical layers and by the scarcity of CPN-specific antigenic markers to identify them as they develop *in vivo*. Few genes have been reported that label neurons of the upper cortical layers (Molyneaux et al., 2007). These include *Satb2* a nuclear matrix protein that was recently reported to be a critical regulator of CPN development, controlling molecular events that induce the formation of callosal connections by CPN during corticogenesis (Britanova et al., 2005; Szemes et al., 2006). In the absence of *Satb2*, postmitotic neuroblasts that are normally destined to become CPN of layers II/III begin to express *Ctip2,* a gene required for the formation of projections to subcerebral targets, and extend axons through the internal capsule instead of through the corpus callosum (Alcamo et al., 2008; Britanova et al., 2008). Other genes, such as *Cux1, Cux2 (Nieto et al., 2004; Zimmer et al., 2004),* and *Unc5d (Tarabykin et al., 2001; Zhong et al., 2004; Sasaki et al., 2008),* are expressed in the SVZ during the generation of upper layer neurons and, postnatally, in neurons of the upper layers. Finally, genes with broader patterns of expression in different neuronal layers have been reported to label neurons in the upper layers of cortex. These include *Lhx2*, a gene that is critical for the specification of the dorsal progenitor domain that gives rise to the cortex, and that postnatally labels layer II/III (Bulchand et al., 2001; Bulchand et al., 2003); *Gpr6,* a marker of postnatal layers II/III-IV (Chenn et al., 2001); *Brn1* and *Brn2*, two markers of layer II/III-V neurons that regulate differentiation and migration of these layers (McEvilly et al., 2002; Sugitani et al., 2002); and *Kitl* and *Dtx4,* markers of layers II/III-IV (Zhong et al., 2004), among others. While these genes can identify the upper cortical layers, their patterns of expression are typically too broad to identify individual neuronal populations within these layers, and it is not currently known whether they specifically label CPN among other upper layer neuron types. Further, there is a paucity of genes that specifically identify CPN of the deep layers, and distinguish them from corticofugal neurons located within the same layers.

Here we provide the first demonstration that distinct classes of callosal neurons can be defined *in vivo* based on the expression of different molecular markers, suggesting distinct molecular controls over their subtype-specific development, connectivity, and function. Some of the CPN genes are expressed by most callosal neurons, spanning layers II/III, V, and VI (e.g. *Lpl, Hspb3*), suggesting that they may play broader roles during the development of all callosal neurons. In contrast, other genes are more restricted to only callosal neurons of selected layers: for example *Cpne4, Btg1, Inhba, Gm879, Tmtc4* are expressed in layer II/III, while *PlexinD1, Gfra2, Tcrβ,* and *Dkk3* mark CPN of the deep layers V and VI. Our data reveal the presence of callosal neuron subpopulations that were not previously recognized at the anatomical and histological levels, by demonstrating that different subtypes of callosal projection neurons can be identified by combinations of molecular markers within subdivisions of the same canonical lamina. The identification of genes that uniquely define distinct callosal subpopulations will now make it possible to investigate the function and connectivity of individual subpopulations via genetic manipulation and targeting of distinct callosal projection neuron types.

Interestingly, we find that callosal projection neurons of the upper layers (II/III) exhibit a higher degree of molecular heterogeneity than those located in the deep layers (V and VI), as indicated by the fact that CPN located in different portions of layer II/III express different genes. For example, genes including *Grsp1, Nnmt, EphA3* and *Cav1* all selectively label CPN located in the most superficial portion of layer II/III, while genes including *Nectin-3, Chn2,* and *Ptn* are preferentially restricted to the deeper part of the same layer. Of note, a number of layer-specific genes have been identified via large-scale *in situ* efforts, including the Allen Brain Atlas (http://www.brain-map.org). Interestingly, examination in the Allen Brain Atlas of the expression profile of the CPN genes identified here reveals that some of these genes maintain layer-specific expression in the adult. For these genes, our data extend these layer-specific expression data to provide an indication of the neuron types that express the individual genes. Many other genes are not identified in the Allen Brain Atlas as layer-specific in the adult, further supporting functional roles during embryonic and early postnatal stages of CPN development. Finally, a small number of the CPN genes reported here (e.g., *Lhx2* and *COUPTF1*) have been shown previously to be expressed only in restricted cortical areas (Nakagawa et al., 1999; Liu et al., 2000), suggesting that additional CPN populations might be distinguished at different rostrocaudal and mediolateral locations. In the future, it will be useful to further define the boundaries of arealization of the CPN genes reported here.

It is interesting to speculate that the presence of a molecularly more diversified population of callosal neurons in the superficial layers of the rodent cortex might reflect the early stages of the expansion and diversification of these layers that occurred during evolution of the primate cortex. Since the divergence of reptiles, birds, and mammals, the cortex has undergone substantial radial expansion, with major addition of new neurons within the superficial cortical layers II-IV of mammalian species (Reiner, 1991; Marín-Padilla, 1992; Aboitiz and Montiel, 2003). For example, the reptilian cortex has only three layers, thought to be homologous to layers I, V and VI of the six-layer mammalian cortex, and they lack neurons with properties of mammalian upper layer projection neurons (Reiner, 1991). Among mammals, the primate cortex exhibits further expansion; the six canonical layers seen in rodents and lower mammals have enlarged to include new subdivisions that can be easily distinguished at the histological level (Rakic and Kornack, 2001). Of particular note is the subdivision of the expanded layer II/III of the rodent into the multiple histologically distinct layers and sublayers seen in primates.

While these layers cannot be distinguished at the histological level in the rodent, it is intriguing to speculate that our identification of genes that mark neurons located in distinct radial positions within layer II/III might support the hypothesis that the specialization of distinct populations of CPN within upper layers is already occurring in the rodent cortex both molecularly and almost certainly with regard to connectivity and function. Future work that investigates the expression of the genes identified here within the cortex of primates will likely provide important insight into the evolution of the neocortex. This subject is further investigated in Chapter 3 of this dissertation.

The expansion of the superficial layers during cortical evolution has been accompanied by the expansion of a new germinal zone, the subventricular zone (SVZ), and by the appearance of intermediate progenitors within the SVZ that are fated to produce neurons of the upper layers(Smart and McSherry, 1982; Martinez-Cerdeno et al., 2006; Molyneaux et al., 2007). This is in contrast to reptiles and birds, in which cortical neurogenesis occurs only in the ventricular zone (VZ)(Cheung et al., 2007). In mammals, it is now becoming clear that VZ progenitors give rise to neurons of the deep cortical layers, while SVZ progenitors largely generate the upper cortical layers (Tarabykin et al., 2001; Wu et al., 2005). In agreement with existing data, we find that callosal neurons of the deep cortical layers (V and VI) express a unique set of genes (e.g. *Tcrβ, Dkk3*) that are not expressed by callosal neurons of the upper layers, likely reflecting the different evolutionary origin of these two populations.

The data presented here provide the first molecular classification of the callosal projection neuron population in the cortex. Distribution analysis of the newly identified CPN genes reveals the presence of molecularly distinct subpopulations that were not previously described at the histological, morphological, or anatomical levels. This likely reflects the distinct origin of different callosal neuron subpopulations, and it might be predictive of their evolutionary diversification in higher mammalian species. It is likely that distinct combinations of molecular developmental controls define key aspects of CPN diversity – subtype-specific differentiation, axon collateralization, synaptic connectivity, and physiologic function – underlying their central roles in interhemispheric association and connectivity. Together, these data provide the foundation for future studies in which molecular and genetic approaches can be combined with anatomical and cellular data to dissect the mechanisms of development of the diverse and likely functionally critical populations of callosal projection neurons.

Funding

This work was partially supported by grants from the NIH (NS41590, NS45523) and the Harvard Stem Cell Institute to J.D.M.. P.A. was supported by a Claflin Distinguished Scholar Award, the Harvard Stem Cell Institute, and the ALS Association. B.J.M. was supported by the Harvard M.S.T.P. and the United Sydney Association. R.M.F. was partially supported by a National Science Foundation Graduate Research Fellowhsip Program (GRFP) fellowship and a National Institutes of Health predoctoral NRSA fellowship F31 NS073136.

Acknowledgments

We thank A. Meleski and K. Quinn for technical assistance; U. Berger for assistance with *in situ* hybridization; D. Dombkowski for assistance and advice on FACS methods; Z. Riley for assistance and advice on fluorescent *in situ* hybridization; J. Menezes and members of the Macklis lab for suggestions and critical reading of the manuscript.

Chapter 3:

Cited2 functions broadly in early intermediate progenitor cell development and in somatosensory callosal projection neuron identity acquisition

Author contributions: This project was an equal collaboration between Jessica L. MacDonald, PhD, a post-doctoral fellow, and me. We jointly designed all experiments and interpreted all data. Jessica performed the bulk of the protein localization work and quantification of cellular number and neocortical lengths, while I selected the gene candidate, performed the bulk of the retrograde labeling experiments, ISH, confocal imaging, and quantification of density, neocortical thickness, and axonal extension and density.

3.1 Abstract

The development of diverse neuronal populations with precise projections for refined patterns of connectivity within the neocortex is essential to its proper function and processing of information. Neocortical excitatory neurons are diverse in the location of their cell bodies, input received from other neurons, and targets of axonal connectivity. In addition to these diverse qualities that define a variety of neuronal types, functional area differences convey additional sybtype specificity to neocortical neuronal populations. Callosal projection neurons (CPN) reside in neocortical layers II/III, V, and VI; extend axons to the contralateral hemisphere across the midline; and connect through all functional areas of the neocortex to integrate sensory and motor information. While molecular controls over neuronal type specification and areal patterning have begun to be explored, there has been no identification and characterization of gene products that function throughout cortical development to integrate both areal and neuron-type information into a definable neuronal subtype. Here we report that the transcriptional co-activator CITED2 (Cbp/p300-interacting transactivator with aspartic acid (E), glutamic acid (D), rich carboxy-terminal domain, family member 2) is required early and broadly for correct neocortical intermediate progenitor number, and later specifically for acquisition of somatosensory (SS) CPN identity. In this later role, CITED2 might act as an integrator of projection neuron subtype identity and areal identity in the specific subpopulation of SS CPN.

3.2 Introduction

Recent investigations into neocortical neuronal diversity have identified many genetic controls both over functional areal specification (O'Leary and Nakagawa, 2002; Rash and Grove, 2006; O'Leary et al., 2007; Joshi et al., 2008), and over neuronal-type specification and developmental fate acquisition(Arlotta et al., 2005; Molyneaux et al., 2005; Molyneaux et al., 2007; Alcamo et al., 2008; Britanova et al., 2008; Molyneaux et al., 2009); however, very little is known about the intersection of areal and neuronal-type identity acquisition and, what, if any, genetic controls function specifically to define areal identity within a specific neuronal population. Callosal projection neurons (CPN) are distributed throughout all functional neocortical areas in rodent, and connect homotypic regions of the two hemispheres to enable interhemisphereic communication and information integration. Therefore, dependent on the areal location of their cell bodies, CPN send distinct projections transmitting assorted information, making them a unique population to address the question of molecular controls over areal subpopulations of neuronal types.

As described in more detail in Chapter 1, specification of neocortical functional areas is a complex, progressive process involving early broad gradients of morphogens and gene expression, refined by functional input and molecular interactions to fully segregate functional areas throughout the process of areal specification. Simultaneous to this arealization process, neuronal type specification and maturation occurs. Additive overlap of molecular controls over these two processes has been shown to induce areal subpopulations of neuronal types. In the case of *AP2-γ* function, *AP2-γ* is expressed broadly in cortical progenitors, and only by overlapping with an arealizing rostro-caudal gradient, such as the one exhibited by *Pax6,* is it required specifically for caudal visual cortex CPN development(Pinto et al., 2009). However, genes that function to integrate this subtype and areal information into a single subpopulation identity likely exist, and would be critical to generate the level of neuron type diversity utilized in complex neocortical function. Areal differences are obvious histologically throughout the neocortex, and CPN have been specifically shown to exhibit area-specific properties in primates, including differential

Figure 3.1: CPN areal diversity **(A)** Schematic representation of the rough distribution of primary neocortical functional areas at P6 as viewed from above and in a sagittal section. **(B)** Schematic representation of differences in axonal fiber thickness across the rostro-caudal extent of the human adult corpus callosum. P, postnatal day; OB, olfactory bulb; Crb, cerebellum; Roman numerals indicate neocortical layer; F, frontal; M, motor; Ss, somatosensory; A, auditory; TP, temporoparietal; V, visual. **(B)** Adapted and expanded from (Aboitiz and Montiel, 2003), with data from(Aboitiz et al., 2003),(Aboitiz et al., 1992b),(Aboitiz et al., 1992a).

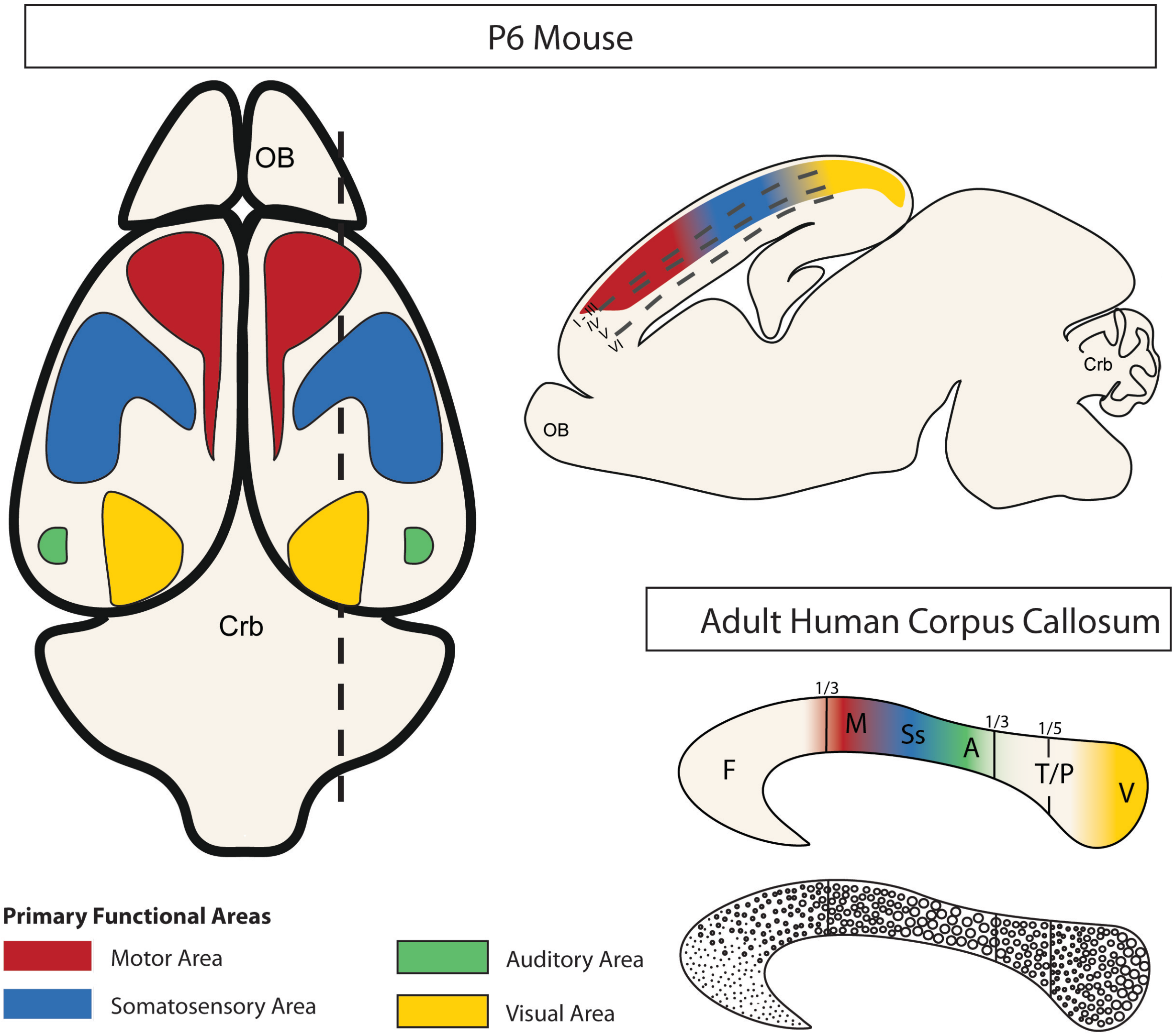

Figure 3.1 (Continued)

axonal thickness and myelination in various areas (Figure 3.1). This known areal diversity further motivates investigation of areal- and subtype-specific controls over CPN identity acquisition.

As areal and subtype identity acquisition proceeds, timing of action is of particular importance for controlling progressive development of neocortical neurons. Gene expression varies over time to act in distinct processes, and single gene products can act at multiple times in different contexts to perform many unique, discrete functions. Examples of differential context-dependent gene function are ubiquitous, though one specific example pertinent to CPN development and identity acquisition that acts critically in neocortical development is the compound action of transcription factor *cut-like homeobox 2 (Cux2)*. *Cux2* is expressed by a subset of dividing cells in the SVZ during generation of superficial layer neurons, and postnatally by some neurons of layers II-IV. Early in cortical development, *Cux2* has been found to be critical for proliferation of intermediate progenitors, while, postmitotically, *Cux2* regulates neuronal maturation, specifically dendritic arborization and synapse formation(Nieto et al., 2004; Zimmer et al., 2004; Cubelos et al., 2007; Cubelos et al., 2010). Thus, maintaining parsimony, gene products have multiple distinct context-dependent purposes in neocortical neuronal development.

One gene highly expressed by CPN, *Cited2*(Cbp/p300-interacting transactivator with aspartic acid (E), glutamic acid (D), rich carboxy-terminal domain, family member 2), is poised to act broadly early, then specifically as an integrator of subtype and areal identity later in development. *Cited2,* like *AP2-γ*, is expressed throughout cortical areas early in development, but, unlike *AP2-γ*, its expression refines to somatosensory cortex postnatally. Far from being a pan-somatosensory control, *Cited2* has previously been identified to be significantly more highly expressed by CPN than by other projection neuron populations (Chapter 2 and (Molyneaux et al., 2009)). CITED2 (also known as MRG1 or P35srj) is a transcriptional coactivator with no DNA binding domains, but with the ability to recruit histone modifying elements, such as the CPB histone acetyltransferase, and link them to one of its many identified DNA-binding partners, regulating their activity. The three other members of the CITED family, CITED1, CITED3, and CITED4 have similar functionalities, but with distinct binding partners.

They are divergent except for three conserved homology domains, one of which (CR2) is required for binding the transcriptional co-activator CBP/p300(Rodriguez et al., 2004). CITED3 is not part of the mammalian genome, however CITED1 and CITED4 have identified functions in mouse. CITED2 has been shown to act in the development of other systems including heart, kidney, neural crest, lens, liver, thymus, and sex determination(Bamforth et al., 2001; Qu et al., 2007; Val et al., 2007; Chen et al., 2008; Michell et al., 2010), and it exhibits abnormal copy number variation (CNV) in a subset of autism spectrum disorder (ASD) patients(Szatmari et al., 2007). In the non-neuronal systems listed above, identified roles of CITED2 can be divided into functional pathway categories, including a general convergence of CITED2 action in pathways critically involved in cell proliferation, differentiation, mobility, and survival (e,g, CITED2 activates TFAP2 (AP2)(Bamforth et al., 2001) and PPARγ(Tien et al., 2004; Gonzalez et al., 2008; Li et al., 2012); co activates WT1 pathways(Val et al., 2007; Buaas et al., 2009); downregulates HIF-1α via binding partner competition(Xu et al., 2007); and is downregulated by TGFβ (including Nodal)(Bamforth et al., 2004; Chou, 2006; Chou and Yang, 2006b; Chou et al., 2012)). All of the above listed interactors are expressed in developing neocortex(Visel et al., 2004), but have no specifically explored neocortical function. Both TGFβ and PPARγ signaling pathways are critical for progenitor proliferation, survival/death, mobility, and differentiation in other systems (Bottner et al., 2000; Roberts-Thomson, 2000; Chou et al., 2012). TFAP2 has been shown to be involved with eye, face, neural crest, neural tube, and limb development(Zhao et al.; Chou and Yang, 2006a), while WT1 signaling regulates mRNA splicing or metabolism to specifically control cell development and survival(Val et al., 2007). Therefore, we hypothesized that *Cited2* likely functions in processes of proliferation, survival, and/or differentiation of CPN within the neocortex.

Several interactors of CITED2 with DNA-binding transcription factor properties have already been implicated in neocortical development, and are expressed in neocortex concurrently with CITED2. Some of these include AP2γ {Braganca, 2003 #2631}(Pinto et al., 2009), Lhx2(Porter et al., 1997; Glenn and Maurer, 1999), and PAX6(Englund et al., 2005; Chen et al., 2008). AP2γ controls developmental regulation of caudal visual cortex CPN(Braganca et al., 2003; Pinto et al., 2009). Lhx2 regulates early cortical hem and neocortical identity(Porter et al., 1997; Glenn and Maurer, 1999). PAX6 controls early neocortical arealization, and radial glia progenitor identity and function(Englund et al., 2005; Chen et al., 2008). In addition, CITED2 has been shown to interact genetically with the critical neocortcical control gene coactivator LIM-domain only 4 (LMO4)(Huang et al., 2009; Michell et al., 2010; Asprer et al., 2011). Thus, CITED2 interacts with a number of critical neocortical developmental controls; this further supports its potential to play critical roles in specific neocortical projection neuron development.

I hypothesize that specific properties of unique CPN subpopulations are controlled progressively, including post-mitotically, on top of a more “default” CPN identity. These progressive steps translate areal identity to specific neuronal subtype identity, and are controlled by genes with the ability to integrate multiple overlapping signals into one specific neuronal subtype identity. To address this hypothesis directly, I investigated function(s) of the transcriptional co-activator CITED2 in broad early CPN development, and in developmental acquisition of unique properties of somatosensory (SS) CPN.

3.3 Materials and Methods

3.3 a. Mouse Lines

C57/Bl6 wildtype mice were obtained from Charles River Laboratories (Wilmington, MA, USA), and were used for retrograde label, Western blotting, and determining gene expression.

Cited2 null mice (C2D) (Bamforth et al., 2001) and *Cited2* conditional floxed mice (C2f) (Preis et al., 2006)were a generous gift from Professor Sally Dunwoodie at the Victor Chang Cardiac Research Institute in Darlinghurst, Australia.

The following PCR primers and genotyping protocols were used:

C2Δ:

WT: F: 5’- GGC CAA ACT GCT TAA TCT TGT- 3’
R: 5’- GAA ATG TTT GCC ACT GAC GA -3’
Product size: ~350bp

Neo: F: 5’-GAC AAC CCC CCC CAA ATG ACT GAC-3’
R: 5’-GGC GAT GCC TGC TTG CCG AAT ATC-3’
Product size: ~650bp

C2f (transgenic):

F: 5’ - GTC TCA GCG TCT GCT CGT TT - 3’
R: 5’- CTG CTG CTG TTG GTG ATG AT -3’
Product sizes: WT: ~166bp
Floxed allele: ~210bp

The following cycling parameters were used: initial denaturation at 94°C for 4 min., denaturation at 94°C for 30 sec., annealing at 58°C for 30 sec., and extension at 72°C for 30 sec. (C2f) or 45 sec. (C2Δ), for 35 cycles, followed by extension for 10 min. (C2f) or 2 min. (C2Δ) at 72°C. The products were separated by gel electrophoresis on a 4% (C2f) or 2% (C2Δ) agarose gel.

Mice with Cre recombinase under the *Emx1* promoter element were generated by (Gorski et al., 2002b) and obtained from The Jackson Laboratory (Bar Harbor, Maine, USA), strain number 005628.

Cre: 5'- TAG CAC CGC AGG TGT AGA GAA GG -3'
5'- CAG ACC AGG CCA GGT ATC TCT GA -3'
Product size: ~300 bp

WT: 5'- GAA GGG TTC CCA CCA TAT CAA CC -3'
5'- CAT AGG GAA GGG GGA CAT GAG AG -3'
Product size: ~500 bp

The following cycling parameters were used: initial denaturation at 94°C for 3 min., denaturation at 94°C for 30 sec., annealing at 65°C for 45 sec., and extension at 72°C for 45 sec. for 33 cycles, followed by extension for 3 min. at 72°C. The products were separated by gel electrophoresis on a 1.5% agarose gel.

3.3 b. Immunocytochemistry

For embryonic tissue collection, timed pregnant females were anesthetized with a lethal dose of Avertin (1.25% 2-2-2 tribromoethanol in 0.63% isoamyl alcohol), death was confirmed by cervical dislocation, and embryos were removed from the uterine horns. Embryos were anesthetized by hypothermia, and the whole head was fixed in 4% paraformaldehyde (PFA) overnight at 4°C, rinsed 3 times for 10 min. in 0.1 M phosphate buffered saline (PBS, pH 7.35), and stored in 0.025% sodium azide in PBS (PBS-azide). Postnatal pups were anaesthetized by hypothermia (P6 and younger) or with a lethal does of Avertin (P7 and older), and mice were perfused transcardially with PBS followed by 4% PFA, post-fixed overnight in 4% PFA at 4°C, and stored in PBS-azide until sectioning. For DAPI and BrdU labeling, brains were cryoprotected overnight in 30% sucrose in 0.1M PB [81mM dibasic sodium phosphate, 18.9 mM monobasic sodium phosphate], and then sectioned on a CM3050S cryostat (Leica Microsystems, Wetzlar, Germany) to a thickness of 14µm in Tissue Freezing Medium (TBS-Triangle Biomedical Sciences). For all other assays, brains were sectioned at 50 µm coronally or sagittally on a VT1000S vibrating microtome (Leica Microsystems).

Antigen retrieval methods were required to expose antigens for some of the primary antibodies, including TUJ1. Sections were incubated in 0.1M citric acid (pH=6.0) for 10 mi. at 95-98°C, and sections were rinsed in PBS prior to blocking. For thymidine analogues (IdU, CldU, BrdU), HCl antigen retrieval was required. Tissue was rinsed quickly in ddH_2O, incubated in 4N HCl for 10 min. at room temperature, treated as described above with 0.1M citric acid, and sections were then rinsed in PBS prior to blocking.

Floating sections were incubated for 30 min. at room temperature in blocking solution (0.3% BSA [Sigma, St. Louis, MO], 0.3% Triton X-100 [Sigma], and 8% goat or donkey serum in 0.025% PBS-azide) before incubation in the primary antibody diluted in blocking solution overnight at 4°C. Primary antibodies and dilutions were used as follows: goat anti-β−galactosidase, 1:2000 (Biogenesis 4600-1409); rabbit anti-Ki67, 1:500 (Abcam ab15580); goat anti-LMO4, 1:200 (Santa Cruz Biotech SC-11122), rabbit anti-TBR2 1:500 (Abcam ab23345); mouse anti-TUJ1,1:500 (Covance mms-435P); mouse anti-PCNA 1:1000 (Sigma WH0005111M2); rabbit anti-activated caspase 3, 1µg/mL (Becton Dickinson 557035); rat anti-CTIP2 1:500 (Abcam ab18465); mouse anti-BrdU, 1:750 (Chemicon); rabbit anti-GFP, 1:500 (Molecular Probes). Sections were washed (3 times 10 min. in PBS) prior to incubation for 3 hours at room temperature in secondary antibodies. Appropriate secondary antibodies were selected from the Molecular Probes Alexa series (Invitrogen, Carlsbad, CA). After incubation, sections were washed again (3 times 10 min. in PBS), counterstained for 1 min. in 1:10,000 4',6-diamidino-2-phenylindole (DAPI) when needed, rinsed in 0.033M PB [27mM dibasic sodium phosphate, 6.3mM monobasic sodium phosphate], and mounted with the aqueous-based Fluoromount-G (Southern Biotech. Inc, Birmingham, Alabama) on Superfrost ® glass slides (Fisher Scientific, Pittsburgh, PA).

3.3 c. In situ hybridization

Nonradioactive colorimetric *in situ* hybridization was performed using probes labeled with digoxigenin (dig)-UTP. Sense probes were used as negative controls in all experiments.

For *in situ* hybridization, fixed (4% PFA) tissue was either sectioned on a CM3050S cryostat (Leica Microsystems) to a thickness of 14μm, as detailed above, or vibratome sectioned on a VT1000S vibrating microtome (Leica Microsystems) to a thickness of 50 μm, as described above. Sections were then mounted on Superfrost plus slides ® (Fisher Scientific) and were postfixed in 4% PFA in PBS for 10 min., rinsed in PBS for 3 min., permeabilized in 0.3% Triton X-100 (Sigma) followed by RIPA cell lysis buffer [150 mM Sodium chloride, 1% Triton X-100, 1% deoxicholic acid sodium salt, 0.1% sodium dodesil sulfate, 50 mM Tris-HCl, pH 7.5, 2mM EDTA], re-fixed in 4% PFA, acetylated for 15 min. in 0.1M triethanolamine/ 0.4% HCl/0.25% acetic anhydride (Sigma), and then preybridizied in 65°C hybridization buffer [50% formamide, 5x SSC, 5x Denhardts [1μg/mL Ficoll 400, 1μg/mL Polyvinilpyrrolidone, 1μg/mL BSA] , 500μg/mL sheared salmon sperm DNA, 250μg/mL Yeast RNA]. Slides were incubated overnight (14-20 hours) at 65°C in 2μg/17mL dig-labeled probe in hybridization buffer in a plastic mailer. Slides were then subjected to stringency washes in 2x SSC/ 50% formamide/ 0.1% Tween-20 at 65°C for 2 hours. Sections were then rinsed in MABT [0.9M maleic acid (Sigma), 0.1M NaCl (Sigma), 0.0005% Tween 20 (Sigma), 0.175M NaOH (Sigma)] at RT, blocked in 10% goat serum in MABT, and incubated overnight in goat alkaline phosphatase-conjugated anti-dig (1:1000, Roche) primary antibody in block. The following day, the slides were rinsed with MABT, followed by a 30 min. wash in alkaline phosphatase reaction buffer [100mM Tris pH 9.5, 50mM $MgCl_2$, 100mM NaCl, 0.1% Tween-20]. The alkaline phosphatase reaction was developed with 0.25 mg/mL nitro-blue tetrazolium (NBT) / 125μg/mL 5-bromo-4-chloro-3'-indolyphosphate (BCIP) in phosphatase reaction buffer, changing to fresh solution every 1-4 hours at RT or every 6-9 hours at 4°C. When the reaction was judged complete (48-100 hours), tissue was rinsed in 0.1% Tween-20 in PBS, postfixed in 4% PFA for 30 min, counterstained for 1 min. in 1:10,000 4',6-diamidino-2-phenylindole (DAPI), and rinsed in 0.033M PB [27mM dibasic sodium phosphate, 6.3mM monobasic sodium phosphate]. Slides were coverslipped with Fluromount ® (Sigma), dried, and edges were protected with clear nailpolish.

The probes were synthesized as described in previous publications: *Cited2*(Molyneaux et al., 2009), *Rorβ, EphrinA5 ((*Allen Brain Atlas Resources, http://www.brain-map.org))*, Eph A7* (Mori et al., 1995), *Cadherin8*(Joshi et al., 2008).

3.3 d. Retrograde labeling of cortical projection neurons

For retrograde projection neuron labeling, P2-P4 pups were anesthetized by hypothermia. Axons were labeled with Alexa555-conjugated cholera toxin subunit B (CTB-555) (2 mg/ml, Molecular Probes, Carlsbad, CA), using a pulled glass micropipette (tip diameter 80-100μm) under ultrasound guided microscopy. For CPN, axons were labeled from the corpus callosum on the contralateral hemisphere with three injection sites along the rostro-caudal axis of the neocortex, each consisting of 10 injections of 4.6 nl each, starting in the white matter, then retracting through the grey matter in a step-wise fashion. For retrograde labeling of CSMN, CTB-555 was injected into the corticospinal tract at cervical vertebrae segment (C2/C3). Six injections of 32 nl per injection site were performed on each side of the midline. Mice were transcardially perfused for analysis at P6, as outlined previously.

3.3 e. Fluorescence activated cell sorting (FACS)

FACS purification was performed essentially as described in (Arlotta et al., 2005) and(Molyneaux et al., 2009), and summarized in Chapter 2.

3.3 f. Western blotting

Immunoblotting was performed as described previously (Cowan et al., 2001; Macdonald et al., 2010). Briefly, neocortical tissue, FACS purified neurons, or HEK cells were isolated. Protein was extracted using 1% sodium dodecyl sulfate (SDS, Sigma) in PBS. Protein homogenates were separated by 10% SDS–polyacrylamide gel electrophoresis, and transferred to nitrocellulose membrane (Bio-Rad Trans-Blot). Membranes were blocked for 1 hour at room temperature with 5% nonfat milk in Tris-buffered saline (TBS), and incubated for 12–20 hours at 4 °C in the following primary antibody diluted in in 2% milk/TBS: sheep anti-CITED2 (R&D Systems, Minneapolis, MN). Membranes were then washed three times for 5 min. each in 0.1% Tween-20 in TBS, and incubated for 1 hour at room temperature in peroxidase-coupled goat anti-rabbit IgG (BioRad) diluted in 2% milk/TBS. Signals were detected with chemiluminescence (Pierce, Rockford, IL).

3.3 g. In utero electroporation

In utero electroporations were performed essentially as described in (Saito and Nakatsuji, 2001) and (Molyneaux et al., 2005). For all *in utero* experiments, the morning of vaginal plug detection was designated as E0.5. At age E15.5, C57/Bl6 or *Cited2 floxed* pregnant mice were deeply anesthetized with Avertin, abdominal hair was removed, and mice were placed on a heating pad for the duration of the surgery and recovery period. A small incision was made at the midline through the skin, a vertical midline laparotomy was performed along the abdominal wall *linea alba*, and the skin and abdominal wall were gently separated using blunt dissection techniques on intervening fascia. 690 nl of purified DNA (1.5 - 2 µg/ µl, endotoxin-free) with 0.005% Fast Green FCF (Sigma) for immediate visualization of injected DNA, and 0.1% DiI for postnatal detection *in vivo* of electroporated pups, were injected under guidance by ultrasound backscatter microscopy into the lateral ventricle (Vevo 770, VisualSonics). Five pulses of 30 volts each of 50 ms duration at 1 second intervals were delivered into the ventricular zone progenitors at the desired orientation using 5 mm diameter CUY650-P5 platinum electrodes (Protech International, San Antonio, Texas) and a Nepa Gene CUY21EDIT square wave electroporater (Nepa Gene, Japan). Non-sequential embryos along each horn (excluding the two closest to the birth canal) underwent DNA delivery and electroporation.

3.3 h. Birthdating

For BrdU birthdating, equimolar delivery of IdU (57.5 mg per kg) or CldU (42.5 mg per kg) at E15.5 was performed(Vega and Peterson, 2005), calculating embryonic age with E0.5 as the morning of observed vaginal plug. We euthanized and perfused mice at P3, and prepared brains for immunocytochemistry. To assess migration of neocortical cells born at E15.5, the neocortical thickness was divided into six equal bins (see Figure 3.15). Superficial layers were denoted as the 2 most superficial bins; validation with CUX2 immunocytochemistry confirmed alignment with layer II/III.

5.3 i. Microscopy and image analysis

Whole mount images were acquired using an SMZ1500 fluorescence dissecting microscope (Nikon, Melville, NY) with a SPOT CCD digital camera (Diagnostic Instruments, Sterling Heights, MI) and SPOT acquisition software.

Tissue sections were imaged on a Nikon E1000 microscope (Nikon Instruments, Melville, NY) equipped with an XCite 120 illuminator (EXFO, Mississauga, ON, Canada) and Q-imaging Retixa EX cooled CCD camera (Q-imaging Corp., Surrey, BC, Canada), or a Nikon 90i microscope using a 1.5 megapixel cooled CCD digital camera (Andor Technology, Dublin, Northern Ireland), or a 5 megapixel color CCD digital camera (Nikon Instruments, Melville, NY). Images were collected and analyzed with Volocity image analysis software (Version 4.0.1; Improvision Inc., Waltham, MA) or Elements acquisition software (Nikon Instruments, Melville, NY). Laser confocal analysis was performed using a BioRad Radiance 2100 confocal microscope with LaserSharp2000 imaging software (BioRad Laboratories, Hercules, CA).

Images were processed using a combination of functions provided by ImageJ (Rasband, W.S., ImageJ, U. S. National Institutes of Health, Bethesda, Maryland, USA, http://imagej.nih.gov/ij/, 1997-2011.) and Adobe Photoshop/ Illustrator software packages (Adobe, San Jose, CA).

3.3 j. Cortical thickness/length quantification

All length and thickness measurements were performed with images of matched sagittal 50μm sections using ImageJ to trace with the curvature of the neocortical surface being measured. Length of E15.5 CP and VZ, N=5 per genotype, was normalized to average of WT. P3 whole mount diagonal length, N=5 per genotype, was normalized to average of WT. P21 cortical length, N=3 per genotype, was normalized to average of WT. Functional areal lengths at P3, (N=5 per genotype), P0 (N=3 per genotype), and P8 (N=5 per genotype), were measured at 4 medio-lateral levels (labeled a, b, c, d; see Figure 3.11). Motor cortex was determined by rostral region expressing high levels of LMO4 in superficial layers; somatosensory cortex was determined by region not expressing LMO4 in superficial layers; and caudal regions were delineated as caudal region expressing high levels of LMO4 in superficial layers. For analysis of SS cortical length with multiple markers, N=4 per genotype, *in situ* hybridization for *Cadh8*-negativity, *EphA7*-negativity*, EphrinA5*-positivity*, and Rorβ*-positivity were used to delineate SS cortex. p-values were calculated using the unpaired two-tailed Student's t-test.

Neocortical thickness at P3, N=4 per genotype, were measured in matched sagittal 50μm sections. Superficial layers were defined as cellular layers superficial to CTIP2 expression (layers II-IV), and deep layers were defined as cellular layers including CTIP2 expression and deeper (layers V-VI). Areas were determined as described above using LMO4 immunoreactivity. p-values were calculated using the unpaired two-tailed Student's t-test.

3.3 k. Axonal quantification

Sections were matched with respect to electroporation location in sensory cortex and matched 50 μm sections where the CC, hippocampus, and AC were all visible at P3 or P8 were selected for analysis. P3 axonal extension, N=4 *Cited2 fl/wt* and N=5 *Cited2 fl/fl*, ratio was calculated normalized to the number of electroporated axons entering whitematter tracts and expressed as a ratio in comparing *Cited2 fl/fl* to

Cited2 fl/wt controls. P8 axonal extension, N=5 per genotype, ratio was calculated normalized to the number of electroporated axons entering contralateral grey matter after crossing through the CC, and expressed as a ratio in comparing *Cited2 fl/fl* to *Cited2 fl/wt* controls. p-values were calculated using the unpaired two-tailed Student's t-test.

3.3 l. Tbr2-positivity, cell proliferation and death, and cellular density quantification

Cell death was quantified at E15.5, N=6 *Cited2cKO* and N=11 *Cited2wt* controls, using immunopositivty for activate cleaved caspase 3. The mitotic fraction was defined as $PCNA^+$ cells, and the postmitotic fraction was defined as $PCNA^-$ cells.

Neocortical cellular density at P3, N=3 per genotype, was measured in matched sagittal 14 μm cryosections stained for DAPI to mark nuclei and immunolabeled for LMO4 and CTIP2 to mark areas and laminae. Superficial layers were defined as described above, using CTIP2 immunoreactivity, neocortical functional areas were defined as described above using LMO4 immunoreactivity. Boxes of standard width were digitally placed over images and volume was calculated using 14 μm thickness, measured laminar thickness for each sample, and 280 μm wide box; and is expressed as cells/100 μm^3. p-values were calculated using the unpaired two-tailed Student's t-test.

3.4 Results

3.4 a. Cited2 is expressed by a restricted population of CPN and excluded from CSMN

Cited2 is more highly expressed by CPN relative to CSMN in the developing neocortex, with a peak of expression as early as retrograde labeling can be used for the purification process (E18.5) (Molyneaux et al., 2009) (Figure 3.2A). We confirmed and more deeply investigated *Cited2* expression by developmental Western blotting, revealing even higher CITED2 expression at E15.5 (Figure 3.2 B); and with retrograde label confirming that *Cited2* is expressed by CPN and excluded from CSMN at P3 (Figure 3.2 C). Developmental *in situ* hybridization reveals that there is no pallial expression of *Cited2* at E13.5, but CITED2 is highly expressed in developing cortex during early CPN development at E15.5, with expression decreasing as differentiation proceeds. Postnatally, *Cited2* expression is maintained in neocortical layers II/III, V, and VI (Figure 3.3). Closer evaluation of the peak E15.5 expression both via *in situ* hybridization and using β-galactosidase expression under the control of the *Cited2* promoter (*Cited2-LacZ*)(Bamforth et al., 2001) reveals that, at E15.5, *Cited2* is most highly expressed in the Tbr2-expressing subventricular zone (SVZ), and mostly excluded from the Ki-67-expressing proliferating ventricular zone (VZ) (Figure 3.4). Embryonically, *Cited2* is expressed across the rostro-caudal extent of neocortex, largely as immature neurons exit the cell cycle and begin migrating, with cortical expression becoming much more restricted to CPN of somatosensory (SS) cortex by P3 (in layers II/III and V) (Figure 3.5). This expression pattern suggests that *Cited2* might function broadly in early specification and development of CPN, and might have an areally-restricted developmental function in postnatal SS cortex.

3.4 b. Cited2 function is not required for early corticogenesis (E10-E15.5)

We performed experiments to investigate development of CPN in *Cited2* null neocortex, both as a general population, and specifically within SS cortex, where *Cited2* expression becomes progressively restricted. To bypass a set of early patterning defects in homozygous *Cited2* null mutants(Bamforth et al., 2001), and to eliminate any role *Cited2* might have in the subpallial domain, we generated forebrain-specific conditional knockouts using *Emx1*-promoter driven cre-recombinase (*Emx1-Cre*)(Guo et al., 2000; Jin et al., 2000) to recombine a floxed locus surrounding the entirety of the *Cited2* translated sequence (exon2) (Figure 3.6). *Emx1* expression begins in the forebrain at E9.5 medially and encompasses the full extent of forebrain by E11 (Yoshida et al., 1997), and therefore bypasses neural tube closure defects and defects in other organ systems including heart and kidney(Bamforth et al., 2001), but removes *Cited2* function before corticogenesis begins. In all experiments, we compared *Cited2 fl/fl*; *Emx1-Cre*+ conditional knockout mice (cKO) to littermate controls, both *Cited2 fl/fl*; *Emx1-Cre*-, and *Cited2 fl/wt*; *Emx1-Cre*+. Because no significant differences were observed between the two control genotypes, they were combined as *Cited2* WT in most analyses.

Because *Cited2* is highly expressed throughout the SVZ at E15.5, the peak of superficial layer CPN birth, we first examined the development of the *Cited2* cKO neocortex at this age. Careful analysis of early neocortical establishment indicates that there is no change in the length or thickness of the cortex, length of the proliferative zone, or thickness of postmitotic Tuj1+ immature migrating neurons ($p>>0.05$) (Figure 3.7). In addition, there is no change in the overall number of proliferating progenitors (Figure 3.8). These results support expression data that *Cited2* is most highly expressed by neocortical cells at E15.5, and confirms specificity of the conditional null scheme with precise excision enabling proper neural tube closure and robust formation of early neocortical progenitor domains.

3.4 c. Cited2 function is required for regulation of Tbr2+ intermediate progenitors in E15.5 neocortex.

While there is no overt change in cortical size or progenitor or post-mitotic domain length/ thickness in the E15.5 *Cited2* conditional null neocoertex, we specifically investigated whether the population of Tbr2+ intermediate progenitor cells (IPCs), which most highly express *Cited2* at E15.5, are altaered in the absence of *Cited2* function. Directed analysis of this population reveals that there is a reduction in the number of IPCs at all regions sampled across the rostro-caudal axis (24% reduction, $p=0.007$) (Figure 3.8). Since a reduced number of Tbr2+ IPCs could be the result of reduced IPC production, IPC death,

Figure 3.2: *Cited2* is developmentally expressed by CPN and excluded from CSMN

(A) Comparative microarray analysis at critical times in development (E18.5, migration; P3, process extenstion; P6, target finding; and P14, connectivity refinement) detects *Cited2* as more highly expressed by a retrogradely labeled, FACS purified population of CPN (red line) than by CSMN (blue line). Error bars indicate standard deviation. **(B)** CITED2 is expressed most highly early in development, as detected by CITED2 immunoblotting. **(C)** Retrograde label combined with *in situ* hybridization confirms comparative microarray data that *Cited2* is expressed by CPN, and excluded from CSMN at P3.

CSMN, corticospinal motor neurons; CPN, callosal projection neurons; E, embryonic day; P, postnatal day. Panel **(A)** taken from Molyneaux, Arlotta, et al. *J. Neurosci.* 2005.

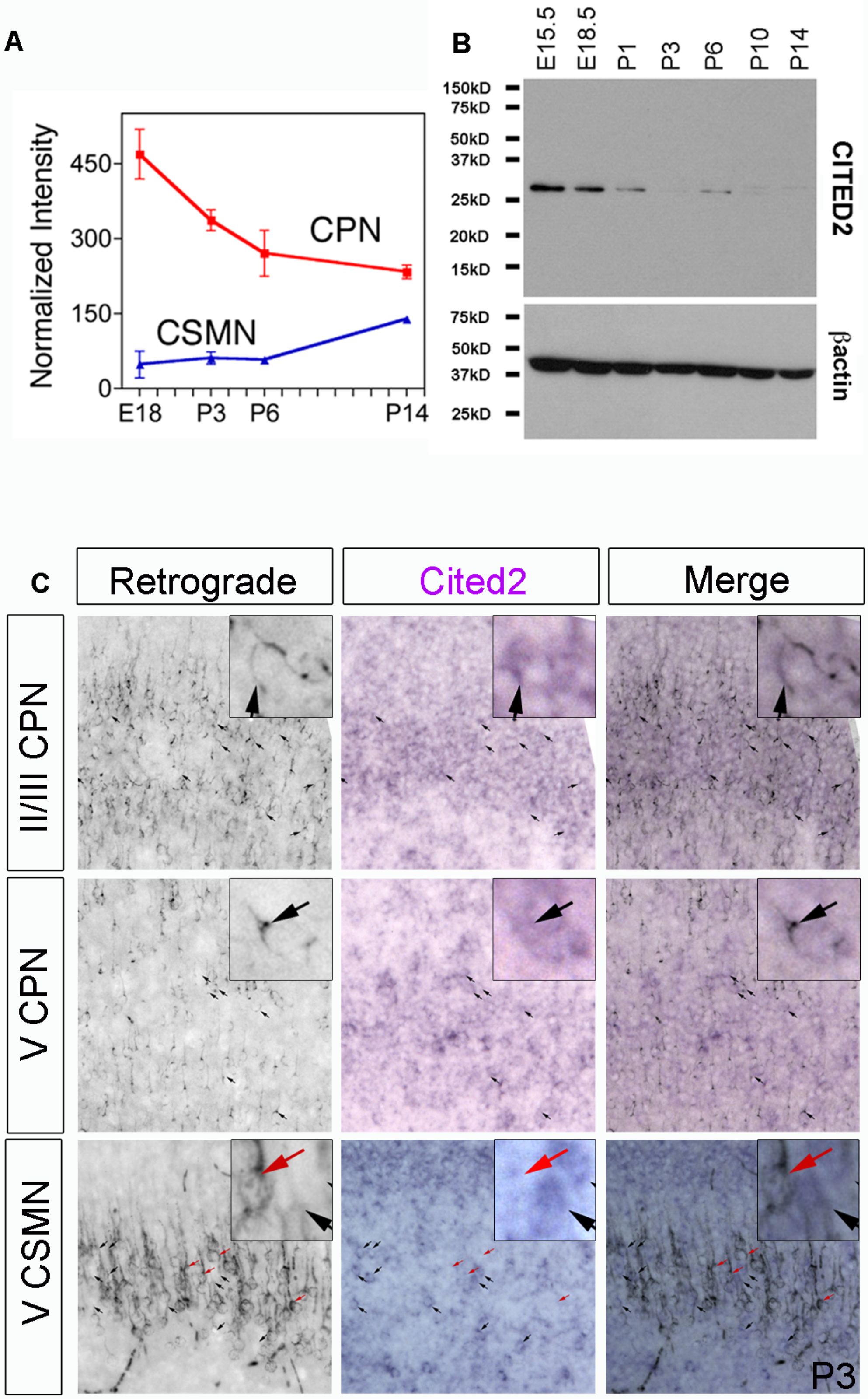

Figure 3.2 (Continued)

Figure 3.3: ***Cited2*** **is expressed at early and mid-stage CPN development (A)** *Cited2* is excluded from pallial progenitors at E13.5, but is expressed in subpallial regions. **(B, C)** At E15.5 and E18.5, *Cited2* is highly expressed in both pallial and subpallial ventricular/ peri-ventricular domains. **(D-F)** Postnatally, *Cited2* is expressed neocortical layers II/III and V, and along the lateral ventricle and in hippocampus.

Scale bars (A, B, C) 500 μm, (D, E, F) 1mm, (D’, D”,E’, E”, F’, F”) 100 μm. E, embryonic day; P, postnatal day.

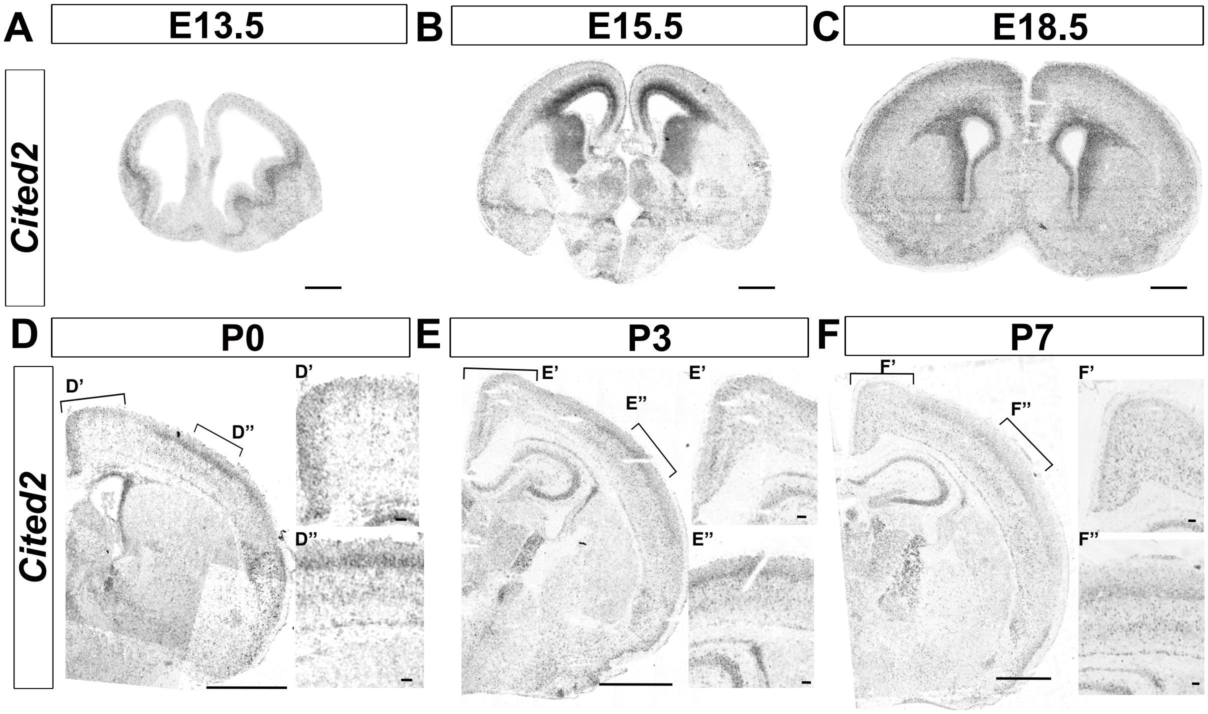

Figure 3.3 (Continued)

Figure 3.4: At E15.5, peak time of neocortical *Cited2* expression, *Cited2* is most highly expressed in immature neurons of the SVZ. (A) *in situ* hybridization for *Cited2* reveals that the highest levels of *Cited2* expression are just basal to the VZ, likely the SVZ. **(A')** magnification of region in **A (B)** Immunocytochemistry against β-galactosidase (red) under the *Cited2* promoter in *Cited2* heterozygous mice reveals that most CITED2-expressing cells are outside of the Ki67-expressing mitotic zone and overlap with the popultion of Tbr2-expressing intermediate progenitors.

Scale bars: **(A)** 1mm, **(A'-B)** 200μm SVZ, subventricular zone; VZ, ventricular zone; LV, lateral ventricle; E, embryonic day; P, postnatal day

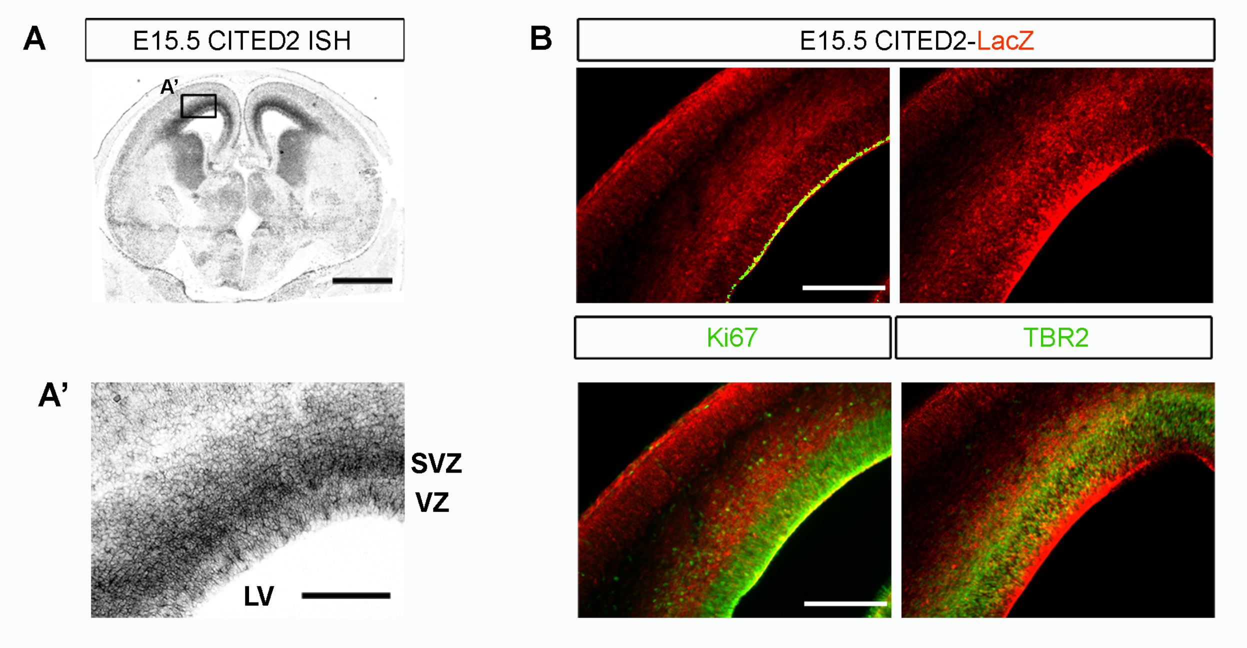

Figure 3.4 (Continued)

Figure 3.5: *Cited2* expression becomes progressively restricted to sensory neocortical areas (A-A") *Cited2* is expressed evenly across the rostro-caudal axis embryonically (E18.5) (arrowheads), but **(B-B")** becomes restricted to SS (arrows) and far caudal cortex postnatally (P3). CP = cortical plate, LV = lateral ventricle

CP, cortical plate; LV, lateral ventricle; SVZ, subventricular zone; VZ, ventricular zone; Roman numberal indicate neocortical layers; E, embryonic day; P, postnatal day. Scale bars (**A, B, A', B'**) 1mm, (**A",B")** 100 μm.

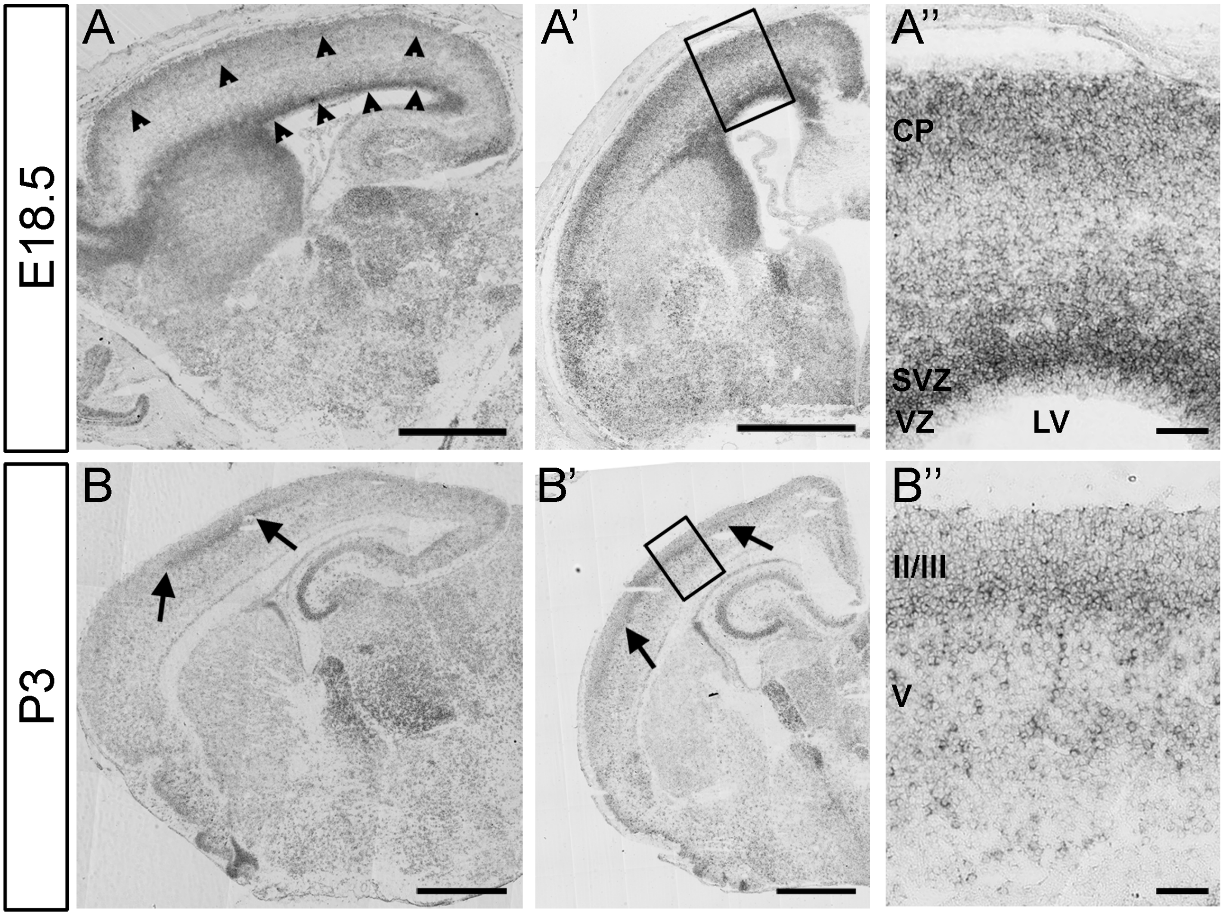

Figure 3.5 (Continued)

Figure 3.6: Conditional deletion of *Cited2* via *Emx1* driven cre recombinase expression results in specific loss of *Cited2* expression in the forebrain (A) Schematic representation of conditional knockout (cKO) approach for *Cited2* in the neocortex using floxed *Cited2* alleles and the *Emx1*Cre line. **(B)** This approach yields forebrain specific loss of *Cited2* mRNA in noecortex (arrows) and hippocapus, but subpallial expression (here in the thalamus), is maintained. Shown here at P3. **(B')** Reported showing *Emx1* Cre excision pattern.

WT, wildtype; IRES, internal ribosomal entry site; CreRecom, Cre Recombinase; UTR, untranslated region; cKO, conditional null. (B') Taken from (Gorski et al., 2002a)

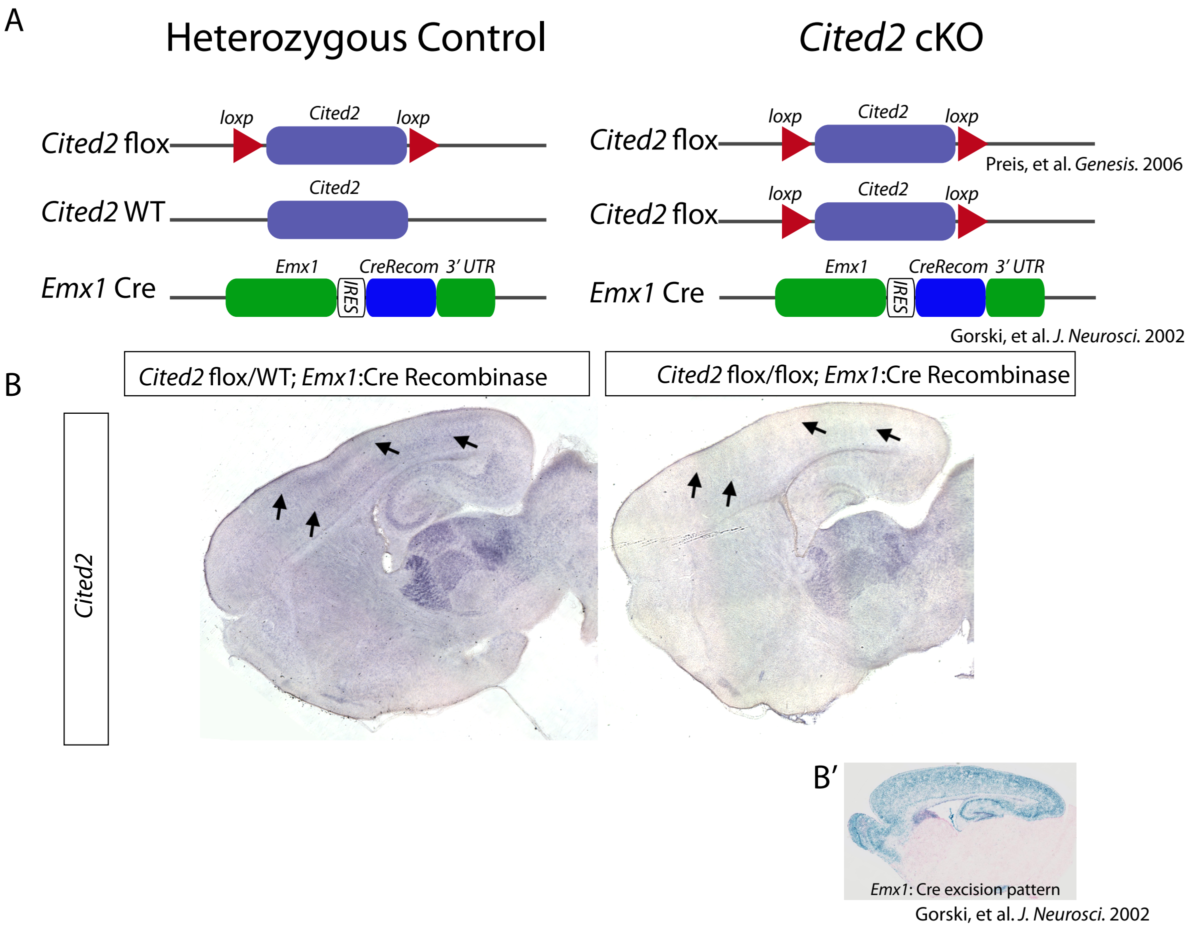

Figure 3.6 (Continued)

Figure 3.7: Specific reduction in IPCs in E15.5 *Cited2* cKO (A) At E15.5, *Cited2* cKO cortex (light grey) has no change in cortical or progenitor domain length or thickness compared to WT cortex (dark grey) (N=5). **(B)** At E15.5, *Cited2* cKO cortex (light grey) has no change in thickness of Tuj1-positive region of immature post-mitotic migrating neurons.

White bars in (A) indicate motor, SS, and caudal region analyzed in (B).

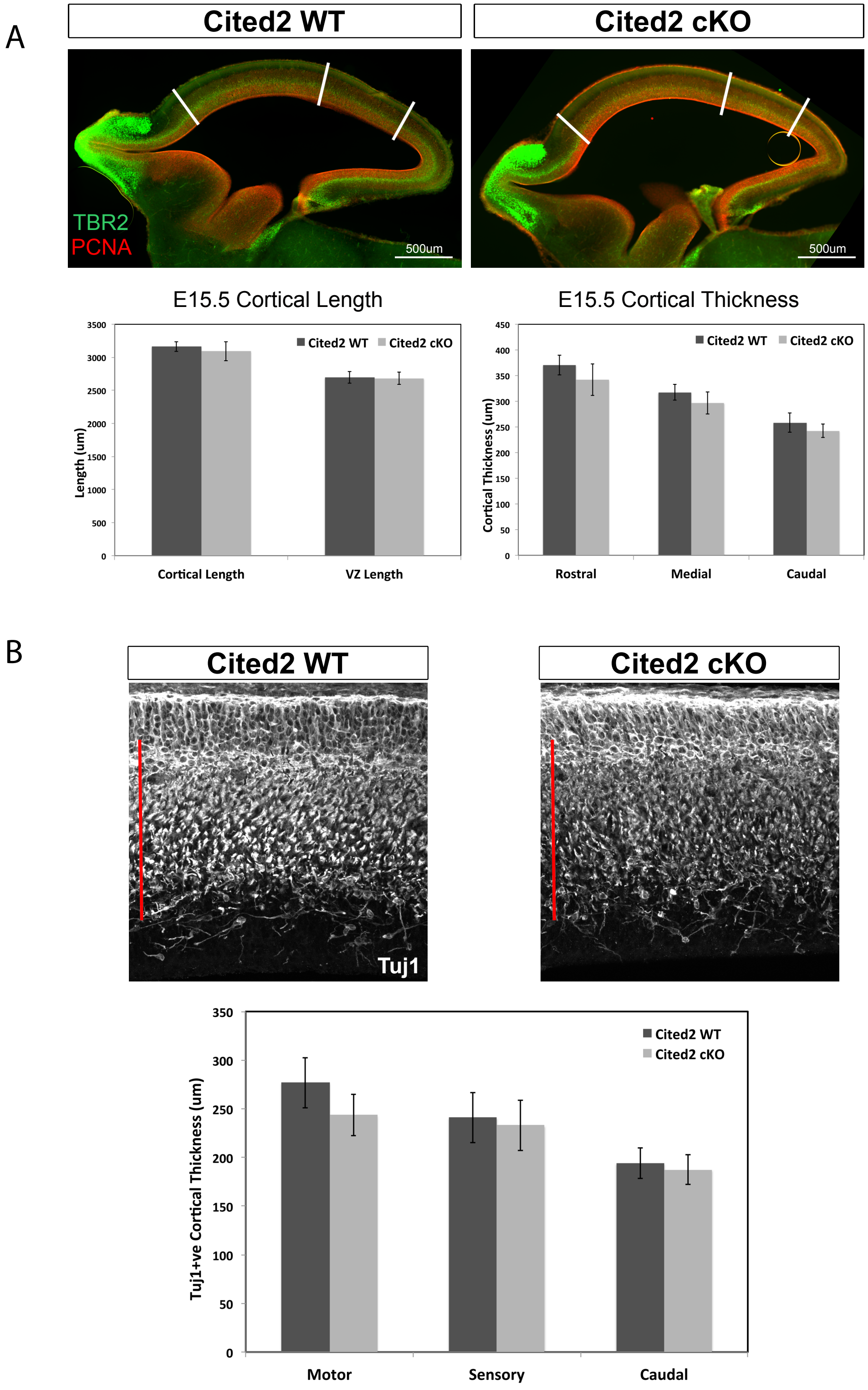

Figure 3.7 (Continued)

Figure 3.8: Loss of *Cited2* function results in a loss of Tbr2+ intermediate progenitors at E15.5

Cited2 cKO is not changed in number of PCNA+ proliferative progenitors, but there is a reduction of Tbr2+IPCs (24% reduction, N=6 cKO and 11 WT, p=0.007).

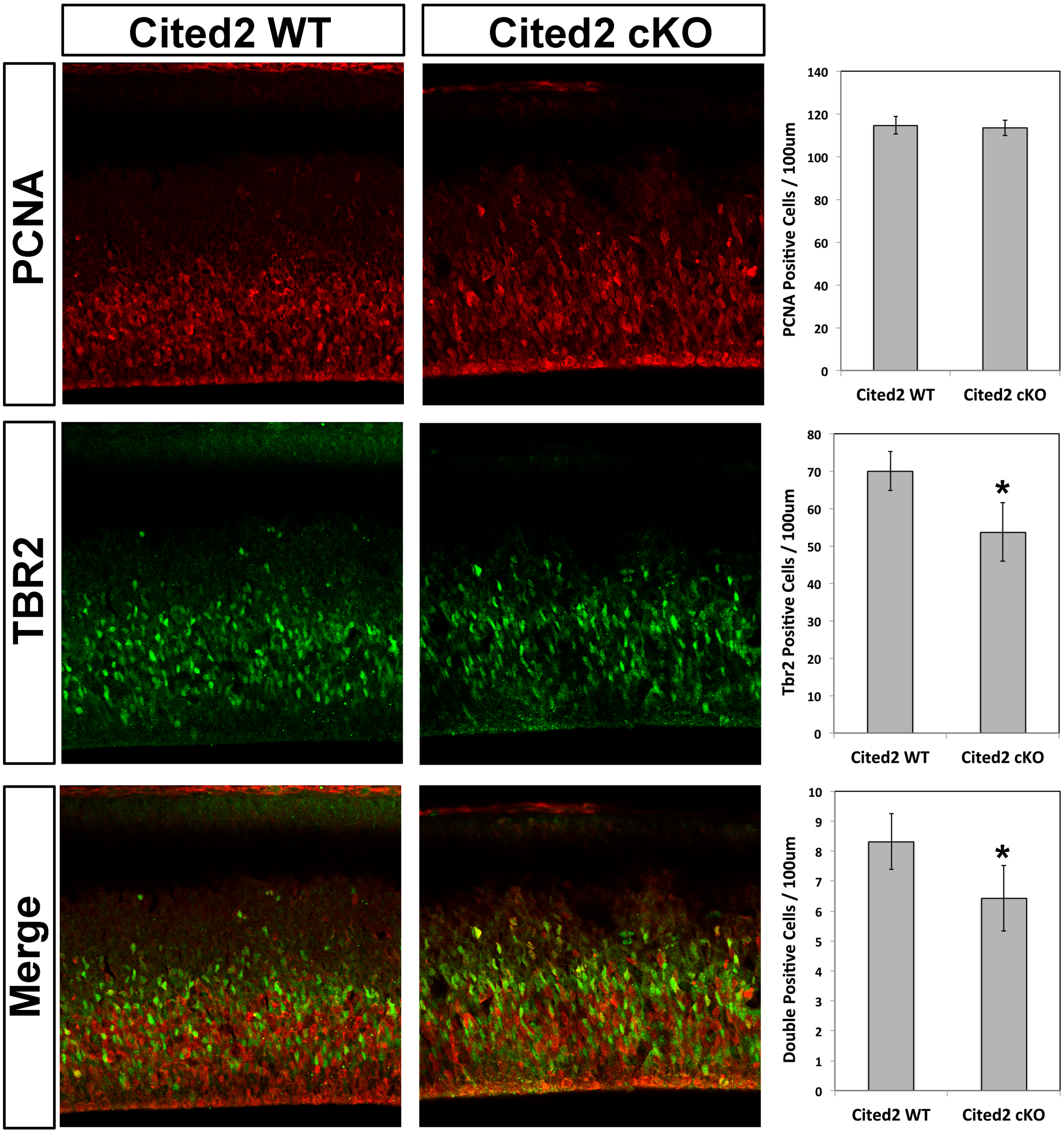

Figure 3.8 (Continued)

loss of IPC maintenance, or a combination of two or three of these processes; we investigated whether any of these processes are affected by loss of *Cited2* function. We began by asking if there is increased cell death in E15.5 developing *Cited2* cKO cortex. Indeed, we found that there is almost double the cell death in E15.5 *Cited2* cKO cortex than WT (p= 0.0006), evenly distributed between mitotic progenitors and post-mitotic neurons (Figure 3.9). However, this increase in death does not likely account for all of the loss of Tbr+ IPCs, and birthdating analyses are currently underway (see Discussion).

3.4 d. Reduced superficial layer thickness in somatosensory and occipital Cited2 cKO neocortex.

Superficial layer CPN arise predominantly from IPCs; therefore, we investigated whether there is a postnatal reduction in superficial layer CPN, resulting either radially in a change in the thickness of the superficial layers, and/or tangentially in the cortical length. Additionally, because the majority of mouse CPN (~80%) reside in layers II/III, and they are the predominant projection neuron subtype in this layer, measurement of thickness of the superficial layers provides a relative approximation of CPN number. Analysis of neocortical layer thickness at P3 reveals a significant reduction in superficial layer thickness (including layers II/III and IV) in the LMO4-negative SS area (17% reduction, p=0.02), and caudal occipital cortex (caudal: 10% reduction, p=0.01; far caudal: 25% reduction, p=0.007), with no apparent change in motor cortex (p=0.11), or within deep layers (where CPN account for only a minority of projection neurons) (Figure 3.10). These data suggest that the reduction in Tbr2+ IPCs observed early in the development of *Cited2* null neocortex is not recovered, and is translated to reduction in superficial layer neurons. Additionally, these results indicate that CPN in different cortical areas are differentially affected by loss of CITED2 function, suggesting that CITED2 might interact with area-specific transcriptional co-activators and/or target genes.

3.4 e. Reduced neocortical length specifically in somatosensory areas of Cited2 cKO neocortex.

In addition to radial reduction in cKO neocortex, early loss of Tbr2+ progenitors could also result in neocortical length decrease on the tangential axis. Measurements of cortical surface length at P3 reveal a

5% smaller cKO diagonal cortical length than WT (p=0.02) (Figure 3.11A). This translates to a 10% reduction in rostro-caudal length in P3 *Cited2* cKO neocortex (p=0.0006) (Figure 3.11B). These data indicate that, not only is there a significant loss in cortical thickness as a result of *Cited2* loss of function, likely through the early reduction of Tbr2+ progenitors along with additional *Cited2* function throughout corticogenesis, it also results in significant reduction in neocortical tangential length. This ~10% loss of cortical length is not recovered, and the *Cited2* cKO neocortex is still significantly shorter at P21 than that of WT littermates (10% reduction, p=0.005) (Figure 3.11C), indicating that the reduction is not a delay in maturation, but a persistent loss of ~10% of the neocortical rostro-caudal length.

Due to restricted *Cited2* expression to SS cortex, and functional areal differences observed upon analysis of *Cited2* cKO neocortical thickness, we also investigated whether there is areal specificity in *Cited2* cKO cortical length reduction. Analysis based on three broad cortical areas divided by LMO4 expression at P3(Joshi et al., 2008) indicates that there is a highly specific and substantial reduction (28% reduction, p=0.003 SS; versus p=0.3 motor and p=0.9 for caudal) in the rostro-caudal length of only SS *Cited2* cKO cortex, resulting in an overall reduction in cortical length (Figure 3.12). At P0, before motor and sensory cortical areas are refined, *Cited2* cKO neocortical length is already reduced in mixed sensory-motor areas. (12% reduction motor, p=0.08; 17% reduction SS, p=0.002). At P8, the specific reduction in somatosensory cortical length is maintained in *Cited2* cKO compared to WT (28% reduction, p=0.0005).

To avoid relying on expression of a single gene as full indication of a neocortical area, we confirmed the SS-specific reduction of cortical length in P3 *Cited2* cKO mice using independent molecular markers of cortical areas. Strikingly, superficial layer measurements of SS cortex length (*Cadh8* (19% reduction, p=0.01), *EphrinA5* (17% reduction, p=0.0009), *EphA7* (13% reduction, p=0.01)) confirmed the reduced length observed with LMO4 measurements, while measurements of acallosal layer IV SS cortex (*EphrinA5*, p=0.25; and *Ror*β, p=0.6) did not detect a significant difference in SS cortex in the *Cited2* cKO (Figure 3.13). These results indicate a highly specific and significant disruption of superficial layer SS cortex in the absence of *Cited2* function, likely SS CPN development.

Figure 3.9: Loss of *Cited2* function results in increased cell death at E15.5 (A) Image of ac-3 immunocytochemistry at E15.5 in WT and **(B)** *Cited2* cKO littermates. **(C)** At E15.5, *Cited2* cKO cortex (light grey) has an increased number of cells undergoing apoptosis compared to WT cortex (dark grey) (~50% reduction, N=6 cKO and 11 WT, p=0.0006). Error bars indicate standard error of the mean.

Scale bar: 100 μm. WT, wildtype; cKO, conditional null; E, embryonic day; ac3, activated (cleaved) caspase-3

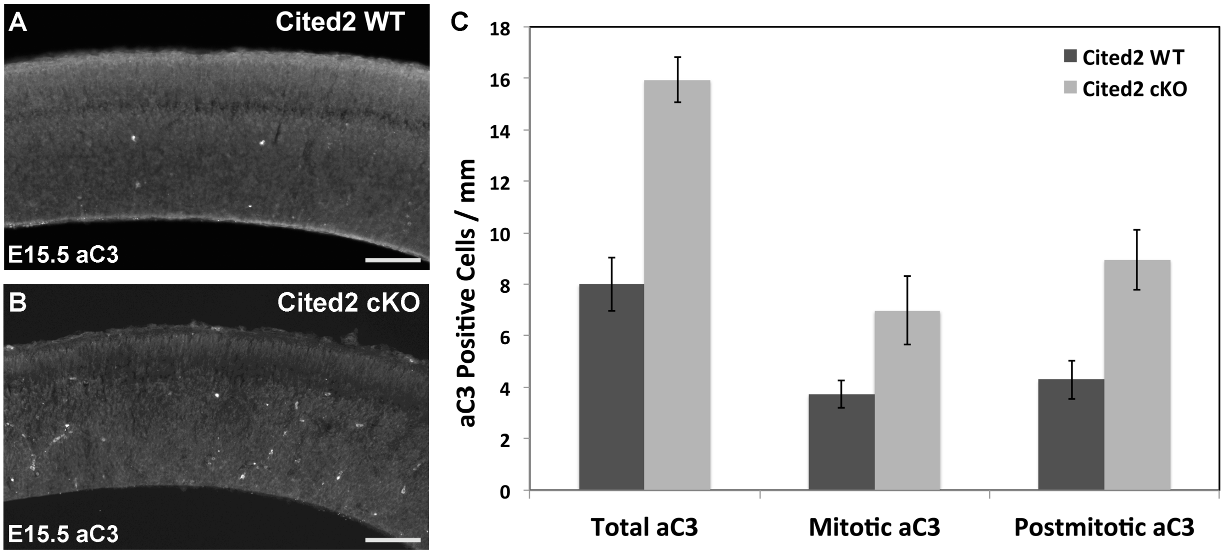

Figure 3.9 (Continued)

Figure 3.10: Loss of *Cited2* function results reduced superficial layer thickness at P3

(A) Sagittal section of P3 neocortex, showing four rostro-caudal regions where thickness measurements were made (a-d), and immunocytochemistry for CTIP2 (green) and LMO4 (red). **(B)** Superficial layers (II-IV) in *Cited2* cKO (light grey bars) have reduced thickness in sensory areas (b-d) as compared to WT (dark grey bars) (SS area: 17% reduction, p=0.02; caudal: 10% reduction, p=0.01; far caudal: 25% reduction, p=0.007), but not motor areas (a) (p=0.11). **(C)** There is no change in deep layer thickness in any region in *Cited2* cKO as compared to WT. (N=4 per genotype)

Scale bar: 1mm. WT, wildtype; cKO, conditional null; P, postnatal day

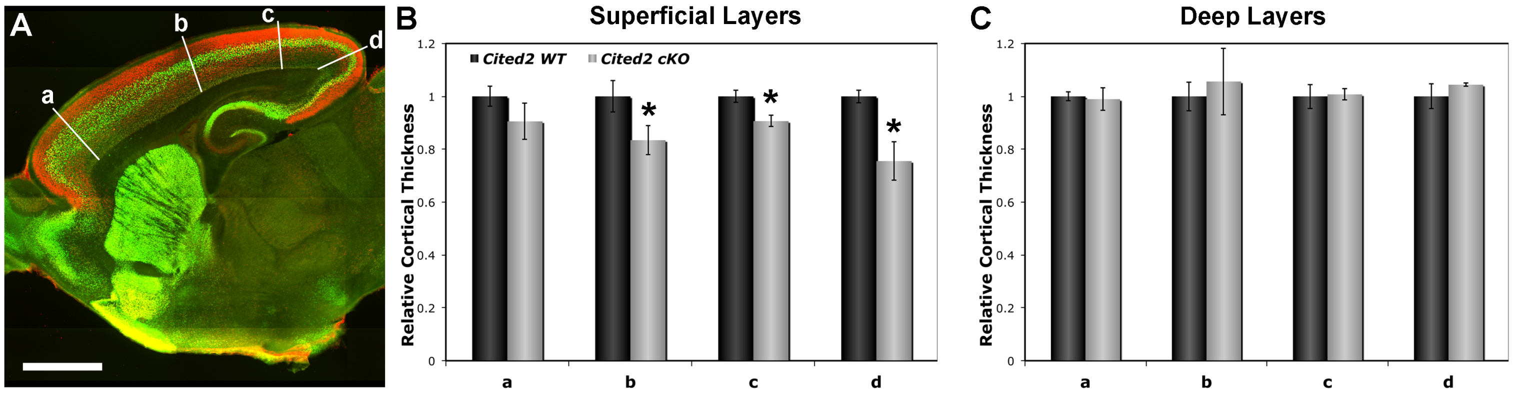

Figure 3.10 (Continued)

Figure 3.11: Loss of *Cited2* function results in reduced cortical length at P3 that is maintained at least until P21. (A) Measurements of cortical surface length at P3 reveal an ~5% smaller cKO diagonal cortical length than WT (N=5 per genotype, p=0.02) **(B)** This translates to an ~10% reduction in rostro-caudal length in P3 *Cited2* cKO neocortex (N=5 per genotyps, p=0.0006) at all but the most lateral of four medio-lateral levels (A-D). **(C)** This ~10% loss of cortical length is not recovered, and the *Cited2* cKO neocortex is still significantly shorter at P21 (~10% reduction, N=3, p=0.005).

Scale Bar: 1mm. WT, wildtype; cKO, conditional null; P, postnatal day

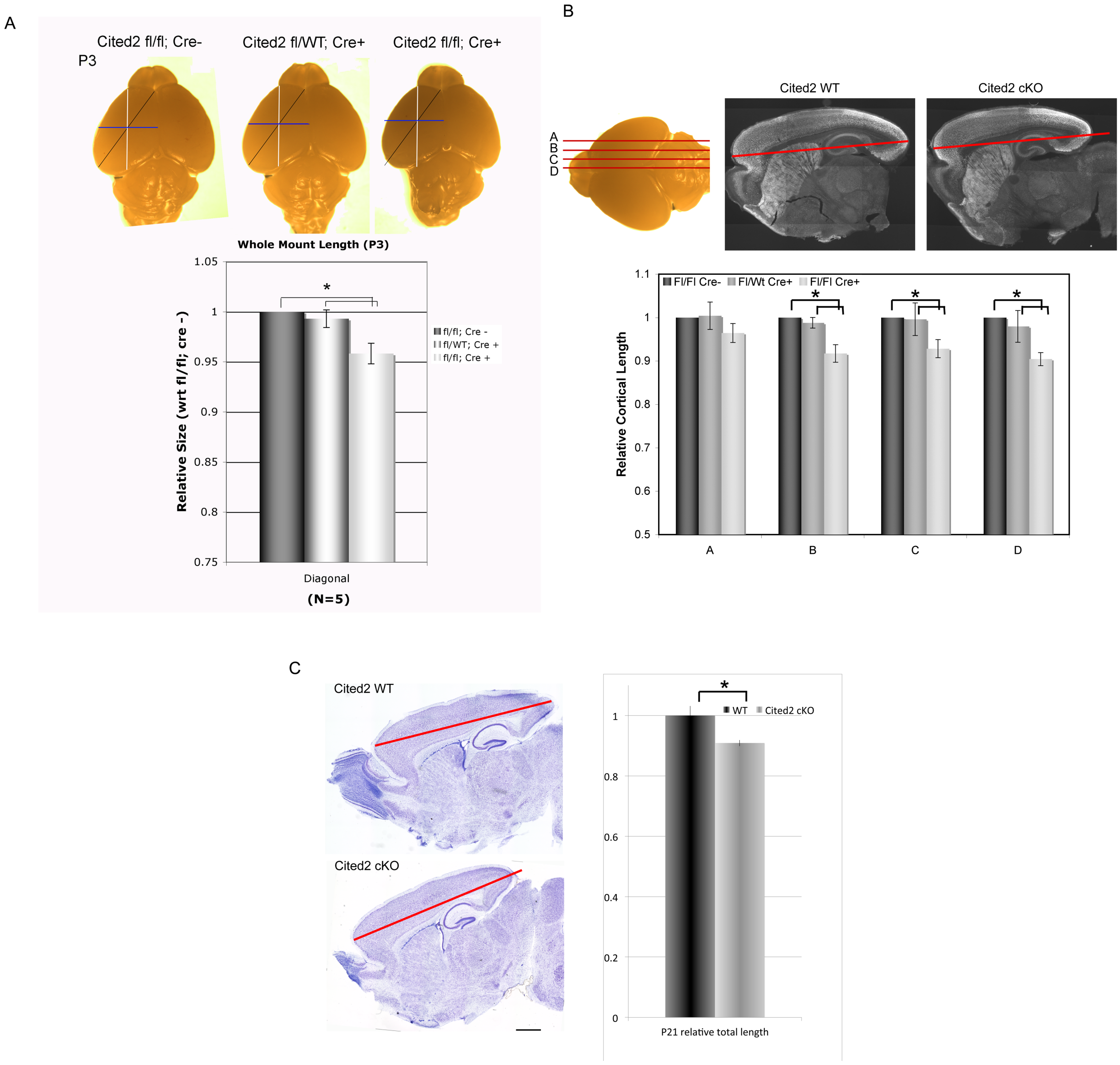

Figure 3.11 (Continued)

Figure 3.12: Loss of *Cited2* function results in reduced cortical length in somatosensory neocortex at P3 that is restricted to the unrefined sensorimotor cortex at P0, and maintained until at least P8. **(A)** Analysis based on three broad cortical areas divided by LMO4 expression at P3 indicates that there is a highly specific and substantial reduction (28% reduction, N=5 per genotype, p=0.003 SS; versus p=0.3 motor and p=0.9 for caudal) in the rostro-caudal length of the somatosensory area in the *Cited2* cKO cortex (light grey bars) comparted to WT controls (darker grey bars). **(B)** The reduction in somatosensory cortex length (red) accounts for nearly all of the total reduction in cortical length with no change in caudal (green) or motor (blue). **(C)** At P0, before motor and sensory cortical areas are refined, *Cited2* cKO (light grey bars) has length reduction in mixed sensory-motor areas. (N=3 per genotype, 12% reduction motor, p=0.08; 17% reduction SS, p=0.002) **(D)** At P8, the specific reduction in somatosensory cortical length is maintained in *Cited2* cKO (light grey bars) compared to WT (dark grey bars) (28% reduction, N=5 per genotype, p=0.0005). Error bars indicate standard error of the mean.

WT, wildtype; cKO, conditional null; P, postnatal day

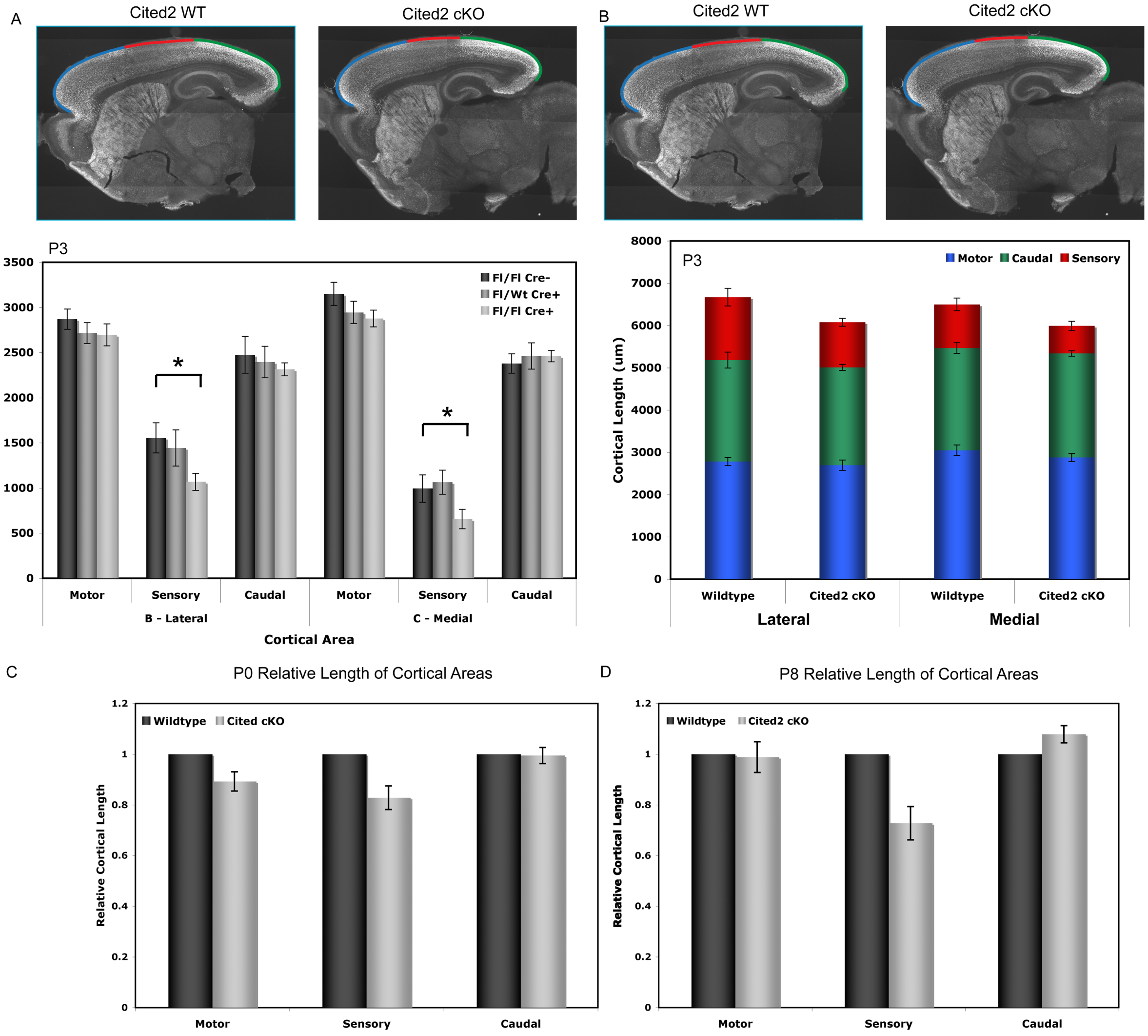

Figure 3.12 (Continued)

Figure 3.13: Loss of *Cited2* function results in reduced cortical length in somatosensory neocortex only in superficial layer neurons, and not in acallosal layer IV.

Superficial layer measurements of SS cortex length (*Cadh8* (19% reduction, p=0.01*)*, *EphrinA5* (17% reduction, p=0.0009*)*, *EphA7* (13% reduction, p=0.01)) confirmed the reduced length in the *Cited2* cKO compared to WT observed with LMO4 measurements (black arrowheads), while measurements of acallosal layer IV SS cortex (*EphrinA5*, p=0.25; and *Ror*β, p=0.6) did not detect a significant difference in SS cortex in the *Cited2* cKO compared to WT (black arrows). (N=4 per genotype).

WT, wildtype; P, postnatal day.

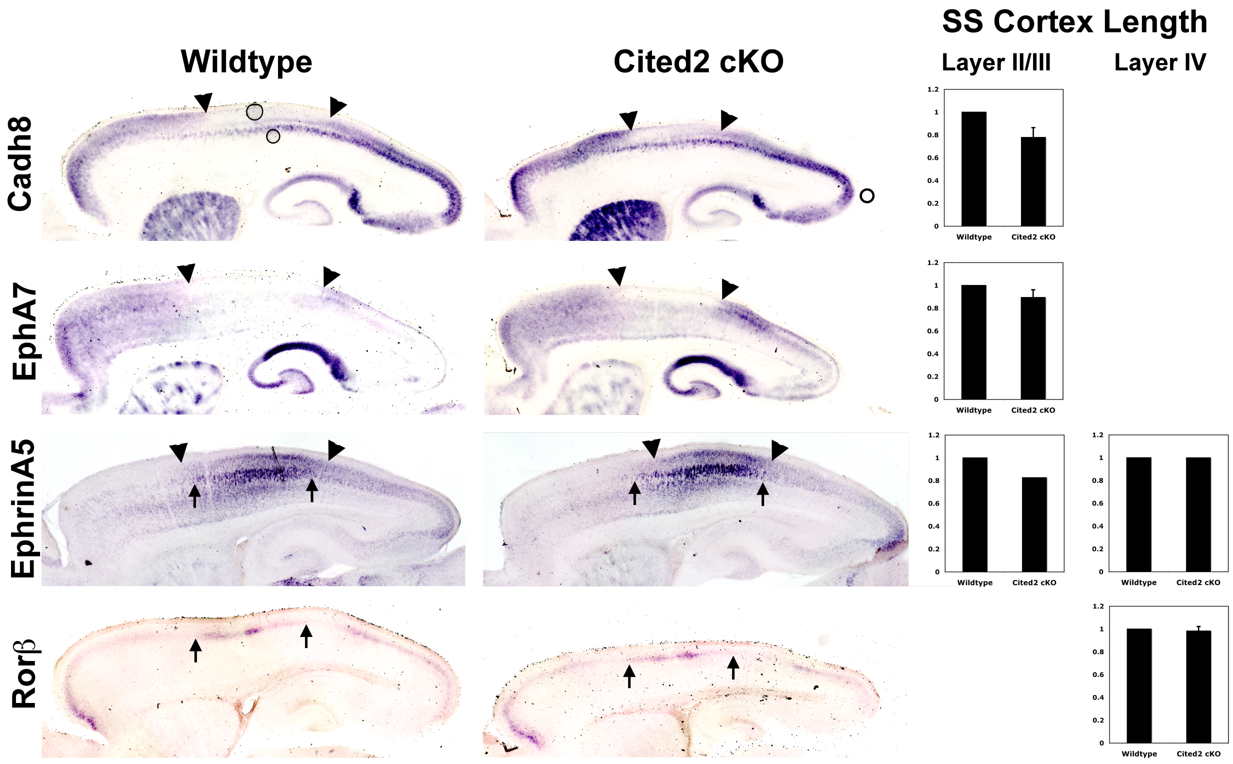

Figure 3.13 (Continued)

To investigate potential causes of this reduction in area size, we explored whether any of the size reduction was be due to increased cellular density, rather than all being accounted for by early IPC reduction. There is an increase in cellular density in superficial neocortical layers of *Cited2* cKO neocortex, but only in SS areas (23% increase in superficial layer cell density, p=0.01) (Figure 3.14). Increased cell density suggests either smaller soma size, reduced neuropil in existing SS superficial layer neurons, or both. Volumetric calculations suggest that a greater than 70% increase in density would be necessary to account entirely for the observed ~28% reduction in SS length (Section 3.4 e.) and ~17% reduction in superficial layer thickness (Section 3.4 d.). Therefore, this observed 23% increase in superficial layer SS cortex density likely accounts for some, but not all of the loss on SS neocortical size. Taken together, these data support the interpretation that the observed reduction in SS cortex size is likely a combination of a reduction in early cell number compounded by reduction in either neuropil size and/or cell soma size.

3.4 f. Cited2 functions cell autonomously in superficial layer CPN migration and axonal extension.

To investigate potential cell autonomous function(s) of CITED2 in development of CPN, we disrupted expression of *Cited2* in a directly targeted subpopulation of superficial layer CPN in SS cortex. We electroporated an expression construct containing Cre recombinase-IRES-farnesylated-GFP into dorsal progenitors at E15.5, the peak of superficial layer formation (Figure 3.15A), in *Cited2* fl/wt control brains and fl/fl littermates. At P0, the vast majority of WT GFP-positive cells within the control neocortex are located in layers II/III, with a few cells with immature, migrating neuronal morphologies observed throughout the layers of the neocortex. In striking contrast, in *Cited2 fl/fl* brains, there are many GFP-positive cells throughout deeper layers of the SS cortex (Figure 3.15B). However, by P3 and P8, the majority of GFP-positive neurons are found in the superficial layers in both *fl/wt* and *fl/fl* brains (Figure 3.15C). This observed migrational delay was also observed in the cKO cortex, as assessed via BrdU birthdating at E15.5, and assessment at P3 across all functional areas. These results reveal an ~15% reduction ($p \leq 0.001$) in the proportion of neurons born at E15.5 that reach superficial layers (Figure

3.15D). These results suggest cell autonomous roles for *Cited2* in CPN development, including migration and/or survival of developing CPN.

Because even a migrational delay can lead to death or extensive dendritic and axonal extension disruption of superficial layer CPN(Alfano et al.), we further investigated the connectivity of *Cited2* null CPN, employing both *Cited2* cKO mice and approaches to more deeply investigate cell autonomous loss of *Cited2*. To observe SS CPN axon extension before the CPN axons reach final targets, we quantified distance extended by axons of individual SS superficial layer neurons of either *Cited2 fl/fl* or *fl/wt* littermate controls with E15.5 *cre* electroporation. At P3, there is a significant delay in axonal extension, first to the ipsilateral CC white matter flexure, and then to the midline itself. Normalized to the total number of electroporated axons entering the white matter, in comparison to *fl/wt* controls, *Cited2 fl/fl* neuron axons were only half as likely to reach the first landmark, and only one quarter as likely to reach the midline (p=0.004 and p=0.003) (Figure 3.16A). By P8, there was no difference between *Cited2* null and WT neurons' ability to extend axons into contralateral cortex parenchyma, normalized to the number entering contralateral grey matter (p=0.5 layer IV, p=0.9 at layer II/III) (Figure 3.16B). However this metric does not assess the proportion of axons able to cross the midline. A sparser electroporation scheme will be needed to allow total initial axon counts in the densely packed CC at this age. At P6, when retrograde label from contralateral grey matter superficial layer targets is possible, SS CPN extend across the midline equally, but *Cited2* cKO CPN axons consistently show evidence of imprecise targeting (Figure 3.16C).

Figure 3.14: Loss of *Cited2* function results in increased somatosensory superficial layer cellular density at P3

At P3, superficial layers (II-IV) of somatosensory *Cited2* cKO noecortex (light grey bars) have increased cellular density in comparison to WT neocortex (dark grey bars) (23% increase in superficial layer cell density N=3 per genotype, p=0.01). There is no change in density in deep layers (V-VI). Error bars indicate standard error of the mean.

Scale bar: 50μm. WT, wildtype; cKO, conditional null; P, postnatal day

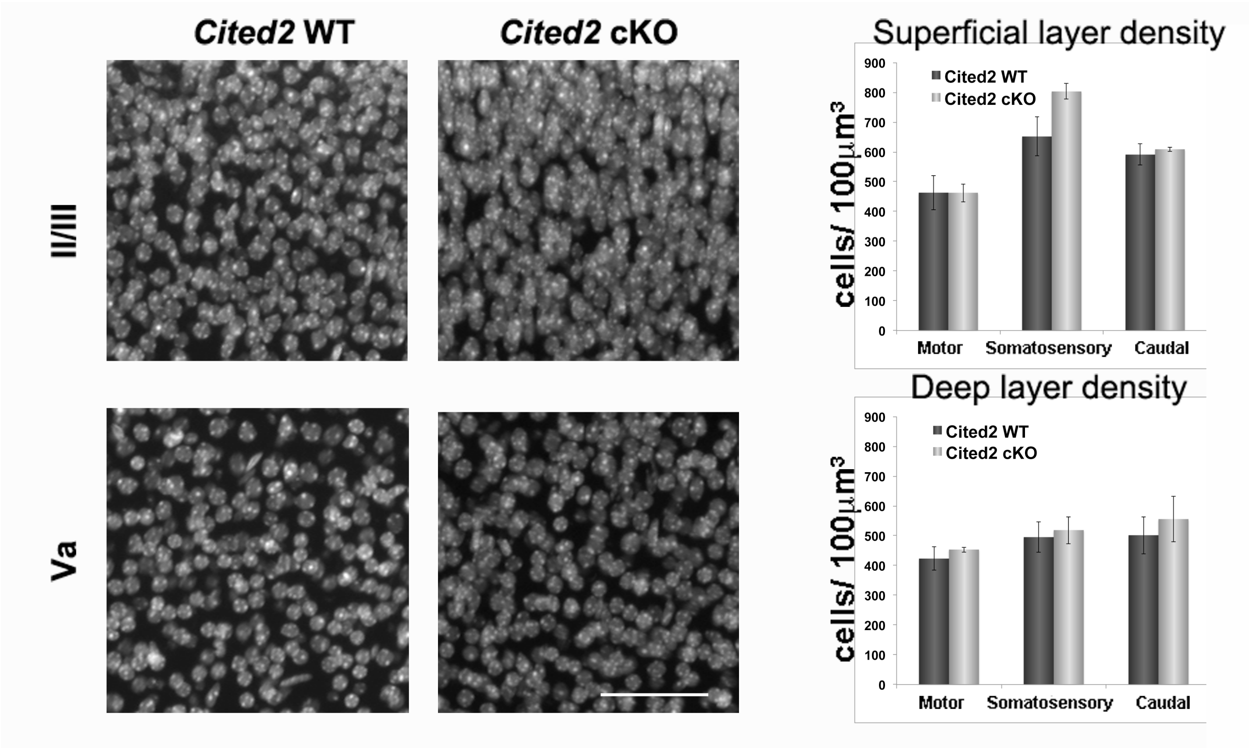

Figure 3.14 (Continued)

Figure 3.15: Loss of *Cited2* function results in cell-autonomous migration delay.

(A) Schematic of approach to dirupt expression of *Cited2* in a directly targeted subpopulation of superficial layer CPN in SS cortex by electroporating an expression construct containing Cre recombinase with GFP into dorsal progenitors at E15.5, the peak of superficial layer formation in *Cited2 fl/wt* control brains and *fl/fl* littermates. **(B)** At P0, the vast majority of WT GFP-positive cells within the control neocortex are located in layers II/III, with a few cells with immature, migrating neuronal morphologies observed throughout the layers of the neocortex. In striking contrast, in *fl/fl* brains, there are many GFP-positive cells throughout the layers of the SS cortex. **(C)** At P3 and P8, the majority of GFP-positive neurons are found in the superficial layers in both fl/wt and fl/fl brains. **(D)** This cell autonomously observed migrational delay was also observed across all functional areas in the P3 cKO cortex (light grey) compared to WT cortex (dark grey), as assessed via both BrdU birthdating at E15.5 and determining what percentage of birthdated cells were in superficial layers by P3 (N=3 per genotype, motor:17% reduction, p=0.001; somatosensory: 15% reduction, p=0.007; caudal: 15% reduction, p=0.003).

WT, wildtype; cKO, conditional null; LV, lateral ventricle; E, embryonic day; P, postnatal day.

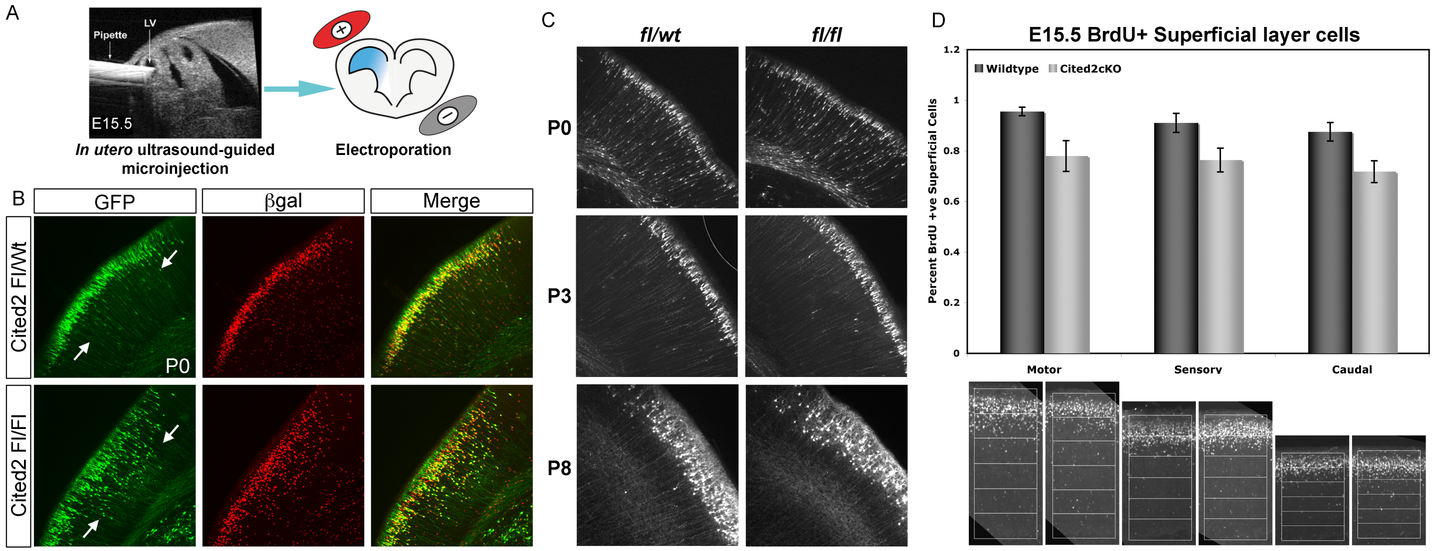

Figure 3.15 (Continued)

Figure 3.16: Loss of *Cited2* function results in cell-autonomous axon extension delay. (A) At P3, there is a significant delay in axonal extenstion to first the ipsilateral CC whitematter flexure and to the midline itself. Normalized to the total number of elecroporated axons entering the white matter, in comparison to *fl/wt* controls (dark grey bars), *Cited2 fl/fl* neuron axons (light grey bars) were half as likely to reach the first landmark and only a quarter as likely to reach the midline (N=4 *fl/wt* and N=5 *fl/fl*, p=0.004 at ipsilateral flexure and p=0.003 at midline) **(B)** By P8, there is no difference between *Cited2* null and WT neurons' ability to extend axons into contralateral cortex normalized to the number entering contralateral grey matter (N= 5 per genotype, p=0.5 layer IV, p=0.9 at layer II/III). **(C)** At P8, when retrograde label from contralateral targets is possible, CPN extend across the midline equally, but consistently show evidence of imprecise targeting. Error bars indicate standard error of the mean.

Scale bar: **(C)** 1mm.WT, wildtype; cKO, conditional null; CPN, callosal projection neurons; P, postnatal day; Ipsiflex, ipsilateral flexure of the corpus callosum.

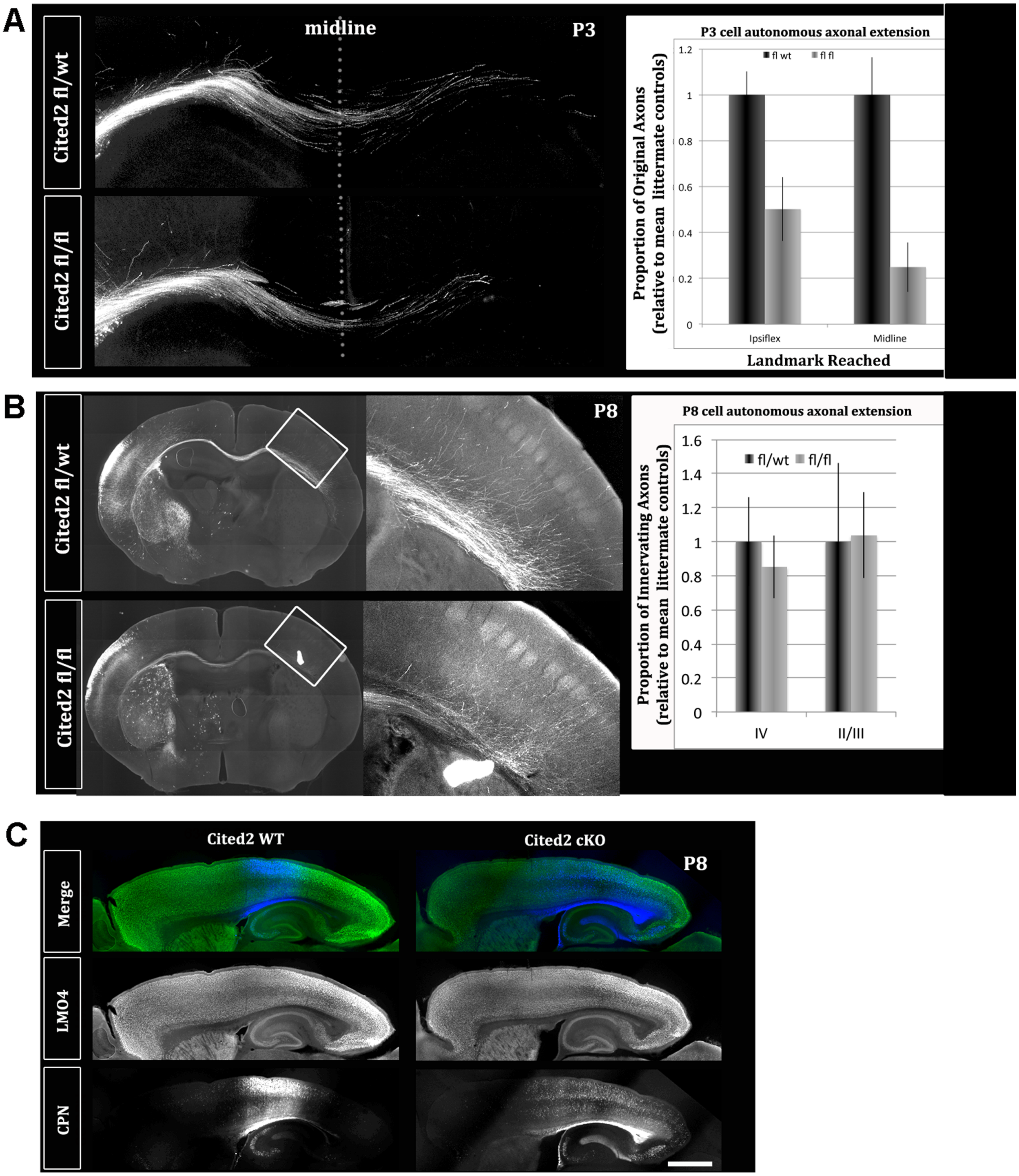

Figure 3.16 (Continued)

3.5 Discussion

Subpopulations of callosal projection neurons (CPN) of the cerebral cortex display heterogeneity with respect to laminar location, connectivity, and gene expression. In addition, CPN reside in, and homotypically connect, distinct functional areas within the cerebral cortex to convey different modalities of information, even though all CPN extend axons to homotopic mirror image targets on the contralateral hemisphere to enable bilateral information integration. Here, I present CITED2 as a broad early control over Tbr2+ intermediate progenitor cells (IPCs), and as a specific, later-acting control over identity acquisition of the specific subpopulation of somatosensory (SS) CPN.

I began investigation of *Cited2* function by confirming and expanding projection neuron-type-specific comparative microarray expression analysis(Molyneaux et al., 2009). I verified that, among projection neuron subtypes, *Cited2* is expressed by CPN, and excluded from CSMN. However, postnatally, *Cited2* is expressed by a restricted population of CPN in cortical layers II/III, V, and VI of SS cortex. Interestingly, early, before CPN axons have extended, *Cited2* is expressed broadly across all areas by immature Tbr2+ IPCs, and by cortical plate neurons. This first broad, then restricted, expression pattern lead me to investigate whether *Cited2* functions broadly, in a restricted fashion, or both, in a context-dependent manner.

We employed *Cited2* conditional null mice with a floxed *Cited2* gene excised with forebrain specific *Emx1*-driven cre recombinase to investigate *Cited2* function in neocortical projection neuron development. After validating the specificity of the system, and confirming that *Cited2* function is not required for early corticogenesis (E10-E15.5) before its peak expression, we directly investigated the Tbr2+ IPCs that express *Cited2*. We find that *Cited2* function is required for regulation of Tbr2+ IPCs in E15.5 cKO mouse brains. The number of Tbr2+ cells in *Cited2* null neocortex is reduced by about 20% in comparison to WT control brains. Such a reduction could theoretically be due to decreased generation, increased death, or both. We find that the 20% reduction in Tbr2+ cells is accompanied by a 50% increase in cell death at E15.5; however, the amount of increased cell death does not fully account for the absolute numbers of decreased Tbr2+ cells. Therefore, while there is excess cell death in *Cited2* cKO cortex, there is likely also reduction in generation of Tbr2+ cells to explain the reduction in Tbr2 positivity. We are currently examining the neurogenic quotient at E14.5 and E15.5 using short pulses of BrdU birthdating, to determine if loss of *Cited2* affects the number of dividing cells at each age giving rise to Tbr2+ IPCs, and how many produce neurons. This will enable direct analysis of the question of how the reduction in generation of Tbr2+ IPCs arises in the absence of *Cited2* function. If fewer IPCs are generated at E15.5, it would suggest either decreased symmetric proliferation of IPCs, or decreased generation of IPCs from radial glia ventricular progenitors, which could be distinguished via shorter time course birthdating analyses or live imaging of living cortical slices expressing a *Pax6*-driven fluorescent reporter (Schedl et al., 1996; Ashery-Padan et al., 2000).

A function for *Cited2* at the transition generating IPCs is compelling, particularly because of its known interaction with Pax6(Englund et al., 2005; Chen et al., 2008). Loss of Pax6 function in Pax6$^{sey/sey}$ mutants has been shown to overproduce Tbr2+ progenitors at E12.5, but drastically increase cell cycle length at E15.5 (Estivill-Torrus et al., 2002), leading to premature neuronal differentiation and reduced later generation of Tbr2+ progenitors. These results are similar to what we observe after loss of *Cited2* function. *Cited2* is, therefore, poised to act by interacting with Pax6 around E15.5 to convey its time dependent change in function. We are currently performing directed immunoprecipitation studies to determine whether Pax6 and CITED2 directly interact in developing neocortex. If there is no detected interaction, these experiments will allow us to rule out direct interaction, but not indirect interaction or function through a co-partner. However, if there is a direct interaction, these results will inform directed experiments to determine how closely the *Cited2* null phenotype resembles the later function of Pax6, and focus on whether there is a specific decrease in Pax6+ cells producing IPCs.

Reduction in progenitors early would likely translate into fewer cortical neurons postnatally. Indeed, superficial layer thickness is reduced in somatosensory and occipital *Cited2* cKO neocortex, but, interestingly, there is no significant change in superficial layer thickness in motor cortex, nor any change in deep layer thickness in any area. The unchanged thickness in deep layers likely reflects the fact that *Cited2* expression is highest during the second half of corticogenesis, when superficial layers are generated, or because CPN make up a minority of deep layer projection neurons. Unchanged thickness in motor cortex superficial layers could be a reflection of the fact that superficial layers in motor cortex are thinner naturally and, therefore, a gross change is harder to detect. However, since far occipital superficial layers are normally even thinner than those in motor cortex, this lack of change in motor cortex is likely representative of an areal specific function of *Cited2*. Strikingly, the thinning of *Cited2* cKO occipital cortex (25% reduction) very closely resembles the reduction in visual cortex in AP2-γ loss-of-function neocortex(Pinto et al., 2009), suggesting that this occipital cortex effect could be altogether separate from the SS cortex effect, and might be modulated by the known CITED2 interaction with AP2-γ (Braganca et al., 2003).

While thickness results indicate a radial reduction in neocortical projection neurons, we also examined potential tangential effects of reduced Tbr2+ IPC numbers. We find reduced neocortical length by ~10% in *Cited2* cKO cortex. However, because we observed areal differences in neocortical thickness, and because *Cited2* expression refines to SS postnatally, we asked if this reduction is specific to a particular functional area. Using LMO4 as a marker of motor and caudal areas that is excluded in superficial layers of SS cortex, we find that the ~10% reduction in cortical length is specifically lost from somatosensory areas of *Cited2* cKO neocortex. Length measurements of motor and caudal cortical areas show no difference between WT and *Cited2* null brains. However, ~30% of SS cortex length is lost in P3 *Cited2* cKO cortex. This area specific loss is maintained at P8, and neocortical length is still reduced at P21, suggesting that there is no later compensation for the loss in SS cortex length. We employed a variety of functional genetic controls over SS cortex identity, either expressed in or excluded from SS cortex, to confirm and expand these results. We find similar reductions in SS cortex as measured by genes expressed in superficial layers. However, there is no change in layer IV SS cortex, suggesting that this reduction is neither a pan-SS nor a pan-superficial layer effect, but rather this reduction is seemingly specific to CPN, none of which reside in layer IV.

Such areal and neuron type-specificity in function, particularly in sensory processing regions of the neocortex, is relevant to diseases of complex sensory information integration as is observed in ASD, in which reduced corpus callosum volume has already been implicated (Egaas et al., 1995; Frazier and Hardan, 2009; Hardan et al., 2009; He et al., 2010). Notably, *Cited2* genetic abnormalities have been identified in ASD patients(Szatmari et al., 2007). Magnetic resonance diffusion tensor imaging (DTI) analysis of *Cited2* null brains is currently underway to assess corpus callosum size, extent, and fiber tract organization in a way that can be compared to human disease morphometry data. Such a global analysis of the fiber tract pattern might also reveal targeting imprecisions that have been difficult to identify using target-based labeling approaches.

The areal specificity for somatosensory cortex reduction in length, with a broad early reduction in Tbr2-expressing progenitors, and broad increase in cellular death in *Cited2* null cortex, suggests two distinct functions for *Cited2* in neocortical development. *Cited2* might have an early, broad function at the time of generation of Tbr2+ IPCs, and a later, more specific function in maintaining the somatosensory neocortical domain of CPN, and their specific subtype identity acquisition. A later function is likely driven by a different set of interactors for CITED2 than its early function(s).

One particularly compelling candidate interactor for late CITED2 function is LMO4. Results presented above indicate that, despite a global reduction in Tbr2+ IPCs, there is highly specific and significant reduction in the length of superficial layers in LMO4-negative SS cortex, in addition to reduced superficial layer thickness in this area. In contrast, motor cortex, where LMO4 is highly expressed, does not appear to be affected. In thymus development, the transcriptional co-regulator *Lmo4* can partially functionally compensate for *Cited2*(Michell et al., 2010), leading us to hypothesize that *Lmo4* might functionally compensate for loss of *Cited2* in some aspects of CPN development in motor cortex.

To test this hypothesis regarding potential LMO4 interaction and compensation, we are currently performing immunoprecipitation experiments to determine if LMO4 and CITED2 interact in neocortex, and we plan to employ two cell autonomous approaches via *in utero* electroporation: 1) disrupt *Lmo4* expression via knock-down in motor cortex of *Cited2* cKO mice; and 2) ectopically express *Lmo4* in superficial layer CPN of SS cortex. These experiments would allow us to ask if *Lmo4* can compensate for *Cited2* loss when ectopically expressed in SS cortex, or if it is compensating for *Cited2* loss in motor cortex. Additionally, at a more global level, we are currently breeding double conditional null mice for *Lmo4* and *Cited2* to investigate whether losing *Lmo4* function as well as *Cited2* function rescues the areal specific size decrease, resulting in all areas being equally reduced in size. Future experiments to distinguish early and late function(s) of *Cited2* include using an inducible cre recombinase mouse line (such as the tamoxifen-inducible *Cux2*-cre line) to disrupt *Cited2* function after E15.5, and to isolate potential late arealization roles of *Cited2*.

Since most of the analyses of *Cited2* function presented here are based in a forebrain null for *Cited2* analyzed on a population level, we investigated *Cited2* loss of function in a chimeric system in which we electroporated a small number of neocortical progenitors at E15.5 with an expression plasmid of cre recombinase to determine which, if any, functions of *Cited2* are cell-autonomous. We observed an early migrational delay, both in cell autonomous studies and in *Cited2* cKO cortex. This is similar to previous studies linking *Cited2* to TGFβ and PPARα signaling pathways that regulate cellular mobility (Bottner et al., 2000; Lai et al., 2008; Molyneauz et al. 2005). We also observed cell-autonomous axonal extension delays, and possible imprecise SS CPN axonal targeting. However, currently ongoing anterograde labeling experiments will better allow for direct investigation of axonal targeting than allowed by the retrograde data presented here. Migration and axonal extension delays could be a result of CITED2 interaction with specific migration pathways including TGFβ and PPARα. However, they could also be a reflection of one of the many other cellular differentiation pathways in which *Cited2* has been shown to function, because disrupted differentiation can also cause arrested migration(Harrison-Uy and Pleasure, 2012). Additional biochemical analyses of what CITED2 binds in developing neocortex will enable more directed pathway analyses.

Since we have shown that *Cited* functions cell autonomously in neocortical development, we are currently investigating what processes *Cited2* is sufficient to affect by overexpressing *Cited*2 at E13.5 in progenitors that do not normally express it. Exogenous expression of *Cited2* might induce opposite functions as does loss of *Cited2* or, perhaps, even opposite functions as have been shown for loss of function of candidate *Cited2* interactors for neocortical *Cited2* function.

Because of the nature of CITED2 as a transcriptional co-activator, knowing what transcription factors and transcriptional modulators it interacts with in developing neocortex is important to dissecting *Cited2* function. We have recently optimized a protocol for performing complete quantitative immunoprecitiation of CITED2 from developmental cortical tissue samples. With this ability, it is now conceivably possible to perform proteomics analysis of CITED2's interactors, first early at E15.5 in the developing cortex, and, separately, later around P0 when areal refinement is underway. We are currently collecting samples to perform non-biased assessment of some context-dependent CITED2 interactors across different developmental times. Results from these experiments will give important mechanistic insight into how CITED2 functions during neocortical development.

Funding

This work, as well as work described in Chapters 4, 5 and 6, was partially supported by grants from the National Institutes of Health (NINDS), the Harvard Stem Cell Institute, and the United Sydney Association. R.M.F. was partially supported by a National Science Foundation Graduate Research Fellowhsip Program (GRFP) fellowship and a National Institutes of Health predoctoral NRSA fellowship F31 NS073136.

Acknowledgements

I thank L. Pasquina, R. Richardson, C. Greppi, T. Keefe, P. Davis, and B. Noble for superb technical assistance; and current and past members of our laboratory for discussions and helpful suggestions.

Chapter 4:

Caveolin1 identifies a specific subpopulation of CPN including dual projecting CPN/FPN

Author contributions: This project was an equal collaboration between Jessica L. MacDonald, PhD, a post-doctoral fellow, and me. We jointly designed all experiments and interpreted all data. Jessica performed the majority of the early post-natal retrograde labeling, ICC, and protein localization work; and I performed the majority of the dual retrograde labeling experiments, ISH, and confocal imaging.

4.1 Abstract

Molecular controls over broad callosal projection neuron (CPN) development have begun to be identified. However, CPN are a broad set of distinct subpopulations each with unique function based on area, laminar, or connectivity properties. The postmitotic development of specific subpopulations of CPN gives rise to their unique connectivity and activity, and, therefore, function in the neocortex. Here, we show that *Caveolin1* (*Cav1*) is a molecular control that is poised to execute one or a few of these postmitotic events in a specific subpopulation of CPN, including CPN with ipsilateral frontal projections to premotor cortex (CPN/FPN). Cav1 is a lipid-bound scaffolding domain protein expressed by over 80% of CPN/FPN, localized to cell bodies and dendritic spines, excluded from the nucleus, with peak expression postmitotically as axon and dendrite targets are being reached and refined. Cav1 function is not required by CPN/FPN for their early specification or for reaching their axonal targets, and, even though Cav1 interacts with neurotransmitter receptors, its expression is not dependent on connectivity. Both of these lines of evidence support a role for Cav1 in maturation. The ability of *Cav1* misexpression to induce aberrant migration delay, its roles as a scaffolding protein for neurotransmitter receptors, and its known interaction with the local adhesion molecule Rac1 all provide insight into potential roles in adhesion and activity-based post-mitotic maturation of CPN subpopulations. The defining properties of this CPN/FPN subpopulation are still being identified and characterized, but this analysis of *Cav1* expression and function identifies and characterizes a first molecular control over this functionally unique projection neuron population.

4.2 Introduction

Callosal projection neurons (CPN) include a diverse set of subpopulations, as described in Chapters 1-3. Multiple properties can describe and identify some of these subpopulations, including cell body location, birthdate, electrophysiological and neurochemical properties, dendritic tree distribution, axonal target(s), and molecular expression. While these properties are convenient for categorization, all of them are also critically interrelated to determine the final function(s) of a neuron. For example, populations of projection neurons with multiple axonal targets send information to diverse brain regions at once and, therefore, likely have critical functions in information integration. One population of dual projecting CPN extend homotopic axonal connections to mirror image locations in the contralateral hemisphere, as well as rostrally to ipsilateral frontal areas, sending information from sensory or motor modalities to higher hierarchical cortical areas (here, referred to as CPN/FPN)(Mitchell and Macklis, 2005). CPN/FPN were identified anatomically in mouse by members of the Macklis lab in 2005 (Mitchell and Macklis, 2005), and they showed that the majority of these CPN/FPN are located in neocortical layer Va primary sensory areas (S1), with a large expansion in caudo-lateral neocortex (S2) (see Figure 4.7A). While this population has been identified anatomically, no molecular controls over this population's unique connectivity or function have been described.

Caveolin 1 ***(Cav1)*** encodes for a membrane-bound scaffolding protein known to play a role in neurotrophin response, and that has the ability to interact with synaptosome complexes (Bilderback et al., 1997; Bilderback et al., 1999; Head and Insel, 2007). Here, I identify *Cav1* to be highly expressed during axonal and dendritic development at P3 in this laminarly and regionally-restricted subset of CPN that enable long distance, complex information integration by maintaining dual projections interhemispherically and to frontal cortex (CPN/FPN). *Cav1* function has been shown to be necessary for a wide range of cellular processes in other systems, including functions related to the unique lipid raft structures that it forms, caveolae. *Cav1* is highly expressed in developing blood vessels and endothelial cells, broadly, and is required for their proper proliferation (Razani et al., 2001) and adhesion to give correct microvascular permeability(Schubert et al., 2002). In addition, *Cav1* is necessary for proper lipid metabolism in mice(Razani et al., 2002), and for smooth muscle calcium influx(Sathish et al., 2012). No caveolae lipid raft structures are present in mice that lack *Cav1* expression.

Members of the *Caveolin* family, of which *Cav1* is the most abundant, have a distinct structure for transmembrane proteins(Williams and Lisanti, 2004). While the 33 amino acid long transmembrane domain is longer than needed to pass the membrane once, it is not long enough for a double pass, and, therefore, results in both the N and C termini localized cytoplasmically(Dupree et al., 1993; Monier et al., 1995). This results in a horseshoe shaped helix-break-helix intramembrane domain, and a palmitoylated residue before membrane exit on the C terminal intracellular region, which establishes membrane curvature and allows for Cav1 to participate in forming its namesake membrane invaginations, caveolae(Lee and Glover, 2012), as well as to have a prominent cytoplasmic scaffolding region.

While the caveolae structure does not exist in neurons(Head and Insel, 2007), *Cav1* knockout mice exhibit neurological abnormalities including limb clasping, abnormal spinning, muscle weakness, reduced activity, and gait abnormalities (Trushina et al., 2006). Interestingly, human *Cav1* is located at the locus 7q31.1, part of autism-linked locus 9 (Auts9), immediately upstream of *MET,* which shows direct pre-transcription start-site mutations associated with ASD (Campbell et al., 2006). This suggests that *Cav1* might also be directly relevant in ASD and potentially contribute to some of the Auts9 linkage to the disorders, perhaps via CPN. *Cav1* is also close genomically to *Foxp2* in Auts9, which had been suspected to underlie ASD language defects, but later shown to not be causal of the Auts9 ASD linkage (Newbury et al., 2002). Other potential gene linkages in this locus (NRCAM and ST7) are relatively weak, indicating that the linkage must be accounted for, at least in part, by other Auts9 genes, potentially by *Cav1*.

As a lipid raft scaffolding molecule, Cav1 has been shown to interact with multiple binding partners, some of which are particularly compelling for neuronal function. Interestingly, Cav1 binds directly to the calmodulin-dependent scaffolding protein striatin(Gaillard et al., 2001a), which acts as a signaling platform in dendritic spine signal transduction (Benoist et al., 2006), and SNAP25, which complexes to Cav1 presynaptically upon synaptic potentiation (Braun and Madison, 2000). Cav1 known functions that are directly linked to neuronal function also include a requirement for Cav1 for estrogen receptor α (ERα) activation of a specific metabotrophic glutamate receptor, mGluR1α, in hippocampal neurons, potentially playing a role in long-term depression through this pathway(Takayasu et al., 2010). Specificity for particular caveolin activity is reflected by caveolin functional diversity in estradiol signaling through mGluRs, since Cav3 is necessary for mGluR2/3 signaling, but not for mGluR1 signaling (Boulware et al., 2007). It was later identified that Cav1 provides a support function for an interaction that regulates transcriptional activity by providing a scaffold for both the ERα voltage-dependent anion receptor and one of its interactors, the IGF-1 receptor(Maggi et al., 2002; Marin et al., 2009), a known positive regulatory factor for corticospinal projection neuron axonal outgrowth (Ozdinler and Macklis, 2006). Cav1 has also been implicated in neuronal differentiation from progenitors (Li et al., 2011), synaptic ribbons in photoreceptors (Kachi et al., 2001), and other neurotransmitter receptor functions including muscarinic cholinergic receptors (Lai et al., 2004). These neuro-specific processes might account for some of the neurological deficits found with *Cav1* loss-of-function described above, and motivates this study of Cav1 in CPN/FPN.

Additionally, a more general role of Cav1, its interaction with Rho-family GTPase RAC1, might underlie a neuronal function for Cav1. In non-neuronal systems, Cav1 and Rac1 have been shown to directly interact (Zuluaga et al., 2007), and Cav1 controls Rac1 protein levels through ubiquitylation and degradation(Nethe et al., 2010). The Cav1/ Rac1 interaction has been directly implicated in neurite outgrowth in induced neuroblastoma cell lines (Kang et al., 2006). In other systems, the Cav1/Rac1 interaction has been shown to play important roles in critical functions relating to cytoskeletal dynamics, focal adhesion, and migration (Beardsley et al., 2005; Joshi et al., 2008a). Further, Rac1 is required for midline crossing of CPN(Chen et al., 2007; Kassai et al., 2008), and Rac1, when recruited by CDKL5, can regulate neuronal migration and dendritic arborization of superficial layer CPN(Chen et al., 2010).

Expression of Cav1 in a specific population of CPN including CPN/FPN during early stages of neuronal maturation, and the known interaction between Cav1 and Rac1 in other systems, suggests a potential function for Cav1 in the specific subpopulation of CPN by which it is expressed, during such processes as early migration, neurite outgrowth, and branching. The identified scaffolding roles of Cav1 at synapses, and its interactions with neurotransmitter receptors, suggest that Cav1 might influence neuronal activity and/or axonal/ dentrite connectivity, and/or function. This study defines neocortical Cav1 expression, and investigates a potential requirement for Cav1 in migration, axonal extension, and branching.

4.3 Materials and Methods

4.3 a. *Mouse Lines*

Caveolin1 null mice on a congenic C57/ Bl6 background (B6.Cg-*Cav1*^{tm1Mls}/J) were obtained from The Jackson Laboratory (Bar Harbor, Maine, USA), strain number 007083. The original targeted null mutation was generated by Michael Lisanti at The Albert Einstein College of Medicine. A 2.2 kb region of the gene including exons 1 and 2 and a portion of the promoter region was replaced with a neomycin resistance cassette via homologous recombination(Razani et al., 2001).

The following PCR primers and genotyping protocols were used:

Cav1^{tm1Mls}/J :

Wild-type:	F: 5'- GTG TAT GAC GCG CAC ACC AAG - 3'
	R: 5'- CTT GAG TTC TCT TCA CCA G -3'

Product size: ~690 bp

Cav1 (transgenic):

F: 5' – CTA GTG AGA CGT GCT ACT TCC - 3'

R: 5'- CTT GAG TTC TCT TCA CCA G -3'

Product size: ~410 bp

The following cycling parameters were used: denaturation at 94°C for 30 sec, annealing at 65°C for 60 sec, and extension at 72°C for 60 sec. for 35 cycles, followed by extension for 2 min. at 72°C. The products were separated by gel electrophoresis on a 1.5% agarose gel.

BTBR acallosal mice on a congenic background (BTBR *T*$^{+}$ *tf*/J) were obtained from The Jackson Laboratory (Bar Harbor, Maine, USA), strain number 002282 (Wahlsten et al., 2003). LP/J mice have been shown to be an appropriate callosal control population for BTBR mice. LP/J mice (LP/J) were obtained from the Jackson Laboratory (Bar Harbor Maine, USA), strain number 000676.

C57/Bl6 wildtype mice were obtained from The Jackson Laboratory (Bar Harbor, Maine, USA), and were used to breed with *Cav1* null mice, and for birthdating and electroporation experiments.

4.3 b. *Immunocytochemistry*

Immunocytochemistry was performed as described in Chapter 3.

Antigen retrieval methods were required to expose antigens for some of the primary antibodies, including Cav1. Sections were incubated in 0.1M citric acid (pH=6.0) for 10 min. at 95-98°C and sections were rinsed in PBS prior to blocking. For thymidine analogues (IdU, CldU, BrdU), HCl antigen retrieval was required. Tissue was rinsed quickly in ddH_2O and incubated in 2N HCl for 2 hours at room temperature and sections were rinsed in PBS prior to blocking.

Primary antibodies and dilutions were used as follows: rabbit anti-Caveolin-1, 1:500 (Cell Signaling #3238); mouse anti-Caveolin-2, 1:500 (BD Biosciences); rat anti-Caveolin-3, 1:500 (BD Biosciences); goat anti-LMO4, 1:200 (Santa Cruz Biotech SC- 11122); rat anti-CTIP2 1:500 (Abcam ab18465), mouse-anti-Map2, 1:500 (Sigma M1406)**;** mouse anti-BrdU, 1:500 (Becton Dickinson) (detects IdU); rat anti-BrdU, 1:500 (Accurate) (detects CldU); mouse anti-BrdU, 1:750 (Chemicon); rabbit anti-GFP, 1:500 (Molecular Probes).

4.3 c. *In situ hybridization*

Nonradioactive colorimetric *in situ* hybridization was performed using probes labeled with dig-UTP as described in Chapter 3. Sense probes were used as negative controls in all experiments.

4.3 d. Retrograde labeling of cortical projection neurons

Perinatal retrograde labeling of CPN and CSMN

Perinatal retrograde labeling of CPN and CSMN was performed as described in Chapter 3.

Post-natal dual CPN/ FPN retrograde labeling

P6 pups were anesthetized with hypothermia. P21 mice were deeply anesthetized with Avertin (0.02mL/g body weight, injected I.P.). Tracers were injected transcranially with sharp pulled glass micropipettes (tip diameter 80-100μm in presumptive premotor and sensory-motor areas, as described below. Double fluorescent tracer injections were performed to label simultaneously:1) CPN in sensory-motor cortex, and 2) frontal projection neurons with long-distance ipsilateral projections to the premotor cortex. CPN with projections to the contralateral neocortex were labeled with Alexa 647 conjugated cholera toxin subunit B (2 mg/ml, Molecular Probes) with 25 injection sites, 46nL (10 injections of 4.6nL) each site at a depth of 250 μm at P6 and 450μm at P21. Ipsilateral corticocortial projections to the premotor cortex were simultaneously retrogradely labeled with injections of Alexa 555 conjugated cholera toxin subunit B (2 mg/ml, Molecular Probes) with 5 injection sites, 46nL each site and a depth of 250 μm at P6 and 450μm at P21 (see Figure 4.7).

Full craniotomies were not performed, rather, small punctures were made in the skull at the location of each injection point with either a pulled glass pipette (P6) or a fine suture needle (P21) prior to lowering the injection needle to the proper depth. This minimized insult and improved recovery while allowing for exact depth measurements to be accurately made.

4.3 e. Birthdating

For IdU and CldU birthdating, equimolar delivery of IdU (57.5 mg per kg) or CldU (42.5 mg per kg) at 12 hour intervals from E11 to E15.5 was performed(Vega and Peterson, 2005), calculating embryonic age with E0.5 as the day of observed vaginal plug. We sacrificed and perfused mice at P6, and prepared brains for immunocytochemistry.

4.3 f. Gain-of-function constructs

For control gain-of-function experiments, a vector containing a constitutively active CMV enhancer / β actin promoter driving GFP after an internal ribosomal entry site (IRES) was used (*GFP*^{control} , generous gift of C. Lois, MIT; (Molyneaux et al., 2005)). For the *Cav1* overexpression construct, called *Cav1*^{GFP}, full length *Cav1* cDNA was cloned into the same vector backbone using a Sal1 /Not1 digest (New England Biolabs, Ipswich, MA) of the *Cav1* cDNA from a pSport1 vector purchased from Open Biosystems (Lafayette, CO; clone ID 30062454). A sequenced clone with perfect alignment to the NCBI reference sequence NM_007616 in both the sense and antisense orientations was selected for experiments.

For 2A tagged constructs (used in Figure 4.11), the following primers were used to amplify the *Cav1* cDNA coding sequence only from the *Cav1*^{GFP} construct, above, and clone it into an AAV plasmid backbone with the 2A sequence from the picornavirus virus to create a bicistronic vector(de Felipe et al., 1999) with a following GFP using an SpeI/NotI digest. This construct is called Cav1^{2AG}. The control vector, called GFP^{2ASTOP}, the GFP was followed by the 2A sequence and a stop codon.

F: 5'- gcACTAGTatgtctgggggcaaatacgt-3' (with 5' SpeI site (capital letters) added on)

R: 5' - ggGCGGCCGC<u>tca</u>tatctctttctgcgtgc -3' (with 3' NotI, (capital letters) and STOP (underlined) added on).

4.3 g. In utero electroporation

In utero electroporations were performed essentially as described in (Saito and Nakatsuji, 2001; Saito, 2006), and (Molyneaux et al., 2005); and summarized in Chapter 3.

4.3 h. Quantification of FPN/CPN

For P8 quantification of Cav1-expressing CPN/FPN, anatomically matched sections were selected (*N*= 4 WT) Cav1 immunocytochemistry was performed. Digital boxes of fixed width indicated the S2 cortical region and the number of CPN/FPN, and Cav1$^+$ CPN/FPN were counted. Percentages of FPN/CPN that express Cav1 in each region were calculated from total numbers. Error bars or "±" indicate the standard error of the mean. It was not possible to count all of the CPN or all of the Cav1-expressing neurons due to high neuronal density.

For P8 quantification of CPN/FPN in the *Cav1*-null, anatomically matched sections were selected (*N* = 5 WT, *N*= 5 *Cav1*$^{-/-}$). Digital boxes of fixed width indicated the S2 cortical region and the number of CPN/FPN, and FPN were counted in S1 and S2. The percent of FPN with concurrent callosal projections was also calculated. No significant differences were detected between WT and *Cav1*$^{-/-}$. Error bars or "±" indicate the standard error of the mean.

4.3 i. Microscopy and image analysis

Whole mount images were acquired using a SMZ1000 fluorescence dissecting microscope (Nikon, Melville, NY) with a SPOT CCD microscope digital camera (Diagnostic Instruments, Sterling Heights, MI) and SPOT acquisition software.

Tissue sections were imaged on a Nikon E1000 microscope (Nikon Instruments, Melville, NY) equipped with an XCite 120 illuminator (EXFO, Mississauga, ON, Canada) and Q-imaging Retixa EX cooled CCD camera (Q-imaging Corp., Surrey, BC, Canada), or a Nikon 90i microscope using a 1.5 megapixel cooled CCD digital camera (Andor Technology, Dublin, Northern Ireland), a 5 megapixel color CCD digital camera (Nikon Instruments, Melville, NY). Images were collected and analyzed with Volocity image analysis software (Version 4.0.1; Improvision Inc., Waltham, MA) or Elements acquisition software (Nikon Instruments, Melville, NY).

Laser confocal analysis was performed using a BioRad Radiance 2100 confocal microscope with LaserSharp2000 imaging software (BioRad Laboratories, Hurcules, CA). Images were processed using a combination of functions provided by ImageJ (Rasband, W.S., ImageJ, U. S. National Institutes of Health, Bethesda, Maryland, USA, http://imagej.nih.gov/ij/, 1997-2011.) and Adobe Photoshop/ Illustrator software packages (Adobe, San Jose, CA).

4.4 Results

4.4 a. Cav1 is expressed by a restricted population of CPN, and is excluded from CSMN

Cav1 is highly expressed by CPN relative to CSMN in the developing neocortex, with a peak of expression between P3 and P6 (Molyneaux et al., 2009) (Figure 4.1A), when CPN are making axonal and dendritic connections. *Cav1* is not detected in CPN by P14. I more thoroughly investigated Cav1 expression by immunocytochemistry, and similarly detected that Cav1 is indeed expressed by CPN, and is excluded from subcerebral projection neurons (SCPN, of which CSMN are a subpopulation) by combining Cav1 immunocytochemistry and dual retrograde labeling of CPN (from the contralateral cortex) and SCPN (from the pons). The Cav1-expressing population of CPN is clearly superficial to the SCPN. This highly restricted expression pattern suggests that Cav1 functions in a very specific subpopulation of CPN, rather than playing a broad role in CPN development (Figure 4.1B).

Additionally, *Cav1* mRNA and Cav1 protein is beginning to be expressed by cortical neurons at E18.5 (in addition to developing blood vessels), is highly expressed at P3 and P6, and is no longer detectable by P14. *Cav1*-expressing cells are distributed uniquely in cortical layer V, and in caudo-lateral areas. This pattern is not a developmental gradient, and is maintained specifically at all developmental agest at which *Cav1* is expressed (Figure 4.1C, D).

Interestingly, at P8, Cav1 is restricted to a subpopulation of CPN extending in layer V throughout somatosensory (SS) cortex, and expanding in the caudo-lateral cortex, but is excluded from motor cortex. This exclusion is shown by comparison between LMO4, which has high motor cortex expression, and Cav1 immunocytochemistry (Figure 4.2A). This area-specific expression further supports a subpopulation-specific function of CAV1 in CPN. Because of the strong expression of Cav1 at all developmental ages in layer V, particularly in caudo-lateral areas close to archicortex, where canonical cortical neuron subpopulations breakdown, I investigated whether Cav1-expressing neurons exclude CTIP2, the canonical SCPN control gene expressed highly in specific SCPN layer V populations. Unexpectedly, a subset of Cav1-expressing neurons in far caudo-lateral S2 do express CTIP2

Figure 4.1: *Caveolin1* is expressed by a restricted population of caudo-lateral CPN

(A) Caveolin1 is more highly expressed by purified CPN than by purified CSMN

Comparative microarray analysis at critical times in development (E18.5, migration; P3, process extenstion; P6, target finding; and P14, connectivity refinement), detects *Caveolin1 (Cav1)* as more highly expressed by a retrogradely labeled, FACS purified population of CPN (red line) than by CSMN (blue line). Error bars indicate standard deviation.

(B) CAV1 is expressed by CPN and excluded from SCPN at P3

Retrograde label at P1 with CAV1 immunocytochemistry at P3 confirms that CAV1 is expressed by CPN and excluded from SCPN at P3. B' inset from B. B'' confocal Z-stack of region in B. Open arrows indicate labeled CPN, closed arrows indicate labeled SCPN.

(C) Caveolin1 is expressed in caudo-lateral cortex during midstage cortical development

Cav1 mRNA is expressed by a restricted population of caudo-lateral, layer Va cells as shown by *in situ* hybridization over time (E18.5, P3, P7, and P14).

(D) CAV1 is expressed in caudo-lateral cortex during midstage cortical development

CAV1 protein is expressed by a restricted population of caudo-lateral, layer Va cells as shown by immunocytochemistry over time (E18.5, P3, P6, and P14). Scale bars: (B) 30μm, (D) 100 μm. SCPN, subcerebral projection neurons; CPN, callosal projection neurons; E embryonic day; P, postnatal day; Va, superficial portion of neocortical layer V. Panel A taken from Molyneaux, Arlotta, et al. *J. Neurosci.* 2005.

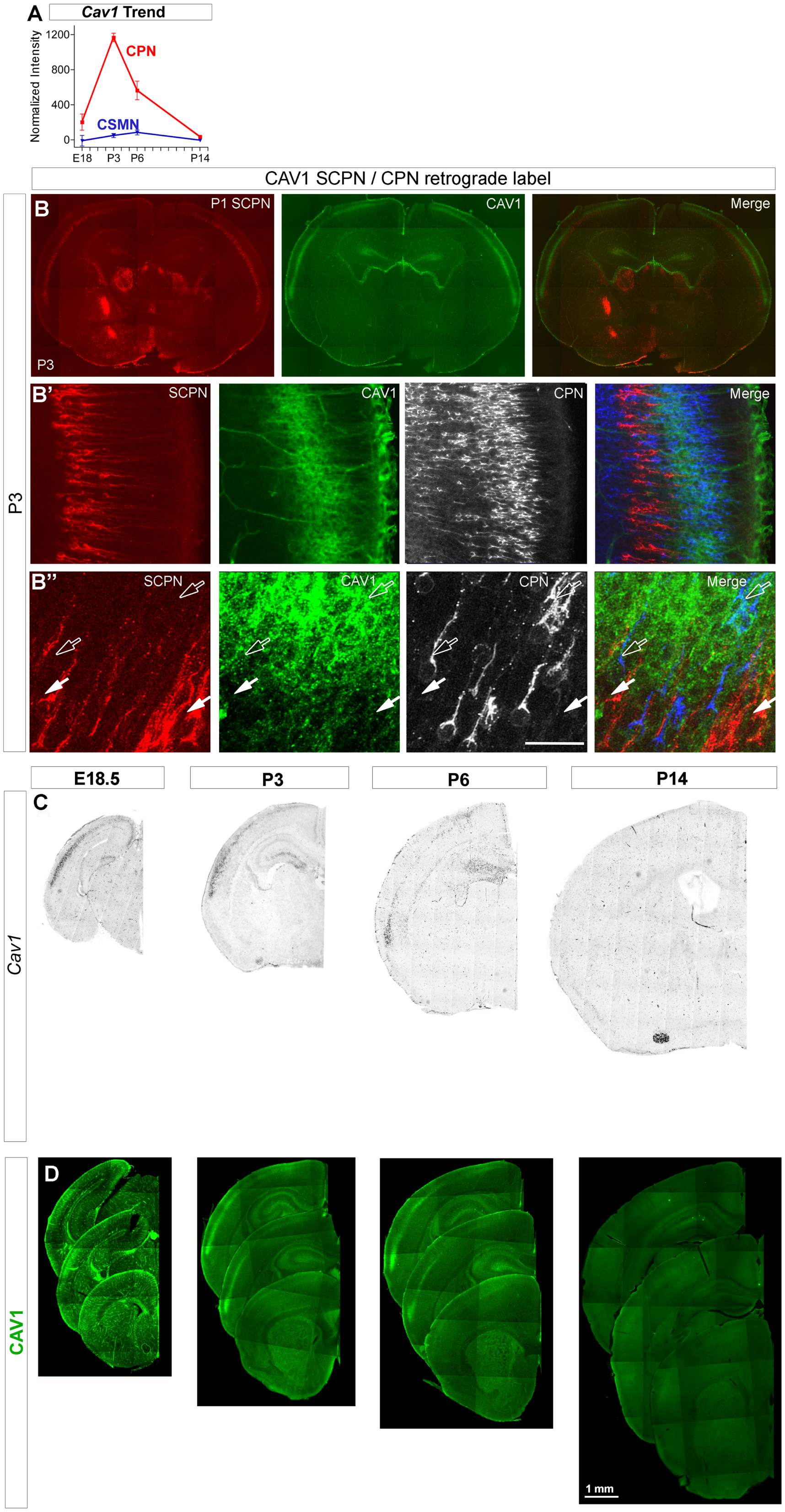

Figure 4.1 (Continued)

Figure 4.2 CAV1 is expressed in an areally restricted fashion at P8, and is excluded from motor cortex

(A) Expression of CAV1 is areally restricted; co-immunocytochemistry against LMO4 and CAV1 at P8 reveals that CAV1 is not expressed in motor cortex CPN. A’, inset from A.

Scale bar: (A’) 500 μm. SCPN, subcerebral projection neurons; CPN, callosal projection neurons; P, postnatal day.

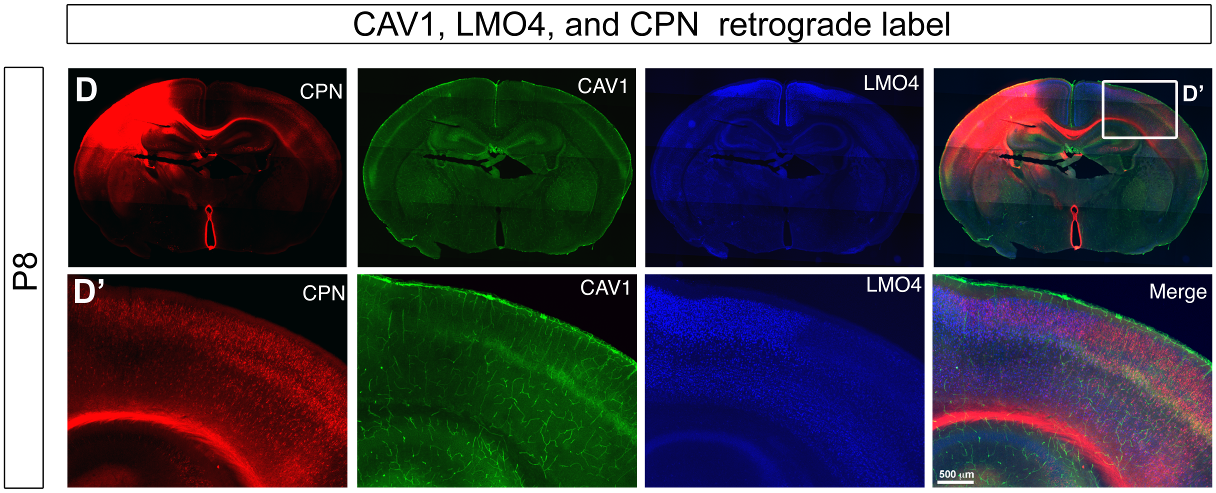

Figure 4.2 (Continued)

(Figure 4.3A), but are not subcerebrally projecting neurons (Figure 4.3 B, C). This quite unique population of non-SCPN, CTIP2$^+$ neurons has not been extensively defined, but they might likely be a subpopulation of neurons with a transient developmental spinal projection that is later lost (Polleux et al., 2001; Arlotta et al., 2005), and which fail to prune these spinal projections in *Ctip2*$^{-/-}$ mice.

In order to investigate more closely what subpopulation(s) of CPN expresses Cav1, both to better define the population(s) and enable correct targeting of the population via *in utero* electroporation in future experiments, I performed birthdating analysis every 12 hours throughout corticogenesis with thymidine analogs. These experiments reveal that Cav1 expressing neurons are born between E12.5 and E13, consistent with the dominant birthdate ranges for neocortical neurons residing in layer V (Figure 4.4). Cav1-expressing neurons in caudo-lateral S2 cortex are born earlier (peak at E12.5) than those of S1 layer V (peak at E13).

4.4 b. Cav1 is expressed by CPN cell bodies and dendrites endogenously, and when overexpressed.

Cav1 is a membrane-bound scaffolding protein, and, thus, its subcellular distribution can provide insight into its function in a given cell type. I examined the expression of Cav1 in P3 CPN, and found it to be highly expressed around the soma, with expression extending throughout the apical dendrite and dendritic tuft (Figure 4.5A). This suggests potential roles for Cav1 in migration and dendrite function. Cav1 is not highly detected in axons. Further, I generated a *Cav1-2A-GFP* over-expression construct to test Cav1 function in later analyses. Over-expressed CAV1 via *in utero* electroporation at E15.5 in superficial layer CPN of the SS cortex, which do not normally express *Cav1*, has a similar cellular distribution as endogenous, and is highly detected in superficial layer CPN cell bodies and dendrites at P6 (Figure 4.5B).

4.4 c. Cav1 is expressed by over 80% of dual-projecting FPN/CPN

Development of CPN does not end when early progenitors are specified, but includes acquisition of specific CPN subpopulation identities. Cav1 is much more highly expressed in CPN versus CSMN, but is expressed in a very restricted pattern in neocortex. Because many uniquely projecting subpopulations of CPN reside in restricted cortical areas, I examined localization of forward projecting neurons from somatosensory cortex to frontal areas (FPN), backward projecting neurons (BPN), CPN with striatal projections ($\mathrm{CStrPN_i}$), and anterior commissure projection neurons (ACN). The pattern of Cav1 expression closely resembles the restricted location of dual projecting frontal/callosal projection neurons (FPN/CPN) (Mitchell and Macklis, 2005) and partially overlaps with $\mathrm{CStrPN_i}$ and ACN. Expression is highest at the time of axon and dendrite elongation, and stabilization of neuronal connections (P3) (Figure 4.6; Figure 4.7 A, B, C, D). Cav1 is not expressed in all dual projecting CPN populations, because the range of BPN does not overlap with the Cav1 expression domain, suggesting that is specifically important for CPN/FPN and not all dual CPN populations.

To test the specific hypothesis that Cav1 might be acting in the dual projecting FPN/CPN subpopulation, I retrogradely co-labeled callosal- and frontal-projecting neurons by stereotaxic injection of the beta subunit of cholera toxin conjugated to two different Alexa fluorophores into the contralateral somatosensory cortex and the ipsilateral premotor cortex (Figure 4.7E). In support of this hypothesis, I found that over 80% of dual projecting CPN/FPN are $\mathrm{Cav1^+}$, and only a small population of non-dual projecting cortical neurons expresses Cav1; therefore, the highly restricted expression of Cav1 almost precisely labels this dual projecting population (Figure 4.7F). Due to the membranous location of Cav1 protein, and the incomplete label achieved by the CTB injections, I have not been able to reciprocally quantify the percentage of $\mathrm{Cav1^+}$ cortical neurons that are dual-projecting. Performing such counting with DAPI counterstain and a more diffusible dye (such as FluoroGold and DiI), might overcome these problems.

Figure 4.3: A subset of CAV1-expressing neurons co-express CTIP2, but CAV1 is not expressed by SCPN.

(A) CAV1 and CTIP2 are co-expressed by a subpopulation of caudo-lateral neurons.

CAV1 is largely excluded from the CTIP2 expression domain, though a subpopulation of CAV1 expressing neurons also expresses the canonical SCPN control gene, CTIP2.

(B) CTIP2 is expressed by SCPN and is excluded from CPN. As has been described in detail elsewhere, CTIP2 is expressed by SCPN and excluded from CPN. This holds true in the far caudo-lateral S2 region as well. Not all CTIP2-expressing neurons are SCPN.

(C) CAV1 and CTIP2 are co-expressed, but Caveolin1 is not expressed by SCPN.

Caudo-lateral (S2) CAV1-expressing neurons are not SCPN, as determined by retrograde label analysis, and are therefore likely to be some of the non-SCPN CTIP2-expressing neurons. A', inset from A.

Scale bars: (A) 500 μm (A') 100 μm (B,C) 60μm,. SCPN, subcerebral projection neurons; CPN, callosal projection neurons; P, postnatal day.

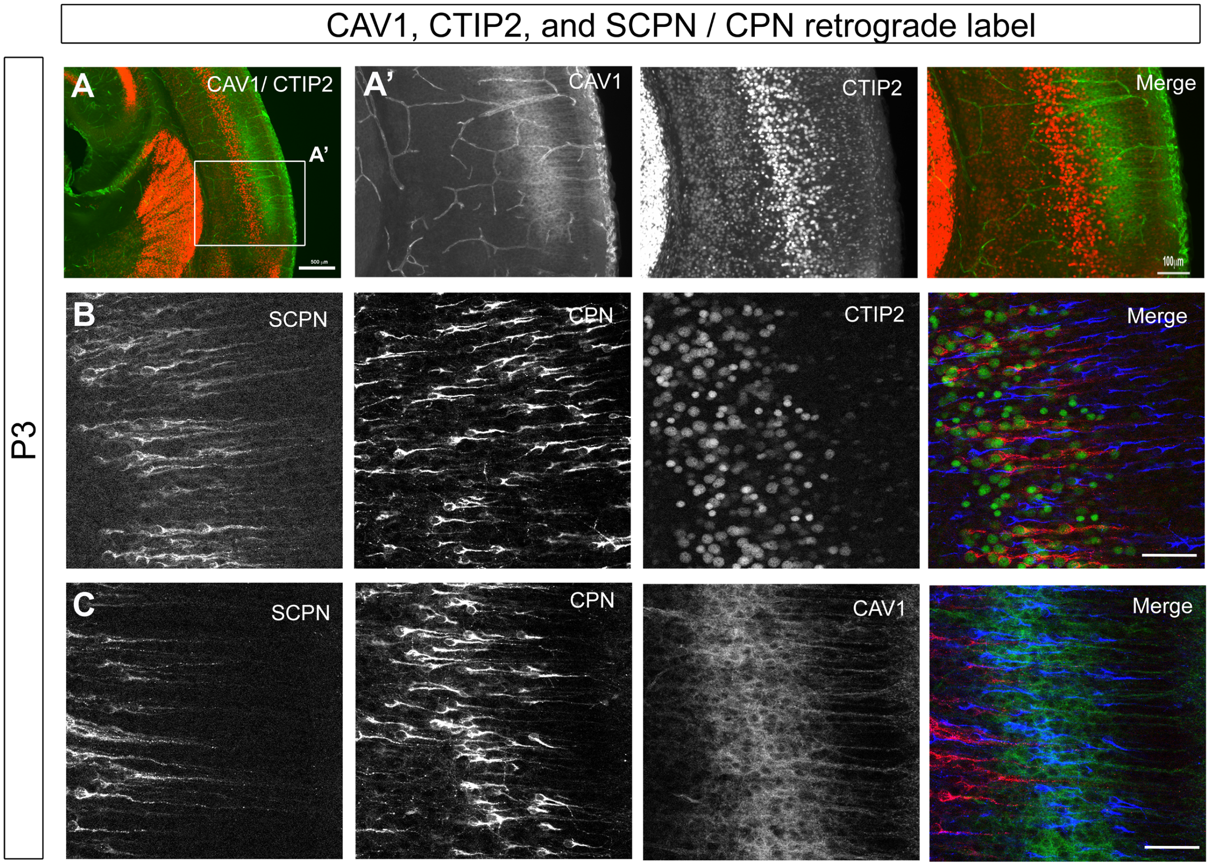

Figure 4.3 (Continued)

Figure 4.4: Caveolin1-expressing neurons are born between days E12.5 and E13

(A) deoxyUridine analog (CldU or IdU) injections at 24-hour intervals throughout corticogenesis reveal that CAV1-expressing neocortical neurons, both in S1(somatosensory layer V) and S2 (caudolateral expansion) are born close to E12.5. **(B)** Focused analysis with deoxyUridine analog injections at 24-hour intervals at peak birth times identified above reveals that the majority of this population is born between E12.5 and E13, with S2 peak CAV1-neurogenesis at E12.5 and S1 peak CAV1- neurogenesis at E13. Scale bars: 100μm. E embryonic day; P, postnatal day; V, neocortical layer V.

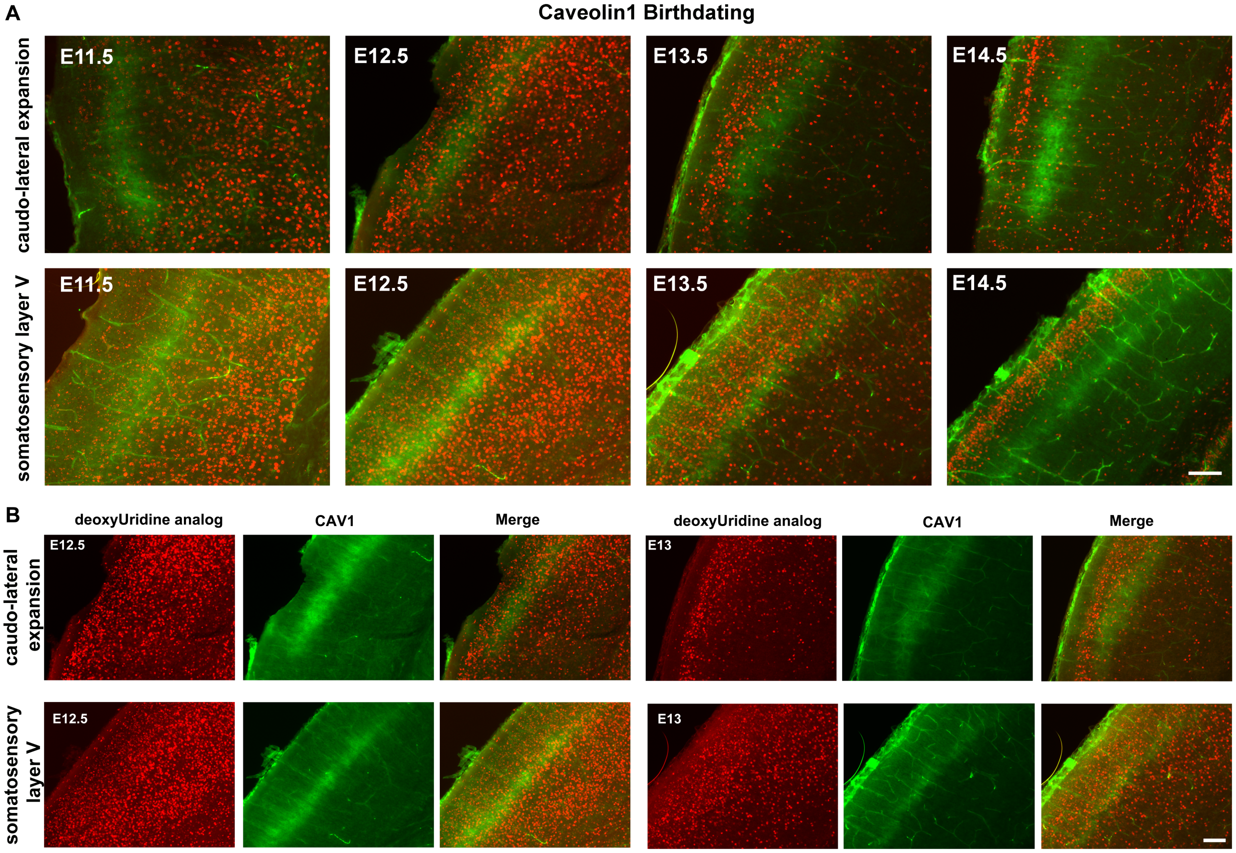

Figure 4.4 (Continued)

Figure 4.5: Caveolin1 is expressed in neuronal cell-bodies and dendrites at postnatal ages

***(A)* Caveolin1 is expressed in neuronal cell bodies and dendrites at P3**

MAP2 immunocytochemistry reveals that CAV1 expression overlaps with the dendritic and cell body compartments of neuronal plasma membrane.

(B) Exogenously expressed CAV1 correctly traffics to localize in the dendritic and cell body compartments of superficial layer neurons at P6.

Exogenously expressing *Cav1* in superficial layer neurons by *in utero* electroporation at E15.5 results in CAV1 protein trafficking that is similar to that of the endogenous protein **(A)**, and localized to the cell body and dendritic compartments of the neuronal plasma membrane. SCPN, subcerebral projection neurons; CPN, callosal projection neurons; E embryonic day; P, postnatal day.

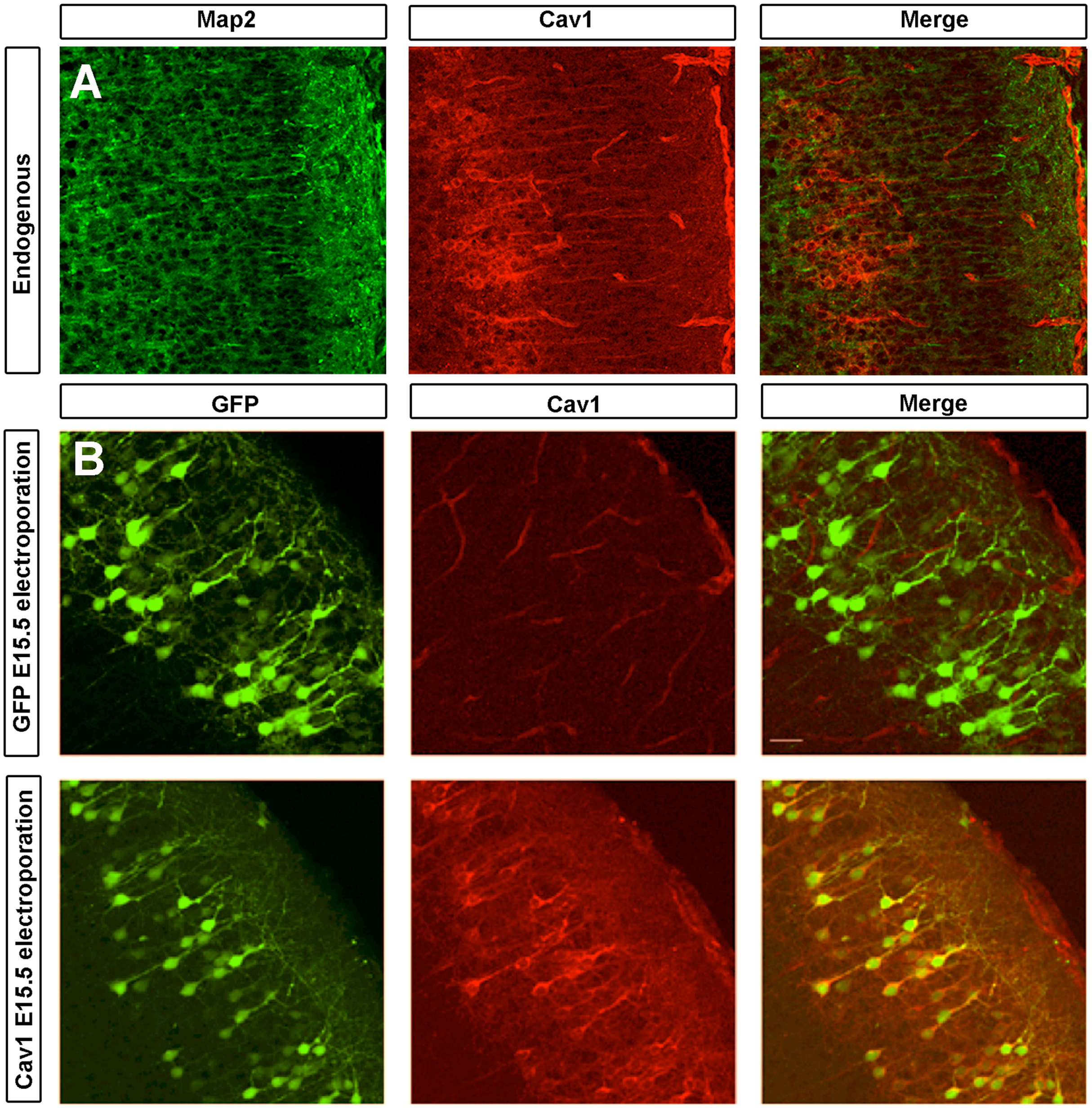

Figure 4.5 (Continued)

4.4 d. Cav1 function is not necessary for dual-projecting FPN/CPN to reach their axonal targets

Because the membrane-bound scaffolding protein Cav1 is expressed by the overwhelming majority of dual-projecting FPN/CPN at P8, and most highly at P3, I hypothesized that Cav1 might be necessary for the correct maturation (pruning, extension, or guidance of neuronal processes) and/or maintenance of this specific population of CPN. I first tested whether axons of FPN/CPN without Cav1 initially reach their targets correctly, which would suggest that Cav1 is not necessary for axonal extension or pathfinding, or establishment of CPN identity. I retrogradely labeled FPN/CPN in both *Cav1* null mice and their WT littermate controls at P6, and examined them at P8. At this early time (P8), when CPN exuberance is most pronounced, there is no change in the overall number of FPN/CPN in nulls, nor in the specific bin corresponding to the secondary somatosensory cortical area (S2), where both Cav1 expression and the abundance of FPN/CPN change dramatically (Figure 4.8). Thus, Cav1 function is not required for CPN/FPN to extend dual-projecting axons to specific targets. Due to the fact that Cav1 is expressed around the neuronal cell body as well as the dendritic tree, but not broadly in the axon or growth cone, it is not surprising that FPN/CPN reach their targets at P8. I am currently testing the hypothesis that Cav1 is required for the maintenance/strengthening of FPN/CPN synapses, by examining the final connectivity pattern in mature (P21) Cav1 null cortex, by performing dual retrograde labeling at P21. I am also examining dendritic morphology via electroporation of farnisylated GFP at the time of Cav1+ CPN birth, over expressing Cav1 tagged with the same membrane-targeted GFP, and examining synapses via synapse-specific antigens on FPN/CPN in *Cav1* null mice.

4.4 e. Cav1 is not expressed by brain cell populations expressing Cav2 or Cav3, and Caveolin family members do not compensate for Cav1 in its absence.

Because there are three members of the *Caveolin* family in the mouse genome, and because these members interact with each other in other systems(Hnasko and Lisanti, 2003), I investigated whether Cav2 or Cav3 are expressed by the same population(s) of neurons expressing Cav1. Both Cav2 and Cav3 are expressed in mouse brain, but are excluded from the Cav1-expressing population(s) at P3. Cav2 is expressed along the surface of the lateral ventricles. Cav3 is expressed by mitral cells, projection neurons in the olfactory bulb (Figure 4.9A, B). This fact is particularly interesting in light of evidence that, in other systems, Cav2 protein localization and, therefore, stability, is dependent on Cav1 expression(Mora et al., 1999). In *Cav1* loss of function mutants, neither family member extends its expression domain into neocortex projection neurons (Figure 4.9C, D), indicating that no *Caveolin* family member is compensating for *Cav1* function in the mutant neocortex. Therefore, findings in the *Cav1* null cortex are not likely explained by a compensation event.

4.4 f. Cav1 expression is not dependent on correct callosal connectivity

Since Cav1 is known to interact with striatins for correct signal transduction at synapses (Gaillard et al., 2001a) and multiple neurotransmitter receptors (Boulware et al., 2007; Takayasu et al., 2010), I hypothesized that Cav1 expression might be regulated by neuronal activity. Since I have shown that Cav1 is expressed by CPN, I asked whether Cav1 expression is altered in the acallosal BTBR mouse strain (Wahlsten et al., 2003). These mice exhibit largely normal cortical development, but no axons extend across the CC; even though they perform quite well on physical coordination tasks, they display behavioral abnormalities. Additionally, these mice exhibit a reduced hippocampal commissure, accompanied by improper wiring reflected by tangles of axons known as probst bundles. I find that Cav1 expression is independent of correct callosal connectivity, and Cav1 is expressed normally in P4 BTBR neocortex (Figure 4.10). Based on the early neonatal expression of Cav1, it might be hypothesized that final connectivity is not needed for Cav1 expression. These results indicate that, although Cav1 had been previously shown to act at synapses(Gaillard et al., 2001a), its expression in CPN is, indeed, not dependent on correct connectivity.

4.4 g. Exogenous Cav1 function is sufficient to cause migrational defects

As discussed in section *4.4 b.*, Cav1 is subcellularly highly concentrated in cell bodies and dendritic arbors within cerebral cortex, and exogenously expressed *Cav1* is correctly trafficked. Cav1 is known to

Figure 4.6: CAV1 developmental expression includes overlap with dual projecting CPN/FPN. (A). Schematic representation of CPN (blue), FPN (red), and CPN/FPN (purple overlap) distribution over neocortical development. **(B)** Schematic representation of CAV1 expression (green) over the same developmental times denoting the similar distribution of CAV1 expressing neurons and CPN/FPN, as quantified in Figure 4.6.

CPN, callosal projection neurons; FPN, ipsilateral frontal projection neurons; P, postnatal day.

A is adapted and expanded from Mitchell and Macklis, *J. Comp. Neurol.*, 2005.

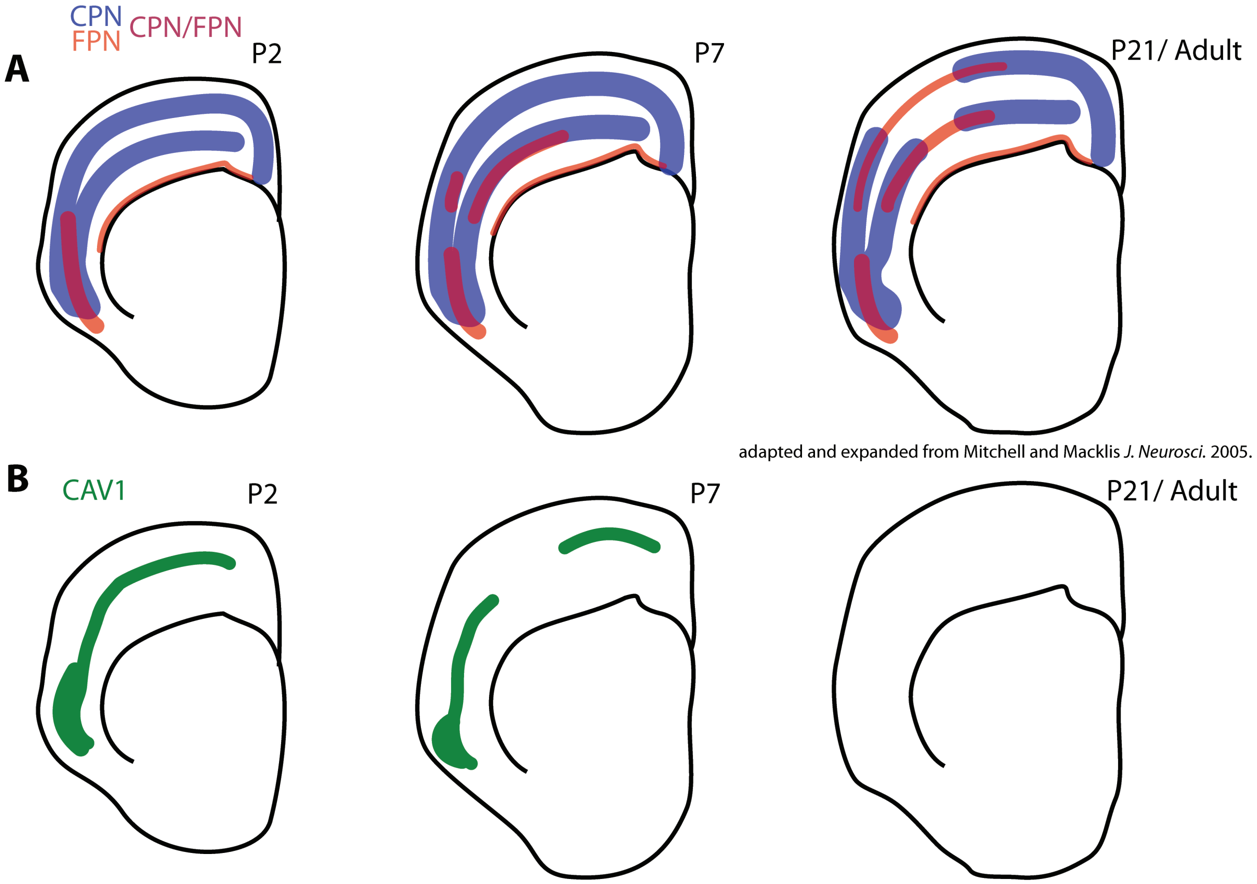

adapted and expanded from Mitchell and Macklis *J. Neurosci.* 2005.

Figure 4.6 (Continued)

Figure 4.7: CAV1 is expressed by restricted subpopulations of neocortical neurons including dual projecting CPN/FPN at P8.

(A, B, C, D) Diverse populations of neocortical projection neurons with CPN projecting subsets including CPN, FPN, BPN, and CStrPNi/ ACN. Schematic representations of diverse cortico-cortical projection neurons labeled (CPN, red; CPN/FPN, blue; CPN/BPN, purple; CStrPNi, green; ACN, yellow). Retrograde labels of CPN (green) **(A)**, FPN **(B)**, BPN **(C)**, and CStrPNi/ ACN **(D)** (all red). Other than CPN, the only pure population of cortico-cortical projection neurons in the CAV1 expression domain are FPN. However, the mixed population of CStrPNi/ ACN also overlaps with the CAV1 expression domain laterally.

(E) Schematic representation of the dual CPN/FPN retrograde labeling scheme. FPN are isolated to layers V, and VIb (subplate) in largely lateral cortical locations, with caudo-lateral S2 expansion. CPN are located in layers II/III, V, and VI. The populations overlap in the subpopulation of dual projecting CPN/FPN. These projections were assessed following CTB injection into ipsilateral premotor cortex, and simultaneously into contralateral somatosensory cortex.

(F) CAV1 is expressed by over 80% of dual projecting CPN/FPN. Dual projecting CPN/FPN were labeled as shown in (E), and the percentage of dual projecting CPN/FPN that also express CAV1 was calculated for four medio-lateral regions with standard error.

CPN, callosal projection neurons; FPN, ipsilateral frontal projection neurons; BPN, ipsilateral backward projecting neurons; CStrPNi, intratelencephalic corticostriatal projection neurons; ACN, anterior commissure projection neurons; E, embryonic day; P, postnatal day. BPN retrograde label by G. Cederquist.

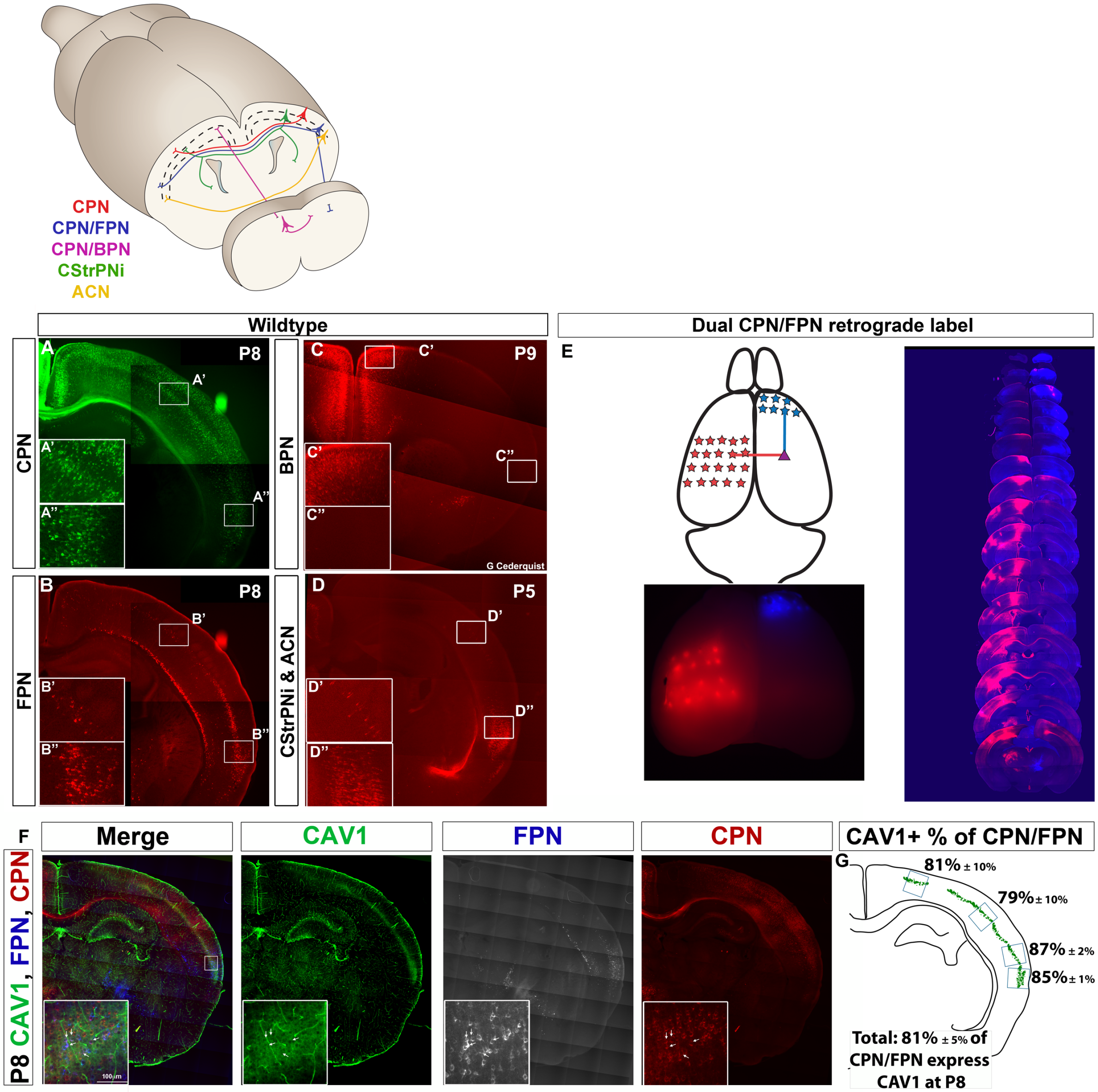

Figure 4.7 (Continued)

Figure 4.8: Loss of *Cav1* function does not disrupt formation of dual projecting CPN/FPN axonal projections at P8.

(A, D) CPN form in the absence of Cav1 function. CPN were retrogradely labeled from contralateral cortex in *Cav1* null animals and WT controls. There is no significant difference between the two genotypes. N=5 WT and 5 *Cav1* null.

(B, E, H) FPN form in the absence of Cav1 function. FPN were labeled as described above, and the number of labeled FPN was calculated for 2 medio-lateral regions (S1 and S2) with standard error. There is no significant difference between the two genotypes. N=5 WT and 5 *Cav1* null.

(C, F, G, I) Dual projecting CPN/FPN form in the absence of Cav1 function. Dual projecting CPN/FPN were labeled as described above, and the percentage of dual projecting CPN/FPN was calculated for 2 medio-lateral regions (S1 and S2) with standard error. The percentage of labeled FPN with a callosal projection was also calculated for 2 medio-lateral regions (S1 and S2) with standard error. There is no significant difference between the two genotypes. N=5 WT and 5 *Cav1* null.

Error bars: standard error of the mean. CPN, callosal projection neurons; FPN, ipsilateral frontal projection neurons; WT, wildtype; P, postnatal day.

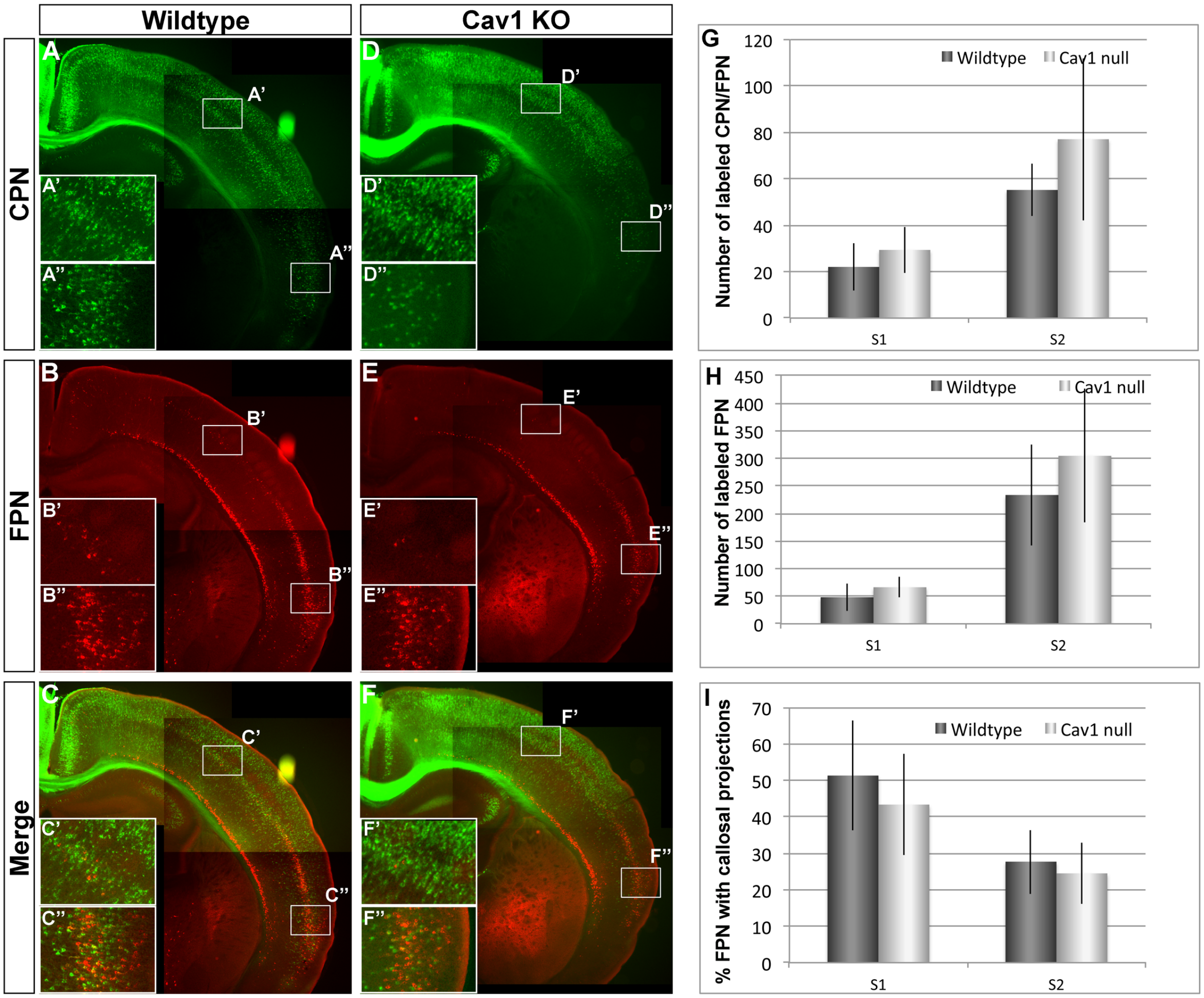

Figure 4.8 (Continued)

Figure 4.9: Caveolin family members are expressed in non-overlapping patterns in the developing brain, and do not appear to compensate for loss of *Cav1* function.

(A) Caveolin family members are expressed in non-overlapping regions of the P6 brain. CAV1 is expressed in layer Va of S1 cortex and more broadly in S2 cortex; CAV2 is expressed along the lateral ventricle; and CAV3 is expressed in mitral cells of the olfactory bulb.

(B) Focused examination of the CAV2 and CAV3 expression domains indicates that CAV1 is not expressed in overlapping regions as its family members, in particular, CAV1 is not expressed along the lateral ventricle or in mitral cells.

(C) Caveolin family members CAV1 and CAV2 do not change expression patterns in the P3 Cav1 loss-of function brain. While CAV1 expression is lost in the Cav1 loss-of-function brain, CAV2 and CAV3 do not have altered expression patterns.

(D) CAV2 and CAV3 are not expressed in Cav1 loss-of-function caudo-lateral cortex. Focused examination of the normal CAV1 expression domains in the CAV1 null brain indicate that CAV2 and CAV3 do not appear to compensate for loss of CAV1 function.

Scale bars: 2mm (A, C), 100μm (B), 200μm (D); WT, wildtype; P, postnatal day; OB, olfactory bulb; LV, lateral ventricle.

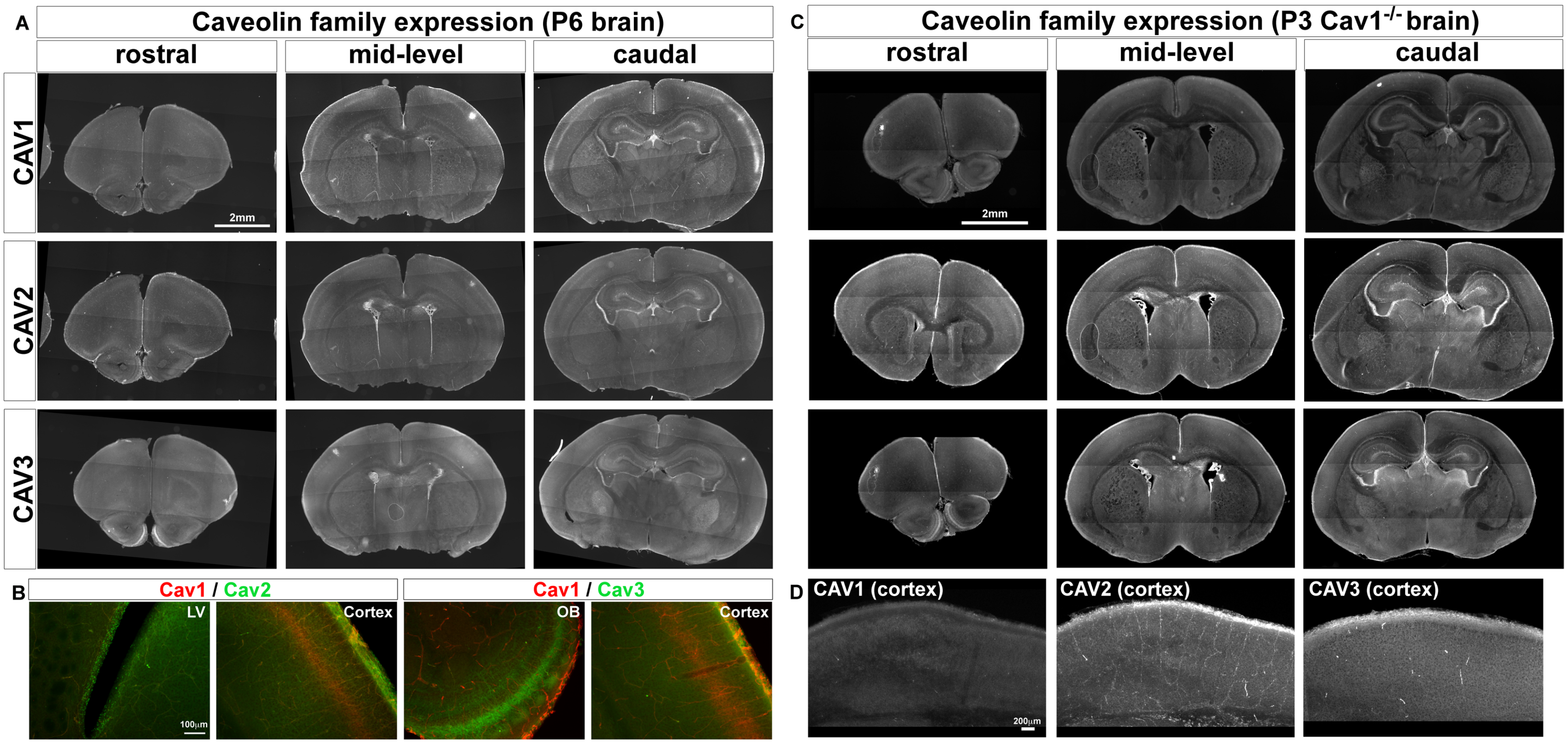

Figure 4.9 (Continued)

Figure 4.10: Correct *Cav1* expression is not dependent on formation of the corpus callosum at P4.

(A) Acallosal BTBR mice express CAV1 at comparable levels, and in an identical pattern, to their closely related callosal LPJ strain, suggesting that CAV1 expression is not dependent on correct CPN connectivity.

Scalebar: 1mm. WT, wildtype; P, postnatal day.

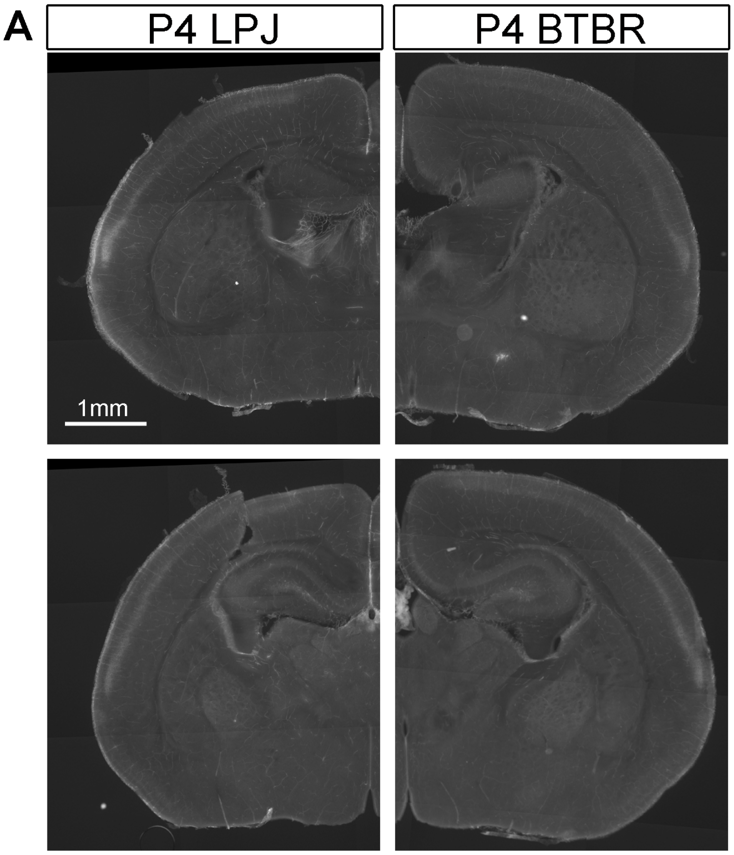

Figure 4.10 (Continued)

Figure 4.11: Exogenous CAV1 expression leads to delayed neuronal migration and excess axonal branching in the CC

Exogenous overexpression (OE) of CAV1 in superficial layer neurons leads to immature neuronal phenotypes at P1, including delayed migration **(A)** and less complex dendrite branching **(B)** as compared to expression of a GFP control (G2A-Stop). At P6, the earlier migration phenotypes are no longer visible **(C).** However, images indicate extra axonal branching in the CC **(D)** when CAV1 is mis-expressed, in contrast to GFP control expression construct (G2A-stop).

Scale bars: 100 μm. CC, corpus callosum; E, embryonic day; P, postnatal day; OE, overexpression.

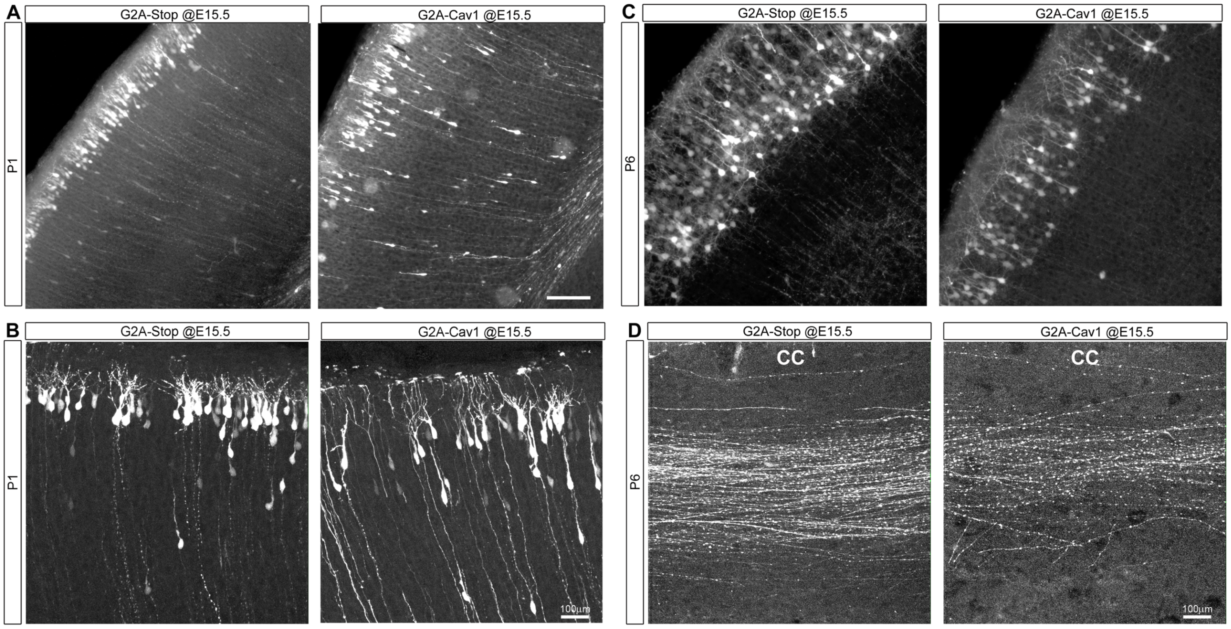

Figure 4.11 (Continued)

interact with striatins at synapses and Rac1 at focal adhesion points in other systems(Gaillard et al., 2001b; Nethe et al., 2010). Therefore, I hypothesized that Cav1 might function in proper neuronal adhesion. Such a role might affect critical neuronal processes such as migration, axonal extension and branching, and/or correct formation and/or maintenance of complex dendritic arbors for this unique population of CPN/FPN.

To investigate a potential function for Cav1 in early neuronal maturation processes, I employed *in utero* electroporation at E15.5 to exogenously express *GFP*^{control} and *Cav1*^{GFP} in superficial layer projection neurons, a population that does not endogenously express *Cav1*. I found that exogenous expression of *Cav1* results in superficial layer neurons that display immature morphologies at P1 (Figure 4.11A, B). These immature phenotypes indicate delayed migration, and suggest potential extra aberrant adhesion points. By P6, no delayed neurons are detected, either due to elimination of improperly located neurons, or due to a recovery of the migrational delay (Figure 4.11C). Interestingly, exogenous *Cav1* expression might also result in excess axonal branching within the developing CC (Figure 4.11D), a phenotype that could also be linked to potential extra aberrant adhesion points or to the dependence of neurotrophin signaling on Cav1 (Bilderback et al., 1997; Bilderback et al., 1999; Rico et al., 2004).

Studies demonstrating Cav1 interaction with Rac1 at focal adhesion sites in non-neuronal cells (Nethe et al., 2010), and of Cav1 regulation of neurotrophin signaling pathways (Bilderback et al., 1997; Bilderback et al., 1999) support a hypothesis of Cav1 function in process ramification. Future directions include extending these overexpression studies to later times, performing focused axonal branching analysis, and employing dendritic analysis techniques already available in the lab to examine dendritic development/ maintenance, both in *Cav1*-mis-expressing neurons and *Cav1*-null CPN/FPN.

4.5 Discussion

Callosal projection neurons (CPN) of the cerebral cortex reside in cortical layers II/III, V, and VI, and all extend axons to homotopic mirror image targets in the contralateral hemisphere. Some subpopulations extend second axons to distinct targets including frontal or caudal ispsilateral neocortex, or even subcortically into ipsi- or contralateral striatum. Identifying molecular determinants of CPN that are neuron subtype-specific or subpopulation-specific will enable specific and thorough study of these unique subpopulations critical for information integration by providing molecular markers. In addition, such studies will also allow for in-depth functional analysis of these determinants themselves throughout development, to gain insight on their roles in establishing the precise connectivity that endows these subpopulations with critical roles in neocortical information transfer and correlation.

Previously, I presented comparative microarray analysis designed to identify molecular determinants of CPN populations, and subsequent evaluation of these data revealing molecular diversity within the broad population of CPN. This diversity includes not only laminar and areal subpopulations, but also includes some unique expression patterns that reflect subpopulations of CPN with diverse axonal projection patterns. Here, I show that Cav1, a lipid raft scaffolding protein enriched in CPN over CSMN, is expressed in a restricted fashion in the neocortex, and is expressed by over 80% of one such subpopulation, dual projecting CPN extending axons contralaterally and to ipsilateral frontal areas (CPN/FPN). Specifically, Cav1 is localized to neuronal cell bodies and to dendrites, but has not been detected in axons. The temporal developmental expression of *Cav1* coincides with the middle time period of CPN development, including low-level expression during neuronal migration, and highest levels of expression from P3 to P6, when CPN are extending and refining axonal and dendritic processes. Together, these results suggest functions for *Cav1* in post-mitotic establishment of innervation or connection pruning.

Cav1 function is not necessary for specification and early development of dual projecting CPN/FPN, as shown by precise dual retrograde labeling approaches in *Cav1* null neocortex, consistent with its later developmental timing of expression, and absence of subcellular localization to axons. This lack of requirement for *Cav1* function in establishment of CPN/FPN is not a result of simple compensation by close family members, as neither Cav2 nor Cav3 are co-expressed with Cav1, nor do these two family members change expression domains in the absence of Cav1 function. Because these CPN/FPN projections continue to prune and establish precise connectivity until P21 (Mitchell and Macklis, 2005), it would be interesting to employ the same dual labeling approaches at P21 to investigate potential changes in axonal pruning that might result from potentially improper dendritic arborization, dendritic synaptogenesis, and/or axonal target-finding. If there is a change in the number of CPN/FPN in *Cav1* null mice at P21, comparison between the number of CPN/FPN detected with retrograde labeling at P21 to the number detected at P21 from retrograde labeling performed at P8 would be able to distinguish between axonal pruning of one or both projections, versus a loss of these neurons altogether.

Because of Cav1's known interaction with neurotransmitter receptors (Boulware et al., 2007) (Lai et al., 2004) (Takayasu et al., 2010), dendritic spine signaling scaffolds(Gaillard et al., 2001a), and synaptosome components (Bilderback et al., 1997; Bilderback et al., 1999; Braun and Madison, 2000) the function of CAV1 in CPN/FPN might only be comprehensible through electrophysiological functional analysis of these neurons lacking their endogenous *Cav1* function in *in vivo* circuits. I find that Cav1 expression is not dependent on correct CPN connectivity by examining Cav1 expression in the acallosal BTBR mouse line; however, Cav1 might be critical for CPN/FPN neuronal activity. Since neuronal activity is very tightly tied to axonal and dendritic connectivity(Wang et al., 2007), especially maintenance and establishment, careful examination of P21 CPN/FPN axonal and dendritic morphologies with loss- or gain-of-function of *Cav1* might very likely reveal a Cav1 function in CPN/FPN activity.

Exogenous expression of *Cav1* in superficial layer CPN that do not endogenously express *Cav1* results in neurons that display immature morphologies at P1, with delayed migration and P6 axonal morphologies that resemble extra branching, suggesting potential additional adhesion points. To investigate whether Cav1 function is sufficient to promote adhesion that gives rise to neurite branching (similar to processes likely necessary for dual axonal projection formation by CPN or to direct or modify dendritic development) the *Cav1* overexpression studies could be extended from Section *4.4g* to a scheme that would allow detailed axonal and dendritic analysis at P6 and later, as CPN/FPN are extending neurites. Electroporating *Cav1-2A-EGFP* and a control GFP construct at E15.5 will produce high EGFP expression throughout CPN axons. It would then be possible to visualize potential bifurcation of *Cav1* overexpression CPN axons and dendrites in comparison to GFP-expressing control CPN, in addition to the precision of their contralateral targeting at specific postnatal time points. Using a construct with the 2A peptide labeling Cav1 protein could allow for higher sensitivity in localizing overexpressed Cav1, to determine if any is in the axon, either at growth cones or at branching points. This single set of experiments would allow for analysis of both axonal and dendritic development of *Cav1* overexpression and control electroporated CPN of the superficial layer SS cortex.

Overexpression studies, like the ones discussed above, should take into account caveats of not only expressing proteins in unnatural cell populations, but also temporal misplacement of expression. Since expression of Cav1 in the caudo-lateral cortex begins around E18.5, and is up-regulated postnatally, over-expression of *Cav1* in progenitors might, therefore, result in gain-of-function phenotypes different from the endogenous function of Cav1 in CPN/FPN. However, these phenotypes might provide valuable mechanistic insight into Cav1 action in cortical projection neurons, and could inform the investigation of general processes in which Cav1 can participate, providing insight regarding potential binding partners. To directly examine the function of Cav1 in the postnatal development of CPN, it would be possible to alter the over-expression strategy to give correct temporal expression in an incorrect neuronal population by employing early postnatal injections of *Cav1* expressing adenovirus, or by the electroporation of an inducible *Cav1* expression construct.

Because Cav1 is highly concentrated in cell bodies and dendritic arbors of CPN/FPN, future work on this project could examine dendritic development and maintenance in *Cav1* null CPN/FPN in comparison to wildtype. Together, these studies would provide important insight into the development of this newly molecularly identified dual projecting population of CPN that likely functions in a variety of complex and critical processes integrating cortical information.

Cav1 is a scaffolding domain protein with a number of known protein interactors from studies in other systems. Informed, directed, and refined by the results of the above proposed experiments, it would be possible to investigate whether Cav1 directly interacts with a carefully selected subset of known Cav1 binding partners in CPN (particularly those shown to act in neuronal-relevant processes), and whether Cav1 functions in the development of defined subpopulations of CPN through these interactions. One particularly compelling potential interacting protein for first analysis is Rac1, for reasons described above, including that it has been shown in other systems to play roles in important neuronal functions relating to cytoskeletal dynamics and focal adhesion, such as neurite growth, adhesion, and migration (Beardsley et al., 2005; Kang et al., 2006; Joshi et al., 2008a). In particular, Rac1 is required for midline crossing of CPN(Chen et al., 2007; Kassai et al., 2008), and Rac1, recruited by CDKL5, can regulate neuronal migration and dendritic arborization of some CPN(Chen et al., 2010). Identification of neocortical binding partners of Cav1 will provide valuable insight into mechanisms of CPN subtype development / refinement through complex networks of discrete protein-protein interactions, with likely implications for subtypes of ASD. The emerging "cortical connectivity/synaptogenic hypothesis" of ASD suggests that such a process change caused by Cav1 function might contribute to ASD phenotypes.

These data are, to my knowledge, the first identification and functional analysis of a potential molecular control over a uniquely projecting subpopulation of CPN. While Cav1 function itself reveals unique properties of CPN/FPN, and reveals itself as a specific direct actor in specific functionalities of CPN/FPN, it will also likely function as a molecular "hook" to identify potential upstream controls over CPN/FPN. The defining properties of this subpopulation, likely critical for "feed forward" information integration, are yet to be completely understood, but this analysis of Cav1 expression and function identifies and characterizes a first molecular control over this functionally unique projection neuron population.

Funding

This work, as well as work described in Chapters 3, 5, and 6, was partially supported by grants from the National Institutes of Health (NINDS), the Harvard Stem Cell Institute, and the United Sydney Association. R.M.F. was partially supported by a National Science Foundation Graduate Research Fellowhsip Program (GRFP) fellowship and a National Institutes of Health predoctoral NRSA fellowship F31 NS073136.

Acknowledgements

I thank E. Gillis-Buck for assistance with the birthdating studies and blinded counting; G. Cederquist for sharing expertise regarding CPN/ BPN; L. Pasquina, R. Richardson, C. Greppi, T. Keefe, and P. Davis for superb technical assistance; and current and past members of our laboratory for discussions and helpful suggestions.

Chapter 5:

TMTC4 is critical for human corpus callosum formation and functions in axonal development of a subpopulation of callosal projection neurons in mice

Author contributions: The murine work on this project was an equal collaboration between Jessica L. MacDonald, PhD, a post-doctoral fellow, and me. We jointly designed all experiments and interpreted all data. Jessica performed the majority of the FACS purification, qPCR, protein gels, and protein localization work; and I performed the majority of the mutant construct design, axonal analysis, ISH, and confocal imaging. All human genetic work presented in the introduction was performed in Elliott Sherr's laboratory at UCSF. Our two labs are collaborating on this project.

5.1 Abstract

Molecular controls over key processes in callosal projection neuron (CPN) development are only very recently being discovered and functionally characterized. However, many developmental disorders involving CPN and the corpus callosum (CC) have already been clinically characterized. The overlap of CPN developmentally expressed genes, and disorders involving improper development of CPN, likely converge on gene products critical to controlling CPN development. *Tmtc4* (Transmembrane and tetratricopeptide repeat containing 4) is a previously uncharacterized protein-binding, transmembrane protein that we identified to have expression increasingly restricted to CPN during the first postnatal week, when CPN axons are crossing the midline and targeting to the contralateral hemisphere. While the function of *Tmtc4* is unknown, mutations in *Tmtc4* were recently identified in human cases of corpus callosum agenesis (AgCC) (Elliott Sherr's lab, UCSF; Li et al., SFN 2008) concurrent with our work in mouse, suggesting that *Tmtc4* might be a critical regulator of CPN axon outgrowth and/or targeting. Here, I show in mice that *Tmtc4* is expressed by CPN of neocortical layers II/III and Va in endoplasmic reticulum, and is excluded from early midline structures and other cortical projection neuron populations. Strikingly, overexpression of disease causing human point mutations affects axonal projections. Specifically, $\mathit{Tmtc4}^{\Delta R506Q}$ drives exogenous axonal CPN branching, and $\mathit{Tmtc4}^{\Delta E463K}$ results in some misrouting of CPN axons on the ipsilateral side. Together, these results suggest that *Tmtc4* can act in CPN development, and that cell-autonomous function of *Tmtc4* in CPN axons potentially causes the effects of mutated *Tmtc4* in human patients with AgCC.

5.2 Introduction

Callosal projection neurons (CPN), the corpus callosum (CC), and their dysfunction have been implicated in numerous neurodevelopmental disorders including autism spectrum disorders (ASD)(Booth et al., 2011), schizophrenia(Innocenti et al., 2003), dyslexia(von Plessen et al., 2002), and agenesis of the corpus callosum (AgCC) (Paul et al., 2007; Kaufman et al., 2008; Wahl et al., 2008; Booth et al., 2011). Therefore, we hypothesized that some of the genes more highly expressed by CPN than by other projection neuron populations might be "disease genes (when mutated or variant), functioning cell-autonomously in CPN.

Recently our group identified *Tmtc4* (Transmembrane and tetratricopeptide repeat containing 4) as more highly expressed by CPN than by CSMN, specifically during early postnatal neuronal development, via comparative developmental gene expression analysis between purified populations of projection neurons (Chapter 2 and (Molyneaux et al., 2009)). Simultaneous to our identification of *Tmtc4* as a candidate gene for functioning in CPN development, Elliott Sherr's lab at the Comprehensive Center for Brain Development at UCSF identified *Tmtc4* as mutated in 3/140 examined patients with AgCC (Li et al., 2008). Together these data suggest that *Tmtc4* might be one such gene acting in CPN development, and whose dysfunction results in human disease.

Tmtc4 is the last identified member of a largely functionally uncharacterized family of proteins; while nothing has been characterized about TMTC4, TMTC1 mutations are associated with heart failure from a genome wide screen (Smith et al., 2010; Della-Morte et al., 2011), and both TMTC2 and TMTC3 have been identified to be localized to endoplasmic reticulum (ER)(Simpson et al., 2000; Racapé et al., 2011). TMTC4 is predicted to contain twelve transmembrane domains, followed by eight tetra-trico-peptide repeat (TPR) domains (www.uniprot.org – ID Q8BG19) (Figure 5.1A). TPRs are protein-protein interaction modules found in multiple copies in many functionally different proteins. More specifically, each TPR motif unit contains two antiparallel **α** helices; and tandem repeats of individual TPR motifs, as present in TMTC4, generate a right-handed helix with an amphipathic channel that can bind such a complimentary region in a target protein(Blatch and Lässle, 1999). Therefore, TPR-containing proteins like TMTC4 are associated with multiprotein complexes, form homodimers, and have been shown to be involved in cell cycle, transcription and splicing, protein transport, protein folding (co-chaperones), and phosphate turnover(Blatch and Lässle, 1999). Some TPR-containing proteins have specifically been implicated in nervous system development and function including: dyslexia susceptibility gene (Dyx1c1), which functions during neuronal migration in the embryonic neocortex(Wang et al., 2006; Rosen et al., 2007) and white matter formation(Darki et al., 2012); and TPR containing Down syndrome gene (TPRD or TTC3), a candidate gene in pathophysiology of Down Syndrome that is highly expressed in human and mouse neocortex, and is critical for neuronal differentiation through RhoA GTPase cell cycle regulation(Berto et al., 2007). Therefore, while no specific function has yet been attributed to TMTC4, family members and other TPR-motif containing proteins play critical roles in critical cellular processes and neuronal development.

Complementary to our work, Elliott Sherr's group at UCSF independently identified *Tmtc4* as a candidate disease gene in an 11-year-old patient with complete AgCC with misrouted axons in bilateral probst bundles. This child has a balanced reciprocal chromosomal translocation between chromosome 1 and chromosome 13, spanning a 10kb sequence in the *Tmtc4* gene intron 6 (mouse intron 5) between the coding sequence producing the 4th and 5th transmembrane domains (Figure 5.1B). After identifying this genomic abnormality, members of the Sherr lab performed focused analysis of *Tmtc4* sequences in their 140 AgCC patients. They found two more AgCC patients with single point missense mutations in *Tmtc4* that result in altered amino acids with dissimilar properties that were predicted to be disease causing: 1. glutamic acid to lysine at amino acid 463 (E463K) in exon 12 (mouse exon 11); and 2. arginine to glutamine at amino acid 506 (R506Q) in exon 13 (mouse exon 12) (both are conserved residues in mouse TMTC4). These variations were not found in the control cohort (Figure 5.1C,D). Due to the complexity of midline formation and correct midline crossing, consensus mutations causing AgCC are rare, and, therefore, *Tmtc4* is a high priority candidate for functional analysis. However, while the Sherr lab

Figure 5.1: Tmtc4 has a predicted structure of 12 transmembrane domains and 8 tetratricopeptide repeats; human mutations occur in the TPR domain. **(A)** Schematic representation of the predicted functional domain structure of TMTC4. **(B)** The identified human chromosome1:chromosome3 balanced translocation with agenesis of the corpus callosum (AgCC) occurs in a 10kb sequence in the *Tmtc4* gene intron 6 (mouse intron 5) between the coding sequence producing the 4th and 5th transmembrane domains. **(C)** Single point missense mutation (black swirl) in *Tmtc4* found in a patient with AgCC results in an amino acid change from glutamic acid (E) to lysine (K) at amino acid 463, which is located at the junction of the last transmembrane domain and the first TPR motif. **(D)** Single point missense mutation (grey swirl) in *Tmtc4* found in a patient with AgCC results in an amino acid change from arginine (R) to glutamine (Q) at amino acid 506, which is located in the second TPR motif. Amino acid "R" groups are depicted on the right-hand side to illustrate changed chemical properties resulting from the mutations. TM, helical transmembrane domain; TPR, tetratricopeptide repeat motif; P, phosphorylation point; Ch, chromosome.

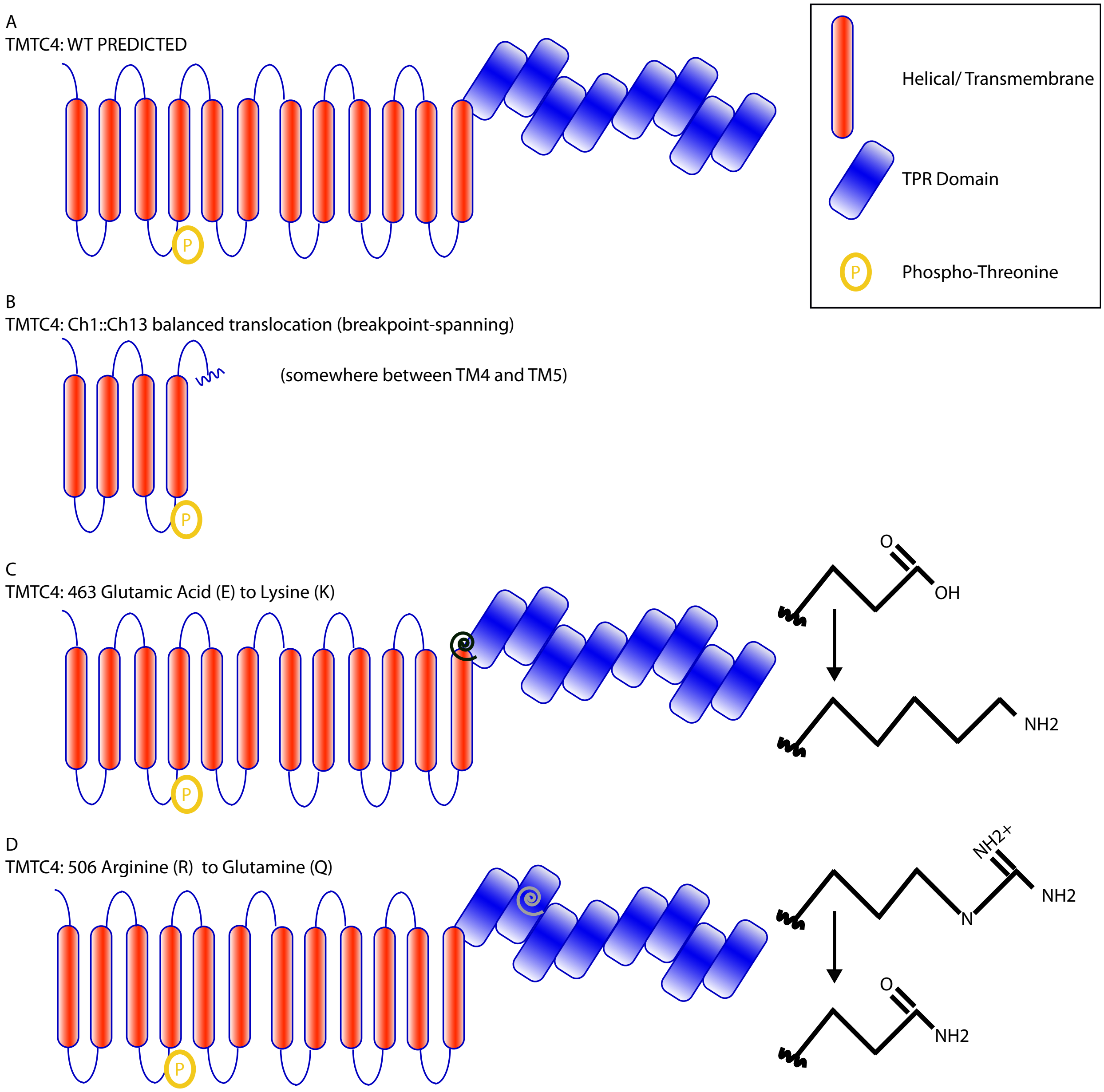

Figure 5.1 (Continued)

specializes in human genetics of AgCC and other brain malformations, they do not pursue directed genetic functional analyses. Our labs agreed to collaborate on this project, so they provided us with their unpublished human mutation data.

Many human congenital syndromes are associated with AgCC, likely because of the many diverse processes required for proper formation of the CC. In fact, AgCC occurs in approximately 1:4,000 individuals(Paul et al., 2007). Most generally, holoprosencephly, or the failure of the telencephalon to form two hemispheres, precludes existence of any CC. However, since holoprosencephly is so severe and not specific to CC, it is customarily categorized as a separate neurological malformation from traditional AgCC(Richards et al., 2004).

After the two hemispheres are formed, the midline must correctly fuse if CPN axons are to cross the midline. Midline fusion occurs around E14 in mouse, and a population of midline cells termed midline zipper glia (MZG) are required for this process to complete(Lindwall et al., 2007). Blockages, or cysts, at this midline structure can also cause AgCC by physically obstructing axons (Richards et al., 2004). By E15.5 in mouse, the first CPN axons have begun to cross the midline. At this stage in development, both CPN-autonomous and CPN-nonautonomous processes must work together to correctly form the CC and avoid AgCC. Midline structures, including the subcallosal sling, glial wedge, and indusium griseum glia, must form and secrete appropriate guidance signals (Lindwall et al., 2007; Paul et al., 2007) (see Figure 5.3A). Inability of CPN themselves, particularly the first to cross, to respond correctly to attractive and repulsive cues, could also result in AgCC(Rash and Richards, 2001; Richards et al., 2004; Lindwall et al., 2007; Paul et al., 2007; Donahoo and Richards, 2009). Finally, CPN axons prune as a result of input received (Cusick and Lund, 1981; Elberger, 1994), and, as a consequence of making incorrect connections on the contralateral side, there is a possibility of partial degeneration of axons that have already crossed the midline. AgCC, therefore, can be caused by defects in any one of these collective critical complex processes, including both those that are CPN-autonomous or CPN-nonautonomous.

Focused analyses of single disturbed processes that cause subtypes of AgCC will allow for specific disease characterization, directed diagnosis, and potentially therapeutic prevention.

Taken together, 1) TMTC4 expression in CPN during a critical period of axonal and dendrite extension and refinement, 2) evidence that related functional TPR domain-containing proteins are involved in neuronal differentiation and white matter formation, and 3) recent unpublished data from the Sherr lab that *Tmtc4* is mutated in in 3/140 patients with corpus callosum agenesis (two missense mutations and one translocation patients with AgCC), suggest that *Tmtc4* plays a critical role in the development of CPN. Further, these data suggest that TMTC4 function is likely necessary cell-autonomously for correct CPN development, particularly in axonal guidance.

5.3 Materials and Methods

5.3 a. Mouse Lines

C57/Bl6 wildtype mice and CD-1 wildtype mice were obtained from Charles River Laboratories (Wilmington, MA, USA), and were used for labeling, primary neuronal culture, and electroporation experiments.

5.3 b. Immunocytochemistry

Immunocytochemistry on tissue sections was performed as described in Chapter 3, with dilutions as follows rabbit-anti-2A 1:500 (Millipore ABS31), rabbit-anti-GFP 1:500 (Invitrogen A-11122), mouse-anti-KDEL 1:150 (Enzo Life Sciences SPA-827).

5.3 c. In situ hybridization

Nonradioactive colorimetric *in situ* hybridization was performed using probes labeled with dig-UTP as described in Chapter 3. Sense probes were used as negative controls in all experiments.

5.3 d. *Retrograde labeling of cortical projection neurons*

Perinatal retrograde labeling of CPN and CSMN

For retrograde CPN labeling, P2-P4 pups were anesthetized by hypothermia. The axons of CPN were labeled from the corpus callosum on the contralateral hemisphere with Alexa555-conjugated Cholera toxin subunit B (CTB-555) (2 mg/ml, Molecular Probes, Carlsbad, CA), under ultrasound guided microscopy, and transcardially perfused at P4 or P6. Three injection sites each consisting of 10 injections of 4.6 nl each, starting in the white matter, then retracting through the grey matter in a step-wise fashion were performed along the rostro-caudal axis of the neocortex.

For retrograde labeling of CSMN, P4 pups were anesthetized by hypothermia. CTB-555 (2 mg/ml, Molecular Probes, Carlsbad, CA) was injected into the corticospinal tract at cervical vertebrae segment

C2/C3 using a pulled glass micropipette (tip diameter 80-100μm) under ultrasound backscatter microscopy. Six injections of 32 nl per injection site were performed on each side of the midline. Mice were transcardially perfused for analysis at P6.

5.3 e. Fluorescence activated cell sorting (FACS)

FACS purification was performed essentially as described in (Arlotta et al., 2005) and(Molyneaux et al., 2009), and summarized in Chapter 2.

5.3 f. Western blotting

Immunoblotting was performed as described previously(Cowan et al., 2001; Macdonald et al., 2010). Briefly, HEK cells were isolated and membrane protein was extracted using 1% sodium dodecyl sulfate (SDS, Sigma) in PBS. Protein homogenates were separated by 10% SDS–polyacrylamide gel electrophoresis, and transferred to nitrocellulose membrane (Bio-Rad Trans-Blot). Membranes were blocked for 1 hr at room temperature with 5% nonfat milk in Tris-buffered saline (TBS), and incubated for 12–20 hours at 4 °C in the following primary antibodies diluted in in 2% milk/TBS: rabbit anti-2A peptide (1:2000; Abcam). Membranes were then washed three times for 5 min. each in 0.1% Tween 20 in TBS, and incubated for 1 hour at room temperature in peroxidase-coupled goat anti-rabbit IgG (BioRad) diluted in 2% milk/TBS. Signals were detected with chemiluminescence (Pierce, Rockford, IL).

5.3 g. Quantitative real-time PCR (qPCR)

RNA was extracted from FACS-purified cells using the StrataPrep Total RNA Micro Kit (Stratagene, La Jolla, CA), and cDNA was synthesized using SuperScript II reverse transcriptase (Invitrogen). qPCR was performed with a LightCycler 1.5 system (Roche, Branford, CT) according to the manufacturer's instructions. Primer pairs for *Tmtc4*_c-terminus, *Tmtc4*_exon7, *Satb2*, *Ctip2*, and *Gapdh* were as follows; each primer of each primer pair was designed in different exons, so as not to amplify genomic DNA:

c-terminus *Tmtc4*:

F: 5’-CTG AAG AGC TGC TGT CGT TG-3’

R: 5’-CTG CTC TGC TTC CTC AAA CC-3’

exon 7 *Tmtc4:*

F: 5’-AGG CAA ACT CGA CAT TCT GG-3’

R: 5’-AGG GCT ATT CGG AAA AGG AG-3’

Satb2 (gift from M. Woodworth, L. Custo-Greig, and K. Liu; Macklis Lab):

F: 5’- CTT TGC AAG AGT GGC ATT CA-3’

R: 5’- GCA GGT TGA GGA AGT TCT GC-3’

Ctip2 (gift from M. Woodworth, L. Custo-Greig, and K. Liu; Macklis Lab):

F: 5’- ACC TAC TGT CAC CCA CGA AA-3’

R: 5’- GTA GAT TCG GAA GCC ATG TG-3

Gapdh:

F: 5’- GGC ATT GCT CTC AAT GAC AA-3’

R: 5’- TGT GAG GGA GAT GCT CAG TG-3’

Each polymerase chain reaction consisted of 1X LightCycler FastStart DNA Master SYBR Green I mixture, 0.125 - 0.25 μM primers, and cDNA. We generated a standard curve for each gene, and performed relative quantification analysis in triplicate for each sample, using three independent RNA samples from each genotype. The results are reported as the ratio of target DNA sequence to a calibrator sample, following normalization to a reference gene, Gapdh. The average of the ratios of wild-type samples were set as “1”. p-values were calculated with an unpaired Student’s t-test. To verify the specificity of the amplicons, we ran the amplicons on agarose gels and confirmed the molecular size of the amplicons, in addition to melting curve analysis. Error bars indicate standard error of mean (SEM).

5.3 h. Loss- and gain-of-function constructs

Gain-of-function

For control expression experiments, vectors constructs of either GFP or full length *Tmtc4*, tagged with the T2A peptide sequence from the *Thosea asigna* virus (T2A) were used. *Tmtc4* cDNA in a pSport6 vector was purchased from Open Biosystems (Lafayette, CO; clone ID 5029461), however the full sequence was not included in that vector. The following primers were used to amplify the missing portion of the *Tmtc4* cDNA coding sequence from a P3 neocortical cDNA library and clone it into pSport6 and then into an AAV plasmid backbone with the chicken β-actin promoter (CβA), woodchuck hepatitis post-transcriptional regulatory element enhancer (WPRE), and the T2A peptide sequence from the *Thosea asigna* virus (T2A) peptide (first identified in the picornavirus virus) to create a bicistronic vector(de Felipe et al., 1999) by taking advantage of a weak proline peptide bond (see figure 5.4). This construct is called *Tmtc4*^{FL}. In the control vector, called GFP^{2ASTOP}, the GFP was followed by the T2A sequence and a stop codon.

Tmtc4 primers for amplification of missing piece from cDNA library are as follows:

F: 5'-gcGAATTC|ACTAGTgccaccatggttgagctggatgctga-3' (with 5' EcoR1 & Spe1 sites (capital letters) and Kozak initiation sequence (underlined))

R$_{small}$: 5' – gGATATCgaacacagcattca-3' (with 3' EcoRV site (capital letters) added on)

The amplicon and pSport6Tmtc4 (Open Biosystems) were digested with EcoR1 and EcoRV and ligated. The following primers were used to amplify the full length coding sequence of *Tmtc4* from the pSport vector:

F: 5'-gcGAATTC|ACTAGTgccaccatggttgagctggatgctga-3' (with 5' EcoR1 & Spe1 sites (capital letters) and Kozak initiation sequence (underlined))

R: -ggCTCGAGgacatctttcttctgcgttt (with 3' Xho1 (capital letters) added on)

The amplicon and pAAV T2A vector was digested with SpeI and XhoI and ligated. A sequenced clone with perfect alignment to the NCBI reference sequence NM_028651.2 in both the sense and antisense orientations was selected for experiments.

For human mutation constructs, the homologous region of mouse *Tmtc4* was identified and point mutations were introduced via PCR site-directed mutagenesis of G → A at nucleotide 1387 in the Tmtc4 coding sequence for $Tmtc4^{\Delta E463K}$ and of G → A at nucleotide 1517 in the *Tmtc4* coding sequence for $Tmtc4^{\Delta R506Q}$.

Loss-of-function

Since no loss-of-function mouse genetic model exists for *Tmtc4*, we employed an RNAinterference (RNAi) knockdown approach using a short-hairpin microRNA precursor RNA (shRNA-miR) (Cullen, 2005; Silva et al., 2005). Three shRNA-mir sequences in the miR-30 context with the following loop sequence and antisense hairpin sequences were selected for their perfect, and unique, homology to *Tmtc4* sequence NM_028651.2:

Loop: 5’-TAG TGA AGC CAC AGA TGT A-3’

1. *shTmtc4F* (Open Biosystems, RMM4431-99009154, clone ID: V2LMM_101825)

Antisense Hairpin: 5’- TTT GCC AAT GAG AAC ATA AGG G-3’

2. *shTmtc4H* (Open Biosystems, RHS4430-99138868, clone ID: V2LHS_177667)

Antisense Hairpin: 5’- AAT TGC CTT GAG GAA TAA AGC T-3’

3. *shTmtc4D (*Open Biosystems, RMM4431-98727668, clone ID: V2LMM_116685).

Antisense Hairpin: 5’- ATG TAT TTG ATC TTG ATG GCG G-3’

All shRNA-mir constructs were received in the pGIPZ lentiviral construct and were cloned into the pAAV expression construct as detailed above. In all experiments, a “scrambled” shRNA-mir that contains no homology to any known gene of the mouse genome was used as a control (Open Biosystems). The non-silencing shRNAmir control antisense hairpin sequence is as follows:

5’-aTC TCG CTT GGG CGA GAG TAA G-3’.

To measure efficiency of translational inhibition, the *Tmtc4* coding sequence or the 3' UTR were cloned using a XhoI /NotI digest into the psi-CHECK2 vector (Promega, Madison, WI) downstream of the *Renilla* luciferase gene STOP codon. ShRNA binding to the mRNA of the gene of interest results in degradation of the fusion mRNA, and reduces expression of the reporter gene *Renilla* luciferase. A second reporter gene, firefly luciferase, was used to normalize *Renilla* luciferase activity. The psiCHECK luminescence assay (Promega) was performed as described in the manufacturer's instructions. Briefly, 293T Human Embryonic Kidney (HEK) cells plated in a 96-well format at 70-80% confluency were transfected with a 1:10 ratio of psiCHECK2-*Tmtc4* and the desired shRNA or control scrambled shRNA, using the Arrestin transfection reagent (Open Biosystems) in 100 μl serum-free medium, which 3-6 hr later was supplemented with serum. 48 hours after transfection, *Renilla* and firefly luciferase activities were measured using the Dual-Luciferase Reporter 1000 Assay System (Promega) on a Victor3 1420 plate reader (Perkin Elmer, Waltham, Massachusetts). *Renilla* luciferase assay reagent (100 μl) was added to each well, incubated for 10 min., and luminescence was measured. The normalization control reading was measured by adding STOP&GLO reagent (100 μl) to each well to quench *Renilla* activity and provide the substrate for firefly activity, followed by measuring luciferase activity. Average luminescence of wells of untransfected HEK cells was subtracted as background. The luminescence of each well was normalized individually, and results from four replicates were averaged for each condition. Percent mRNA levels are expressed as average luminescence normalized to the average luminescence of control scrambled shRNA (scrambled shRNA) wells, ± SEM. *shTmtc4F* gave the most knockdown of about 80%.

5.3 i. In utero electroporation

In utero electroporations were performed essentially as described in (Saito and Nakatsuji, 2001; Saito, 2006), and (Molyneaux et al., 2005); and summarized in Chapter 3.

5.3 j. Microscopy and image analysis

Tissue sections were imaged on a Nikon E1000 microscope (Nikon Instruments, Melville, NY) equipped with an XCite 120 illuminator (EXFO, Mississauga, ON, Canada) and Q-imaging Retixa EX cooled CCD camera (Q-imaging Corp., Surrey, BC, Canada), or a Nikon 90i microscope using a 1.5 megapixel cooled CCD digital camera (Andor Technology, Dublin, Northern Ireland), a 5 megapixel color CCD digital camera (Nikon Instruments, Melville, NY). Images were collected and analyzed with Volocity image analysis software (Version 4.0.1; Improvision Inc., Waltham, MA) or Elements acquisition software (Nikon Instruments, Melville, NY). Laser confocal analysis was performed using a BioRad Radiance 2100 confocal microscope with LaserSharp2000 imaging software (BioRad Laboratories, Hurcules, CA). Images were processed using a combination of functions provided by ImageJ (Rasband, W.S., ImageJ, U. S. National Institutes of Health, Bethesda, Maryland, USA, http://imagej.nih.gov/ij/, 1997-2011.) and Adobe Photoshop/ Illustrator software packages (Adobe, San Jose, CA).

5.3 k. *Axonal quantification*

Contralateral axonal branching quantification:

Sections were matched with respect to electroporation location in sensory cortex and matched 50 μm sections where the CC, hippocampus, and AC were all visible at P8 were selected for analysis. From 4x montages of the contralateral cortex electroporated axons, four curves were drawn with the curvature of the cortex as follows: 1. immediately above the white matter tract when axons turn to enter the grey matter, 2. just below the layer VI barrel cortex, 3. just above the layer VI barrel cortex in layer II/III, and 4. in the process-dense, nearly acellular layer I (See figure 5.7). All axons and axon branches crossing each of these lines were counted using ImageJ cell counter plugin. The number of axons and axon branches in cortical layers was then normalized to the number of axons entering the grey matter and expressed as the averaged normalized proportion of axons entering the cortical grey matter ± S.E.M. for each GFP^{2ASTOP} (N= 5), *Tmtc4*^{FL}(N=6), *Tmtc4*$^{\Delta E463K}$ (N=6), *and* *Tmtc4*$^{\Delta R506Q}$ (N=5). p-values were calculated using the unpaired two-tailed Student's t-test.

Axon target quantification:

Sections were matched with respect to electroporation location in SS cortex and matched 50 μm sections where the CC, hippocampus, and AC were all visible at P8 were selected for analysis. From 4x montages of the electroporated axons in the entire section, brains were given a discrete score of 1 (axons present) or 0 (axons absent) in the following locations : 1. ipsilateral striatum, 2. ipsilateral globus pallidus, 3. high density in ipsilateral globus pallidus, 4. ipsilateral anterior commissure, and 5. contralateral anterior commissure. The proportion of brains with electroporated axons in each of these regions was calculated for each GFP^{2ASTOP} (n= 8), *Tmtc4*^{FL}(n=6), *Tmtc4*$^{\Delta E463K}$ (n=9), *and* *Tmtc4*$^{\Delta R506Q}$ (n=5). p-values were calculated using the parametric z-test for comparing two proportions (XLSTAT, Addinsoft SARL).

5.4 Results

5.4 a. TMTC4 is expressed by a restricted population of CPN, and is excluded from CSMN

Previously published comparative microarray data show that *Tmtc4* is highly expressed by CPN compared to CSMN during the first postnatal week ((Molyneaux et al., 2009) and Chapter 2), suggesting that TMTC4 functions post-mitotically at the time of axonal targeting and refinement (Figure 5.2A). We more specifically investigated *Tmtc4* expression by combining retrograde labeling of CPN (from the contralateral cortex) and subcerebral projection neurons (SCPN) (from the pons), followed by FACS purification and qPCR. We validated the purification method by priming for *Ctip2* and *Satb2*, which at P4 are virtually segregated between SCPN and CPN, respectively(Arlotta et al., 2005; Alcamo et al., 2008; Britanova et al., 2008; Chen et al., 2008a). *Ctip2* is enriched in SCPN three-fold over CPN, and *Satb2* is enriched in CPN over two-fold over SCPN, validating our sorting efficacy. We find, that in this validated population of CPN at P4, *Tmtc4* is two-and-a-half-times enriched in CPN over SCPN (Figure 5.2B).

Two major splice variants of *Tmtc4* have been identified in mouse, one “canonical” isoform including all 18 exons (17 coding exons), and a second isoform containing only 8 exons, and excluding the c-terminus. Since the *in situ* hybridization probe recognizes regions of the c-terminus and, therefore, the long isoform, we asked if the short variant is expressed at different levels, in different populations, or at different developmental times from the full length isoform in mouse cortex. We designed PCR primers to exon 7 (which would identify the full length and alternative sequence) and to the c-terminus (which would identify the full length isoform only), and find no difference in the level or timing of expression between the two, suggesting that it is the full length isoform that is expressed in developing mouse neocortex from E12.5 to P14, and not the splice variant (Figure 5.2C). Additionally, we confirmed and expanded the microarray developmental expression data with developmental *in situ* hybridization, and find that *Tmtc4* becomes restricted to superficial layer and layer Va CPN at P3 and P6 (Figure 5.3). These data combined indicate that *Tmtc4* is expressed by CPN during the first postnatal week of mouse brain development and is, therefore, poised to act specifically in CPN during axon and dendrite extension.

These results, taken together with microarray, qPCR, and retrograde labeling/*in situ* hybridization data, indicate that *Tmtc4* is indeed specifically expressed in the developing neocortex by CPN during the first postnatal week.

5.4 b. Tmtc4 is not expressed in early midline structures

The analysis presented above indicates that postnatally, *Tmtc4* is specifically expressed by CPN over other projection neuron subtypes. However, because *Tmtc4* has been implicated in human AgCC, we investigated in mice whether it could be acting early in development during midline formation, one of the most commonly malformed structures leading to AgCC(Richards et al., 2004; Paul et al., 2007; Donahoo and Richards, 2009). At the time of midline formation by glial and neuronal populations (from E15.5-E17.5) (Lindwall et al., 2007), *Tmtc4* is not expressed at the midline (Figure 5.3A,B), indicating that by extension any effects of *Tmtc4* mutations in human AgCC are not likely a result from a change in midline structure formation, but, rather, are likely the result of CPN-autonomous function for TMTC4.

5.4 c. Tmtc4-T2A is localized subcellularly to endoplasmic reticulum

To identify where TMTC4 acts in developing neurons, we investigated the subcellular localization of overexpressed TMTC4-T2A in conjunction with subcellular molecular markers. No antibody able to detect endogenous TMTC4 in tissue has been identified (although we have tried multiple native polyclonal and affinity purified monoclonal versions); therefore, we took advantage of the short T2A peptide sequence tagged onto TMTC4 in the expression plasmid, and performed immunocytochemistry against 2A in electroporated neocortical superficial layer neurons expressing the tagged protein (Figure 5.4A,C). The T2A peptide was differentially localized subcellularly when it was on TMTC4 versus GFP (Figure 5.5A,B). TMTC4-T2A localization closely resembles the pattern of endoplasmic reticulum (ER).

To further investigate whether TMTC4-T2A is localized to the ER, we took advantage of the fact that most lumenal ER proteins have COOH-terminal Lys-Asp- Glu-Leu (KDEL)(Ellgaard et al., 1999), and co-stained for KDEL to identify ER. Even though TMTC4 does not contain the canonical KDEL

Figure 5.2: *Tmtc4* is expressed by CPN at mid-stage CPN development (A) *Tmtc4* is more highly expressed by CPN than by CSMN via comparative microarray analysis of FACS purified retrogradely labeled neurons. **(B)** Tmtc4 is more highly expressed by FACS-purified CPN than by CSMN via q-PCR on purified neuronal populations at P4. **(C)** *Tmtc4* full length mRNA is expressed at equal levels in the cortex to exon 7 of *Tmtc4*, indicating that the short splice variant of *Tmtc4* is not a major contributor to *Tmtc4* expression.

CSMN, corticospinal motor neurons; CPN, callosal projection neurons; E, embryonic day; P, postnatal day; FACS, fluorescence activated cell sorting. **A** from(Molyneaux et al., 2009).

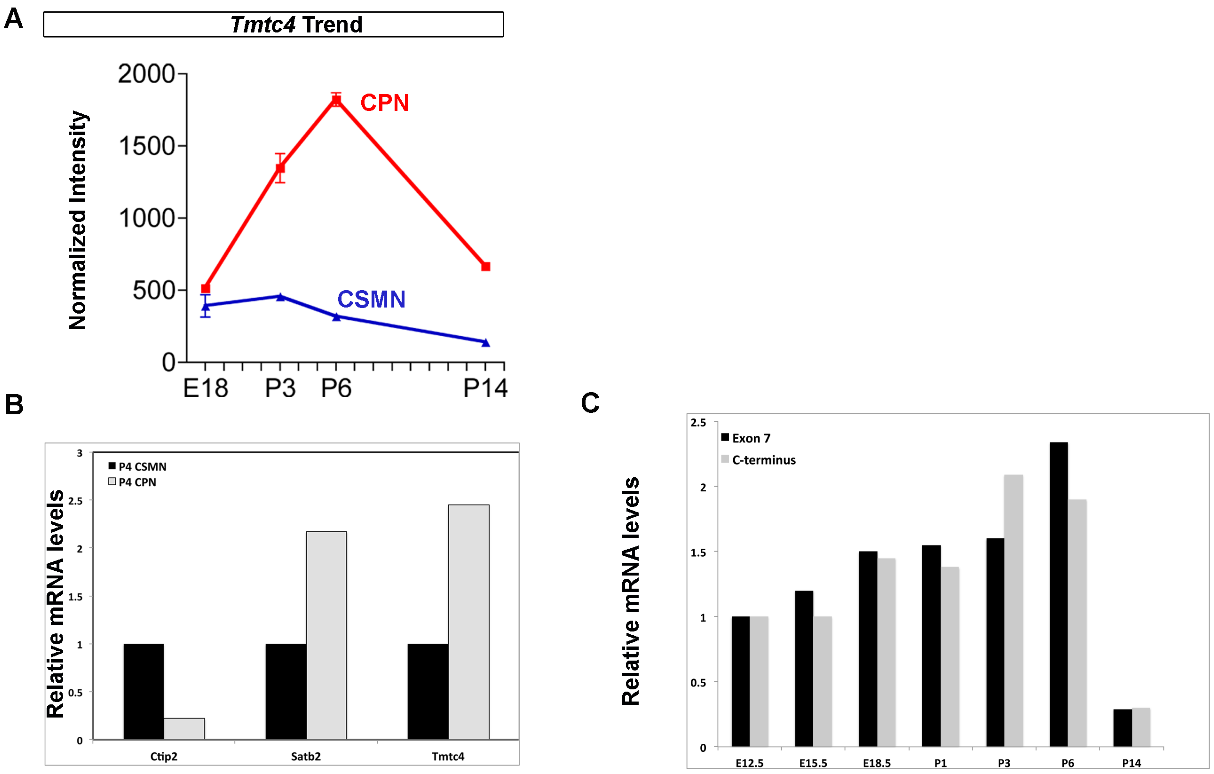

Figure 5.2 (Continued)

Figure 5.3: *Tmtc4* is not expressed at the midline at the time of midline structure formation, and is expressed postnatally by superficial layer and layer Va neurons. (A) Schematic representation of early midline structures and first-crossing CPN axons. **(B)** *Tmtc4* is not expressed in early midline structures at E15.5 or E17.5 **(C-E)** *Tmtc4* is expressed by postmitotic superficial layer and layer Va neurons of the early postnatal neocortex.

Scale bars (B) 500 μm, (C, D, E) 1mm, (C', C",D', D", E', E") 100 μm. **A** from(Fame et al., 2011), **B-E** *in situ* hybridization. CP, cortical plate; IZ, intermediate zone; SVZ, subventricular zone; VZ, ventricular zone; IGG, indusium gresium glia; GW, glial wedge; SCS, subcallosal sling; MZG, midline zipper glia; E, embryonic day; P, postnatal day.

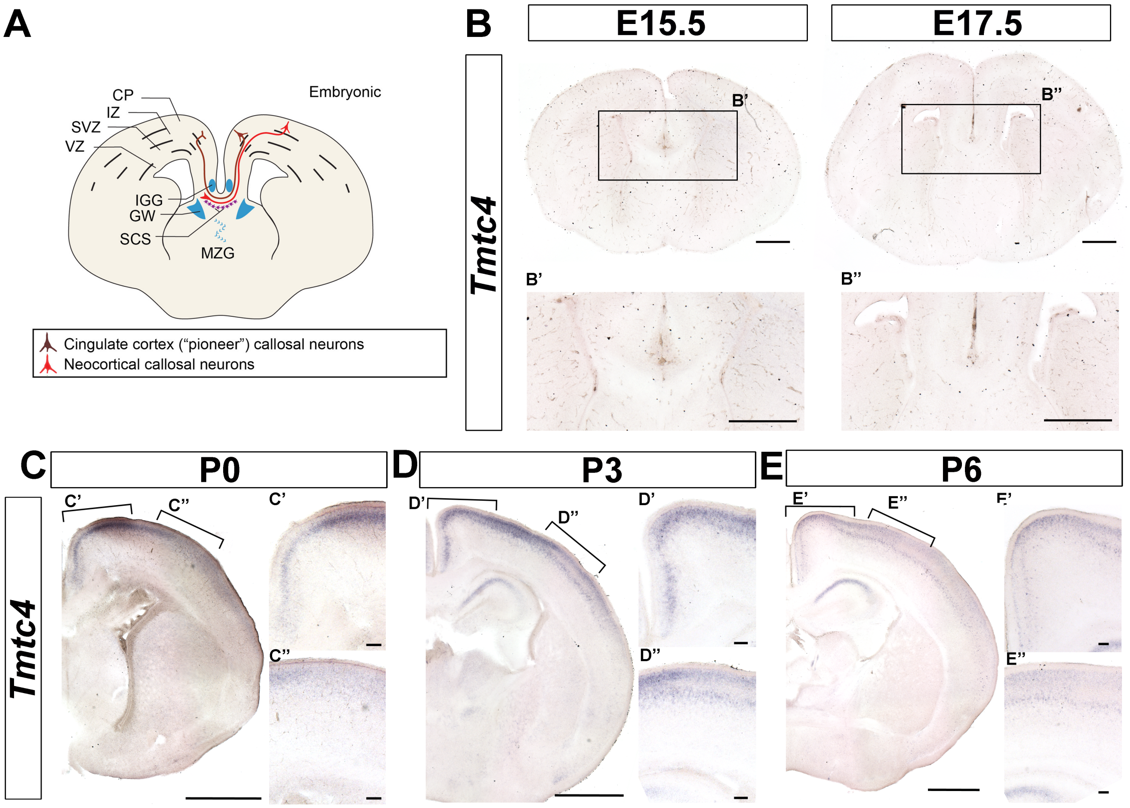

Figure 5.3 (Continued)

Figure 5.4: Overexpression scheme for analyzing human mutations of *Tmtc4*, which produce full-length protein. (A) Schematic representation of *Tmtc4*-T2A overexpression construct including the CβA promoter, the WPRE enhancer, and the T2A peptide that both tags the preceeding protein product, and also allows for peptide cleavage between the two peptide products **(B)** All of the overexpressed TMTC4 variations (*Tmtc4*^{FL}, *Tmtc4*$^{\Delta E463K}$, and *Tmtc4*$^{\Delta R506Q}$) produce full-length TMTC4 protein, and result in dimerization, as detected by 2A immunoblotting. **(C)** Schematic representation of *in utero* electroporation approach at E15.5 to target superficial layer cortical projection neurons at the peak time of their birth.

CβA, chicken beta-actin; T2A, *Thoseaasigna* virus 2A peptide; GFP, green fluorescent protein; WPRE, woodchuck hepatitis post-transcriptional regulatory element; bp, basepairs; kD, kilodaltons; LV, lateral ventricle; E, embryonic day; P, postnatal day.

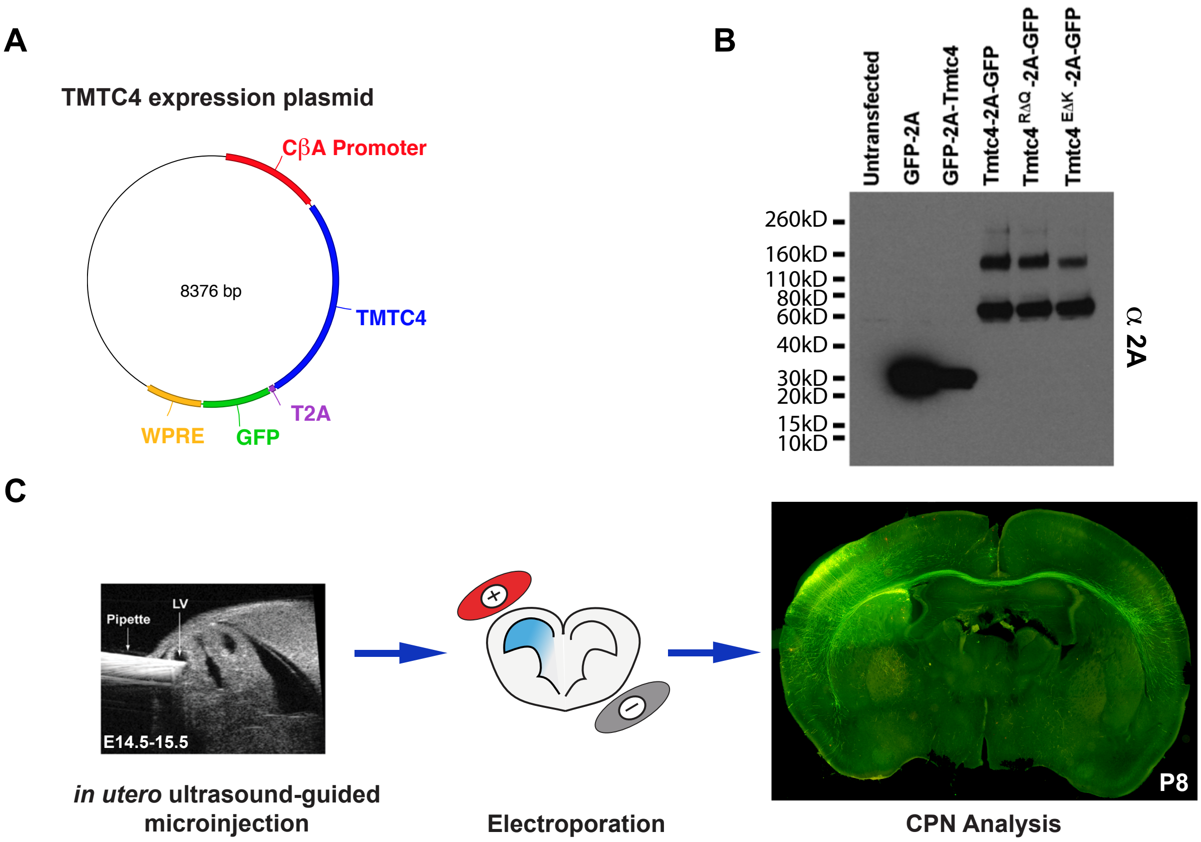

Figure 5.4 (Continued)

Figure 5.5: Wildtype Tmtc4-2A and human mutations of Tmtc4-2A are localized to neuronal endoplasmic reticulum. (A) At P8, overexpressed GFP-T2A fills the cytoplasm and processes of superficial layer pyramidal neurons. **(B)** At P8, overexpressed full-length Tmtc4-T2A is trafficked to superficial layer neuronal ER. **(C)** At P8, overexpressed *Tmtc4*$^{\Delta R506Q}$ -T2A is trafficked to superficial layer neuronal ER. **(D)** At P8, overexpressed *Tmtc4*$^{\Delta E463K}$ -T2A is trafficked to superficial layer neuronal ER.

Scale bar indicates 100 μm. ER, endoplasmic reticulum; T2A, *Thoseaasigna* virus 2A peptide; GFP, green fluorescent protein; KDEL, lysine-aspartic acid-glutamic acid-leucine endoplasmic retention peptide sequence; P, postnatal day. White arrows indicate examples of electroporated cells analyzed.

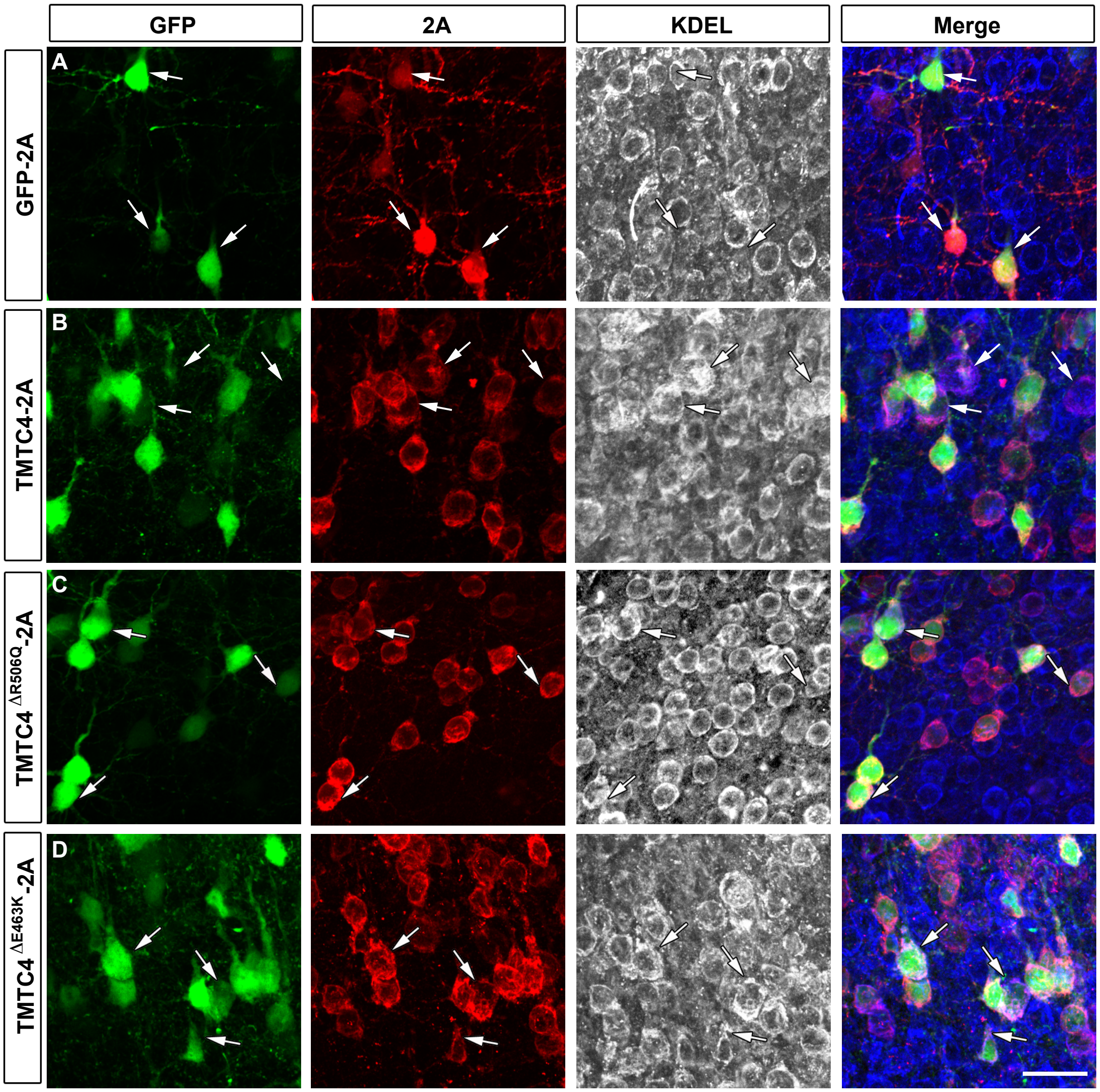

Figure 5.5 (Continued)

carboxy-terminus, TMTC4-T2A localization overlaps with KDEL expression in ER, while GFP-T2A localization is much more broad (Figure 5.4A,B). While overexpression of proteins can sometimes lead to trafficking defects, these localization data, combined with evidence that other TMTC family members localize to and act in ER, strengthen the interpretation that TMTC4 might also act in ER.

5.4 d. Eighty percent knockdown of Tmtc4 in vitro does not result in significant knockdown in vivo

To test the hypothesis that TMTC4 function is critical for CPN maturation and CC development, we selected a short-hairpin RNA (shRNA) knockdown approach, introduced via *in utero* electroporation at E15.5, the peak of superficial layer CPN birth (Figure 5.6A). The shRNA constructs for knockdown of *Tmtc4* were first validated using the psiCheck system (Promega), and we identified an shRNA construct (*shTmtc4F*) with unique homology to mouse *Tmtc4* that gives greater than 80% knockdown consistently *in vitro* (Figure 5.6B). This results in knockdown at the protein level in 293T HEK cells (Figure 5.6C). This construct also contains GFP, and therefore allows visualization of the cell body, axon, and principal dendrites.

Because the artificial system of knocking down an overexpressed construct in non-neuronal cells is quite different than knocking down gene expression *in vivo* at endogenous levels, we closely examined the level of *Tmtc4* knockdown *in vivo* in superficial layer neurons. In this system, even the best construct from the psiCheck and protein level validation did not give sufficient *Tmtc4* knockdown at the mRNA level *in vivo* (Figure 5.6D). Without sufficient knockdown *in vivo*, and with no observed differences between knockdown and control neurons, this system is not suitable for studying reduced *Tmtc4* function *in vivo*.

5.4 e. Human point mutations of TMTC4 generate full-length transcripts that correctly localize to ER in superficial layer CPN

Since human AgCC patients with *Tmtc4* mutations have mutations on only one of the two copies, and because point mutations, especially in transmembrane proteins like members of the TMTC family that bind to protein partners, can act as a dominant negative by sequestering binding partners, we designed overexpression vectors for homologous point mutations in mouse *Tmtc4* as were identified in human patients to investigate whether the mutated protein has an effect when expressed in otherwise wildtype neurons. The amino acids and nucleotide sequences where the identified mutations occurred are 100% conserved in human and mouse. To determine whether the mutations affect completion of transcription or translation, we overexpressed *Tmtc4*^{FL}*,* *Tmtc4*$^{\Delta E463K}$*,* and *Tmtc4*$^{\Delta R506Q}$ in 293T HEK cells, and determined protein size via Western blot analysis. All three are translated and generate full-length proteins of the same molecular weight at the wildtype protein (predicted size ~70 kd) that likely duplex, as TPR domain proteins are known to do (Figure 5.B).

To investigate whether the mutations affect *Tmtc4* trafficking to ER, we performed immunological colocalization of the 2A and KDEL peptides in superficial layer CPN that had been electroporated at E15.5 with mutated *Tmtc4* constructs. *Tmtc4*$^{\Delta R506Q}$ trafficked to the ER, as did *Tmtc4*$^{\Delta E463K}$ (Figure 5.5C,D). Together, these results suggest that TMTC4 is localized to, and therefore acts in, neuronal ER.

5.4 f. Overexpression of human mutations of Tmtc4 in superficial layer CPN cause axonal defects in mouse CPN development

Because AgCC results in misrouted CPN axons in Probst bundles, and improper CPN axonal targeting, we investigated whether the human disease-causing mutations in *Tmtc4* affected CPN axonal outgrowth. We performed systematic investigation of CPN axons expressing GFP only, *Tmtc4*^{FL}*,* *Tmtc4*$^{\Delta E463K}$*,* or *Tmtc4*$^{\Delta R506Q}$. Since axons do cross the midline through the CC in the overexpression model, we investigated axonal branching and targeting in contralateral cortex. Strikingly, overexpression of *Tmtc4*$^{\Delta R506Q}$ results in extra branching of CPN axons in layer I as compared to the GFP control (18% increase; p=0.02), *Tmtc4*^{FL} control (26% increase, p=0.004)*,* and *Tmtc4*$^{\Delta E463K}$ experimental (18% increase, p=0.009) (Figure 5.7A, B). Interestingly, the *Tmtc4*^{FL} control showed significantly less branching than *Tmtc4*$^{\Delta R506Q}$ in layer II/III as well (22% less, p=0.01)*,* suggesting that potentially *Tmtc4*^{FL} has an opposite

Figure 5.6: shRNA construct that provides eighty percent knockdown of *Tmtc4 in vitro* does not result in significant *Tmtc4* mRNA knockdown *in vivo.* (A) Schematic representation of the miR-30 context shRNA hairpin design. **(B)** Luciferase assay for candidate shRNA efficacy indicates that, relative to scrambled shRNA control, sh*Tmtc4*D causes 20% knockdown, sh*Tmtc4*H causes 70% knockdown, andshRNA*Tmtc4*F gives the best knockdown at 80% reduction of mRNA levels. **(C)** At the protein level, shRNA*Tmtc4*F gives product knockdown in 293T HEK cells. **(D)** Expression of the sh*Tmtc4*F knockdown construct *in vivo* does not result in significant reduction of *Tmtc4* mRNA levels.

Scale bars: D, 1mm; D', 100 μm; D" 20 μm. Error bars: standard error of the mean. shRNA, short-hairpin RNA, scramshRNA, scrambled control shRNA, T2A, *Thoseaasigna* virus 2A peptide; kD, kiloDaltons; P, postnatal day. White arrows **(D)** indicate limits of knockdown electroporation, white arrows in **(D')** indicate eletroporated cells magnified in **D"**. Dashed lines in **D"** indicate cellular outline of electroporated cells.

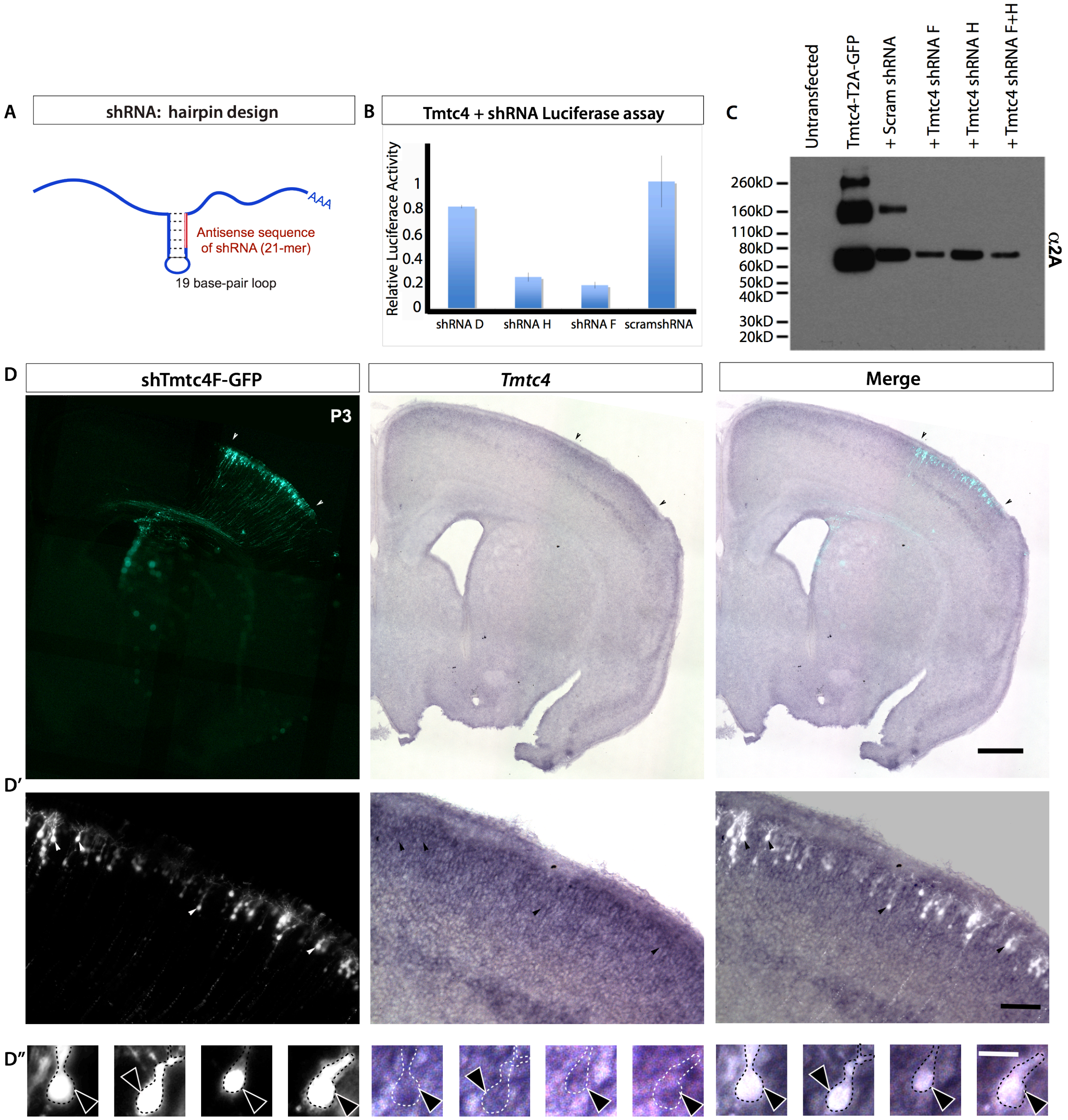

Figure 5.6 (Continued)

Figure 5.7: Human mutations of *Tmtc4*$^{\Delta R506Q}$ result in aberrant axonal branching/ failure to stop in mouse superficial layer neurons at P8. (A) Quantification of number of axon branches of superficial layer neurons electroporated with *Tmtc4* expression constructs reaching each noted radial cortical landmark in the contralateral cortex. Results are expressed as the average relative number of axonal branches normalized to the number of axons reaching the contralateral grey matter ±S.E.M. Quantification at P8 reveals an increase in axonal branches in superficial layer I by neurons expressing *Tmtc4*$^{\Delta R506Q}$ by 18% (N=6, p = 0.02) compared to GFP control, 26% increase (N=5, p=0.004) compared to *Tmtc4*^{FL} wildtype control, and 18% increase (N=6, p=0.009) compared to *Tmtc4*$^{\Delta E463K}$ experimental. The *Tmtc4*^{FL} control-expressing neurons showed significantly less branching than those expressing *Tmtc4*$^{\Delta R506Q}$ in layer II/III as well (22% less, p=0.01), suggesting that potentially *Tmtc4*^{FL} has an opposite effect to that of the *Tmtc4*$^{\Delta R506Q}$ mutated form, although neither is different from the GFP control in layer II/III **(B)** Representative images of contralateral axonal innervation for each condition **(B')** GFP **(B'')** *Tmtc4*^{FL}, **(B"')** *Tmtc4*$^{\Delta R506Q}$, and **(B"")** *Tmtc4*$^{\Delta E463K}$.

Error bars: standard error of the mean. Roman numerals indicate neocortical layers. Scale bar: 500 μm.

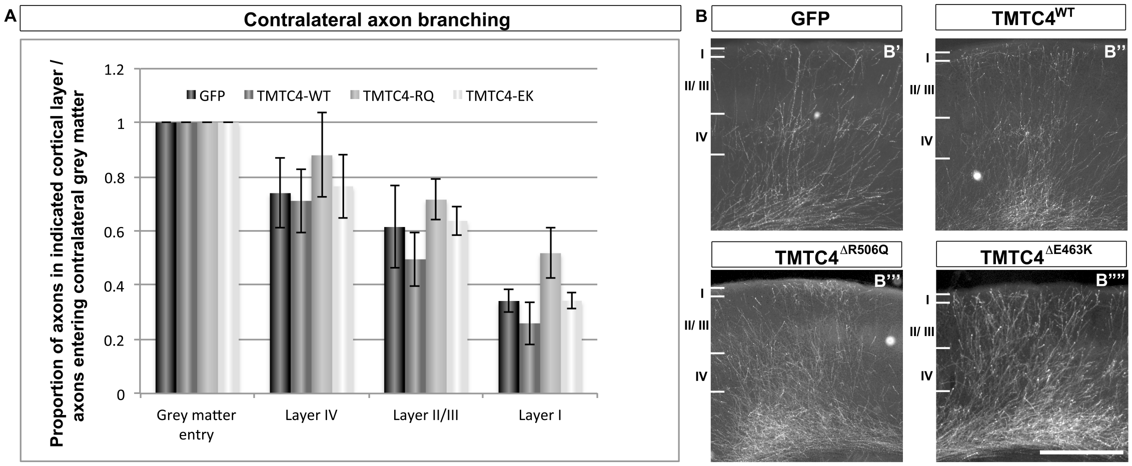

Figure 5.7 (Continued)

effect as the *Tmtc4*$^{\Delta R506Q}$ mutated form, although neither is different from the GFP control in layer II/III (Figure 5.7A). No other significant differences were observed in this analysis. Therefore, correct *Tmtc4* function might be critical for appropriate local target finding, and/or accurate response to inhibitory stop signals.

Additionally, we investigated axonal targeting to areas other than contralateral cortex through the CC, since some populations of CPN axons expressing mutant forms of TMTC4 might not cross through the CC at all. In all conditions, CPN axons projected to ipsilateral striatum, as expected. TMTC4 overexpressing axons of all types – WT and both mutations – trend toward being more likely to have axons targeting the globus pallidus, a typical target for striatal neurons, but not cortical neurons, than those electroporated with GFP control. However, only *Tmtc4*$^{\Delta E463K}$ - expressing experimental neurons were significantly more likely than the GFP control neurons to extend axons to the globus pallidus (64% increase, $p=0.001$). Although absolute quantification was not performed, large numbers of axons expressing the *Tmtc4*$^{\Delta E463K}$ mutated protein were repeatedly detected densely covering the entirety of the globus pallidus domain, while only a few axons overexpressing the other *Tmtc4* variations were found in the globus pallidus (67% more than GFP, $p<0.0001$; 50% more than *Tmtc4*^{FL}, $p=0.02$; 47% more than *Tmtc4*$^{\Delta R506Q}$, $p= 0.05$). Interestingly, brains with neurons expressing the *Tmtc4*$^{\Delta E463K}$ mutated protein were more likely to have axons crossing to the contralateral hemisphere in the anterior commissure compared with either the GFP control (43% increase, $p=0.03$) or the *Tmtc4*$^{\Delta R506Q}$ experimental (55% increase, $p=0.001$).

This result is particularly compelling because ~10% of canonical AgCC includes enlargement of the AC(Paul et al., 2007), and the initial patient identified by the Sherr lab with the translocation in *Tmtc4* exhibits an enlarged anterior commissure in addition to AgCC. These axon targeting data are interesting, and encourage further study of axon targeting in the overexpression system to determine how and when the mistargeting occurs, particularly looking at earlier developmental times. These two sets of data combined suggest that TMTC4 can play critical roles in axonal branching, targeting, and stopping, and that the human missense mutations of TMTC4 likely disrupt important and potentially distinct functions of this protein that could result in CPN malfunction and mistargeting.

Figure 5.8: Human mutations of *Tmtc4*$^{\Delta E463K}$ result in aberrant axonal targeting in mouse superficial layer neurons at P8.

(A) TMTC4 overexpressing axons of all types –WT and both mutations – trend toward being more likely to have axons targeting the globus pallidus (GP), a typical target for striatal neurons, but not cortical neurons, than those electroporated with GFP control. However, only *Tmtc4*$^{\Delta E463K}$ experimental-expressing neurons were significantly more likely than the GFP control neurons to extend axons to the GP (N=9, 64% increase, p=0.001). Although normalized quantification was not performed, large numbers of axons expressing the *Tmtc4*$^{\Delta E463K}$ mutated protein were repeatedly detected densely covering the entire GP domain, while only small numbers of axons expressing the other *Tmtc4*-expression constructs were found in the GP (67% more than GFP, N=8, p<0.0001; 50% more than *Tmtc4*^{FL}, N=5, p=0.02; 47% more than *Tmtc4*$^{\Delta R506Q}$, N=6, p= 0.05). Brains with neurons expressing the *Tmtc4*$^{\Delta E463K}$ mutated protein were more likely to have axons crossing to the contralateral hemisphere in the anterior commissure than either the GFP control (43% increase, N=8, p=0.03) or the *Tmtc4*$^{\Delta R506Q}$ experimental (55% increase, N=6, p=0.001). **(B)** Representative images of axon targeting for each condition **(B')** GFP **(B'')** *Tmtc4*^{FL}, **(B"')** *Tmtc4*$^{\Delta R506Q}$, and **(B"")** *Tmtc4*$^{\Delta E463K}$.

*, p <0.05; **, p<0.001; ***, p< 0.0001, WT, wildtype; P, postnatal day; Str, striatum; GP, globus pallidus; AC, anterior commissure.

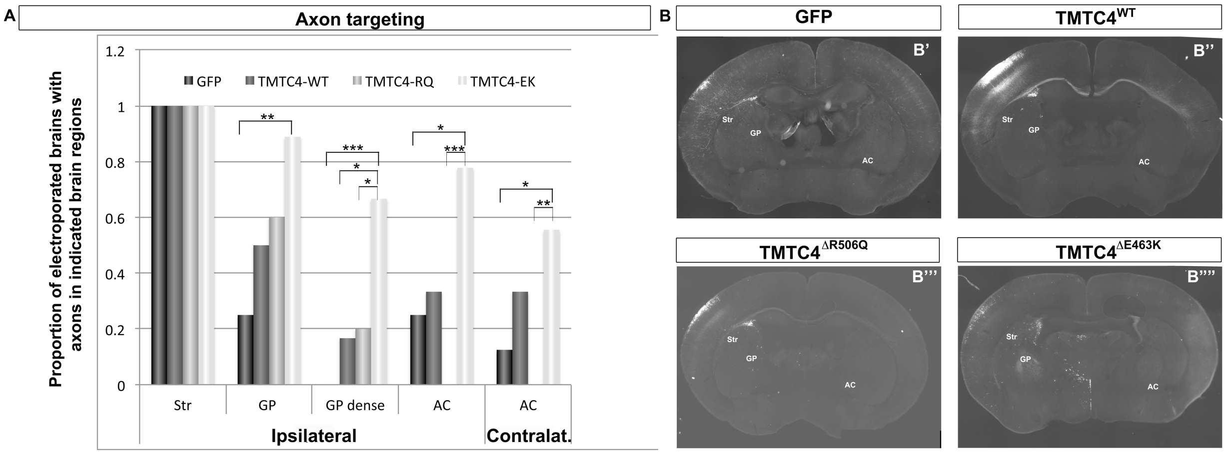

Figure 5.8 (Continued)

5.5 Discussion

Callosal projection neurons (CPN) of the cerebral cortex reside in cortical layers II/III, V, and VI,and all extend axons to homotopic mirror image targets on the contralateral hemisphere enabling bilateral information integration within the cerebral cortex. Dysfunction and malformation of CPN have been implicated in diseases of associative function, including autism spectrum disorders (ASD), schizophrenia, and agenesis of the corpus callosum (AgCC). Some CPN subpopulations likely play preferential roles in specific disorders of CPN development and associative function. We hypothesized that some of the molecular determinants expressed by specific populations of CPN would not only be likely developmental regulators of this specific neuronal population, but their absence or mutation could also be associated with incorrect development or function of CPN in human disease. Identifying disease genes within the set of genes expressed by CPN provides a useful filter to enrich for genes whose functions are likely specific and cell-autonomous. *Tmtc4* is one such gene at the intersection of human disease, AgCC, and CPN-enriched developmental expression. Focused in-depth functional analysis of these determinants throughout development in unique subpopulations of CPN will likely provide insight into critical processes disrupted in human disease.

In Chapter 2, comparative microarray analysis designed to identify molecular determinants of CPN populations is presented. In subsequent chapters, functional investigation of some of these determinants in CPN development is presented. Data revealing molecular diversity within the broad population of CPN has identified regulators of CPN development. Here, I show that *Tmtc4,* a transmembrane protein with a TPR protein interaction domain whose mutated forms are associated with patients with a deformation of CPN, AgCC, is enriched in CPN over CSMN, and is expressed in a restricted fashion in the neocortex. Specifically, *Tmtc4* expression is restricted to neocortical layer II/III and Va CPN. The temporal developmental expression of *Tmtc4* coincides with an intermediate time period of CPN development, including low-level expression during neuronal migration, and highest levels of expression from P3 to P6, after neuronal birth and migration when CPN are extending and refining axonal and dendritic processes. Together, these data suggest that *Tmtc4* might function in post-mitotic establishment of innervation or connection pruning. In addition, *Tmtc4* is not expressed in developing midline structures in mice, indicating that it does not function in formation of the midline in mice; rather, function of *Tmtc4* in mouse and human CC development is likely CPN-autonomous. Strengthening this interpretation for specificity of *Tmtc4* function, no isoforms of *Tmtc4* other than the canonical isoform measured by *in situ hybridization* and qPCR are expressed in the developing neocortex. This suggests that the spatially and temporally restricted expression pattern detected by *in situ* hybridization and qPCR of canonical full-length *Tmtc4* denotes the only restricted involvement of *Tmtc4* in neocortical development.

Peptide tagged TMTC4 localizes to the endoplasmic reticulum, as has been shown for other TMTC family members; this suggests that TMTC4 might function in ER-specific roles in CPN. With an artificial overexpression scheme, there is always the possibility that the large amount of protein results in mistrafficking. However, data that other family members act in the ER (Racapé et al., 2011) reinforces the current results showing TMTC4 specific localization to the ER. The ER plays many roles in cellular processes, including being the site of synthesis and maturation of proteins destined for secretion, for the plasma membrane, and for the secretory and endocytic organelles(Ellgaard et al., 1999); being the site of lipid and steroid synthesis; being the location of carbohydrate and toxin metabolism; and acting as a regulator of cytosolic Ca^{2+} levels(Tojima, 2012). Some of these roles are specifically critical for neuronal development and function. While the protein synthesis function of ER acts more generally in all cell types, the metabolic and folding chaperone roles of ER have been connected to neurodegeneration of large excitatory neurons such as CSMN and spinal motor neurons that degenerate in amyotrophic lateral sclerosis (ALS)(Riboldi et al., 2011). Additionally, closely regulated Ca^{2+} levels plays critical roles in apoptosis, axonal outgrowth, guidance, and neurotransmission(Limke et al., 2004; Shen and Shuai, 2011; Tojima, 2012). These crucial functions of ER in neuronal development and survival suggest the possibility that ER-localized TMTC4 might be acting in one of these important processes either directly, or through chaperone/ protein sorting roles acting on other critical players in these processes.

While any of these roles of ER could be applicable to TMTC4 function in AgCC, those involved in cytosolic Ca^{2+} level regulation are most directly connected to axonal development. Cytosolic Ca^{2+} levels are generally kept quite low in neurons (50–100 nM). However, in response to axon guidance cues or neurotransmitters, Ca^{2+} stores in the ER can be released into the cytosol through the opening of inositol triphosphate receptor (IP_3R) channels by IP_3 upon hydrolysis of PIP_2 from cellular membrane(Shen and Shuai, 2011). This, in turn, signals either growth cone attraction or replusion(Limke et al., 2004; Tojima, 2012), or signal propagation(Shen and Shuai, 2011).

A number of axonal growth cone behaviors, including turning, stopping, extension, and responding to external cues, have been shown to require precise regulation of intracellular Ca^{2+}(Kater and Mills, 1991; Aridor and Fish, 2009), and could be affected by TMTC4 mutations – particularly by mutations in the protein binding TRP region, like those described here. Data presented in this chapter show that expression of disease-associated mutations in *Tmtc4* can result in excess axonal branching (*Tmtc4*$^{\Delta R506Q}$) or mistargeting (*Tmtc4*$^{\Delta E463K}$). These phenotypes could be results of an inability of axons to respond to stop signals, or inappropriate axonal response to attractive and repulsive guidance cues, respectively. These axon guidance data from overexpression of human disease associated mutations of *Tmtc4* additionally lend support to the hypothesis that TMTC4 acts in neuronal ER to control correct growth cone targeting. The function of intracellular Ca^{2+} regulation in how guidance cues are interpreted is particularly pertinent to the above results suggesting potential mistargeting as a result of *Tmtc4* mutations. Cues involving cellular membrane Ca^{2+} that result in intracellular ER Ca^{2+} release cause growth cone attraction, while cues involving cellular membrane Ca^{2+} without intracellular ER Ca^{2+} release cause growth cone repulsion.(Tojima, 2012). Therefore, controlled regulation of ER protein localization and Ca^{2+} release are critical for appropriate interpretation of attractive and repulsive guidance cues, and *Tmtc4* is poised to be involved with these processes in the ER.

In addition to axonal growth cone response, the ER and ER-localized proteins play critical roles in neuronal activity(Shen and Shuai, 2011). This role for ER in neuronal activity is also connected to cytosolic Ca^{2+} levels, and the fact that ER is a continuous network that extends to all parts of the neuron, including the axon and dendrites. Individual IP_3R channels can release a small amount of Ca^{2+} locally, a small cluster of IP_3R channels can have a larger effect releasing more Ca^{2+}, and slowly propagating waves of Ca^{2+} release along large portions of the ER can affect the neuron globally(Parker et al., 1996). While investigations reported in this chapter do not directly address neurofunctional activity after the artificial expression of *Tmtc4* mutant gene products, functional aberrations could affect neuron migration, target finding, and axon maintenance (Koralek and Killackey, 1990; Innocenti and Price, 2005). Since *Tmtc4* is poised to potentially affect such processes, further analysis including electrophysiological functional assays of neurons with inappropriate *Tmtc4* expression or loss of *Tmtc4* function might contribute to understanding roles of *Tmtc4* in projection neuron development.

These experimental results, while informative and motivating for further analysis of TMTC4 function in neuronal development, do not fully recapitulate either the human AgCC disease state or a full loss-of-function. For example, chromosomal translocation mutations such as the one detected in the first human patient to be identified, are inexact and difficult to correctly recapitulate with an expression plasmid. While the resulting situation is likely a functional null of the protein product, there is also the possibility of producing a product with some chimeric properties. This possibility could potentially be illuminated by full sequencing of the chromosomal abnormality in the human patient with the translocation mutation. Additionally, in the overexpresssion system used here, all neurons still express two wildtype copies of *Tmtc4* and, therefore, neurons in which mutant *Tmtc4* has been misexpressed likely retain more TMTC4 function than patients carrying the mutations. In addition, in this chimeric system of *in utero* electroporation, neurons expressing mutant forms of *Tmtc4* might be able to cross the corpus callosum by following neighboring wildtype neurons, which would not be possible in the case of human patients.

To thoroughly investigate *Tmtc4* function in developing CPN it will be necessary either to design and test new *Tmtc4* shRNA constructs that more completely reduce mRNA levels *in vivo,* or to generate a set of *Tmtc4* targeted gene deletion mice (global and conditional nulls). While such mice are not yet available, the International Knockout Mouse Consortium has now successfully created a *Tmtc4* deletion line in embryonic stem cells, and it will be quite interesting and useful for basic developmental analysis of *Tmtc4* function to perform subsequent investigations of CPN and CC development in *Tmtc4* heterozygote and null mice when they are generated. These analyses will likely inform future research into AgCC disease causing properties of *Tmtc4,* in addition to providing a loss-of-function tool that will allow investigators to more deeply study basic functional requirement(s) of TMTC4 in CPN development.

Taken together with the involvement of *Tmtc4* mutations in human AgCC, the data presented in this chapter showing: 1) *Tmtc4* expression by developing CPN at the time of axon and dendrite extension; 2) ER localization of TMTC4; 3) aberrant axon targeting with $Tmtc4^{\Delta E463K}$ expression; and 4) exuberant and inappropriate layer I axonal branching with $Tmtc4^{\Delta R506Q}$ expression, suggest that TMTC4 might likely function in axonal guidance during neuronal development. Critical function in ER-influenced growth cone response to stop or guidance cues might result in axonal pathfinding roles for TMTC4, potentially including cytosolic Ca^{2+} levels, and are supported by the mutant overexpression data revealing atypical axonal development. The excess layer I axonal branching in $Tmtc4^{\Delta R506Q}$ aligns with known roles of ER Ca^{2+} in proper response to stop signals (Kater and Mills, 1991), while aberrant axon targeting with $Tmtc4^{\Delta E463K}$ supports a connection to many studies implicating correct Ca^{2+} levels and ER protein retention in attraction, repulsion, and targeting(Kater and Mills, 1991; Aridor and Fish, 2009; Shen and Shuai, 2011; Tojima, 2012). Further studies of *Tmtc4* null CPN, and of direct connections between *Tmtc4* function and neuronal activity/ axonal pathfinding, might likely prove fruitful for understanding roles of *Tmtc4* in CPN development, and critical processes in CPN development that contribute to AgCC.

Funding

This work, as well as work described in Chapters 3, 4 and 6, was partially supported by grants from the National Institutes of Health (NINDS), the Harvard Stem Cell Institute, and the United Sydney Association. R.M.F. was partially supported by a National Science Foundation Graduate Research Fellowhsip Program (GRFP) fellowship and a National Institutes of Health predoctoral NRSA fellowship F31 NS073136.

Acknowledgements

I thank L. Pasquina, R. Richardson, C. Greppi, T. Keefe, and P. Davis for superb technical assistance; Dr. A. Poulopoulos for sharing his protein biochemistry insight and expertise; Dr. M. Galazo, for communicating some of her vast knowledge of non-cortical brain anatomy and connectivity; Dr. J. Li, L. Fernandez, and Prof. E. Sherr for sharing their unpublished human data; and current and past members of our laboratory for discussions and helpful suggestions.

Chapter 6:

Subtype-specific genes that identify distinct subpopulations of callosal projection neurons in mice identify molecularly homologous populations in macaque cortex

Author contributions: I performed all planning, laboratory work, imaging, and data interpretation on this project, except for tissue harvesting and preparation performed in Professors Colette Dehay's and Henry Kennedy's laboratories at INSERM U846 / Stem Cell and Brain Research Institute in Lyon, France.

6.1 Abstract

Callosal projection neurons (CPN) as a population have undergone striking differential expansion throughout recent evolution. This is evident from the disproportionately large, histologically recognizable variety of primate superficial layers (that contain~90% of CPN), as compared to rodent superficial layers (that contain only ~80% of CPN), and from the noticeably larger relative volume of cortical white matter tracts found in primates than rodents, including the corpus callosum, through which CPN axons project (Smart et al., 2002a). Recent studies in mouse have identified genes enriched in distinct populations of CPN, including those of deep layers, superficial layers, and sublaminae within each population (Chapter 2 and (Molyneaux et al., 2009)).

In the work presented here, I address the hypothesis that cortical neuronal diversity in primates might include molecular expression conserved with that in rodent, revealing more comparative commonality and subpopulation diversity in subpopulations of CPN in macaque and mice than previously recognized. Newly identified molecular controls over CPN subtype diversity in mouse might reflect a non-histologically recognizable molecular pattern shared among mammals that likely arose before the divergence of rodents and primates, and the dramatic expansion of primate superficial layers. I find that, while expression of CPN-enriched genes in early cortex (*Ptn*, *Nnmt, Dkk3, Lmo4, Inhba,* and *Tmtc4)* and later deep neocortical layers are conserved (*Cited2, Dkk3, Plexin-D1,* and *Gfra2)*, gene expression in superficial layer CPN shows more varied levels of conservation of expression, suggesting conservation and/or expansion of some superficial CPN populations in macaque (*Nnmt* ,*Chn2*, and *EphA3*), independent expansion of some in mouse (*Limch1*), and even emergence of others in macaque (*Gfra2)*. Together, these data inform future comparative studies of the many subpopulations of CPN that can be effectively studied in mouse, which ones are unique to primates, and evolutionary relationship(s) between the two.

6.2 Introduction

The neocortex is the seat of complex cognitive, perceptive, and motor function in mammals(Rakic, 1988). As such, it has undergone dramatic expansion throughout mammalian evolution, reflected in taxonomical size and complexity increase in primates not present in rodents.

The fossil record of soft tissues, including the nervous system, is lacking(de Sousa, 2007); therefore, comparative analysis of current species enables study of conserved features that likely arose from common ancestors containing the shared features that were then independently selected upon by evolutionary forces to produce contemporary species present today. Since the divergence of mammalian ancestors from the sauropsid ancestors of reptiles and birds over 315 million years ago, the cortex has undergone considerable radial expansion with substantial, disproportionate increase in neuronal numbers in the superficial cortical layers II-IV among mammalian species (Reiner, 1991; Marín-Padilla, 1992; Reiner, 1993; Aboitiz et al., 2003). The sauropsid cortex contains only three layers, which are thought to be homologous to layers I, V and VI of the six-layered mammalian cortex because of the output properties of the neurons present, and because of a lack of neurons with properties of mammalian superficial layer projection neurons (Reiner, 1991). Distinct members of the mammalian class exhibit neocortical expansion as complexity arises, with the primate cortex exhibiting further expansion than rodents. The basal state of six canonical layers seen in mammals has enlarged in primates to include new subdivisions that can be easily distinguished at the histological level, while rodents and other small-brained mammals have less prominent neocortical variety(Rakic and Kornack, 2001; Smart et al., 2002b).

Of particular note and of direct relevance to callosal projection neurons (CPN), is the disproportionately large expansion of superficial layers in primate cortex. Rodent layer II/III is histologically indistinguishable. Hhowever, in primate neocortex, superficial layers are discrete layers II and III, containing multiple histologically distinct sublayers, not found in rodents (Figure 6.1). Since there is definitive support for the SVZ origin of superficial layer neurons (Wu et al., 2005), expansion of the SVZ might represent an evolutionary mechanism to increase the number of neurons within the neocortex, especially during generation of neurons of superficial layers (Smart et al., 2002a; Kriegstein et al., 2006).

Most CPN are contained within superficial cortical layers not present in sauropsids (Manzoni et al., 1986). In fact, the corpus callosum (CC), and thus CPN, are found exclusively in placental mammals (eutheria) and have not been observed in any non-placental animal species studied(Aboitiz and Montiel, 2003; Mihrshahi, 2006). The presence of cortical superficial layers correlates quite well with emergence of CPN, although a significant proportion of CPN reside in deeper layers (~10% in primates; ~20% in rodents). However, not all six-layered cortices contain CPN. Particularly interesting are non-placental mammals, including marsupials. For example, the marsupial short-tailed opossum possesses a six-layered cortex quite similar histologically and molecularly to that of rodents (Puzzolo and Mallamaci, 2010), but does not have a CC. Together, these data suggest that a six-layered cortex with superficial layer neurons is required for, but not sufficient to guarantee modern CPN. However, the presence of deep layer CPN suggests that the first CPN might have arisen in a cortical structure without superficial layer neuronal populations.

With delineation of layers II and III in primate cerebral cortex, it is possible to address distinct cell types that populate these neuroarchitecturally distinct laminar units. Just as in rodents, both layers II and III contain associative local neurons. The expanded superficial layers also reflect a larger population of CPN since (as noted above) only ~80% of mouse CPN are in superficial layers, while over 90% of primate CPN are located in superficial layers, with layer V CPN remaining a significant, but smaller population of CPN (Manzoni et al., 1986). In addition, expansion of cortical superficial layers correlates with expansion of cortical and interhemispheric white matter, indicating that expansion of superficial layers is, at least in part, due to expansion of CPN populations. However, while CPN in mouse are evenly distributed throughout layer II/III (See Figure 6.2D), essentially all superficial layer primate CPN in sensorimotor neocortex are restricted to layer III, and most specifically concentrated in deeper layer III (IIIb) (Jones and Wise, 1977; Killackey et al., 1983; Manzoni et al., 1986). Layer II in primate cortex (external granular layer) is very dense, and contains small local interneurons (granule cells) and some slightly larger ipsilateral associative pyramidal cells(Lund et al., 1993; Swenson, 2006), but essentially no contralateral projecting CPN. These data suggest that either mouse layers II/III contain a mixture of all of

Figure 6.1: Schematic representation and cytoarchitectural view of mouse and macaque somatosensory neocortex.

(A) Schematic representation of developing and adult mouse and macaque cortex in S1, drawn to a common internal scale. **(B)** DAPI nuclear stain at mid-corticogenesis (E14/ E94) and after neuronal migration (P3/ E108) in macaque to show cytoarchitectural layers in S1.

Scale bars: **B**,100 μm. E, embryonic day; P, postnatal day; VZ, ventricular zone; SVZ, subventricular zone; SP, subplate; ISVZ, inner subventricular zone; IFL, inner fibrous layer; OSVZ, outer subventricular zone; OFL, outer fibrous layer; CP, cortical plate; S1, primary somatosensory area; Roman numerals indicate cortical layers. **A** adapted from (Fame et al., 2011)

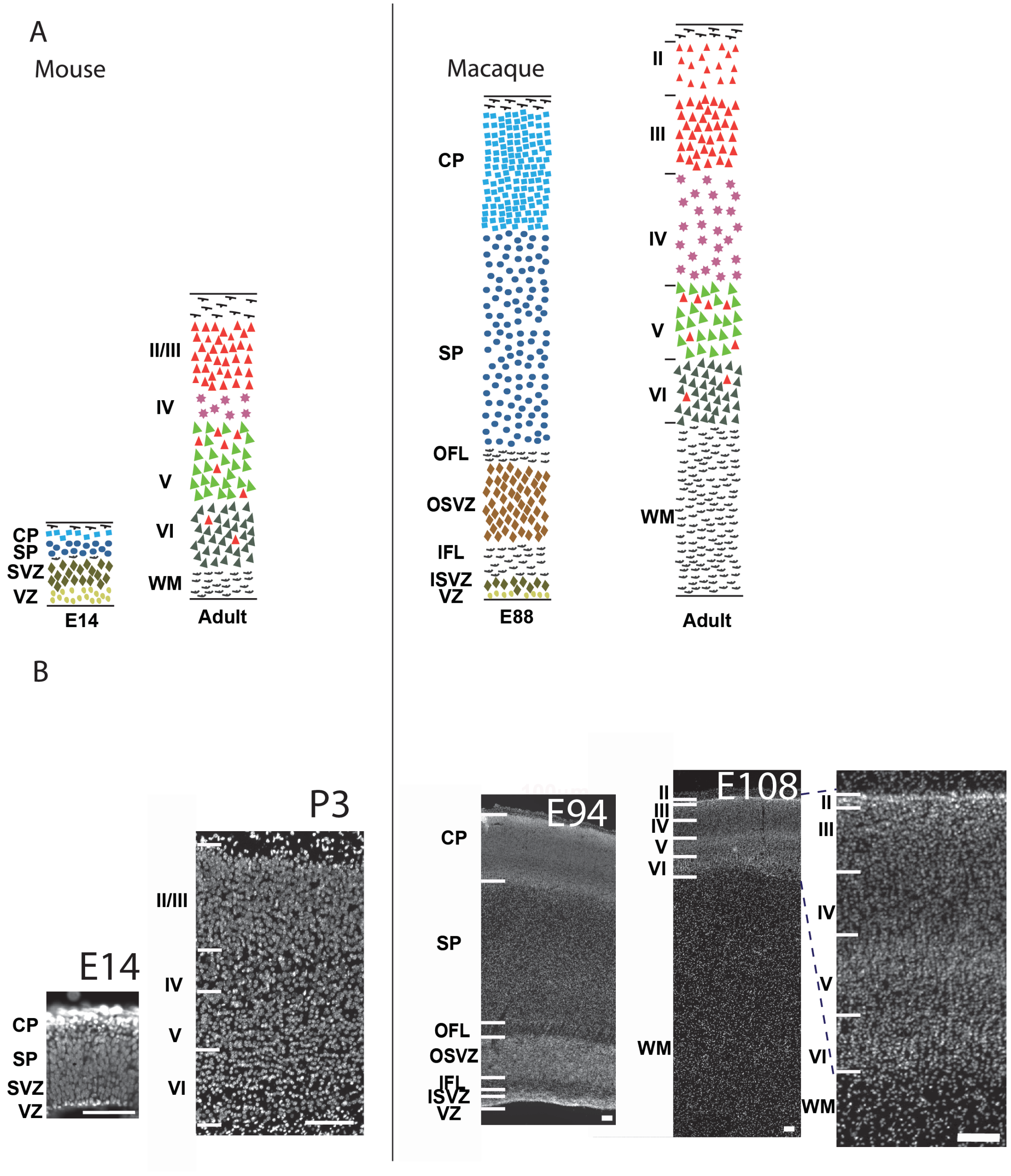

Figure 6.1 (Continued)

these neuron types that segregated upon expansion in primate cortex, and/or new neuron types have emerged to populate the expanded regions of primate neocortex.

By routine histology, it has appeared that the level of diversity evident in primates does not exist in mouse; however, our recently published data revealing molecular diversity of rodent CPN (Molyneaux et al., 2009) potentially reveals parallel diversity in mouse. Cortical neuronal diversity in primates might have molecular correlates in mice, and newly identified molecular controls over CPN subtype diversity in mice might reflect an evolutionarily older, non-histologically recognizable, shared molecular expression, and therefore function, not revealed by examining the overall expansion of superficial layer size in primates. To test this hypothesis, I have selected a set of genes expressed by distinct populations in mice that I hypothesize might be new candidates to identify heterogeneity within laminar populations in primates and investigate whether they are likely homologous populations with conserved gene expression patterns between the two species.

Unlike many genome-wide, layer-specific, or microdissection regional-specific gene expression analyses in primate and mouse (Donoghue and Rakic, 1999b; Donoghue and Rakic, 1999a; Johnson et al., 2009; Wang et al., 2009; Ip et al., 2011; Bernard et al., 2012), this study addresses the intersection of laminar molecular diversity within a specific population of neocortical projection neurons, CPN, and which subtypes of this evolutionarily-motivated population have been conserved or expanded molecularly during primate evolution. In addition, many studies of comparative genomics have identified a trend that most mutations in developmentally acting genes occur in regulatory regions rather than coding regions, further motivating the importance of examining gene expression patterns and timing to gain insight into conservation of critical developmental controls(Stern and Orgogozo, 2008). Here, I report that many of the molecular controls over CPN diversity are conserved in general expression between mouse and macaque, with notable distinctions, predominantly in superficial layer CPN. These distinctions in superficial layer CPN likely reveal cell-type complexity in mouse and macaque that has not yet been correlated between the two species, nor molecularly defined in macaque.

6.3 Materials and Methods

6.3 a. In situ hybridization probe design

All macaque *in situ* hybridization probes were designed to closely match homologous regions of corresponding mouse mRNA that were recognized by Molyneaux, et al (Molyneaux et al., 2009), reported here in Chapter 2. Optimized primers were then chosen to amplify between 400 and 900 bp of this conserved region (see Table 6.1). Since the macaque genome is not fully annotated, not all of the sequences could be obtained from verified sequences and, therefore, some were obtained from NCBI predicted homologs or whole chromosome shotgun sequencing data.

6.3 b. RNA extraction, and first strand cDNA synthesis and library construction

Total RNA was extracted from frozen E85 macaque neocortex tissue following the product insert instructions for organic RNA extraction with TRIzol ® Reagent (Invitrogen Life Sciences). First-strand cDNA was synthesized using Oligo(dT) primers (25ng/μL) and total RNA (0.5ng/μL), following the product insert instructions for Superscript II ® reverse transcriptase (Ambion Life Sciences). To remove RNA complementary to the cDNA, *E. coli* RNase H (0.1U/μL) was added and incubated at 37° C for 20 min. This single stranded DNA was then used as template for PCR (sequences of all primers used are listed in table 6.1), and cloned into TOPO II ® (Invitrogen Life Sciences) bacterial vectors using appropriate restriction enzymes (New England Biolabs).

6.3 c. In situ hybridization

Nonradioactive colorimetric *in situ* hybridization was performed using probes labeled with dig-UTP. Sense probes were used as negative controls in all experiments.

For *in situ* hybridization, 25 μm cryosections of fixed (4% PFA), cryoprotected (30% sucrose) E94 or E108 macaque forebrain were mounted on superfrost plus slides ® (Fisher Scientific) and were postfixed in 4% PFA in PBS for 10 min., rinsed in PBS for 3 min., permeabilized in 0.3% Triton X-100 (Sigma) followed by RIPA cell lysis buffer [150 mM Sodium chloride, 1% Triton X-100, 1% deoxicholic acid sodium salt, 0.1% sodium dodesyl sulfate, 50 mM Tris-HCl, pH 7.5, 2mM EDTA], re-fixed in 4% PFA, acetylated for 15 min. in 0.1M triethanolamine/ 0.4% HCl/0.25% acetic anhydride (Sigma), and then preybridizied for 1 hour in 65°C hybridization buffer [50% formamide, 5x SSC, 5x Denhardts [1μg/mL Ficoll 400, 1μg/mL Polyvinilpyrrolidone, 1μg/mL BSA] , 500μg/mL sheared salmon sperm DNA, 250μg/mL Yeast RNA]. Slides were incubated overnight (14-20 hours) at 65°C in 2μg/mL dig-labeled probe in hybridization buffer coverslipped with GeneFrame ® adhesive spacers (Thermo Scientific) in a well-humidified oven. Slides were then subjected to stringency washes in 2x SSC/ 50% formamide/ 0.1% Tween-20 at 65°C for 1 hour each. Sections were then rinsed in MABT [0.9M maleic acid (Sigma), 0.1M NaCl (Sigma), 0.0005% Tween 20 (Sigma), 0.175M NaOH (Sigma)] at RT, blocked in 10% goat serum in MABT, and incubated overnight in goat alkaline phosphatase-conjugated anti-dig (1:1000, Roche) primary antibody in block, rinsed with MABT, followed by 30 a min. wash in alkaline phosphatase reaction buffer [100mM Tris pH 9.5, 50mM $MgCl_2$, 100mM NaCl, 0.1% Tween-20]. The alkaline phosphatase reaction was developed with NBT/BCIP in phosphatase reaction buffer, changing to fresh solution every 1-4 hours at RT or every 6-9 hours at 4°C. When the reaction was judged complete (48-100 hours), tissue was rinsed in 0.1% Tween-20 in PBS, postfixed in 4% PFA for 30 min, counterstained for 1 min. in 1:10,000 4',6-diamidino-2-phenylindole (DAPI), and rinsed in 0.033M PB [27mM dibasic sodium phosphate, 6.3mM monobasic sodium phosphate]. Slides were coverslipped with Fluromount ® (Sigma), dried, and edges were protected with clear nailpolish.

For older E108 tissuse, an additional permeabilization step with proteinase K (Sigma) treatment [10μg /mL enzyme in 0.005M EDTA, 0.05M Tris, pH 8.0] for 10 min. at room temperature was added after the RIPA permeabilization.

6.3 d. Immunocytochemstry

Immunostaining was largely performed as described in Chapter 3. However, all immmunocytochemical reactions were performed on 25 μm cryosections of fixed (4% PFA), cryoprotected (30% sucrose) E94 or E108 macaque forebrain mounted on superfrost plus slides ® (Fisher Scientific). These were then warmed to room temperature and postfixed in 4% PFA in PBS for 10 min., rinsed in PBS for 3 min. and stained as previously described. Antigen retrieval in 0.1M citric acid (pH=6.0) for 10 min. at 95-98°C was used for CAV1 and LMO4 staining as described in Chapters 3 and 4. Primary antibodies were used as follows: mouse-anti-CAV1, 1:500 (Cell Signaling #3238), goat-anti-LMO4, 1:200 (Santa Cruz Biotech SC- 11122), rabbit-anti-Nectin-3, 1:500 (Abcam ab63931).

6.3 e. Microscopy and image analysis

Images were acquired using a Nikon E90i microscope, using a 1.5 megapixel cooled CCD digital camera (Andor Technology, Dublin, Northern Ireland), a 5 megapixel color CCD digital camera (Nikon Instruments, Melville, NY), and Elements acquisition software (Nikon Instruments, Melville, NY). All analysis was performed in primary somatosensory area (S1) unless otherwise noted.

Table 6.1: Detailed Information About the Clones Used for *In Situ* Hybridization

Gene	**GenBank/ Ensembl ID**	**Left primer**	**Right primer**	**Amplicon**
Chn2	NM_001261577.1	ATGAGCCTTTCACACCAA	ATGCTTTGCCTTCCATTTA	444 bp
Cited2	XM_001096152.2	AAAGAAATCAAACCCCCA	GCCACCAAAGGTAACAAT	900 bp
Dkk3	NM_001265749.1	CAGTTATCACGTCTGTGG	GAGCTGAATAAATGCACA	823 bp
Epha3	XM_001083136.1	GGCTGTGGAAGGTGTAGC	GGCTCTAAGCACCAGAGC	955 bp
Gfra2	XM_001105178.2	TTTGACATGACGCCCAAC	GGCATTTCTAGAGCCTCGT	955 bp
Inhba	XM_001098421.1	TTTCTGTTGGCAAGTTGCT	CATCCCCCTCCTCTTCTTT	781 bp
Limch1	NW_001118139	GGCCAAGAAAGGAGTCA	CTCCATGAGAAGTCCTGG	517 bp
Nnmt	XM_001086727.1	GGAACAGAGTCAAGGGTC	CCACCAGGGAGAAAAGTC	414 bp
PlxnD1	ENSMMUG000000127	GCAAGGTTCTCAACTCCA	CAGCTCTCAGGAATCTTCC	865 bp
Ptn	NM_001194354.1	TGCAACAAAGGCAGACTG	TCTCCTGTTTCTTGCCTTC	540 bp
Tmtc4	XM_001094711.2	ACCGGATGGCAATTAAAC	CAAGCTGCAAGGAGATTT	429 bp
Fezf2	(Arlotta et al., 2005)			

Table 6.1 (Continued)

6.4 Results

6.4 a. In situ hybridization protocol detects mRNA in macaque tissue

Because each new tissue preparation and worksite setup is different and can influence the outcome of *in situ* hybridization results, and particularly because this tissue was prepared in a different lab than that in which analysis of gene expression was to be performed, I chose a control probe known to be highly conserved with laminar expression in layers V (high expression) and VI (low expression) between mouse and primate, *Fezf2* (Molyneaux et al., 2005; Ip et al., 2011) (Kwan et al., 2008) (Padmanabhan, HK and Sohur, US; unpublished observations). In mouse, *Fezf2* is expressed at high levels by corticospinal motor neurons (CSMN) at at lover levels by corticothalamic projection neurons (related corticofugal neurons), and is necessary and sufficient to produce CSMN, but is excluded from CPN. I confirmed that the macaque tissue, handling, and protocol can provide accurate gene expression results.

At E94 in macaque (mid-corticogenesis), *Fezf2* expression is conserved as strongly expressed in the cortical plate. (Figure 6.2A). At E108, when neocortical projection neurons have fully migrated to their final laminar positions, *Fezf2* is expressed highly in layer V, and at lower levels in layer VI (Figure 6.2B). This is similar to reported expression of *Fezf2* in mouse by layer V CSMN (high level) and layer VI CThPN(Chen et al., 2005a; Chen et al., 2005b; Molyneaux et al., 2005; Rouaux and Arlotta, 2010). This expression in macaque both confirms previous findings (Ip et al., 2011) (Kwan et al., 2008), and validates the chosen approach for comparing macaque and mouse gene expression.

6.4 b. Genes expressed by CPN early in mouse development are similarly expressed in macaque

Because some of the CPN subtype-specific genes are expressed very highly early in development, and because early expression is thought to be more likely conserved between species than later (Donoghue and Rakic, 1999b; Donoghue and Rakic, 1999a), I examined expression of 7 genes in E94 macaque cortex that are expressed early in mouse CPN development. Strikingly, subventricular zone (SVZ) expressed genes are conserved in expression between mouse and macaque, including *Ptn*, *Nnmt, Dkk3,* and *Lmo4*. In addition, most post-mitotic, cortical plate gene expression is also conserved with *Lmo4,* *Nnmt, Dkk3, and Inhba..* In addition, cortical plate gene *Epha3* has been shown previously to have similar cortical plate expression in macaque earlier at E65, but restricted to caudal cortex(Donoghue and Rakic, 1999b; Donoghue and Rakic, 1999a). Together, thes data suggest that these early populations of progenitors and immature post-mitotic neurons are extremely similar in early gene expression between mouse and macaque.

Populations of neurons and progenitors are molecularly defined not only by positive expression of genes, but also by the lack of expression of other, inappropriate factors. Therefore, I also investigated expression of 3 genes expressed by CPN at late stages in development, but not expressed early in mouse: *Gfra2 and Tmtc4*. Neither of these exclusively later genes were expressed in the early E94 macaque cortical plate or progenitor zone, suggesting that the examined CPN genes expressed in early macaque cortex are both positively and negatively regulated in similar populations as in mouse.

A notable exception to the largely conserved early expression of developmentally regulated neocortical control genes is that of the cell adhesion and guidance molecule *Plexin-D1*. By E14 in mouse, *Plexin-D1* is strongly expressed by immature neurons of the cortical plate as they begin to extend their axons, however no *Plexin-D1* expression is observed in E94 macaque cortical plate (Figure 6.3D). In section *6.4c*, below, I show that postmigratory expression of *Plexin-D1* is conserved between mouse and macaque. Therefore, this lack of *Plexin-D1* expression in early macaque cortex likely reflects changes in gene regulation affecting timing of *Plexin-D1* expression by migrating immature neurons.

The above data add to a growing body of work revealing similarities and differences between rodents and primates in this population of progenitors and early post-mitotic neurons(Donoghue and Rakic, 1999b; Donoghue and Rakic, 1999a; Johnson et al., 2009; Ip et al., 2011; Bernard et al., 2012). This current focused study specifically examines radial similarities between mouse and primate, and finds general conservation of expression during early developmental processes in mouse and macaque neocortex. This work does not, however, address tangential areal molecular compartmentalization, which have been shown to be additionally complex in primates compared to mouse (Donoghue and Rakic, 1999b; Donoghue and Rakic, 1999a). At the earliest areal organization stages of development, most

Figure 6.2: *Fezf2* is detectable in macaque tissue using current *in situ* hybridization approach **(A)** *in situ* hybridization at E94 in macaque and E14 in mouse for *Fezf2*, showing early similarities in expression between mouse and macaque. **(B)** *in situ* hybridization at E108 in macaque and P3 in mouse for *Fezf2*, confirming early similarities in expression between mouse and macaque, and validating the chosen approach.

Scale bars: **A**, µm; **B**,100 µm. E, embryonic day; P, postnatal day; VZ, ventricular zone; SVZ, subventricular zone; IZ, intermediate zone; CP, cortical plate; S1, primary somatosensory area; Roman numerals indicate cortical layers. E14 mouse *in situ* from GenePaint digital expression atlas www.genepaint.org

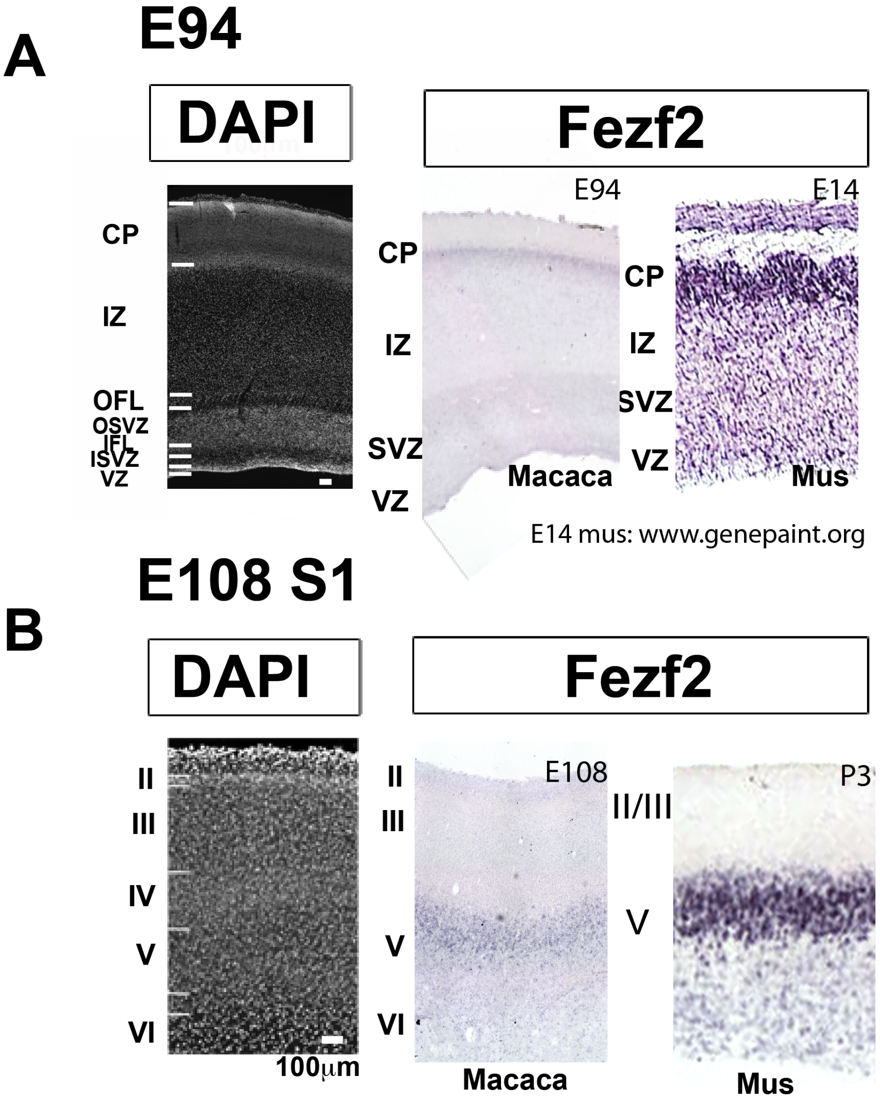

Figure 6.2 (Continued)

Figure 6.3: At E14.5 and E94, early expressed CPN genes are similarly expressed in mouse and macaque **(A)** *in situ* hybridization at E94 in macaque and E14 in mouse for early expressed CPN genes, shows early similarities in expression between mouse and macaque. **(B)** *in situ* hybridization at E94 in macaque for exclusively later expressed CPN genes in mouse demonstrates negative, as well as positive, molecular similarities between radial populations in mouse and macaque neocortex. (**C)** *in situ* hybridization at E94 in macaque reveals some non-conserved timing in gene expression by early neocortical neurons.

Scale bar: **A,** 100 mm. E, embryonic day; P, postnatal day; VZ, ventricular zone; SVZ, subventricular zone; IZ, intermediate zone; CP, cortical plate; S1, primary somatosensory area; Roman numerals indicate cortical layers. E14 mouse *in situ* from GenePaint digital expression atlas www.genepaint.org, except *Tmtc4*, which was performed in house as described in Chapter 5.

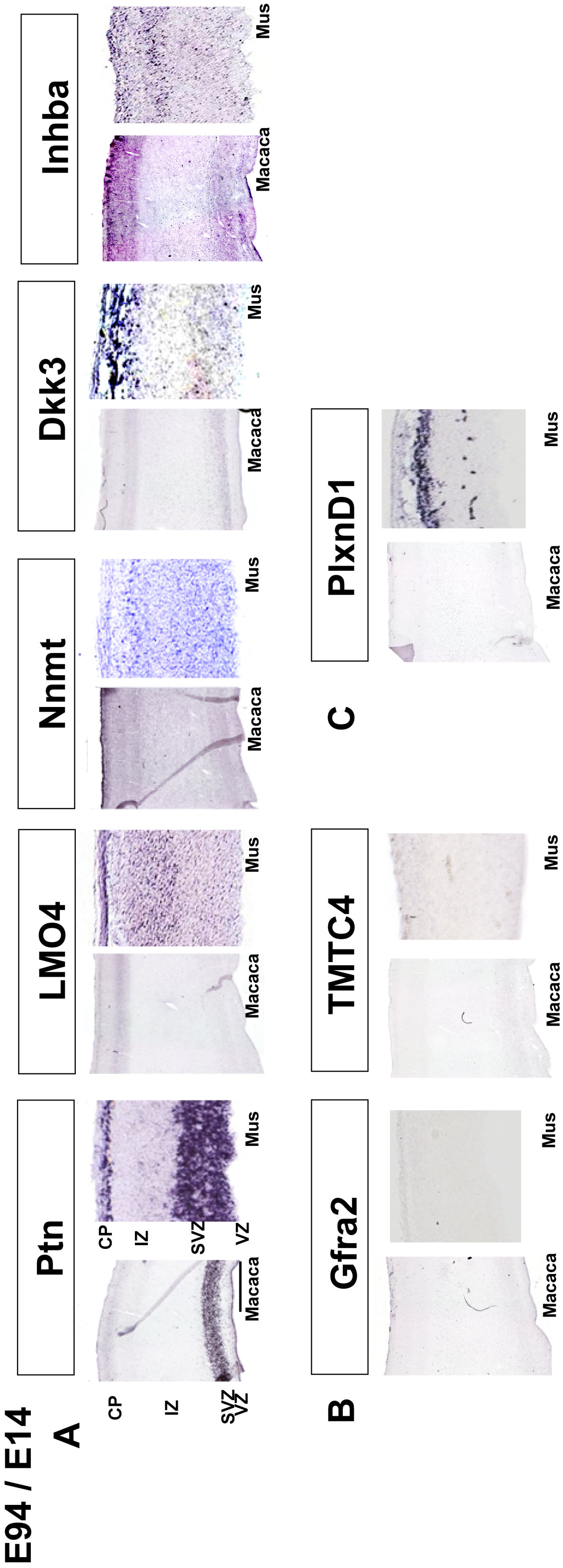

E14 mus: www.genepaint.org

Figure 6.3 (Continued)

CPN have not yet emerged, though radial similarities found in this early population lend support for further investigations (addressed below) of these genes in specific, cell-type specific roles when the neocortex has formed.

6.4 c. CPN genes expressed after migration reveal related CPN populations in mouse and macaque superficial cortical layers

Throughout independent evolutionary divergence between rodent and primate neocortex, the superficial layers, which contain over 80% of CPN in rodents, have expanded the most of any of the laminar populations. These expanded superficial layers in primate exhibit discernable subpopulations of cellular density and cell size that are not recognizable in mouse superficial layers. Since some of the diversity identified in primate cortex superficial layers by traditional histology might exist as molecular diversity within superficial layer CPN in mouse, but might simply not be possible to observe by traditional histological analyses (Molyneaux et al., 2009), I directly compared expression of CPN-enriched genes in mouse and macaque. By E108 in macaque, all cortical neurons have migrated to their final laminar locations, but the neurons are still immature and likely to express genes critical to neocortical developmental processes. Therefore, I chose E108 to first study CPN expressed genes in macaque.

Both *Nnmt* and *Chn2* very closely match expression between mouse and macaque. *Nnmt* is expressed exclusively in the superficial portion of mouse layer II/III, and is limited to macaque layer II. *Chn2* is expressed in the deeper portion of mouse layer II/III, and is restricted layer III in macaque. Interestingly, *Chn2* is not expressed throughout macaque layer III, only in the more superficial regions of this layer, suggesting an even more segregated population of *Chn2*-expressing neurons in macaque(Figure 6.4A). Potentially, these might include populations of local associative neurons or even dual CON/local association neurons, since most CPN in macaque S1 are in deeper portions of layer III (Jones and Wise, 1977; Killackey et al., 1983; Manzoni et al., 1986), but this would have to be verified by retrograde labeling or other hodological analyses.

The selected subset of superficial layer CPN genes also hints at populations of neurons that, while present in both rodent and macaque, are differentially dominant. *EphA3*$^{+}$ neurons are a quite restricted population in mouse cortex, yet they extend more broadly in macaque. *Limch1* is expressed in a specifically defined microlayer of most superficial layer II in macaque, but *Limch1* is expressed throughout layer II/III in mouse (Figure 6.4A). These examples suggest that mouse molecular diversity of CPN provides insight into some expanded populations of primate CPN, but does not contain all of the primate molecular diversity.

6.4 d. CPN genes expressed after migration reveal related CPN populations in mouse and macaque deep cortical layers

Deep cortical layers have not undergone the dramatic expansion of the superficial layers(Smart et al., 2002b; Fame et al., 2011), however a significant proportion of CPN reside in deep layers (~20% in mouse and ~10% in macaque), and, therefore CPN are a very interesting deep layer population to study to gain insight into what expanded diversity, and if any, exists within deep layers. Strikingly, all of the deep layer mouse CPN genes examined (*Cited2, Dkk3, Plexin-D1,* and *Gfra2)* are conserved in their deep layer expression in macaque, suggesting that deep layer CPN are likely to be evolutionarily consistent from rodent to primate (Figure 6.4B). Interestingly, in addition to its conserved expression in layer Va and VI CPN in mouse and macaque, *Gfra2* is also expressed strongly in superficial layer neurons in macaque, suggesting a potentially novel neuronal population of superficial layer macaque CPN. Together these data suggest that, while expanded superficial layer CPN populations likely have refined and expanded, deep layer, evolutionarily older CPN have remained largely molecularly, and therefore potentially functionally, consistent.

Figure 6.4: At early postnatal times in mouse, and at E108 in macaque CPN genes reveal related CPN populations in mouse and macaque superficial and deep cortical layers.

(A) *in situ* hybridization at E108 in macaque, and at P3/P6/P14 in mouse, for subpopulation-specific CPN genes, showing molecular similarities and differences in distinct populations of CPN in subcompartments within the canonical superficial cortical layers between mouse and macaque. **(B)** *in situ* hybridization at E108 in macaque and P3/P6 in mouse for subpopulation specific CPN genes, showing molecular similarities between deep layer radial populations in mouse and macaque neocortex

Scale bars: **A, B** 100 μm. E, embryonic day; VZ, ventricular zone; SVZ, subventricular zone; IZ, intermediate zone; CP, cortical plate. Postnatal mouse *in situ* from (Molyneaux et al., 2009).

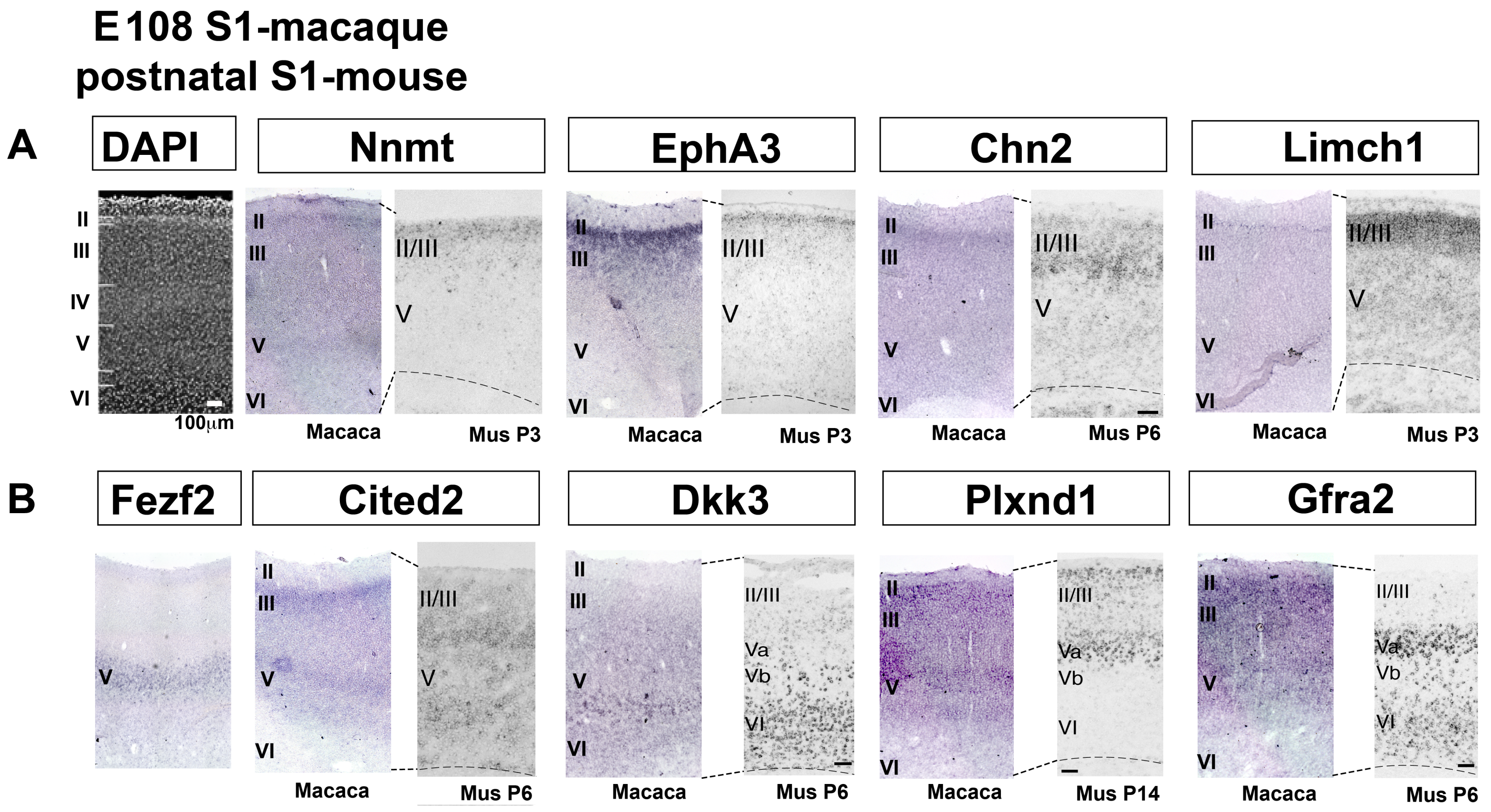

P3/P6/P14 mus: Molyneaux, Arlotta, Fame, MacDonald, McQuarrie, Macklis, *J.Neurosci.* 2010

Figure 6.4 (Continued)

6.4 e. Subcellular and functional areal localization of CPN-expressed proteins suggest related functions for conserved genes expressed by CPN populations

The above analyses reveal molecular conservation and divergence between populations of CPN in distinct laminar locations within somatosensroy neocortical areas. While comparative genomics has found many more changes in regulatory regions than in coding regions(Stern and Orgogozo, 2008), it remains unknown if genes expressed in mouse and macaque CPN have shared functionality within these neurons. As a second read-out of potential conserved gene function (after temporal and laminar specific expression, as investigated above), I investigated whether proteins developmentally expressed in macaque cortex shared subcelular localization with those expressed by mouse CPN.

To compare subcellular localization of subtype-specific proteins, I selected three proteins with distinct subcellular localization in mouse CPN: Nectin-3, with axonal white matter expression by superficial layer CPN axons in the CC (see Chapter 2), CAV1, with cell body and dendritic localization by a subpopulation of deep layer CPN (see Chapter 4), and LMO4, with nuclear expression in deep layer CPN of somatosensory cortex (see Chapter 3). Strikingly, at E94, Nectin-3 is expressed specifically in white matter tracts in macaque developing neocortex (Figure 6.5A). There is low expression in the cell-dense cortical plate, higher expression throughout the cell-sparse subplate, and very high, fiber-localized expression in both the outer and inner fibrous layers. With similar conservation, at E108, CAV1 is localized to neuronal cell membranes and apical dendrites, as well as to developing blood vessels, and LMO4 is expressed in nucleae of deep layer somatosensory neocortical neurons, as is seen in mouse. These data strongly support conserved function within shared neuronal populations for these gene products, suggesting not only that rodents and primates likely arose from shared ancestors with specific genetic controls over complex neocortical neuronal populations, but also support the viability of relating rodent studies of these proteins' functions to human development and disease.

Interestingly, both LMO4 and CAV1 are differentially expressed in particular neocortical areas in mouse. I investigated whether this was a shared property between mouse and macaque, even though it might be modified by the increasingly complex process of primate cortical arealization as compared to rodent. Strikingly, areal restriction for both LMO4 and CAV1 are conserved. LMO4 expression in motor cortex is throughout all neocortical layers instead of the more restricted expression in somatosensory cortex. CAV1 expression is reduced in motor cortex in comparison to somatosensory. Together, these data suggest that gene product function is likely shared for Nectin-3, CAV1, and LMO4 in rodents and primates, based on conserved protein subcellular localization and areal-specific expression between the two species, highly motivating current and future functional analyses of these proteins in mouse neocortical development, especially for human disease-linked genes.

Figure 6.5: Subcellular and functional areal localization of CPN-expressed proteins suggests related functions for conserved genes expressed by CPN populations

Three proteins with distinct subcellular localization in mouse CPN were selected: LMO4, with nuclear expression in deep layer CPN of somatosensory cortex (see Chapter 3); Nectin-3, with axonal white matter expression by superficial layer CPN axons in the CC (see Chapter 2); and CAV1, with cell body and dendritic localization by a subpopulation of deep layer CPN (see Chapter 4). **(A)** At E94, Nectin-3 is expressed specifically in white matter tracts in macaque developing neocortex. There is low level expression in the cell-dense cortical plate, higher level expression throughout the cell-sparse subplate, and very high level, fiber-localized expression in both the outer and inner fibrous layers. **(B)** LMO4 shows nuclear localization in deep layer somatosensory neocortical neurons, and CAV1 is localized to neuronal cell membranes and apical dendrites, as well as to developing blood vessels, as is seen in mouse. **(C),** Areal restriction for both LMO4 and CAV1 are conserved. LMO4 expression in motor cortex is throughout all neocortical layers, instead of the more restricted expression in somatosensory cortex. CAV1 expression is reduced in motor cortex compared to somatosensory cortex.

Scale bars: 100 μm. E, embryonic day; P, postnatal day; VZ, ventricular zone; SVZ, subventricular zone; SP, subplate; ISVZ, inner subventricular zone; IFL, inner fibrous layer; OSVZ, outer subventricular zone; OFL, outer fibrous layer; CP, cortical plate; S1, primary somatosensory area; MCtx, motor cortex; Roman numerals indicate cortical layers.

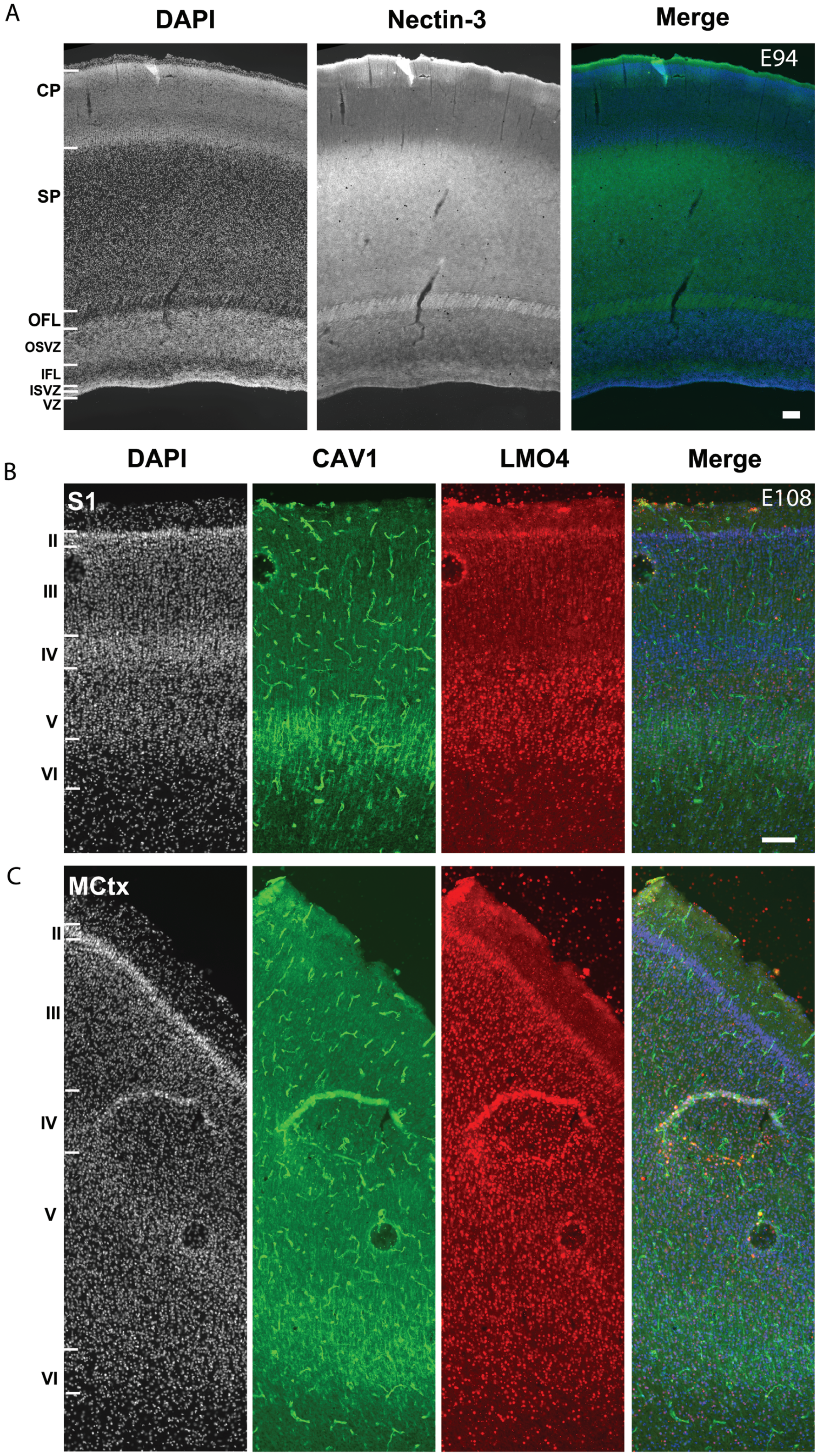

Figure 6.5 (Continued)

6.5 Discussion

It is interesting to speculate that the presence of a molecularly more diversified population of callosal neurons in the superficial layers of the rodent cortex (Molyneaux et al., 2009) might reflect a common ancestor for rodent and primate that had already undergone early stages of the expansion and diversification of these layers that occurred conspicuously during evolution of the primate cortex. While these layers cannot be distinguished at the histological level in rodents, genes that mark neurons located in distinct radial positions within layer II/III might support the hypothesis that specialization of distinct populations of CPN within upper layers are at least partially conserved in rodent cortex molecularly, and likely, then, also with regard to connectivity and function. This work directly investigates the expression of genes identified in distinct populations of mouse CPN within the macaque neocortex, to provide insight into cortical evolution and conservation/ expansion of neocortical projection neuron populations.

The expansion of the superficial layers during cortical evolution has been accompanied by the expansion of a new germinal zone, the subventricular zone (SVZ), and by the appearance of intermediate progenitors within the SVZ that are larely fated to produce neurons of the superficial layers(Smart and McSherry, 1982; Martinez-Cerdeno et al., 2006; Molyneaux et al., 2007). This is in contrast to reptiles and birds, in which cortical neurogenesis is reported to occur only in the ventricular zone (VZ)(Cheung et al., 2007). In mammals, progenitor populations have greatly expanded as cortical complexity has expanded(Smart et al., 2002a) from VZ and SVZ in rodent, to include and inner and outer SVZ region in primate cortex. The progenitors of the inner SVZ (ISVZ) more closely resemble rodent SVZ intermediate progenitors; they express *Tbr2*, but down-regulate *Pax6* (Fietz et al., 2010). The progenitors of the primate outer SVZ (OSVZ), conversely, are more similar to radial glial cells, both molecularly and morphologically (Smart et al., 2002a; Fietz et al.; Hansen et al.). Further, the radial glial-like progenitors of the OSVZ can undergo both symmetric, self-renewing divisions, as well as asymmetric, neurogenic and self-renewing divisions (Fietz et al., 2010; Hansen et al.). This capacity of OSVZ progenitors to undergo self-renewing asymmetric divisions to also generate progenitors that can further proliferate greatly enhances neuronal output, and may have been an important evolutionary step in the expansion of the neocortex. I find that many of the early expressed genes are consistent between rodent and primate (*Ptn*, *Nnmt, Inhba, and Dkk3)*, but none are overtly restricted to any of the primate-specific progenitor zones. This likely reflects a more ancient evolutionary origin of CPN than previously identified, but also the potential for additional molecular complexity in primate progenitor domains than is observed in mouse.

Superficial neocortical layers contain the overwhelming majority of CPN (~80% in mouse and ~90% in macaque), and have undergone extensive expansion over mammalian evolution. Therefore, I hypothesized that some of the newly identified molecular controls over CPN development that divide superficial layers in mice might reflect a common origin for superficial layer CPN expansion identified in primates. I found that some gene expression identified in mouse, including *Nnmt* and *Chn2,* very closely matches expression in macaque. However, while mouse molecular diversity of CPN can suggest correlates to some expanded populations of primate CPN, it does not contain all of the primate molecular diversity, and has likely independently acquired unique populations critical for rodent cortical function. For example, *EphA3* and *Limch1*, while both are expressed in rodent and macaque superficial layers, are expressed by differentially expansive populations. This suggests that some CPN populations common to mouse and macaque were additionally expanded in primates, whereas others were preferentially expanded in rodents. These populations might reveal functional processing differences between mouse and macaque, and provide insight into CPN functions that are more dominant in human cognition.

Deep neocortical layers contain a significant proportion of CPN (~20% in mouse and ~10% in macaque), but have undergone less extensive expansion over mammalian evolution than superficial layers. Therefore, I hypothesized that most of the newly identified molecular controls over deep layer CPN development in mouse might be conserved in macaque. I found that, indeed, all of the deep layer CPN genes that I studied are conserved between mouse and macaque (*Cited2, Dkk3, Plexin-D1,* and *Gfra2)*. Unexpectedly, *Gfra2*, expressed exclusively in layer Va and VI CPN in mouse, is, in addition to deep layer expression, also expressed strongly by superficial layer neurons in macaque, suggesting a potentially entirely new population of CPN that acquired genetic controls first employed by deep layer

CPN. Deep layer CPN cross the midline before superficial layer CPN in development, and are related molecularly and by birthdate to corticofugal neurons, leading to the hypothesis that deep layer CPN were modified from existing corticofugal neuronal populations to become the first to cross the midline early in evolution(Lai et al., 2008; Azim et al., 2009a; Fame et al., 2011). Therefore, similar mechanisms of repurposing existing populations might be at play in the *Gfra2*-expressing population of superficial layer neurons in macaque, to expand superficial layer CPN from other populations, potentially from associative neurons.

In addition to CPN, both superficial and deep neocortical layers contain other populations of neurons. Deep layers predominately contain corticofugal neurons. Superficial layers, while mostly CPN, also contain large populations of local associative neurons. In addition, all layers contain interneurons. While the genes examined here were identified in a comparative microarray analysis to identify genes more highly expressed by CPN than by CSMN, and while many were validated as CPN-expressed in mouse (Chapter 2 and (Molyneaux et al., 2009)), knowing the connectivity of the neurons expressing these genes in macaque will likely give significant insight into CPN populations in macaque. Due to the difficultly of manipulating embryonic macaques, we were not able to perform retrograde labeling early enough to have E108 tissue with labeled CPN. However, now that expression of some of the target genes is validated at this age, it will now be possible to perform CPN retrograde labeling, and look for expression of these CPN genes later in development. While expression levels for most of the superficial layer genes decrease as neurons mature in mouse, it is possible that some could still be expressed in macaque at a time when CPN retrograde labeling is possible.

Complementary to comparative gene expression results in radially expanded neocortical neuronal populations, I also investigated comparative subcellular localization of CPN-expressed gene products between mouse and macaque to gain insight into conserved gene function within these comparative subpopulations of CPN. I found that protein subcellular localization for Nectin-3, CAV1, and LMO4 is conserved between mouse and macaque, with Nectin-3 in axonal white matter, CAV1 in cell membranes and apical dendrites, and LMO4 localized to nuclei. Additionally, differential expression in distinct cortical functional areas is also conserved for CAV1 and LMO4. While conserved gene expression reflects conserved gene regulatory regions, this identified conserved protein localization also suggests conserved gene product function.

While evident differential expansion has occurred in rodent and primate neocortices, both contain CPN, and, therefore, it is likely that conserved gene expression at least partially maps onto conserved CPN populations. However, cortical expansion in marsupials is not as easily compared. Significant cortical expansion to distinct layers II and III in some marsupial species has occurred without CPN. Therefore, understanding relationships between gene expression in particular CPN subpopulations in mouse and macaque, and comparing with large cortices in marsupials, might give interesting insight into evolutionary origins of marsupial connectivity and cortical expansion.

The data presented here provide the first molecular comparison of callosal projection neuron subpopulations in the rodent and primate cortex. Such comparative information will likely be useful for defining both abilities and limits of rodent research to understand some of the complex integrative functions of primate neocortex. Laminar distribution analysis of some recently identified mouse CPN genes in macaque reveals the comparative identity of molecularly distinct subpopulations that had not yet been previously described at the histological, morphological, or anatomical levels in mouse. It is likely that distinct combinations of molecular developmental controls define key aspects of CPN diversity in both species – subtype-specific differentiation, axon collateralization, synaptic connectivity, and physiologic function – underlying their central roles in interhemispheric association and connectivity. Together, these data provide a foundation of evolutionary relationships to inform future studies about which complex subpopulations of primate CPN can be studied with molecular and genetic approaches in mouse and which are uniwue to primate neocortex.

Funding

This work was partially supported by grants from the NIH (NS41590, NS45523), the Harvard Stem Cell Institute, and the United Sydney Association to J.D.M. R.M.F. was partially supported by a National Science Foundation Graduate Research Fellowhsip Program (GRFP) fellowship and a National Institutes of Health predoctoral NRSA fellowship F31 NS073136.

Acknowledgments

I thank R. Richardson and N. Doerflinger for excellent technical assistance with probe synthesis and histology, respectively; and Dr. J. MacDonald, Dr. H. Padmanabhan, and Dr. M. Jose-Galazo for stimulating discussions and helpful suggestions regarding neocortical molecular evolution and primate tissue handling.

Chapter 7:

Discussion

7.1 Discussion

Around the beginning of the 19th century, a building fascination with the brain and nervous system began to focus on the neuron as the basic cellular unit of the brain, enabling its function. Santiago Ramón y Cajal, armed with the Golgi method to sparsely label individual neurons, argued passionately in support of the “neuron hypothesis”, and against contemporaneous “protoplasmic” and “diffuse” network hypotheses(Cimino, 1999; López-Muñoz et al., 2006; DeFelipe, 2010). Even though the debate continued for almost another century, it was clear that neurons were not merely identical, repeating units of neural tissue, but, rather, great diversity of neuronal types from distinct areas of the nervous system were described by physical features, and their organization in relation to one another suggested diversity even within populations of neurons with the same general location and cell body properties. The cerebral cortex is particularly interesting because it is highly organized into laminae, with all layers containing large pyramidal projection neurons.

With the emergence of advanced optical, molecular, connectivity tracing, and electrophysiological techniques, more and more evidence supports functionally important diversity among pyramidal neocortical projection neurons, clearly indicating that better understanding of neuronal subtypes and their development is essential to understanding brain function. Within this decade, molecular controls over specification, development, and maturation of neocortical projection neuron subtypes have begun to be identified, and their functions characterized(Ma et al., 2002; Arlotta et al., 2005; Chen et al., 2005a; Chen et al., 2005b; Mitchell and Macklis, 2005; Molyneaux et al., 2005; Molnár and Cheung, 2006; Hattox and Nelson, 2007; Alcamo et al., 2008; Britanova et al., 2008; Chen et al., 2008a; Joshi et al., 2008b; Kwan et al., 2008; Lai et al., 2008; Anderson et al., 2010; Cubelos et al., 2010) (Leone et al., 2008).

Here, in this dissertation, I describe further diversity between subtypes within one broad projection neuron population, callosal projection neurons (CPN). CPN are excitatory pyramidal neurons that connect the two cerebral hemispheres via axons that pass through the corpus callosum (CC). They are restricted to placental mammals, and are a disproportionately large portion of the neocortical projection neurons of animals with larger brains, suggesting their critical roles in information processing and cognition. I begin by identifying new molecularly defined subpopulations of CPN that reside within distinct neocortical laminae(Molyneaux et al., 2009). I follow this identification with functional analysis of three genes and their products that are candidate controls over development of CPN diversity: 1) *Cited2* early in broad development of intermediate progenitor cells, and later specifically in CPN of somatosensory cortex; 2) *Caveolin1 (Cav1)* in a specific population of dual projecting CPN with an additional connection to ipsilateral frontal neocortex; and 3) *Tmtc4* in axonal development of CPN projections. I end with a comparative molecular analysis of genes expressed by specific CPN subpopulations in mice compared to expression in macaque, which contain disproportionately more CPN compared to other neocortical projection neurons in their large cerebral cortex. Together, the results support the hypotheses that 1) CPN are an immensely diverse set of subpopulations controlled by specific, combinatorialy interacting genes that function progressively to enable acquisition of CPN subtype identities in addition to broad laminar, cell type, or areal controls over neocortical development; and 2) that many of these combinatorially interacting genes are conserved between rodents and primates, while others have diverged in their expression over evolution.

7.1 a. Progressive acquisition of neocortical projection neuron identity

Establishing progenitor domains

In the neocortex, the first broad division of neuron type, excitatory versus inhibitory, is segregated at the progenitor domain level. Neocortical excitatory projection neurons arise from dorsal, or pallial, progenitors, while inhibitory neurons arise from ventral, or subpallial, progenitors. Upon induction of the telencephalon by gradients of extracellular signaling molecules such as sonic hedgehog, fibroblast growth factors, and bone morphogenetic proteins (Rallu et al., 2002), a set of repressive transcription factor interactions establish a pallial neocortical progenitor identity as distinct from subpallial progenitor identity. These transcription factors include *Lhx2*, *Foxg1*, *Emx2*, *Pax6*, and *Sox6*, each of which plays crucial roles in specifying the progenitors that give rise to projection neurons of the neocortex. Together, these five transcriptional regulators establish the neocortical progenitor domain by repressing dorsal midline (*Lhx2* and *Foxg1*) and subpallial fates (*Emx2*, *Pax6,* and *Sox6*), a critical first step in the initial specification of neocortical projection neuron identity.

Work described in the Appendix of this dissertation further explores this early process of progenitor domain formation involving the SRY-type HMG box (SOX)-containing transcription factors *Sox5* and *Sox6,* which play a critical cross-repressive role in parcellation of the proliferative neuroepithelium at the pallial-subpallial boundary(Azim et al., 2009a). *Sox6* and *Sox5* are complementarily expressed in pallial and subpallial progenitors, respectively, and *Sox6* controls the segregation of pallial from subpallial progenitors by repressing the expression of *Mash1* and downstream subpallium-specific programs in pallial progenitors(Azim et al., 2009a). Interestingly, despite the partial ventralization of *Sox6* null pallial progenitors, *Pax6* and *Ngn2* are expressed normally in the *Sox6* null pallium, and projection neuron laminar distribution and subtype- and layer-specific molecular expression are largely normal, though inappropriate subpallial and interneuron genes are co-expressed, forming seemingly “confused” neurons. Thus, *Sox6* critically maintains pallial progenitor identity by repressing subpallial programs of gene expression, but redundant and/or compensatory controls (for example, *Ngn2* and *Ngn1*) persist that are sufficient to ensure somewhat appropriate pallial corticogenesis, indicating that *Sox6* likely acts cooperatively with *Ngn2* to control the segregation of telencephalic progenitor domains during development(Azim et al., 2009a).

Projection neuron type specification

All neocortical projection neurons arise from pallial progenitors that progressively generate projection neuron types. The broad types of neocortical projection neurons are corticofugal projection neurons (CFuPN), including corticothalamic projection neurons (CThPN) and subcerebral projection neurons (SCPN), which in turn include corticospinal motor neurons (CSMN) and corticotectal projection neurons (CTPN); and commissural callosal projection neurons (CPN). Differences in birthdate translate to differences in laminar location, with deep layers born early, and more superficial layers born later. CThPN all reside in layer VI, and are, therefore, born from early progenitors. SCPN reside in layer V and are born from slightly later progenitors than CThPN. A molecularly controlled temporal shift in progenitor capacity can help explain generation of these distinct neuron types. In addition to progenitor change, sequential generation of neuronal types is postmitotically controlled from subplate neurons (earliest born corticofugal projection neurons), through corticothalamic neurons, to corticospinal motor neurons. *Sox5* controls this sequential generation of corticofugal projection neuron subtypes by progressively reducing its repression (via Sox5 down-regulation) of genes required for differentiation of later generated subtypes, ultimately CSMN, preventing premature emergence of normally later-born neurons during early stages of corticogenesis (Lai et al., 2008).

CPN, however, are generated throughout neocortical development, and reside in layers II/III, V, and VI; they are intermingled with CFuPN, and temporal differences in generation cannot alone explain their neuron type identity. In 2008, the first critical molecular regulator of broad CPN specification, special AT-rich sequence-binding protein 2 (SATB2), was identified and characterized as a DNA-binding transcription factor expressed by CPN(Alcamo et al., 2008; Britanova et al., 2008). SATB2 is necessary for specification of CPN through repression of COUP-TF interacting protein 2 (CTIP2), a transcription factor critical for CSMN axon outgrowth and fasciculation(Arlotta et al., 2005; Molyneaux et al., 2007). In the absence of SATB2 function, neurons that would have extended axons across the corpus callosum instead project subcortically through the internal capsule and take on some molecular and electrophysiological characteristics of CFuPN(Chen et al., 2008a). Other pan-callosally expressed genes such as *Lpl* and *Hspb3,* identified in work presented here in Chapter 2, might similarly be broad controls over CPN identity, specifying them from other projection neuron types.

Projection neuron subtype identities

Subtypes exist within all populations of neocortical projection neurons and have been identified by physical cell body location or shape, connectivity, electrophysiological properties, or molecular expression. As a first level of diversity, many of these subtypes have been defined by axonal projection specificity and cell body location. For example, CThPN are defined by their projections from the neocortex to the thalamus, however subpopulations within this broad population exist that project to unique functional thalamic nuclei(Galazo et al., 2008{Miller, 1993 #2653; Watakabe et al., 2012)}. Similarly, tightly regulated subpopulations of CSMN are diverse and extend axons to specific levels of the spinal cord to control motor function in diverse body sections(Penfield, 1937). Within CPN, subpopulations are found in distinct functional areas and laminae(Koralek et al., 1990; Conti and Manzoni, 1994; Reiner et al., 2003; Ramos et al., 2008; Molyneaux et al., 2009), with homotopic and, sometimes, additional heterotopic axonal connections}(Wilson, 1987; Cauller et al., 1998; Mitchell and Macklis, 2005). Thus, subpopulations within broad types of neocortical projection neurons exist and have critical functions that are distinct and specialized even more than those of the more general neuron type.

7.1 b. CPN diversity

Results published earlier, and those presented here, indicate many categories of subtype diversity within the broad population of CPN(Wilson, 1987; Cauller et al., 1998; Mitchell and Macklis, 2005; Molyneaux et al., 2009)}(Koralek et al., 1990; Conti and Manzoni, 1994; Reiner et al., 2003; Ramos et al., 2008). These include birthdate, laminar location, axonal projection connectivity, areal identity, and molecular expression. These levels of diversity are all significant, and likely influence one another. Molecular expression is rarely simply a marker of no function but, rather, expressed genes are typically controls over specific properties or developmental processes. Location of CPN cell bodies in multiple cortical laminae not only reflects distinct birthdates from progenitors with distinct potential and/or subtype restriction, but also indicates distinct connectivity patterns. In rat, deep layer CPN (layers V and VI) provide about 80% of the CPN collaterals connecting primary motor cortex to primary somatosensory cortex, and some deep layer CPN have also been shown to project to secondary somatosensory cortex and the claustrum, in addition to the striatum(Veinante and Deschenes, 2003). In contrast, superficial layer CPN more likely participate in local column circuitry, sending short collaterals to pyramidal neurons within layer II/III, more strongly to layer V, and to pyramidal and stellate neurons in layer VI, in both ipsilateral and contralateral hemispheres (Petreanu et al., 2007). CPN in distinct functional areas have been shown to be differentially myelinated in human brain (Aboitiz et al., 1992a), they respond differently to activity-based pruning(Innocenti et al., 1977; Norris and Kalil, 1992), and they send homotypic axons to different functional areas to transmit diverse functional modalities. Gene expression in distinct populations of CPN might convey some of these attributes, and restricted CPN gene expression in not yet functionally uncategorized populations, might allow identification of new functional subtypes.

Recently, molecular controls that act specifically in subclasses of CPN have begun to be identified. The transcription factor activator enhancing binding protein 2 gamma (AP2γ) acts specifically in a subset of radial glia cortical progenitors to specify SVZ intermediate progenitors to enable the switch from proliferative to neurogenic division, and generating a specific subpopulation of superficial layer CPN in visual cortex(Pinto et al., 2009). Interestingly, while the action of AP2γ is highly area specific, the expression of AP2γ is not, suggesting an areally-restricted partner or compensatory activity. In addition, *Cux1* and *Cux2,* previously discussed as layer-specific identifiers, regulate dendrite branching, spine development, and synapse formation specifically in layer II/III CPN(Cubelos et al., 2010). These subtype-specific controls are important for understanding the diversity that exists within, and is integral to, the broad CPN population.

Data presented in this dissertation begin to identify and functionally characterize molecular controls over CPN subpopulations. Identification of genes expressed by CPN in distinct sublaminae suggest controls over birthdate and connectivity, such as those presented in Chapter 2. *Cav1* identifies a unique subpopulation of CPN in deep layers that includes dual projecting CPN/FPN, and potentially other specific populations of dual projecting CPN. Functional analysis of *Cav1* in CPN in Chapter 4 indicates that, while it is not necessary for generic establishment of CPN projections, its expression in dendrites and its ability to affect early migration suggest that it might be acting in unique dendritic branching or activity required for relaying information from dual projecting CPN. Analysis of *Cited2* function in somatosensory CPN presented in Chapter 3 indicates it as a molecular control that specifically acts in CPN of different functional areas. These examples provide functional evidence in support of the overall hypothesis that these genes expressed in restricted populations of CPN act to control and identify the unique properties of these subpopulations.

7.1 c. Mechanisms of progressive generation of diverse CPN subpopulations

Identifying which gene products control which phenotypic properties, anatomic and function, of distnct CPN subtypes identity and function will be useful at least three levels: 1) to molecularly identify subpopulations so that they are genetically accessible for in-depth study; 2) to provide understanding into how individual populations develop their unique properties; and 3) to identify human "disease genes" that are likely critical for proper function of specific, functionally important CPN subpopulations. More broadly, however, investigation into functions of subtype-specifically expressed genes will provide insight into how subtype identity is acquired by CPN. More specifically, this work will elucidate whether the cumulative overlap of a general CPN control with areal and laminar controls alone defines subpopulations of CPN, or whether there are specific molecular controls acting in these diverse subpopulations to integrate overlapping signals into distinct neuron types.

The investigation of *Cited2* function presented in Chapter 3 most directly addresses this final, broad question. *Cited2* is more highly expressed by CPN by than other projection neuron subtypes, and its expression becomes refined to somatosensory functional areas postnatally. *Cited2* function is required for proper formation of somatosensory (SS) superficial layers, where ~80% of mouse CPN reside. In the absence of *Cited2* function, there is a significant, specific reduction in superficial layer thickness in SS cortex, but not in deep layers or motor cortex. The reduction in SS superficial layers is neither a pan-SS nor a pan-superficial layer effect, because both superficial layers in motor cortex, and SS acallosal layer IV, are unaffected by loss of *Cited2* function. Therefore, it is probable that *Cited2* function is areal and neuron subtype-specific, integrating diverse controls to endow the subtype identity of CPN of sensory processing regions of the neocortex. These data support the hypothesis that specific projection neuron areal subtype populations are defined and controlled by specific genes, such as *Cited2*, acting in this role, rather than by strict addition of two distinct, more broadly acting signals.

A combined goal of the research presented here, and all investigation of molecular control over neocortical development, more broadly, is not only to understand mechanism determining final subtype identity and characteristics, but, rather, to identify functional steps required to generate unambiguous, functional neurons. My early work presented in the Appendix on specification and parcellation of pallial and subpallial progenitor domains(Azim et al., 2009a) builds on earlier work in the field identifying broad controls over telencephalon identity. *Sox6*-expressing, pallial progenitors progressively acquire CPN subtype identity, first by specification as CPN through mechanisms involving *Satb2* (Alcamo et al., 2008; Britanova et al., 2008; Chen et al., 2008a; Gyorgy et al., 2008), and likely by broad CPN controls identified in Chapter 2(Molyneaux et al., 2009). Built on this braod CPN identity, subtype identities are acquired by what current data suggests as directed and specific molecular mechanisms, likely induced collaboratively controlled by broad subtype, areal, and laminar controls. My work elucidates two such subtype controls: *Cited2* over somatosensory CPN; and *Cav1* over specific properties of subtypes of dual projecting CPN in layer V and far lateral neocortex.

Interestingly, a single molecular control such as *Cited2* can act at multiple levels in these progressive processes in distinct temporal and areal contexts. The areal specificity for *Cited2* function in somatosensory cortex superficial layer length is preceded in development by a broad early requirement of *Cited2* for proper development of Tbr2-expressing intermediate progenitors (IPCs), and loss of *Cited2* function also results in a broad increase in cellular death in *Cited2* null cortex early in development. This suggests at least two distinct functions for *Cited2* in neocortical development, with a broad, early function at the time of generation of specific basal progenitors, Tbr2+ IPCs, and later function in maintaining the somatosensory neocortical domain of CPN and their specific subtype identity acquisition. These two functions are likely controlled combinatorially by different sets of interactors for CITED2, a transcriptional co-activator that binds multiple distinct transcription factors.

Thus, this work adds support for the general interpretation that mechanisms of cell-type identity acquisition are controlled progressively throughout development. This work also specifically addresses how individual neuronal subtype identities can be acquired, supporting the hypothesis that there are specific molecular controls acting in diverse subpopulations to integrate various axes of signals into distinct neuron type identities.

7.1 d. Evolutionary neocortical expansion, implications for CPN disease, and future directions

CPN have been implicated in many human diseases of subtle behavioral, language, or cognitive dysfunction, including autism spectrum disorders (ASD)(Booth et al., 2011), schizophrenia(Innocenti et al., 2003), dyslexia(von Plessen et al., 2002), and agenesis of the corpus callosum (AgCC) (Paul et al., 2007; Kaufman et al., 2008; Wahl et al., 2008; Booth et al., 2011). Mice lacking CPN exhibit largely normal survival, breeding, and motor output, but show reduced social interactions, impaired play, low exploratory behavior, unusual vocalizations, and high anxiety as compared to other inbred strains (McFarlane et al., 2008) (Scattoni et al., 2008) (Moy et al., 2007). Association of CPN with such disorders of higher cognitive functions that are more fully developed in humans suggest that CPN function in some of the most complex intellectual processes. In addition, the proportion of neocortical projection neurons that are CPN increases with increased intellectual and computational capacity(Manzoni et al., 1986), suggesting a dependence on many CPN (and potentially expanded subtypes of CPN) for high-level cognitive processing.

In this dissertation, I pursued comparative analysis of some of the molecular CPN subtypes identified in mouse with macaque cortex. I identified many CPN-expressed genes as conserved in expression between the mice and macaques, and others that have subtly diverged in expression. Studies of comparative gene expression by CPN are particularly interesting because CPN as a population have undergone differential expansion throughout recent mammalian evolution. This expansion is reflected by the disproportionately large and varied primate superficial layers (that contain~90% of CPN), as compared to rodent superficial layers (that contain only ~80% of CPN), and the noticeably larger relative volume of cortical white matter tracts in primates as compared to rodents, including the CC (Smart et al., 2002a). I find that expression of CPN-enriched genes in early cortex and later deep neocortical layers is conserved, supporting the hypothesis that early developmental processes and deep layer neurons (present in birds and reptiles, in addition to mammals) are highly conserved. I also show that gene expression by superficial layer CPN, which are recent evolutionarily additions in mammals, exhibits more varied levels of conservation of expression. These results suggest that, in these more recently emerged populations, there is specific conservation and/or expansion of some superficial CPN populations in macaque, independent expansion of others in mouse, and even emergence of distinct populations in macaque.

This dissertation research enables both extended comparative evolutionary analysis of this broad neocortical population of CPN, and also contributes toward understanding which human disease genes and affected CPN subpopulations can be effectively studied in mouse, and how these studies can be related back to human patients. All three of the genes (each expressed by distinct subsets of CPN) regarding which I pursued functional analysis in this dissertation are closely related to human cognitive disease. *Cited2* exhibits abnormal copy number variation (CNV) in a subset of ASD patients(Szatmari et al., 2007). Human *Caveolin1* is located at the locus 7q31.1, part of autism-linked locus 9 (*Auts9*). Other potential gene linkages in the *Auts9* locus (*Nrcam, Foxp2, and ST7*) are relatively weak, indicating that the linkage must be accounted for, at least in part, by other *Auts9* genes, potentially *Cav1*. Finally, and most directly connected to human disease, *Tmtc4* was identified in a forward genetic screen of human AgCC patients to occur in 3/140 patients in the cohort(Li et al., 2008) concurrently with our identification of *Tmtc4* as a candidate control over CPN development in mouse(Molyneaux et al., 2009). My comparative studies in mouse and macaque identified conservation of gene expression for all three of these genes in CPN subpopulations. These results reinforce the views that mouse developmental biology is higly relevant to human development and disease, and that directed functional analyses of human "disease genes" in mouse can provide understanding of what neuron populations are affected, and how they contribute to human disease.

Data presented in this dissertation – identifying molecular subtypes of CPN, and functionally investigating three of these gene products as candidate controls over specific CPN subpopulations – enables a range of future studies that were not previously possible. Each gene with restricted CPN subpopulation expression identified in Chapter 2 is a candidate control over these subpopulations.

Directed functional analyses of well-motivated candidates will likely reveal controls over individual populations. The mechanisms by which each of these gene products controls CPN development will provide insight into characteristics of CPN subsets that are important for their diversity and function. In addition, using molecular expression of select genes/ products as markers for specific subpopulations of CPN will enable deeper and more insightful instigation of previously identified molecular controls over CPN, identifying with more precision which CPN subpopulations are affected, and how. Use of new markers will potentially also enable isolation of distinct CPN subpopulations, and identification of additional subtype-specific genes enabling deeper investigation of each subpopulation's role in brain organization, and, therefore, function. For example, isolation of *Cav1*–expressing neurons, followed by additional gene expression analysis, might identify earlier molecular controls over the development of CPN with dual projecting axons, and over formation of dual projection axons, more broadly. Identification of both similarities and differences in CPN gene expression between rodents and primates will not only enable investigations of and connections to human disease as discussed above, but might also direct further analysis of neuron subtypes that most specifically express these genes in primates. Taken together, these comparative connections between mouse and primate, coupled with functional analyses of candidate controls over development and function in mice, begin to identify additional characteristics and subtleties of neuronal subtypes making precise, complex, and diverse connections from between functional cortical areas, in particular that enable the most complex integrative functions of the cerebral cortex.

References

Abelson, J. F., Kwan, K. Y., O'Roak, B. J., Baek, D. Y., Stillman, A. A., Morgan, T. M., Mathews, C. A., Pauls, D. L., Rasin, M. R., Gunel, M. et al. (2005) Sequence variants in SLITRK1 are associated with Tourette's syndrome, *Science* 310(5746): 317-20.

Aboitiz, F., Scheibel, A. B., Fisher, R. S. and Zaidel, E. (1992a) Fiber composition of the human corpus callosum, *Brain Res* 598(1-2): 143-53.

Aboitiz, F., Scheibel, A. B., Fisher, R. S. and Zaidel, E. (1992b) Individual differences in brain asymmetries and fiber composition in the human corpus callosum, *Brain Res* 598(1-2): 154-61.

Aboitiz, F. and Montiel, J. (2003) One hundred million years of interhemispheric communication: the history of the corpus callosum, *Braz J Med Biol Res* 36(4): 409-20.

Aboitiz, F., Morales, D. and Montiel, J. (2003) The evolutionary origin of the mammalian isocortex: towards an integrated developmental and functional approach, *Behav Brain Sci* 26(5): 535-52; discussion 552-85.

Alcamo, E. A., Chirivella, L., Dautzenberg, M., Dobreva, G., Farinas, I., Grosschedl, R. and McConnell, S. K. (2008) Satb2 regulates callosal projection neuron identity in the developing cerebral cortex, *Neuron* 57(3): 364-77.

Alfano, C., Viola, L., Heng, J. I., Pirozzi, M., Clarkson, M., Flore, G., De Maio, A., Schedl, A., Guillemot, F. and Studer, M. COUP-TFI promotes radial migration and proper morphology of callosal projection neurons by repressing Rnd2 expression, *Development* 138(21): 4685-97.

Allen-Institute-for-Brain-Science (©2009a) Allen Developing Mouse Brain Atlas [Internet], Available from: http://developingmouse.brain-map.org.

Allen-Institute-for-Brain-Science (©2009b) Allen Human Cortex Study [Internet], Available from: http://humancortex.alleninstitute.org. .

Alvarez-Bolado, G., Rosenfeld, M. G. and Swanson, L. W. (1995) Model of forebrain regionalization based on spatiotemporal patterns of POU-III homeobox gene expression, birthdates, and morphological features, *J Comp Neurol* 355(2): 237-95.

Amir, R. E., Van den Veyver, I. B., Wan, M., Tran, C. Q., Francke, U. and Zoghbi, H. Y. (1999) Rett syndrome is caused by mutations in X-linked MECP2, encoding methyl-CpG-binding protein 2, *Nat Genet* 23(2): 185-8.

Anderson, C. T., Sheets, P. L., Kiritani, T. and Shepherd, G. M. (2010) Sublayer-specific microcircuits of corticospinal and corticostriatal neurons in motor cortex, *Nat Neurosci* 13(6): 739-44.

Anderson, S. A., Kaznowski, C. E., Horn, C., Rubenstein, J. L. and McConnell, S. K. (2002) Distinct origins of neocortical projection neurons and interneurons in vivo, *Cereb Cortex* 12(7): 702-9.

Andrews, W., Liapi, A., Plachez, C., Camurri, L., Zhang, J., Mori, S., Murakami, F., Parnavelas, J. G., Sundaresan, V. and Richards, L. J. (2006) Robo1 regulates the development of major axon tracts and interneuron migration in the forebrain, *Development* 133(11): 2243-52.

Angevine, J. B. and Sidman, R. L. (1961) Autoradiographic study of cell migration during histogenesis of cerebral cortex in the mouse, *Nature* 192: 766-8.

Anthony, T. E., Klein, C., Fishell, G. and Heintz, N. (2004) Radial glia serve as neuronal progenitors in all regions of the central nervous system, *Neuron* 41(6): 881-90.

Aridor, M. and Fish, K. N. (2009) Selective targeting of ER exit sites supports axon development, *Traffic* 10(11): 1669-84.

Arion, D., Unger, T., Lewis, D. A. and Mirnics, K. (2007) Molecular markers distinguishing supragranular and infragranular layers in the human prefrontal cortex, *Eur J Neurosci* 25(6): 1843-54.

Arlotta, P., Molyneaux, B. J., Chen, J., Inoue, J., Kominami, R. and Macklis, J. D. (2005) Neuronal subtype-specific genes that control corticospinal motor neuron development in vivo, *Neuron* 45(2): 207-21.

Arlotta, P., Molyneaux, B. J., Jabaudon, D., Yoshida, Y. and Macklis, J. D. (2008) Ctip2 controls the differentiation of medium spiny neurons and the establishment of the cellular architecture of the striatum, *J Neurosci* 28(3): 622-32.

Armentano, M., Chou, S. J., Tomassy, G. S., Leingartner, A., O'Leary, D. D. and Studer, M. (2007) COUP-TFI regulates the balance of cortical patterning between frontal/motor and sensory areas, *Nat Neurosci* 10(10): 1277-86.

Arnold, S. J., Huang, G. J., Cheung, A. F., Era, T., Nishikawa, S., Bikoff, E. K., Molnar, Z., Robertson, E. J. and Groszer, M. (2008) The T-box transcription factor Eomes/Tbr2 regulates neurogenesis in the cortical subventricular zone, *Genes Dev* 22(18): 2479-84.

Ashery-Padan, R., Marquardt, T., Zhou, X. and Gruss, P. (2000) Pax6 activity in the lens primordium is required for lens formation and for correct placement of a single retina in the eye, *Genes Dev* 14(21): 2701-11.

Asprer, J. S. T., Lee, B., Wu, C.-S., Vadakkan, T., Dickinson, M. E., Lu, H.-C. and Lee, S.-K. (2011) LMO4 functions as a co-activator of neurogenin 2 in the developing cortex, *Development* 138(13): 2823-32.

Azim, E., Jabaudon, D., Fame, R. M. and Macklis, J. D. (2009a) SOX6 controls dorsal progenitor identity and interneuron diversity during neocortical development, *Nat Neurosci* 12(10): 1238-1247.

Azim, E., Shnider, S. J., Cederquist, G. Y., Sohur, U. S. and Macklis, J. D. (2009b) Lmo4 and Clim1 progressively delineate cortical projection neuron subtypes during development, *Cereb Cortex* 19 Suppl 1: i62-9.

Baala, L., Briault, S., Etchevers, H. C., Laumonnier, F., Natiq, A., Amiel, J., Boddaert, N., Picard, C., Sbiti, A., Asermouh, A. et al. (2007) Homozygous silencing of T-box transcription factor EOMES leads to microcephaly with polymicrogyria and corpus callosum agenesis, *Nat Genet* 39(4): 454-6.

Bagri, A., Marin, O., Plump, A. S., Mak, J., Pleasure, S. J., Rubenstein, J. L. and Tessier-Lavigne, M. (2002) Slit proteins prevent midline crossing and determine the dorsoventral position of major axonal pathways in the mammalian forebrain, *Neuron* 33(2): 233-48.

Bamforth, S. D., Bragança, J., Eloranta, J. J., Murdoch, J. N., Marques, F. I., Kranc, K. R., Farza, H., Henderson, D. J., Hurst, H. C. and Bhattacharya, S. (2001) Cardiac malformations, adrenal agenesis, neural crest defects and exencephaly in mice lacking Cited2, a new Tfap2 co-activator, *Nat Genet* 29(4): 469-74.

Bamforth, S. D., Bragança, J., Farthing, C. R., Schneider, J. E., Broadbent, C., Michell, A. C., Clarke, K., Neubauer, S., Norris, D., Brown, N. A. et al. (2004) Cited2 controls left-right patterning and heart development through a Nodal-Pitx2c pathway, *Nat Genet* 36(11): 1189-96.

Barnabe-Heider, F., Wasylnka, J. A., Fernandes, K. J., Porsche, C., Sendtner, M., Kaplan, D. R. and Miller, F. D. (2005) Evidence that embryonic neurons regulate the onset of cortical gliogenesis via cardiotrophin-1, *Neuron* 48(2): 253-65.

Barres, B. A., Silverstein, B. E., Corey, D. P. and Chun, L. L. (1988) Immunological, morphological, and electrophysiological variation among retinal ganglion cells purified by panning, *Neuron* 1(9): 791-803.

Bayer, S. A. and Altman, J. (1991) *Neocortical Development*, New York: Raven Press.

Beardsley, A., Fang, K., Mertz, H., Castranova, V., Friend, S. and Liu, J. (2005) Loss of caveolin-1 polarity impedes endothelial cell polarization and directional movement, *J Biol Chem* 280(5): 3541-7.

Bedogni, F., Hodge, R. D., Elsen, G. E., Nelson, B. R., Daza, R. A. M., Beyer, R. P., Bammler, T. K., Rubenstein, J. L. R. and Hevner, R. F. (2010) Tbr1 regulates regional and laminar identity of postmitotic neurons in developing neocortex, *Proc Natl Acad Sci USA*.

Benoist, M., Gaillard, S. and Castets, F. (2006) The striatin family: A new signaling platform in dendritic spines, *J Physiol-Paris*.

Berger, U. V. and Hediger, M. A. (2001) Differential distribution of the glutamate transporters GLT-1 and GLAST in tanycytes of the third ventricle, *J Comp Neurol* 433(1): 101-14.

Bernard, A., Lubbers, L. S., Tanis, K. Q., Luo, R., Podtelezhnikov, A. A., Finney, E. M., McWhorter, M. M., Serikawa, K., Lemon, T., Morgan, R. et al. (2012) Transcriptional architecture of the primate neocortex, *Neuron* 73(6): 1083-99.

Berto, G., Camera, P., Fusco, C., Imarisio, S., Ambrogio, C., Chiarle, R., Silengo, L. and Di Cunto, F. (2007) The Down syndrome critical region protein TTC3 inhibits neuronal differentiation via RhoA and Citron kinase, *J Cell Sci* 120(Pt 11): 1859-67.

Bilderback, T. R., Grigsby, R. J. and Dobrowsky, R. T. (1997) Association of p75(NTR) with caveolin and localization of neurotrophin-induced sphingomyelin hydrolysis to caveolae, *J Biol Chem* 272(16): 10922-7.

Bilderback, T. R., Gazula, V. R., Lisanti, M. P. and Dobrowsky, R. T. (1999) Caveolin interacts with Trk A and p75(NTR) and regulates neurotrophin signaling pathways, *J Biol Chem* 274(1): 257-63.

Bishop, K. M., Goudreau, G. and O'Leary, D. D. (2000) Regulation of area identity in the mammalian neocortex by Emx2 and Pax6, *Science* 288(5464): 344-9.

Bishop, K. M., Rubenstein, J. L. and O'Leary, D. D. (2002) Distinct actions of Emx1, Emx2, and Pax6 in regulating the specification of areas in the developing neocortex, *J Neurosci* 22(17): 7627-38.

Blatch, G. L. and Lässle, M. (1999) The tetratricopeptide repeat: a structural motif mediating protein-protein interactions, *Bioessays* 21(11): 932-9.

Booth, R., Wallace, G. L. and Happé, F. (2011) Connectivity and the corpus callosum in autism spectrum conditions: insights from comparison of autism and callosal agenesis, *Prog Brain Res* 189: 303-17.

Bottner, M., Krieglstein, K. and Unsicker, K. (2000) The transforming growth factor-betas: structure, signaling, and roles in nervous system development and functions, *J Neurochem* 75(6): 2227-40.

Boulware, M. I., Kordasiewicz, H. and Mermelstein, P. G. (2007) Caveolin proteins are essential for distinct effects of membrane estrogen receptors in neurons, *J Neurosci* 27(37): 9941-50.

Braganca, J., Eloranta, J. J., Bamforth, S. D., Ibbitt, J. C., Hurst, H. C. and Bhattacharya, S. (2003) Physical and functional interactions among AP-2 transcription factors, p300/CREB-binding protein, and CITED2, *J Biol Chem* 278(18): 16021-9.

Braun, J. E. and Madison, D. V. (2000) A novel SNAP25-caveolin complex correlates with the onset of persistent synaptic potentiation, *J Neurosci* 20(16): 5997-6006.

Brill, M. S., Ninkovic, J., Winpenny, E., Hodge, R. D., Ozen, I., Yang, R., Lepier, A., Gascon, S., Erdelyi, F., Szabo, G. et al. (2009) Adult generation of glutamatergic olfactory bulb interneurons, *Nat Neurosci* 12(12): 1524-33.

Britanova, O., Akopov, S., Lukyanov, S., Gruss, P. and Tarabykin, V. (2005) Novel transcription factor Satb2 interacts with matrix attachment region DNA elements in a tissue-specific manner and demonstrates cell-type-dependent expression in the developing mouse CNS, *Eur J Neurosci* 21(3): 658-68.

Britanova, O., Alifragis, P., Junek, S., Jones, K., Gruss, P. and Tarabykin, V. (2006) A novel mode of tangential migration of cortical projection neurons, *Dev Biol* 298(1): 299-311.

Britanova, O., de Juan Romero, C., Cheung, A., Kwan, K. Y., Schwark, M., Gyorgy, A., Vogel, T., Akopov, S., Mitkovski, M., Agoston, D. et al. (2008) Satb2 is a postmitotic determinant for upper-layer neuron specification in the neocortex, *Neuron* 57(3): 378-92.

Brunelli, S., Innocenzi, A. and Cossu, G. (2003) Bhlhb5 is expressed in the CNS and sensory organs during mouse embryonic development, *Gene Expr Patterns* 3(6): 755-9.

Buaas, F. W., Val, P. and Swain, A. (2009) The transcription co-factor CITED2 functions during sex determination and early gonad development, *Hum Mol Genet* 18(16): 2989-3001.

Bulchand, S., Grove, E. A., Porter, F. D. and Tole, S. (2001) LIM-homeodomain gene Lhx2 regulates the formation of the cortical hem, *Mech Dev* 100(2): 165-75.

Bulchand, S., Subramanian, L. and Tole, S. (2003) Dynamic spatiotemporal expression of LIM genes and cofactors in the embryonic and postnatal cerebral cortex, *Dev Dyn* 226(3): 460-9.

Bulfone, A., Smiga, S. M., Shimamura, K., Peterson, A., Puelles, L. and Rubenstein, J. L. (1995) T-brain-1: a homolog of Brachyury whose expression defines molecularly distinct domains within the cerebral cortex, *Neuron* 15(1): 63-78.

Calegari, F., Haubensak, W., Haffner, C. and Huttner, W. B. (2005) Selective lengthening of the cell cycle in the neurogenic subpopulation of neural progenitor cells during mouse brain development, *J Neurosci* 25(28): 6533-8.

Campbell, D. B., Sutcliffe, J. S., Ebert, P. J., Militerni, R., Bravaccio, C., Trillo, S., Elia, M., Schneider, C., Melmed, R., Sacco, R. et al. (2006) A genetic variant that disrupts MET transcription is associated with autism, *Proc Natl Acad Sci USA* 103(45): 16834-9.

Caric, D., Gooday, D., Hill, R. E., McConnell, S. K. and Price, D. J. (1997) Determination of the migratory capacity of embryonic cortical cells lacking the transcription factor Pax-6, *Development* 124(24): 5087-96.

Catapano, L. A., Arnold, M. W., Perez, F. A. and Macklis, J. D. (2001) Specific neurotrophic factors support the survival of cortical projection neurons at distinct stages of development, *J Neurosci* 21(22): 8863-72.

Catapano, L. A., Arlotta, P., Cage, T. A. and Macklis, J. D. (2004) Stage-specific and opposing roles of BDNF, NT-3 and bFGF in differentiation of purified callosal projection neurons toward cellular repair of complex circuitry, *Eur J Neurosci* 19(9): 2421-34.

Cauller, L. J., Clancy, B. and Connors, B. W. (1998) Backward cortical projections to primary somatosensory cortex in rats extend long horizontal axons in layer I, *J Comp Neurol* 390(2): 297-310.

Caviness, V. S. and Takahashi, T. (1995) Proliferative events in the cerebral ventricular zone, *Brain Dev* 17(3): 159-63.

Charvet, C. J., Owerkowicz, T. and Striedter, G. F. (2009) Phylogeny of the telencephalic subventricular zone in sauropsids: evidence for the sequential evolution of pallial and subpallial subventricular zones, *Brain Behav Evol* 73(4): 285-94.

Chen, B., Schaevitz, L. R. and McConnell, S. K. (2005a) Fezl regulates the differentiation and axon targeting of layer 5 subcortical projection neurons in cerebral cortex, *Proc Natl Acad Sci USA* 102(47): 17184-9.

Chen, B., Wang, S. S., Hattox, A. M., Rayburn, H., Nelson, S. B. and McConnell, S. K. (2008a) The Fezf2-Ctip2 genetic pathway regulates the fate choice of subcortical projection neurons in the developing cerebral cortex, *Proc Natl Acad Sci U S A* 105(32): 11382-7.

Chen, J., Magavi, S. S. and Macklis, J. D. (2004) Neurogenesis of corticospinal motor neurons extending spinal projections in adult mice, *Proc Natl Acad Sci U S A*.

Chen, J.-G., Rasin, M.-R., Kwan, K. Y. and Sestan, N. (2005b) Zfp312 is required for subcortical axonal projections and dendritic morphology of deep-layer pyramidal neurons of the cerebral cortex, *Proc Natl Acad Sci USA* 102(49): 17792-7.

Chen, L., Liao, G., Waclaw, R. R., Burns, K. A., Linquist, D., Campbell, K., Zheng, Y. and Kuan, C. Y. (2007) Rac1 controls the formation of midline commissures and the competency of tangential migration in ventral telencephalic neurons, *J Neurosci* 27(14): 3884-93.

Chen, Q., Zhu, Y. C., Yu, J., Miao, S., Zheng, J., Xu, L., Zhou, Y., Li, D., Zhang, C., Tao, J. et al. (2010) CDKL5, a protein associated with rett syndrome, regulates neuronal morphogenesis via Rac1 signaling, *J Neurosci* 30(38): 12777-86.

Chen, Y., Doughman, Y.-Q., Gu, S., Jarrell, A., Aota, S.-I., Cvekl, A., Watanabe, M., Dunwoodie, S. L., Johnson, R. S., Van Heyningen, V. et al. (2008b) Cited2 is required for the proper formation of the hyaloid vasculature and for lens morphogenesis, *Development* 135(17): 2939-2948.

Chenn, A. and McConnell, S. K. (1995) Cleavage orientation and the asymmetric inheritance of Notch1 immunoreactivity in mammalian neurogenesis, *Cell* 82(4): 631-41.

Chenn, A., Levin, M. E. and McConnell, S. K. (2001) Temporally and spatially regulated expression of a candidate G-protein-coupled receptor during cerebral cortical development, *J Neurobiol* 46(3): 167-77.

Cheung, A. F., Pollen, A. A., Tavare, A., DeProto, J. and Molnar, Z. (2007) Comparative aspects of cortical neurogenesis in vertebrates, *J Anat* 211(2): 164-76.

Chou, S.-J., Perez-Garcia, C. G., Kroll, T. T. and O'Leary, D. D. M. (2009) Lhx2 specifies regional fate in Emx1 lineage of telencephalic progenitors generating cerebral cortex, *Nat Neurosci*: 1-10.

Chou, Y.-T. and Yang, Y.-C. (2006a) Post-transcriptional control of Cited2 by transforming growth factor beta. Regulation via Smads and Cited2 coding region, *J Biol Chem* 281(27): 18451-62.

Chou, Y. T. (2006) Cited2, an Autoregulated Transcriptional Modulator, in TGF-beta Signaling, *Case Western Reserve University Dissertation*.

Chou, Y. T. and Yang, Y. C. (2006b) Post-transcriptional control of Cited2 by transforming growth factor beta. Regulation via Smads and Cited2 coding region, *J Biol Chem* 281(27): 18451-62.

Chou, Y. T., Hsieh, C. H., Chiou, S. H., Hsu, C. F., Kao, Y. R., Lee, C. C., Chung, C. H., Wang, Y. H., Hsu, H. S., Pang, S. T. et al. (2012) CITED2 functions as a molecular switch of cytokine-induced proliferation and quiescence, *Cell death and differentiation*.

Cimino, G. (1999) Reticular theory versus neuron theory in the work of Camillo Golgi, *Physis; rivista internazionale di storia della scienza* 36(2): 431-72.

Conti, F. and Manzoni, T. (1994) The neurotransmitters and postsynaptic actions of callosally projecting neurons, *Behav Brain Res* 64(1-2): 37-53.

Courchesne, E. and Pierce, K. (2005) Why the frontal cortex in autism might be talking only to itself: local over-connectivity but long-distance disconnection, *Curr Opin Neurobiol* 15(2): 225-30.

Cowan, C. M., Thai, J., Krajewski, S., Reed, J. C., Nicholson, D. W., Kaufmann, S. H. and Roskams, A. J. (2001) Caspases 3 and 9 send a pro-apoptotic signal from synapse to cell body in olfactory receptor neurons, *J Neurosci* 21(18): 7099-109.

Cubelos, B., Sebastian-Serrano, A., Kim, S., Moreno-Ortiz, C., Redondo, J., Walsh, C. and Nieto, M. (2007) Cux-2 Controls the Proliferation of Neuronal Intermediate Precursors of the Cortical Subventricular Zone, *Cereb Cortex* 18(8): 1758-1770.

Cubelos, B., Sebastian-Serrano, A., Beccari, L., Calcagnotto, M. E., Cisneros, E., Kim, S., Dopazo, A., Alvarez-Dolado, M., Redondo, J. M., Bovolenta, P. et al. (2010) Cux1 and Cux2 Regulate Dendritic Branching, Spine Morphology, and Synapses of the Upper Layer Neurons of the Cortex, *Neuron* 66(4): 523-535.

Cullen, B. R. (2005) RNAi the natural way, *Nat Genet* 37(11): 1163-5.

Cusick, C. G. and Lund, R. D. (1981) The distribution of the callosal projection to the occipital visual cortex in rats and mice, *Brain Research* 214(2): 239-59.

Darki, F., Peyrard-Janvid, M., Matsson, H., Kere, J. and Klingberg, T. (2012) Three Dyslexia Susceptibility Genes, DYX1C1, DCDC2, and KIAA0319, Affect Temporo-Parietal White Matter Structure, *Biol Psychiat*.

de Felipe, P., Martin, V., Cortes, M. L., Ryan, M. and Izquierdo, M. (1999) Use of the 2A sequence from foot-and-mouth disease virus in the generation of retroviral vectors for gene therapy, *Gene therapy* 6(2): 198-208.

de Sousa, A. A. W., B.A. (2007) The hominin fossil record and the emergence of the modern human central nervous system. in J. H. K. T.M. Preuss (ed.) *The Evolution of Primate Nervous Systems*, vol. 4. Oxford: Academic Press.

DeFelipe, J. (2010) *Cajal's Butterflies of the Soul: Science and Art*, New York: Oxford University Press.

Dehay, C. and Kennedy, H. (2007) Cell-cycle control and cortical development, *Nat Rev Neurosci* 8(6): 438-50.

Della-Morte, D., Beecham, A., Rundek, T., Wang, L., McClendon, M. S., Slifer, S., Blanton, S. H., Di Tullio, M. R. and Sacco, R. L. (2011) A follow-up study for left ventricular mass on chromosome 12p11 identifies potential candidate genes, *BMC medical genetics* 12: 100.

Desai, A. R. and McConnell, S. K. (2000) Progressive restriction in fate potential by neural progenitors during cerebral cortical development, *Development* 127(13): 2863-72.

Dinstein, I., Pierce, K., Eyler, L., Solso, S., Malach, R., Behrmann, M. and Courchesne, E. (2011) Disrupted neural synchronization in toddlers with autism, *Neuron* 70(6): 1218-25.

Donahoo, A. L. S. and Richards, L. J. (2009) Understanding the Mechanisms of Callosal Development Through the Use of Transgenic Mouse Models, *YSPEN* 16(3): 127-142.

Donoghue, M. J. and Rakic, P. (1999a) Molecular evidence for the early specification of presumptive functional domains in the embryonic primate cerebral cortex, *J Neurosci* 19(14): 5967-79.

Donoghue, M. J. and Rakic, P. (1999b) Molecular gradients and compartments in the embryonic primate cerebral cortex, *Cereb Cortex* 9(6): 586-600.

Dou, C. L., Li, S. and Lai, E. (1999) Dual role of brain factor-1 in regulating growth and patterning of the cerebral hemispheres, *Cereb Cortex* 9(6): 543-50.

Dugas, J., Mandemakers, W., Rogers, M., Ibrahim, A., Daneman, R. and Barres, B. (2008) A Novel Purification Method for CNS Projection Neurons Leads to the Identification of Brain Vascular Cells as a Source of Trophic Support for Corticospinal Motor Neurons, *Journal of Neuroscience* 28(33): 8294-8305.

Dupree, P., Parton, R. G., Raposo, G., Kurzchalia, T. V. and Simons, K. (1993) Caveolae and sorting in the trans-Golgi network of epithelial cells, *The EMBO journal* 12(4): 1597-605.

Egaas, B., Courchesne, E. and Saitoh, O. (1995) Reduced size of corpus callosum in autism, *Arch Neurol* 52(8): 794-801.

Elberger, A. J. (1994) Transitory corpus callosum axons projecting throughout developing rat visual cortex revealed by DiI, *Cereb Cortex* 4(3): 279-99.

Ellgaard, L., Molinari, M. and Helenius, A. (1999) Setting the standards: quality control in the secretory pathway, *Science* 286(5446): 1882-8.

Englund, C., Fink, A., Lau, C., Pham, D., Daza, R. A., Bulfone, A., Kowalczyk, T. and Hevner, R. F. (2005) Pax6, Tbr2, and Tbr1 are expressed sequentially by radial glia, intermediate progenitor cells, and postmitotic neurons in developing neocortex, *J Neurosci* 25(1): 247-51.

Estivill-Torrus, G., Pearson, H., van Heyningen, V., Price, D. J. and Rashbass, P. (2002) Pax6 is required to regulate the cell cycle and the rate of progression from symmetrical to asymmetrical division in mammalian cortical progenitors, *Development* 129(2): 455-66.

Fame, R. M., MacDonald, J. L. and Macklis, J. D. (2011) Development, specification, and diversity of callosal projection neurons, *Trends Neurosci* 34(1): 41-50.

Fazeli, A., Dickinson, S. L., Hermiston, M. L., Tighe, R. V., Steen, R. G., Small, C. G., Stoeckli, E. T., Keino-Masu, K., Masu, M., Rayburn, H. et al. (1997) Phenotype of mice lacking functional Deleted in colorectal cancer (Dcc) gene, *Nature* 386(6627): 796-804.

Ferland, R. J., Cherry, T. J., Preware, P. O., Morrisey, E. E. and Walsh, C. A. (2003) Characterization of Foxp2 and Foxp1 mRNA and protein in the developing and mature brain, *J Comp Neurol* 460(2): 266-79.

Fietz, S. A., Kelava, I., Vogt, J., Wilsch-Brauninger, M., Stenzel, D., Fish, J. L., Corbeil, D., Riehn, A., Distler, W., Nitsch, R. et al. (2010) OSVZ progenitors of human and ferret neocortex are epithelial-like and expand by integrin signaling, *Nat Neurosci* 13(6): 690-9.

Finlay, B. L. and Darlington, R. B. (1995) Linked regularities in the development and evolution of mammalian brains, *Science* 268(5217): 1578-84.

Fode, C., Ma, Q., Casarosa, S., Ang, S. L., Anderson, D. J. and Guillemot, F. (2000) A role for neural determination genes in specifying the dorsoventral identity of telencephalic neurons, *Genes Dev* 14(1): 67-80.

Franco, S.J., Gil-Sanz, C., Martinez-Garay, I., Espinosa, A., Harkins-Perry S.R., Ramos, C., Müller, U. (2012) Fate-restricted neural progenitros in the mammalian cerebral cortex, *Science* 337(6095): 746-9.

Frantz, G. D., Bohner, A. P., Akers, R. M. and McConnell, S. K. (1994a) Regulation of the POU domain gene SCIP during cerebral cortical development, *J Neurosci* 14(2): 472-85.

Frantz, G. D., Weimann, J. M., Levin, M. E. and McConnell, S. K. (1994b) Otx1 and Otx2 define layers and regions in developing cerebral cortex and cerebellum, *J Neurosci* 14(10): 5725-40.

Frantz, G. D. and McConnell, S. K. (1996) Restriction of late cerebral cortical progenitors to an upper-layer fate, *Neuron* 17(1): 55-61.

Frazier, T. W. and Hardan, A. Y. (2009) A Meta-Analysis of the Corpus Callosum in Autism, *Biol Psychiatry* 66(10): 935-941.

Freitag, C. M., Luders, E., Hulst, H. E., Narr, K. L., Thompson, P. M., Toga, A. W., Krick, C. and Konrad, C. (2009) Total brain volume and corpus callosum size in medication-naïve adolescents and young adults with autism spectrum disorder, *Biol Psychiatry* 66(4): 316-9.

Fukumitsu, H., Ohtsuka, M., Murai, R., Nakamura, H., Itoh, K. and Furukawa, S. (2006) Brain-derived neurotrophic factor participates in determination of neuronal laminar fate in the developing mouse cerebral cortex, *J Neurosci* 26(51): 13218-30.

Gage, F. H., Coates, P. W., Palmer, T. D., Kuhn, H. G., Fisher, L. J., Suhonen, J. O., Peterson, D. A., Suhr, S. T. and Ray, J. (1995) Survival and differentiation of adult neuronal progenitor cells transplanted to the adult brain, *Proc Natl Acad Sci U S A* 92(25): 11879-83.

Gaillard, S., Bartoli, M., Castets, F. and Monaghan, A. P. (2001a) Striatin, a calmodulin-dependent scaffolding protein, directly binds caveolin-1, *FEBS Letters*.

Gaillard, S., Bartoli, M., Castets, F. and Monneron, A. (2001b) Striatin, a calmodulin-dependent scaffolding protein, directly binds caveolin-1, *FEBS Lett* 508(1): 49-52.

Gal, J. S., Morozov, Y. M., Ayoub, A. E., Chatterjee, M., Rakic, P. and Haydar, T. F. (2006) Molecular and morphological heterogeneity of neural precursors in the mouse neocortical proliferative zones, *J Neurosci* 26(3): 1045-56.

Galazo, M. J., Martinez-Cerdeño, V., Porrero, C. and Clascá, F. (2008) Embryonic and postnatal development of the layer I-directed ("matrix") thalamocortical system in the rat, *Cereb Cortex* 18(2): 344-63.

Gao, W. J. and Zheng, Z. H. (2004) Target-specific differences in somatodendritic morphology of layer V pyramidal neurons in rat motor cortex, *J Comp Neurol* 476(2): 174-85.

Garcez, P. P., Henrique, N. P., Furtado, D. A., Bolz, J., Lent, R. and Uziel, D. (2007) Axons of callosal neurons bifurcate transiently at the white matter before consolidating an interhemispheric projection, *Eur J Neurosci* 25(5): 1384-94.

Geschwind, D. H. and Levitt, P. (2007) Autism spectrum disorders: developmental disconnection syndromes, *Curr Opin Neurobiol* 17(1): 103-11.

Glenn, D. J. and Maurer, R. A. (1999) MRG1 binds to the LIM domain of Lhx2 and may function as a coactivator to stimulate glycoprotein hormone alpha-subunit gene expression, *J Biol Chem* 274(51): 36159-67.

Gong, S., Zheng, C., Doughty, M. L., Losos, K., Didkovsky, N., Schambra, U. B., Nowak, N. J., Joyner, A., Leblanc, G., Hatten, M. E. et al. (2003) A gene expression atlas of the central nervous system based on bacterial artificial chromosomes, *Nature* 425(6961): 917-25.

Gong, S., Doughty, M., Harbaugh, C. R., Cummins, A., Hatten, M. E., Heintz, N. and Gerfen, C. R. (2007) Targeting Cre recombinase to specific neuron populations with bacterial artificial chromosome constructs, *J Neurosci* 27(37): 9817-23.

Gonzalez, Y. R., Zhang, Y., Behzadpoor, D., Cregan, S., Bamforth, S., Slack, R. S. and Park, D. S. (2008) CITED2 signals through peroxisome proliferator-activated receptor-gamma to regulate death of cortical neurons after DNA damage, *J Neurosci* 28(21): 5559-69.

Gorski, J. A., Talley, T., Qiu, M., Puelles, L., Rubenstein, J. L. and Jones, K. R. (2002a) Cortical excitatory neurons and glia, but not GABAergic neurons, are produced in the Emx1-expressing lineage, *J Neurosci* 22(15): 6309-14.

Gorski, J. A., Talley, T., Qiu, M., Puelles, L., Rubenstein, J. L. R. and Jones, K. R. (2002b) Cortical excitatory neurons and glia, but not GABAergic neurons, are produced in the Emx1-expressing lineage, *J Neurosci* 22(15): 6309-14.

Gotz, M. and Huttner, W. B. (2005) The cell biology of neurogenesis, *Nat Rev Mol Cell Biol* 6(10): 777-88.

Gray, P. A., Fu, H., Luo, P., Zhao, Q., Yu, J., Ferrari, A., Tenzen, T., Yuk, D. I., Tsung, E. F., Cai, Z. et al. (2004) Mouse brain organization revealed through direct genome-scale TF expression analysis, *Science* 306(5705): 2255-7.

Gu, C., Rodriguez, E. R., Reimert, D. V., Shu, T., Fritzsch, B., Richards, L. J., Kolodkin, A. L. and Ginty, D. D. (2003) Neuropilin-1 conveys semaphorin and VEGF signaling during neural and cardiovascular development, *Dev Cell* 5(1): 45-57.

Guillemot, F., Molnar, Z., Tarabykin, V. and Stoykova, A. (2006) Molecular mechanisms of cortical differentiation, *Eur J Neurosci* 23(4): 857-68.

Guo, H., Hong, S., Jin, X. L., Chen, R. S., Avasthi, P. P., Tu, Y. T., Ivanco, T. L. and Li, Y. (2000) Specificity and efficiency of Cre-mediated recombination in Emx1-Cre knock-in mice, *Biochem Biophys Res Commun* 273(2): 661-5.

Gyorgy, A. B., Szemes, M., de Juan Romero, C., Tarabykin, V. and Agoston, D. V. (2008) SATB2 interacts with chromatin-remodeling molecules in differentiating cortical neurons, *Eur J Neurosci* 27(4): 865-73.

Hack, M. A., Sugimori, M., Lundberg, C., Nakafuku, M. and Gotz, M. (2004) Regionalization and fate specification in neurospheres: the role of Olig2 and Pax6, *Mol Cell Neurosci* 25(4): 664-78.

Hamasaki, T., Leingartner, A., Ringstedt, T. and O'Leary, D. D. (2004) EMX2 regulates sizes and positioning of the primary sensory and motor areas in neocortex by direct specification of cortical progenitors, *Neuron* 43(3): 359-72.

Hanashima, C., Li, S. C., Shen, L., Lai, E. and Fishell, G. (2004) Foxg1 suppresses early cortical cell fate, *Science* 303(5654): 56-9.

Hansen, D. V., Lui, J. H., Parker, P. R. and Kriegstein, A. R. (2010) Neurogenic radial glia in the outer subventricular zone of human neocortex, *Nature* 464(7288): 554-561.

Hardan, A. Y., Pabalan, M., Gupta, N., Bansal, R., Melhem, N. M., Fedorov, S., Keshavan, M. S. and Minshew, N. J. (2009) Corpus callosum volume in children with autism, *Psychiatry Res* 174(1): 57-61.

Harel, N. Y. and Strittmatter, S. M. (2006) Can regenerating axons recapitulate developmental guidance during recovery from spinal cord injury?, *Nat Rev Neurosci* 7(8): 603-16.

Harrison-Uy, S. J. and Pleasure, S. J. (2012) Wnt signaling and forebrain development, *Cold Spring Harb Perspect Biol* 4(7).

Hartfuss, E., Galli, R., Heins, N. and Gotz, M. (2001) Characterization of CNS precursor subtypes and radial glia, *Dev Biol* 229(1): 15-30.

Hattox, A. M. and Nelson, S. B. (2007) Layer V neurons in mouse cortex projecting to different targets have distinct physiological properties, *J Neurophysiol*.

Haubensak, W., Attardo, A., Denk, W. and Huttner, W. B. (2004) Neurons arise in the basal neuroepithelium of the early mammalian telencephalon: a major site of neurogenesis, *Proc Natl Acad Sci USA* 101(9): 3196-201.

He, Q., Duan, Y., Karsch, K. and Miles, J. (2010) Detecting corpus callosum abnormalities in autism based on anatomical landmarks, *Psychiatry Res* 183(2): 126-32.

Head, B. P. and Insel, P. A. (2007) Do caveolins regulate cells by actions outside of caveolae?, *Trends Cell Biol* 17(2): 51-7.

Heins, N., Malatesta, P., Cecconi, F., Nakafuku, M., Tucker, K. L., Hack, M. A., Chapouton, P., Barde, Y. A. and Gotz, M. (2002) Glial cells generate neurons: the role of the transcription factor Pax6, *Nat Neurosci* 5(4): 308-15.

Heintz, N. (2004) Gene expression nervous system atlas (GENSAT), *Nat Neurosci* 7(5): 483.

Herbert, M. R. and Kenet, T. (2007) Brain abnormalities in language disorders and in autism, *Pediatr Clin North Am* 54(3): 563-83, vii.

Heuer, H., Christ, S., Friedrichsen, S., Brauer, D., Winckler, M., Bauer, K. and Raivich, G. (2003) Connective tissue growth factor: a novel marker of layer VII neurons in the rat cerebral cortex, *Neuroscience* 119(1): 43-52.

Hevner, R. F., Shi, L., Justice, N., Hsueh, Y., Sheng, M., Smiga, S., Bulfone, A., Goffinet, A. M., Campagnoni, A. T. and Rubenstein, J. L. (2001) Tbr1 regulates differentiation of the preplate and layer 6, *Neuron* 29(2): 353-66.

Hevner, R. F., Daza, R. A., Rubenstein, J. L., Stunnenberg, H., Olavarria, J. F. and Englund, C. (2003) Beyond laminar fate: toward a molecular classification of cortical projection/pyramidal neurons, *Dev Neurosci* 25(2-4): 139-51.

Hinds, J. W. and Ruffett, T. L. (1971) Cell proliferation in the neural tube: an electron microscopic and golgi analysis in the mouse cerebral vesicle, *Z Zellforsch Mikrosk Anat* 115(2): 226-64.

Hirata, T., Suda, Y., Nakao, K., Narimatsu, M., Hirano, T. and Hibi, M. (2004) Zinc finger gene fez-like functions in the formation of subplate neurons and thalamocortical axons, *Dev Dyn* 230(3): 546-56.

Hlushchuk, Y. and Hari, R. (2006) Transient suppression of ipsilateral primary somatosensory cortex during tactile finger stimulation, *J Neurosci* 26(21): 5819-24.

Hnasko, R. and Lisanti, M. P. (2003) The biology of caveolae: lessons from caveolin knockout mice and implications for human disease, *Mol Interv* 3(8): 445-64.

Hoerder-Suabedissen, A., Paulsen, O. and Molnar, Z. (2008) Thalamocortical maturation in mice is influenced by body weight, *J Comp Neurol* 511(3): 415-20.

Hoerder-Suabedissen, A., Wang, W. Z., Lee, S., Davies, K. E., Goffinet, A. M., Rakic, S., Parnavelas, J., Reim, K., Nicolic, M., Paulsen, O. et al. (2009) Novel markers reveal subpopulations of subplate neurons in the murine cerebral cortex, *Cereb Cortex* 19(8): 1738-50.

Hu, Z., Yue, X., Shi, G., Yue, Y., Crockett, D. P., Blair-Flynn, J., Reuhl, K., Tessarollo, L. and Zhou, R. (2003) Corpus callosum deficiency in transgenic mice expressing a truncated ephrin-A receptor, *J Neurosci* 23(34): 10963-70.

Huang, Z., Kawase-Koga, Y., Zhang, S., Visvader, J., Toth, M., Walsh, C. A. and Sun, T. (2009) Transcription factor Lmo4 defines the shape of functional areas in developing cortices and regulates sensorimotor control, *Dev Biol* 327(1): 132-42.

Innocenti, G. M., Fiore, L. and Caminiti, R. (1977) Exuberant projection into the corpus callosum from the visual cortex of newborn cats, *Neurosci Lett* 4(5): 237-42.

Innocenti, G. M., Ansermet, F. and Parnas, J. (2003) Schizophrenia, neurodevelopment and corpus callosum, *Mol Psychiatry* 8(3): 261-74.

Innocenti, G. M. and Price, D. J. (2005) Exuberance in the development of cortical networks, *Nat Rev Neurosci* 6(12): 955-65.

Inoue, K., Terashima, T., Nishikawa, T. and Takumi, T. (2004) Fez1 is layer-specifically expressed in the adult mouse neocortex, *Eur J Neurosci* 20(11): 2909-16.

Ip, B. K., Bayatti, N., Howard, N. J., Lindsay, S. and Clowry, G. J. (2011) The corticofugal neuron-associated genes ROBO1, SRGAP1, and CTIP2 exhibit an anterior to posterior gradient of expression in early fetal human neocortex development, *Cereb Cortex* 21(6): 1395-407.

Irizarry, R. A., Hobbs, B., Collin, F., Beazer-Barclay, Y. D., Antonellis, K. J., Scherf, U. and Speed, T. P. (2003) Exploration, normalization, and summaries of high density oligonucleotide array probe level data, *Biostatistics* 4(2): 249-64.

Isshiki, T., Pearson, B., Holbrook, S. and Doe, C. Q. (2001) Drosophila neuroblasts sequentially express transcription factors which specify the temporal identity of their neuronal progeny, *Cell* 106(4): 511-21.

Jabaudon, D., Shnider, S. J., Tischfield, D. J., Galazo, M. J. and Macklis, J. D. (2012) RORbeta induces barrel-like neuronal clusters in the developing neocortex, *Cereb Cortex* 22(5): 996-1006.

Jessell, T. M. (2000) Neuronal specification in the spinal cord: inductive signals and transcriptional codes, *Nat Rev Genet* 1(1): 20-9.

Jin, X. L., Guo, H., Mao, C., Atkins, N., Wang, H., Avasthi, P. P., Tu, Y. T. and Li, Y. (2000) Emx1-specific expression of foreign genes using "knock-in" approach, *Biochem Biophys Res Commun* 270(3): 978-82.

Jinnai, K. and Matsuda, Y. (1979) Neurons of the motor cortex projecting commonly on the caudate nucleus and the lower brain stem in the cat, *Neuroscience letters* 13(2): 121-6.

Johnson, M. B., Kawasawa, Y. I., Mason, C. E., Krsnik, Z., Coppola, G., Bogdanovic, D., Geschwind, D. H., Mane, S. M., State, M. W. and Sestan, N. (2009) Functional and evolutionary insights into human brain development through global transcriptome analysis, *Neuron* 62(4): 494-509.

Jones, E. G. and Wise, S. P. (1977) Size, laminar and columnar distribution of efferent cells in the sensory-motor cortex of monkeys, *J Comp Neurol* 175(4): 391-438.

Joshi, B., Strugnell, S. S., Goetz, J. G., Kojic, L. D., Cox, M. E., Griffith, O. L., Chan, S. K., Jones, S. J., Leung, S.-P., Masoudi, H. et al. (2008a) Phosphorylated caveolin-1 regulates Rho/ROCK-dependent focal adhesion dynamics and tumor cell migration and invasion, *Cancer Res* 68(20): 8210-20.

Joshi, P. S., Molyneaux, B. J., Feng, L., Xie, X., Macklis, J. D. and Gan, L. (2008b) Bhlhb5 regulates the postmitotic acquisition of area identities in layers II-V of the developing neocortex, *Neuron* 60(2): 258-72.

Kachi, S., Yamazaki, A. and Usukura, J. (2001) Localization of caveolin-1 in photoreceptor synaptic ribbons, *Invest Ophthalmol Vis Sci* 42(3): 850-2.

Kang, M.-J., Seo, J.-S. and Park, W.-Y. (2006) Caveolin-1 inhibits neurite growth by blocking Rac1/Cdc42 and p21-activated kinase 1 interactions, *Neuroreport* 17(8): 823-7.

Kashani, A. H., Qiu, Z., Jurata, L., Lee, S. K., Pfaff, S., Goebbels, S., Nave, K. A. and Ghosh, A. (2006) Calcium activation of the LMO4 transcription complex and its role in the patterning of thalamocortical connections, *J Neurosci* 26(32): 8398-408.

Kassai, H., Terashima, T., Fukaya, M., Nakao, K., Sakahara, M., Watanabe, M. and Aiba, A. (2008) Rac1 in cortical projection neurons is selectively required for midline crossing of commissural axonal formation, *Eur J Neurosci* 28(2): 257-267.

Kater, S. B. and Mills, L. R. (1991) Regulation of growth cone behavior by calcium, *J Neurosci* 11(4): 891-9.

Kaufman, J. A., Paul, L. K., Manaye, K. F., Granstedt, A. E., Hof, P. R., Hakeem, A. Y. and Allman, J. M. (2008) Selective reduction of Von Economo neuron number in agenesis of the corpus callosum, *Acta Neuropathol* 116(5): 479-489.

Kawaguchi, A., Ikawa, T., Kasukawa, T., Ueda, H. R., Kurimoto, K., Saitou, M. and Matsuzaki, F. (2008) Single-cell gene profiling defines differential progenitor subclasses in mammalian neurogenesis, *Development* 135(18): 3113-24.

Keeble, T. R., Halford, M. M., Seaman, C., Kee, N., Macheda, M., Anderson, R. B., Stacker, S. A. and Cooper, H. M. (2006) The Wnt receptor Ryk is required for Wnt5a-mediated axon guidance on the contralateral side of the corpus callosum, *J Neurosci* 26(21): 5840-8.

Killackey, H. P., Gould, H. J., 3rd, Cusick, C. G., Pons, T. P. and Kaas, J. H. (1983) The relation of corpus callosum connections to architectonic fields and body surface maps in sensorimotor cortex of new and old world monkeys, *J Comp Neurol* 219(4): 384-419.

Killackey, H. P., Koralek, K. A., Chiaia, N. L. and Rhodes, R. W. (1989) Laminar and areal differences in the origin of the subcortical projection neurons of the rat somatosensory cortex, *J Comp Neurol* 282(3): 428-45.

Koester, S. E. and O'Leary, D. D. (1992) Functional classes of cortical projection neurons develop dendritic distinctions by class-specific sculpting of an early common pattern, *J Neurosci* 12(4): 1382-93.

Koester, S. E. and O'Leary, D. D. (1994) Axons of early generated neurons in cingulate cortex pioneer the corpus callosum, *J Neurosci* 14(11 Pt 1): 6608-20.

Koralek, K. A. and Killackey, H. P. (1990) Callosal projections in rat somatosensory cortex are altered by early removal of afferent input, *Proc Natl Acad Sci U S A* 87(4): 1396-400.

Koralek, K. A., Olavarria, J. and Killackey, H. P. (1990) Areal and laminar organization of corticocortical projections in the rat somatosensory cortex, *J Comp Neurol* 299(2): 133-50.

Kowalczyk, T., Pontious, A., Englund, C., Daza, R. A., Bedogni, F., Hodge, R., Attardo, A., Bell, C., Huttner, W. B. and Hevner, R. F. (2009) Intermediate neuronal progenitors (basal progenitors) produce pyramidal-projection neurons for all layers of cerebral cortex, *Cereb Cortex* 19(10): 2439-50.

Kriegstein, A. and Parnavelas, J. G. (2003) Changing concepts of cortical development, *Cereb Cortex* 13(6): 541.

Kriegstein, A., Noctor, S. and Martinez-Cerdeno, V. (2006) Patterns of neural stem and progenitor cell division may underlie evolutionary cortical expansion, *Nat Rev Neurosci* 7(11): 883-90.

Kroll, T. T. and O'Leary, D. D. (2005) Ventralized dorsal telencephalic progenitors in Pax6 mutant mice generate GABA interneurons of a lateral ganglionic eminence fate, *Proc Natl Acad Sci U S A* 102(20): 7374-9.

Kwan, K. Y., Lam, M. M. S., Krsnik, Z., Kawasawa, Y. I., Lefebvre, V. and Sestan, N. (2008) SOX5 postmitotically regulates migration, postmigratory differentiation, and projections of subplate and deep-layer neocortical neurons, *Proc Natl Acad Sci USA* 105(41): 16021-6.

Lai, H., Boone, T., Yang, G., Smith, C., Kiss, S. and al., e. (2004) Loss of caveolin-1 expression is associated with disruption of muscarinic cholinergic activities in the urinary bladder, *Neurochem Int*.

Lai, T., Jabaudon, D., Molyneaux, B. J., Azim, E., Arlotta, P., Menezes, J. R. and Macklis, J. D. (2008) SOX5 Controls the Sequential Generation of Distinct Corticofugal Neuron Subtypes, *Neuron* 57(2): 232-247.

Land, P. W. and Monaghan, A. P. (2003) Expression of the transcription factor, tailless, is required for formation of superficial cortical layers, *Cereb Cortex* 13(9): 921-31.

Lanier, L. M., Gates, M. A., Witke, W., Menzies, A. S., Wehman, A. M., Macklis, J. D., Kwiatkowski, D., Soriano, P. and Gertler, F. B. (1999) Mena is required for neurulation and commissure formation, *Neuron* 22(2): 313-25.

Lee, J. and Glover, K. J. (2012) The transmembrane domain of caveolin-1 exhibits a helix-break-helix structure, *Biochimica et biophysica acta*.

Legg, C. R., Mercier, B. and Glickstein, M. (1989) Corticopontine projection in the rat: the distribution of labelled cortical cells after large injections of horseradish peroxidase in the pontine nuclei, *J Comp Neurol* 286(4): 427-41.

Lein, E. Hawrylycz, M. Ao, N. Ayres, M. Bensinger, A. Bernard, A. Boe, A. Boguski, M. Brockway, K. Byrnes, E. et al. (2007) Genome-wide atlas of gene expression in the adult mouse brain, *Nature* 445(7124): 168-176.

Leone, D., Srinivasan, K., Chen, B., Alcamo, E. and McConnell, S. (2008) The determination of projection neuron identity in the developing cerebral cortex, *Curr Opin Neurobiol*.

Li, J., Strominger, Z., Wakahiro, M. and Sherr, E. H. (2008) 'A novel gene TMTC4 in a female with absence of the corpus callosum, mental retardation and a balanced translocation between chromosomes t (1; 13)(p32; q32)', given at a conference 'Society for Neuroscience Conference', Washington, D.C.

Li, L., Hutchins, B. I. and Kalil, K. (2009) Wnt5a Induces Simultaneous Cortical Axon Outgrowth and Repulsive Axon Guidance through Distinct Signaling Mechanisms, *J Neurosci* 29(18): 5873-5883.

Li, Q., Pan, H., Guan, L., Su, D. and Ma, X. (2012) CITED2 mutation links congenital heart defects to dysregulation of the cardiac gene VEGF and PITX2C expression, *Biochem Biophys Res Commun* 423(4): 895-9.

Li, Y., Luo, J., Lau, W.-M., Zheng, G., Fu, S., Wang, T.-T., Zeng, H.-P., So, K.-F., Chung, S. K., Tong, Y. et al. (2011) Caveolin-1 Plays a Crucial Role in Inhibiting Neuronal Differentiation of Neural Stem/Progenitor Cells via VEGF Signaling-Dependent Pathway, *PLoS ONE* 6(8): e22901.

Limke, T. L., Heidemann, S. R. and Atchison, W. D. (2004) Disruption of intraneuronal divalent cation regulation by methylmercury: are specific targets involved in altered neuronal development and cytotoxicity in methylmercury poisoning?, *Neurotoxicology* 25(5): 741-60.

Lindwall, C., Fothergill, T. and Richards, L. J. (2007) Commissure formation in the mammalian forebrain, *Curr Opin Neurobiol* 17(1): 3-14.

Liu, Q., Dwyer, N. D. and O'Leary, D. D. (2000) Differential expression of COUP-TFI, CHL1, and two novel genes in developing neocortex identified by differential display PCR, *J Neurosci* 20(20): 7682-90.

Liu, Y., Shi, J., Lu, C. C., Wang, Z. B., Lyuksyutova, A. I., Song, X. J. and Zou, Y. (2005) Ryk-mediated Wnt repulsion regulates posterior-directed growth of corticospinal tract, *Nat Neurosci* 8(9): 1151-9.

López-Bendito, G., Flames, N., Ma, L., Fouquet, C., Di Meglio, T., Chedotal, A., Tessier-Lavigne, M. and Marín, O. (2007) Robo1 and Robo2 cooperate to control the guidance of major axonal tracts in the mammalian forebrain, *J Neurosci* 27(13): 3395-407.

López-Muñoz, F., Boya, J. and Alamo, C. (2006) Neuron theory, the cornerstone of neuroscience, on the centenary of the Nobel Prize award to Santiago Ramon y Cajal, *Brain Res Bull* 70(4-6): 391-405.

Lukaszewicz, A., Savatier, P., Cortay, V., Kennedy, H. and Dehay, C. (2002) Contrasting effects of basic fibroblast growth factor and neurotrophin 3 on cell cycle kinetics of mouse cortical stem cells, *J Neurosci* 22(15): 6610-22.

Lund, J. S., Yoshioka, T. and Levitt, J. B. (1993) Comparison of intrinsic connectivity in different areas of macaque monkey cerebral cortex, *Cereb Cortex* 3(2): 148-62.

Ma, L., Harada, T., Harada, C., Romero, M., Hebert, J. M., McConnell, S. K. and Parada, L. F. (2002) Neurotrophin-3 is required for appropriate establishment of thalamocortical connections, *Neuron* 36(4): 623-34.

Ma, Q., Kintner, C. and Anderson, D. J. (1996) Identification of neurogenin, a vertebrate neuronal determination gene, *Cell* 87(1): 43-52.

Macdonald, J. L., Verster, A., Berndt, A. and Roskams, A. J. (2010) MBD2 and MeCP2 regulate distinct transitions in the stage-specific differentiation of olfactory receptor neurons, *Mol Cell Neurosci* 44(1): 55-67.

MacDonald, J. L., Fame, R. M., Azim, E., Shnider, S. J., Molyneaux, B. J., Arlotta, P. and Macklis, J. D. (in press) *Developmental Neuroscience: A Comprehensive Reference*: Elsevier.

Magavi, S. S., Leavitt, B. R. and Macklis, J. D. (2000) Induction of neurogenesis in the neocortex of adult mice, *Nature* 405(6789): 951-5.

Magdaleno, S., Jensen, P., Brumwell, C. L., Seal, A., Lehman, K., Asbury, A., Cheung, T., Cornelius, T., Batten, D. M., Eden, C. et al. (2006) BGEM: an in situ hybridization database of gene expression in the embryonic and adult mouse nervous system, *PLoS Biol* 4(4): e86.

Maggi, D., Biedi, C., Segat, D., Barbero, D., Panetta, D. and al., e. (2002) IGF-I induces caveolin 1 tyrosine phosphorylation and translocation in the lipid rafts, *Biochem Biophys Res Commun*.

Malatesta, P., Hartfuss, E. and Gotz, M. (2000) Isolation of radial glial cells by fluorescent-activated cell sorting reveals a neuronal lineage, *Development* 127(24): 5253-63.

Malatesta, P., Hack, M. A., Hartfuss, E., Kettenmann, H., Klinkert, W., Kirchhoff, F. and Gotz, M. (2003) Neuronal or glial progeny: regional differences in radial glia fate, *Neuron* 37(5): 751-64.

Mallamaci, A., Muzio, L., Chan, C. H., Parnavelas, J. and Boncinelli, E. (2000) Area identity shifts in the early cerebral cortex of Emx2-/- mutant mice, *Nat Neurosci* 3(7): 679-86.

Mallamaci, A. and Stoykova, A. (2006) Gene networks controlling early cerebral cortex arealization, *Eur J Neurosci* 23(4): 847-56.

Mangale, V. S., Hirokawa, K. E., Satyaki, P. R., Gokulchandran, N., Chikbire, S., Subramanian, L., Shetty, A. S., Martynoga, B., Paul, J., Mai, M. V. et al. (2008) Lhx2 selector activity specifies cortical identity and suppresses hippocampal organizer fate, *Science* 319(5861): 304-9.

Manzoni, T., Conti, F. and Fabri, M. (1986) Callosal projections from area SII to SI in monkeys: anatomical organization and comparison with association projections, *J Comp Neurol* 252(2): 245-63.

Marin, R., Díaz, M., Alonso, R., Sanz, A., Arévalo, M. A. and Garcia-Segura, L. M. (2009) Role of estrogen receptor α in membrane-initiated signaling in neural cells: Interaction with IGF-1 receptor, *J Steroid Biochem Mol Biol* 114(1-2): 2-7.

Marín-Padilla, M. (1992) Ontogenesis of the pyramidal cell of the mammalian neocortex and developmental cytoarchitectonics: a unifying theory, *J Comp Neurol* 321(2): 223-40.

Markram, H., Toledo-Rodriguez, M., Wang, Y., Gupta, A., Silberberg, G. and Wu, C. (2004) Interneurons of the neocortical inhibitory system, *Nat Rev Neurosci* 5(10): 793-807.

Martinez-Cerdeno, V., Noctor, S. C. and Kriegstein, A. R. (2006) The role of intermediate progenitor cells in the evolutionary expansion of the cerebral cortex, *Cereb Cortex* 16 Suppl 1: i152-61.

Mcalonan, G. M., Cheung, C., Cheung, V., Wong, N., Suckling, J. and Chua, S. E. (2009) Differential effects on white-matter systems in high-functioning autism and Asperger's syndrome, *Psychol. Med.* 39(11): 1885.

McConnell, S. K., Ghosh, A. and Shatz, C. J. (1989) Subplate neurons pioneer the first axon pathway from the cerebral cortex, *Science* 245(4921): 978-82.

McConnell, S. K. and Kaznowski, C. E. (1991) Cell cycle dependence of laminar determination in developing neocortex, *Science* 254(5029): 282-5.

McConnell, S. K., Ghosh, A. and Shatz, C. J. (1994) Subplate pioneers and the formation of descending connections from cerebral cortex, *J Neurosci* 14(4): 1892-907.

McEvilly, R. J., de Diaz, M. O., Schonemann, M. D., Hooshmand, F. and Rosenfeld, M. G. (2002) Transcriptional regulation of cortical neuron migration by POU domain factors, *Science* 295(5559): 1528-32.

McFarlane, H. G., Kusek, G. K., Yang, M., Phoenix, J. L., Bolivar, V. J. and Crawley, J. N. (2008) Autism-like behavioral phenotypes in BTBR T+tf/J mice, *Genes Brain Behav* 7(2): 152-63.

Mendes, S. W., Henkemeyer, M. and Liebl, D. J. (2006) Multiple Eph receptors and B-class ephrins regulate midline crossing of corpus callosum fibers in the developing mouse forebrain, *J Neurosci* 26(3): 882-92.

Michell, A. C., Bragança, J., Broadbent, C., Joyce, B., Franklyn, A., Schneider, J. E., Bhattacharya, S. and Bamforth, S. D. (2010) A novel role for transcription factor Lmo4 in thymus development through genetic interaction with Cited2, *Dev. Dyn.* 239(7): 1988-1994.

Migliore, M. and Shepherd, G. M. (2005) Opinion: an integrated approach to classifying neuronal phenotypes, *Nat Rev Neurosci* 6(10): 810-8.

Mihrshahi, R. (2006) The corpus callosum as an evolutionary innovation, *J Exp Zool B Mol Dev Evol* 306(1): 8-17.

Minshew, N. J. and Williams, D. L. (2007) The new neurobiology of autism: cortex, connectivity, and neuronal organization, *Arch Neurol* 64(7): 945-50.

Mitchell, B. D. and Macklis, J. D. (2005) Large-scale maintenance of dual projections by callosal and frontal cortical projection neurons in adult mice, *J Comp Neurol* 482(1): 17-32.

Miyata, T., Kawaguchi, A., Saito, K., Kawano, M., Muto, T. and Ogawa, M. (2004) Asymmetric production of surface-dividing and non-surface-dividing cortical progenitor cells, *Development* 131(13): 3133-45.

Mizuno, H., Hirano, T. and Tagawa, Y. (2007) Evidence for activity-dependent cortical wiring: formation of interhemispheric connections in neonatal mouse visual cortex requires projection neuron activity, *J Neurosci* 27(25): 6760-70.

Mizuno, H., Hirano, T. and Tagawa, Y. (2010) Pre-synaptic and post-synaptic neuronal activity supports the axon development of callosal projection neurons during different post-natal periods in the mouse cerebral cortex, *Eur J Neurosci* 31(3): 410-24.

Mizutani, K. and Saito, T. (2005) Progenitors resume generating neurons after temporary inhibition of neurogenesis by Notch activation in the mammalian cerebral cortex, *Development* 132(6): 1295-304.

Mo, Z., Moore, A. R., Filipovic, R., Ogawa, Y., Kazuhiro, I., Antic, S. D. and Zecevic, N. (2007) Human cortical neurons originate from radial glia and neuron-restricted progenitors, *J Neurosci* 27(15): 4132-45.

Molnár, Z. and Cheung, A. F. P. (2006) Towards the classification of subpopulations of layer V pyramidal projection neurons, *Neurosci Res* 55(2): 105-15.

Molnár, Z., Metin, C., Stoykova, A., Tarabykin, V., Price, D. J., Francis, F., Meyer, G., Dehay, C. and Kennedy, H. (2006) Comparative aspects of cerebral cortical development, *Eur J Neurosci* 23(4): 921-34.

Molyneaux, B. J., Arlotta, P., Hirata, T., Hibi, M. and Macklis, J. D. (2005) Fezl is required for the birth and specification of corticospinal motor neurons, *Neuron* 47(6): 817-31.

Molyneaux, B. J., Arlotta, P., Menezes, J. R. and Macklis, J. D. (2007) Neuronal subtype specification in the cerebral cortex, *Nat Rev Neurosci* 8(6): 427-37.

Molyneaux, B. J., Arlotta, P., Fame, R. M., MacDonald, J. L., MacQuarrie, K. L. and Macklis, J. D. (2009) Novel subtype-specific genes identify distinct subpopulations of callosal projection neurons, *J Neurosci* 29(39): 12343-54.

Monier, S., Parton, R. G., Vogel, F., Behlke, J., Henske, A. and Kurzchalia, T. V. (1995) VIP21-caveolin, a membrane protein constituent of the caveolar coat, oligomerizes in vivo and in vitro, *Molecular biology of the cell* 6(7): 911-27.

Monuki, E. S., Porter, F. D. and Walsh, C. A. (2001) Patterning of the dorsal telencephalon and cerebral cortex by a roof plate-Lhx2 pathway, *Neuron* 32(4): 591-604.

Mora, R., Bonilha, V. L., Marmorstein, A., Scherer, P. E., Brown, D., Lisanti, M. P. and Rodriguez-Boulan, E. (1999) Caveolin-2 localizes to the golgi complex but redistributes to plasma membrane, caveolae, and rafts when co-expressed with caveolin-1, *J Biol Chem* 274(36): 25708-17.

Mori, T., Wanaka, A., Taguchi, A., Matsumoto, K. and Tohyama, M. (1995) Differential expressions of the eph family of receptor tyrosine kinase genes (sek, elk, eck) in the developing nervous system of the mouse, *Mol Brain Res* 29(2): 325-35.

Morrow, T., Song, M. R. and Ghosh, A. (2001) Sequential specification of neurons and glia by developmentally regulated extracellular factors, *Development* 128(18): 3585-94.

Moy, S. S., Nadler, J. J., Young, N. B., Perez, A., Holloway, L. P., Barbaro, R. P., Barbaro, J. R., Wilson, L. M., Threadgill, D. W., Lauder, J. M. et al. (2007) Mouse behavioral tasks relevant to autism: phenotypes of 10 inbred strains, *Behavioural brain research* 176(1): 4-20.

Muzio, L., DiBenedetto, B., Stoykova, A., Boncinelli, E., Gruss, P. and Mallamaci, A. (2002) Conversion of cerebral cortex into basal ganglia in Emx2(-/-) Pax6(Sey/Sey) double-mutant mice, *Nat Neurosci* 5(8): 737-45.

Muzio, L. and Mallamaci, A. (2005) Foxg1 confines Cajal-Retzius neuronogenesis and hippocampal morphogenesis to the dorsomedial pallium, *J Neurosci* 25(17): 4435-41.

Nakagawa, Y., Johnson, J. E. and O'Leary, D. D. (1999) Graded and areal expression patterns of regulatory genes and cadherins in embryonic neocortex independent of thalamocortical input, *J Neurosci* 19(24): 10877-85.

Nakagawa, Y. and O'Leary, D. D. (2003) Dynamic patterned expression of orphan nuclear receptor genes RORalpha and RORbeta in developing mouse forebrain, *Dev Neurosci* 25(2-4): 234-44.

Nethe, M., Anthony, E. C., Fernandez-Borja, M., Dee, R., Geerts, D., Hensbergen, P. J., Deelder, A. M., Schmidt, G. and Hordijk, P. L. (2010) Focal-adhesion targeting links caveolin-1 to a Rac1-degradation pathway, *J Cell Sci* 123(11): 1948-1958.

Newbury, D. F., Bonora, E., Lamb, J. A., Fisher, S. E., Lai, C. S., Baird, G., Jannoun, L., Slonims, V., Stott, C. M., Merricks, M. J. et al. (2002) FOXP2 is not a major susceptibility gene for autism or specific language impairment, *Am J Hum Genet* 70(5): 1318-27.

Nicolelis, M. A. and Shuler, M. (2001) Thalamocortical and corticocortical interactions in the somatosensory system, *Prog Brain Res* 130: 90-110.

Nieto, M., Monuki, E. S., Tang, H., Imitola, J., Haubst, N., Khoury, S. J., Cunningham, J., Gotz, M. and Walsh, C. A. (2004) Expression of Cux-1 and Cux-2 in the subventricular zone and upper layers II-IV of the cerebral cortex, *J Comp Neurol* 479(2): 168-80.

Niquille, M., Garel, S., Mann, F., Hornung, J.-P., Otsmane, B., Chevalley, S., Parras, C., Guillemot, F., Gaspar, P., Yanagawa, Y. et al. (2009) Transient neuronal populations are required to guide callosal axons: a role for semaphorin 3C, *PLoS Biol* 7(10): e1000230.

Noctor, S. C., Flint, A. C., Weissman, T. A., Dammerman, R. S. and Kriegstein, A. R. (2001) Neurons derived from radial glial cells establish radial units in neocortex, *Nature* 409(6821): 714-20.

Noctor, S. C., Flint, A. C., Weissman, T. A., Wong, W. S., Clinton, B. K. and Kriegstein, A. R. (2002) Dividing precursor cells of the embryonic cortical ventricular zone have morphological and molecular characteristics of radial glia, *J Neurosci* 22(8): 3161-73.

Noctor, S. C., Martinez-Cerdeno, V., Ivic, L. and Kriegstein, A. R. (2004) Cortical neurons arise in symmetric and asymmetric division zones and migrate through specific phases, *Nat Neurosci* 7(2): 136-44.

Noctor, S. C., Martínez-Cerdeño, V. and Kriegstein, A. R. (2008) Distinct behaviors of neural stem and progenitor cells underlie cortical neurogenesis, *J Comp Neurol* 508(1): 28-44.

Norris, C. R. and Kalil, K. (1991) Guidance of callosal axons by radial glia in the developing cerebral cortex, *J Neurosci* 11(11): 3481-92.

Norris, C. R. and Kalil, K. (1992) Development of callosal connections in the sensorimotor cortex of the hamster, *J Comp Neurol* 326(1): 121-32.

O'Leary, D. D. and Terashima, T. (1988) Cortical axons branch to multiple subcortical targets by interstitial axon budding: implications for target recognition and "waiting periods", *Neuron* 1(10): 901-10.

O'Leary, D. D. (1992) Development of connectional diversity and specificity in the mammalian brain by the pruning of collateral projections, *Curr Opin Neurobiol* 2(1): 70-7.

O'Leary, D. D. and Koester, S. E. (1993) Development of projection neuron types, axon pathways, and patterned connections of the mammalian cortex, *Neuron* 10(6): 991-1006.

O'Leary, D. D. and Nakagawa, Y. (2002) Patterning centers, regulatory genes and extrinsic mechanisms controlling arealization of the neocortex, *Curr Opin Neurobiol* 12(1): 14-25.

O'Leary, D. D., Chou, S. J. and Sahara, S. (2007) Area patterning of the mammalian cortex, *Neuron* 56(2): 252-69.

Ozaki, H. S. and Wahlsten, D. (1998) Timing and origin of the first cortical axons to project through the corpus callosum and the subsequent emergence of callosal projection cells in mouse, *J Comp Neurol* 400(2): 197-206.

Ozdinler, P. H. and Macklis, J. D. (2006) IGF-I specifically enhances axon outgrowth of corticospinal motor neurons, *Nat Neurosci* 9(11): 1371-81.

Parker, I., Choi, J. and Yao, Y. (1996) Elementary events of InsP3-induced Ca2+ liberation in Xenopus oocytes: hot spots, puffs and blips, *Cell calcium* 20(2): 105-21.

Paul, L. K., Brown, W. S., Adolphs, R., Tyszka, J. M., Richards, L. J., Mukherjee, P. and Sherr, E. H. (2007) Agenesis of the corpus callosum: genetic, developmental and functional aspects of connectivity, *Nat Rev Neurosci* 8(4): 287-99.

Pearson, B. J. and Doe, C. Q. (2003) Regulation of neuroblast competence in Drosophila, *Nature* 425(6958): 624-8.

Penfield, W., and Boldrey, E. (1937) Somatic motor and sensory representation in the cerebral cortex of man as studied by electrical stimulation, *Brain* 60: 389-443.

Peters, A. and Jones, E. G. (1984) Cellular Components of the Cerebral Cortex *Cerebral Cortex*, vol. 1. New York: Plenum Press.

Petreanu, L., Huber, D., Sobczyk, A. and Svoboda, K. (2007) Channelrhodopsin-2-assisted circuit mapping of long-range callosal projections, *Nat Neurosci* 10(5): 663-8.

Pinto, L., Drechsel, D., Schmid, M.-T., Ninkovic, J., Irmler, M., Brill, M. S., Restani, L., Gianfranceschi, L., Cerri, C., Weber, S. N. et al. (2009) AP2γ regulates basal progenitor fate in a region- and layer-specific manner in the developing cortex, *Nat Neurosci* 12(10): 1229-1237.

Piper, M., Plachez, C., Zalucki, O., Fothergill, T., Goudreau, G., Erzurumlu, R., Gu, C. and Richards, L. J. (2009) Neuropilin 1-Sema Signaling Regulates Crossing of Cingulate Pioneering Axons during Development of the Corpus Callosum, *Cereb Cortex*: 11.

Plachez, C., Lindwall, C., Sunn, N., Piper, M., Moldrich, R. X., Campbell, C. E., Osinski, J. M., Gronostajski, R. M. and Richards, L. J. (2008) Nuclear factor I gene expression in the developing forebrain, *J Comp Neurol* 508(3): 385-401.

Polleux, F., Dehay, C., Goffinet, A. and Kennedy, H. (2001) Pre- and post-mitotic events contribute to the progressive acquisition of area-specific connectional fate in the neocortex, *Cereb Cortex* 11(11): 1027-39.

Pontious, A., Kowalczyk, T., Englund, C. and Hevner, R. F. (2008) Role of intermediate progenitor cells in cerebral cortex development, *Dev Neurosci* 30(1-3): 24-32.

Porter, F. D., Drago, J., Xu, Y., Cheema, S. S., Wassif, C., Huang, S. P., Lee, E., Grinberg, A., Massalas, J. S., Bodine, D. et al. (1997) Lhx2, a LIM homeobox gene, is required for eye, forebrain, and definitive erythrocyte development, *Development* 124(15): 2935-44.

Preis, J. I., Wise, N., Solloway, M. J., Harvey, R. P., Sparrow, D. B. and Dunwoodie, S. L. (2006) Generation of conditional Cited2 null alleles, *genesis* 44(12): 579-83.

Puzzolo, E. and Mallamaci, A. (2010) Cortico-cerebral histogenesis in the opossum Monodelphis domestica: generation of a hexalaminar neocortex in the absence of a basal proliferative compartment, *Neural Develop* 5(1): 8.

Qu, X., Lam, E., Doughman, Y.-Q., Chen, Y., Chou, Y.-T., Lam, M., Turakhia, M., Dunwoodie, S. L., Watanabe, M., Xu, B. et al. (2007) Cited2, a coactivator of HNF4alpha, is essential for liver development, *Embo J* 26(21): 4445-56.

Quinn, J. C., Molinek, M., Martynoga, B. S., Zaki, P. A., Faedo, A., Bulfone, A., Hevner, R. F., West, J. D. and Price, D. J. (2007) Pax6 controls cerebral cortical cell number by regulating exit from the cell cycle and specifies cortical cell identity by a cell autonomous mechanism, *Dev Biol* 302(1): 50-65.

Racapé, M., Duong Van Huyen, J.-P., Danger, R., Giral, M., Bleicher, F., Foucher, Y., Pallier, A., Pilet, P., Tafelmeyer, P., Ashton-Chess, J. et al. (2011) The Involvement of SMILE/TMTC3 in Endoplasmic Reticulum Stress Response, *PLoS ONE* 6(5): e19321.

Rakic, P. (1972) Mode of cell migration to the superficial layers of fetal monkey neocortex, *J Comp Neurol* 145(1): 61-83.

Rakic, P. (1974) Neurons in rhesus monkey visual cortex: systematic relation between time of origin and eventual disposition, *Science* 183(123): 425-7.

Rakic, P. (1988) Specification of cerebral cortical areas, *Science* 241(4862): 170-6.

Rakic, P. and Kornack, D. R. (2001) Neocortical expansion and elaboration during primate evolution: a view from neuroembryology. in D. Falk and K. R. Gibson (eds.) *In: Evolutionary anatomy of the primate cerebral cortex* Cambridge, UK: Cambridge UP.

Rakic, P. (2003) Developmental and evolutionary adaptations of cortical radial glia, *Cereb Cortex* 13(6): 541-9.

Rallu, M., Corbin, J. G. and Fishell, G. (2002) Parsing the prosencephalon, *Nat Rev Neurosci* 3(12): 943-51.

Ramón y Cajal, S. (1995) *Histology of the nervous system of man and vertebrates*, New York: Oxford University Press.

Ramos, R. L., Tam, D. M. and Brumberg, J. C. (2008) Physiology and morphology of callosal projection neurons in mouse, *Neuroscience* 153(3): 654-63.

Rash, B. G. and Richards, L. J. (2001) A role for cingulate pioneering axons in the development of the corpus callosum, *J Comp Neurol* 434(2): 147-57.

Rash, B. G. and Grove, E. A. (2006) Area and layer patterning in the developing cerebral cortex, *Curr Opin Neurobiol* 16(1): 25-34.

Razani, B., Engelman, J. A., Wang, X. B., Schubert, W., Zhang, X. L., Marks, C. B., Macaluso, F., Russell, R. G., Li, M., Pestell, R. G. et al. (2001) Caveolin-1 null mice are viable but show evidence of hyperproliferative and vascular abnormalities, *J Biol Chem* 276(41): 38121-38.

Razani, B., Combs, T. P., Wang, X. B., Frank, P. G., Park, D. S., Russell, R. G., Li, M., Tang, B., Jelicks, L. A., Scherer, P. E. et al. (2002) Caveolin-1-deficient mice are lean, resistant to diet-induced obesity, and show hypertriglyceridemia with adipocyte abnormalities, *J Biol Chem* 277(10): 8635-47.

Reid, C. B. and Walsh, C. A. (2002) Evidence of common progenitors and patterns of dispersion in rat striatum and cerebral cortex, *J Neurosci* 22(10): 4002-14.

Reiner, A. (1991) A comparison of neurotransmitter-specific and neuropeptide-specific neuronal cell types present in the dorsal cortex in turtles with those present in the isocortex in mammals: implications for the evolution of isocortex, *Brain Behav Evol* 38(2-3): 53-91.

Reiner, A. (1993) Neurotransmitter organization and connections of turtle cortex: implications for the evolution of mammalian isocortex, *Comp Biochem Physiol Comp Physiol* 104(4): 735-48.

Reiner, A., Jiao, Y., Del Mar, N., Laverghetta, A. V. and Lei, W. L. (2003) Differential morphology of pyramidal tract-type and intratelencephalically projecting-type corticostriatal neurons and their intrastriatal terminals in rats, *J Comp Neurol* 457(4): 420-40.

Reiner, A., Hart, N. M., Lei, W. and Deng, Y. (2010) Corticostriatal projection neurons - dichotomous types and dichotomous functions, *Front Neuroanat* 4: 142.

Ren, T., Zhang, J., Plachez, C., Mori, S. and Richards, L. J. (2007) Diffusion tensor magnetic resonance imaging and tract-tracing analysis of Probst bundle structure in Netrin1- and DCC-deficient mice, *J Neurosci* 27(39): 10345-9.

Riboldi, G., Nizzardo, M., Simone, C., Falcone, M., Bresolin, N., Comi, G. P. and Corti, S. (2011) ALS genetic modifiers that increase survival of SOD1 mice and are suitable for therapeutic development, *Prog Neurobiol* 95(2): 133-48.

Richards, L. J., Plachez, C. and Ren, T. (2004) Mechanisms regulating the development of the corpus callosum and its agenesis in mouse and human, *Clin Genet* 66(4): 276-89.

Rico, B., Beggs, H. E., Schahin-Reed, D., Kimes, N., Schmidt, A. and Reichardt, L. F. (2004) Control of axonal branching and synapse formation by focal adhesion kinase, *Nat Neurosci* 7(10): 1059-69.

Roberts-Thomson, S. J. (2000) Peroxisome proliferator-activated receptors in tumorigenesis: targets of tumour promotion and treatment, *Immunol Cell Biol* 78(4): 436-41.

Rodriguez, T. A., Sparrow, D. B., Scott, A. N., Withington, S. L., Preis, J. I., Michalicek, J., Clements, M., Tsang, T. E., Shioda, T., Beddington, R. S. et al. (2004) Cited1 is required in trophoblasts for placental development and for embryo growth and survival, *Mol Cell Biol* 24(1): 228-44.

Rosen, G. D., Bai, J., Wang, Y., Fiondella, C. G., Threlkeld, S. W., LoTurco, J. J. and Galaburda, A. M. (2007) Disruption of neuronal migration by RNAi of Dyx1c1 results in neocortical and hippocampal malformations, *Cereb Cortex* 17(11): 2562-72.

Rouaux, C. and Arlotta, P. (2010) Fezf2 directs the differentiation of corticofugal neurons from striatal progenitors in vivo, *Nat Neurosci* 13(11): 1345-7.

Roy, K., Kuznicki, K., Wu, Q., Sun, Z., Bock, D., Schutz, G., Vranich, N. and Monaghan, A. P. (2004) The Tlx gene regulates the timing of neurogenesis in the cortex, *J Neurosci* 24(38): 8333-45.

Sahara, S., Kawakami, Y., Izpisua Belmonte, J. C. and O'Leary, D. D. (2007) Sp8 exhibits reciprocal induction with Fgf8 but has an opposing effect on anterior-posterior cortical area patterning, *Neural Dev* 2: 10.

Saito, T. and Nakatsuji, N. (2001) Efficient gene transfer into the embryonic mouse brain using in vivo electroporation, *Dev Biol* 240(1): 237-46.

Saito, T. (2006) In vivo electroporation in the embryonic mouse central nervous system, *Nat Protoc* 1(3): 1552-8.

Saitoh, O. and Courchesne, E. (1998) Magnetic resonance imaging study of the brain in autism, *Psychiatry and clinical neurosciences* 52 Suppl: S219-22.

Sansom, S. N., Hebert, J. M., Thammongkol, U., Smith, J., Nisbet, G., Surani, M. A., McConnell, S. K. and Livesey, F. J. (2005) Genomic characterisation of a Fgf-regulated gradient-based neocortical protomap, *Development* 132(17): 3947-61.

Sasaki, S., Tabata, H., Tachikawa, K. and Nakajima, K. (2008) The cortical subventricular zone-specific molecule Svet1 is part of the nuclear RNA coded by the putative netrin receptor gene Unc5d and is expressed in multipolar migrating cells, *Mol Cell Neurosci* 38(4): 474-83.

Sathish, V., Abcejo, A. J., Thompson, M. A., Sieck, G. C., Prakash, Y. S. and Pabelick, C. M. (2012) Caveolin-1 regulation of store-operated Ca2+ influx in human airway smooth muscle, *Eur Respir J.*

Scattoni, M. L., Gandhy, S. U., Ricceri, L. and Crawley, J. N. (2008) Unusual repertoire of vocalizations in the BTBR T+tf/J mouse model of autism, *PLoS ONE* 3(8): e3067.

Schaeren-Wiemers, N., Andre, E., Kapfhammer, J. P. and Becker-Andre, M. (1997) The expression pattern of the orphan nuclear receptor RORbeta in the developing and adult rat nervous system suggests a role in the processing of sensory information and in circadian rhythm, *Eur J Neurosci* 9(12): 2687-701.

Schedl, A., Ross, A., Lee, M., Engelkamp, D., Rashbass, P., van Heyningen, V. and Hastie, N. D. (1996) Influence of PAX6 gene dosage on development: overexpression causes severe eye abnormalities, *Cell* 86(1): 71-82.

Schipul, S. E., Keller, T. A. and Just, M. A. (2011) Inter-regional brain communication and its disturbance in autism, *Front Syst Neurosci* 5: 10.

Schoenemann, P. T., Sheehan, M. J. and Glotzer, L. D. (2005) Prefrontal white matter volume is disproportionately larger in humans than in other primates, *Nat Neurosci* 8(2): 242-52.

Schreyer, D. J. and Jones, E. H. (1988) Topographic sequence of outgrowth of corticospinal axons in the rat: a study using retrograde axonal labeling with Fast blue, *Brain Res* 466(1): 89-101.

Schubert, W., Frank, P. G., Woodman, S. E., Hyogo, H., Cohen, D. E., Chow, C.-W. and Lisanti, M. P. (2002) Microvascular hyperpermeability in caveolin-1 (-/-) knock-out mice. Treatment with a specific nitric-oxide synthase inhibitor, L-NAME, restores normal microvascular permeability in Cav-1 null mice, *J Biol Chem* 277(42): 40091-8.

Schuurmans, C. and Guillemot, F. (2002) Molecular mechanisms underlying cell fate specification in the developing telencephalon, *Curr Opin Neurobiol* 12(1): 26-34.

Schuurmans, C., Armant, O., Nieto, M., Stenman, J. M., Britz, O., Klenin, N., Brown, C., Langevin, L. M., Seibt, J., Tang, H. et al. (2004) Sequential phases of cortical specification involve Neurogenin-dependent and -independent pathways, *Embo J* 23(14): 2892-902.

Serafini, T., Colamarino, S. A., Leonardo, E. D., Wang, H., Beddington, R., Skarnes, W. C. and Tessier-Lavigne, M. (1996) Netrin-1 is required for commissural axon guidance in the developing vertebrate nervous system, *Cell* 87(6): 1001-14.

Sessa, A., Mao, C. A., Hadjantonakis, A. K., Klein, W. H. and Broccoli, V. (2008) Tbr2 directs conversion of radial glia into basal precursors and guides neuronal amplification by indirect neurogenesis in the developing neocortex, *Neuron* 60(1): 56-69.

Seuntjens, E., Nityanandam, A., Miquelajauregui, A., Debruyn, J., Stryjewska, A., Goebbels, S., Nave, K. A., Huylebroeck, D. and Tarabykin, V. (2009) Sip1 regulates sequential fate decisions by feedback signaling from postmitotic neurons to progenitors, *Nat Neurosci* 12(11): 1373-80.

Shen, Q., Wang, Y., Dimos, J., Fasano, C., Phoenix, T., Lemischka, I., Ivanova, N., Stifani, S., Morrisey, E. and Temple, S. (2006) The timing of cortical neurogenesis is encoded within lineages of individual progenitor cells, *Nat Neurosci* 9(6): 743-751.

Shen, R. and Shuai, J. W. (2011) Neuronal modeling with intracellular calcium signaling, *Sheng Li Xue Bao* 63(5): 442-52.

Shihabuddin, L. S., Horner, P. J., Ray, J. and Gage, F. H. (2000) Adult spinal cord stem cells generate neurons after transplantation in the adult dentate gyrus, *J Neurosci* 20(23): 8727-35.

Shu, T., Valentino, K. M., Seaman, C., Cooper, H. M. and Richards, L. J. (2000) Expression of the netrin-1 receptor, deleted in colorectal cancer (DCC), is largely confined to projecting neurons in the developing forebrain, *J Comp Neurol* 416(2): 201-12.

Shu, T., Li, Y., Keller, A. and Richards, L. J. (2003a) The glial sling is a migratory population of developing neurons, *Development* 130(13): 2929-37.

Shu, T., Puche, A. C. and Richards, L. J. (2003b) Development of midline glial populations at the corticoseptal boundary, *J Neurobiol* 57(1): 81-94.

Shu, T., Sundaresan, V., McCarthy, M. M. and Richards, L. J. (2003c) Slit2 guides both precrossing and postcrossing callosal axons at the midline in vivo, *J Neurosci* 23(22): 8176-84.

Silva, J. M., Li, M. Z., Chang, K., Ge, W., Golding, M. C., Rickles, R. J., Siolas, D., Hu, G., Paddison, P. J., Schlabach, M. R. et al. (2005) Second-generation shRNA libraries covering the mouse and human genomes, *Nat Genet* 37(11): 1281-8.

Silver, J., Lorenz, S. E., Wahlsten, D. and Coughlin, J. (1982) Axonal guidance during development of the great cerebral commissures: descriptive and experimental studies, in vivo, on the role of preformed glial pathways, *J Comp Neurol* 210(1): 10-29.

Simpson, J. C., Wellenreuther, R., Poustka, A., Pepperkok, R. and Wiemann, S. (2000) Systematic subcellular localization of novel proteins identified by large-scale cDNA sequencing, *EMBO reports* 1(3): 287-92.

Smart, I. H. (1973) Proliferative characteristics of the ependymal layer during the early development of the mouse neocortex: a pilot study based on recording the number, location and plane of cleavage of mitotic figures, *J Anat* 116(Pt 1): 67-91.

Smart, I. H. and McSherry, G. M. (1982) Growth patterns in the lateral wall of the mouse telencephalon. II. Histological changes during and subsequent to the period of isocortical neuron production, *J Anat* 134 (Pt 3): 415-42.

Smart, I. H., Dehay, C., Giroud, P., Berland, M. and Kennedy, H. (2002a) Unique morphological features of the proliferative zones and postmitotic compartments of the neural epithelium giving rise to striate and extrastriate cortex in the monkey, *Cereb Cortex* 12(1): 37-53.

Smart, I. H. M., Dehay, C., Giroud, P., Berland, M. and Kennedy, H. (2002b) Unique morphological features of the proliferative zones and postmitotic compartments of the neural epithelium giving rise to striate and extrastriate cortex in the monkey, *Cereb Cortex* 12(1): 37-53.

Smith, K. M., Ohkubo, Y., Maragnoli, M. E., Rasin, M.-R., Schwartz, M. L., Sestan, N. and Vaccarino, F. M. (2006) Midline radial glia translocation and corpus callosum formation require FGF signaling, *Nat Neurosci* 9(6): 787-97.

Smith, N. L., Felix, J. F., Morrison, A. C., Demissie, S., Glazer, N. L., Loehr, L. R., Cupples, L. A., Dehghan, A., Lumley, T., Rosamond, W. D. et al. (2010) Association of genome-wide variation with the risk of incident heart failure in adults of European and African ancestry: a prospective meta-analysis from the cohorts for heart and aging research in genomic epidemiology (CHARGE) consortium, *Circ Cardiovass Genet* 3(3): 256-66.

Stancik, E. K., Navarro-Quiroga, I., Sellke, R. and Haydar, T. F. (2010) Heterogeneity in Ventricular Zone Neural Precursors Contributes to Neuronal Fate Diversity in the Postnatal Neocortex, *Journal of Neuroscience* 30(20): 7028-7036.

Stanojevic, D., Small, S. and Levine, M. (1991) Regulation of a segmentation stripe by overlapping activators and repressors in the Drosophila embryo, *Science* 254(5036): 1385-7.

Stern, D. L. and Orgogozo, V. (2008) The loci of evolution: how predictable is genetic evolution?, *Evolution* 62(9): 2155-77.

Stoykova, A., Treichel, D., Hallonet, M. and Gruss, P. (2000) Pax6 modulates the dorsoventral patterning of the mammalian telencephalon, *J Neurosci* 20(21): 8042-50.

Sugino, K., Hempel, C. M., Miller, M. N., Hattox, A. M., Shapiro, P., Wu, C., Huang, Z. J. and Nelson, S. B. (2006) Molecular taxonomy of major neuronal classes in the adult mouse forebrain, *Nat Neurosci* 9(1): 99-107.

Sugitani, Y., Nakai, S., Minowa, O., Nishi, M., Jishage, K., Kawano, H., Mori, K., Ogawa, M. and Noda, T. (2002) Brn-1 and Brn-2 share crucial roles in the production and positioning of mouse neocortical neurons, *Genes Dev* 16(14): 1760-5.

Sugiyama, Y., Suzuki, A., Kishikawa, M., Akutsu, R., Hirose, T., Waye, M. M., Tsui, S. K., Yoshida, S. and Ohno, S. (2000) Muscle develops a specific form of small heat shock protein complex composed of MKBP/HSPB2 and HSPB3 during myogenic differentiation, *J Biol Chem* 275(2): 1095-104.

Suhonen, J. O., Peterson, D. A., Ray, J. and Gage, F. H. (1996) Differentiation of adult hippocampus-derived progenitors into olfactory neurons in vivo, *Nature* 383(6601): 624-7.

Sundaresan, V., Mambetisaeva, E., Andrews, W., Annan, A., Knoll, B., Tear, G. and Bannister, L. (2004) Dynamic expression patterns of Robo (Robo1 and Robo2) in the developing murine central nervous system, *J Comp Neurol* 468(4): 467-81.

Swenson, R. (2006) The Cerebral Cortex. in R. Swenson (ed.) *Review of Clinical and Functional Neuroscience*.

Szatmari, P. Paterson, A. D. Zwaigenbaum, L. Roberts, W. Brian, J. Liu, X. Q. Vincent, J. B. Skaug, J. L. Thompson, A. P. Senman, L. et al. (2007) Mapping autism risk loci using genetic linkage and chromosomal rearrangements, *Nat Genet* 39(3): 319-28.

Szemes, M., Gyorgy, A., Paweletz, C., Dobi, A. and Agoston, D. V. (2006) Isolation and characterization of SATB2, a novel AT-rich DNA binding protein expressed in development- and cell-specific manner in the rat brain, *Neurochemical research* 31(2): 237-46.

Takahashi, M., Palmer, T. D., Takahashi, J. and Gage, F. H. (1998) Widespread integration and survival of adult-derived neural progenitor cells in the developing optic retina, *Mol Cell Neurosci* 12(6): 340-8.

Takahashi, T., Nowakowski, R. S. and Caviness, V. S., Jr. (1994) Mode of cell proliferation in the developing mouse neocortex, *Proc Natl Acad Sci U S A* 91(1): 375-9.

Takahashi, T., Nowakowski, R. S. and Caviness, V. S., Jr. (1995) Early ontogeny of the secondary proliferative population of the embryonic murine cerebral wall, *J Neurosci* 15(9): 6058-68.

Takayasu, Y., Takeuchi, K., Kumari, R., Bennett, M. V. L., Zukin, R. S. and Francesconi, A. (2010) Caveolin-1 knockout mice exhibit impaired induction of mGluR-dependent long-term depression at CA3-CA1 synapses, *Proc Natl Acad Sci USA*: 1-6.

Takeuchi, A. and O'Leary, D. D. M. (2006) Radial migration of superficial layer cortical neurons controlled by novel Ig cell adhesion molecule MDGA1, *J Neurosci* 26(17): 4460-4.

Tan, S. S., Kalloniatis, M., Sturm, K., Tam, P. P., Reese, B. E. and Faulkner-Jones, B. (1998) Separate progenitors for radial and tangential cell dispersion during development of the cerebral neocortex, *Neuron* 21(2): 295-304.

Tarabykin, V., Stoykova, A., Usman, N. and Gruss, P. (2001) Cortical upper layer neurons derive from the subventricular zone as indicated by Svet1 gene expression, *Development* 128(11): 1983-93.

Tien, E. S., Davis, J. W. and Vanden Heuvel, J. P. (2004) Identification of the CREB-binding protein/p300-interacting protein CITED2 as a peroxisome proliferator-activated receptor alpha coregulator, *J Biol Chem* 279(23): 24053-63.

Tojima, T. (2012) Intracellular signaling and membrane trafficking control bidirectional growth cone guidance, *Neurosci Res* 73(4): 269-74.

Tole, S., Gutin, G., Bhatnagar, L., Remedios, R. and Hébert, J. M. (2006) Development of midline cell types and commissural axon tracts requires Fgfr1 in the cerebrum, *Dev Biol* 289(1): 141-51.

Tomasch, J. (1954) Size, distribution, and number of fibres in the human corpus callosum, *Anat Rec* 119(1): 119-35.

Tomassy, G. S., De Leonibus, E., Jabaudon, D., Lodato, S., Alfano, C., Mele, A., Macklis, J. D. and Studer, M. (2010) Area-specific temporal control of corticospinal motor neuron differentiation by COUP-TFI, *Proc Natl Acad Sci USA*: 1-6.

Toresson, H., Potter, S. S. and Campbell, K. (2000) Genetic control of dorsal-ventral identity in the telencephalon: opposing roles for Pax6 and Gsh2, *Development* 127(20): 4361-71.

Trushina, E., Ducharme, J., Parisi, J. and Mcmurray, C. (2006) Neurological abnormalities in caveolin-1 knock out mice, *Behav Brain Res* 172(1): 24-32.

Tuoc, T. C., Radyushkin, K., Tonchev, A. B., Pinon, M. C., Ashery-Padan, R., Molnar, Z., Davidoff, M. S. and Stoykova, A. (2009) Selective cortical layering abnormalities and behavioral deficits in cortex-specific Pax6 knock-out mice, *J Neurosci* 29(26): 8335-49.

Tusher, V. G., Tibshirani, R. and Chu, G. (2001) Significance analysis of microarrays applied to the ionizing radiation response, *Proc Natl Acad Sci U S A* 98(9): 5116-21.

Val, P., Martinez-Barbera, J.-P. and Swain, A. (2007) Adrenal development is initiated by Cited2 and Wt1 through modulation of Sf-1 dosage, *Development* 134(12): 2349-2358.

Vega, C. J. and Peterson, D. A. (2005) Stem cell proliferative history in tissue revealed by temporal halogenated thymidine analog discrimination, *Nat Methods* 2(3): 167-9.

Veinante, P. and Deschenes, M. (2003) Single-cell study of motor cortex projections to the barrel field in rats, *J Comp Neurol* 464(1): 98-103.

Vidal, C. N., Nicolson, R., DeVito, T. J., Hayashi, K. M., Geaga, J. A., Drost, D. J., Williamson, P. C., Rajakumar, N., Sui, Y., Dutton, R. A. et al. (2006) Mapping corpus callosum deficits in autism: an index of aberrant cortical connectivity, *Biol Psychiatry* 60(3): 218-25.

Vilaro, S., Camps, L., Reina, M., Perez-Clausell, J., Llobera, M. and Olivecrona, T. (1990) Localization of lipoprotein lipase to discrete areas of the guinea pig brain, *Brain Research* 506(2): 249-53.

Visel, A., Thaller, C. and Eichele, G. (2004) GenePaint.org: an atlas of gene expression patterns in the mouse embryo, *Nucleic Acids Res* 32(Database issue): D552-6.

Vlamings, P. H. J. M., Jonkman, L. M., Hoeksma, M. R., Van Engeland, H. and Kemner, C. (2008) Reduced error monitoring in children with autism spectrum disorder: an ERP study, *European Journal of Neuroscience* 28(2): 399-406.

Voelker, C. C., Garin, N., Taylor, J. S., Gahwiler, B. H., Hornung, J. P. and Molnar, Z. (2004) Selective neurofilament (SMI-32, FNP-7 and N200) expression in subpopulations of layer V pyramidal neurons in vivo and in vitro, *Cereb Cortex* 14(11): 1276-86.

von Plessen, K., Lundervold, A., Duta, N., Heiervang, E., Klauschen, F., Smievoll, A. I., Ersland, L. and Hugdahl, K. (2002) Less developed corpus callosum in dyslexic subjects--a structural MRI study, *Neuropsychologia* 40(7): 1035-44.

Vyas, A., Saha, B., Lai, E. and Tole, S. (2003) Paleocortex is specified in mice in which dorsal telencephalic patterning is severely disrupted, *J Comp Neurol* 466(4): 545-53.

Wahl, M., Strominger, Z., Jeremy, R. J., Barkovich, A. J., Wakahiro, M., Sherr, E. H. and Mukherjee, P. (2008) Variability of Homotopic and Heterotopic Callosal Connectivity in Partial Agenesis of the Corpus Callosum: A 3T Diffusion Tensor Imaging and Q-Ball Tractography Study, *American Journal of Neuroradiology* 30(2): 282-289.

Wahlsten, D., Metten, P. and Crabbe, J. C. (2003) Survey of 21 inbred mouse strains in two laboratories reveals that BTBR T/+ tf/tf has severely reduced hippocampal commissure and absent corpus callosum, *Brain Research* 971(1): 47-54.

Wang, C.-L., Zhang, L., Zhou, Y., Zhou, J., Yang, X.-J., Duan, S.-M., Xiong, Z.-Q. and Ding, Y.-Q. (2007) Activity-Dependent Development of Callosal Projections in the Somatosensory Cortex, *J Neurosci* 27(42): 11334-11342.

Wang, W. Z., Oeschger, F. M., Lee, S. and Molnar, Z. (2009) High quality RNA from multiple brain regions simultaneously acquired by laser capture microdissection, *BMC molecular biology* 10: 69.

Wang, Y., Paramasivam, M., Thomas, A., Bai, J., Kaminen-Ahola, N., Kere, J., Voskuil, J., Rosen, G. D., Galaburda, A. M. and Loturco, J. J. (2006) DYX1C1 functions in neuronal migration in developing neocortex, *Neuroscience* 143(2): 515-22.

Ware, M. L., Tavazoie, S. F., Reid, C. B. and Walsh, C. A. (1999) Coexistence of widespread clones and large radial clones in early embryonic ferret cortex, *Cereb Cortex* 9(6): 636-45.

Watakabe, A., Hirokawa, J., Ichinohe, N., Ohsawa, S., Kaneko, T., Rockland, K. S. and Yamamori, T. (2012) Area-specific substratification of deep layer neurons in the rat cortex, *J Comp Neurol*.

Wedeen, V. J., Rosene, D. L., Wang, R., Dai, G., Mortazavi, F., Hagmann, P., Kaas, J. H. and Tseng, W.-Y. I. (2012) The Geometric Structure of the Brain Fiber Pathways, *Science* 335(6076): 1628-1634.

Weimann, J. M., Zhang, Y. A., Levin, M. E., Devine, W. P., Brulet, P. and McConnell, S. K. (1999) Cortical neurons require Otx1 for the refinement of exuberant axonal projections to subcortical targets, *Neuron* 24(4): 819-31.

Williams, B. P. and Price, J. (1995) Evidence for multiple precursor cell types in the embryonic rat cerebral cortex, *Neuron* 14(6): 1181-8.

Williams, T. M. and Lisanti, M. P. (2004) The Caveolin genes: from cell biology to medicine, *Annals of medicine* 36(8): 584-95.

Wilson, C. J. (1987) Morphology and synaptic connections of crossed corticostriatal neurons in the rat, *J Comp Neurol* 263(4): 567-80.

Wise, S. P. and Jones, E. G. (1976) The organization and postnatal development of the commissural projection of the rat somatic sensory cortex, *J Comp Neurol* 168(3): 313-43.

Wise, S. P. and Jones, E. G. (1977) Cells of origin and terminal distribution of descending projections of the rat somatic sensory cortex, *J Comp Neurol* 175(2): 129-57.

Wonders, C. P. and Anderson, S. A. (2006) The origin and specification of cortical interneurons, *Nat Rev Neurosci* 7(9): 687-96.

Woodworth, M. A. and Macklis, J. D. (2009) 'Dissecting autonomous and non autonomous functions of CTIP2 in CSMN development', given at a conference 'Society for Neuroscience Annual Meeting', Chicago, IL.

Wu, S. X., Goebbels, S., Nakamura, K., Nakamura, K., Kometani, K., Minato, N., Kaneko, T., Nave, K. A. and Tamamaki, N. (2005) Pyramidal neurons of upper cortical layers generated by NEX-positive progenitor cells in the subventricular zone, *Proc Natl Acad Sci U S A* 102(47): 17172-7.

Xu, B., Doughman, Y., Turakhia, M., Jiang, W., Landsettle, C. E., Agani, F. H., Semenza, G. L., Watanabe, M. and Yang, Y. C. (2007) Partial rescue of defects in Cited2-deficient embryos by HIF-1alpha heterozygosity, *Dev Biol* 301(1): 130-40.

Yoneshima, H., Yamasaki, S., Voelker, C. C., Molnar, Z., Christophe, E., Audinat, E., Takemoto, M., Nishiwaki, M., Tsuji, S., Fujita, I. et al. (2006) Er81 is expressed in a subpopulation of layer 5 neurons in rodent and primate neocortices, *Neuroscience* 137(2): 401-12.

Yoshida, M., Suda, Y., Matsuo, I., Miyamoto, N., Takeda, N., Kuratani, S. and Aizawa, S. (1997) Emx1 and Emx2 functions in development of dorsal telencephalon, *Development* 124(1): 101-11.

Yun, K., Potter, S. and Rubenstein, J. L. (2001) Gsh2 and Pax6 play complementary roles in dorsoventral patterning of the mammalian telencephalon, *Development* 128(2): 193-205.

Zembrzycki, A., Griesel, G., Stoykova, A. and Mansouri, A. (2007) Genetic interplay between the transcription factors Sp8 and Emx2 in the patterning of the forebrain, *Neural Dev* 2: 8.

Zhao, F., Bosserhoff, A. K., Buettner, R. and Moser, M. A heart-hand syndrome gene: Tfap2b plays a critical role in the development and remodeling of mouse ductus arteriosus and limb patterning, *PLoS ONE* 6(7): e22908.

Zhong, Y., Takemoto, M., Fukuda, T., Hattori, Y., Murakami, F., Nakajima, D., Nakayama, M. and Yamamoto, N. (2004) Identification of the genes that are expressed in the upper layers of the neocortex, *Cereb Cortex* 14(10): 1144-52.

Zhou, C., Tsai, S. Y. and Tsai, M. J. (2001) COUP-TFI: an intrinsic factor for early regionalization of the neocortex, *Genes Dev* 15(16): 2054-9.

Zimmer, C., Tiveron, M. C., Bodmer, R. and Cremer, H. (2004) Dynamics of Cux2 expression suggests that an early pool of SVZ precursors is fated to become upper cortical layer neurons, *Cereb Cortex* 14(12): 1408-20.

Zuluaga, S., Gutierrez-Uzquiza, A., Bragado, P., Alvarez-Barrientos, A., Benito, M., Nebreda, A. R. and Porras, A. (2007) p38alpha MAPK can positively or negatively regulate Rac-1 activity depending on the presence of serum, *FEBS Lett* 581(20): 3819-25.

Appendix-Chapter 8:

SOX6 controls dorsal progenitor identity and interneuron diversity during neocortical development

Author contributions: I joined this project during my rotation in the Macklis lab. I worked closely with first author Eiman Azim, who designed the overall experimental directions, specific analyses, and figures. Denis Jabaudon co-performed the microarray experiments and assisted with interneuron quantification, microarray data evaluation, experimental design and data analysis, and manuscript writing and editing. I optimized whole embryo *in situ* hybridization and immunolaeling to generate Figure A1b, c. I also assisted with BrdU/PH3 pallial progenitor analysis, and developed and implemented the quantification scheme for evaluating interneuron migration delay in the marginal zone stream, quantified in Figure A8b, c, and described in Figure A9. Additionallly, I worked with first and second authors Eiman Azim and Denis Jabaudon to systematically analyze candidate genes from the *Sox6* null vs wildtype comparative microarray analysis (Table A1), quantify interneuron subtypes Figures A10-A13), and edit the manuscript.

Publication: Eiman Azim, Denis Jabaudon, Ryann Fame, and Jeffrey D Macklis· "SOX6 controls dorsal progenitor identity and interneuron diversity during neocortical development." *Nat. Neurosci*. 2009 Oct;12(10):1238-47.

This chapter has been kept largely unchanged from its published form, with the exception of minor changes in figure organization and numbering.

8.1 Abstract

The neuronal diversity of the CNS emerges largely from controlled spatial and temporal segregation of cell type-specific molecular regulators. We report that the transcription factor SOX6 controls the molecular segregation of dorsal (pallial) from ventral (subpallial) telencephalic progenitors and the differentiation of cortical interneurons, regulating forebrain progenitor and interneuron heterogeneity. During corticogenesis in mice, SOX6 and SOX5 are largely mutually exclusively expressed in pallial and subpallial progenitors, respectively, and remain mutually exclusive in a reverse pattern in postmitotic neuronal progeny. Loss of SOX6 from pallial progenitors causes their inappropriate expression of normally subpallium-restricted developmental controls, conferring mixed dorsal-ventral identity. In postmitotic cortical interneurons, loss of SOX6 disrupts the differentiation and diversity of cortical interneuron subtypes, analogous to SOX5 control over cortical projection neuron development. These data indicate that SOX6 is a central regulator of both progenitor and cortical interneuron diversity during neocortical development.

8.2 Introduction

Two broad functional classes of cortical neurons, excitatory projection neurons and inhibitory interneurons, arise from spatially and molecularly segregated pallial (dorsal) and subpallial (ventral) proliferative ventricular zones of the telencephalon, respectively(Schuurmans and Guillemot, 2002; Wonders and Anderson, 2006; Molyneaux et al., 2007). Parcellation of these proliferative regions into molecularly segregated domains separated at the pallial-subpallial boundary (PSB) is critical for the generation of these distinct classes of neurons. Within these broad excitatory and inhibitory neuronal classes, tremendous subtype diversity arises largely from the dynamic temporal expression of progenitor and postmitotic transcriptional regulators. Both of these developmental mechanisms (inter- and intra-domain segregation of molecular regulators) combine to give rise to the extraordinary neuronal diversity of the adult mammalian brain.

The parcellation of the proliferative neuroepithelium at the PSB is defined and maintained by the interactions of several critical early patterning transcription factors, exemplified by the repressive interaction of pallium-expressed Neurogenin2 (Ngn2, also known as Neurog2) on the generally subpallium-expressed Mash1 (also known as Ascl1)(Schuurmans and Guillemot, 2002). Accordingly, loss of Ngn2 function results in dorsal expansion of Mash1 expression and a consequent ventralization of pallial progenitors, which aberrantly give rise to subpallial-like neurons(Fode et al., 2000; Parras et al., 2002). The dynamic interaction between this pair of transcription factors exemplifies the delicate balance of molecular regulators required to establish and maintaining the PSB.

Throughout corticogenesis, these pallial and subpallial progenitors give rise to neurons whose fates depend largely on the location and time at which they are born(Butt et al., 2005; Flames et al., 2007; Miyoshi et al., 2007; Molyneaux et al., 2007; Wonders et al., 2008). In the pallium, distinct excitatory projection neuron subtypes are born sequentially under the control of temporally coordinated programs that guide their subtype specification and differentiation(Molyneaux et al., 2007). Simultaneously, inhibitory cortical interneurons, which constitute approximately 25% of all cortical neurons, are primarily born in the subpallial medial (MGE) and caudal ganglionic eminences (CGE)(Wonders and Anderson, 2006). Acquisition of distinct interneuron subtype identities, distinguishable by molecular, morphological, and electrophysiological phenotypes, depends on both the place and time of birth in the MGE and CGE(Butt et al., 2005; Flames and Marin, 2005; Wonders and Anderson, 2006; Flames et al., 2007; Fogarty et al., 2007; Miyoshi et al., 2007; Ascoli et al., 2008; Wonders et al., 2008). Differentiating interneurons then migrate tangentially toward and then radially into the cortex to populate their final laminar destinations alongside concurrently born pallium-derived excitatory projection neurons(Corbin et al., 2001; Wonders and Anderson, 2006). Because cortical interneurons are implicated in several developmental disorders(Levitt et al., 2004), including epilepsy(Armijo et al., 2002), autism(Rubenstein and Merzenich, 2003), and schizophrenia(Lewis, 2000), understanding the molecular controls over their subtype diversity might clarify some causes of and potential therapeutic approaches to these important disorders.

Although major progress has been made in understanding the regulation of broad aspects of neuronal heterogeneity during development(Schuurmans and Guillemot, 2002), only recently have specific controls over excitatory(Molyneaux et al., 2007) (Arlotta et al., 2005; Chen et al., 2005a; Chen et al., 2005b; Molyneaux et al., 2005; Alcamo et al., 2008; Britanova et al., 2008; Joshi et al., 2008; Kwan et al., 2008; Lai et al., 2008) and inhibitory(Cobos et al., 2005; Liodis et al., 2007; Butt et al., 2008; Du et al., 2008; Zhao et al., 2008) cortical neuron subtype differentiation been characterized. We recently reported that SOX5 postmitotically controls the sequential generation of distinct pallium-derived excitatory corticofugal projection neuron populations, regulating their subtype diversity (Kwan et al., 2008; Lai et al., 2008). Motivated by the complementary and largely redundant functions of SOX5 and SOX6 in other systems(Smits et al., 2001; Stolt et al., 2006), we hypothesized that SOX6 might also function in the generation of forebrain neuronal diversity.

SOX6 and SOX5 belong to the SRY-type HMG box (SOX)-containing transcription factor family, which is composed of 20 members in mammals, many of which have precise temporal and spatial functions in cell-fate specification and differentiation in multiple organ systems including the CNS(Wegner, 1999; Wegner and Stolt, 2005). SOX6 and SOX5, which share 93% identity in their HMG DNA-binding domains and 61% overall identity(Connor et al., 1995), interact and functionally overlap during chondrogenesis and oligodendroglial development in the spinal cord. During chondrogenesis, SOX6 and SOX5 are coexpressed in prechondrocytes, where they have overlapping and additive roles in promoting appropriate and timely differentiation into chondroblasts. The loss of either gene alone produces mild skeletal defects and perinatal death, while the loss of both genes results in major cartilage dysgenesis and death during late gestation(Smits et al., 2001). Similarly, SOX6 and SOX5 are coexpressed in developing oligodendroglia in the spinal cord, where they act as functionally equivalent repressors of specification and terminal differentiation(Stolt et al., 2006). SOX6 is expressed in the forebrain during mid-gestation, as seen by whole-mount *in situ* hybridization(Connor et al., 1995), and in the early postnatal brain, as determined by northern blot and real-time quantitative RT-PCR(Narahara et al., 2002), but its cell type-specific expression and function in the brain have not been investigated.

We found that, in contrast with their overlapping expression and largely redundant functions in other systems, SOX6 and SOX5 are almost entirely mutually exclusively expressed in the forebrain and have distinct, complementary functions. SOX6 and SOX5 are complementarily expressed in pallial and subpallial progenitors, respectively, and this expression is reversed in differentiating postmitotic neurons, as progeny of subpallial progenitors (at least largely composed of cortical interneurons) express SOX6, and corticofugal projection neuron progeny of pallial progenitors express SOX5. During development, SOX6 controls the segregation of pallial from subpallial progenitors by repressing the expression of Mash1 and downstream subpallium-specific programs in pallial progenitors. Postmitotically, SOX6 regulates multiple aspects of cortical interneuron differentiation, ultimately controlling the molecular diversity of cortical interneuron subtypes. We conclude that SOX6 and SOX5 have independent and complementary roles in the generation of neuronal diversity during neocortical development.

8.3 Materials and Methods

8.3 a. Mice.

Sox6$^{+/-}$ and *Sox5*$^{+/-}$ mice were the generous gift of V. Lefebvre (Cleveland Clinic)(Smits et al., 2001) (*Sox6* GeneID 20679; *Sox5* GeneID 20678). The *GAD67-gfp* (delta-neo) mice were the generous gift of Y. Yanagawa (Gunma University)(Narahara et al., 2002; Liodis et al., 2007). *Ngn2*$^{+/-}$; *Ngn1*$^{+/-}$ mice were a generous gift from F. Guillemot (NIMR)[4]. The *Sox6* and *Sox5* transgenic mice are on a pure C57BL/6 background. The *Ngn2; Ngn1* transgenic mice are on a pure CD1 background. The *Sox6; GAD67-gfp* transgenic crosses are a mix between C57BL/6 and Swiss Webster; controls always had the same degree of mixed background. The day of vaginal plug detection was designated as E0.5. The day of birth was designated as P0. All mouse studies were approved by the Massachusetts General Hospital Institutional Animal Care and Use Committee and were performed in accordance with institutional and federal guidelines.

7.3 b. Immunocytochemistry and in situ hybridization.

Brains were fixed and stained using standard methods(Arlotta et al., 2005). For primary antibodies, we used rabbit antibody to SOX6 (1:500, Abcam), goat antibody to SOX5 (1:250, Santa Cruz Biotech), mouse antibody to BrdU (1:500, Becton Dickinson; detects IdU), rat antibody to BrdU (1:500, Accurate; detects CldU), mouse antibody to BrdU (1:750, Chemicon), rabbit antibody to PH3 (1:200, Upstate); mouse antibody to PH3 (1:400, Abcam), mouse antibody to PCNA (1:5,000, Sigma), rabbit antibody to TBR1 (1:1,500, gift of R. Hevner (University of Washington)), rabbit antibody to TBR1 (1:500, Abcam), rat antibody to CTIP2 (1:1,000, Abcam), mouse antibody to Reelin (1:500, Chemicon), rabbit antibody to GFP (1:500, Molecular Probes), mouse antibody to PV (1:500, Sigma), rat antibody to SST (1:100, Chemicon), mouse antibody to calbindin (1:500, Chemicon), rabbit antibody to calretinin (1:1,000, Chemicon), mouse antibody to calretinin (1:400, Chemicon), rabbit antibody to NPY (1:500, Immunostar), rabbit antibody to VIP (1:100, Immunostar), and rabbit antibody to LHX6 (1:1,000, gift of V. Pachnis (NIMR)). Appropriate secondary antibodies were from the Molecular Probes Alexa series. When double immunocytochemistry was performed with two primary antibodies raised in the same species (only in the case of SOX6 colocalization with NPY and VIP and NPY colocalization with TBR1 and LHX6), immunocytochemistry for each antibody was performed sequentially using different secondary antibodies, tissue was fixed for 30 min in 4% paraformaldehyde (by weight) and rinsed in phosphate-buffered saline before application of the second primary antibody. In instances of minor cross-reactivity, nuclear versus cytoplasmic localization of fluorescence was used to distinguish between the two.

Riboprobes were generated and nonradioactive *in situ* hybridization was performed as previously described[18]. The *Sox6* cDNA clone was a gift from V. Lefebvre(Smits et al., 2001). RT-PCR was used to generate the following cDNA clones: *Ngn2* (NM_009718.2, BGEM), *Mash1* (RP_050927_04_D07, Allen Brain Atlas), *Olig2* (NM_016967.2, BGEM), *Pax6* (RP_050927_01_H01, Allen Brain Atlas), *Cux2* (ref. 19), *PlexinD1* (ref. 19), *Lhx6* (MTF#274, Gudmap), and *Vglut2* (nucleotides 2477–2933 of NM_080853).

8.3c Molecular and mitotic characterization of progenitors.

For examination of pallial progenitor phenotype, we performed immunocytochemistry for SOX5 (*n* = 5 wild-type and *n* = 4 *Sox6*$^{-/-}$ at E13.5, *n* = 4 wild-type and *n* = 4 *Sox6*$^{-/-}$ at P0; in Figure A4) and *in situ* hybridization for *Mash1* (*n* = 3 wild-type, *n* = 3 *Sox6*$^{-/-}$, *n* = 1 *Sox5*$^{-/-}$, *n* = 1 *Sox6*$^{-/-}$*; Sox5*$^{-/-}$ at E13.5; *n* = 2 wild-type and *n* = 1 *Ngn2*$^{-/-}$*; Ngn1*$^{-/-}$ at E14.5; *n* = 1 wild-type and *n* = 1 *Sox6*$^{-/-}$ at E17.5; in Figures A5 and A6), *Sox6* (*n* = 2 wild-type and *n* = 1 *Ngn2*$^{-/-}$*; Ngn1*$^{-/-}$ at E14.5; in Figure A5), *Olig2* (*n* = 1 wild-type and *n* = 1 *Sox6*$^{-/-}$ at E13.5; in Figure A6) and *Pax6* (*n* = 1 wild-type and *n* = 1 *Sox6*$^{-/-}$ at E13.5; in Figure A6). For examination of subpallial progenitor phenotype, we performed *in situ* hybridization for *Sox6* (*n* = 3 wild-type and *n* = 2 *Sox6*$^{-/-}$ at E13.5; *n* = 3 wild-type and *n* = 3 *Sox6*$^{-/-}$ at P0; in Figure A4) and *Ngn2* (*n* = 3 wild-type, *n* = 2 *Sox6*$^{-/-}$, *n* = 1 *Sox5*$^{-/-}$, *n* = 1 *Sox6*$^{-/-}$*; Sox5*$^{-/-}$ at E13.5; *n* = 1 wild-type and *n* = 1 *Sox6*$^{-/-}$ at E17.5; in Figures A5 and A6).

For BrdU birthdating and PH3 quantification, timed pregnant females received a single intraperitoneal injection of BrdU (50 mg per kg of body weight) at E13.5 (pallial progenitor analysis) or E14.5 (subpallial progenitor analysis in Figure A3). Embryos were collected 1 h later and processed for BrdU immunocytochemistry(Molyneaux et al., 2005). For pallial progenitor quantification, we selected four anatomically matched cortical sections from each mouse (*n* = 3 wild-type, *n* = 3 *Sox6*$^{-/-}$), carried out BrdU and PH3 immunocytochemistry (2 h of 2N HCl treatment preceded BrdU immunocytochemistry), obtained fluorescent images, and selected two anatomically matched areas (130 μm × 200 μm) from each hemisphere of each section (one medial and one lateral) for blinded quantification of BrdU positivity (defined *a priori* as having strong and homogenous nuclear labeling) and PH3 positivity by two independent investigators. Normal distribution was confirmed, and the unpaired, two-tailed *t* test was used for statistical analysis.

8.3 d. Microarray analysis.

Each embryo from four E13.5 litters (generated by mating male and female *Sox6*$^{+/-}$ mice) was placed in cold Hank's Buffered Salt Solution (HBSS), the pallium was microdissected and immediately preserved in RNAlater (Ambion), and the remaining embryo tissue was subsequently genotyped. RNA extraction, quality assessment, and amplification followed previously reported methods(Arlotta et al., 2005). Briefly, to ensure biological significance and reproducibility, biological replicate RNA samples from four wild-type and four *Sox6*$^{-/-}$ embryos were extracted using the StrataPrep Total RNA Mini Prep Kit (Stratagene), RNA was quantified using a NanoDrop (Thermo Fisher Scientific), and the quality was assessed with a Nanochip in a Bioanalyzer (Agilent Technologies). RNA was amplified via two rounds of *in vitro* transcription and biotinylated using a BioArray HighYield RNA Transcript Labeling Kit (Enzo), yielding approximately 20–50 μg of labeled cRNA for hybridization(Arlotta et al., 2005), and the quality of the amplified RNA was assessed with a Nanochip in a Bioanalyzer before hybridization on Affymetrix 430.2 GeneChips.

Homotypic (biological replicates) and heterotypic comparisons (wild-type versus *Sox6*$^{-/-}$) were performed using Rosetta Resolver software (Rosetta Inpharmatics). Differentially expressed genes with an absolute fold change of more than 1.8 and a *P* value of less than 0.005 were selected for further analysis. To rigorously ensure statistical significance of identified candidate genes, we normalized the data via three additional independent methods (RMA (Robust Multi-Array Analysis), GCRMA (Guanine Cytosine Robust Multi-Array Analysis) and MAS 5.0-Affymetrix in Bioconductor and cross-referenced the significance of candidate genes with the Rosetta Resolver normalized dataset. Additional cross-referencing was performed with genes identified as significant with a Significance Analysis of Microarrays (SAM) approach using an absolute fold change of more than 1.8 and a *d* value of 0.772 for gcRMA-normalized data and a *d* value of 0.35 for RMA-normalized data. The biological relevance of candidate genes was assessed in an integrated gene analysis platform developed in our laboratory (Jabaudon, D., Azim, E., Macklis, J.D., unpublished data), using online *in situ* hybridization, gene ontology, protein function, and literature databases to individually assess expression and function of each gene. Statistically significant genes with normally segregated pallial or subpallial expression during development were identified (reported in Table A1).

8.3 e. Mis-expression of SOX6 and SOX5 via electroporation.

For control experiments, a vector containing *IRES-egfp* under the control of a constitutively active CMV/β-actin promoter was used(Molyneaux et al., 2005) (a generous gift of C. Lois (Picower Institute)). *Sox6* and *Sox5* (ref. 22) were cloned upstream of *IRES-egfp* for mis-expression. We mixed 750 nl of purified DNA (1.0 μg/μl) with 0.005% Fast Green (for visualization), injected it *in utero* into the lateral ventricle of CD1 embryos at E12.5 under ultrasound guidance (Vevo 770, VisualSonics), and electroporated into the subpallial (*Sox6*) or pallial (*Sox5*) ventricular zone, as described previously(Molyneaux et al., 2005; Lai et al., 2008). Embryos were analyzed at E16.5 (*n* = 3 subpallial control, *n* = 3 subpallial *Sox6*, *n* = 3 pallial control, *n* = 3 pallial *Sox5*, multiple independent litters were examined in each condition).

8.3 f. Interneuron quantification.

For quantification of the tangential distance between the leading edges of the marginal zone and intermediate zone/SVZ interneuron tangential migratory streams at E13.5, we selected anatomically matched sections (*n* = 3 *Sox6*$^{+/+}$*; GAD67-gfp*$^{+/–}$, *n* = 3 *Sox6*$^{–/–}$*; GAD67-gfp*$^{+/–}$; 10–12 hemispheres per mouse, spanning the rostro-caudal extent of the telencephalon), and carried out GFP immunocytochemistry. The distance was measured in micrometers between the position of the soma of the leading neuron of the marginal zone stream, radially projected to the pial surface, and the corresponding position of the soma of the leading neuron in the intermediate zone/SVZ stream, radially projected to the pial surface, determined by drawing imaginary lines radially from the marginal zone and intermediate zone/SVZ streams perpendicular to the surface of the brain (described in FigureA9).

For quantification of interneuron number at E13.5, anatomically matched sections were selected (*n* = 3 *Sox6*$^{+/+}$*; GAD67-gfp*$^{+/–}$, *n* = 3 *Sox6*$^{–/–}$*; GAD67-gfp*$^{+/–}$, 10–12 hemispheres per mouse spanning the rostro-caudal extent of the telencephalon), GFP immunocytochemistry was performed, and Grid Confocal (Improvision) images were obtained of a single plane of GFP-positive neurons. Digital boxes of fixed area (marginal zone stream, 85 mm × 175 mm; intermediate zone/SVZ stream, 115 μm × 175 μm) were superimposed at predetermined anatomical landmarks at the base, middle, and leading edge of each migratory stream of each hemisphere, and GFP-positive neurons were quantified (described in Figure A9).

For P0 quantification, anatomically matched sections were selected (*n* = 3 wild-type, *n* = 3 *Sox6*$^{–/–}$; 10–12 hemispheres per mouse spanning the rostro-caudal extent of the telencephalon), GFP immunocytochemistry was performed, digital boxes of fixed width were equally divided into four bins (see Figure A10) and superimposed on the cortices adjacent to the PSB of each hemisphere, and height was adjusted to extend from the bottom of layer VI to directly under the marginal zone (at P0, the marginal zone was still very interneuron dense and was therefore not included in the quantification). GFP-positive neurons were quantified, and density values were calculated on the basis of the area of the box in each image; densities are expressed as neurons per mm^2. Laminar distributions were determined by dividing the proportion of neurons in each bin by the total number of neurons in all bins.

For P14 quantification, anatomically matched sections were selected (*n* = 3 wild-type, *n* = 3 *Sox6*$^{–/–}$; 8–12 hemispheres per mouse spanning the rostro-caudal extent of the telencephalon), and SOX6, GFP, PV, SST, NPY (*n* = 6 wild-type, *n* = 6 *Sox6*$^{–/–}$), VIP (*n* = 4 wild-type, *n* = 4 *Sox6*$^{–/–}$), calretinin, calbindin, and LHX6 immunocytochemistry was performed. Digital boxes of fixed width were equally divided into four bins (see Figure A10b), superimposed on the cortices adjacent to the PSB of each hemisphere, and height was adjusted to extend from the top of the white matter to the cortical surface. The percentages of wild-type interneurons that express SOX6 (in Figure A12b) were calculated from the total numbers in all four bins. Density values and laminar distributions in wild-type and *Sox6*$^{-/-}$ were calculated as above.

For IdU and CldU interneuron birthdating, equimolar delivery of IdU (57.5 mg per kg) at E11.5 and CldU (42.5 mg per kg) at E15.5 was performed(Vega and Peterson, 2005). We sacrificed and perfused mice at P14, genotyped, and prepared brains for immunocytochemistry. Anatomically matched sections were selected, and IdU, CldU, PV, SST and NPY immunocytochemistry was performed (IdU and PV, IdU and NPY: $n = 2$ wild-type, $n = 3$ *Sox6*$^{-/-}$; IdU and SST, CldU and PV, CldU and SST, CldU and NPY: $n = 2$ wild-type, $n = 2$ *Sox6*$^{-/-}$; 7–8 hemispheres per mouse spanning the rostro-caudal extent of the telencephalon). Digital boxes of fixed width were superimposed on the cortices adjacent to the PSB, and height was adjusted to extend from the top of the white matter to the cortical surface. Interneurons coexpressing SST, PV, or NPY, and either IdU or CldU (defined *a priori* as having strong and homogenous nuclear labeling) were quantified (colabeling was defined as clear nuclear label surrounded by cytoplasmic PV, SST, or NPY label; in Figure A13a) and density values were calculated on the basis of the area of the box in each image.

All quantification was performed on 50 μm vibratome sections using well-established modified stereological methods, beginning at the rostral limit of the corpus callosum and continuing caudally, skipping four sections between samples, so that no cell could be counted twice in an adjacent section. We used strict *a priori* criteria, whereby the entire soma of a cell needed to be present to be counted, which was effectively accomplished by counting with high numerical aperture optics in the central approximately 30 μm of the thick 50 μm sections, avoiding cut neurons present in the top or bottom approximately 10 μm of each section. All quantifications were blinded, normal distribution was confirmed, and the unpaired, two-tailed *t* test was used for statistical analysis. Welch corrections were performed in the rare instances when the s.d. of the two groups varied significantly. All results are expressed as the mean ± s.e.m.

8.3 g. Microscopy and image analysis.

Tissue sections were viewed on a Nikon E1000 microscope equipped with an X-Cite 120 illuminator (EXFO), and images were collected and analyzed with Volocity image analysis software (Improvision, v4.0.1). Images were optimized for size, color, and contrast using Photoshop 7.0 (Adobe). Single plane fluorescence images for E13.5 interneuron quantification were obtained using the Volocity Grid Confocal microscopy system (Improvision). Images were collected at the approximate midpoint between the top and bottom planes of focus.

8.4 Results

8.4 a. SOX6 and SOX5 are mutually exclusively expressed

To determine whether SOX6 and SOX5 have complementary or interactive roles during neocortical development, we characterized their expression at important stages of corticogenesis. *In situ* hybridization and immunocytochemistry revealed that SOX6 and SOX5 are expressed in complementary and almost entirely mutually exclusive populations of progenitors and cortical neurons: SOX6 in pallial progenitors and postmitotic subpallial neurons, and SOX5 in subpallial progenitors and postmitotic pallial corticofugal projection neurons(Lai et al., 2008) (Figure A1a–e). Early in corticogenesis, SOX6 is expressed in the telencephalon in a slight dorsal-high to ventral-low gradient (Figure A1b), whereas SOX5 is expressed in a spatially reciprocal ventral-high to dorsal-low gradient (Figure A1c). During mid- to late corticogenesis, SOX6 and SOX5 are mutually exclusively expressed in pallial (SOX6) and subpallial (SOX5) ventricular zone progenitors (Figure A1d,e and Figure A2). Their expression overlaps exclusively in a discrete portion of the dorsal subpallial ventricular zone at the PSB (Figure A2), a region that gives rise to the lateral cortical stream, populating basal telencephalic structures, including the amygdala and piriform cortex(Puelles et al., 2000; Carney et al., 2006).

The postmitotic progeny of pallial and subpallial progenitors mutually exclusively express SOX6 and SOX5 in a reverse pattern; SOX6 is expressed in the MGE and CGE mantle zones, which contain, among other neuronal populations, developing cortical interneurons that maintain SOX6 expression as they mature in the neocortex, whereas SOX5 is expressed by corticofugal projection neurons in the cortical plate(Lai et al., 2008) (Figure A1d,e and Figure A2; also **Fig. 6a**). Notably, SOX6 is not expressed in the mantle zone of the lateral ganglionic eminence (LGE), where medium spiny neurons that populate the striatum will later mature (Figure A1d). Immunocytochemical analysis of the S-phase marker BrdU, the pan-mitotic marker PCNA, and the M-phase marker phospho-histone 3 (PH3) revealed that subpallial expression of SOX6 is overwhelmingly postmitotic (Figure A3). Taken together, these data indicate that SOX6 and SOX5 are expressed in spatially abutting, almost entirely non-overlapping populations of progenitors and postmitotic neurons, suggesting cross-repressive interactions during development.

7.4 b. SOX6 and SOX5 progenitor expression is cross-repressive

We hypothesized that if cross-repressive interactions exist, either direct or indirect, loss of either SOX6 or SOX5 would result in the corresponding ectopic expression of the other. Accordingly, loss of SOX6 function in *Sox6*$^{-/-}$ mice(Smits et al., 2001) results in an expansion of SOX5 expression into the pallial ventricular zone that normally expresses SOX6 (Figure A4a). During corticogenesis, this ectopic SOX5 expression in *Sox6*$^{-/-}$ pallium gradually expands from the lateral to the medial extent of the pallial ventricular zone, suggesting a developmental gradient of SOX5 expression. Conversely, in *Sox5*$^{-/-}$

Figure A1: SOX6 and SOX5 are expressed in complementary populations of telencephalic progenitors and neuronal progeny during corticogenesis. (**a**) Schematic illustrating the relative position of the neocortex, LGE, MGE, and CGE in the developing brain. A, anterior; D, dorsal; P, posterior; V, ventral. (**b**,**c**) *Sox6* (**b**, black arrow) is expressed in a slight dorsal-high ventral-low gradient (analyzed by *in situ* hybridization, ISH) and SOX5 (**c**, black arrow) is expressed in a ventral-high dorsal-low gradient (analyzed by immunocytochemistry, ICC) in the telencephalon (white dotted circles) at E10.5, as corticogenesis is beginning. Insets show higher-magnification view of the telencephalon. (**d**,**e**) During corticogenesis, shown here at E13.5 and E15.5, *Sox6* (**d**, *in situ* hybridization) is expressed in progenitors of the pallial ventricular zone (red arrows) and in postmitotic neurons in the MGE and CGE mantle zones (red arrowheads), but it is not expressed in subpallial ventricular zone progenitors (blue arrows). SOX5 (**e**, immunocytochemistry) is expressed in subpallial ventricular zone progenitors (blue arrows) and postmitotic neurons in the cortical plate (blue arrowheads), but it is not expressed in pallial ventricular zone progenitors (red arrows). Panel **a** is adapted from (Corbin et al., 2001). Scale bars represent 100 µm and 150 µm for E.13.5 and E.15.5, respectively.

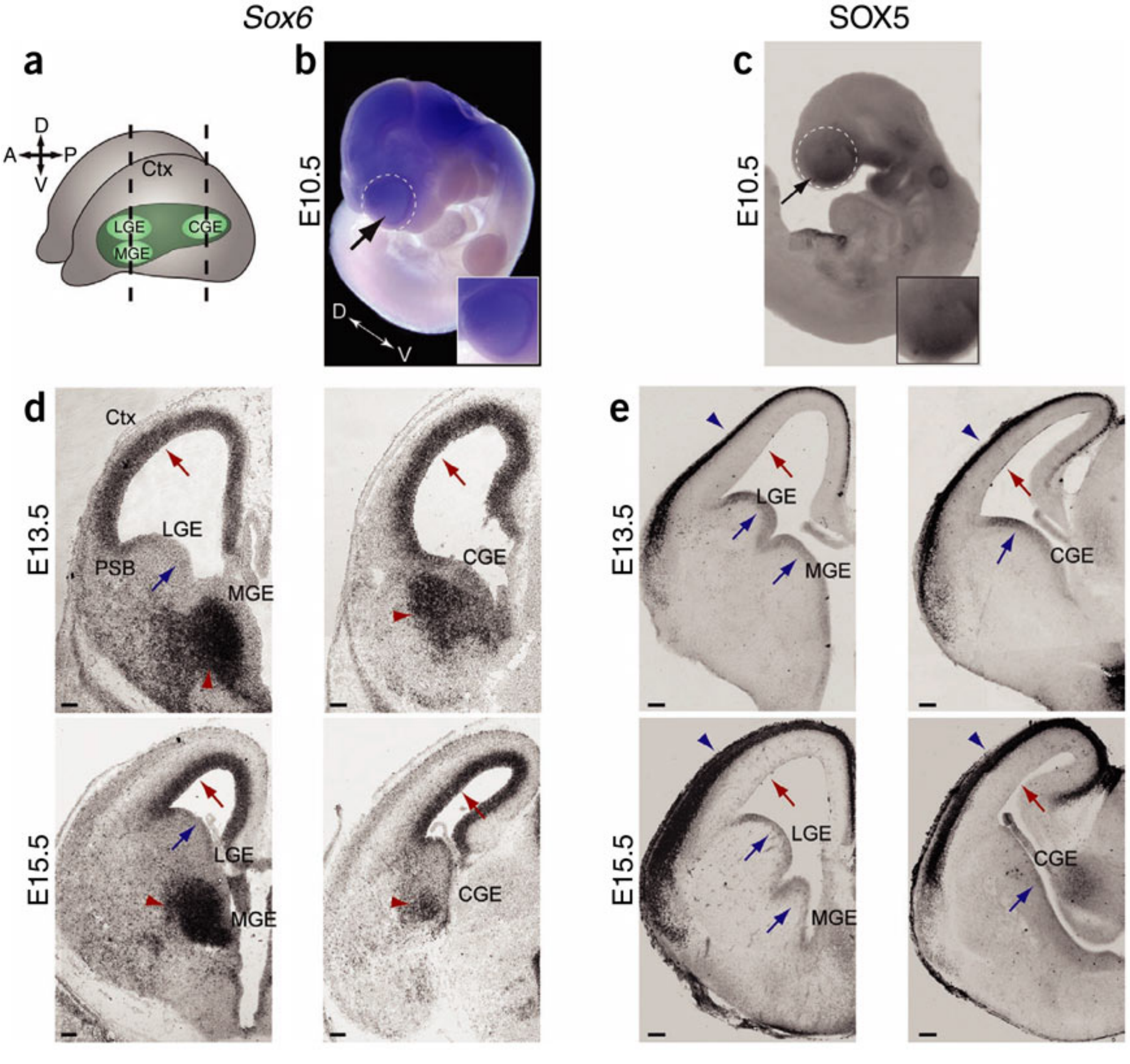

Figure A1 (Continued)

mice(Smits et al., 2001), SOX6 expression expands ventrally into the subpallial ventricular zone during neocortical development (Figure A4b). This cross-repressive interaction is restricted to progenitors and is not apparent in postmitotic neurons that express SOX6 or SOX5, indicating that progenitor-specific, and possibly indirect, interactions are occurring between these two transcription factors, most likely in coordination with other progenitor patterning genes.

Notably, the dorsal subpallial ventricular zone coexpresses SOX6 and SOX5 (Figure A2), indicating that there is a unique relationship between the two transcription factors in this distinct developmental domain, and suggesting that the expression of either one alone is not sufficient to repress the expression of the other. To investigate whether SOX6 and SOX5 are sufficient to repress the expression of each other in progenitors, we mis-expressed *Sox6* in the subpallial ventricular zone and *Sox5* in the pallial ventricular zone via *in utero* electroporation at embryonic day 12.5 (E12.5) for analysis at E16.5. Many progenitors transfected with one of the genes continued to express the other gene, which is not surprising, given their normal coexpression in a discrete region of dorsal subpallial progenitors (Figure A2), as well as in other developing systems(Smits et al., 2001; Stolt et al., 2006). Taken together, these data indicate that SOX6 and SOX5 are necessary, but not sufficient, to repress the expression of each other in forebrain progenitors, strongly suggesting that there are combinatorial interactions with other regional patterning signals during telencephalic development.

8.4 c. SOX6 and Ngn2 cooperatively control pallial identity

The complementary and mutually exclusive expression of SOX6 and SOX5 in forebrain progenitor domains is highly reminiscent of the generally non-overlapping expression of the patterning transcription factors Ngn2 (pallial) and Mash1 (subpallial)(Ma et al., 1997; Fode et al., 2000). Loss of Ngn2 causes ectopic expansion of Mash1 expression into pallial progenitors, activating downstream subpallial differentiation programs(Fode et al., 2000; Parras et al., 2002). Because the patterns of SOX6 and Ngn2 expression in telencephalic progenitors are similar, we examined whether the loss of SOX6 function would result in a similar ventralization of the pallium. Indeed, loss of SOX6 causes a marked expansion of Mash1 expression into the pallial ventricular zone throughout corticogenesis (Figure A5a and Figure A6). Olig2, a transcription factor that is also expressed by subpallial progenitors during corticogenesis, is also ectopically expressed in *Sox6*$^{-/-}$ pallial ventricular zone (Figure A6). This domain-parcellating function is specific for SOX6, as loss of SOX5 function does not cause a reciprocal ventral expansion of pallium-specific Ngn2 expression, and simultaneous loss of both SOX6 and SOX5 function largely replicates the phenotype of *Sox6*$^{-/-}$ mice (Figure A6). These data indicate that SOX6 functions centrally in the molecular segregation of the pallial from the subpallial progenitor domain.

We next examined whether the partial ventralization of pallial progenitors in *Sox6*$^{-/-}$ mice is a result of the disruption of the expression of mostly pallium-restricted Pax6 or its direct downstream target Ngn2 (ref. 41). Pax6 (Figure A6) and Ngn2 (Figure A5b) are still normally expressed in the *Sox6*$^{-/-}$ pallium, indicating that their expression is not centrally driven by SOX6. Because Ngn2 is known to normally repress Mash1 (Fode et al., 2000), and because this repression is lost in *Sox6*$^{-/-}$ pallial progenitors (where Ngn2 and Mash1 are abnormally coexpressed; Figure A5a, b), we hypothesized that SOX6 maintains pallial identity either in and transcriptionally activated by the well-described Pax6 → Ngn2 —| Mash1 pathway, mediating Ngn2 repression of Mash1, or in a previously undefined genetic cascade that does not require the Ngn2 pathway for transcriptional activation. To discriminate between these two possibilities, we examined the expression of SOX6 in the abnormally ventralized pallium of *Ngn2*$^{-/-}$*; Ngn1*$^{-/-}$ mice(Fode et al., 2000), in which the repression of Mash1 by Ngn2 (supplemented by additive repression by Ngn1) is lost(Fode et al., 2000) (Figure A5c). Loss of SOX6 expression in the *Ngn2*$^{-/-}$*; Ngn1*$^{-/-}$ pallium would suggest that SOX6 is a downstream transcriptional target of Ngn signaling, acting in this canonical pathway. The data exclude this alternative, as SOX6 expression is maintained in *Ngn2*$^{-/-}$*; Ngn1*$^{-/-}$ pallium (Figure A5d). Just as Ngn2 is normally expressed in the pallial ventricular zone in the absence of SOX6, SOX6 is normally expressed in the absence of Ngn2. These data indicate that the cooperative convergence of both SOX6 and Ngn2 pathways is necessary to repress Mash1 and maintain the dorsal identity of pallial progenitors, while neither is sufficient on its own. In the absence of either of these critical regulators, pallial progenitors adopt a mixed dorsal-ventral identity, inappropriately coexpressing genes that are normally specific to one or the other developmental domain.

Despite the partial ventralization of *Sox6*$^{-/-}$ pallial progenitors, projection neuron laminar distribution and subtype- and layer-specific molecular expression appear to be largely normal (Figure A7). Similarly, pallial progenitor proliferation is not affected by loss of SOX6 function, as assessed by BrdU uptake and PH3 expression (data not shown). To determine whether the expansion of Mash1 expression into the *Sox6*$^{-/-}$ pallium is indicative of the initiation of subpallium-specific programs of gene expression, we carried out comparative microarray analysis between wild-type and *Sox6*$^{-/-}$ pallium during mid-corticogenesis at E13.5 and identified several normally subpallium-expressed genes that are ectopically expressed in the *Sox6*$^{-/-}$ pallium, including *Dlx1*, *Dlx2*, *Dlx4*, *Gsh2*, *Isl1*, *Meis1* and *Sox5* (Table A1). These data indicate that SOX6 critically maintains pallial progenitor identity by repressing subpallial programs of gene expression, but redundant and/or compensatory controls (for example, Ngn2 and Ngn1) persist that are sufficient to ensure largely appropriate pallial corticogenesis(Britz et al., 2006). We conclude that SOX6 acts cooperatively with Ngn2 to control the segregation of telencephalic progenitor domains during development.

Figure A2: Sox6, expressed in pallial progenitors, and SOX5 expressed in subpallial progenitors, overlap in the dorsal subpallial VA, and are not sufficient to repress expression of eachother. (**a**) During corticogenesisi, shown here at E13.5, E15.5, and P0, SOX6 is expressed in progenitors of the pallial ventricular zonw (VZ) (white areeows), and in neurons that originate in the MGE and CGE mantle zones (white arrowheads). (**b**) SOX6 and SOX5 expression in the telencephalon is essentially nutually exclusive, with overlap uniquely in the dorsal subpallial VZ (white arrow). (**c, d**) Mis-expression of *Sox6* (*IRES-EGFP*) in the subpallial VZ via *in utero* electroporation (**c**) at E12.5 for analysis at E16.5 reveals that many transfected cells both do (white arrows) and do not (white arrowheads) express SOX5. Mis-expression of *Sox5* (*IRES-EGFP*) in the pallial VZ (**d**) at E12.5 for analysis at E16.5, reveals extensive co-expression of SOX5 and SOX6 (white arrows). Electroporation of a control EGFP vector in the pallial or subpoallial VZ also does not affect SOX6 or SOX5 expresion in transfected progenitors, respectively (data not shown). Both the *Sox6* and *Sox5* constructs were immunocytochemically verified to express both the gene of interest as well as EGFP. (a-d) immunocytochemistry. Ctx, cortex; LGE, lateral ganglionic eminence; MGE, medial ganglionic eminence; CGE, caudal ganglionic eminence; PSB, pallial-subpallial boundary. Dotted lines (c,d) indicate lateral ventricle boundary. Scale bars, (a; E13.5) 100 μm, (a; E15.5) 150 μm, (a; P0, low magnification) 200 μm, (a; P0, high magnification) 50 μm, (b) 50 mm, (c,d) 20 μm.

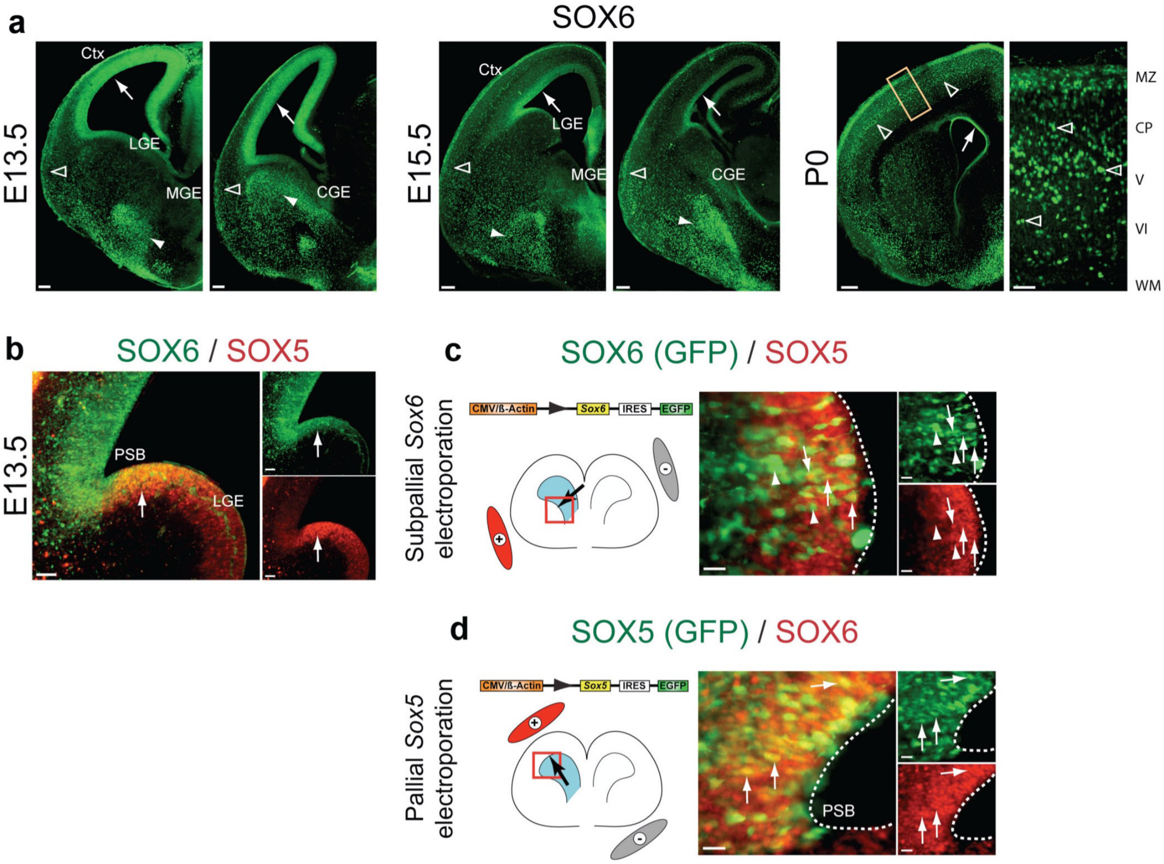

Figure A2 (Continued)

Figure A3: SOX6 subpallial mantle zone expression is postmitotic. (**a**) At E14.5, SOX6 expression (white arrowheads) and BrdU label (white arros) are non-overlapping in the MGE mantle zone following a one hour pulse of BrdU to label cells in S-phase (as well as some cells in G2), with very rare exceptions (as expected in a dense transistion zone between mitotic and postmitotic cells). (**b**) At E15.5, SOX6 (white arrowheads) and the pan-mitotic marker PCNA (white arrows) are not co-expressed, with very rare exceptions (again, as expected, with potential protein perdurance, and in a dense region of transition from mitotic to postmitotic state). (**c**) At E15.5, SOX6 (white arrowheads) and the M-phase marker PH3 (white arrows) are not co-expressed in the MGE mantle zone. IN order to assess co-localization with surrounding mantle zone SOX6 expression, all analyses were preformed at later stages of cortico genesis (E14.5 and E15.5), when SVZ proliferatios predominate. (a-c) immunocytochemistry. Ctx, cortex; LGE, lateral ganglionic eminence; MGE, medial ganglionic eminence**.** Scale bars, (a-c; low magnification) 300 μm, (a-c; intermediate magnification) 50 μm, (a-c; high magnification) 10 μm.

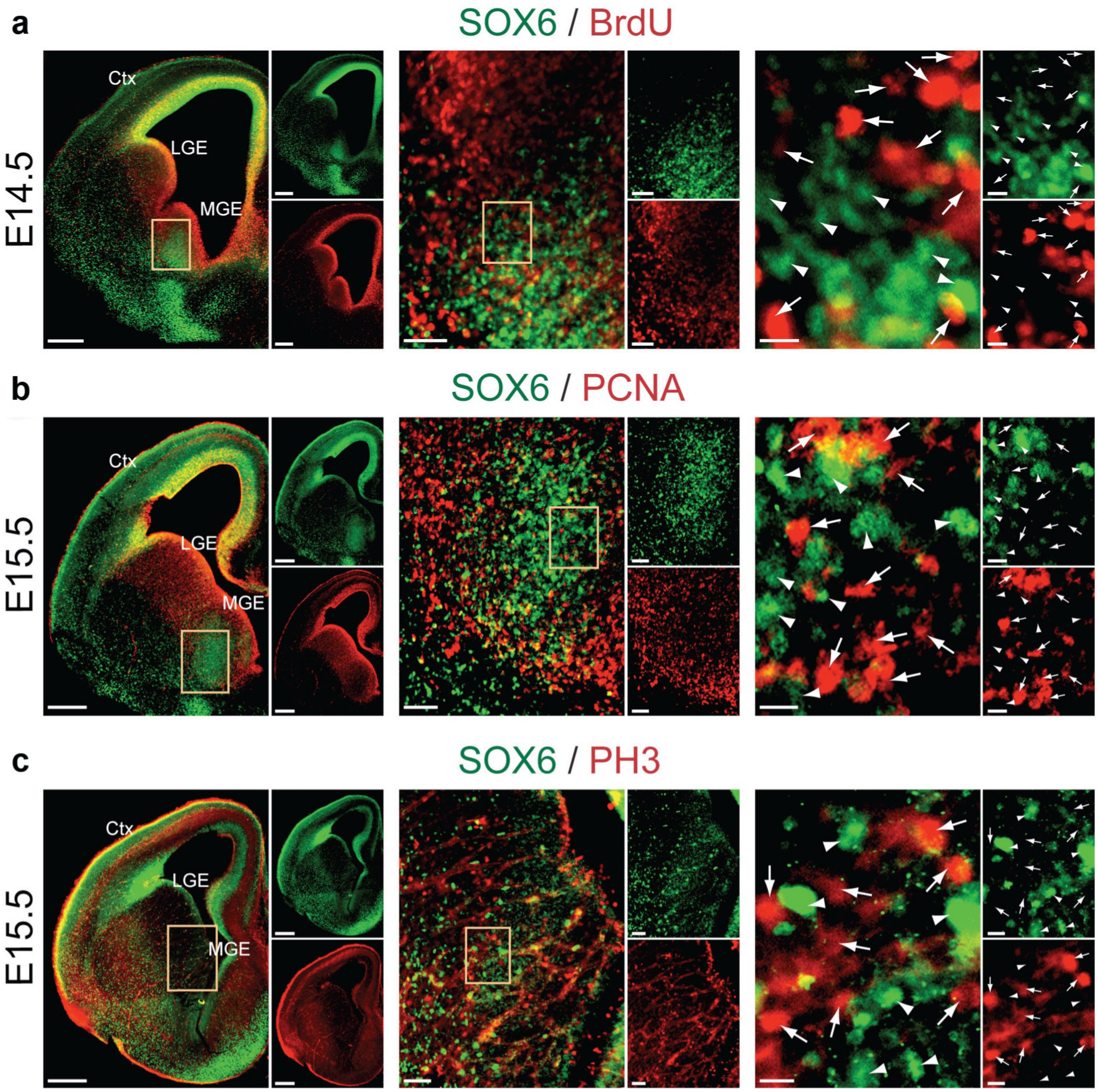

Figure A3 (Continued)

8.4 d SOX6 controls cortical interneuron subtype differentiation

SOX6 is also expressed in postmitotic interneurons as they reside in the subpallium and populate the neocortex (Figures A1d, A2, and A3). We therefore examined whether the loss of SOX6 function would affect key sequential steps of interneuron differentiation: early postmitotic molecular identity; cortical laminar location and morphology; and interneuron molecular subtype differentiation. Our data indicate that SOX6 acts postmitotically, at all three of these stages of cortical interneuron differentiation, controlling their appropriate development.

As the early molecular programs of immature postmitotic cortical interneurons in the subpallial mantle zones largely determine and predict their appropriate differentiation(Batista-Brito et al., 2008), we first examined early cortical interneuron molecular identity. We found that *Sox6*$^{-/-}$ MGE and CGE mantle zones abnormally express the proneural transcription factors Mash1 and Ngn2 (Figure A5a,b). SOX6 repression of the ectopic and persistent expression of Mash1 (normally progenitor- and subpallium-specific) and Ngn2 (normally progenitor and pallium-specific) in subpallial mantle zones strongly suggests that SOX6 controls the temporal segregation of transcriptional programs between progenitors and postmitotic neurons.

Because MGE and CGE *Sox6*$^{-/-}$ mantle zone cells ectopically express Ngn2, which normally represses subpallial and maintains pallial identity(Fode et al., 2000), we hypothesized that these cells might abnormally initiate pallium-like gene expression. Consistent with this hypothesis, *Sox6*$^{-/-}$ subpallial mantle zone cells inappropriately express Vglut2, a vesicular glutamate transporter whose expression is normally restricted to pallium-born excitatory projection neurons (Figure A8a). This indicates that at least a subpopulation of *Sox6*$^{-/-}$ subpallial immature neurons in the mantle zone are inappropriately acquiring pallial properties.

To determine whether this abnormal coexpression of pallial/subpallial and progenitor/postmitotic molecular regulators (Mash1, Ngn2 and Vglut2) in *Sox6*$^{-/-}$ immature subpallial neurons affects their ability to broadly differentiate into GABAergic neurons, we examined whether they express GAD67 (also known as Gad1), an enzyme that is necessary for the synthesis of the inhibitory neurotransmitter GABA, a fundamental indicator of their identity. Using *in situ* hybridization for *GAD67* (data not shown), and confirming this with *GAD67-gfp* (delta-neo) transgenic mice, in which green fluorescent protein (GFP) is expressed in the vast majority of GABA-positive neurons(Tamamaki et al., 2003; Liodis et al., 2007), we found that GAD67 is expressed in neurons leaving the subpallial mantle zones in *Sox6*$^{-/-}$*; GAD67-gfp* mice (Figure A8b), suggesting appropriate GABAergic neuron specification. However, as cortical interneurons continue their migration tangentially in one of two streams toward the cortex (a superficial marginal zone stream or a deeper intermediate zone/subventricular zone (SVZ) stream), they fail to migrate properly in *Sox6*$^{-/-}$ cortex, as indicated by the consistently less advanced leading edge of the marginal zone stream compared with the leading edge of the intermediate zone/SVZ stream (Figures A8 b,c and A9). There is no change in the number of interneurons in either migratory stream at E13.5 (Figures A8d and A9). From these data, we conclude that loss of SOX6 function perturbs the initial temporal segregation of progenitor-specific factors from postmitotic neurons, potentially causing their abnormal tangential migration, without affecting overall GABAergic neuron specification and abundance.

To further investigate whether the molecular and migratory irregularities at early stages of *Sox6*$^{-/-}$ subpallial neuron differentiation are associated with abnormalities in subsequent stages of interneuron cortical invasion, we examined the laminar location and morphology of these interneurons as they populate the cortex. In *GAD67-gfp* mice at postnatal day 0 (P0; Figure A10a), just after the interneurons have begun their radial migration into the maturing cortex, and at P14 (Figure A10b), as they have more fully adopted their mature phenotypes, *Sox6*$^{-/-}$ interneurons preferentially populate deeper neocortical layers (Figure A10c,d), without any change in their total numbers. (Although the large majority of *Sox6*$^{-/-}$ mice die perinatally, small numbers survive a few weeks postnatally, which allowed us to analyze them at P14 (Smits et al., 2001). *Sox6*$^{+/-}$ mice survive to adulthood, with a small number exhibiting occasional seizure behavior.) We also examined the morphology of GAD67-GFP-positive neurons at P0 and found that *Sox6*$^{-/-}$ interneurons have abnormal tangential orientation, in contrast with the mostly radial orientation of wild-type interneurons (reflecting their transition from tangential to radial migration) (Figure A10a). These laminar distribution and morphological abnormalities were confirmed by analysis of the broad (at P0) interneuron marker calbindin (Figure A11). These data indicate that SOX6 is necessary for the appropriate differentiation of cortical interneurons as they integrate into the neocortical circuitry, manifested by their inappropriately deep laminar location and abnormal morphology in the absence of SOX6.

To determine whether SOX6 differentially affects the development of distinct cortical interneuron subtypes, we examined interneuron subpopulations using subtype-defining molecular markers(Wonders and Anderson, 2006; Ascoli et al., 2008). By P14, the calcium-binding protein parvalbumin (PV) and the peptide hormone somatostatin (SST) are expressed by two non-overlapping subclasses of predominantly MGE-born interneurons, many of which are born early in corticogenesis. The peptide neurotransmitter neuropeptide Y (NPY) is expressed by later-born MGE and CGE-derived interneurons, many of which coexpress SST. The peptide hormone vasoactive intestinal peptide (VIP) is predominantly expressed by late-born, CGE-derived interneurons, although a subpopulation of VIP-positive interneurons coexpress SST and might be of MGE origin. The calcium-binding protein calretinin is predominantly expressed by late-born CGE interneurons, although a subpopulation also coexpresses SST and might be of MGE

Figure A4: SOX6 and SOX5 are cross-repressive in pallial and subpallial telencephalic progenitor domains. (**a**) SOX5 expression (analyzed by immunocytochemistry), which normally extends to the ventral edge of the pallial-subpallial boundary (blue arrows in wild-type, WT) and is absent from pallial ventricular zone progenitors, ectopically expands into *Sox6*$^{-/-}$ pallial ventricular zone progenitors (blue arrows in *Sox6*$^{-/-}$) at E13.5 and P0. This SOX5 expansion is most pronounced near the PSB at E13.5 and extends evenly throughout the entire pallial ventricular zone by P0. (**b**) Conversely, *Sox6* expression (analyzed by *in situ* hybridization), which normally extends to the dorsal edge of the PSB (red arrows in WT) and is absent from subpallial progenitors, ectopically expands into *Sox5*$^{-/-}$ subpallial ventricular zone progenitors (red arrows in *Sox5*$^{-/-}$) at E13.5 and P0. This *Sox6* expansion is most pronounced near the PSB in the LGE at E13.5 and extends throughout the entire subpallial ventricular zone by P0. Scale bars represent 50 µm.

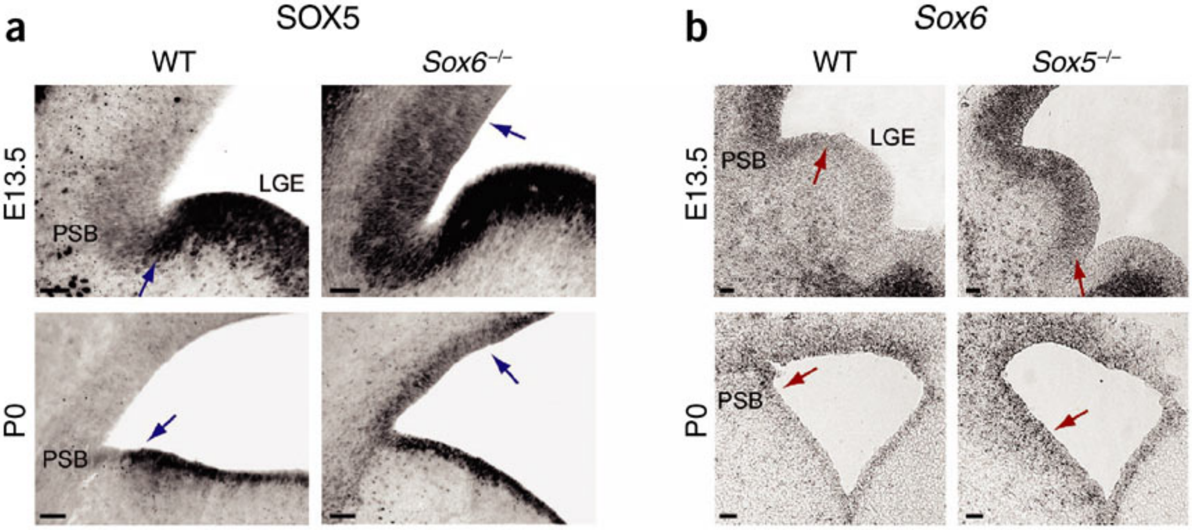

Figure A4 (Continued)

Figure A5: Loss of SOX6 function results in ectopic proneural gene expression in pallial progenitors and subpallial mantle zones. (**a**) *Mash1*, which is normally restricted to subpallial ventricular zone progenitors and is not expressed by pallial ventricular zone progenitors (red arrows) or by postmitotic neurons in subpallial mantle zones (red arrowheads), is ectopically expressed in *Sox6*$^{-/-}$ pallial ventricular zone progenitors and in the MGE and CGE mantle zones at E13.5. (**b**) *Ngn2*, which is normally restricted to pallial ventricular zone progenitors and is not expressed by postmitotic neurons in subpallial mantle zones (red arrowheads), is ectopically expressed in *Sox6*$^{-/-}$ MGE and CGE mantle zones at E13.5. (**c**) As previously reported[4], *Mash1*, which is normally not strongly expressed in pallial ventricular zone progenitors, is ectopically expressed in progenitors of the *Ngn2*$^{-/-}$*; Ngn1*$^{-/-}$ pallial ventricular zone at E14.5 (red arrows). (**d**) As in the wild-type, SOX6 continues to be expressed in *Ngn2*$^{-/-}$*; Ngn1*$^{-/-}$ pallial ventricular zone progenitors (red arrows). SOX6 is ectopically expressed in *Ngn2*$^{-/-}$*; Ngn1*$^{-/-}$ postmitotic pallium-derived neurons in the cortical plate (red arrowheads), consistent with the ectopic expression of subpallial postmitotic signals in pallium-born neurons in the absence of Ngn2 function, as previously described(Fode et al., 2000; Parras et al., 2002). All expression was analyzed by *in situ* hybridization. Scale bars represent 100 µm.

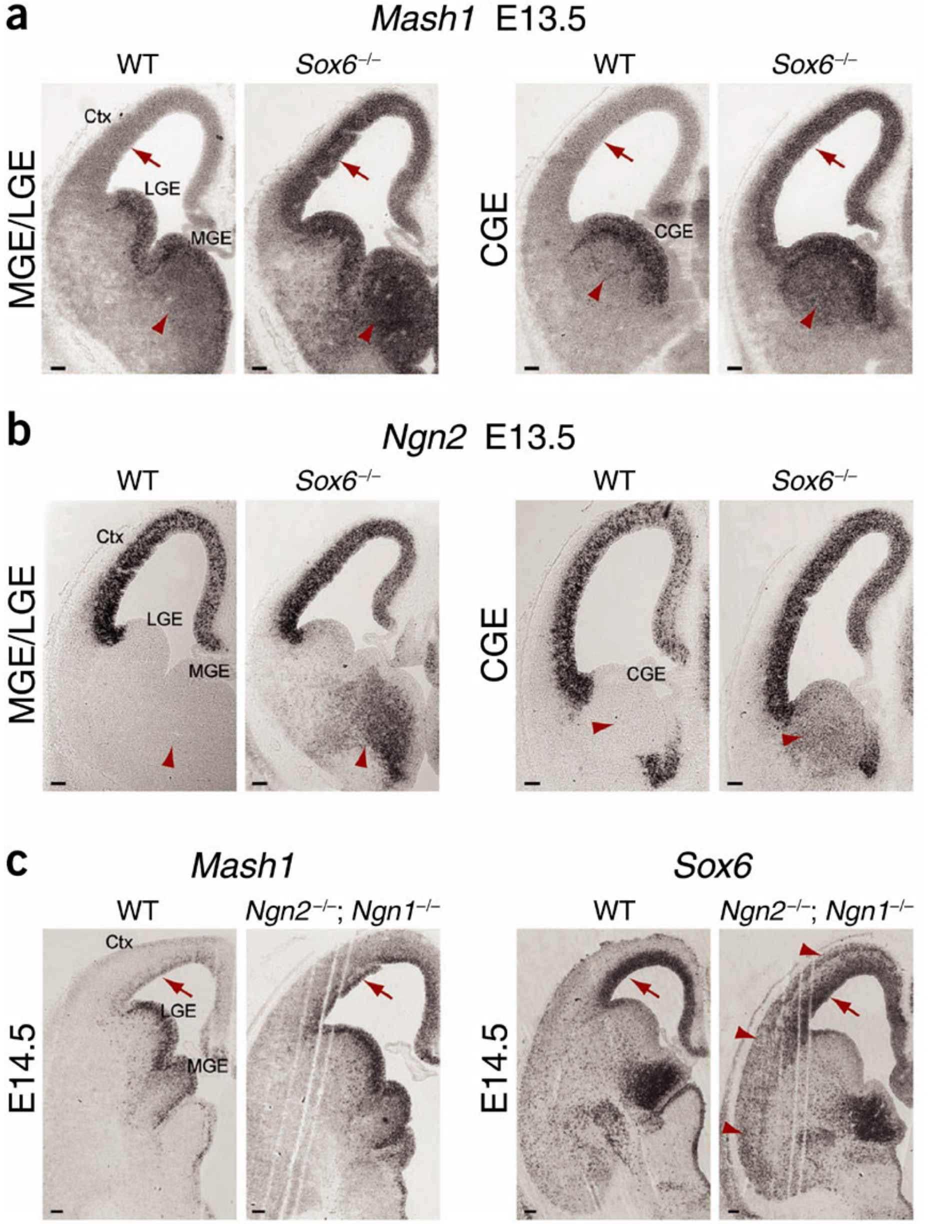

Figure A5 (Continued)

Figure A6: SOX6 regulates transcription factor expression during development. (**a**) *Mash1*, normally absent from pallial VZ progenitors (red arrow) and subpallial mantle zome (red arrowhead), is extopically expressed in these cells in *Sox6*$^{-/-}$ mice, shown here at E17.5. (**b**) *Olig2* , normally expressed in subpallial, but not pallial, VZ progenitors (red arrow), is ectopically expressed in *Sox6*$^{-/-}$ pallial VZ progenitors, shown here at E17.5. (**c**) *Mash1* is not expressed in pallial progenitors (red arrow) and subpallial mantle zones (red arrowhead) in WT and *Sox5*$^{-/-}$ brains, and is equivalently ectopically expressed in both of these cellular populations in *Sox6*$^{-/-}$ and *Sox6*$^{-/-}$/ *Sox5*$^{-/-}$ brains, shown here at E13.5. (WT and *Sox6*$^{-/-}$ panels are reproduced here from Figure A5 for comparison). (**d**) *Ngn2* is not expressed in subpallial mantle zones (red arrowhead) in WT and *Sox5*$^{-/-}$ brains, and is equivalently extopically expressed in these populations in *Sox6*$^{-/-}$ and *Sox6*$^{-/-}$/ *Sox5*$^{-/-}$ brains, shown here at E13.5. Additionally, *Ngn2* expression expands slightly into the dorsal LGE in *Sox6*$^{-/-}$/ *Sox5*$^{-/-}$ brains (red arrow). (WT and *Sox6*$^{-/-}$ panels are reproduced here from Figure A5 for comparison). (**e**) *Pax6* retains its normal mostly pallial VZ progenitor –specific expression (red arrow) in *Sox6*$^{-/-}$ brains, shown here at E13.5. (**f**) *Ngn2* expression, normally absent from subpallial mantle zones (red arrowhead), is extopically expressed in these populations in *Sox6*$^{-/-}$ mice, shown here at E17.5. (a-f) *in situ* hybridization. WT, wildtype; Ctx, cortex; LGE, lateral ganglionic eminence; MGE, medial ganglionic eminence**.** Scale bars, (a-f) 100 µm.

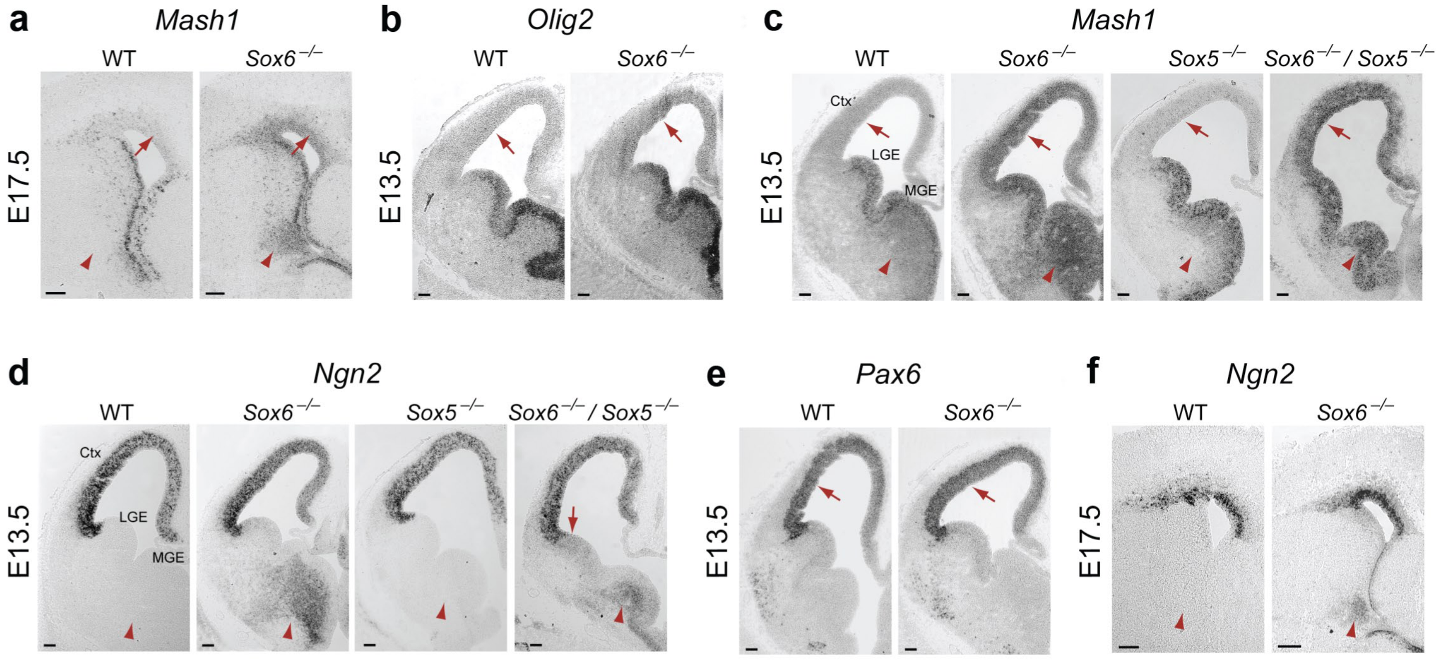

Figure A6 (Continued)

Figure A7: Pallium –derived cortical neuron specification and laminar location is broadly normal in *Sox6*$^{-/-}$ neocortex. At P0, neurons in layer VI and V expression TBR1 **(a)**,CTIP2 **(b),** and SOX5 **(c);** neurons in layers II/III expression *PlexinD1* **(d)**; neurons in layer II-IV expressing *Cux2* **(e);** and cells in layer I expressing Reelin (**f**) have roughtly equivalent expression and laminar location ni WT and *Sox6*$^{-/-}$ neocortex. (a-c, f) innunocytochemistry, (d-e) *in situ* hybridization. WT, wildtype; MZ, marginal zone; CP, cortical plate; WM, white matter. Dotted lines indicate pial surface. Scale bars, (a-f) 50 μm.

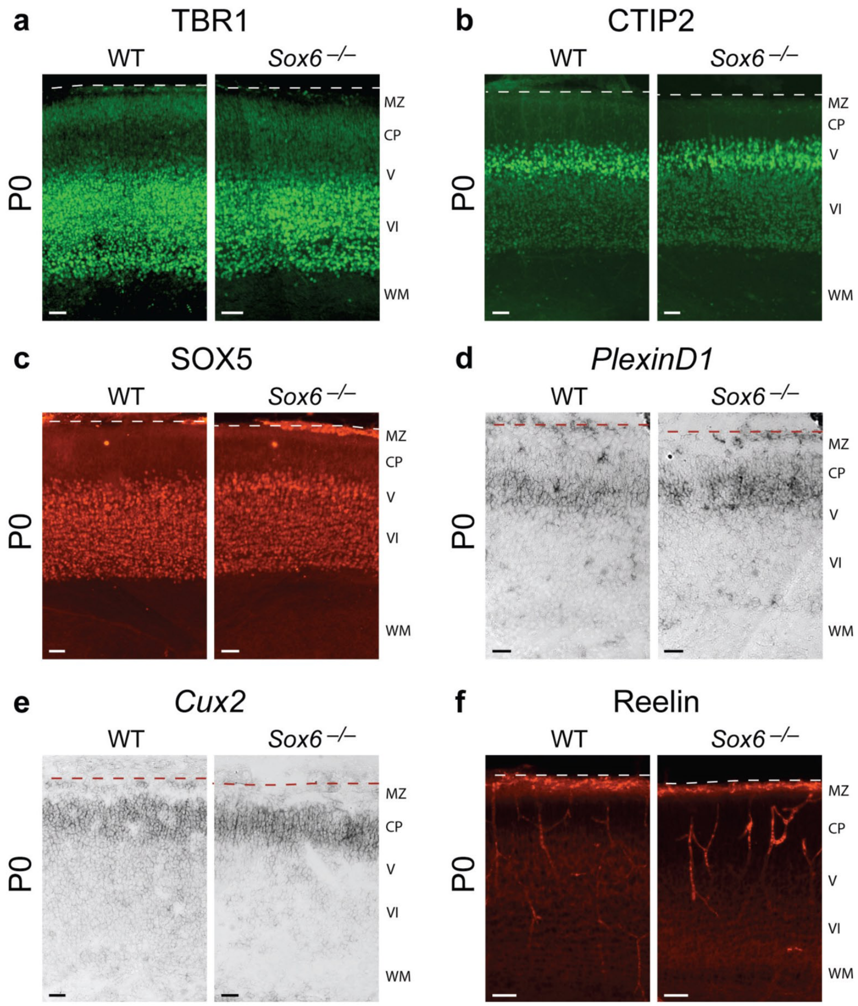

Figure A7 (Continued)

Table A1: Loss of SOX6 function cuases a partial ventralization of the pallial VZ. Microarray comparison (Affymetrix 430.2 GeneChips) between WT (n=4) and *Sox6*$^{-/-}$ (n=4) pallium at E13.5 reveals aberrant expression of genes normally restricted to the subpallium, and decreased expression of genes normally restricted to the pallium. (in addition to its subpallial VZ progenitor expression, *Sox5* is also expressed in the thin cortical plate at E13.5) Fold change indicated change in expression in *Sox6*$^{-/-}$ pallium compared to WT. Change in *Sox6* expression is provided as a positive control. WT, wildtype.

Gene	Fold Change	p-value	WT Expression Domain	WT Normalized Intensity	*Sox6*$^{-/-}$ Normalized Intensity
Dlx1	27.19	5.65E-10	Subpallial	0.01543	0.53511
Dlx2	2.41	4.86E-03	Subpallial	0.09966	0.22774
Dlx4 (7)	6.69	1.20E-03	Subpallial	0.01105	0.07086
Dlx6os1	3.89	6.30E-04	Subpallial	0.11904	0.49277
Gsh2	14.80	4.00E-05	Subpallial	0.03005	0.21532
Isl1	10.09	1.00E-05	Subpallial	0.01884	0.14475
Meis1	1.89	1.33E-06	Subpallial	0.25469	0.48171
Sox5	3.01	4.78E-03	Subpallial	0.06589	0.18576
Boc	-2.1	7.60E-04	Pallial	2.17109	1.07424
Cdon	-57.13	3.04E-11	Pallial	0.22801	0.01149
Chrna	-10.21	8.9E-04	Pallial	0.07319	0.01009
Sox6	-15.40	1.22E-27	Pallial	3.8922	0.22086

Table A1

origin(Cavanagh and Parnavelas, 1988; Cavanagh and Parnavelas, 1990; Butt et al., 2005; Wonders and Anderson, 2006; Miyoshi et al., 2007).

We found that at P14, ~65% of all GAD67-GFP-positive interneurons express SOX6, including essentially all of the PV-positive (86%) and SST-positive (96%) interneurons (both the calretinin-positive (83%) and calretinin-negative (95%) subpopulations), and over one-third of the NPY-positive interneurons (37%). Essentially no VIP-positive interneurons (3%) and only a small minority of calretinin-positive interneurons (11%) express SOX6 (Figure A12a,b). Loss of SOX6 function results in a marked reduction in the number of interneurons expressing PV (93% reduction, $P < 0.0001$) and SST (70% reduction, $P = 0.002$), including the small population of SST and calretinin double-positive interneurons (79% reduction, $P = 0.03$), and the SST-positive and calretinin-negative interneurons (70% reduction, $P = 0.001$). Conversely, there is a corresponding marked increase in the number of NPY-positive interneurons (137% increase; $P = 0.0009$), and no change in the number of VIP- and calretinin-positive interneurons (Figures A11 and A12c,d). Notably, as observed with the general interneuron marker GAD67, all interneuron subtypes that normally express SOX6 inappropriately redistribute to deeper cortical layers in *Sox6*$^{-/-}$ cortex (Figure A11). At P0, when SST expression is normally seen in lateral neocortex and piriform cortex, there are already markedly reduced numbers of *Sox6*$^{-/-}$ SST-positive interneurons (Figure A11), indicating that SOX6 function is necessary at early stages of cortical interneuron molecular differentiation. Together, these data indicate that loss of SOX6 function causes a decrease in the abundance of specific molecularly-defined subtypes of cortical interneurons, many of which are normally MGE-derived during early corticogenesis, without affecting overall cortical interneuron number.

To investigate potential temporal control by SOX6 over cortical interneuron subtype differentiation, particularly given its preferential effects on largely early-born PV- and SST-positive MGE-derived interneurons(Butt et al., 2005; Wonders and Anderson, 2006; Miyoshi et al., 2007) (Cavanagh and Parnavelas, 1988), we performed dual birthdating of interneuron subtypes born at E11.5 and E15.5 using the halogenated thymidine analogs iododeoxyuridine (IdU) and chlorodeoxyuridine (CldU), respectively(Vega and Peterson, 2005), for examination at P14 (Figure A13). We found that in wild-type cortex, NPY-positive interneurons are preferentially born during late versus early corticogenesis (about twice as many CldU and NPY double-positive neurons as there were IdU and NPY double-positive neurons, 180%, $P = 0.02$; Figure A13a), confirming previous reports(Cavanagh and Parnavelas, 1990). In addition, although the number of early- and late-born neurons are equivalent between wild-type and *Sox6*$^{-/-}$ cortices, far fewer *Sox6*$^{-/-}$ early- and late-born interneurons are PV- and SST^{-}positive (early PV:

83% decrease, *P* = 0.002; early SST: 65% decrease, *P* = 0.009; late PV: 88% decrease, *P* = 0.02; late SST: 93% decrease, *P* = 0.04), while an increased number of *Sox6*$^{-/-}$ early- and late-born cortical interneurons are NPY positive (early NPY: 40% increase, *P* = 0.03; late NPY: 90% increase, *P* = 0.04; Figure A13b). These data strongly suggest that, when SOX6 function is absent, many early- and late-born cortical interneurons that would normally differentiate into PV- and/or SST-positive subtypes inappropriately express NPY, which is normally preferentially expressed by later-born subtypes. Taken together, these data suggest that, much like the function of SOX5 in corticofugal projection neurons(Kwan et al., 2008; Lai et al., 2008), SOX6 is necessary for appropriate cortical interneuron molecular subtype diversity, ensuring the appropriate temporal expression of subtype- and function-defining proteins.

Given the pronounced effects of loss of SOX6 function on the largely MGE-derived PV- and SST-positive interneurons and the lack of an effect on overall cortical interneuron numbers, we next examined whether loss of SOX6 function affects the expression of LHX6, a transcription factor that is necessary for the appropriate development of MGE-derived cortical interneuron subtypes(Liodis et al., 2007; Zhao et al., 2008). In *Sox6*$^{-/-}$ mice, LXH6 is expressed in MGE-born interneurons, but these neurons are disorganized as they segregate into migratory streams and populate the cortex at E13.5 (Figure A14a), confirming the tangential migratory abnormalities that we observed in *Sox6*$^{-/-}$*; GAD67-gfp* mice (Figure A8b,c). These data indicate that SOX6 is required for appropriate subtype-specific differentiation from these early stages of interneuron development. At P14, after maturing interneurons have populated the cortex, while there is a modest drop in the abundance of LHX6-positive neurons in *Sox6*$^{-/-}$ cortex (35% reduction, *P* = 0.04), most LHX6-positive interneurons populate the cortex (Figure A14b). LHX6 is not ectopically expressed in neurons born from abnormally ventralized *Sox6*$^{-/-}$ pallial progenitors (Figure A14a) or in *Sox6*$^{-/-}$ CGE (data not shown), indicating that, as in the normal brain, LHX6-positive neurons in *Sox6*$^{-/-}$ cortex are MGE-derived.

To determine whether the abnormally abundant NPY-positive interneurons arise from the *Sox6*$^{-/-}$ MGE population itself (population autonomous, rather than a result of changes outside of this population), we investigated whether there is an increase in the number of MGE-derived LHX6-positive interneurons that express NPY in *Sox6*$^{-/-}$ cortex. In wild-type cortex, very few LHX6-positive neurons coexpress NPY (1% ± 0.5% of LHX6-positive neurons), whereas the number that coexpress NPY in *Sox6*$^{-/-}$ cortex markedly increases (23% ± 3% of LHX6-positive neurons; ~11.5-fold increase, *P* = 0.004; Figure A14c,d). Similarly, there is a very large increase in the number of NPY-positive neurons that immunocytochemically colabel with LHX6 in *Sox6*$^{-/-}$ cortex (22% ± 3% of NPY-positive neurons) as compared with wild-type (4% ± 2% of NPY-positive neurons). In addition, the large majority of these

Sox6$^{-/-}$ LHX6 and NPY double-positive neurons are found in deep cortical layers (81% ± 5%), further suggesting they are of early-born MGE origin (Figure A14d). Taken together, these interneuron subtype analyses indicate that SOX6 functions in a population autonomous manner, controlling the appropriate molecular differentiation of MGE-derived cortical interneuron subtypes.

An additional (although not mutually exclusive) potential explanation for the increase in the number of *Sox6*$^{-/-}$ NPY-positive interneurons is that they might be born from abnormally ventralized *Sox6*$^{-/-}$ pallial progenitors. However, our data indicate that *Sox6*$^{-/-}$ NPY-positive neurons are not pallium-derived: LHX6-positive interneurons in *Sox6*$^{-/-}$ cortex do not express TBR1 (Figure A15), a transcription factor that is broadly expressed by pallium-derived pyramidal neurons through P14, and all NPY-positive neurons in *Sox6*$^{-/-}$ cortex express GAD67-GFP (Figure A15), which is not expressed by neurons born from partially ventralized *Sox6*$^{-/-}$ pallial progenitors (Figure A8b).

In sum, we found that SOX6 is largely mutually exclusively expressed and cross-repressively interacts with highly related SOX5 during telencephalic development, critically controlling pallial progenitor identity and cortical interneuron differentiation and diversity. We previously found that subtype differentiation in the complementary population of corticofugal projection neurons is analogously controlled by SOX5 (Lai et al., 2008). Taken together, these simultaneous, independent, and functionally parallel controls critically underlie much of the tremendous neuronal diversity in the neocortex (Figure A16).

Figure A8: Loss of SOX6 function results in abnormal early cortical interneuron differentiation, without a change in interneuron number. (**a**) Although excitatory neuron-specific *Vglut2* is not normally expressed in neurons born in the subpallium, it is ectopically expressed in the subpallial mantle zone in $Sox6^{-/-}$ mice at E15.5 (red arrowheads; analyzed by *in situ* hybridization). (**b**,**c**) GAD67-GFP-positive neurons are born in both wild-type and $Sox6^{-/-}$ MGE (white arrowheads, analyzed by immunocytochemistry). However, as GABAergic cortical interneurons tangentially migrate into the cortex, the leading edge of the marginal zone (MZ) migratory stream is consistently less advanced in the $Sox6^{-/-}$ cortex compared with the wild-type cortex (white arrows; 60% reduction in distance, $P = 0.03$; **c**). Dotted lines (**b**) indicate lateral ventricle boundary. IZ, intermediate zone. (**d**) There is no difference between wild-type and $Sox6^{-/-}$ cortex in the number of migrating cortical interneurons in either the marginal zone or intermediate zone/SVZ migratory streams. Scale bars represent 150 μm (low magnification, **a**), 100 μm (high magnification in **a** and low magnification in **b**), and 50 μm (high magnification, **b**). Results are expressed as mean ± s.e.m.

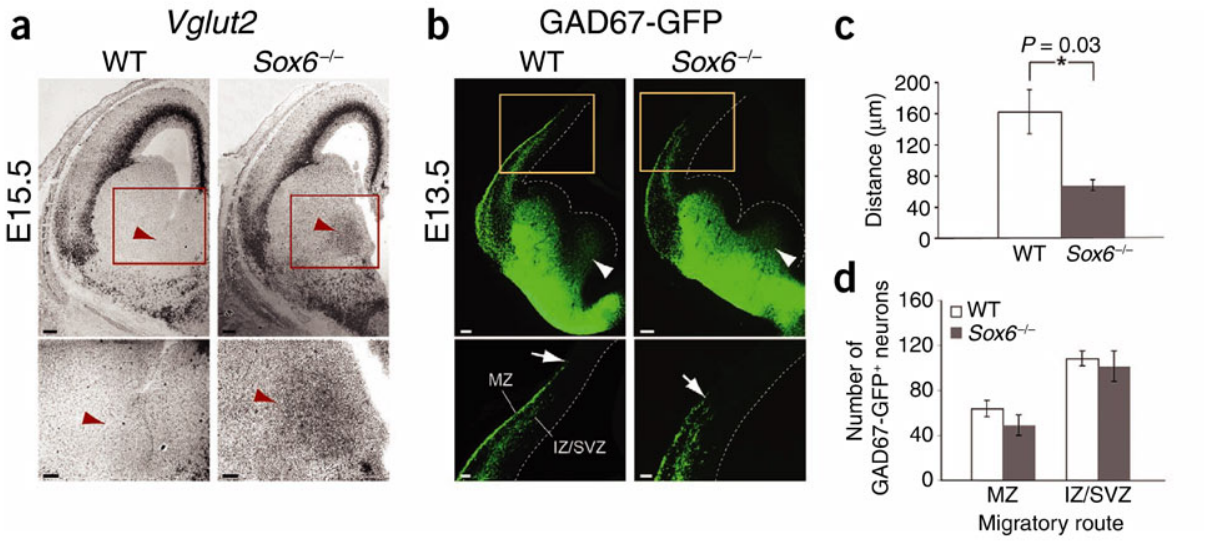

Figure A8 (Continued)

Figure A9: Measurement of the tangential distance between the leading edge of the MZ and IZ/SVZ cortical interneuron migratory streams, and the number of interneurons migrating within each of these streams. **(a)** The distance (solid yellow line) was measured in μm between the position of the soma of the leading neuron of the MZ stream (white arrow), radially projected to the pial surface, and the correspondinf position of the soma of the leading neuron in the IZ/SVZ streasm (white arrowhead), radially projected to the pioal surface, determined by drawing imaginary lines (dotted white lines) radially from the MZ and IZ/SVZ strease perpendicular to the surface of the brain (see Methods). **(b)** Tangentially migrating cortical interneurons were quantified at three anatomically defined points in both the MZ and IZ/SVZ migratory streams in *GAD67-GFP* WT and *Sox6*$^{-/-}$ mice at E13.5 (see Methods). (a,b) immunosytochemistry. WT, wildtype; MZ, marginal zone; IZ, intermediate zone; SVZ, subventricular zone. Scale bars, (a,b) 25 μm.

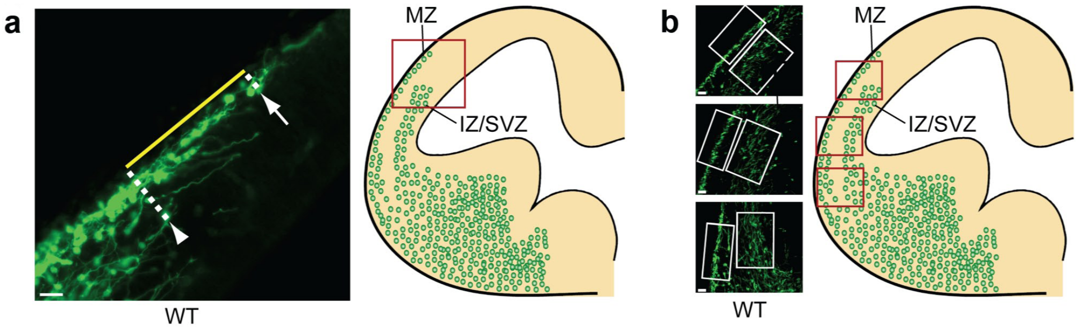

Figure A9 (Continued)

Figure A10: Loss of SOX6 function disrupts the normal laminar position and morphology of cortical interneurons. (**a**–**d**) Analysis of *GAD67-gfp* mice revealed that, although there are equal numbers of cortical interneurons at P0 (**a**) and P14 (**b**) in wild-type and *Sox6*$^{-/-}$ cortex, there is a redistribution of interneurons toward deeper cortical layers in *Sox6*$^{-/-}$ cortex compared with wild-type (**c**,**d**). Quantification at P0 (**c**) revealed a proportional increase in interneuron density in the deepest bin, bin 1, by 13% (P = 0.01) and bin 2 by 5% (P = 0.04), and a proportional decrease in the more superficial bin 3 by 7% (P = 0.05) and bin 4 by 10% (P = 0.004). Quantification at P14 (**d**) revealed an increase in interneuron density in bin 1 by 10% (P = 0.001) and a decrease in the more superficially located bin 3 by 5% (P = 0.0003). Red lines (**a**,**b**) indicate subdivision into four bins for quantification (see Online Methods). Interneurons have abnormal tangential morphology in *Sox6*$^{-/-}$ cortex compared with the radially oriented interneurons in wild-type cortex (**a**, red arrowheads). (**a**,**b**) immunocytochemistry. CP, cortical plate; I-VI, cortical layers I-VI; WM, white matter. Dotted lines indicate pial surface. Scale bars represent 200 μm (low magnification, **a**), 50 μm (intermediate magnification, **a**), 25 μm (high magnification, **a**), 300 μm (low magnification, **b**) and 100 μm (high magnification, **b**). Results are expressed as mean ± s.e.m.

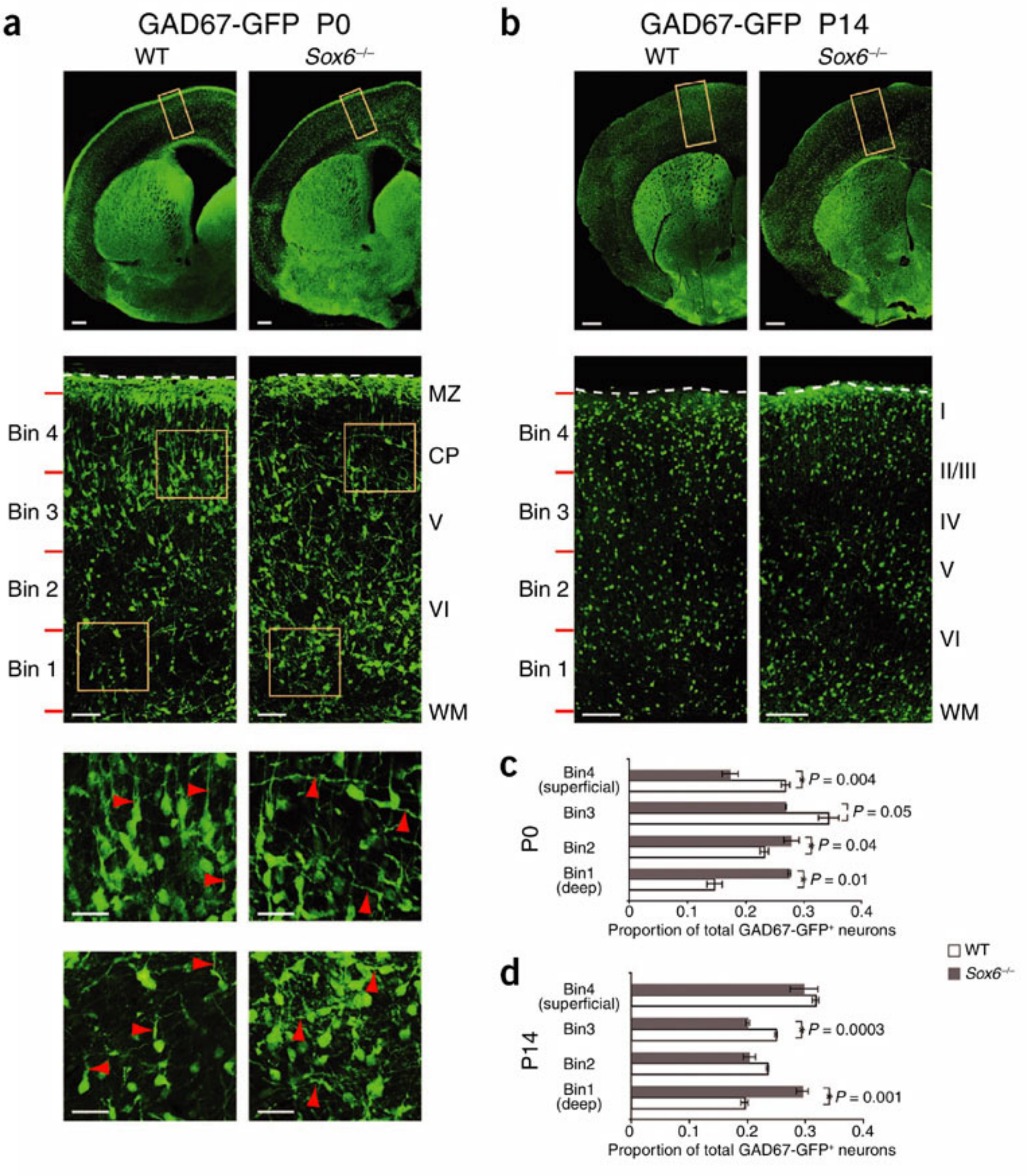

Figure A10 (Continued)

Figure A11: SOX6 controls interneuron subtype development and laminar location. **(a)** At P0, Calb$^+$ interneurons have abnormal laminar distribution and tangentially oriented morphology (red arrowheads) in *Sox6*$^{-/-}$ neocortex comparte to WT. **(b)** At P0, SST is predominantly expressed in neurons in the lateral neocortex, piriform cortex, and striatum in WT brains (white arrowheads); the number of SST$^+$ interneurons is strikingly reduced in *Sox6*$^{-/-}$ brains. **(c-i)** The density of PV$^+$ interneurons **(c)** is dramatically reduced in *Sox6*$^{-/-}$ cortical layers in bin 2 ($p=0.02$), at the expense of more superficial layer in bin 3($p=0.04$). The density of SST$^+$ interneurons **(d)** is also reduced in *Sox6*$^{-/-}$ cortex (70% decrease; $p=0.002$), with those remaining preferentially populating the lowest cortical layers in bin1 ($p=0.03$), at the expsense of the more superficial layers in bin 2 ($p=0.04$) and bin 3 ($p=0.01$). The density of NPY$^+$ interneurons **(e)** is greatly increased in *Sox6*$^{-/-}$ neocortex (136% increase; $p=0.0009$), especially in the lowest cortical layers in bin 1 ($p=0.006$), at the expense of the most superficial layers in bin 4 ($p=0.006$). There is no change in the density of VIP$^+$ interneurons in *Sox6*$^{-/-}$ neocortex **(f).** The density of all Calret$^+$ interneurons is not changed in *Sox6*$^{-/-}$ neocortex **(g),** but there is a laminar redistribution, whith more Calret$^+$ interneurons occupying deeper cortical layers in bin 2 ($p=0.01$), at the expense of the most superficial layers in bin 4 ($p=0.04$), most likely representing a change in the small population of SST$^+$/Calret$^+$ interneurons **(h),** whose density is dramatically reduced in *Sox6*$^{-/-}$ neocortex (79% reduction; $p=0.03$), whith the reduction occurring predominantly superficially in the uppermost bin 4 ($p=0.0002$). The density of SST$^+$/Calret$^-$ interneurons **(i)** is reduced in *Sox6*$^{-/-}$ neocortex (70% reduction; $p=0.001$), with those remaining preferentially population the deepest cortical layers in bin 1 ($p=0.01$) at the expense of more superficial layers in bin 3 ($p=0.005$). See figure A10 for bin placement. (a,b) immunocytochemistry. WT, wildtype; MZ marginal zone; CP, cortical plate; WM, white matter. Scale bar, (a,b; low magnification) 200 μm, (a; high magnification) 50 μm; (b; high magnification) 100 μm. Resuts are expessed at the mean ± SEM.

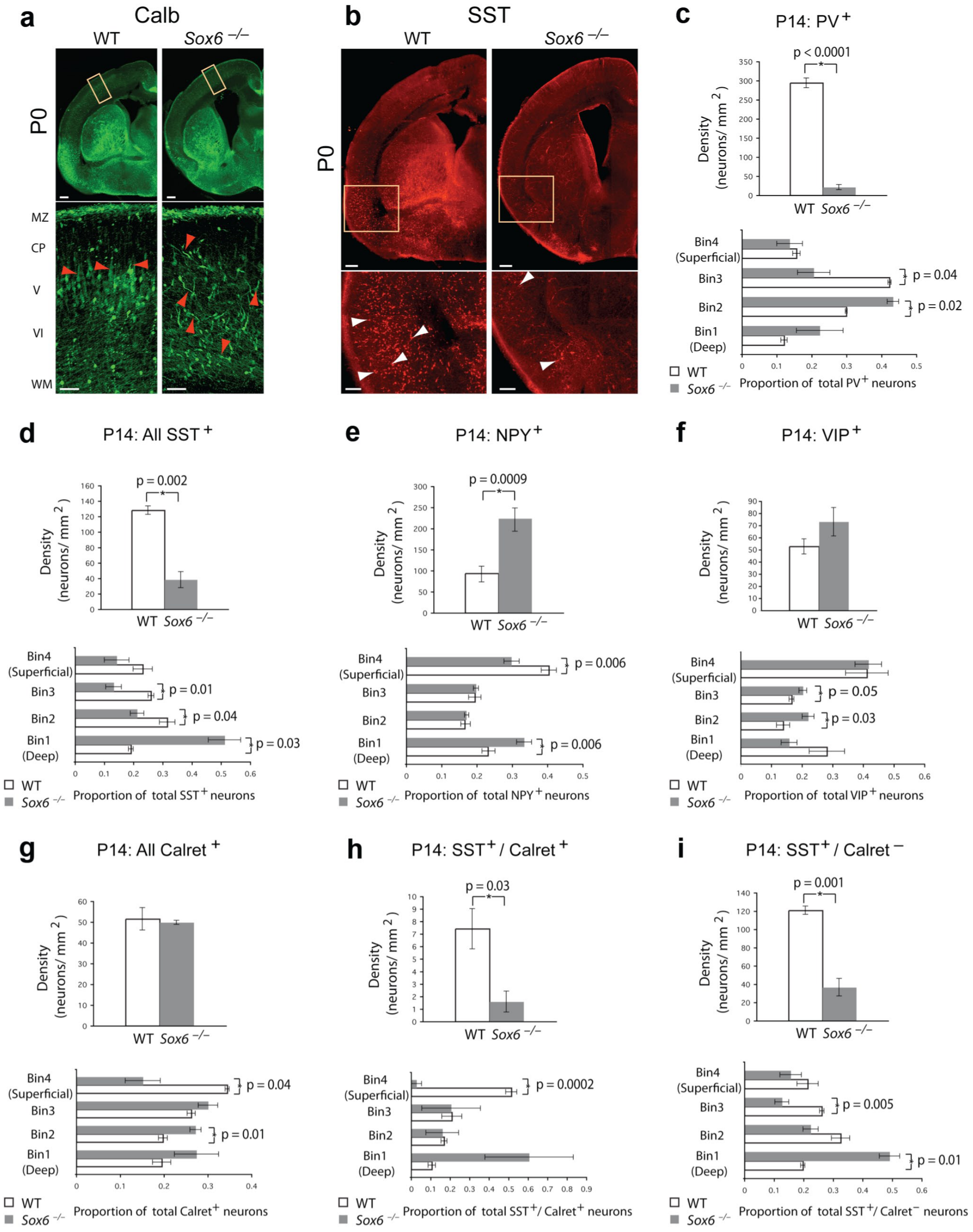

Figure A11 (Continued)

Figure A12: SOX6 is necessary for cortical interneuron subtype development. (**a**,**b**) At P14, SOX6 is expressed in ~65% of all neocortical GAD67-GFP-positive interneurons (analyzed by immunocytochemistry), including essentially all PV-positive (86%), SST-positive (96%), SST and calretinin (Calret) double-positive (83%) (white arrowheads), and SST-positive and calretinin-negative (95%) interneurons. SOX6 is expressed in more than one-third of all NPY-positive interneurons (37%) (white arrowheads; open arrowheads indicate NPY-positive, SOX6-negative interneurons), in essentially no VIP-positive interneurons (3%; open arrowheads indicate VIP-positive, SOX6-negative interneurons) and in very few calretinin-positive interneurons (11%; open arrowheads indicate calretinin-positive, SOX6-negative interneurons). Red lines in **a** indicate approximate regions of magnification in **b**. (**c**,**d**) At P14, PV-positive cortical interneuron numbers (white arrowheads) are diminished in *Sox6*$^{-/-}$ compared with wild-type cortex (93% reduction, $P < 0.0001$), as are SST-positive cortical interneuron numbers (red neurons, white arrowheads; 70% reduction, $P = 0.002$). There is no change in the number of calretinin-positive interneurons (green neurons, open arrowheads), although the subset of SST and calretinin double-positive interneurons (yellow neurons, white arrows) is reduced in number in *Sox6*$^{-/-}$ compared with wild-type cortex (79% reduction, $P = 0.03$). The subset of SST-positive, calretinin-negative interneurons is also reduced (70% reduction, $P = 0.001$). The number of NPY-positive cortical interneurons (white arrowheads) is increased in *Sox6*$^{-/-}$ compared with wild-type cortex (137% increase, $P = 0.0009$). There is no change in the number of VIP-positive interneurons (white arrowheads). The positions of the yellow boxes in the low-magnification panels (**c**) are representative of the neocortical position examined in the high-magnification panels. Quantification is represented as the percentage of neuron density in *Sox6*$^{-/-}$ compared with wild-type. Dotted lines indicate pial surface (**a**,**c**). Scale bars represent 300 μm (low magnification, **a**,**c**), 100 μm (high magnification, **a**,**c**) and 50 μm. (**b**). Results are expressed as mean ± s.e.m.

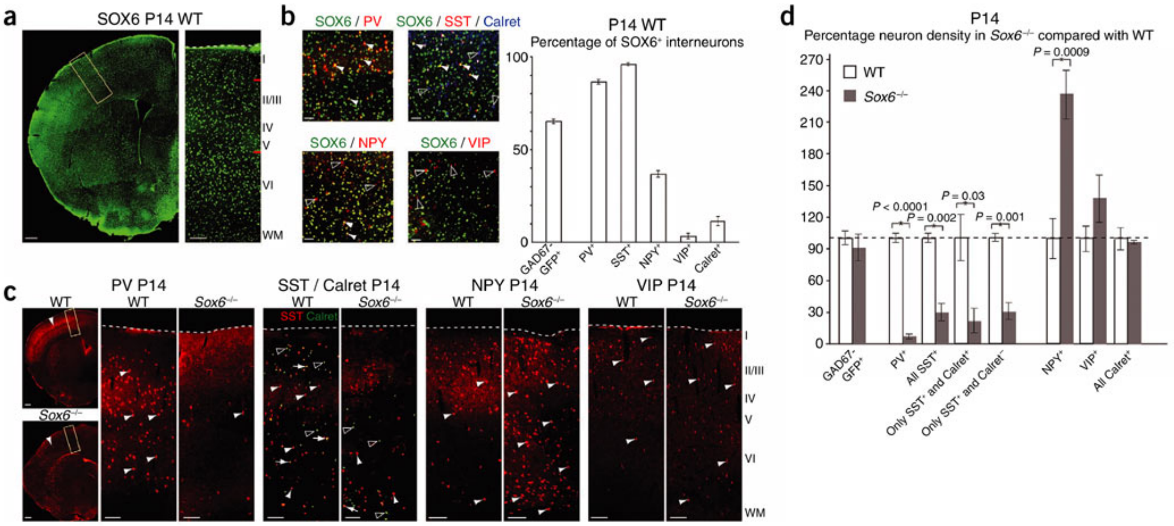

Figure A12 (Continued)

Figure A13: Loss of SOX6 function produces an increased number of early- and late-born NPY-positive cortical interneurons. (**a**,**b**) Dual birthdating of cortical interneurons using IdU (E11.5) and CldU (E15.5) (analyzed by immunocytochemistry) reveals a decrease in the number of PV- and SST-positive early- and late-born interneurons (early PV: 83% decrease, $P = 0.002$; early SST: 65% decrease, $P = 0.009$; late PV: 88% decrease, $P = 0.02$; late SST: 93% decrease, $P = 0.04$; **b**) and a large increase in the number of NPY-positive early- (white arrowheads) and late-born (white arrows) interneurons (early NPY: 40% increase, $P = 0.03$; late NPY: 90% increase, $P = 0.04$; **b**). Colocalization was strictly assessed as homogenous, strong nuclear IdU or CldU label surrounded by cytoplasmic PV, SST or NPY labeling (NPY/IdU colocalization provided as a representative example in **a**, white arrowhead). Quantification is represented as the percentage of neuron density in *Sox6*$^{-/-}$ cortex compared with wild-type. Dotted lines in **a** indicate pial surface. Scale bars represent 100 μm (low magnification, **a**) and 10 μm (high magnification, **a**). Results are expressed as mean ± s.e.m.

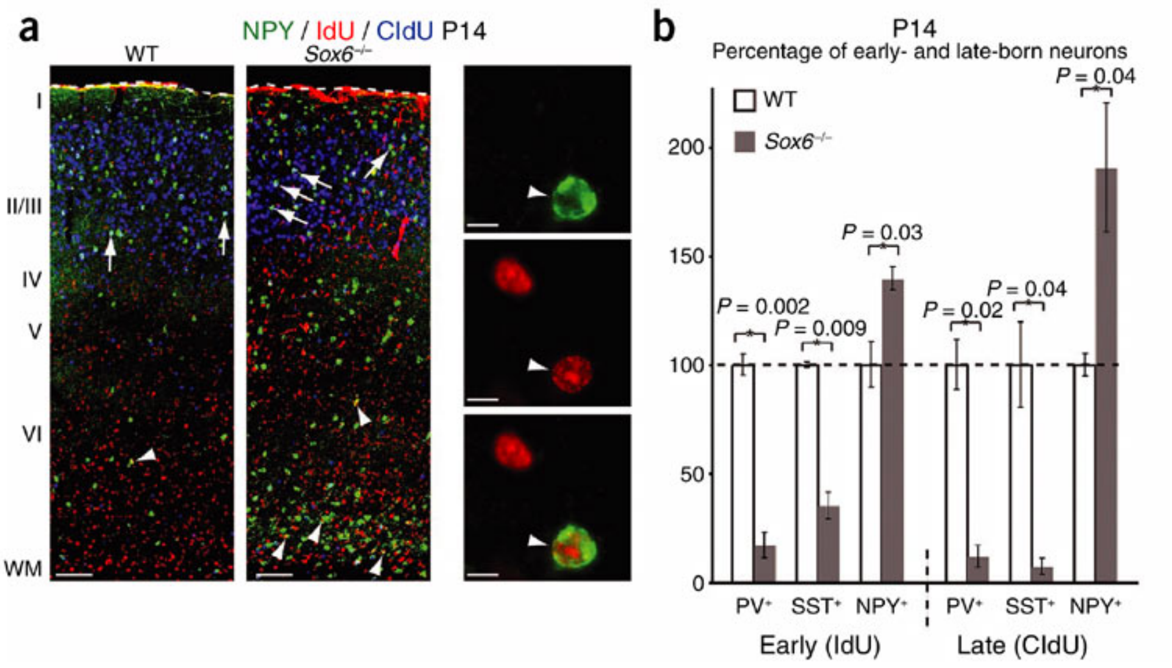

Figure A13 (Continued)

Figure A14: SOX6 control over MGE-derived cortical interneuron subtype differentiation is population autonomous. (**a**) At E13.5, during the early stages of cortical interneuron differentiation, MGE-born interneurons in wild-type and *Sox6*$^{-/-}$ telencephalon express *Lhx6* (low magnification; red arrowheads; *in situ* hybridization), but the development of these neurons is disrupted in *Sox6*$^{-/-}$ mice. The migratory streams are disorganized compared with wild-type mice (high magnification, red arrowheads), and the leading edge of the marginal zone migratory stream compared with the intermediate zone/SVZ stream is consistently shorter in *Sox6*$^{-/-}$ compared with wild-type mice (red arrows). (**b**) By P14, a large subset of *Lhx6*-positive neurons present in the cortex of wild-type mice have populated the maturing *Sox6*$^{-/-}$ cortex (red arrowheads; *in situ* hybridization). (**c**,**d**) At P14 in wild-type cortex, the vast majority of LHX6-positive neurons (99% ± 0.5%) do not express NPY (**d**, white arrowheads; immunocytochemistry), whereas LHX6-positive neurons increased their coexpression of NPY in *Sox6*$^{-/-}$ cortex (**d**, white arrows) (~11.5-fold increase, $P = 0.004$; **c**), especially in deeper layers (81% ± 5% of colocalization in the two deepest bins; see **Fig. 5b** for bin placement). Quantification is represented as the density of neurons per mm^2 (**c**). Dotted lines in **b** and **d** indicate pial surface. Scale bars represent 100 µm (low magnification in **a**, **b**, and **d**), 50 µm (high magnification, **a**) and 25 µm (high magnification, **d**). Results are expressed as mean ± s.e.m.

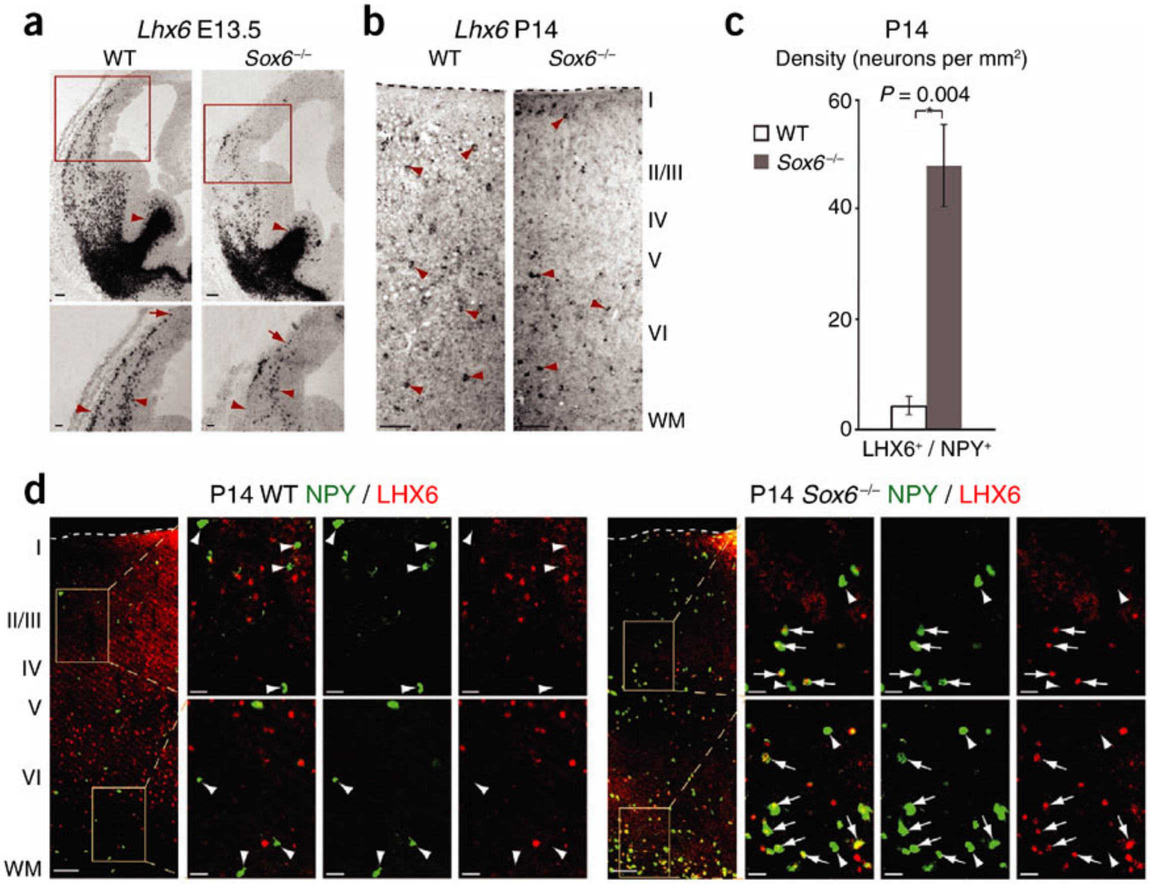

Figure A14 (Continued)

Figure A15: NPY$^+$ neurons in *Sox6*$^{-/-}$ cortex are not pallium-born. **(a)** TBR1, broadly expressed by pallium-derived neurons through the second postnatal week, is not expressed by NPY$^+$ neurons in WT or *Sox6*$^{-/-}$ cortex (white arrowheads). **(b)** All NPY$^+$ neurons in WT and *Sox6*$^{-/-}$ cortex are GAD67$^+$ interneurons (white arrowheads), as assessed in *GAD67-GFP* mice. (a,b) immunocytochemistry. WT, wildtype; WM, white matter. Dotted lines indicate pial surface. Scale bars, (a,b; low magnification) 100 μm, (a,b; high magnification) 25 μm.

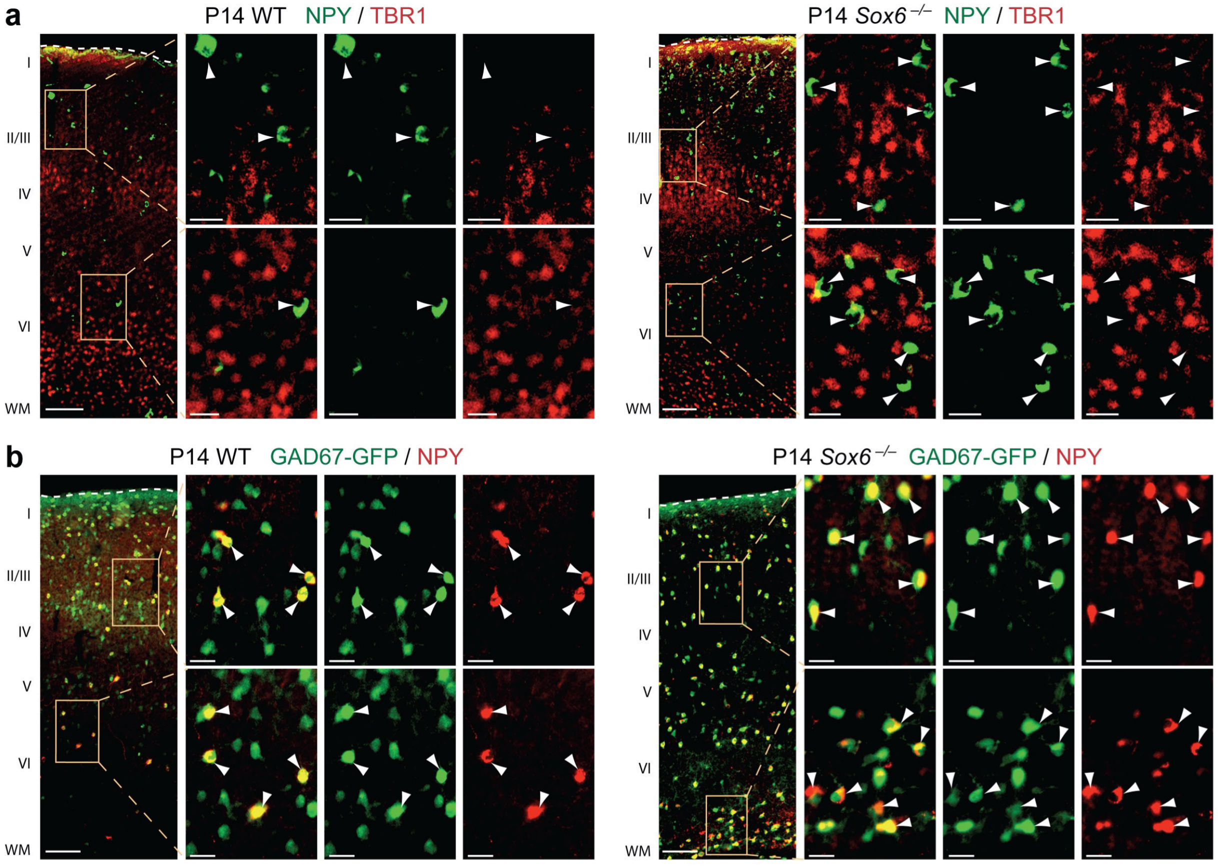

Figure A15 (Continued)

Figure A16: Schematic model for cross-repressive and network interactive function of SOX6 and SOX5 in progenitors and postmitotic cortical neurons. SOX6 and SOX5 are cross-represseive in pallial and subpallial progenitors, respectively. The purple area at the PSB indicated a discrete region of SOX6 and SOX5 co-expression in the dorsal subpallium, encompassing the source of the lateral cortical streasm, which populates more ancient basal telencephalic structures including anygdala and piriform cortex. Within the pallial and subpallial domains, SOX6 and SOX5 integrate and interact with key telencephalic patterning molecular controls. SOX6 and Ngn2 are both necessary, but neither is alone sufficient, to repress Mash1 expression and maintain dorsal identity in pallial progenitors. Postmitotically, SOX5 controls the subtype development of deep layer, corticofugal projection neurons(Kwan et al., 2008; Lai et al., 2008), while SOX6 represses the expression of progenitor-specific genes in subpallial mantle zones, and controls cortical interneuron subtype differentiation, potentially acting downstream of NKX2-1, and interacting with LHX6 (dashed lines). These diverse functions in mutally exclusice, but complementary populations of cells are required for the establishment of appropriate cortical neurons diversity. PSB, pallial-subpallial boundary; VZ, ventricular zone. Adapted from(Schuurmans and Guillemot, 2002).

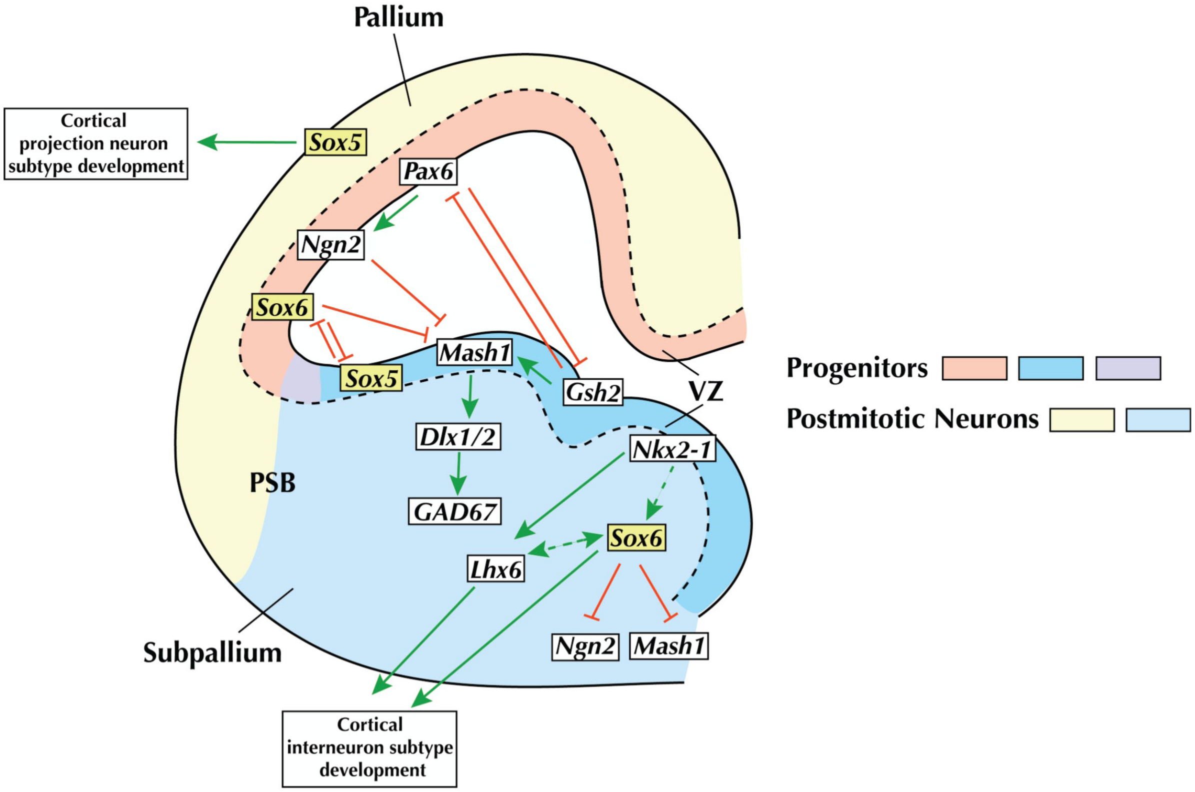

Figure A16 (Continued)

8.5 Discussion

The cellular diversity of the CNS arises largely from the parsimonious use of a relatively small number of genes across distinct cell types, exemplified here by the multiple and distinct functions of SOX6 during neocortical development. We found that the highly related transcription factors SOX6 and SOX5 (which are coexpressed with largely overlapping functions in other organ systems(Smits et al., 2001; Stolt et al., 2006)) are expressed and function in the telencephalon in a cross-repressive and complementary fashion. SOX6 functions cooperatively with previously described pallial/subpallial parcellation programs to control pallial progenitor identity, and it is critical for the subtype diversity of cortical interneurons, parallel to SOX5 function in pallium-derived corticofugal projection neurons(Lai et al., 2008).

In the developing telencephalon, the repressive action of SOX6 and Ngn2 (Fode et al., 2000) on Mash1 expression is critical for maintaining pallial progenitor identity. Our data indicate that the expression of SOX6 and Ngn2 are independent, that these two Mash1-repressive interactions are cooperative, and that both are individually necessary, although neither of them is sufficient alone, for repressing subpallial identity. Although Pax6 directly activates Ngn2 expression in the telencephalon, spinal cord, and retina(Scardigli et al., 2003), it does not appear to act transcriptionally upstream or downstream of SOX6, as others have shown that microarray analysis of *Pax6*$^{-/-}$ pallium does not reveal a change in SOX6 expression(Holm et al., 2007), and we found that the *Sox6*$^{-/-}$ pallium continues to express Pax6. This strongly suggests that there are at least two pathways that restrict Mash1 expression to the subpallium: a classic Pax6-Ngn2 pathway, and a cooperative pathway in which SOX6 is expressed independently of Pax6 and Ngn2.

Despite dorsal ectopic expression of Mash1, SOX5, and other subpallial ventricular zone signals in *Sox6*$^{-/-}$ pallial progenitors, postmitotic projection neuron progeny appear to develop normally. This contrasts with the apparently more severe ventralization of these neurons in *Ngn2*$^{-/-}$ mice (including ectopic expression of GAD67)(Fode et al., 2000; Parras et al., 2002), suggesting that, although initial stages of ventralization occur in *Sox6*$^{-/-}$ pallium (Table A1), dorsal identity regulators that persist in *Sox6*$^{-/-}$ pallial progenitors, including perhaps Ngn2 and Ngn1, are sufficient to override and mask Mash1 and other subpallial fate programs, as has been suggested previously(Britz et al., 2006). Therefore, SOX6 likely functions in concert with additional pallial patterning regulators to control dorsal identity.

Notably, SOX6 and SOX5 are coexpressed in a discrete region of the dorsal subpallial ventricular zone near the PSB. This region encompasses a proliferative source for the lateral cortical stream, which populates structures of the basal limbic system, including the amygdala and piriform cortex(Puelles et al., 2000; Carney et al., 2006). These paleopallial structures are of older evolutionary origin than the neocortex of the neopallium. SOX6 and SOX5 may have been evolutionarily selected to act cooperatively in this unique population of progenitors, as they do in chondrocytes and spinal cord oligodendrocytes. In contrast, the later evolution of the neocortex may have driven the separation of these transcription factors, contributing to the evolution of mammalian neocortical development(Molnar and Butler, 2002). Further molecular phylogenetic analysis might elucidate whether SOX6 and SOX5 cooperate during paleopallium development, and at what point SOX6 and SOX5 function diverged into discrete telencephalic progenitor and neuronal populations.

SOX6 is also necessary for successive stages of cortical interneuron postmitotic differentiation. Immature neurons in *Sox6*$^{-/-}$ subpallial mantle zones have mixed progenitor/postmitotic and dorsal-ventral molecular identity, aberrantly expressing subpallial progenitor-restricted Mash1, pallial progenitor-restricted Ngn2 and pallial postmitotic-restricted Vglut2. As *Sox6*$^{-/-}$ cortical interneurons mature, they are broadly specified as GABAergic and populate the cortex in correct numbers, but finer molecular analysis revealed aberrant subtype differentiation, as exemplified by MGE-born cortical interneuron populations. In the absence of SOX6 function, there is a large increase in the abundance of NPY-positive interneurons at the expense of PV- and SST-positive interneurons, revealing abnormal subtype-defining neurotransmitter/molecular identity, one of multiple core contributing factors to the overall subtype identity and function of a neuron. Additional morphological and electrophysiological analyses might further examine whether these aberrant NPY-positive interneurons fully adopt functions that are normally associated with NPY expression.

Three potential (and not mutually exclusive) processes might account for the loss of *Sox6*$^{-/-}$ cortical interneuron molecular subtype diversity, without an overall reduction of interneuron number. One possibility is that population autonomous subtype specification is primarily affected, such that MGE-derived interneurons that would normally differentiate into subtypes that express PV and/or SST abnormally differentiate and express NPY. Another possibility is that MGE-born interneurons that normally would have been PV- and SST-positive might selectively not populate the cortex, and CGE progenitors might simultaneously increase their NPY-positive interneuron output. A third, similar possibility is that abnormally partially ventralized *Sox6*$^{-/-}$ pallial progenitors are a source of these new NPY-positive neurons, which populate the cortex in place of MGE-born interneurons.

Our data very strongly favor the first interpretation of SOX6 control over population autonomous subtype differentiation. 1) There is a very large increase in the number of MGE-derived LHX6-positive interneurons that express NPY concomitant with their loss of PV and SST expression. 2) Our birthdating analysis revealed that, although the overall numbers of both early- and late-born neurons are unaffected by the loss of SOX6 function, a large number of early-born interneurons, which tend to arise from the MGE rather than the CGE, do not express PV or SST, but instead inappropriately express NPY. 3) Abnormal molecular identity in the *Sox6*$^{-/-}$ MGE mantle zone (Ngn2, Mash1, Vglut2), observed as soon as the interneurons are born, strongly suggests a population autonomous effect of SOX6 function very early in neuronal differentiation. 4) There is no evidence of a substantial increase in the number of GAD67-GFP-positive migrating interneurons originating from *Sox6*$^{-/-}$ CGE, or any from the pallium, that would be required to compensate for the hypothetical loss of MGE-born interneurons (predicted for the second and third possibilities listed above). 5) Regarding the second possibility, that the NPY-positive neurons are all CGE-derived, it is neither likely nor supported by any of the data that *Sox6*$^{-/-}$ CGE progenitor populations would increase their neurogenic rate in the absence of SOX6, as SOX6 is not normally expressed in CGE ventricular zone progenitors. 6) Finally, regarding the third possibility, that the NPY-positive neurons are pallium derived, in *Sox6*$^{-/-}$ cortex, all of the NPY-positive neurons express GAD67, which is not ectopically expressed in *Sox6*$^{-/-}$ pallium-born neurons, and they do not express TBR1, which is broadly expressed by pallium-derived projection neurons, indicating that the NPY-positive neurons are not born from pallial progenitors. Taken together, these results reinforce previous findings on the population autonomous functions of SOX6 both in and outside of the nervous system(Smits et al., 2001; Stolt et al., 2006), indicating that SOX6 functions as a critical control over the appropriate molecular differentiation of MGE-derived cortical interneuron subtypes.

Additional interneuron developmental deficits might be occurring in the absence of SOX6 function. Although all of the LHX6-positive neurons in *Sox6*$^{-/-}$ cortex express GAD67-GFP, indicating their broad differentiation into GABAergic interneurons, some do not express NPY, PV, SST, or other major cortical interneuron subtype molecular markers. This suggests that some *Sox6*$^{-/-}$ MGE-derived interneurons might stall during later stages of subtype differentiation. In addition, these data do not exclude the possibility that SOX6 also functions in the population autonomous subtype differentiation of SOX6-positive CGE-derived cortical interneurons, or perhaps via additional non-population autonomous pathways.

NKX2-1 is a transcription factor that acts upstream of LHX6 (Du et al., 2008), and was recently shown to be critical for multiple stages of cortical interneuron development, including the temporal fate specification of cortical interneuron subtypes(Butt et al., 2008; Nobrega-Pereira et al., 2008) Loss of NKX2-1 function results in a reduction in the number of PV- and SST-positive cortical interneurons and a corresponding increase in the number of VIP- and calretinin-positive interneurons. Given our results, SOX6 might be functioning, at least partially, in the postmitotic downstream execution of NKX2-1 signaling, potentially interacting with LHX6 (Liodis et al., 2007; Zhao et al., 2008), thereby regulating the temporal pacing of MGE-derived cortical interneuron fate specification and differentiation (Figure A16).

Additional gain- and loss-of-function analyses might reveal potential functional interactions between these transcription factors during interneuron subtype specification and differentiation.

Much like pallium-born projection neuron subtypes, cortical interneuron subtype identity is largely determined by the time of birth. Fate-mapping experiments using H^3-thymidine labeling and, more recently, genetic tools investigating subtype specification in MGE-born interneurons have shown that SST-positive interneurons, which are diminished in number in *Sox6*$^{-/-}$ cortex, are on average born at earlier stages of corticogenesis, whereas NPY-, VIP- and CR-positive interneurons, whose numbers are either increased or maintained in *Sox6*$^{-/-}$ cortex, are born later (Cavanagh and Parnavelas, 1988; Cavanagh and Parnavelas, 1990; Miyoshi et al., 2007; Butt et al., 2008). These data raise the hypothesis that, during cortical interneuron development, SOX6 participates in setting the pace for the proper timing of developmental transitions. In this model, loss of SOX6 might result in premature differentiation into neurons that are normally born at later developmental stages, at the expense of those born at earlier stages. Supporting this interpretation, our dual IdU/CldU birthdating analysis of the molecular differentiation of early- and late-born neurons in *Sox6*$^{-/-}$ cortex revealed that early-born neurons aberrantly differentiate and express the later-born subtype-defining protein NPY. As the lineage relationships of particular cortical interneuron subtypes are further clarified, it will be possible to discern whether loss of SOX6 function alters temporal development in a lineage (for example, those that would normally be SST-positive neurons aberrantly differentiate into NPY-positive neurons born later from potentially the same lineage) and/or whether loss of SOX6 function results in inappropriate differentiation across lineages (for example, those that would normally be PV-positive neurons aberrantly differentiate into NPY-positive neurons born later from a potentially distinct lineage).

We recently reported that the loss of SOX5 function in pallium-derived corticofugal projection neurons results in the premature adoption of subcerebral projection neuron features that are characteristic of later stages of cortical projection neuron development(Lai et al., 2008). Therefore, it is possible that SOX6 and SOX5 both suppress coordinately regulated controls that promote premature transition into later stages of subtype differentiation. Consistent with this interpretation are the largely redundant roles of both SOX6 and SOX5 in chondroblasts during cartilage development and in oligodendroglial progenitors in the spinal cord in preventing the premature transition of these cell types to subsequent stages of development(Smits et al., 2001; Stolt et al., 2006). Given their analogous loss-of-function phenotypes, it is interesting to speculate that SOX6 and SOX5 separated in function during the evolution of the increasingly complex neuronal diversity of the telencephalon, and assumed complementary, but distinct, roles.

Funding

This work was partially supported by grants from the US National Institutes of Health (NS49553 and NS45523; additional infrastructure supported by NS41590), the Travis Roy Foundation, the Spastic Paraplegia Foundation, the Massachusetts Spinal Cord Injury research program, and the Harvard Stem Cell Institute to J.D.M., and by the Jane and Lee Seidman Fund for CNS Research, and the Emily and Robert Pearlstein Fund for Nervous System Repair. E.A. was partially supported by a US National Institutes of Health individual predoctoral National Research Service Award fellowship (F31 NS060421). D.J. was partially supported by fellowships from the Swiss National Science Foundation and the Holcim Foundation. R.F. was partially supported by a National Science Foundation Graduate Research Fellowship.

Acknowledgements

We thank K. Billmers, A. Palmer, L. Pasquina, K. Quinn, D. Schuback, E. Sievert, A. Wheeler, and T. Yamamoto for superb technical assistance; G. Fishell, R. Batista-Brito, G. Miyoshi, P. Arlotta, B. Molyneaux, H. Padmanabhan, F. Guillemot, Q. Ma, C. Cepko, and L. Goodrich for helpful discussions and input; U. Berger for technical assistance with *in situ* hybridization; C. Lois, R. Hevner, V. Lefebvre, F. Guillemot, V. Pachnis and Y. Yanagawa for generously sharing mice, antibodies and reagents; and current and past members of our laboratory for helpful suggestions.

Appendix References

Alcamo, E. A., Chirivella, L., Dautzenberg, M., Dobreva, G., Farinas, I., Grosschedl, R. and McConnell, S. K. (2008) Satb2 regulates callosal projection neuron identity in the developing cerebral cortex:: Supplemental Data, *Neuron* 57(3): 364-77.

Arlotta, P., Molyneaux, B. J., Chen, J., Inoue, J., Kominami, R. and Macklis, J. D. (2005) Neuronal subtype-specific genes that control corticospinal motor neuron development in vivo, *Neuron* 45(2): 207-21.

Armijo, J. A., Valdizan, E. M., De Las Cuevas, I. and Cuadrado, A. (2002) [Advances in the physiopathology of epileptogenesis: molecular aspects], *Rev Neurol* 34(5): 409-29.

Ascoli, G. A., Alonso-Nanclares, L., Anderson, S. A., Barrionuevo, G., Benavides-Piccione, R., Burkhalter, A., Buzsaki, G., Cauli, B., Defelipe, J., Fairen, A. et al. (2008) Petilla terminology: nomenclature of features of GABAergic interneurons of the cerebral cortex, *Nat Rev Neurosci* 9(7): 557-68.

Batista-Brito, R., Machold, R., Klein, C. and Fishell, G. (2008) Gene expression in cortical interneuron precursors is prescient of their mature function, *Cereb Cortex* 18(10): 2306-17.

Britanova, O., de Juan Romero, C., Cheung, A., Kwan, K. Y., Schwark, M., Gyorgy, A., Vogel, T., Akopov, S., Mitkovski, M., Agoston, D. et al. (2008) Satb2 is a postmitotic determinant for upper-layer neuron specification in the neocortex, *Neuron* 57(3): 378-92.

Britz, O., Mattar, P., Nguyen, L., Langevin, L. M., Zimmer, C., Alam, S., Guillemot, F. and Schuurmans, C. (2006) A role for proneural genes in the maturation of cortical progenitor cells, *Cereb Cortex* 16 Suppl 1: i138-51.

Butt, S. J., Fuccillo, M., Nery, S., Noctor, S., Kriegstein, A., Corbin, J. G. and Fishell, G. (2005) The temporal and spatial origins of cortical interneurons predict their physiological subtype, *Neuron* 48(4): 591-604.

Butt, S. J., Sousa, V. H., Fuccillo, M. V., Hjerling-Leffler, J., Miyoshi, G., Kimura, S. and Fishell, G. (2008) The requirement of Nkx2-1 in the temporal specification of cortical interneuron subtypes, *Neuron* 59(5): 722-32.

Carney, R. S., Alfonso, T. B., Cohen, D., Dai, H., Nery, S., Stoica, B., Slotkin, J., Bregman, B. S., Fishell, G. and Corbin, J. G. (2006) Cell migration along the lateral cortical stream to the developing basal telencephalic limbic system, *J Neurosci* 26(45): 11562-74.

Cavanagh, M. E. and Parnavelas, J. G. (1988) Development of somatostatin immunoreactive neurons in the rat occipital cortex: a combined immunocytochemical-autoradiographic study, *J Comp Neurol* 268(1): 1-12.

Cavanagh, M. E. and Parnavelas, J. G. (1990) Development of neuropeptide Y (NPY) immunoreactive neurons in the rat occipital cortex: a combined immunohistochemical-autoradiographic study, *J Comp Neurol* 297(4): 553-63.

Chen, B., Schaevitz, L. R. and McConnell, S. K. (2005a) Fezl regulates the differentiation and axon targeting of layer 5 subcortical projection neurons in cerebral cortex, *Proc Natl Acad Sci USA* 102(47): 17184-9.

Chen, J.-G., Rasin, M.-R., Kwan, K. Y. and Sestan, N. (2005b) Zfp312 is required for subcortical axonal projections and dendritic morphology of deep-layer pyramidal neurons of the cerebral cortex, *Proc Natl Acad Sci USA* 102(49): 17792-7.

Cobos, I., Calcagnotto, M. E., Vilaythong, A. J., Thwin, M. T., Noebels, J. L., Baraban, S. C. and Rubenstein, J. L. (2005) Mice lacking Dlx1 show subtype-specific loss of interneurons, reduced inhibition and epilepsy, *Nat Neurosci* 8(8): 1059-68.

Connor, F., Wright, E., Denny, P., Koopman, P. and Ashworth, A. (1995) The Sry-related HMG box-containing gene Sox6 is expressed in the adult testis and developing nervous system of the mouse, *Nucleic Acids Res* 23(17): 3365-72.

Corbin, J. G., Nery, S. and Fishell, G. (2001) Telencephalic cells take a tangent: non-radial migration in the mammalian forebrain, *Nat Neurosci* 4 Suppl: 1177-82.

Du, T., Xu, Q., Ocbina, P. J. and Anderson, S. A. (2008) NKX2.1 specifies cortical interneuron fate by activating Lhx6, *Development* 135(8): 1559-67.

Flames, N. and Marin, O. (2005) Developmental mechanisms underlying the generation of cortical interneuron diversity, *Neuron* 46(3): 377-81.

Flames, N., Pla, R., Gelman, D. M., Rubenstein, J. L., Puelles, L. and Marin, O. (2007) Delineation of multiple subpallial progenitor domains by the combinatorial expression of transcriptional codes, *J Neurosci* 27(36): 9682-95.

Fode, C., Ma, Q., Casarosa, S., Ang, S. L., Anderson, D. J. and Guillemot, F. (2000) A role for neural determination genes in specifying the dorsoventral identity of telencephalic neurons, *Genes Dev* 14(1): 67-80.

Fogarty, M., Grist, M., Gelman, D., Marin, O., Pachnis, V. and Kessaris, N. (2007) Spatial genetic patterning of the embryonic neuroepithelium generates GABAergic interneuron diversity in the adult cortex, *J Neurosci* 27(41): 10935-46.

Holm, P. C., Mader, M. T., Haubst, N., Wizenmann, A., Sigvardsson, M. and Gotz, M. (2007) Loss- and gain-of-function analyses reveal targets of Pax6 in the developing mouse telencephalon, *Mol Cell Neurosci* 34(1): 99-119.

Joshi, P. S., Molyneaux, B. J., Feng, L., Xie, X., Macklis, J. D. and Gan, L. (2008) Bhlhb5 regulates the postmitotic acquisition of area identities in layers II-V of the developing neocortex, *Neuron* 60(2): 258-72.

Kwan, K. Y., Lam, M. M. S., Krsnik, Z., Kawasawa, Y. I., Lefebvre, V. and Sestan, N. (2008) SOX5 postmitotically regulates migration, postmigratory differentiation, and projections of subplate and deep-layer neocortical neurons, *Proc Natl Acad Sci USA* 105(41): 16021-6.

Lai, T., Jabaudon, D., Molyneaux, B. J., Azim, E., Arlotta, P., Menezes, J. R. and Macklis, J. D. (2008) SOX5 Controls the Sequential Generation of Distinct Corticofugal Neuron Subtypes, *Neuron* 57(2): 232-247.

Levitt, P., Eagleson, K. L. and Powell, E. M. (2004) Regulation of neocortical interneuron development and the implications for neurodevelopmental disorders, *Trends Neurosci* 27(7): 400-6.

Lewis, D. A. (2000) GABAergic local circuit neurons and prefrontal cortical dysfunction in schizophrenia, *Brain Res Brain Res Rev* 31(2-3): 270-6.

Liodis, P., Denaxa, M., Grigoriou, M., Akufo-Addo, C., Yanagawa, Y. and Pachnis, V. (2007) Lhx6 activity is required for the normal migration and specification of cortical interneuron subtypes, *J Neurosci* 27(12): 3078-89.

Ma, Q., Sommer, L., Cserjesi, P. and Anderson, D. J. (1997) Mash1 and neurogenin1 expression patterns define complementary domains of neuroepithelium in the developing CNS and are correlated with regions expressing notch ligands, *J Neurosci* 17(10): 3644-52.

Miyoshi, G., Butt, S. J., Takebayashi, H. and Fishell, G. (2007) Physiologically distinct temporal cohorts of cortical interneurons arise from telencephalic Olig2-expressing precursors, *J Neurosci* 27(29): 7786-98.

Molnar, Z. and Butler, A. B. (2002) The corticostriatal junction: a crucial region for forebrain development and evolution, *Bioessays* 24(6): 530-41.

Molyneaux, B. J., Arlotta, P., Hirata, T., Hibi, M. and Macklis, J. D. (2005) Fezl is required for the birth and specification of corticospinal motor neurons, *Neuron* 47(6): 817-31.

Molyneaux, B. J., Arlotta, P., Menezes, J. R. and Macklis, J. D. (2007) Neuronal subtype specification in the cerebral cortex, *Nat Rev Neurosci* 8(6): 427-37.

Narahara, M., Yamada, A., Hamada-Kanazawa, M., Kawai, Y. and Miyake, M. (2002) cDNA cloning of the Sry-related gene Sox6 from rat with tissue-specific expression, *Biol Pharm Bull* 25(6): 705-9.

Nobrega-Pereira, S., Kessaris, N., Du, T., Kimura, S., Anderson, S. A. and Marin, O. (2008) Postmitotic Nkx2-1 controls the migration of telencephalic interneurons by direct repression of guidance receptors, *Neuron* 59(5): 733-45.

Parras, C. M., Schuurmans, C., Scardigli, R., Kim, J., Anderson, D. J. and Guillemot, F. (2002) Divergent functions of the proneural genes Mash1 and Ngn2 in the specification of neuronal subtype identity, *Genes Dev* 16(3): 324-38.

Puelles, L., Kuwana, E., Puelles, E., Bulfone, A., Shimamura, K., Keleher, J., Smiga, S. and Rubenstein, J. L. (2000) Pallial and subpallial derivatives in the embryonic chick and mouse telencephalon, traced by the expression of the genes Dlx-2, Emx-1, Nkx-2.1, Pax-6, and Tbr-1, *J Comp Neurol* 424(3): 409-38.

Rubenstein, J. L. and Merzenich, M. M. (2003) Model of autism: increased ratio of excitation/inhibition in key neural systems, *Genes Brain Behav* 2(5): 255-67.

Scardigli, R., Baumer, N., Gruss, P., Guillemot, F. and Le Roux, I. (2003) Direct and concentration-dependent regulation of the proneural gene Neurogenin2 by Pax6, *Development* 130(14): 3269-81.

Schuurmans, C. and Guillemot, F. (2002) Molecular mechanisms underlying cell fate specification in the developing telencephalon, *Curr Opin Neurobiol* 12(1): 26-34.

Smits, P., Li, P., Mandel, J., Zhang, Z., Deng, J. M., Behringer, R. R., de Crombrugghe, B. and Lefebvre, V. (2001) The transcription factors L-Sox5 and Sox6 are essential for cartilage formation, *Dev Cell* 1(2): 277-90.

Stolt, C. C., Schlierf, A., Lommes, P., Hillgartner, S., Werner, T., Kosian, T., Sock, E., Kessaris, N., Richardson, W. D., Lefebvre, V. et al. (2006) SoxD proteins influence multiple stages of oligodendrocyte development and modulate SoxE protein function, *Dev Cell* 11(5): 697-709.

Tamamaki, N., Yanagawa, Y., Tomioka, R., Miyazaki, J., Obata, K. and Kaneko, T. (2003) Green fluorescent protein expression and colocalization with calretinin, parvalbumin, and somatostatin in the GAD67-GFP knock-in mouse, *J Comp Neurol* 467(1): 60-79.

Vega, C. J. and Peterson, D. A. (2005) Stem cell proliferative history in tissue revealed by temporal halogenated thymidine analog discrimination, *Nat Methods* 2(3): 167-9.

Wegner, M. (1999) From head to toes: the multiple facets of Sox proteins, *Nucleic Acids Res* 27(6): 1409-20.

Wegner, M. and Stolt, C. C. (2005) From stem cells to neurons and glia: a Soxist's view of neural development, *Trends Neurosci* 28(11): 583-8.

Wonders, C. P. and Anderson, S. A. (2006) The origin and specification of cortical interneurons, *Nat Rev Neurosci* 7(9): 687-96.

Wonders, C. P., Taylor, L., Welagen, J., Mbata, I. C., Xiang, J. Z. and Anderson, S. A. (2008) A spatial bias for the origins of interneuron subgroups within the medial ganglionic eminence, *Dev Biol* 314(1): 127-36.

Zhao, Y., Flandin, P., Long, J. E., Cuesta, M. D., Westphal, H. and Rubenstein, J. L. (2008) Distinct molecular pathways for development of telencephalic interneuron subtypes revealed through analysis of Lhx6 mutants, *J Comp Neurol* 510(1): 79-99.